FERROPTOSIS AS NEW THERAPEUTIC TARGETS IN CANCER: FROM MOLECULAR MECHANISMS TO THERAPEUTIC OPPORTUNITIES

EDITED BY: Xu Chen, Jiaoti Huang, Yasusei Kudo and Jian Chen

PUBLISHED IN: Frontiers in Pharmacology and Frontiers in Oncology

frontiers Research Topics

frontiers

ISSN 1664-8714
ISBN 978-2-83250-427-7
DOI 10.3389/978-2-83250-427-7

About Frontiers

Frontiers is more than just an open-access publisher of scholarly articles: it is a pioneering approach to the world of academia, radically improving the way scholarly research is managed. The grand vision of Frontiers is a world where all people have an equal opportunity to seek, share and generate knowledge. Frontiers provides immediate and permanent online open access to all its publications, but this alone is not enough to realize our grand goals.

Frontiers Journal Series

The Frontiers Journal Series is a multi-tier and interdisciplinary set of open-access, online journals, promising a paradigm shift from the current review, selection and dissemination processes in academic publishing. All Frontiers journals are driven by researchers for researchers; therefore, they constitute a service to the scholarly community. At the same time, the Frontiers Journal Series operates on a revolutionary invention, the tiered publishing system, initially addressing specific communities of scholars, and gradually climbing up to broader public understanding, thus serving the interests of the lay society, too.

Dedication to Quality

Each Frontiers article is a landmark of the highest quality, thanks to genuinely collaborative interactions between authors and review editors, who include some of the world's best academicians. Research must be certified by peers before entering a stream of knowledge that may eventually reach the public - and shape society; therefore, Frontiers only applies the most rigorous and unbiased reviews.
Frontiers revolutionizes research publishing by freely delivering the most outstanding research, evaluated with no bias from both the academic and social point of view. By applying the most advanced information technologies, Frontiers is catapulting scholarly publishing into a new generation.

What are Frontiers Research Topics?

Frontiers Research Topics are very popular trademarks of the Frontiers Journals Series: they are collections of at least ten articles, all centered on a particular subject. With their unique mix of varied contributions from Original Research to Review Articles, Frontiers Research Topics unify the most influential researchers, the latest key findings and historical advances in a hot research area! Find out more on how to host your own Frontiers Research Topic or contribute to one as an author by contacting the Frontiers Editorial Office: frontiersin.org/about/contact

FERROPTOSIS AS NEW THERAPEUTIC TARGETS IN CANCER: FROM MOLECULAR MECHANISMS TO THERAPEUTIC OPPORTUNITIES

Topic Editors:
Xu Chen, Guilin Medical University, China
Jiaoti Huang, Duke University, United States
Yasusei Kudo, Tokushima University, Japan
Jian Chen, Guilin Medical University, China

Citation: Chen, X., Huang, J., Kudo, Y., Chen, J., eds. (2022). Ferroptosis as New Therapeutic Targets in Cancer: From Molecular Mechanisms to Therapeutic Opportunities. Lausanne: Frontiers Media SA. doi: 10.3389/978-2-83250-427-7

Table of Contents

frontiers | Frontiers in Pharmacology

TYPE Editorial
PUBLISHED 23 September 2022
DOI 10.3389/fphar.2022.1019395

OPEN ACCESS

EDITED AND REVIEWED BY
Olivier Feron,
Université catholique de Louvain,
Belgium

*CORRESPONDENCE
Xu Chen,
chenxu@glmc.edu.cn

SPECIALTY SECTION
This article was submitted to Pharmacology of Anti-Cancer Drugs, a section of the journal Frontiers in Pharmacology

RECEIVED 15 August 2022
ACCEPTED 05 September 2022
PUBLISHED 23 September 2022

CITATION
Chen J and Chen X (2022), Editorial: Ferroptosis as new therapeutic targets in cancer: From molecular mechanisms to therapeutic opportunities. *Front. Pharmacol.* 13:1019395. doi: 10.3389/fphar.2022.1019395

Editorial: Ferroptosis as new therapeutic targets in cancer: From molecular mechanisms to therapeutic opportunities

Jian Chen[1] and Xu Chen[2]*

[1]School of Basic Medical Sciences, Guilin Medical University, Guilin, China, [2]College of Pharmacy, Guilin Medical University, Guilin, China

KEYWORDS

ferroptosis, molecular mechanism, pharmacology, cancer therapy, programmed cell death

Editorial on the Research Topic
Ferroptosis as new therapeutic targets in cancer: from molecular mechanisms to therapeutic opportunities

Ferroptosis is a new form of programmed cell death characterized by iron-dependent accumulation of lipid reactive oxygen species (ROS). In the process of ferroptosis, excessive iron accumulation can trigger Fenton reaction in cells, induce massive production of ROS, and finally cause lipid peroxidation, DNA damage and protein degradation (Dixon et al., 2012). In the last decade, there has been an increased interest in the process and function of ferroptosis due to its relationship to various diseases including cancer. Following treatment with ferroptosis inducers (e.g., erastin, RSL3 and sorafenib), the anti-tumor response can be achieved in various cancer types and models, highlighting the need for better understanding of molecular mechanism of ferroptosis (Zhao et al., 2020). In this editorial, we provide a platform for most recent advances in the mechanism of ferroptosis initiation and execution in cancer cells, along with the potential clinical application of ferroptosis-related drugs to cancer therapy. The Research Topic represents a collection of 10 original research articles, seven review articles ranging from theory to application.

There are three main metabolic pathways in ferroptosis, namely, iron metabolism, lipid metabolism and amino acid metabolism. Among them, the first two metabolism types contribute to increased generation of lipid peroxide, whereas the latter is known to be responsible for antioxidant response. Lipid peroxidation plays an essential part in the mechanism of ferroptosis. Its major process is to convert the polyunsaturated fatty acids (PUFA) to toxic PUFA-PE-OH, leading to initiation of cell death cascades (Conrad et al., 2018). These reactions were successively catalyzed by the acyl-CoA synthetase long-chain family member 4 (ACSL4), polyunsaturated fatty acids-phosphatidylethanolamine (LPCAT3) catalysis and arachidonic acid lipoxygenases ($ALOX_S$). Interestingly,

ACSL4 facilitates ferroptotic cell death, but recent studies showed that ACSL4 levels are up-regulated in multiple cancer types and is associated with cancer malignancy (Hou et al., 2022). As expected, ACSL4 down-regulation by Yiqi Huayu Decoction (YQHY), a traditional Chinese herbal medicine compound, induced ferroptosis, and inhibited gastric cancer proliferation and metastasis (Song et al.). Moreover, KEGG pathway enrichment analysis showed the hub targets of YQHY mainly enriched in the JAK2-STAT3 signaling pathway. On the other hand, ACSL4 expression was notably decreased in ferroptosis-resistant cells, and its up-regulation promoted the sensitivity to ferroptosis, indicating the role of ACSL4 in chemoresistance (Doll et al., 2017).

In the process of amino acid metabolism, cystine is transferred into cells with the help of glutamate-cystine antiporter system X_c^- (xCT), consisting of SLC3A2 and SLC7A11. Next, intracellular cystine is converted to cysteine and participates in synthesis of Glutathione (GSH) that is then rapidly oxidized to glutathione disulfide (GSSG) via glutathione peroxidase 4 (GPX4) (Badgley et al., 2020). Functioning as an active peroxidase, GPX4 has protective effect against oxidative damage by catalyzing the degradation of lipid peroxides. Until now, several drugs targeting this antioxidant line of defense have been demonstrated to inhibit tumor growth by promoting ferroptosis. Erastin and its derivatives, for example, could prevent the system X_c^- antiporter and decrease cystine import, thus decreasing GSH bioavailability (Koppula et al., 2021). Huang et al. further examined the mechanism of GSH-targeting ferroptosis using network pharmacology and molecular docking in oral cancer. Total 14 core targets of GSH were identified to be involved in ferroptosis. Moreover, GSH was predicted to bind directly to EGFR, PTGS2 and HIF1A proteins, all of which have been demonstrated to correlate with ferroptosis in human cancers. These bioinformatic data provides new mechanistic insights into GSH action in ferroptosis, as well as the GSH-based cancer therapies.

In addition, there is involvement of organelles-specific regulation in the initiation or avoidance of ferroptosis, including mitochondria, endoplasmic reticulum (ER), Golgi and lysosome (Zhang et al.). On the one hand, mitochondria electron transport chain (ETC) are the main sources of ROS production. On the other hand, mitochondria are also involved in the intracellular iron homeostasis via regulation of iron transportation in mitochondria, which could affect the production of mitochondrial ROS (mitoROS) (Battaglia et al., 2020). ER is a continuous membrane system and the main site of protein, lipid and carbohydrate synthesis. The activation of ER stress sensors, IRE1, PERK and ATF6, are capable of emitting pro-apoptotic signaling pathways, causing ER stress-mediated ferroptosis (Lee et al., 2018). Otherwise, the location of ACSL4 to the Golgi apparatus suggests that lipid peroxide may also occur in Golgi membranes (Alborzinia et al., 2018). Actually, the lipid peroxides accumulate subsequent to Golgi stress, and induce ferroptosis by reducing intracellular glutathione. Autophagy is a conserved lysosome-mediated degradation process, which is crucial for maintenance of cellular homeostasis. Recent studies have shown that the treatment of RSL3 can decrease GPX4 levels, promote autophagy degradation of intracellular lipid, and enhance accumulation of free fatty acids, leading to ferroptosis in human tumor cell lines (Wang et al., 2019). In agreement with these results, Li et al. demonstrated that the expression of E3 ubiquitin ligase F-box only protein 22 (FBXO22), a key regulator of cellular protein degradation degradation, was significantly increased in epithelial ovarian cancer tissues and was closely correlated with clinical pathological variables. What's more, FBXO22 promoted cell proliferation and metastasis *via* MAPK/ERK pathway, whereas inhibited the autophagy flux in a p-ERK-dependent manner, suggesting its potential as a target for epithelial ovarian cancer therapy, With better understanding of the pathways involved in ferroptosis, an increasing number of ferroptosis regulators have been demonstrated. Tabnak et al. roughly classified these regulators into suppressors (mainly System X_c^-, GPX4, FSP1, NRF2 and NFS1) and inducers (mainly ACSL4) in the context of lung cancer. Further, these ferroptosis regulators can predict the prognosis of patients with lung cancer, as well as the overall survival. Among them, nuclear factor E2-related factor 2 (Nrf2) plays a essential role in ferroptotic cell death through regulation of multiple downstream targets (Dempke and Reck, 2021). For example, Nrf2 activates the GPX4 and SLC7A11 expression to exert inhibitory effects on lipid peroxidation (Gao et al., 2020). Also regulated by Nrf2 are heme oxygenase 1 (HO1) and ferritin. HO1 catalyzes the heme to choline, and thus inhibit the production of ROC (Wei et al., 2021). Ferritin is a protein composed of light chain (FTL) and heavy chain (FTH1) subunits and has the function of storing iron (Horniblow et al., 2022). Xiang et al. reported that erianin, a natural product derived from *Dendrobium chrysotoxum Lindl*, significantly triggered ferroptosis and cell cycle arrest in bladder cancer cells both *in vitro* and *in vivo*, as demonstrated by decreased ROS accumulation and GSH depletion. Moreover, Nrf2 was a key factor in erianin-triggered ferroptosis, as Nrf2 reduction resulted in downregulation of GPX4, xCT/SLC7A11, HO-1, FTH1 and GLS.

Unlike Nrf2 pathway, p53 pathway has a dual role in ferroptosis. It can function as ferroptosis suppressor by inducing cyclin-dependent kinase inhibitor (CDKN1A), iPLA2β and parkinson disease 2 (PARK2), which may be associated with decreased ROS production and attenuated GSH depletion (Kang et al., 2019). Also, p53 pathway promoted ferroptosis in tumor cells. Once activated, p53 can inhibit SLC7A11expression by binding to the promoter region of SLC7A11, thus depleting intracellular cysteine and impairing the antioxidant program in cells (Jiang et al., 2015). Additionally, p53 activation is subject to multiple post-translational modifications including ubiquitination, phosphorylation, methylation, acetylation, O-GlcNAcylation and SUMOylation (Zhang et al.). Therefore, dysfunction of p53 has a complex impact on carcinogenesis.

The epigenetic regulation in ferroptosis presents a new direction for therapeutic intervention in cancer. Epigenetic mechanism underlying ferroptosis includes DNA methylation, histone modification, RNA modification and non-coding RNAs (Pei et al.). Recent research mainly focused on the role of non-coding RNAs in regulating key genes of ferroptosis. It was found that some microRNAs (miRNAs) such as miRNA-17-92, miRNA-4715-3p and miRNA-137 could respectively trigger the translational inhibition of ACSL4, GPX4 and SLC1A5 through targeting the 3′-UTR region of mRNA to promote or inhibit ferroptosis in cancer cells (Zhang et al., 2020). Wang et al. analyzed ovarian cancer-related long noncoding RNA (lncRNA) expression profile and clinical follow-up information, and reported that high ferroptosis-related lncRNA expression in patients with ovarian cancer may be more sensitive to conventional chemotherapy or ferroptosis inducers.

Drug resistance is a big challenge facing the successful application of chemotherapy. Therefore, the role of ferroptosis in drug sensitivity of tumors has been attracting more attention. As an important antioxidant, Nrf2 plays a key role in the crosstalk between ferroptosis-related oxidative stress and drug resistance. In Hepatocellular carcinoma (HCC) cells, the overexpression of Nrf2 by PI3K/Akt pathway produced residence to sorafenib (Liu et al.). The activation of PI3K/Akt/Nrf2 pathway was mediated by up-regulation of fibronectin type III domain containing 5 (FNDC5), a transmembrane protein associated with electron transport in mitochondrial oxidative respiration. Subsequent to the activation of PI3K/Akt pathway by FNDC5, Nrf2 translocates into the nucleus, binds to DNA and initiates the transcription of antioxidant enzymes, thereby reducing sorafenib-induced ferroptosis and causing resistance. It suggests that induction of ferroptosis may has promising potential for treatment of chemotherapy-resistant cancers. Accordingly, the cooperation of cisplatin and ferroptosis inducers (e.g., erastin and RSL3) was found to promote ferroptosis and reverse resistance in a variety of cancers (Nie et al.). Notably, evidence shows that the ferroptosis induction can also prevent tumor resistance to immunotherapy. Zhou et al. revealed that cisplatin induced ferroptosis in NSCLC cells, followed by recruitment of neutrophils in tumor tissues. Next, these neutrophils were polarized to a proinflammatory N1 phenotype by ferroptosis and helped to remolded the “cold” tumor TME towards a “hot” one where T cell infiltration and Th1 differentiation were augmented. It seems that the application of cisplatin enhance immune response of cancer cells to immunotherapy due to ferroptosis.

As the field of ferroptosis-inducing therapy with more essential target genes being introduced and new drugs being developed, its application in cancer treatment becomes increasingly significant. For example, Yun et al. used the latest DepMap release CRISPR data to construct a novel prognostic signature based on seven ferroptosis-related genes (ISCU, NFS1, MTOR, EIF2S1, HSPA5, AURKA, RPL8) to predict and monitor clinical outcomes in patients with glioma. Similarly, by using bioinformatics methods, two ferroptosis-related proteins ALB and VEGFA were identified as main potential biomarkers for detecting and directing pharmacological treatment for HCC (Qin et al.). Remarkably, better understanding of ferroptosis-related regulatory mechanisms helps to provide new applications for an old drug. Li et al. proved that PI3K/Akt/mTOR inhibitor NVP BEZ235 significantly suppressed growth and metastasis in renal cell carcinoma (RCC) cell lines, which was mediated by dual regulation of PI3K/Akt/mTOR and TAK1 signaling pathways. Considering the involvement of these pathways in ferroptosis induction, the combination of NVP BEZ235 with ferroptosis inducers may be a new strategy for treating cancers. Actually, the combined therapy using conventional chemotherapeutic agents with clinically available ferroptosis-inducing drugs has been suggested as a possible way to improve anti-cancer efficacy and overcome resistance. In view of the low sensitivity of pancreatic ductal adenocarcinoma (PDAC) to all current treatment regimens, inducing ferroptotic cell death may provide more effective therapeutic strategy to treat PDAC (Liu et al.).

Overall, this Research Topic elucidate the mechanism of action of ferroptosis in cancers, and highlight the key role of ferroptosis in cancer therapy. Indeed, more in-depth research is

needed to better understand the mechanisms and regulation of ferroptosis, ascertain the relationship and cross talk between ferroptosis and other types of cell death, and verify its clinical utility. However, it will undoubtedly provide us with new direction in the treatment of cancer.

Author contributions

All authors listed have made a substantial, direct, and intellectual contribution to the work and approved it for publication.

Funding

This research was supported by the National Natural Science Foundation of China (Grant Nos. 81973574 and 82174082) and the Natural Science Foundation of Guangxi (Grant No. 2019GXNSFFA245001).

Acknowledgments

We are grateful to all the authors and reviewers for their excellent contributions and insightful comments to this Research Topic.

Conflict of interest

The authors declare that the research was conducted in the absence of any commercial or financial relationships that could be construed as a potential conflict of interest.

Publisher's note

References

Alborzinia, H., Ignashkova, T. I., Dejure, F. R., Gendarme, M., Theobald, J., Wölfl, S., et al. (2018). Golgi stress mediates redox imbalance and ferroptosis in human cells. *Commun. Biol.* 1, 210. doi:10.1038/s42003-018-0212-6

Badgley, M. A., Kremer, D. M., Maurer, H. C., DelGiorno, K. E., Lee, H. J., Purohit, V., et al. (2020). Cysteine depletion induces pancreatic tumor ferroptosis in mice. *Science* 368, 85–89. doi:10.1126/science.aaw9872

Battaglia, A. M., Chirillo, R., Aversa, I., Sacco, A., Costanzo, F., and Biamonte, F. (2020). Ferroptosis and cancer: Mitochondria meet the "iron maiden" cell death. *Cells* 9, 1505. doi:10.3390/cells9061505

Conrad, M., Kagan, V. E., Bayir, H., Pagnussat, G. C., Head, B., Traber, M. G., et al. (2018). Regulation of lipid peroxidation and ferroptosis in diverse species. *Genes Dev.* 32, 602–619. doi:10.1101/gad.314674.118

Dempke, W. C. M., and Reck, M. (2021). KEAP1/NRF2 (NFE2L2) mutations in NSCLC-Fuel for a superresistant phenotype? *Lung Cancer* 159, 10–17. doi:10.1016/j.lungcan.2021.07.006

Dixon, S. J., Lemberg, K. M., Lamprecht, M. R., Skouta, R., Zaitsev, E. M., Gleason, C. E., et al. (2012). Ferroptosis: An iron-dependent form of nonapoptotic cell death. *Cell* 149, 1060–1072. doi:10.1016/j.cell.2012.03.042

Doll, S., Proneth, B., Tyurina, Y. Y., Panzilius, E., Kobayashi, S., Ingold, I., et al. (2017). ACSL4 dictates ferroptosis sensitivity by shaping cellular lipid composition. *Nat. Chem. Biol.* 13, 91–98. doi:10.1038/nchembio.2239

Gao, X., Guo, N., Xu, H., Pan, T., Lei, H., Yan, A., et al. (2020). Ibuprofen induces ferroptosis of glioblastoma cells via downregulation of nuclear factor erythroid 2-related factor 2 signaling pathway. *Anticancer. Drugs* 31, 27–34. doi:10.1097/CAD.0000000000000825

Horniblow, R. D., Pathak, P., Balacco, D. L., Acharjee, A., Lles, E., Gkoutos, G., et al. (2022). Iron-mediated epigenetic activation of NRF2 targets. *J. Nutr. Biochem.* 101, 108929. doi:10.1016/j.jnutbio.2021.108929

Hou, J., Jiang, C., Wen, X., Li, C., Xiong, S., Yue, T., et al. (2022). ACSL4 as a potential target and biomarker for anticancer: From molecular mechanisms to clinical therapeutics. *Front. Pharmacol.* 13, 949863. doi:10.3389/fphar.2022.949863

Jiang, L., Kon, N., Li, T., Wang, S. J., Su, T., Hibshoosh, H., et al. (2015). Ferroptosis as a p53-mediated activity during tumour suppression. *Nature* 520, 57–62. doi:10.1038/nature14344

Kang, R., Kroemer, G., and Tang, D. (2019). The tumor suppressor protein p53 and the ferroptosis network. *Free Radic. Biol. Med.* 133, 162–168. doi:10.1016/j.freeradbiomed.2018.05.074

Koppula, P., Zhuang, L., and Gan, B. (2021). Cystine transporter SLC7A11/xCT in cancer: Ferroptosis, nutrient dependency, and cancer therapy. *Protein Cell* 12, 599–620. doi:10.1007/s13238-020-00789-5

Lee, Y. S., Lee, D. H., Choudry, H. A., Bartlett, D. L., and Lee, Y. J. (2018). Ferroptosis-induced endoplasmic reticulum stress: Cross-talk between ferroptosis and apoptosis. *Mol. Cancer Res.* 16, 1073–1076. doi:10.1158/1541-7786.MCR-18-0055

Wang, X., Lu, S., He, C., Wang, C., Wang, L., Piao, M., et al. (2019). RSL3 induced autophagic death in glioma cells via causing glycolysis dysfunction. *Biochem. Biophys. Res. Commun.* 518, 590–597. doi:10.1016/j.bbrc.2019.08.096

Wei, R., Zhao, Y., Wang, J., Yang, X., Li, S., Wang, Y., et al. (2021). Tagitinin C induces ferroptosis through PERK-Nrf2-HO-1 signaling pathway in colorectal cancer cells. *Int. J. Biol. Sci.* 17, 2703–2717. doi:10.7150/ijbs.59404

Zhang, X., Wang, L., Li, H., Zhang, L., Zheng, X., and Cheng, W. (2020). Crosstalk between noncoding RNAs and ferroptosis: New dawn for overcoming cancer progression. *Cell Death Dis.* 11, 580. doi:10.1038/s41419-020-02772-8

Zhao, Y., Li, Y., Zhang, R., Wang, F., Wang, T., and Jiao, Y. (2020). The Role of erastin in ferroptosis and its prospects in cancer therapy. *Onco. Targets. Ther.* 13, 5429–5441. doi:10.2147/OTT.S254995

frontiers in Pharmacology

ORIGINAL RESEARCH
published: 17 September 2021
doi: 10.3389/fphar.2021.742349

Integrated Analysis and Finding Reveal Anti–Liver Cancer Targets and Mechanisms of Pachyman (*Poria cocos* Polysaccharides)

*Li Qin, Dongning Huang, Jian Huang, Fuhui Qin and Haixin Huang**

Department of Oncology, Liuzhou Worker's Hospital, Liuzhou, China

This bioinformatics study aimed to characterize and certify crucial anti-cancer targets, functional processes, and molecular mechanisms of Pachyman in treating hepatocellular carcinoma (HCC) by using pharmacology network and molecular docking analyses, by experimental validation. The crucial anti-HCC targets of Pachyman, including ALB, VEGFA, TNF, CASP3, SRC, EGF, CXCR4, STAT3, HRAS, HSP90AA1, MMP9, BCL2L1, FGF2, and PTPRC, were identified. In addition, the correlative networks of all crucial biotargets of Pachyman in treating HCC were created accordingly. Functionally, these crucial genes were correlated using angiogenesis and neoplastic metastasis of HCC. Interestingly, the molecular docking findings indicated that ALB and VEGFA in HCC might be potent pharmacological targets of Pachyman. In experimental validation, the clinical samples of HCC showed reduced ALB protein expression and increased VEGFA protein level. Following Pachyman treatments *in vitro*, the intracellular level of ALB protein was elevated, whereas the cellular content of VEGFA protein was downregulated. Taken together, current bioinformatics findings based on pharmacology network and molecular docking analyses elucidate the detailed molecular targets and signaling mechanisms of Pachyman in treating HCC. Interestingly, validated biotargets of ALB and VEGFA may be main potential biomarkers for detecting HCC medically.

Keywords: liver cancer, Pachyman, network pharmacology, molecular docking, biomarkers 3

OPEN ACCESS

Edited by:
Xu Chen,
Guilin Medical University, China

Reviewed by:
Liming Zhou,
Sichuan University, China
Manisha Kumari,
Thomas Jefferson University, United States

****Correspondence:***
Haixin Huang
hhxliuzhou@163.com

Specialty section:
This article was submitted to Pharmacology of Anti-Cancer Drugs, a section of the journal Frontiers in Pharmacology

Received: *16 July 2021*
Accepted: *23 August 2021*
Published: *17 September 2021*

Citation:
*Qin L, Huang D, Huang J, Qin F and Huang H (2021) Integrated Analysis and Finding Reveal Anti–Liver Cancer Targets and Mechanisms of Pachyman (*Poria cocos *Polysaccharides). Front. Pharmacol. 12:742349. doi: 10.3389/fphar.2021.742349*

INTRODUCTION

Hepatocellular carcinoma (HCC) refers to a malignant tumor, occurring in liver tissue *in situ*. Statistically, HCC cases account for a majority of cancer-causing deaths worldwide (McGlynn et al., 2021). As revealed in epidemiological assay, HCC is one of the deadly tumors in China, featured with elevated morbidity and mortality yearly (Fu and Wang, 2018). Notably, early symptoms of HCC may be inconspicuous during clinical characterization before the tumor develops as malignant and invasive. Accordingly, most of the HCC patients are diagnosed with advanced stages during initial examination, eventually leading to high mortality and undesired metastasis (Llovet et al., 2018; Llovet et al., 2021). For precision medicine, it is particularly necessary to identify more candidate anti-HCC targets for effective diagnosis, prognosis, and treatment (Anwanwan et al., 2020). In addition, some naturally occurring ingredients may be used for HCC treatment. Pachyman, *Poria cocos* polysaccharides, is a biologically active component that is isolated from the *Poria cocos* plant (Sun, 2014). Beneficially, Pachyman has been proven to exert potent pharmacological properties,

such as antioxidation, anti-tumor action, hepatoprotection, enhancing immunity, and eliminating free radicals (Wu et al., 2018; Li et al., 2019; Liu et al., 2020). Although well-evidenced anti-cancer benefits have been found, there are still only few studies regarding the pharmacological effects of Pachyman in treating HCC. Intriguingly, an attractive strategy using network pharmacology and molecular docking analyses can function as an emerging and promising tool for revealing detailed biotargets and molecular mechanisms of candidate natural agents for treating medical diseases (Li et al., 2020a; Li et al., 2021a), including liver disease (Su et al., 2019), coronavirus disease 2019 (COVID-19) (Qin et al., 2021), and meningitis (Li et al., 2021b). Therefore, the present study was designed to optimize network pharmacology and molecular docking methods in identifying the bioinformatics findings of Pachyman in treating HCC, including detailed biological targets, functional processes, and signaling pathways. Experimentally, some bioinformatics data were validated for potential clinical use of Pachyman in treating HCC in future.

MATERIALS AND METHODS

Screening of Anti-HCC Candidate Targets of Pachyman

All pharmacological targets of Pachyman were collected from databases of PharmMapper and Swiss Target Prediction databases. In addition, HCC-related targets were obtained from databases of OncoDB.HCC and Liverome. Furthermore, these identifiable targets of Pachyman and HCC were determined by using the FunRich software to construct an intersection map of Pachyman in treating HCC, as described by Li et al. (2021c).

Construction of an Integrated Network in Anti-HCC Targets of Pachyman

The available anti-HCC targets of Pachyman were imported to the STRING database for presenting protein–protein interaction (PPI) data with the confidence score greater than 0.9, and then introduced to the Cytoscape software for constructing a PPI map of Pachyman against HCC targets. The PPI network was modeled as a visualized graph, in which the nodes represented genes and the edges indicated the interaction proteins encoded by the related genes (Li et al., 2021d).

Identification and Construction Hub Network of Crucial Targets

Additionally, Network Analyzer in Cytoscape tool was used to determine topological parameters, such as average degree and maximum degree of PPI network of Pachyman in treating HCC, and then the crucial targets were screened and identified according to the contrivable degree value of the targets. Moreover, these crucial targets with interaction network were featured and visualized by using a software platform of Cytoscape for integrating complex networks, as described by Li et al. (2021e).

Enrichment and Function Analyses of Crucial Targets

Subsequently, Gene Ontology (GO) function and Kyoto Encyclopedia of Genes and Genomes (KEGG) pathway enrichment assays were generated by using the Metascape online platform. Additionally, the biological functions and pathway enrichment findings of all crucial targets were featured and visualized by using the OmicShare cloud platform before generating advanced bubble diagrams according to their *p*-values. Furthermore, the crucial target-signaling pathway network of Pachyman in treating HCC was constructed by using the Cytoscape software (Li et al., 2020b).

Molecular Docking Analysis

The molecular structure of the Pachyman compound was obtained from the PubChem database. The crucial target/protein structure in HCC was obtained from the Protein Data Bank database. Magnetometric minimum force field was obtained by using the three-dimensional structure of ChemBio3D Draw module in the ChemBioOffice software (version 2010). The PDBQT structure file necessary for virtual screening was created through the Raccoon software, and the docking active center was defined through the grid box function setting in the software. Data reliability was determined according to the size of the root-mean-square deviation of the docked and the original ligand molecules. Generally, it was designed in a way that the root-mean-square deviation that is ≤4 was the threshold for conforming the docked ligand to match the related original ligand (Nong et al., 2020).

Clinical Study

In a human study, 10 patients with HCC were detected, and clinical samples were collected for experimentative verification. All patients were medically diagnosed for HCC through clinical images and histological staining examination. HCC and HCC-free samples were harvested through surgical operation, followed by immunostaining and analyzing. These human protocols were approved by the Liuzhou Worker's Hospital ethics committee, and correlative experiments were conducted based on the principles of the Declaration of Helsinki (Li et al., 2020c; Li et al., 2021f).

Cell Culture Study

A human liver cancer cell line of HepG2 was treated with Pachyman (Shanghai Yuanye Biotechnology Co., Ltd. China) at different doses of 0, 25, and 50 μM for 48 h. The cell proliferation was determined by using the commercially available reagents of Cell Counting Kit 8. In addition, the protein expressions of ALB and VEGFA were measured by using enzyme-linked immunosorbent assay (ELISA) kits. More experimental procedures have been described in previous reports (Wu et al., 2017; Wu et al., 2019).

Statistical Analyses

The statistical results were indicated as mean ± standard deviations (SD). Statistical assay was performed by using the Statistical Product and Service Solutions 19.0 software (IBM

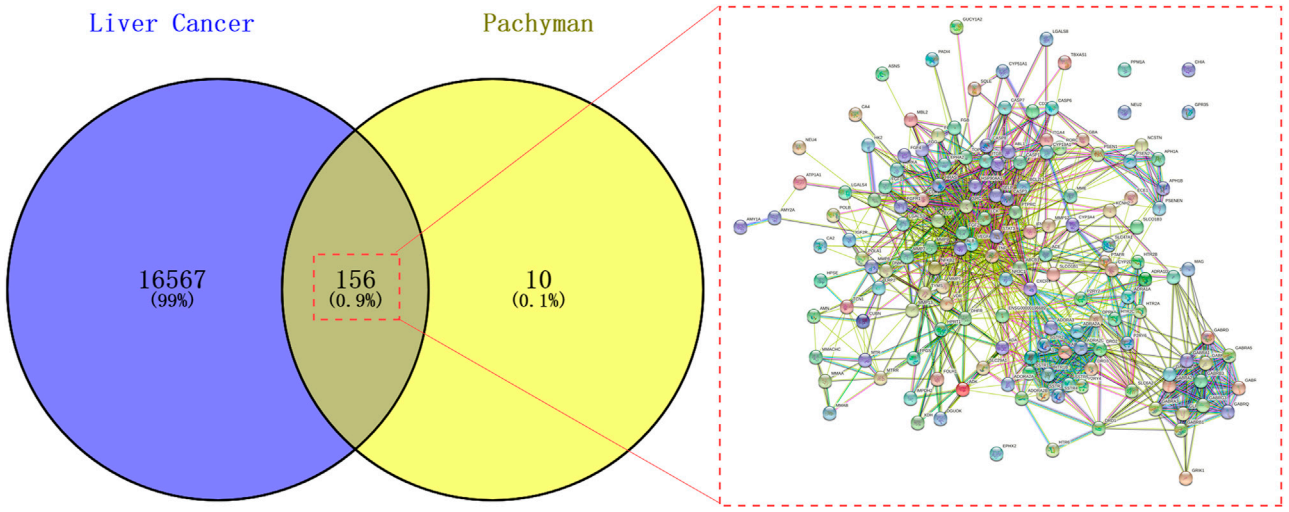

FIGURE 1 | Candidate targets of a PPI network of Pachyman in treating HCC for identifying pharmacological and pathological biotargets.

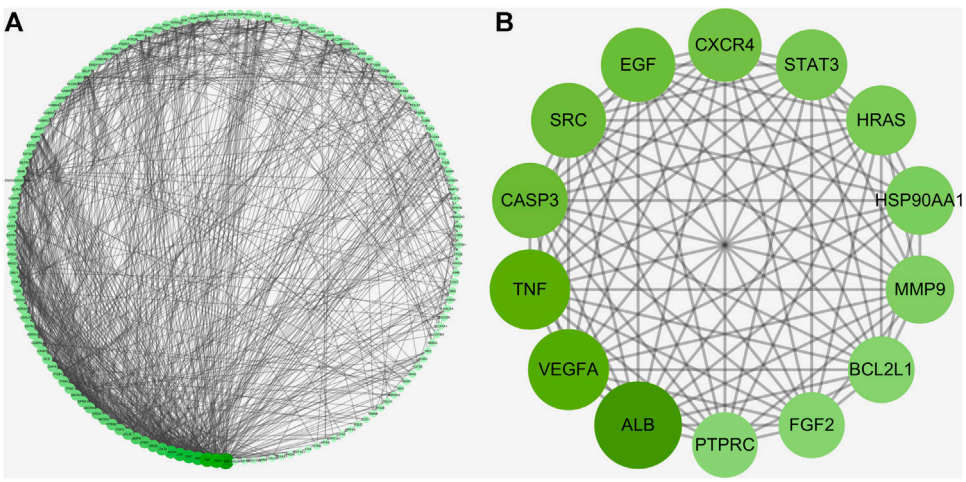

FIGURE 2 | Hub targets of a PPI network **(A)** for uncovering all crucial targets of Pachyman in treating HCC **(B)**.

Corporation, Chicago, IL, United States). Two different comparison groups were determined through one-way analysis of variance, followed by Tukey's post hoc test. The statistical significance was set as $p < 0.05$.

RESULTS

Potential Targets and Establishment of the PPI Network

As shown in the Venn diagram (**Figure 1**), the data reported a total of 16,763 HCC-associated genes and 166 Pachyman-associated genes. As a result, 156 intersection genes of Pachyman and HCC were obtained when all duplicate genes were excluded. Visibly, the PPI network of the intersection genes showed 57 nodes and 139 edges (**Figure 1**).

Identification of Crucial Targets in Anti-HCC Targets of Pachyman

The topological data indicated a close relevance among the intersection genes, characterized in the PPI network map (**Figure 2A**). As revealed in **Figure 2B**, the top 14 crucial targets of ALB, VEGFA, TNF, CASP3, SRC, EGF, CXCR4, STAT3, HRAS, HSP90AA1, MMP9, BCL2L1, FGF2, and PTPRC were identified accordingly.

GO and KEGG Enrichment Findings of Crucial Targets

The biological functional processes and molecular pathways of the crucial targets in Pachyman for treating HCC were enriched and characterized respectively. The top 20 biological processes of Pachyman in treating HCC are illustrated in **Figure 3A–C**. The

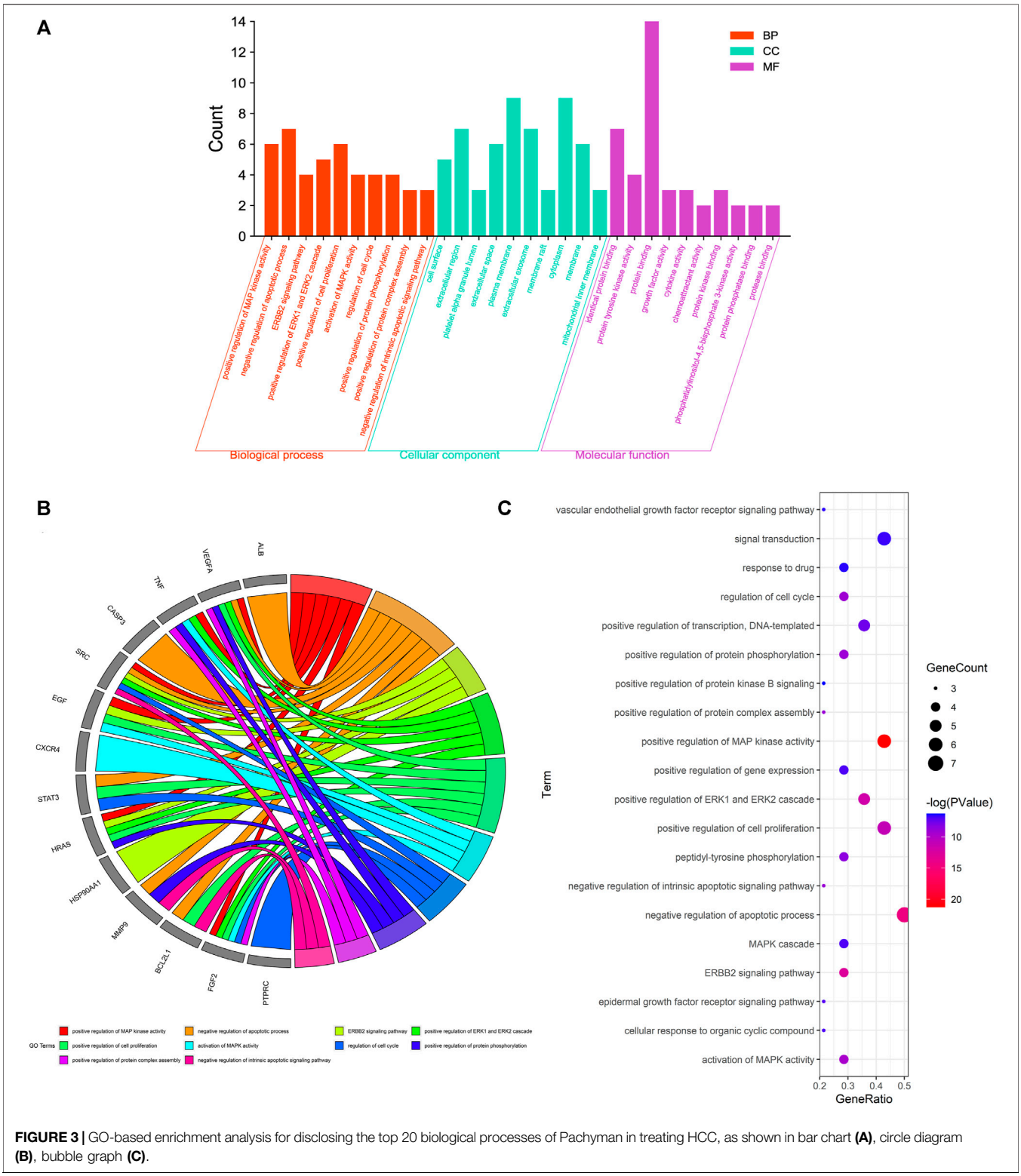

FIGURE 3 | GO-based enrichment analysis for disclosing the top 20 biological processes of Pachyman in treating HCC, as shown in bar chart **(A)**, circle diagram **(B)**, bubble graph **(C)**.

anti-cancer effects of Pachyman in treating HCC were mainly related to the regulation of the following: positive regulation of MAP kinase activity, negative regulation of apoptotic process, ERBB2 signaling pathway, positive regulation of extracellular signal-regulated kinase (ERK)—ERK1 and ERK2—cascades, positive regulation of cell proliferation, activation of mitogen-activated protein kinase (MAPK) activity, regulation of the cell cycle, positive regulation of protein phosphorylation, positive regulation of the protein complex assembly, negative regulation of the intrinsic apoptotic signaling pathway, peptidyl-tyrosine phosphorylation, positive regulation of

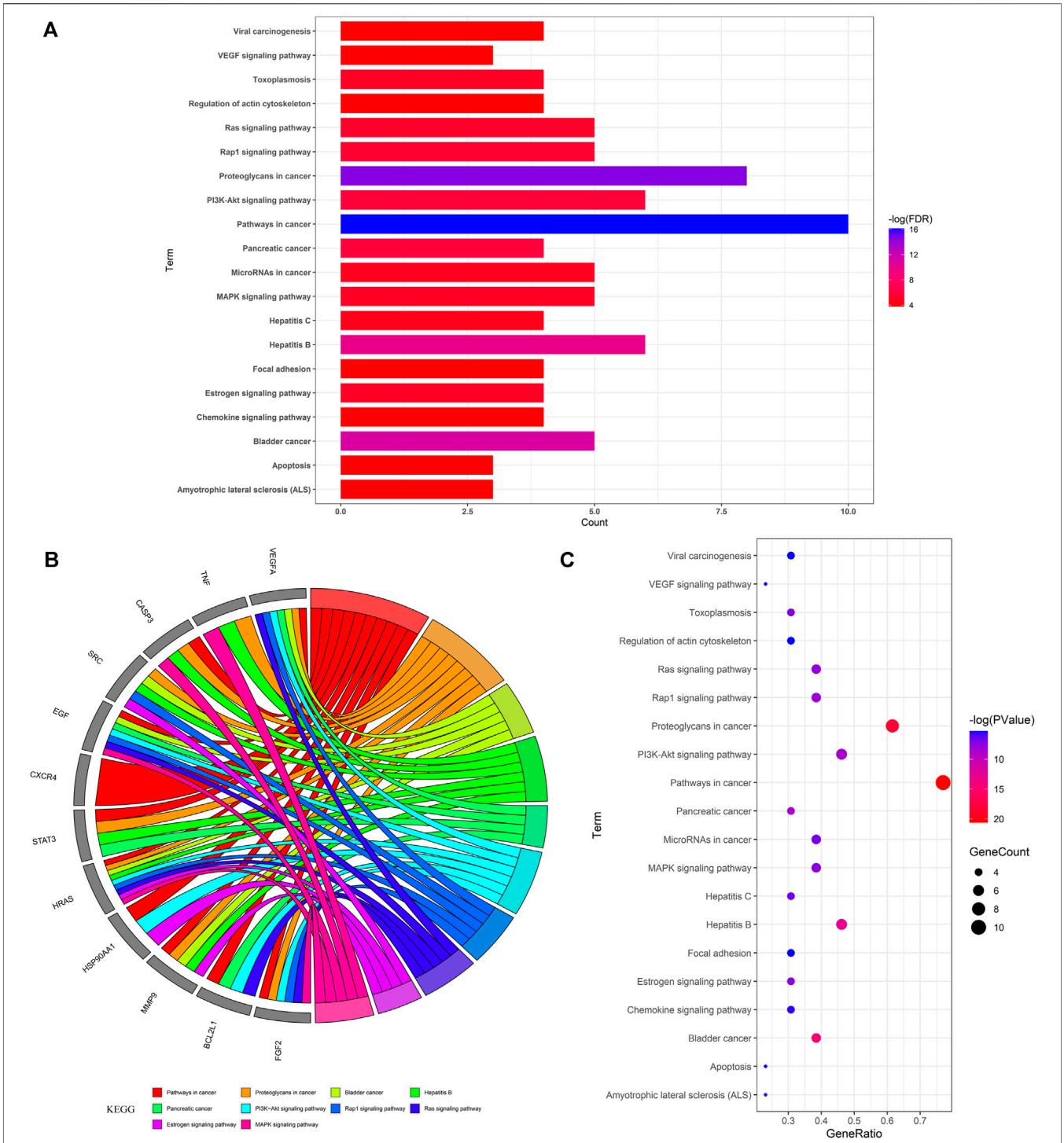

FIGURE 4 | KEGG-based enrichment analysis for revealing the top 20 molecular pathways of Pachyman in treating HCC as shown in bar chart **(A)**, circle diagram **(B)**, bubble graph **(C)**.

DNA-templated transcription, regulation of the epidermal growth factor receptor signaling pathway, regulation of cellular response to organic cyclic compound, MAPK cascade, positive regulation of gene expression, signal transduction, vascular endothelial growth factor receptor signaling pathway, response to drug, and positive regulation of protein kinase B signaling. As is revealed in pharmacological mechanisms, the KEGG pathways of Pachyman in treating HCC included the following: pathways in cancer, proteoglycans in cancer, bladder cancer, hepatitis B, pancreatic cancer, PI3K-Akt signaling pathway, Rap1 signaling pathway, Ras signaling pathway, estrogen

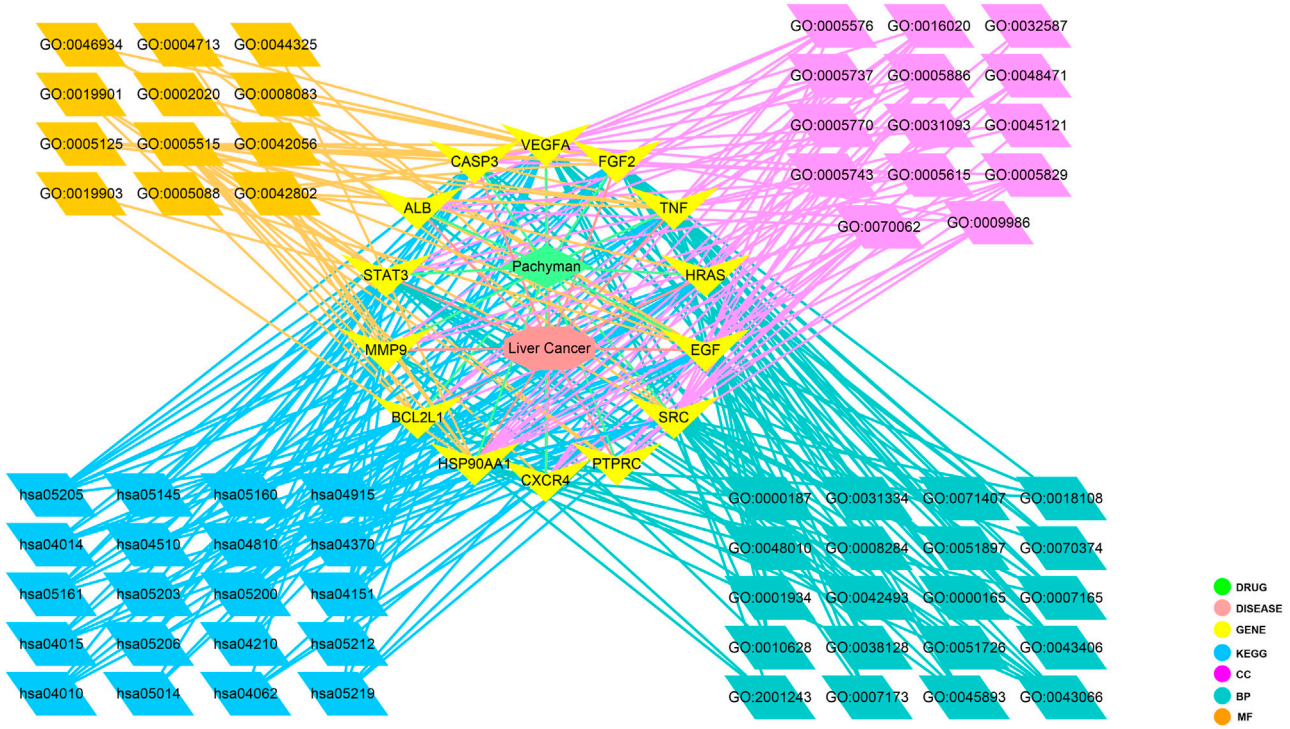

FIGURE 5 | An integrative map of disease and ingredient-target-signaling pathway network of Pachyman in treating HCC.

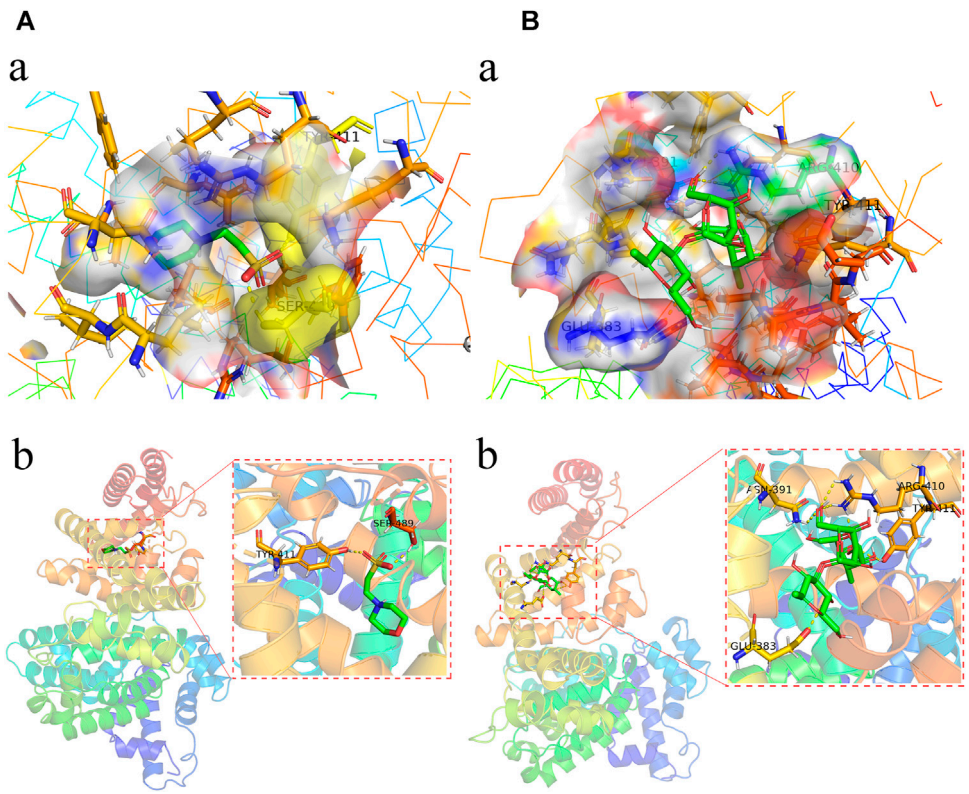

FIGURE 6 | The molecular docking analysis shows potent binding activities of Pachyman with 6QIO in ALB as a crucial target in HCC.

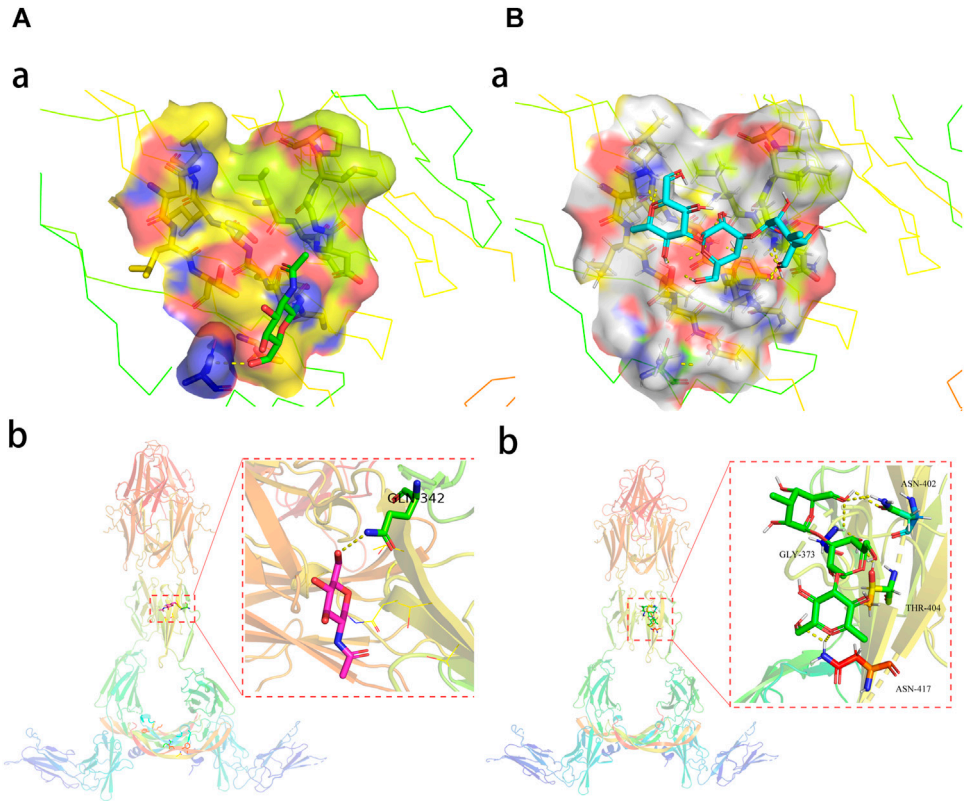

FIGURE 7 | The molecular docking data–suggested potent binding activities of Pachyman with 5T89 in VEGFA as a crucial target in HCC.

signaling pathway, MAPK signaling pathway, toxoplasmosis, microRNAs in cancer, hepatitis C, amyotrophic lateral sclerosis (ALS), chemokine signaling pathway, viral carcinogenesis, focal adhesion, VEGF signaling pathway, apoptosis, and regulation of actin cytoskeleton (**Figures 4A–C**). Collectively, the integrated network diagram with detailed Pachyman–anti-HCC findings can be visualized in **Figure 5**.

Molecular Docking Findings

As shown in the ALB protein (**Figure 6**), the root-mean-square deviation of the original ligand is 2.713 Å. The hydrogen bonding of the pro-ligand MES to 6QIO protein acted on the amino acid residues TYR-411 (1.6Å) and SER-489 (2.0 Å). Pachyman formed bonds with the amino acid residues of TYR-411 (1.7 Å), ASN-391 (2.6 Å), ARG-410 (2.6 Å), and GLU-383 (2.2 Å) (**Figure 6**). As shown for VEGFA protein, the root-mean-square deviation of the original ligand was 2.586 Å. The hydrogen bonding of the pro-ligand NAG and 5T89 protein acted on the amino acid residues of GLN-342 (3.2 Å). Pachyman formed bonds with amino acid residues of ASN-402 (2.6 Å), THR-404 (2.5 Å), GLY-373 (2.8 Å), and ASN-417 (2.6 Å) (**Figure 7**).

Validated Data in Clinical HCC Samples

To further validate the molecular docking findings, the HCC and HCC-free clinical samples were collected for experimental tests. The HCC cases were well characterized medically with medical imaging scans and pathological diagnosis (hematoxylin and eosin stain (HE) and positive cells for hepatocyte, CD34, Ki-67, and EGFR expressions). Additionally, the data from the fluorescence immunostaining assay showed that the HCC samples resulted in significant downregulation of ALB expression and elevation of VEGFA expression when compared with those in HCC-free controls ($p < 0.05$) (**Figure 8**).

Validated Data in Pachyman-Treated HCC Cells

The experimental data *in vitro* suggested that Pachyman-treated HepG2 cells showed markedly reduced cell proliferation in comparison with the non-treated control ($p < 0.05$) (**Figure 9A**). In the quantitative test performed by using ELISA, the Pachyman-treated HepG2 cells exhibited increased ALB expression ($p < 0.05$) and reduced VEGFA content ($p < 0.05$) (**Figure 9B**).

DISCUSSION

In the current bioinformatics findings of this study, network pharmacology–based analysis had identified individual and crucial targets, biological processes, and signaling pathways

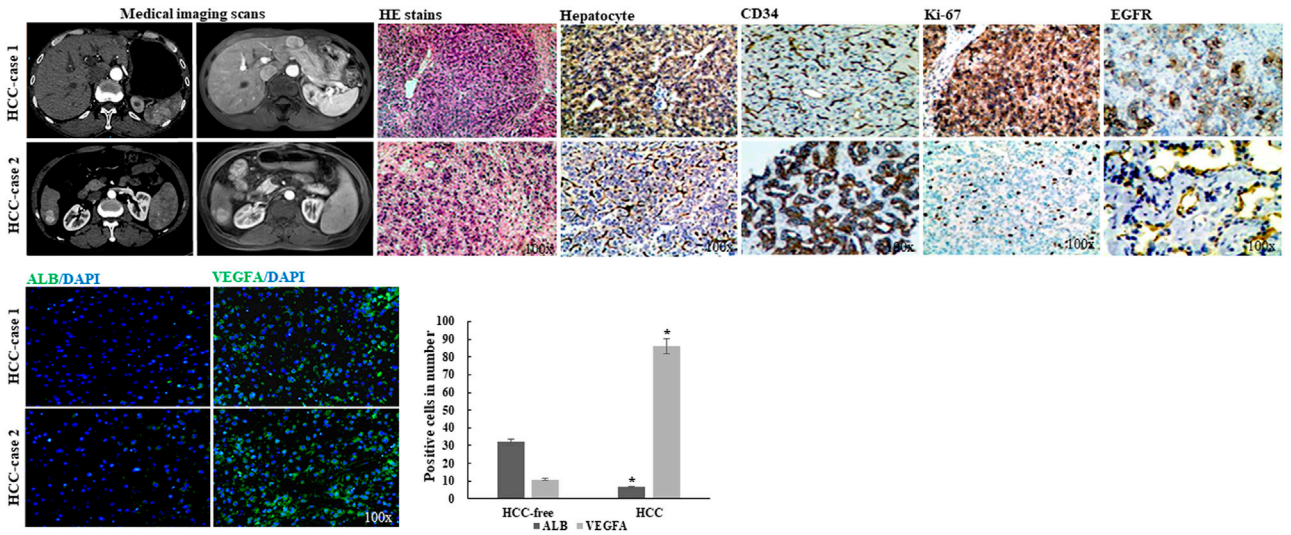

FIGURE 8 | Characterized imaging and immunostaining findings of clinical HCC samples, and validated data based on molecular docking analysis.

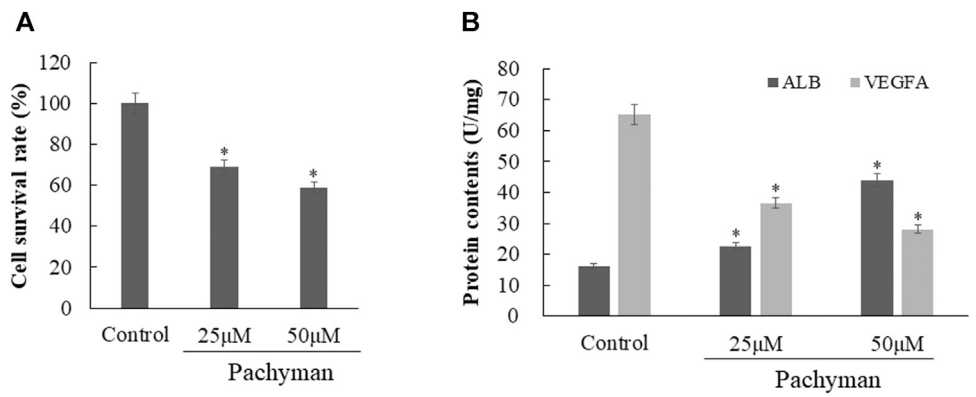

FIGURE 9 | Validated data *in vitro* with Pachyman-treated liver cancer cells according to molecular docking findings, as shown in cell proliferation test **(A)**, target protein determination **(B)**.

of Pachyman in treating HCC. The anti-HCC actions of Pachyman might be related to inducing cell death, enhancing immunologic function, and meliorating tumor microenvironmental regulation, as has been revealed in the GO-based analysis. Additionally, anti-proliferation pathways (such as apoptosis, and PI3K-Akt and MAPK signaling pathways), anti-invasiveness pathway (such as Ras and Rap1 signaling pathway), anti-angiogenesis pathway (such as VEGF signaling pathway), and other pathways (such as MicroRNAs in cancer) were all identified in Pachyman treating HCC actions, as revealed in the KEGG-based findings. During further screening of crucial targets by using molecular docking analysis, the Pachyman-activated anti-HCC core targets, including ALB and VEGFA, were identified accordingly, characterized with potent binding activities of Pachyman with 6QIO and 5T89 proteins in HCC. ALB, a monomeric protein, plays principally as a carrier protein for fatty acids, steroids, and thyroid hormones (Garcia-Martinez et al., 2013). Medically, serum ALB may be used for evaluating the nutritional condition in cancer patients, as malnutrition can be a function of prognostic significance in cancer cases (Gupta and Lis, 2010). It has been reported by using *in situ* hybridization test that endogenous albumin mRNA may serve as a sensitive marker for detecting primary hepatic carcinoma (Chen et al., 2021). In addition, the prognostic value of the albumin score in HCC cases has been identified clinically (Feng et al., 2020). VEGFA, a glycosylated mitogen, can induce vascular permeability, vasculogenesis, and endothelial cell proliferation or growth (Ballmer-Hofer, 2018). In tumor-related angiogenesis, VEGFA-based response mediates numerous functional effectors, including phosphoinositide 3 kinase (PI3K)/Akt, p38 MAPK, and ERKs (Claesson-Welsh and Welsh, 2013). In addition, VEGFA-induced HCC

development and pathogenesis may be a potential pharmacological target for treating hepatocellular carcinoma (Morse et al., 2019). In the present validated experiments, clinical HCC samples showed decreased ALB expression and elevated VEGFA content. As shown in *in vitro* Pachyman treatments, intracellular protein of ALB was upregulated and VEGFA protein expression was reduced. These validated findings demonstrated that ALB and VEGFA may be the anti-HCC pharmacological targets activated by Pachyman. The limitation of the present study is that further *in vivo* experimental validation is needed for potential use of Pachyman in clinical application.

CONCLUSION

Collectively, the bioinformatics and validation findings revealed the pharmacological targets and mechanisms of Pachyman in treating HCC. Specially, computational identification of ALB and VEGFA proteins/genes may functionally serve as potential biomarkers in screening for and treating HCC.

DATA AVAILABILITY STATEMENT

The original contributions presented in the study are included in the article/Supplementary Material; further inquiries can be directed to the corresponding author.

AUTHOR CONTRIBUTIONS

HH contributed to the conception, design of the manuscript. LQ, DH, JH, and FQ contributed to the acquisition, analyses, and interpretation of the data in this manuscript. HH and LQ drafted this manuscript. HH revised this manuscript. All authors agree to be accountable for all aspects of work ensuring integrity and accuracy.

FUNDING

This study was supported by the Liuzhou Scientific Research and Technology Development Project (No. 2017BH20305).

REFERENCES

Anwanwan, D., Singh, S. K., Singh, S., Saikam, V., and Singh, R. (2020). Challenges in Liver Cancer and Possible Treatment Approaches. *Biochim. Biophys. Acta Rev. Cancer.* 1873, 188314. doi:10.1016/j.bbcan.2019.188314

Ballmer-Hofer, K. (2018). Vascular Endothelial Growth Factor, from Basic Research to Clinical Applications. *Int. J. Mol. Sci.* 19, 3750. doi:10.3390/ijms19123750

Chen, D. A., Koehne de Gonzalez, A., Fazlollahi, L., Coffey, A., Remotti, H. E., and Lagana, S. M. (2021). *In Situ* Hybridisation for Albumin RNA in Paediatric Liver Cancers Compared with Common Immunohistochemical Markers. *J. Clin. Pathol.* 74, 98–101. doi:10.1136/jclinpath-2020-206663

Claesson-Welsh, L., and Welsh, M. (2013). VEGFA and Tumour Angiogenesis. *J. Intern. Med.* 273, 114–127. doi:10.1111/joim.12019

Feng, D., Wang, M., Hu, J., Li, S., Zhao, S., Li, H., et al. (2020). Prognostic Value of the Albumin-Bilirubin Grade in Patients with Hepatocellular Carcinoma and Other Liver Diseases. *Ann. Transl Med.* 8, 553. doi:10.21037/atm.2020.02.116

Fu, J., and Wang, H. (2018). Precision Diagnosis and Treatment of Liver Cancer in China. *Cancer Lett.* 412, 283–288. doi:10.1016/j.canlet.2017.10.008

Garcia-Martinez, R., Caraceni, P., Bernardi, M., Gines, P., Arroyo, V., and Jalan, R. (2013). Albumin: Pathophysiologic Basis of Its Role in the Treatment of Cirrhosis and Its Complications. *Hepatology* 58, 1836–1846. doi:10.1002/hep.26338

Gupta, D., and Lis, C. G. (2010). Pretreatment Serum Albumin As a Predictor of Cancer Survival: a Systematic Review of the Epidemiological Literature. *Nutr. J.* 9, 69. doi:10.1186/1475-2891-9-69

Li, R., Guo, C., Li, Y., Liang, X., and Su, M. (2021). Functional Benefit and Molecular Mechanism of Vitamin C against Perfluorooctanesulfonate-Associated Leukemia. *Chemosphere* 263, 128242. doi:10.1016/j.chemosphere.2020.128242

Li, R., Guo, C., Li, Y., Liang, X., Yang, L., and Huang, W. (2020). Therapeutic Target and Molecular Mechanism of Vitamin C-Treated Pneumonia: a Systematic Study of Network Pharmacology. *Food Funct.* 11, 4765–4772. doi:10.1039/d0fo00421a

Li, R., Guo, C., Li, Y., Qin, Z., and Huang, W. (2021). Therapeutic Targets and Signaling Mechanisms of Vitamin C Activity against Sepsis: a Bioinformatics Study. *Brief Bioinform* 22, bbaa079. doi:10.1093/bib/bbaa079

Li, R., Guo, C., Tse, W. K. F., Su, M., Zhang, X., and Lai, K. P. (2020). Metabolomic Analysis Reveals Metabolic Alterations of Human Peripheral Blood Lymphocytes by Perfluorooctanoic Acid. *Chemosphere* 239, 124810. doi:10.1016/j.chemosphere.2019.124810

Li, R., Huang, C., Ho, J. C. H., Leung, C. C. T., Kong, R. Y. C., Li, Y., et al. (2021). The Use of Glutathione to Reduce Oxidative Stress Status and Its Potential for Modifying the Extracellular Matrix Organization in Cleft Lip. *Free Radic. Biol. Med.* 164, 130–138. doi:10.1016/j.freeradbiomed.2020.12.455

Li, R., Huang, X., Liang, X., Su, M., Lai, K. P., and Chen, J. (2021). Integrated Omics Analysis Reveals the Alteration of Gut Microbe-Metabolites in Obese Adults. *Brief Bioinform.* 22 (3), bbaa165. doi:10.1093/bib/bbaa165

Li, R., Li, Y., Liang, X., Yang, L., Su, M., and Lai, K. P. (2021). Network Pharmacology and Bioinformatics Analyses Identify Intersection Genes of Niacin and COVID-19 as Potential Therapeutic Targets. *Brief Bioinform.* 22, 1279–1290. doi:10.1093/bib/bbaa300

Li, R., Wu, K., Li, Y., Liang, X., Lai, K. P., and Chen, J. (2021). Integrative Pharmacological Mechanism of Vitamin C Combined with Glycyrrhizic Acid against COVID-19: Findings of Bioinformatics Analyses. *Brief Bioinform.* 22, 1161–1174. doi:10.1093/bib/bbaa141

Li, R., Wu, K., Li, Y., Liang, X., Tse, W. K. F., Yang, L., et al. (2020). Revealing the Targets and Mechanisms of Vitamin A in the Treatment of COVID-19. *Aging (Albany NY).* 12, 15784–15796. doi:10.18632/aging.103888

Li, X., He, Y., Zeng, P., Liu, Y., Zhang, M., Hao, C., et al. (2019). Molecular Basis for Poria Cocos Mushroom Polysaccharide Used As an Antitumour Drug in China. *J. Cell Mol Med.* 23, 4–20. doi:10.1111/jcmm.13564

Liu, J., Yu, J., and Peng, X. (2020). Poria Cocos Polysaccharides Alleviates Chronic Nonbacterial Prostatitis by Preventing Oxidative Stress, Regulating Hormone Production, Modifying Gut Microbiota, and Remodeling the DNA Methylome. *J. Agric. Food Chem.* 68, 12661–12670. doi:10.1021/acs.jafc.0c05943

Llovet, J. M., Kelley, R. K., Villanueva, A., Singal, A. G., Pikarsky, E., Roayaie, S., et al. (2021). Hepatocellular Carcinoma. *Nat. Rev. Dis. Primers.* 7, 6. doi:10.1038/s41572-020-00240-3

Llovet, J. M., Montal, R., Sia, D., and Finn, R. S. (2018). Molecular Therapies and Precision Medicine for Hepatocellular Carcinoma. *Nat. Rev. Clin. Oncol.* 15, 599–616. doi:10.1038/s41571-018-0073-4

McGlynn, K. A., Petrick, J. L., and El-Serag, H. B. (2021). Epidemiology of Hepatocellular Carcinoma. *Hepatology* 73, 4–13. doi:10.1002/hep.31288

Morse, M. A., Sun, W., Kim, R., He, A. R., Abada, P. B., Mynderse, M., et al. (2019). The Role of Angiogenesis in Hepatocellular Carcinoma. *Clin. Cancer Res.* 25, 912–920. doi:10.1158/1078-0432.CCR-18-1254

Nong, Y., Liang, Y., Liang, X., Li, Y., and Yang, B. (2020). Pharmacological Targets and Mechanisms of Calycosin against Meningitis. *Aging (Albany NY).* 12, 19468–19492. doi:10.18632/aging.103886

Qin, X., Huang, C., Wu, K., Li, Y., Liang, X., Su, M., et al. (2021). Anti-coronavirus Disease 2019 (COVID-19) Targets and Mechanisms of Puerarin. *J. Cell Mol Med.* 25, 677–685. doi:10.1111/jcmm.16117

Su, M., Guo, C., Liu, M., Liang, X., and Yang, B. (2019). Therapeutic Targets of Vitamin C on Liver Injury and Associated Biological Mechanisms: A Study of Network Pharmacology. *Int. Immunopharmacol* 66, 383–387. doi:10.1016/j.intimp.2018.11.048

Sun, Y. (2014). Biological Activities and Potential Health Benefits of Polysaccharides from Poria Cocos and Their Derivatives. *Int. J. Biol. Macromol.* 68, 131–134. doi:10.1016/j.ijbiomac.2014.04.010

Wu, K., Fan, J., Huang, X., Wu, X., and Guo, C. (2018). Hepatoprotective Effects Exerted by Poria Cocos Polysaccharides against Acetaminophen-Induced Liver Injury in Mice. *Int. J. Biol. Macromol* 114, 137–142. doi:10.1016/j.ijbiomac.2018.03.107

Wu, K., Guo, C., Yang, B., Wu, X., and Wang, W. (2019). Antihepatotoxic Benefits of Poria Cocos Polysaccharides on Acetaminophen-Lesioned Livers *In Vivo* and *In Vitro*. *J. Cell Biochem.* 120, 7482–7488. doi:10.1002/jcb.28022

Wu, X., Liang, M., Yang, Z., Su, M., and Yang, B. (2017). Effect of Acute Exposure to PFOA on Mouse Liver Cells *In Vivo* and *In Vitro*. *Environ. Sci. Pollut. Res. Int.* 24, 24201–24206. doi:10.1007/s11356-017-0072-5

Conflict of Interest: The authors declare that the research was conducted in the absence of any commercial or financial relationships that could be construed as a potential conflict of interest.

Publisher's Note: All claims expressed in this article are solely those of the authors and do not necessarily represent those of their affiliated organizations, or those of the publisher, the editors and the reviewers. Any product that may be evaluated in this article, or claim that may be made by its manufacturer, is not guaranteed or endorsed by the publisher.

frontiers in Pharmacology

ORIGINAL RESEARCH
published: 29 October 2021
doi: 10.3389/fphar.2021.775506

OPEN ACCESS

Edited by:
Jiang-Jiang Qin,
Institute of Cancer and Basic Medicine, (CAS), China

Reviewed by:
Jinming Zhang,
Chengdu University of Traditional Chinese Medicine, China
Spencer Gibson,
University of Manitoba, Canada
Weixing Shen,
Nanjing University of Chinese Medicine, China
Nam Deuk Kim,
Pusan National University, South Korea

***Correspondence:**
Xinbing Sui
hzzju@hznu.edu.cn
Tian Xie
xbs@hznu.edu.cn
Deqiang Wang
deqiang_wang@aliyun.com
Qibiao Wu
qbwu@must.edu.mo

†These authors made equal contributions to this work

Specialty section:
This article was submitted to Pharmacology of Anti-Cancer Drugs, a section of the journal Frontiers in Pharmacology

Received: 14 September 2021
Accepted: 04 October 2021
Published: 29 October 2021

Citation:
Xiang Y, Chen X, Wang W, Zhai L, Sun X, Feng J, Duan T, Zhang M, Pan T, Yan L, Jin T, Gao Q, Wen C, Ma W, Liu W, Wang D, Wu Q, Xie T and Sui X (2021) Natural Product Erianin Inhibits Bladder Cancer Cell Growth by Inducing Ferroptosis via NRF2 Inactivation. Front. Pharmacol. 12:775506. doi: 10.3389/fphar.2021.775506

Natural Product Erianin Inhibits Bladder Cancer Cell Growth by Inducing Ferroptosis via NRF2 Inactivation

Yu Xiang[1,2†], Xiaying Chen[1,2†], Wengang Wang[3†], Lijuan Zhai[4], Xueni Sun[1,2], Jiao Feng[1,2], Ting Duan[1,2], Mingming Zhang[1,2], Ting Pan[1,2], Lili Yan[1,2], Ting Jin[1,2], Quan Gao[1,2], Chengyong Wen[1,2], Weirui Ma[1,2], Wencheng Liu[1,2], Deqiang Wang[5], Qibiao Wu[6]*, Tian Xie[1,3,2]* and Xinbing Sui[1,2,5,6]**

[1]School of Pharmacy and Department of Medical Oncology, The Affiliated Hospital of Hangzhou Normal University, Hangzhou Normal University, Hangzhou, China, [2]Key Laboratory of Elemene Class Anti-Cancer Chinese Medicines, Engineering Laboratory of Development and Application of Traditional Chinese Medicines, Collaborative Innovation Center of Traditional Chinese Medicines of Zhejiang Province, Hangzhou Normal University, Hangzhou, China, [3]College of Pharmacy, Chengdu University of Traditional Chinese Medicine, Chengdu, China, [4]Zhejiang Chinese Medical University, Hangzhou, China, [5]Department of Medical Oncology, Affiliated Hospital of Jiangsu University, Jiangsu University, Zhenjiang, China, [6]State Key Laboratory of Quality Research in Chinese Medicines, Faculty of Chinese Medicine, Macau University of Science and Technology, Macau, China

Erianin, a natural product derived from *Dendrobium chrysotoxum Lindl*, has been proved to play antitumor activity in various cancers. However, the effects and molecular mechanisms of erianin in bladder cancer cells remain unexplored. In this study, we found that erianin triggered cell death and cell cycle arrest in bladder cancer cells. Then we demonstrated that erianin could promote the accumulation of lethal lipid-based reactive oxygen species (ROS) and the depletion of glutathione (GSH), suggesting the induction of ferroptosis. In the further study, the ferroptosis inhibitor deferoxamine (DFO), N-Acetylcysteine (NAC) and GSH but not necrostatin-1, CQ or Z-VAD-FMK rescued erianin-caused cell death, showing ferroptosis played a major role in erianin-caused cell death. *In vivo*, we also showed that erianin suppressed the tumor growth by inducing ferroptosis. Mechanistically, we demonstrated that nuclear factor E2-related factor 2 (NRF2) inactivation was a key determinant of ferroptosis caused by erianin. In bladder cancer cells, the compound tert-butylhydro-quinone (TBHQ), an activator of NRF2, suppressed erianin-induced ferroptosis. Whereas, NRF2 inhibition used shRNA augmented the ferroptosis response induced by erianin treatment. In conclusion, our data provide the first evidence that erianin can initiate ferroptosis-like cell death and lipid peroxidation in bladder cancer, which will hopefully become a promising anticancer compound for the treatment of bladder cancer.

Keywords: Erianin, ferroptosis, bladder cancer, nuclear factor E2-related factor 2, natural product

INTRODUCTION

Ferroptosis is a newly defined form of regulated cell death, which is characterized by iron-dependent peroxidation of the lipid membrane induced by reactive oxygen species (ROS) (Yu et al., 2020). Increasing evidence has depicted an essential role for ferroptosis as either the cause or consequence for the pathophysiological process of many human diseases, including acute lung injury (Li et al., 2020), intervertebral disc degeneration (Zhang et al., 2020), ulcerative colitis (Wang et al., 2020), and so on. Recently, more and more studies have provided intriguing insights into the interplay between ferroptosis and cancer because ferroptosis could eliminate cancer cells with an apoptosis-independent manner (Badgley et al., 2020; Lee et al., 2020). In consequence, ferroptosis has attracted more and more attention and will hopefully offer a novel strategy for cancer treatment.

It's our knowledge that a lot of anticancer drugs come from natural sources, including naturally occurring forms and synthetic derivatives. Recently, increasing evidence show that several natural compounds can either induce or inhibit ferroptosis, further expanding their therapeutic potentials. Erianin, extracted from rare traditional Chinese medicine *Dendrobium chrysotoxum Lindl*, was a small-molecule natural compound with a wide range of anticancer potential. Erianin has been reported to inhibit colorectal cancer cells growth by downregulating the transcriptional activity of β-catenin (Sun et al., 2020), induce apoptosis in nasopharyngeal carcinoma by decreasing the phosphorylation of ERK1/2 (Liu et al., 2019), and suppress bladder cancer cell growth through JNK pathways and the mitochondrial apoptosis (Zhu et al., 2004). In our previous study, erianin inhibited the growth and migration via inducing Ca/CaM-dependent ferroptosis and inhibiting cell migration in lung cancer cells (Chen et al., 2020a). However, the underlying molecular mechanism and the anticancer effect of erianin are not well exploited in bladder cancer.

In this study, we focused the effect of erianin on the viability in two different bladder cancer cells KU-19–19 and RT4. The result showed that erianin exerted its anticancer potential through inducing cell death and G2/M-phase arrest in a dose-dependent manner. Then for the first time we showed that ferroptosis facilitated erianin-induced cell death of bladder cancer *in vitro* and *in vivo*, that was confirmed by accompanied with ROS accumulation, GSH depletion, and lipid peroxidation. Moreover, erianin-induced cell death could be rescue by co-treatment with ROS inhibitor N-acetyl-l-cysteine (NAC) or glutathione (GSH) in bladder cancer cells. Mechanistically, we demonstrated that nuclear factor E2-related factor 2 (NRF2) inactivation was a key determinant of erianin-caused ferroptosis. In bladder cancer cells, the compound tert-butylhydro-quinone (TBHQ), an activator of NRF2, suppressed erianin-induced ferroptosis. Whereas, NRF2 inhibition by shRNA augmented the ferroptosis response induced by erianin treatment. In conclusion, our data for the first time demonstrated that erianin suppressed bladder cancer cell growth by inducing ferroptosis via inhibition of NRF2 signaling pathway.

MATERIALS AND METHODS

Cell Culture

RT4 and KU-19–19 cell lines were acquired from ATCC (American Type Culture Collection, Manassas, VA, United States). RT4 and KU-19–19 were cultivated in McCoy's 5A Medium Modified and 1640 Medium Modified comprising 10% fetal bovine serum and double antibiotic, requiring the temperature at 37°C with the routine cultivated conduction (5% CO_2, 95% air).

Reagents and Antibodies

Purified erianin (>98%) (Cat: B20844) was gained from Shanghai Yuanye Biological Co., Ltd. All antibody follow-up experiments used were anti-xCT (Cat: ab175186), anti-Glutaminase (Cat: ab93424), anti-GPX4 (Cat: ab125066), anti-Heme Oxygenase-1 (Cat: ab189491) were from Abcam (Cambridge, United Kingdom), anti-FTH1 (Cat: 4393S), anti-NRF2 (Cat: 12721S), anti-GAPDH (Cat: 5174S) were provided by Cell Signaling Technology (Danvers, United States). And inhibitors mentioned in experiments were deferoxamine (Cat: S5742) (Selleck, Houston, United States), chloroquine (Cat: C6628) (Sigma-Aldrich, St. Louis, United States), Z-VAD-FMK (Cat: HY-16658B), N-Acetylcysteine (Cat: HY-B0215), necrostatin-1 (Cat: HY-15760), L-Glutathione reduced (Cat: HY-D0187), TBHQ (Cat:HY-100489) were obtained from MedChem Express (New Jersey, United States), pLVX-U6-NRF2-shRNA1-PGK-EGFP-E2A-Puro (Cat:p24452) (miaolingbio, Wuhan, China).

Cell Viability Assay

The CCK-8 (Cat: MA0218) (meilunbio, Dalian, China) proliferation assay was used to examine cell viability of KU-19–19 and RT4 after different treatments. About of 5×10^3 cells/well were added into a 96-well plate. And then erianin or inhibitors were used with diverse concentrations for 24 h. After treating for 24 h, CCK-8 solution 10 μl/100 μl to a well was added and placed for 2 h at 37°C before the absorbance at a test wave length of 450 nm.

Apoptosis Assays

Following the manufacturer's instruction, the percentage of cell death used the Annexin V: FITC Apoptosis Detection kit (Cat: 556547) (BD, San Jose, United States). Approximately 6×10^5 cells/well were added in 6-well plate and erianin was given to treatment. The cells to be tested were collected in 100 μl 1×binding buffer placed in an ice box, and stained with FITC Annexin V and PI at room temperature out of Sun for 15 min. Then 200 μl 1×binding buffer was added. Cells were processed and analyzed with a FACS Calibur Flow Cytometer (CytoFLEX S) (Beckman Coulter, United States).

Cell Cycle Staining Assay

The cell cycle was made according to the requirement of cell cycle staining kit (Cat: CCS012) (Multi Science, Hangzhou, China). Cells were adherent and incubated with erianin in 6-well plate for

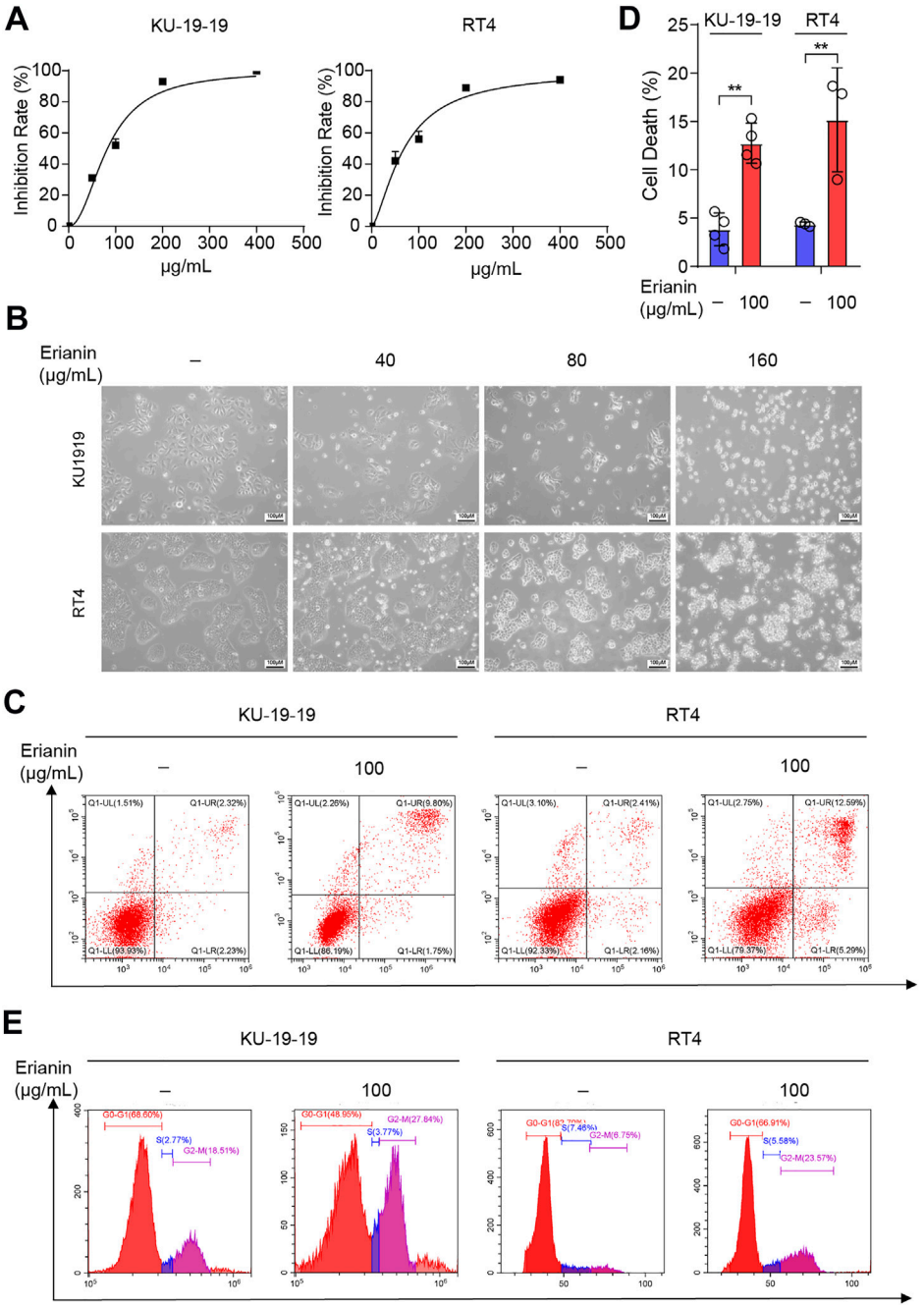

FIGURE 1 | Erianin inhibited cell proliferation and triggered cell death in bladder cancer cells. **(A)** Cell proliferation of KU-19–19 and RT4 was assessed by CCK-8 assay after the treatment with different dose of erianin treatment for 24 h. **(B)** The cell morphology was observed by microscope. **(C,D)** Flow cytometry analysis of cell death by Annexin V-FITC/PI staining in KU-19–19 and RT4 cells were treated with erianin or DMSO control for 24 h, and the quantification of percentage of the cell death was shown. $^{*}p < 0.05$,$^{**}p < 0.01$. **(E)** The percentage of cells treated with erianin in each phase was assessed by flow cytometry.

24 h. Cells collected after treatments were dyed with PI and analyzed by Flow Cytometer.

Measurement of Reactive Oxygen species

Approximately 6×10^5 cells/well were grown in 6-well plate. Cells were treated differently for 24 h after attachment, then 10 μM H2DCF-DA (Cat: S0033) (Beyotime Biotechnology, Shanghai, China) was added to incubate for 1 h. Rinsing the cells twice with PBS to remove residual H2DCF-DA. After that, the labeled cells were trypsinized and 200 μl PBS was added. H2DCF-DA is used to staining and detect ROS generation. The results were processed and analyzed by the

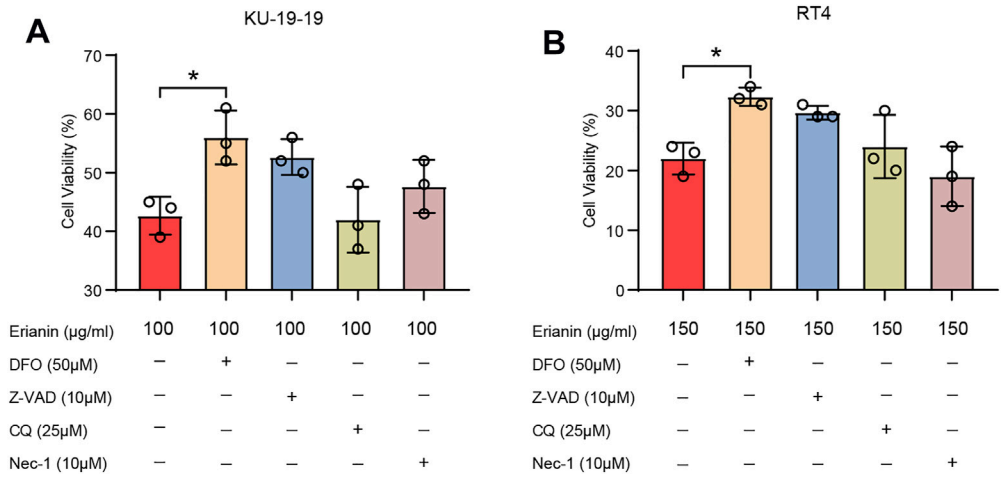

FIGURE 2 | KU-19–19 and RT4 were treated with erianin in combination with or without other cell death inhibitors Nec-1, DFO, Z-VAD and CQ for 24 h, then cell viability was assayed. *$p < 0.05$.

FACS. Each condition was demanded to collect minimum of 10,000 cells.

Measurement of Glutathione

Approximately 6×10^5 cells/well were placed into 6-well plate. After attached, KU-19–19 and RT4 were treated as described previously for 24 h. Protein concentration was determined with BCA assay kit (Cat: P0010S) (Beyotime Biotechnology, Shanghai, China). Following the manufacturer's instruction, total glutathione was measured as instruction of GSH assay kit (Cat: A006-2-1) (Nanjing Jiancheng, Nanjing, China).

Malondialdehyde Assay

Cells were plated and incubated with erianin in 6-well plate for 24 h. Following the manufacturer's instructions, malondialdehyde was detected of MDA assay kit (Cat: S0131S) (Beyotime Biotechnology, Shanghai, China) based on the protein concentration.

Measurement of Ferrous Ion

Approximately 6×10^5 cells/well were placed into 6-well plate. Following the manufacturer's instructions, ferrous ion was detected of Phen Green SK (Cat: P14313) (Thermo Scientific, Rockford, United States). The results were processed and analyzed by the FACS. Each condition was demanded to collect minimum of 10,000 cells.

Western Blot Analysis

Approximately 3×10^6 cells were placed into 10 cm dish. After attached, KU-19–19 and RT4 were dealt with differently for 24 h. And the cells were collected and lysed for 30 min on ice. Then collecting the supernatant after centrifugation at 10^4 rpm/min, then the concentration of protein was measured by BCA kit. Protein was dissolved in SDS-PAGE (12%), and electro-transferred to PVDF membranes. The Membranes were blocked, washed, antibody incubation, and enhanced chemiluminescence detection.

In vivo Tumor Model

The experimental mice were permited by the Animals Use and Care Committee at Hangzhou Normal university (No. 2021–1112). 4-weeks-old female BALB/c nude mice aged were injected into 5×10^5 cells. Every 2 days mice weight and tumor size were assessed, and the tumor volume (V) was calculated with the formula: (maximum length) × (maximum width)^2/2. Once tumors were found, the mice were stochastically divided into 2 groups: the control (PBS) group and the treatment (erianin 100 mg/kg) group. For 14 days, mice were injected intraperitoneally with drugs once a day, then puting the mice to death, after that tumors were taken for IHC (immunohistochemical) analysis.

Statistical Analysis

The results were expressed as mean ± SD. The significance of the statistical results used the *t*-test of GraphPad Prism. Unless otherwise indicated, all studies are conducted at least three times.

RESULTS

Erianin Inhibited Cell Proliferation and Triggered Cell Death in Bladder Cancer Cells

In order to explore the antitumor potential of erianin in bladder cancer, erianin was treated with different concentrations for 24 h in KU-19–19 and RT4 cells, and the cell growth potential was evaluated by CCK-8 assay. As a result, erianin treatment decreased cell viability in a dose-dependent (**Figures 1A,B**) and time-dependent (**Supplementary Figure S1A,B**) manner. In order to determine whether erianin could inhibit the growth of

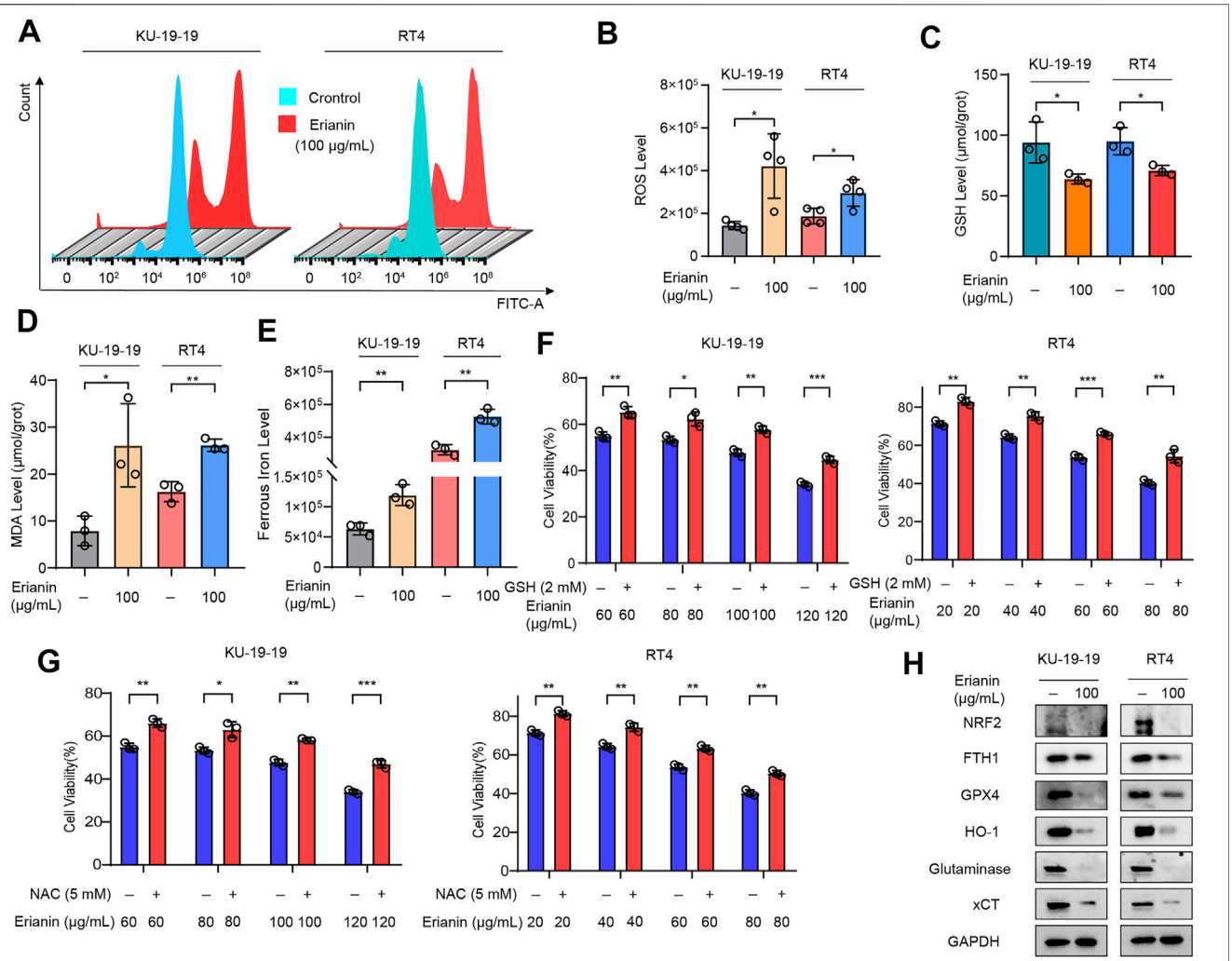

FIGURE 3 | Erianin triggered ferroptosis in bladder cancer cells. **(A,B)** KU-19–19 and RT4 cells were treated with erianin for 24 h and ROS level was analyzed by a flow cytometer, the mean ± s.d. is shown. *$p < 0.05$. **(C)** The GSH level in KU-19–19 and RT4 cells was detected after the treatment with erianin for 24 h, *$p < 0.05$. **(D)** The MDA level in KU-19–19 and RT4 cells was detected after the treatment with erianin for 24 h, *$p < 0.05$,**$p < 0.01$. **(E)** The iron level in KU-19–19 and RT4 cells was detected after the treatment with erianin for 24 h, **$p < 0.01$. **(F)** KU-19–19 and RT4 cells were treated with erianin with or without the oxygen-derived free radicals scavenger GSH for 24 h, and cell viability was assayed, **$p < 0.01$, ***$p < 0.001$. **(G)** KU-19–19 and RT4 cells were treated with erianin with or without the ROS scavenger NAC for 24 h, and cell viability was assayed, **$p < 0.01$, ***$p < 0.001$. **(H)** Several ferroptosis related proteins were determined by western blotting.

bladder cancer cells by inducing the cell death, we performed Annexin V-FITC/PI staining and analyzed by flow cytometry. In **Figures 1C,D**, a markedly high percentage of the dead cells was discovered in bladder cancer cells after the treatment with erianin. Then flow cytometry was performed to confirm whether erianin inhibited the cell proliferation through inducing cell cycle arrest. The result revealed erianin treatment significantly improved the proportion in G2/M phase (**Figure 1D**).

Ferroptosis Predominantly Contributed to Cell Death Inducing by Erianin in Bladder Cancer

The inhibitors of several different signaling pathway were utilized to confirm which cell death program mainly caused the cell death induced by erianin. The results showed that Z-VAD-FMK (inhibitor of pan-caspase), necrostatin-1 (Nec-1, inhibitor of necroptosis) or chloroquine (CQ, inhibitor of autophagy) could not reverse cell death in KU-19–19 and RT4 after the treatment with erianin. Whereas, iron chelator deferoxamine mesylate (DFO) remarkably reduced erianin-induced cell death, indicating ferroptosis is the dominated method generated erianin-caused cell death (**Figures 2A,B**).

It is well known that lipid peroxidation and GSH depletion are important phenomena in ferroptosis. Thus, the level of intracellular ROS, GSH and malondialdehyde (MDA) in KU-19–19 and RT4 cells were further detected following treatment with erianin. The results showed that the increased level of ROS (**Figures 3A,B**) and the decreased level of GSH (**Figure 3C**) were observed after erianin treatment. Meanwhile, erianin treatment obviously upregulated the MDA level (**Figure 3D**) and triggered ferrous iron accumulation

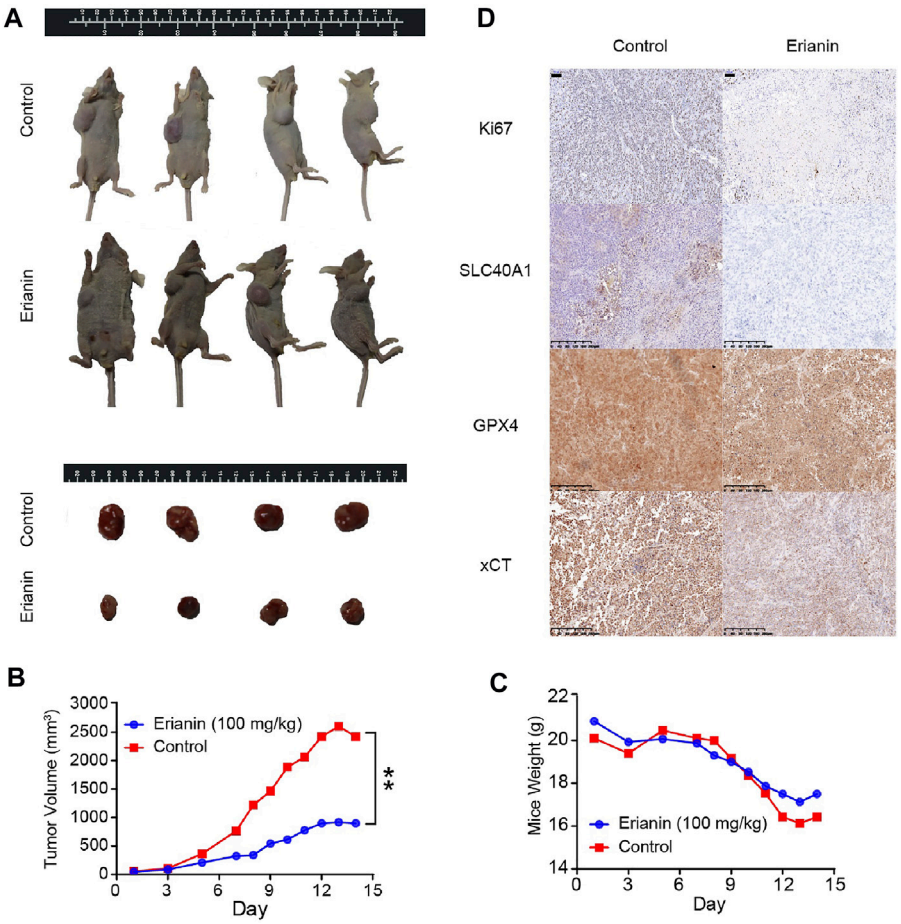

FIGURE 4 | Erianin suppressed tumor growth by inducing ferroptosis *in vivo*. **(A)** Representative image of mice and xenograft tumors at the endpoint of experiment. **(B)** The average tumor volume from different groups. Values are shown as mean ± SD, $^{**}p < 0.01$. **(C)** The average mice weight from different groups. Values are shown as mean ± SD. **(D)** The expression of Ki67, GPX4, SLC40A1 and xCT were detected by IHC.

(**Figure 3E**) in these bladder cancer cells. Furthermore, the anticancer activity of erianin could be dramatically rescued by co-treatment with oxygen-derived free radicals scavenger GSH (**Figure 3F**) and ROS scavenger N-ace-tylcysteine (NAC) (**Figure 3G**).

Subsequently, the effect of erianin on several ferroptotic proteins was detected by western blotting. As shown in **Figure 3H**, the protein levels of nuclear factor E2-related factor 2 (NRF2), ferritin heavy chain 1 (FTH1), glutathione peroxidase 4 (GPX4), heme oxygenase 1 (HO-1), glutaminase (GLS) and solute carrier family 7 member 11 (xCT/SLC7A11) were significantly decreased in KU-19–19 and RT4 cells after erianin treatment compared with the control group (**Figure 3G**). In conclusion, these results suggested that ferroptosis predominantly contributed to erianin-caused cell death in bladder cancer cells.

Erianin Exerted Antitumor Effect by Inducing Ferroptosis *in vivo*

Based on the above findings, we considered whether erianin administration could contribute to ferroptosis-like cell death in a subcutaneous xenograft tumor model. Therefore, BALB/c nude mice with KU-19–19 subcutaneous xenografts were stochasticly divided into two experimental groups: the control group (DMSO) and the erianin treatment group (100 mg/kg). Our data revealed that the growth of KU-19–19 xenograft tumors was dramatically reduced upon erianin treatment (**Figures 4A,B**). However, the body weight between the vehicle control group and erianin-treated group was no statistically significant difference (**Figure 4C**).

We next investigated the expression of Ki67 and several ferroptotic proteins by immunohistochemical (IHC). Ki67 staining showed that erianin treatment suppressed Ki67 expression in tumor tissues (**Figure 4D**), suggesting erianin could suppress the growth of bladder tumor. Also, the protein levels of SLC40A1, GPX4 and xCT were obviously decreased in tumors from erianin treatment group (**Figure 4D**). These results collectively support the idea that erianin suppressed tumor growth by inducing ferroptosis *in vivo*.

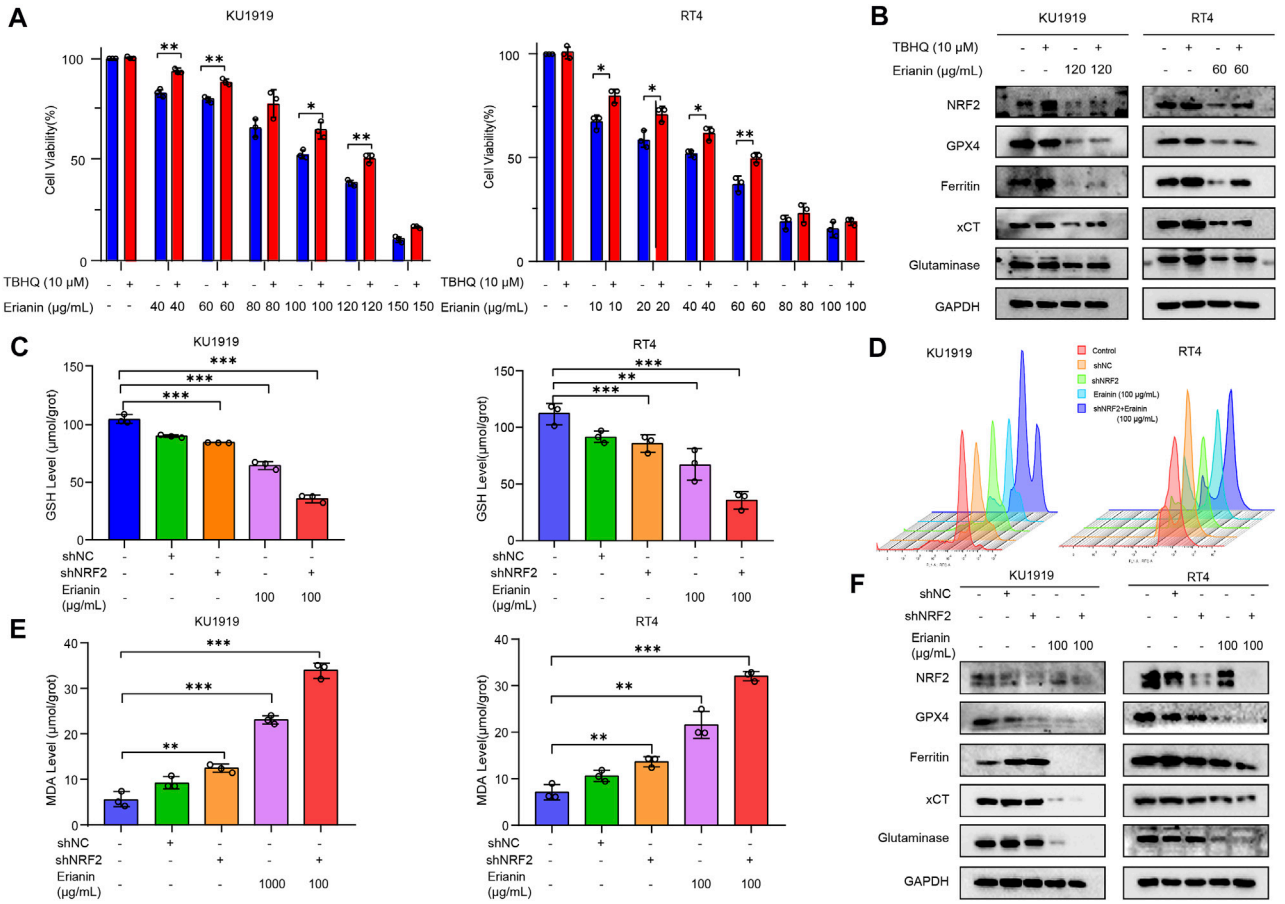

FIGURE 5 | Erianin triggered ferroptosis via the NRF2 pathway. **(A)** Cell viability was quantified by CCK-8 assay in KU-19–19 and RT4 cells treated with the combination of erianin and TBHQ. *$p < 0.05$,**$p < 0.01$. **(B)** The expression of NRF2, GPX4, ferritin, xCT and glutaminase was analyzed in KU-19–19 and RT4 cells treated with the combination of erianin and TBHQ. **(C)** The GSH level in KU-19–19 and RT4 cells was detected after the treatment with erianin and shNRF2, **$p < 0.01$,***$p < 0.001$. **(D)** The ROS level in KU-19–19 and RT4 cells was detected after the treatment with erianin and shNRF2, **$p < 0.01$. **(E)** The MDA level in KU-19–19 and RT4 cells was detected after the treatment with erianin and shNRF2, **$p < 0.01$,***$p < 0.001$. **(F)** The expression of NRF2, GPX4, ferritin, xCT and glutaminase was analyzed in KU-19–19 and RT4 cells treated with erianin and shNRF2.

Erianin Triggered Ferroptosis via the Nuclear Factor E2-Related Factor 2 Pathway

Recent studies have established that NRF2 signaling has a key role in cancer development and ferroptosis inhibition. Therefore, we speculated whether erianin might also induce ferroptosis in bladder cancer through modulation of NRF2. As shown in **Figure 3H**, the treatment of erianin inhibited the activation of NRF2. In order to further evaluate the relationship between erianin-induced ferroptosis and NRF2 signaling, we specifically enhanced NRF2 activation by using tert-butylhydro-quinone (TBHQ), a pharmacological NRF2 activator. We found that TBHQ treatment (10 μM) protected against erianin-induced cell death in KU-19–19 and RT4 cells (**Figure 5A**). Moreover, upregulation of GPX4, ferritin, xCT and glutaminase expression is also observed after the co-treatment with erianin and TBHQ (**Figure 5B**). This result suggests that erianin-mediated NRF2 inhibition probably promotes ferroptosis as a pro-death effect on bladder cancer cells.

Next, we used short hairpin RNA (shRNA) to knockdown NRF2 expression in KU-19–19 and RT4 cells and tested the effect of such inhibition on erianin-triggered ferroptosis. As a result, GSH level were significantly reduced (**Figure 5C**), but the activity of ROS and MDA were greatly increased after being pretreated with shNRF2 (**Figures 5D,E**). Meanwhile, the blockage of NRF2 decreased the protein level of GPX4, ferritin, xCT and glutaminase (**Figure 5F**) and increased the cell death induced by erianin treatment (Figure S1C,D). In general, these results indicated that NRF2 signaling is a key mediator of erianin-triggered ferroptosis in bladder cancer cells.

CONCLUSION

Ferroptosis, a new kind of cell death accompanied by iron-dependent lipid peroxidation, has recently been recognized as

an important role in degenerative diseases, infection diseases and cancer (Chen et al., 2019; Yu et al., 2019; Chen et al., 2020b). Therefore, activating ferroptosis may be a potential strategy for the treatment of cancer, particularly for eradicating traditional therapies-resistant aggressive malignancies. Recently, great progress has been made in the study of novel anticancer drugs induced by ferroptosis. As a critical sources of novel compounds used for anticancer drugs, natural molecules inducing ferroptosis are attracting increasing interest in cancer.

Erianin, the major bioactive flavones extracted from *Dendrobium chrysotoxum Lindl*, also called as shihu in traditional Chinese medicine. Growing evidence supports that erianin exerts antitumor activity in various cancer types. Erianin could suppressed cell proliferation and migration (Zhang et al., 2019), triggered mitochondrial apoptosis (Zhu et al., 2019), autophagy (Chen YT. et al., 2020) and cell cycle arrest (Chen YT. et al., 2020). However, the function of erianin has not been well explored in bladder cancer.

Here, we first showed that erianin inhibited cell proliferation and triggered cell death in bladder cancer cells. Next, we demonstrated that ferroptosis as the predominant method contributed to erianin-induced cell death of bladder cancer both *in vitro* and *in vivo*, which was confirmed by accompanied with ROS accumulation, GSH depletion, lipid peroxidation and downregulation of FTH1, GPX4, HO-1, GLS and xCT/SLC7A11. Moreover, ROS inhibitor NAC or glutathione GSH could rescue erianin-induced ferroptotic cell death. Mechanistically, we showed NRF2 was a key determinant for erianin-triggered ferroptosis. NRF2 activation by TBHQ treatment protected against erianin-induced cell death and increased the expression of GPX4, ferritin, xCT and glutaminase. On the other hand, NRF2 knockdown shRNA increased the activity of ROS and MDA but decreased GSH level and the expression of negative regulatory proteins for ferroptosis.

In brief, our data indicate that inducing ferroptosis is the main mechanism mediating antitumor activity of erianin, and erianin is expected to serve as a promising compound for the treatment of bladder cancer.

DATA AVAILABILITY STATEMENT

The raw data supporting the conclusions of this article will be made available by the authors, without undue reservation.

ETHICS STATEMENT

The animal study was reviewed and approved by Hangzhou Normal University.

AUTHOR CONTRIBUTIONS

XS, TX, QW, and DW conceived the idea and designed the study. YX, XC, and WW performed all the experiments. YX and XC analyzed the data and co-wrote the paper. LZ, XS, JF, TD, MZ, TP, LY, TJ, QG, CW, WM, and WL provided technical support. All the authors read and approved the final version of the manuscript prior to submission.

FUNDING

This work is supported by grants Zhejiang Provincial Natural Science Foundation of China for Distinguished Young Scholars (grant No. LR18H160001); National Natural Science Foundation of China (82104207); Zhejiang Provincial Natural Science Foundation of China (grant No. LQ20H160013 and LQ21H160038); Zhejiang province science and technology project of TCM (grant No. 2019ZZ016 and 2021ZQ058); Opening Project of Zhejiang Provincial Preponderant and Characteristic Subject of Key University (Chinese Traditional Medicine), Zhejiang Chinese Medical University (ZYX2018007).

SUPPLEMENTARY MATERIAL

The Supplementary Material for this article can be found online at: https://www.frontiersin.org/articles/10.3389/fphar.2021.775506/full#supplementary-material

REFERENCES

Badgley, M. A., Kremer, D. M., Maurer, H. C., DelGiorno, K. E., Lee, H. J., Purohit, V., et al. (2020). Cysteine Depletion Induces Pancreatic Tumor Ferroptosis in Mice. *Science* 368, 85–89. doi:10.1126/science.aaw9872

Chen, P., Li, X., Zhang, R., Liu, S., Xiang, Y., Zhang, M., et al. (2020b). Combinative Treatment of β-elemene and Cetuximab Is Sensitive to KRAS Mutant Colorectal Cancer Cells by Inducing Ferroptosis and Inhibiting Epithelial-Mesenchymal Transformation. *Theranostics* 10, 5107–5119. doi:10.7150/thno.44705

Chen, P., Wu, Q., Feng, J., Yan, L., Sun, Y., Liu, S., et al. (2020a). Erianin, a Novel Dibenzyl Compound in Dendrobium Extract, Inhibits Lung Cancer Cell Growth and Migration via Calcium/calmodulin-dependent Ferroptosis. *Signal. Transduct Target. Ther.* 5, 51. doi:10.1038/s41392-020-0149-3

Chen, W., Wu, G., Zhu, Y., Zhang, W., Zhang, H., Zhou, Y., et al. (2019). HOXA10 Deteriorates Gastric Cancer through Activating JAK1/STAT3 Signaling Pathway. *Cancer Manag. Res.* 11, 6625–6635. doi:10.2147/CMAR.S201342

Chen, Y. T., Hsieh, M. J., Chen, P. N., Weng, C. J., Yang, S. F., and Lin, C. W. (2020c). Erianin Induces Apoptosis and Autophagy in Oral Squamous Cell Carcinoma Cells. *Am. J. Chin. Med.* 48, 183–200. doi:10.1142/S0192415X2050010X

Gong, Y.-Q., Fan, Y., Wu, D.-Z., Yang, H., Hu, Z.-B., Wang, Z.-T., et al. (2004). *In Vivo* and *In Vitro* Evaluation of Erianin, a Novel Anti-angiogenic Agent. *Eur. J. Cancer* 40, 1554–1565. doi:10.1016/j.ejca.2004.01.041

Lee, H., Zandkarimi, F., Zhang, Y., Meena, J. K., Kim, J., Zhuang, L., et al. (2020). Energy-stress-mediated AMPK Activation Inhibits Ferroptosis. *Nat. Cel Biol.* 22, 225–234. doi:10.1038/s41556-020-0461-8

Li, Y., Cao, Y., Xiao, J., Shang, J., Tan, Q., Ping, F., et al. (2020). Inhibitor of Apoptosis-Stimulating Protein of P53 Inhibits Ferroptosis and Alleviates Intestinal Ischemia/reperfusion-Induced Acute Lung Injury. *Cell Death Differ* 27, 2635–2650. doi:10.1038/s41418-020-0528-x

Liu, Y. T., Hsieh, M. J., Lin, J. T., Chen, G., Lin, C. C., Lo, Y. S., et al. (2019). Erianin Induces Cell Apoptosis through ERK Pathway in Human Nasopharyngeal Carcinoma. *Biomed. Pharmacother.* 111, 262–269. doi:10.1016/j.biopha.2018.12.081

Sun, Y., Li, G., Zhou, Q., Shao, D., Lv, J., and Zhou, J. (2020). Dual Targeting of Cell Growth and Phagocytosis by Erianin for Human Colorectal Cancer. *Drug Des. Devel Ther.* 14, 3301–3313. doi:10.2147/DDDT.S259006

Wang, S., Liu, W., Wang, J., and Bai, X. (2020). Curculigoside Inhibits Ferroptosis in Ulcerative Colitis through the Induction of GPX4. *Life Sci.* 259, 118356. doi:10.1016/j.lfs.2020.118356

Yu, B., Choi, B., Li, W., and Kim, D. H. (2020). Magnetic Field Boosted Ferroptosis-like Cell Death and Responsive MRI Using Hybrid Vesicles for Cancer Immunotherapy. *Nat. Commun.* 11, 3637. doi:10.1038/s41467-020-17380-5

Yu, M., Gai, C., Li, Z., Ding, D., Zheng, J., Zhang, W., et al. (2019). Targeted Exosome-Encapsulated Erastin Induced Ferroptosis in Triple Negative Breast Cancer Cells. *Cancer Sci.* 110, 3173–3182. doi:10.1111/cas.14181

Zhang, X., Huang, Z., Xie, Z., Chen, Y., Zheng, Z., Wei, X., et al. (2020). Homocysteine Induces Oxidative Stress and Ferroptosis of Nucleus Pulposus via Enhancing Methylation of GPX4. *Free Radic. Biol. Med.* 160, 552–565. doi:10.1016/j.freeradbiomed.2020.08.029

Zhang, X., Wang, Y., Li, X., Yang, A., Li, Z., and Wang, D. (2019). The Anti-carcinogenesis Properties of Erianin in the Modulation of Oxidative Stress-Mediated Apoptosis and Immune Response in Liver Cancer. *Aging (Albany NY)* 11, 10284–10300. doi:10.18632/aging.102456

Zhu, Q., Sheng, Y., Li, W., Wang, J., Ma, Y., Du, B., et al. (2019). Erianin, a Novel Dibenzyl Compound in Dendrobium Extract, Inhibits Bladder Cancer Cell Growth via the Mitochondrial Apoptosis and JNK Pathways. *Toxicol. Appl. Pharmacol.* 371, 41–54. doi:10.1016/j.taap.2019.03.027

Conflict of Interest: The authors declare that the research was conducted in the absence of any commercial or financial relationships that could be construed as a potential conflict of interest.

Publisher's Note: All claims expressed in this article are solely those of the authors and do not necessarily represent those of their affiliated organizations, or those of the publisher, the editors, and the reviewers. Any product that may be evaluated in this article, or claim that may be made by its manufacturer, is not guaranteed or endorsed by the publisher.

frontiers in Oncology

REVIEW
published: 02 December 2021
doi: 10.3389/fonc.2021.792827

Ferroptosis in Lung Cancer: From Molecular Mechanisms to Prognostic and Therapeutic Opportunities

Peyman Tabnak[1*], *Zanyar HajiEsmailPoor*[1†] *and Soroush Soraneh*[2†]

[1] Faculty of Medicine, Tabriz University of Medical Sciences, Tabriz, Iran, [2] Faculty of Medicine, Urmia University of Medical Sciences, Urmia, Iran

OPEN ACCESS

Edited by:
Jian Chen,
Guilin Medical University, China

Reviewed by:
Xiao Zhang,
Shanghai Jiaotong University, China
Michael Wayne Epperly,
University of Pittsburgh, United States

***Correspondence:**
Peyman Tabnak
drtabnak@gmail.com;
tabnakp@tbzmed.ac.ir

[†]*These authors have contributed equally to this work and share second authorship*

Specialty section:
This article was submitted to Pharmacology of Anti-Cancer Drugs, a section of the journal Frontiers in Oncology

Received: *11 October 2021*
Accepted: *15 November 2021*
Published: *02 December 2021*

Citation:
Tabnak P, HajiEsmailPoor Z and Soraneh S (2021) Ferroptosis in Lung Cancer: From Molecular Mechanisms to Prognostic and Therapeutic Opportunities. Front. Oncol. 11:792827. doi: 10.3389/fonc.2021.792827

Lung cancer is the second commonly diagnosed malignancy worldwide and has the highest mortality rate among all cancers. Tremendous efforts have been made to develop novel strategies against lung cancer; however, the overall survival of patients still is low. Uncovering underlying molecular mechanisms of this disease can open up new horizons for its treatment. Ferroptosis is a newly discovered type of programmed cell death that, in an iron-dependent manner, peroxidizes unsaturated phospholipids and results in the accumulation of radical oxygen species. Subsequent oxidative damage caused by ferroptosis contributes to cell death in tumor cells. Therefore, understanding its molecular mechanisms in lung cancer appears as a promising strategy to induce ferroptosis selectively. According to evidence published up to now, significant numbers of research have been done to identify ferroptosis regulators in lung cancer. Therefore, this review aims to provide a comprehensive standpoint of molecular mechanisms of ferroptosis in lung cancer and address these molecules' prognostic and therapeutic values, hoping that the road for future studies in this field will be paved more efficiently.

Keywords: lung cancer, ferroptosis, biomarkers, cell death, Nrf2, iron metabolism, ROS, immunity

HIGHLIGHTS

- GPX4, system X_c^-, NRF2, p53, and UPS are the main ferroptosis regulators in lung cancer.
- Ferroptosis has a close relationship with the immune system status in lung cancer.
- The expression of ferroptosis-related genes including, ALOX15, PEBP1, GLS2, and PHKG2, positively predict prognosis.
- The expression of ferroptosis-related genes, including CISD1, ACSL3, FANCD2, and SLC7A11, negatively predict prognosis.
- Combining ferroptosis inhibitors with radiotherapy or chemotherapy synergistically kills lung tumors.

1 INTRODUCTION

With 11.4% and 18% of prevalence and total cancer death rate, respectively, lung cancer is the second common cancer and the leading cause of cancer death worldwide (1). Though tobacco smoking still is the critical risk factor for lung cancer, the importance of non-tobacco risk factors such as environmental and occupational exposures, chronic lung disease, and lifestyle factors is growing (2). Based on cell origin, lung cancers are divided into two primary subtypes, including non-small-cell lung carcinoma (NSCLC, more common form) and small-cell lung carcinoma (SCLC, less common form). Lung adenocarcinoma (LUAD), as the most common histological subtype of NSCLC, accounts for 38.5% of all lung cancer cases (3). Currently, conventional treatment choices include surgery and adjuvant therapies (e.g., chemotherapy, radiotherapy, and targeted therapy); however, half of the patients succumb within the first year of diagnosis, and five years overall survival is below 18 percent (4). Given the facts mentioned above, the health burden caused by lung cancer is remarkable and extensive efforts have been made to improve the disease in recent years. Understanding the molecular mechanism of lung cancer opens up new horizons for developing novel strategies to manage and fight against this malignancy (5). Ferroptosis, discovered in 2012, was first identified as a type of oxidative iron-dependent programmed cell death (PCD) different from apoptosis, necrosis, and autophagy. Following treatments with small molecules such as erastin, some morphological changes like chromatin condensation, cytoplasmic and organelle swelling, formation of double-membrane vesicles, shrunken mitochondria, and plasma membrane rupture were observed in affected cells (6). This process initiates with the accumulation of various pro-ferroptotic molecules contributing to lipid peroxidation through the production of reactive oxygen species (ROS) under the assistance of iron (7). Our understanding of ferroptosis has been growing over the last decade, and the numbers of ferroptosis regulators are increasing (8). Two main inhibitors of ferroptosis, including system X_c^- and glutathione peroxidase 4 (GPX4), prevent phospholipid peroxidation under physiological conditions. Control of cellular metabolism by different nutrients, intra/intercellular signaling pathways (e.g., p53 and NRF2), and environmental stress play an essential role in the synthesis of ferroptosis stimulators such as ROS and phospholipids containing polyunsaturated fatty acid chains (PUFA-PLs) (9). Ferroptosis is effective in eliciting a therapeutic response by experimental reagents (e.g., erastin and RSL3), approved drugs (e.g., sulfasalazine and artemisinin), ionizing radiation, and cytokines (e.g., IFNγ and TGFβ1), leading to inhibition of tumor growth in various cancer types (10). Therefore, cell death caused by ferroptosis is a great step toward cancer therapy. A study has shown that in Xuanwei area of China which the incidence of lung cancer is very high, ferroptosis dysregulation may implicate in the development of the disease (11). In this study, we particularly aimed to review the role of ferroptosis in lung cancer and provide insights into molecular mechanisms, prognostic and therapeutic importance of ferroptosis regulators.

2 FERROPTOSIS REGULATORS IN LUNG CANCER

2.1 Ferroptosis Suppressors

2.1.1 System X_c^-

System X_c^- (xCT) is a cystine/glutamate antiporter consisting of two subunits, including SLC3A2 and SLC7A11, which is responsible for exporting glutamate and importing cystine (12). Upon this transportation, cystine in the cytosol following an NADPH-consuming reduction reaction by thioredoxin reductase 1 (TXNRD1) is converted to cysteine, an antioxidant amino acid and precursor of tripeptide glutathione (GSH). Moreover, GSH is also a potent antioxidant that is used by glutathione peroxidase 4 (GPX4) for inhibition of ferroptosis by preventing the accumulation of lipid hydroperoxides (LOOHs) and converting them to lipid alcohols (LOHs) (**Figure 1**). Therefore, system X_c^- as a membrane heterodimer is implicated in inhibition of ferroptosis under oxidative stress to provide cancer cell survival (13). Up to now, various studies have pointed to the role of this system in the regulation of ferroptosis in *lung cancer*, most of them representing SLC7A11 as the targets of various novel drugs and upstream regulators (**Figure 1**). For example, a recent study has elucidated that there is a positive relationship between the level of transcription factor SOX2 and SLC7A11 in lung cancer stem-like cells (CSLC), and upregulation of SOX2 in lung tumors can highly inhibit ferroptosis and increase resistance to imidazole ketone erastin (IKE), a strong inducer of ferroptosis (14). Likewise, a similar relationship was observed between RNA binding protein RBMS1 and SLC7A11, in a way that depletion of RBMS1 sensitizes lung cancer cells to ferroptosis and radiotherapy (15). Moreover, Ma et al. have reported that YT521-B homology domain containing 2 (YTHDC2) is a downregulated tumor suppressor in lung adenocarcinoma (LUAD), which can suppress the activity of system X_c^- through targeting mRNA encoding SLC7A11 (16). However, their further investigations revealed that inhibition of SLC7A11 by YTHDC2 is not enough to induce ferroptosis in lung adenocarcinoma. Therefore, they proposed that SLC3A2 as another subunit of system X_c^- should be inhibited by YTHDC2 as well. High-level induction of YTHDC2 could inhibit the expression of SLC3A2 indirectly by inhibiting the expression of HOXA13. Further *in vivo* experiments also confirmed that the induction of YTHDC2 can highly contribute to ferroptosis. Therefore, elevating the levels of YTHDC2 was shown to be a promising strategy in LUAD to induce ferroptosis by selectively inhibiting the expression of both subunits of system X_c^- in tumor cells (17).

2.1.2 GPX4

GPX4, a selenoperoxidase and a key upstream regulator of ferroptosis, plays two roles at the same time including, converting GSH to glutathione disulfide (GSSG) and reducing phospholipid hydroperoxides (PLOOHs) to their corresponding alcohol (PLOHs), thereby preventing the accumulation of lipid peroxides and leading to suppression of ferroptosis. In addition, GSSG can be recycled to GSH under the action of glutathione–

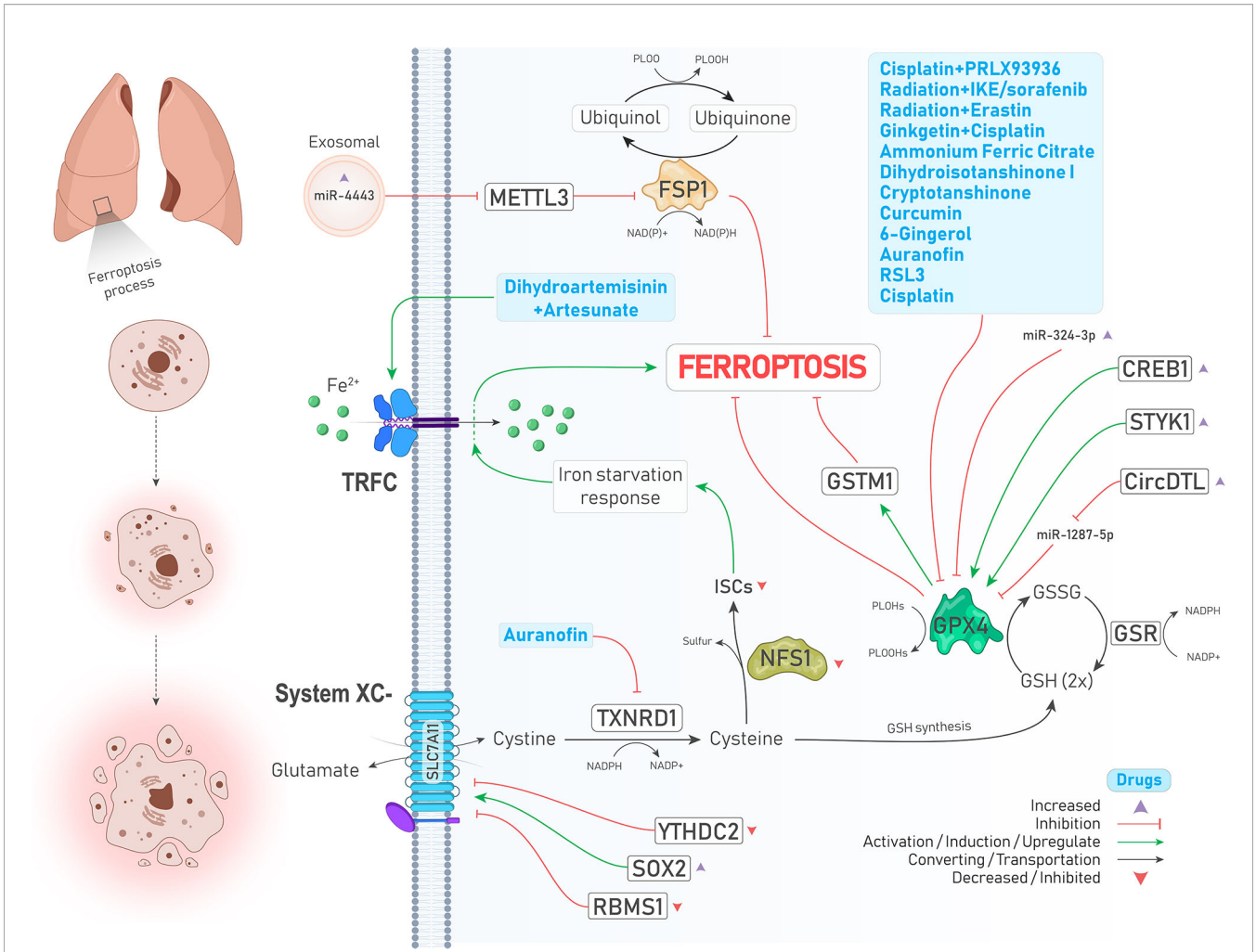

FIGURE 1 | An illustration showing regulation of ferroptosis suppressors, including system X_c^-,GPX4, FSP1, and NFS1 in lung cancer by different molecules and treatments. System X_c^- is upregulated and downregulated due to increase of SOX2 (↓ Ferroptosis) and decrease of YTHDC2 levels (↑ Ferroptosis), respectively. TXNRD1 is inhibited by auranofin (↑ Ferroptosis). Inhibited NFS1 and subsequently decreased ISCs biosynthesis leads to an iron starvation response which causes Fe^{2+} influx to cells by TRFC (↑ Ferroptosis). As a ferroptosis inhibitor, GPX4 is suppressed by a group of drugs depicted in the blue box (↑ Ferroptosis). In addition, GPX4 is positively upregulated by enhanced expressions of CREB and STYK1 (↓ Ferroptosis). FSP1, which inhibits ferroptosis independently, is upregulated upon increased expression of oncogenic miR-4443 (↑ Ferroptosis).

disulfide reductase (GSR) using the electrons provided by $NADPH/H^+$ (9) (**Figure 1**). Various studies have reported that GPX4 is upregulated in different cancers, including LUAD, and is associated with poor prognosis of patients and chemotherapy resistance. Suppression of GPX4 by a small molecule inhibitor named RSL3 strongly enhances the anticancer effects of cisplatin *in vivo*. In other words, RSL3 combined with cisplatin could induce ferritinophagy/ferroptosis (18). Another study has also shown that the levels of GPX4 and mTORC1 are higher in NSCLC cells, and inhibition of these molecules provides a promising strategy to overcome lapatinib resistance *in vivo* (19). cAMP response element-binding protein (CREB) is also an upregulated oncogene in LUAD tissues that positively regulates the expression of GPX4, and their levels are closely related to tumor size and stage (20). A similar relationship was also observed between serine threonine tyrosine kinase 1 (STYK1) and GPX4 in NSCLC. In brain metastasis of lung adenocarcinoma, Glutathione S-transferase M1 (GSTM1) is another protein that is stablized by GPX4 and concurrently result in inhibition of ferroptosis and subsequent resistance to platinum through increasing GSH consumption (21). We will further show that many drugs and upstream signaling pathways significantly affect the regulation of GPX4 in lung cancer (22) (**Figure 1** and **Table 2**).

2.1.3 FSP1

Recent studies have identified that GPX4 is not the only ferroptosis suppressor in human cancer cells, and ferroptosis suppressor protein 1 (FSP1, formerly known as AIFM2) independent of GSH suppresses lipid peroxidation and

subsequent ferroptosis through converting ubiquinone (coenzyme Q10, CoQ10) to ubiquinol (CoQH2, reduced form of CoQ10) using an NADPH-consuming reduction reaction (**Figure 1**). Therefore, this pathway is also referred to as the CoQ-dependent pathway (9). Bersuker et al. showed that FSP1 expression positively correlates with ferroptosis resistance in various cell lines, particularly in the xenograft mouse model of *lung cancer (*23).

2.1.4 NFS1

Cysteine desulfurase nitrogen fixation 1 homolog (NFS1) is an enzyme that extracts sulfur from cysteine for the biosynthesis of iron-sulfur clusters (ISCs) and is expressed at higher levels in differentiated lung adenocarcinomas. A study has demonstrated that suppressing NFS1 as well as ISCs biosynthesis triggers an iron-starvation response and subsequent iron influx to cells by molecules such as transferrin receptor protein (TRFC), thereby promoting ferroptosis and inhibiting tumor growth in lung tumors (24, 25) (**Figure 1**).

2.1.5 NRF2

Transcription factor nuclear factor erythroid 2-related factor 2 (NFE2L2 or NRF2) is an overriding antioxidant transcription regulator of genes involved in lipid peroxidation and the accumulation of free iron (26). Takahashi et al. emphasized that hyperactivation of NRF2 is required for proliferation and survival of 3D culture models of lung tumors through preventing ferroptosis. However, NRF2 downregulation was not enough to suppress ferroptosis since GPX4 levels were increased, proposing that enhanced oxidative stress caused by NRF2 downregulation might activate other cytoprotective signaling pathways, including nuclear factor-κB (NF-κB), involved in activating downstream antioxidant enzymes. Notably, simultaneous inhibition of NRF2 and GPX4 could efficiently induce ferroptosis (27). The study by Liu et al. showed that Wnt signaling pathway through provoking NRF2 increases the activity of GPX4 in brain metastasis of lung adenocarcinoma cells, thereby resulting in chemoresistance to platinum (21). In addition, the activity of NRF2 positively reflects erastin resistance in isogenic lung cancer cell models, regardless of Kelch-like ECH-associated protein 1(KEAP1) mutation (28), a molecule that represses NRF2 *via* its ubiquitin proteasomal degradation in normal conditions (29). Likewise, KEAP1-mutant lung cancer cells were shown to have higher levels of NRF2 and its downstream target SLC7A11. In addition, KEAP1 deficient lung tumors were shown to be sensitive to inhibition of glucose transporter 1 (GLUT1) due to their glucose dependency (30). Similarly, Wohlhieter et al. (31) showed that LUAD tumors with concurrent mutations in serine/threonine kinase 11 (STK11) and KEAP1 were more resistant to ferroptosis since the activity of NRF2 pathway and targets involved in ferroptosis such as SLC7A11 and GPX4 were increased, leading to worse overall survival and enhanced tumor proliferation both *in vivo* and *in vitro* (**Figure 2**). Moreover, their further investigations turned out that stearoyl-CoA desaturase (SCD1, SCD) was necessary for the proliferation of the cells mentioned above (**Figure 2**). SCD1 was previously shown to participate in aberrant lipid metabolism and promoted cell growth in lung cancer (32); therefore, its genetic and pharmacological inhibition could sensitize STK11/KEAP1 co-mutant cells to ferroptosis induction even *in vivo*. Noteworthy to mention, the role of mitochondria and the tricarboxylic acid (TCA) cycle has been highlighted recently in regulating ferroptosis (33). NRF2 can also affect mitochondrial function. For example, in NSCLC, FOCAD-FAK signaling was shown to be involved in cysteine deprivation-induced ferroptosis, and NRF2 was shown to inhibit the FOCAD-FAK signaling axis and induce ferroptosis *via* increasing the activity of Complex I in the mitochondrial electron transport chain (ETC) and TCA cycle. However, inhibiting NRF2 is not enough for ferroptosis induction since the FOCAD-FAK axis does not affect GPX4. Therefore, adding an NRF2 inhibitor such as brusatol concurrent with erastin can promote ferroptosis induction better in NSCLC cells (34) (**Figure 2**). Similarly, a novel study conducted by Kang et al. has highlighted the role of the NRF2 signaling pathway in cystine depletion conditions. NSCLC cells with higher expression levels of NRF2 produce many γ-glutamyl-peptides due to increased activity of glutamate-cysteine ligase catalytic subunit (GCLC). Following production of γ-glutamyl-peptide, glutamate is not accumulated in the cytosol anymore and this process leads to ferroptosis inhibition (35). Activating transcription factor 2 (ATF2) is another protein with an oncogenic role in lung cancer and increases NRF2 expression following treatments with a group of drugs named BET inhibitors (BETi, with the ability to induce ferroptosis in breast cancer) in LUAD, leading to ferroptosis resistance (36). In addition, a very recent study has shown that the expression of E3 ubiquitin ligase Mindbomb 1 (MIB1) is upregulated in a group of lung squamous and adenocarcinoma cells and correlates negatively with patients' survival. Nevertheless, cells overexpressing MIB1 are more sensitive to ferroptosis due to proteasomal degradation of NRF2 by MIB1 (37). Taken together, due to the prominent role of NRF2 in regulating ferroptosis, targeting it by various treatments can significantly induce ferroptosis (see **Table 2**).

2.2 Ferroptosis Inducer

2.2.1 ACSL4

Acyl-CoA synthetase long-chain family member 4 (ACSL4) is a crucial enzyme responsible for lipid metabolism, which converts PUFAs to PUFA-CoAs, and following the action of LPCAT3, the products of this reaction are esterified into phospholipid containing polyunsaturated fatty acid chain (PUFA-PLs). Then, these PUFA-PLs are oxidized by another enzyme named ALOX15 into PL-PUFA-OOHs. Since PL-PUFA-OOHs can trigger ferroptotic cell death, the activity of the abovementioned enzymes contributes to the promotion of ferroptosis (38). Surprisingly, although ALOX15 and ACSL4 facilitate the ferroptosis process, recent studies showed that higher expression of these molecules was associated with increased cancer malignant features. Thereby, these molecules can act as double-edged swords either by promoting or inhibiting cancer progression (39). However in SCLC, Bebber et al. showed that ACSL4 and LPCAT3 are expressed at higher levels in non-

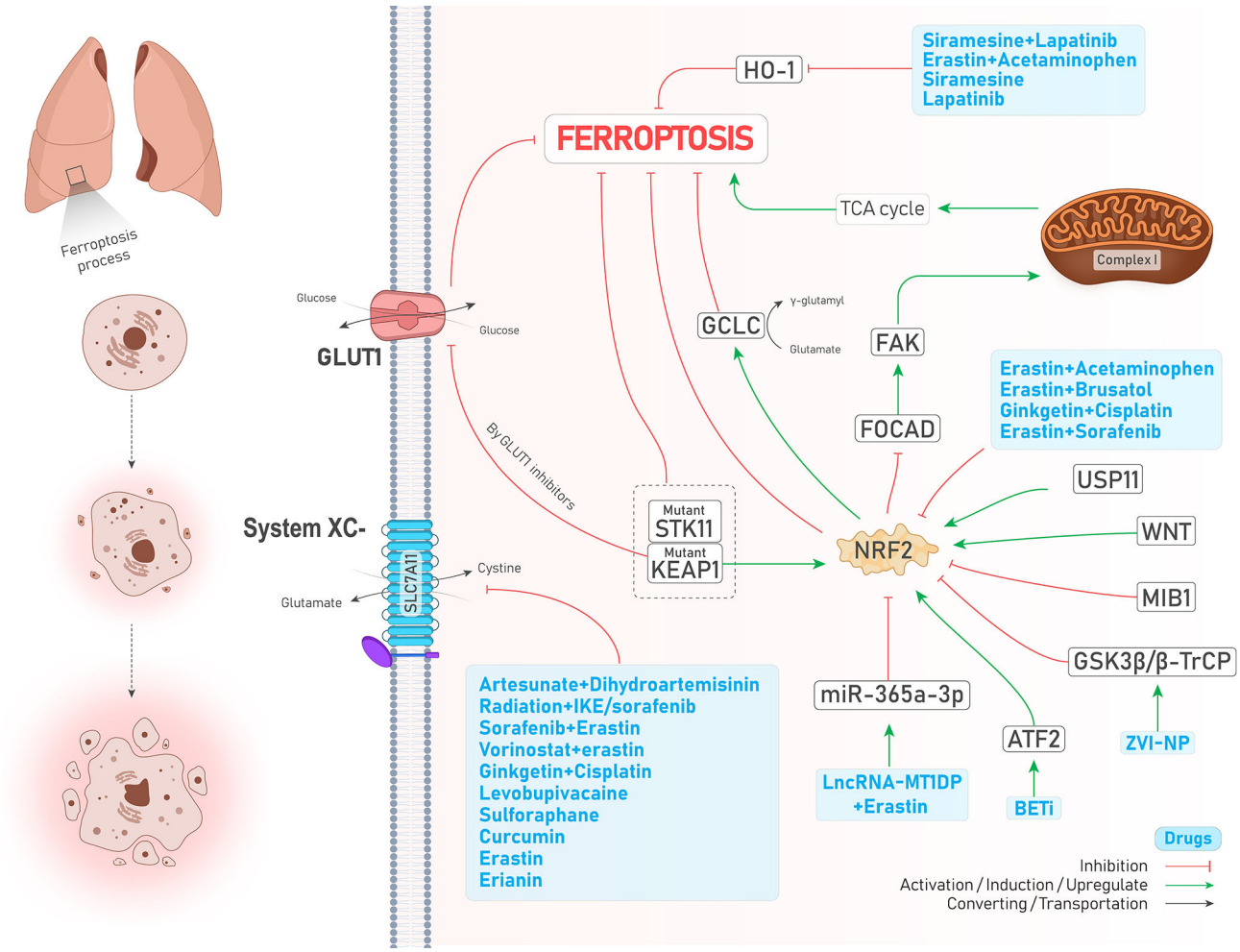

FIGURE 2 | An illustration showing the role of NRF2 in regulating ferroptosis in lung cancer and its control by different molecules and treatments. NRF2 inhibits ferroptosis. KEAP1-mutant cells overexpress NRF2 and inhibit ferroptosis; while using GLUT1 inhibitor agents in these cells induces ferroptosis. Co-mutant STK11 and KEAP1 cells (depicted by dotted box) are more resistant to ferroptosis (↓ Ferroptosis) due to increased levels of GPX4 and SLC7A11 (which is not shown here). The combination of lncRNA-MT1DP and erastin inhibits NRF2 by increasing the activity of miR-365a-3p (↑ Ferroptosis). ATF2 activation by BET inhibitors causes NRF2 upregulation (↓ Ferroptosis). ZVI-NP mediates NRF2 degradation by inducing GSK3β/β-TrCP (↑ Ferroptosis). USP11 activation causes NRF2 induction (↓ Ferroptosis). A significant number of drugs (depicted in the blue box) inhibits NRF2 (↑ Ferroptosis). FOCAD-FAD axis, which mediates ferroptosis by induction of TCA cycle and complex I in the mitochondria, is inhibited by NRF2 (↓ Ferroptosis). Higher levels of NRF2 increase the activity of GCLC (↓ Ferroptosis). A large group of drugs (the biggest blue box) could inhibit system X_c^- (↑ Ferroptosis). HO-1 naturally causes ferroptosis (not shown here); while its degradation by another group of drugs (depicted in the blue box) inhibits ferroptosis (↓ Ferroptosis).

neuroendocrine (non-NE-SCLC) than NE-SCLC, contributing to ferroptosis sensitivity and resistance, respectively in the abovementioned cells. Moreover, they proposed that TRX antioxidant pathway is overactivated in NE-SCLC cells, and its inhibition by auranofin alongside treatment with buthionine sulfoximine (BSO), as a GSH level reducer, could successfully induce ferroptosis and inhibit tumor progression in mice with xenograft NE-SCLC tumors (40). In addition, ACSL4 was found to act as a tumor suppressor and a favorable prognostic factor in patients with LUAD and promoted ferroptosis but inhibited tumor cell survival, invasion, and migration. Most interestingly, a high-fat diet could reverse these effects *via* downregulating ACSL4 both *in vivo* and *in vitro* (41).

2.3 Signaling Pathways and Their Crosstalk With Ferroptosis in Lung Cancer

2.3.1 EGFR and MAPK

The epidermal growth factor receptor (EGFR) pathway is involved in the progression of various cancers, and its mutation is frequently seen in lung adenocarcinomas (42). It is noteworthy to mention that the previously mentioned SCD1 is stabilized by EGFR *via* Y55 phosphorylation and contributes to cancer progression in lung cancer (32). Moreover, activation of mitogen-activated protein kinase (MAPK) as a downstream target of the EGFR pathway is required to induce ferroptosis (**Figure 3**). Following cystine-deprived conditions, those NSCLC cells with the highest MAPK signaling activity significantly lose

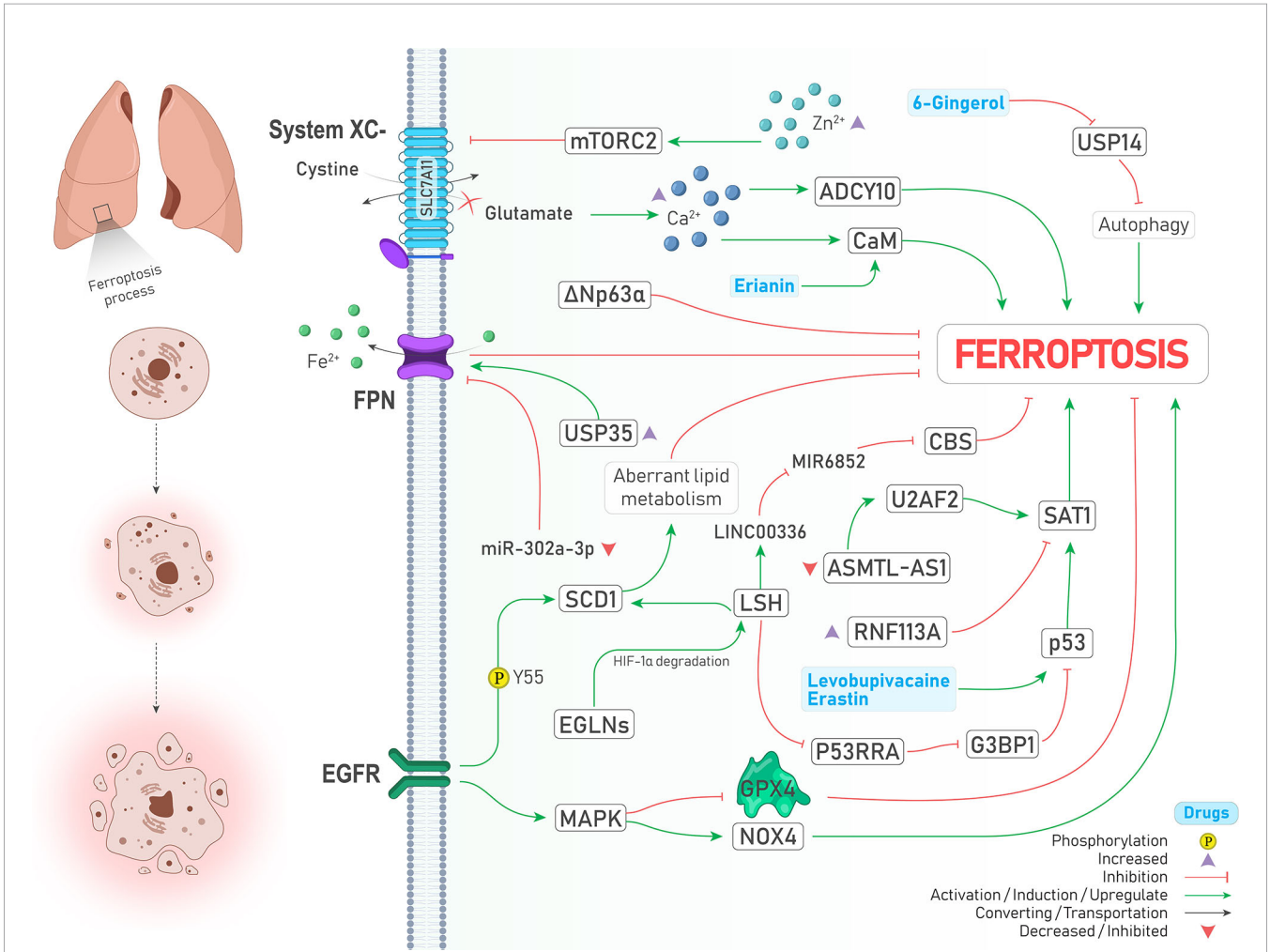

FIGURE 3 | An illustration showing signaling pathways involved in regulating ferroptosis in lung cancer and their possible crosstalk together. MAPK activation leads to GPX4 inhibition and NOX4 activation (↑ Ferroptosis). SCD1 stabilization by EGFR *via* its Y55 phosphorylation inhibits ferroptosis through aberrant lipid metabolism (↓ Ferroptosis). Under the hypoxic condition, EGLNs degrades HIF-1α. Therefore, LSH expression is increased and induces SCD1 expression (↓ Ferroptosis). LSH can upregulate lncRNA-LINC00336. This interaction results in CBS inhibition *via* sponging/inhibiting MIR6852 (↓ Ferroptosis). In addition, LSH downregulates lncRNA-NEAT1 and inhibits p53 *via* G3BP1 downregulation (↓ Ferroptosis). Upregulation of SAT1 by p53 promotes ferroptosis, and RNF113A deficiency causes ferroptosis by increasing SAT1. Two drugs induce the expression of p53 and drive the cell toward ferroptosis (↑ Ferroptosis). ΔNp63α inhibits ferroptosis. USP35 overexpression leads to ferroptosis suppression by stabilization of FPN (↑ Ferroptosis). Moreover, FPN is inhibited upon decreased expression of miR-302a-3p (↑ Ferroptosis). Zinc intoxication causes ferroptosis by inhibition of the System X_c^- inhibition circumstances, glutamate is accumulated in the cell, which results in the calcium ions accumulation. This accumulation induces ferroptosis by CaM and ADCY10 activation (↑ Ferroptosis). Erianin activates CaM (↑ Ferroptosis). USP14 inhibition by 6-Gingerol leads to autophagy induced ferroptosis (↑ Ferroptosis).

their viability through a ferroptosis process caused by inhibited and promoted expression of GPX4 and NOX4, respectively (43).

2.3.2 HIF-1α

Hypoxia, as a hallmark of cancer, leads to excess tumor vascularization and progression (44). Activation of both MAPK and EGFR pathways can induce the expression of hypoxia-inducible factor 1-alpha (HIF-1α) (44, 45). In addition, induction of HIF-1 by EGFR can make A549 lung cancer cells resistant to another type of PCD called anoikis under the lipid raft-disrupting stress (45). Emerging evidence also supports the role of HIFs in the induction of ferroptosis (46, 47). Jiang et al. showed that iron-dependent enzymes Egl nine homolog (EGLNs) under hypoxia conditions degrades HIF-1α (**Figure 3**), leading to increased lymphoid-specific helicase (LSH) expression, a chromatin remodeling factor that acts as an oncogene and ferroptosis inhibitor in lung cancer *via* increasing the expression of SCD1 (48, 49).

2.3.3 P53

Tumor suppressor P53 has a dual role in regulating ferroptosis. Spermidine/spermine N1-acetyltransferase (SAT1) is one of those proteins which is upregulated by p53 and responsible for oxidative stress and ferroptosis (50, 51). However, SAT1 is under

the control of factors other than p53. For instance, RNF113A is an oncogene RNA-binding protein whose deficiency provokes ferroptosis *via* promoting SAT1 expression (**Figure 3**) and was upregulated and contributed to cisplatin resistance in lung adenocarcinomas (52). Recently, it has been discovered that ΔNp63α as a major isoform of p63 can inhibit ferroptosis and oxidative stress independent of p53 and NRF2 activity in lung cancer through transcriptional controlling the expression of genes involved in glutathione synthesis (53).

2.3.4 Proteasomal Degradation Pathway

Ubiquitin–proteasome system (UPS) belongs to a degradation pathway that controls lipid peroxidation and iron accumulation *via* degradation of molecules involved in ferroptosis (8). A recent review has also highlighted the role of ubiquitination in ferroptosis (54). Ubiquitin-specific protease 35 (USP35) is a deubiquitinase that is overexpressed in lung cancer, and its knockdown, in addition to promoting ferroptosis and chemotherapeutic sensitivity to cisplatin and paclitaxel, inhibits lung cancer cell growth, colony formation, and tumor progression. The mechanism by which USP35 overexpression led to ferroptosis was attributed to ferroportin (FPN) stabilization, a protein responsible for exporting iron to the outside of the cells (**Figure 3**) (55). In the same way, a similar relationship between deubiquitinase USP11 and NRF2 was found in patients with NSCLC (SCC subtype), leading to ferroptosis resistance and cell proliferation (**Figure 3**) (56). Noteworthy to mention, the effects of some drugs in inducing ferroptosis are also carried out by the proteasome degradation system. For instance, concurrent treatment with siramesine alongside lapatinib was shown to induce ferroptosis *via* proteasome degradation of heme oxygenase-1 (HO-1) (57).

2.3.5 Autophagy

Autophagy is another intracellular degradation pathway in which various molecules and organelles in the cell are engulfed and then degraded following the formation of lysosomal structures (8). There is close crosstalk between ferroptosis and autophagy, in a way that some of the recent reviews consider ferroptosis as a type of autophagy-dependent cell death (58, 59). The reason behind this assumption is that in the presence of some ferroptosis inducers such as erastin and RSL3, the formation of autophagosomes and components of the autophagy system is also provoked, and thereby ferroptosis is promoted (58). Some pieces of evidence support this relationship in lung cancer. Following inhibition of USP14 by 6-Gingerol (a natural product) in A549 lung cancer cells, the levels of ROS, iron concentration, and autophagosomes started to increase and contributed to increased expression of ferroptosis and autophagy-related proteins *in vivo* and *in vitro* (**Figure 3**). Therefore, it can be concluded that USP proteins are a common executer among autophagy and ferroptosis process (60). Similarly, treatment with curcumin, a well-known natural derived product, could significantly induce cell death both *in vivo* and *in vitro* through an autophagy-dependent ferroptosis mechanism and inhibition of autophagy reversed ferroptosis caused by curcumin in NSCLC (61).

2.3.6 Hippo/YAP Pathway

Hippo is an evolutionarily conserved signaling pathway with potent tumor suppressor activities involved in determining cell fate. Its dysregulation highly induces cancer progression and therapy resistance through aberrant activation of two transcriptional coactivators, including yes-associated protein (YAP) and transcriptional coactivator with PDZ-binding motif (TAZ). When hippo signaling is off, YAP and TAZ are translocated to the nucleus and interact with DNA binding transcription factors named TEA domain family member (TEAD) to provoke the expression of genes involved in cell proliferation (62). Recently the role of Hippo/YAP/TAZ axis in regulating ferroptosis was described as dependent on the distance between cells and their contact. In other words, when there is no contact between the cells (low-density conditions), due to the inactivation of Hippo signaling, YAP and TAZ trigger the expression of genes responsible for ferroptosis induction rather than apoptosis. While this process is reversed when cells get closer to each other and extracellular E-cadherin stimulates Hippo pathway activation, leading to increased apoptosis (62). In LUAD, Zhang et al. demonstrated that the magnitude of YAP suppression is a crucial determiner of ferroptosis sensitivity. While inhibiting system X_c^- by sorafenib could induce ferroptosis and decrease YAP levels, suppressing GPX4 could not, proposing that subsequent glutamate accumulation in the cytosol might sensitize cells to ferroptosis. Their further experiments showed that glutamate repletion conditions (e.g., system X_c^- inhibition) provokes Ca^{2+} ions accumulation in the cytosol and ADCY10 initiates a cascade of reactions leading to YAP destabilization and subsequent ferroptosis (**Figure 3**). Since ADCY10 is expressed higher in advanced stage and therapy resistance LUAD cells, targeting ADCY10 as a molecule linked with YAP and ferroptosis was shown to have clinical significance (63).

2.3.7 Calcium and Zinc Effects

The latest review on ferroptosis insists that ions other than iron (e.g., zinc) cannot induce ferroptosis (8); however, other ions can indirectly affect ferroptosis. As just mentioned earlier, at least in lung cancer, accumulation of Ca^{2+} subsequently triggers the reactions that lead to ferroptosis sensitivity (63). Likewise, treating lung cancer cells with erianin (a natural product) promoted ferroptosis *via* calcium/calmodulin (CaM) signaling activation, a pathway involved in increasing intracellular Ca^{2+} levels (**Figure 3**) (64). Moreover, zinc intoxication in NSCLC cells upregulates the mTORC2/RICTOR pathway, resulting in system X_c^- phosphorylation and subsequent ferroptosis (**Figure 3**). However, it should be noted that these effects of zinc are reversed after a specific time and are limited using iron chelator deferoxamine and vitamin E (65).

2.3.8 mTOR Pathway

The mechanistic target of rapamycin (mTOR) is an essential negative regulator of autophagy (8). Moreover, GPX4 is also involved in regulating ferroptosis, and the levels of mTOR are positively correlated with GPX4 levels; therefore, mTOR inhibitors can induce autophagy-dependent ferroptosis (66).

For this reason, "inhibition of GPX4 or mTORC1 overcomes resistance to Lapatinib *via* promoting ferroptosis in NSCLC cells" (19), while zinc intoxication increases mTORC2 activity and ferroptosis (65). This proposes the theory that mTORC1 and mTORC2 may have distinct impacts on regulating ferroptosis, at least in lung cancer. Moreover, it has been proposed that lung tumors, which in them NRF2 signaling pathway is activated more than usual, are more dependent on the mTOR pathway, and synergistic cooperation between NRF2 and mTOR signaling can enhance cell proliferation in 3D cultures (27).

2.4 Non-Coding RNAs

Non-coding-RNAs (ncRNAs) make up a considerable part of the human transcriptome. They are the hot topic of interest these days since they are involved in many physiologic and pathologic conditions, particularly cancer (67). Recent studies have highlighted the role of ncRNAs in regulating the expression of genes involved in ferroptosis in cancer (68). microRNAs (miRNAs) long non-coding RNAs (lncRNAs), and circular RNAs belong to ncRNAs whose roles in regulating gene expression have been frequently emphasized. Their role in regulating ferroptosis in lung cancer is discussed as below:

2.4.1 miRNAs

miRNAs are a class of ncRNAs with 18-25 nucleotides long that can inhibit protein translation by affecting the expression of their target mRNAs (69). Tumor suppressor miRNAs are downregulated in cancers, and their targets are oncogenic proteins. miR-302a-3p is one of those downregulated tumor suppressor miRNAs that induces ferroptosis *via* targeting 3'-UTR of FPN mRNA in NSCLC. Ectopic induction of miR-302a-3p mimics provides a promising strategy against NSCLCs and sensitizes them to erastin, RSL3, cisplatin, and paclitaxel (70). Similarly, miR-324-3p expression is downregulated in cisplatin-resistant NSCLC cells, and its overexpression sensitizes resistant cells to cisplatin *via* targeting GPX4 (**Figure 1**) (71). Moreover, tumor cells can release exosomes containing miRNAs to their surrounding microenvironment. miR-4443 is an oncogenic miRNA found abundantly in exosomes released from cisplatin-resistant NSCLCs and suppresses ferroptosis *in vivo* and *in vitro* through increasing FSP1 protein level indirectly by targeting methyltransferase-like 3 (METTL3), a molecule that causes N^6-methyladenosine (m^6A) methylation of FSP1 (72) (**Figure 1**).

2.4.2 lncRNAs

lncRNAs are a group of non-coding RNAs which are more than 200 nucleotides in length. Similar to miRNAs, these molecules affect gene expression through an extensive range of mechanisms. Moreover, they may act as sponges for miRNAs and inhibit their activity (73). For example, LSH can increase the expression of lncRNA-LINC00336 in lung cancer and thereby inhibit ferroptosis through sponging the activity of MIR6852, a miRNA that targets mRNA of a ferroptosis suppressor named cystathionine-β-synthase (CBS) (74) (**Figure 3**). Similarly, LSH is responsible for the downregulation of tumor suppressor lncRNA-P53RRA in NSCLC. P53RRA activates the p53 signaling pathway and induces ferroptosis *via* interacting with Ras GTPase-activating protein-binding protein 1 (G3BP1) (**Figure 3**) (75). Furthermore, lncRNA-NEAT1 was shown to induce ferroptosis in NSCLC by increasing the expression levels of ACSL4 mRNA (76). Recently, Sui et al. showed that SAT1 mRNA could be stabilized by an RNA binding protein named U2AF2 and consequently lead to ferroptosis in LUAD. However, lncRNA-ASMTL-AS1, which is responsible for recruiting U2AF2 and promoting SAT1 expression, is downregulated in LUAD cells, and thereby recovering its expression can inhibit malignant features of the cancer cells (77). Targeted delivery of ncRNAs can be considered a promising strategy against cancer. Gai et al. adopted a novel strategy to induce ferroptosis in NSCLC tumors by deploying folate-modified liposomes containing lncRNA-MT1DP combined with erastin. Since MT1DP increases the activity of miR-365a-3p, a miRNA that targets NRF2, subsequent deactivation of NRF2 (**Figure 2**) confers sensitivity to erastin-induced ferroptosis *in vivo* and *in vitro (*78).

2.4.3 circRNAs

circRNAs are more stable than miRNAs and lncRNA due to their covalently-closed structures, and their dysregulation is implicated in the progression of various cancer, including lung cancer (79). CircDTL is an upregulated oncogene circular RNA in NSCLC cells that inhibits ferroptosis *via* acting as a sponge for miR-1287-5p, a miRNA that targets GPX4. Moreover, inhibition of circDTL can increase the sensitivity of lung cancer cells to erastin *in vivo (*80).

3 FERROPTOSIS AND PROGNOSIS OF PATIENTS WITH LUNG CANCER

Up to now, thanks to The Cancer Genome Atlas (TCGA) and Gene Expression Omnibus (GEO) datasets, a significant number of studies have been conducted to analyze the expression profile of genes involved in ferroptosis in patients with lung cancer, particularly LUAD (81–93). As seen in **Table 1**, these studies have shown that *ferroptosis regulator genes* can predict the prognosis and overall survival of patients very efficiently. For example, various studies have shown that the expression of ALOX15, PEBP1, GLS2, and PHKG2 was associated with better prognosis and overall survival (low hazard ratio). In contrast, the expression of CISD1, ACSL3, FANCD2, SLC7A11, PGD, and GCLC was associated with poor prognosis (high hazard ratio). Therefore, the expression of these genes has the applicability of being used as biomarkers for predicting the prognosis of patients. Moreover, pathway analyses of ferroptosis-related genes have revealed that there is a close relationship between ferroptosis and immune system response, suggesting that future studies should pay more attention to this aspect of ferroptosis in lung cancer. Regarding the relationship between the immune system and ferroptosis, Huang et al. have shown that AKR1C1 negatively correlates with infiltrating level of immune cells, including $CD4^+$ T cells, neutrophils, and dendritic cells in NSCLC. Moreover, its high-

TABLE 1 | Bioinformatic studies predicting prognosis of patients based on the expression of ferroptosis-related genes and non-coding RNAs.

Dataset used in the study	Low-risk	High-risk	Highlights of the study	Ref.
TCGA, GSE68465, and GSE72094	TLR4, PHKG2, PEBP1, GLS2, FLT3, and ALOX15	VDAC2, PGD, PANX1, KRAS, ALOX12B, ACSL3, CISD1, FANCD2, and SLC3A2	* "The expression of KRAS and PGD was positively related to tumor mutation burden, indicating that *KRAS and PGD* could serve as *novel biomarkers* for predicting *immunotherapy response rate*" * "VDAC2, GLS2, FLT3, TLR4, PGD, PANX1, PEBP1, ACSL3, CISD1, FANCD2, and SLC3A2 were of statistical significance" * "The four ferroptosis suppressor genes, ACSL3, CISD1, FANCD2, and SLC3A2, increased the *tumor's stem cell-like* features and were all positively associated with *CD133 and CD44*" * "Ferroptosis process involves the *development of tumor immune evasion* (e.g., IL-17 signaling pathway)." * "*PEBP1* could be a promising treatment target and is positively related to *chemotherapy sensitivity*."	(81)
TCGA and GSE68465	ALOX15, IL33, and GDF15	DDIT4 and HNF4A	* "Ferroptosis-related gene signatures can be used as a potential *predictor* for the prognosis of LUAD." * "TCGA cohort showed *lower scores* in *immune-related cells, such as mast cells, neutrophils, dendritic cells (DCs), and T helper cells, with only natural killer (NK) cells showing higher scores*." * "The *high-risk group* in the two cohorts *showed lower scores for type II and type I IFN responses*."	(82)
TCGA, GSE72094, and GSE68465	NCOA4, GLS2, ALOX15, PEBP1, and PHKG2	ACSL3, PGD, ATP5G3, CISD1, and ALOX12B	* "The enriched gene sets in the *high-risk* group were mainly involved in pathways related to *glycolysis, mTORC1, MYC, G2/M checkpoint, unfolded protein response, E2F, hypoxia, mitotic spindle assembly, epithelial-mesenchymal transition, and late response to estrogen*." * "Resting mast cells and resting dendritic cells can be identified as having a potential prognostic capacity in LUAD." * "A total of 62.85% (308/490) of *autophagy-related genes* were found to be significantly correlated with risk scores."	(83)
TCGA, GSE72094, and GPL15048	ANGPTL7, SLC1A4, GDF15, DUOX1, PHKG2, CDO1, LINC00472, DPP4, LINC00336, ALOX15, and GLS2	TXNRD1, DDIT4, SLC7A5, SLC2A1, RRM2, AURKA, ALOXE3, SLC7A11, and GCLC	* "The relationship between the ferroptosis-related genes and *tumor-infiltrating immune cells* was revealed by ANGPTL7 and M2 macrophages, ANGPTL7 and monocytes, GDF15 and M1 macrophages, LINC00472 and M2 macrophages, RRM2 and M1 macrophages, RRM2 and monocytes, and SLC2A1 and M1 macrophages."	(84)
TCGA, GSE11969, GSE13213, GSE30219, GSE31210, and GSE41271	DUOX1, ALOX15, DPP4, CDO1, GDF15, and IL33	SLC7A11, GCLC, FANCD2, HELLS, ALOX12B, ALOXE3, TXNRD1, SRXN1, GPX2, DDIT4, SLC7A5, SLC2A1, RRM2, and AURKA	* "ALOX12B, ALOX15, GPX2, DDIT4, and GDF15 were increased and SLC2A1 and were decreased after erastin treatment." * "ALOX15 was significantly low expressed in Ki67-high samples, while GPX2, DDIT4, and SLC2A1 were high expressed in Ki67-high samples." * "Down-regulation of either GPX2 or DDIT4 could partially reverse the cell proliferation arrest." * "Significantly enriched KEGG pathways include *cell cycle, complement, and coagulation cascades, p53 signaling, cellular senescence, and fatty acid metabolism*."	(85)
TCGA, GSE72094, and GSE30219	AGER, ALOX15B, DPP4, GLS2, ISCU, PEBP1, PHKG2, SLC11A2,	ATP5MC3, CISD1, EGLN1, FANCD2, ITGA6, ITGB4, KRAS, NEDD4, SLC38A1, SLC7A5, STYK1, TFAP2A, VDAC1 AND VDAC2	* "Top five pathways enriched in the high-risk group were the *cell cycle, ubiquitin-mediated proteolysis, oocyte meiosis, homologous recombination and p53 signaling*." * "The top five pathways enriched in the low-risk group were the *arachidonic acid metabolism, primary bile acid biosynthesis, alpha-linolenic acid metabolism, asthma, and intestinal immune network for IgA production pathways*." * "Pathways of the *immune response* were significantly enriched in the 15-gene ferroptosis signature."	(86)
TCGA	ALOX15, and PEBP1	ACSL4, GSS, ACSL3 and PGD	* "Gene's mutation frequencies were higher in the high-risk group [*TP53* (53%), *TTN* (50%), *MUC16* (42%), *CSMD3* (40%), and *RYR2* (39%)]." * "The mainly enriched pathways included the neuroactive ligand-receptor interaction, metabolism of xenobiotics by cytochrome P450, steroid hormone biosynthesis, staphylococcus aureus infection pathway, IL-17 signaling pathway, retinol metabolic pathway."	(87)
GSE68465, GSE41271, and GPL6884	CYBB and SAT2	CISD1, FADD and VDAC2	* "Several *immune-related pathways* were enriched in low-risk group, such as B cell receptor signaling pathway, T cell receptor signaling pathway, Intestinal immune network for IgA production, NOD line receptor signaling pathway, Fc epsilon Ri signaling pathway, Fc gamma R signaling pathway, and Graft *versus* host disease." * "GSEA analysis showed the FRGS was highly associated with *immune status*. The enrichment score of aDCs, DCs, iDCs, pDCs, B cells, Macrophages, Mast cells, Neutrophils, T helper cells, Th1 cells, TIL and Treg was significantly increased in low-risk group. Meanwhile, low-risk group had a higher score of C–C chemokine receptor (CCR), the activity of checkpoint molecules, HLA, T cell co–stimulation and IFN Response Type II."	(88)

(Continued)

TABLE 1 | Continued

Dataset used in the study	Low-risk	High-risk	Highlights of the study	Ref.
TCGA GSE3141, GSE30219, and GSE31210	NOX1 and ALOX15	GSS, ACSL4, CISD1, SLC3A2, and FANCD2	* "Overall, the 12 top-ranked with highest mutations genes were shared between both sets KEAP1, NAV3, and FAT3, were expressed only in the high-risk group, while COL11A1, CSMD1, and ZNF536 were specifically expressed in the low-risk group." * "The enrichment results revealed that processes related to poor survival in lung cancer patients, cancer microenvironment, immature B lymphocytes, early T lymphocytes and lung metastasis were significantly enriched in the high-risk group while processes related to COMP, lectin, TCRA, NOTCH1 target and hypoxia were significantly enriched in the low-risk group." * "Ferroptosis-related risk score (FRRS) is involved in several *immune-signaling pathways*." * "The gene expression levels of potential *immunotherapy targets, including CD276, PD-L1, and NKG2A, were significantly upregulated in the high-risk group*. Meanwhile, the expression levels of *VSIR and CD27 were significantly higher in the low-risk group than in the high-risk group*." * "The *top three* genes that contributed most to FRRS were *CISD1, FANCD2 and SLC3A2*. The results illustrated that low CISD1 expression was significantly associated with favorable immunotherapeutic responses"	(89)
TCGA, GSE13213, and GSE72904	ALOX15, and DPP4	FANCD4, GCLC, and SLC7A11	* "Differentially expressed genes (DEGs) were mostly enriched in the ferroptosis pathway and immune-related pathways, such as human T-cell leukemia virus 1 (HTLV-1) infection pathway. These findings suggested that there exists crosslinking between ferroptosis and *tumor immunity* in NSCLC." * "The GSE13213 dataset revealed differences in the scores of HLA class and type-I and -II immune interferon response." * "The immune score of the subgroups in both TCGA cohort and the GSE13213 dataset was significantly different, especially the score of macrophages and mast cells."	(90)
TCGA, GSE72094, and GSE68465	ARNTL, GLS2, HERPUD1, LPIN1, NCOA4, PEBP1, and TLR4	ACSL3, CISD1, DDIT4, EIF2S1, PANX1, RELA, RRM2, and YWAHE	* "ACSL3, YWHAE, DDIT4, PANX1, RELA, CISD1, EIF2S1, and RRM2 were overexpressed, while GLS2, PEBP1, ARNTL, NCOA4, LPIN1, HERPUD1, and TLR4 were downregulated in high-risk groups." * "GAPDH, BIRC5, ERO1L, EIF2S1, SPHK1, ATIC, GNAI3, NAMPT, EIF4EBP1, and FADD are the top 10 autophagy-related genes that positively corrected with the risk score; 8/10 showed a significant elevated hazard ratio in LUAD." * "ERN1, ATG16L2, CCR2, IKBKB, HSPB8, PRKCD, DAPK1, DRAM1, DLC1, and DAPK2 are the leading 10 that have negative relationships with the 15-gene signature risk score; three of them exhibited a decreased hazard ratio." * "Enriched gene sets of HALLMARK collection in the high-risk group were mainly involved in pathways related to glycolysis, unfolded protein response, *mTORC1*, MYC, G2/M checkpoint, E2F, DNA repair, mitotic spindle assembly, ultraviolet radiation, hypoxia, cholesterol homeostasis, and reactive oxygen species, whereas the gene set concerned with metabolism of bile acids and salts was primary enriched in the low-risk group."	(91)
TCGA	PEBP1, DPP4, ALOX15, GLS2, NCOA4 and PHKG2	ACSL3, GSS, PGD, FANCD2, SLC7A11, GCLC, CISD1, and ATP5MC3	* "PEBP1, ACSL3, NCOA4, PHKG2, and CISD1 were independent prognostic factors for overall survival." * "Four kinds of immune cells showed higher infiltration levels in the high-risk group, including CD4 memory-activated T cells, M0 macrophages, M1 macrophages and activated dendritic cells, and three kinds of immune cells showed higher infiltration levels in the low-risk group, including resting mast cells, activated mast cells and eosinophils." * "The results showed that the high-risk group had higher immune and stromal scores than those of the low-risk group." * "PEBP1, CISD1 and NCOA4 were significantly down-regulated in the LUAD tissues."	(92)
TCGA and GSE31210	ALOX15, DPP4, GLS2, PHKG2, and PEBP1	ATP5MC3, CISD1, FANCD2, GCLC, SLC7A11, ACSL3, ABCC1, and PGD	* "The higher risk group was significantly associated with *higher tumor stage, TP53 mutation, sex, and advanced tumor node metastasis (TNM) stage* in the TCGA cohort" * "Four immune-related biological processes or molecular functions in KEGG were changed between the high- and low-risk groups in the TCGA cohort, including the *intestinal immune network for IGA production, chemokine signaling pathway, TGF beta signaling pathway, and TOLL-like receptor signaling pathway*" * "Four immune-related biological processes or molecular functions in KEGG were changed between the high- and low-risk groups in the TCGA cohort, including the *intestinal immune network for IGA production, chemokine signaling pathway, TGF beta signaling pathway, and TOLL-like receptor signaling pathway*" * "Six immune-related biological processes or molecular functions in GO were changed between the high- and low-risk groups in the TCGA cohort, including somatic diversification of immune receptors, positive regulation of production of molecular, positive regulation of myeloid leukocyte cytokines, positive regulation of cytokine production, regulation of innate	(93)

(Continued)

TABLE 1 | Continued

Dataset used in the study	Low-risk	High-risk	Highlights of the study	Ref.
			immune response, and activation of the innate immune response" * "The score of CD8+ T cells, iDCs, macrophages, mast cells, NK cells, Th1 cells, Th2 cells, Treg, antigen-presenting cells (APC) coi-nhibition, cytolytic activity, HLA, inflammation-promoting, MHC class I, para-inflammation, and T cell co-inhibition were significantly different between the low- and high-risk groups in both TCGA"	
TCGA	AC026355.1, AC124045.1, and AC025048.4	LINC01843, MIR193BHG, AC124045.1, AC091185.1, AC027031.2, ALO21707.2, ALO31667.3, and AL606834.1	* "lncRNA AL031667.3 increased with age, AC027031.2 was abundantly expressed in female patients, the expression of AC091185.1 and AC124045.1 was associated with TNM stage, that of AC091185.1, AC124045.1, AL021707.2, and LINC01843 was associated with pT stage, and that of AC124045.1, AL021707.2, AL031667.3, and MIR193BHG was associated with pN stage. Patients with decreased AC124045.1 expression were more likely to have distant metastases"	(94)
TCGA and GSE37745	CRNDE, AC106047.1, AC090559.1, AL691432.2, AC026355.1, AL034397.3, AC087752.3, VIM-AS1, HLA-DQB1-AS1, AC092171.5, LINCO0996, AC123595.1, ACO011477.2, and HSPC324	AL606489.1, LINC02081, AP000695.2, LINC01843, FAM83A-AS1, AP000695.1, and AC010980.2,	* "The Gene Ontology (GO) terms activation of innate immune response, innate immune response activating signal transduction, positive regulation of innate immune response, interleukin 1 mediated signaling pathway, and regulation of apoptotic signaling pathway were enriched in LUAD samples with high-risk scores. In contrast, CD8+ alpha beta T cell activation, T cell-mediated immunity, MAST cell-mediated immunity, regulation of leukocyte-mediated immunity, and regulation of lymphocyte-mediated immunity were enriched in LUAD samples with low-risk scores." * "KEGG pathways were identified. Cell cycle, pancreatic cancer, *p53 signaling pathway*, pathogenic Escherichia coli, and *small cell lung cancer signaling pathways* were enriched in the high-risk group. Several immune response pathways, such as the intestinal immune network for IgA production, FC epsilon RI signaling pathway, autoimmune thyroid disease, allograft rejection, and graft *versus* host disease, were enriched in the low-risk group."	(95)
TCGA, GSE3141, and GSE37745	ARHGEF26-AS1 C20orf197 MGC32805 LINC00324	LINC01116, LINC01137, and TMPO-AS1	* "The correlation expression between 7 lncRNAs and four most common ferroptosis-related mRNAs (FTH1, GPX4, ACSL4, PTGS2) verified the relationship between 7 lncRNAs and ferroptosis from another perspective." * "Comparative analysis of immune cells and pathways confirmed the differences of HLA, MHC class I, para-inflammation, type I IFN response, type II IFN response, B cell, iDCs, mast cell, neutrophils, NK cell, T helper cell and TIL between two risk groups."	(96)
TCGA, GSE30219, GES31210, and GSE31546	C5orf64, LINC01800, LINC00968, LINC01352, and PGM5-AS1	LINC02097, DEPDC1-AS1, WWC2-AS2, SATB2-AS1, LINC00628, LINC01537, and LMO7DN	* "The KEGG analysis results show that the 12 prognostic lncRNAs are mainly enriched in DNA replication pathway, B cell receptor signaling pathways, hematopoietic cell lineage pathway, and cell cycle pathway"	(97)

level expression negatively predicts overall survival and inhibits ferroptosis in NSCLC (98). Consistent with pathways discussed earlier, the involvement of signaling pathways including p53, fatty acid metabolism, ubiquitin-mediated proteolysis, and mTORC1 in ferroptosis is notable. In addition, several studies have evaluated the expression of ferroptosis-related long non-coding RNAs and their risk ratio (94–97). Descriptions and highlights of each conducted study are summarized in **Table 1**.

4 TREATMENTS FOR INDUCTION OF FERROPTOSIS IN LUNG CANCER

Molecules such as system X_c^- and GPX4 are potent inhibitors of the ferroptosis process, and two well-known small molecules which can inhibit them are erastin (99) and RSL3 (18), respectively. However, with a more detailed look, it can be concluded that the involvement of other signaling pathways might regulate key molecules of ferroptosis. For instance, Huang et al. have mentioned that treatment with erastin induces ROS production in NSCLC cells, which activate the p53 signaling pathway. Moreover, p53 can also inhibit the expression of SCL7A11 post-transcriptionally and subsequently induce ferroptosis (99). Recently, cisplatin (DDP) as a conventional chemotherapeutic agent has been shown to induce ferroptosis in different human cancer cell lines such as NSCLC by inhibiting GSH-GPX system activity, and its combination with erastin synergistically promoted treatment efficacy (100). Similarly, PRLX93936 is an analog of erastin, which its concurrent treatment with DDP can induce ferroptosis *via* GPX4 inhibition (101). Therefore, it seems that combining ferroptosis inhibitors with other treatments is an effective strategy to induce ferroptosis more potently. As seen in **Table 2**, the combination of erastin with other treatments has shown stunning anticancer properties through ferroptosis induction. In addition, the role of natural products in regulating ferroptosis has been highlighted in recent studies, suggesting them as future potential candidates in ferroptosis

TABLE 2 | Treatments for induction of ferroptosis in lung cancer.

Treatment	Cancer type	Target genes	Model	Description	Ref.
Chemotherapy:					
Erastin	NSCLC	↑p53/↓SCL7A11	*In vitro*	* "Erastin-induced ROS lead to the DNA damage response and stimulate p53 in A549 cells" * "Expression of p53 induced by erastin exposure contributes to the cytotoxic effect on A549 cells, leading to ferroptotic and apoptotic death." * "p53 induced by erastin exposure exerts cytostatic effects on A549 cells"	(99)
Cisplatin	NSCLC	↓GSH-GPXs	*In vitro*	* "Cisplatin induced both ferroptosis and apoptosis in A549 cells" * "Silencing iron-responsive element binding protein 2 (IREB2) partially reversed the cytotoxicity of cisplatin, indicating the involvement of iron in cisplatin induced cell death" * "Additive effect observed in combination therapy of cisplatin and erastin"	(100)
Cisplatin (CDDP) with PRLX93936	NSCLC	↓GPX4	*In vitro*	* "Nrf2/Keap1 regulates sensitivity to RPLX93936/cisplatin in NSCLC cells." * "Ferroptosis inhibitors and forced expression of GPX4 attenuated cell death caused by cisplatin and PRLX93936."	(101)
Vorinostat with erastin	EGFR mutant LUAD	↓ xCT	*In vitro*	* "Vorinostat, a clinically used inhibitor targeting histone deacetylase, can robustly enhance the efficacy of ferroptosis inducers." * "Cells with intrinsic or acquired resistance to EGFR-TKI display high sensitivity to ferroptosis inducers."	(102)
Brusatol and erastin	NSCLC	↓ NRF2 ↑FOCAD-FAK	*In vitro/ in vivo*	* "Treatment with NRF2 inhibitor, brusatol, increased the sensitivity of NSCLC cells to erastin-induced ferroptosis *in vitro* and *in vivo*, which depended on the upregulation of FOCAD partially" * "Brusatol can enhance the efficacy of chemotherapy *via* inhibiting NRF2 signaling pathway"	(34)
Erastin with acetaminophen (APAP)	NSCLC	↓NRF2/HO-1	*In vitro/ in vivo*	* "Combination of erastin and APAP inhibited cell proliferation and induced ferroptosis" * Erastin and/OR APAP regulated intracellular ferrous iron * Erastin and/or APAP-induced cell death *via* overgeneration of lipid peroxidation	(103)
Sorafenib combined with erastin	NSCLCs resistant to CDDP	↓ Nrf2/xCT	*In vitro/ in vivo*	* "Sensitivity of NSCLC cells to CDDP is negatively associated with Nrf2 pathway activation" * "Erastin and sorafenib effectively induce ferroptosis in CDDP resistance cells by inhibiting the Nrf2/xCT pathway" * "Erastin/sorafenib restrains *in vivo* tumour growth in nude mice xenograft models"	(104)
Siramesine with lapatinib	LUAD	↓ HO-1	*In vitro*	* "Lapatinib and siramesine induce synergistic cell death in lung adenocarcinoma" * "Lapatinib and siramesine treatment increased reactive iron, ROS, and induced ferroptosis through decreasing heme oxygenase-1 (HO-1) protein expression." * "Decrease in HO-1 expression was due to *proteasome degradation* and confirms that *Nrf2 is not implicated* in the regulation of HO-1"	(57)
Levobupivacaine (local anesthetic) and erastin	NSCLC	↑p53-↓SLC7A11-↓GPX4	*In vitro/ in vivo*	* "Levobupivacaine inhibits proliferation and promotes apoptosis of NSCLC cells and represses invasion and migration of NSCLC cells." * "Levobupivacaine induces ferroptosis of NSCLC cells"	(105)
Auranofin (AF, an antirheumatic drug)	NSCLC	↓TrxR ↓GPX4 ↑ HMOX1	*In vitro/ in vivo*	* "p53 R273H cells were more vulnerable to AF-induced ferroptotic cell death due to downregulation of GPX4 and lipid peroxidation." * "AF primes mutant p53 NSCLC cells for IL-15-stimulated NK cell mediated killing." * "*Contrary*, it was observed that mutant p53 was no limiting factor in the activation of NRF2 and GSH levels, despite *reduced* expression of *SLC7A11* in the mutant p53 NCI–H1299 cells" * "To overcome the toxicity of AF-mediated TrxR inhibition, the data showed that all mutant p53 NSCLC cells *first* boosted their antioxidant defense capacities by *upregulation of pro-survival molecules, such as NRF2 and GSH*, to maintain their redox balance"	(106)
Natural product therapy:					
Artemisinin derivatives: Artesunate (ART) and Dihydroartemisinin (DHA)	NSCLC	↓VDAC and xCT ↑TFRC	*In vitro*	* "Artemisinin derivatives induce apoptosis and ferroptosis." * "ROS is a key regulator of ART/DHA-induced apoptosis and ferroptosis" * "TFRC and VDAC were closely associated with the survival of lung cancer patients and can be used as potential therapeutic targets in lung cancer."	(107)
Dihydroisotanshinone I (DT)	NSCLC	↓GPX4	*In vitro* and *in vivo*	* "DT inhibited the growth of lung cancer cells through apoptosis and ferroptosis and *in vivo* study inhibited metastasis of A549 cells in the nude mice model."	(108)
Cryptotanshinone (CTN)	NSCLC	↓GPX4	*In vitro*	* "Cryptotanshinone induces ROS generation and caspase activity in lung cancer cell lines" * "CTN induces the lipid peroxidation iron-dependent" * "CTN induces apoptosis to the lower level than ferroptosis"	(109)

(Continued)

TABLE 2 | Continued

Treatment	Cancer type	Target genes	Model	Description	Ref.
Curcumin	NSCLC	↑ACSL4 ↓ SLC7A11 ↓ GPX4	*In vivo* and *in vitro*	* 'Curcumin inhibits tumor growth and promotes cells death *in vivo*" * "Curcumin suppresses cell proliferation and promotes cell death *in vitro*" * "Curcumin induces characteristic changes of ferroptosis in mice" * "Inhibition of autophagy attenuated curcumin-induced ferroptosis in A549 and H1299 cells"	(61)
Sulforaphane (SFN)	SCLC	↓SLC7A11	*in vitro*	* SFN inhibits growth and induces cell death in the SCLC cells * "SFN exhibits anticancer effects against SCLC cells *via* induction of ferroptosis" * "SFN-induced cell death was mediated *via* ferroptosis and inhibition of the mRNA and protein expression levels of SLC7A11"	(110)
6-Gingerol	Lung cancer	↓USP14 ↓GPX4 ↓ATF4 ↑NCOA4 and TfR1	*In vitro* and *in vivo*	* "6-Gingerol suppresses tumor growth and enhances the accumulation of ROS and iron." * "6-Gingerol regulates the expression of autophagy and ferroptosis related proteins *in vivo* and *in vitro*."	(60)
Ginkgetin with cisplatin(DDP)	NSCLC	↓NRF2/HO-1 axis ↓ GPX4 ↓ SLC7A11	*In vitro*/ *in vivo*	* "Ginkgetin is synergized with DDP to increase cytotoxicity in NSCLC cells." * "Ginkgetin disrupted redox hemostasis in DDP-treated cells, as demonstrated by the enhanced ROS formation and inactivation of the Nrf2/HO-1 axis." * "Ginkgetin increased labile iron pool and lipid peroxidation and caused elevation of ROS formation, and apoptosis in DDP-treated NSCLC cells."	(111)
Erianin	Lung cancer	↑Ca^{2+}/CaM-dependent ferroptosis ↓SLC7A11	*In vitro*/ *in vivo*	* "Erianin triggers cell death, inhibits cell proliferation, migration, and promotes cell cycle arrest in G2/M in lung cancer cells" * "Ferroptosis contributes to erianin-induced cell death in lung cancer cells" * "Erianin results in ferroptosis induction and exerts antitumor efficacy *in vivo*"	(64)
Food additive for iron supplementation:					
Ammonium Ferric Citrate (AFC)	NSCLC	↓GPX4-GSS/GSR-GGT axis	*In vitro*	* "Decreased the autophagy and cause elevated Fe2+ content and inducing oxidative stress injury consequently ferroptosis." * "Inhibited the proliferation and invasion of NSCLC cell lines *in vitro*." * "Promoted differential gene expression profiles of proliferation and autophagy."	(112)
Nanoparticle therapy:					
ZVI-NP (Zero-valent Iron Nanoparticles)	Lung cancer	↑GSK3β/β-TrCP-dependent degradation of NRF2	*In vitro*/ *in vivo*	* "Attenuated self-renewal ability of cancer and downregulated angiogenesis-related genes and caused lipid peroxidation, increased ROS, and ferroptosis." * "Inhibited NRF2 activity and lung metastases *in vivo*." * "ZVI-NP treatment promoted the M1 polarization induction-derived overexpression of *TNF-α*, while attenuated the expression of the M2 polarization gene *DC-SIGN*" * "ZVI-NP modulates immune cell profile in mouse model *in vivo*".	(113)
Folate (FA)-modified liposome (FA-LP) enriched with erastin and MT1DP (E/M@FA-LPs)	NSCLCs	↓NRF2	*In vitro*/ *in vivo*	* "E/M@FA-LPs sensitizes erastin-induced ferroptosis *in vitro*." * "E/M@FA-LPs represses NRF2 levels to enhance oxidative stress." * "E/M@FA-LPs could powerfully inhibit growth of subcutaneous xenografts."	(78)
Magnetic field therapy:					
Magnetic field (MF) therapy concurrent with DDP and PTX treatments	Lung epithelial cancer cells (A549)	–	*In vitro*/ *in vivo*	* "MF selectively inhibited malignant tumor cells" * "*Ferroptosis* was detected by co-incubation with ferrostatin-1" * "MF exposure led to ROS-dependent DNA damage and subsequent activation of DNA repair pathways" * "MF induced intracellular oxidative stress" * "MF sensitized tumor cells to conventional chemotherapy(DDP and PTX)"	(114)
Radiation therapy:					
Radiation combined with IKE and sorafenib	LUAD	↓ GPX4 ↓xCT	*In vitro*/ *in vivo*	* "IKE and sorafenib, combined with stereotactic radiation therapy, suppress tumor growth in a mouse xenograft model of sarcoma and a patient-derived xenograft model of lung adenocarcinoma." * "Radiation-induced cancer cell death is suppressed by ferroptosis inhibitors"	(115)
Radiation with erastin treatment	NSCLC	↓GPX4	*In vitro*	* "Erastin and IR exhibit a combined effect on killing cells" * "GPX4 expression is increased in the radioresistant cells and erastin inhibits GPX4 expression in the radioresistant cells" * "Knocking down GPX4 expression radiosensitizes NSCLCs cell to radiation in the radioresistant cell lines"	(116)

↓, *Decreases the expression of;* ↑, *Increases the expression of.*

therapy, particularly in lung cancer. For better drug delivery, nanomaterials have received a lot of attention during recent years due to their ability for ferroptosis induction (117). Zero-valent-iron nanoparticle (ZVI-NP) is a type of nanomaterials conventionally used to remove pollutants from groundwater due to its high ability to produce ROS. Recently, their anticancer activity has been investigated *in vivo* and *in vitro* against lung cancer. Hsieh et al. have reported that silver-coated

ZVI-NP (ZVI@Ag) can strongly induce lipid peroxidation and ferroptosis in lung cancer *via* GSK3β/β-TrCP-dependent degradation of NRF2. Moreover, it can provoke immune system activity by increasing cytotoxic $CD8^+$ T cells and M1 ($CD8^+$) anti-tumor macrophages (113). Another example of the applicability of nanoparticles for induction of ferroptosis in lung cancer is the synthesis of folate (FA)-modified liposome (FA-LP) nanoparticles containing erastin and lncRNA-MT1DP (E/M@FA-LPs), which has been mentioned earlier (78). Finally, another novel application of ferroptosis inhibitors such as erastin, IKE, RSL3 and sorafenib is administering them concurrent with radiotherapy to overcome radioresistance in NSCLC cells (116).

5 CONCLUSION AND FUTURE PERSPECTIVES

This review provided an overall viewpoint and understanding of ferroptosis in lung cancer from molecular basis to prognostic and therapeutic significance. Although our understanding of ferroptosis is still insufficient, impressive efforts have been made during recent years to uncover the underlying mechanisms of ferroptosis, especially in NSCLC. To our knowledge, recent evidence has mainly focused on the role of system X_c^- and GPX4 as main inhibitors of ferroptosis and other regulators and signaling pathways such as NRF2, p53, and UPS. These molecules have prominent roles in the ferroptosis process in lung cancer and are targeted by different treatments. Targeted delivery of drugs and ncRNAs involved in regulating ferroptosis and concurrent use of ferroptosis inhibitors alongside chemotherapy or radiotherapy have shown promising cytotoxic effects against lung cancer. Moreover, recent conducted bioinformatic analyses specifically address the impact of ferroptosis regulators in predicting patients' overall survival and their close relationship with immune response. Therefore, it is suggested that future studies investigate the link between ferroptosis and immune response in lung cancer. As another limitation, the majority of these studies have focused on NSCLC, and there are very few studies that have evaluated ferroptosis in other subtypes of lung cancer (e.g., SCLC). These data together indicate that ferroptosis as a newly discovered cell death appears a promising target in lung cancer that can serve as a new candidate for its future treatment.

AUTHOR CONTRIBUTIONS

PT wrote the original draft. ZH drew the figures and their captions. SS assisted PT in writing the manuscript. SS and ZH both should be considered second authors. All authors contributed to the article and approved the submitted version.

ACKNOWLEDGMENTS

We would like to add our special thanks to Frontiers Fee Support Office, Frontiers in Oncology Editorial Office, and Frontiers in Oncology Production Office.

REFERENCES

1. Sung H, Ferlay J, Siegel RL, Laversanne M, Soerjomataram I, Jemal A, et al. Global Cancer Statistics 2020: GLOBOCAN Estimates of Incidence and Mortality Worldwide for 36 Cancers in 185 Countries. *CA Cancer J Clin* (2021) 71:209–49. doi: 10.3322/caac.21660
2. Bade BC, Dela Cruz CS. Lung Cancer 2020: Epidemiology, Etiology, and Prevention. *Clin Chest Med* (2020) 41:1–24. doi: 10.1016/j.ccm.2019.10.001
3. Rodriguez-Canales J, Parra-Cuentas E, Wistuba II. Diagnosis and Molecular Classification of Lung Cancer. *Lung Cancer* (2016) 170:25–46. doi: 10.1007/978-3-319-40389-2_2
4. Zappa C, Mousa SA. Non-Small Cell Lung Cancer: Current Treatment and Future Advances. *Transl Lung Cancer Res* (2016) 5:288. doi: 10.21037/tlcr.2016.06.07
5. Cooper WA, Lam DCL, O'Toole SA, Minna JD. Molecular Biology of Lung Cancer. *J Thorac Dis* (2013) 5:S479. doi: 10.3978/j.issn.2072-1439.2013.08.03
6. Dixon SJ, Lemberg KM, Lamprecht MR, Skouta R, Zaitsev EM, Gleason CE, et al. Ferroptosis: An Iron-Dependent Form of Nonapoptotic Cell Death. *Cell* (2012) 149:1060–72. doi: 10.1016/j.cell.2012.03.042
7. Hirschhorn T, Stockwell BR. The Development of the Concept of Ferroptosis. *Free Radic Biol Med* (2019) 133:130–43. doi: 10.1016/j.freeradbiomed.2018.09.043
8. Tang D, Chen X, Kang R, Kroemer G. Ferroptosis: Molecular Mechanisms and Health Implications. *Cell Res* (2021) 31:107–25. doi: 10.1038/s41422-020-00441-1
9. Jiang X, Stockwell BR, Conrad M. Ferroptosis: Mechanisms, Biology and Role in Disease. *Nat Rev Mol Cell Biol* (2021) 22:266–82. doi: 10.1038/s41580-020-00324-8
10. Chen X, Kang R, Kroemer G, Tang D. Broadening Horizons: The Role of Ferroptosis in Cancer. *Nat Rev Clin Oncol* (2021) 18:280–96. doi: 10.1038/s41571-020-00462-0
11. Li G, Yang J, Zhao G, Shen Z, Yang K, Tian L, et al. Dysregulation of Ferroptosis may Involve in the Development of Non-Small-Cell Lung Cancer in Xuanwei Area. *J Cell Mol Med* (2021) 25:2872–84. doi: 10.1111/jcmm.16318
12. Shin C-S, Mishra P, Watrous JD, Carelli V, D'Aurelio M, Jain M, et al. The Glutamate/Cystine xCT Antiporter Antagonizes Glutamine Metabolism and Reduces Nutrient Flexibility. *Nat Commun* (2017) 8:1–11. doi: 10.1038/ncomms15074
13. Koppula P, Zhuang L, Gan B. Cystine Transporter SLC7A11/xCT in Cancer: Ferroptosis, Nutrient Dependency, and Cancer Therapy. *Protein Cell* (2021) 12:599–620. doi: 10.1007/s13238-020-00789-5
14. Wang X, Chen Y, Wang X, Tian H, Wang Y, Jin J, et al. Stem Cell Factor SOX2 Confers Ferroptosis Resistance in Lung Cancer via Upregulation of SLC7A11. *Cancer Res* (2021) 81:5217–29. doi: 10.1158/0008-5472.CAN-21-0567
15. Zhang W, Sun Y, Bai L, Zhi L, Yang Y, Zhao Q, et al. RBMS1 Regulates Lung Cancer Ferroptosis Through Translational Control of SLC7A11. *J Clin Invest* (2021) 131(22):1–20. doi: 10.1172/JCI152067
16. Ma L, Chen T, Zhang X, Miao Y, Tian X, Yu K, et al. The M6a Reader YTHDC2 Inhibits Lung Adenocarcinoma Tumorigenesis by Suppressing SLC7A11-Dependent Antioxidant Function. *Redox Biol* (2021) 38:101801. doi: 10.1016/j.redox.2020.101801
17. Ma L, Zhang X, Yu K, Xu X, Chen T, Shi Y, et al. Targeting SLC3A2 Subunit of System XC– Is Essential for M6a Reader YTHDC2 to be an Endogenous Ferroptosis Inducer in Lung Adenocarcinoma. *Free Radic Biol Med* (2021) 168:25–43. doi: 10.1016/j.freeradbiomed.2021.03.023
18. Zhang X, Sui S, Wang L, Li H, Zhang L, Xu S, et al. Inhibition of Tumor Propellant Glutathione Peroxidase 4 Induces Ferroptosis in Cancer Cells and Enhances Anticancer Effect of Cisplatin. *J Cell Physiol* (2020) 235:3425–37. doi: 10.1002/jcp.29232
19. Ni J, Chen K, Zhang J, Zhang X. Inhibition of GPX4 or mTOR Overcomes Resistance to Lapatinib *via* Promoting Ferroptosis in NSCLC Cells. *Biochem Biophys Res Commun* (2021) 567:154–60. doi: 10.1016/j.bbrc.2021.06.051

20. Wang Z, Zhang X, Tian X, Yang Y, Ma L, Wang J, et al. CREB Stimulates GPX4 Transcription to Inhibit Ferroptosis in Lung Adenocarcinoma. *Oncol Rep* (2021) 45:1–12. doi: 10.3892/or.2021.8039
21. Liu W, Zhou Y, Duan W, Song J, Wei S, Xia S, et al. Glutathione Peroxidase 4-Dependent Glutathione High-Consumption Drives Acquired Platinum Chemoresistance in Lung Cancer-Derived Brain Metastasis. *Clin Transl Med* (2021) 11:1–22. doi: 10.1002/ctm2.517
22. Lai Y, Zhang Z, Li J, Li W, Huang Z, Zhang C, et al. STYK1/NOK Correlates With Ferroptosis in Non-Small Cell Lung Carcinoma, Biochem. *Biophys Res Commun* (2019) 519:659–66. doi: 10.1016/j.bbrc.2019.09.032
23. Bersuker K, Hendricks JM, Li Z, Magtanong L, Ford B, Tang PH, et al. The CoQ Oxidoreductase FSP1 Acts Parallel to GPX4 to Inhibit Ferroptosis. *Nature* (2019) 575:688–92. doi: 10.1038/s41586-019-1705-2
24. Alvarez SW, Sviderskiy VO, Terzi EM, Papagiannakopoulos T, Moreira AL, Adams S, et al. NFS1 Undergoes Positive Selection in Lung Tumours and Protects Cells From Ferroptosis. *Nature* (2017) 551:639–43. doi: 10.1038/nature24637
25. Alvarez SW, Possemato R. Leveraging the Iron-Starvation Response to Promote Ferroptosis. *Oncotarget* (2018) 9:10830. doi: 10.18632/oncotarget.24395
26. Dodson M, Castro-Portuguez R, Zhang DD. NRF2 Plays a Critical Role in Mitigating Lipid Peroxidation and Ferroptosis. *Redox Biol* (2019) 23:101107. doi: 10.1016/j.redox.2019.101107
27. Takahashi N, Cho P, Selfors LM, Kuiken HJ, Kaul R, Fujiwara T, et al. 3D Culture Models With CRISPR Screens Reveal Hyperactive NRF2 as a Prerequisite for Spheroid Formation *via* Regulation of Proliferation and Ferroptosis. *Mol Cell* (2020) 80:828–44. doi: 10.1016/j.molcel.2020.10.010
28. Kwon O-S, Kwon E-J, Kong H-J, Choi J-Y, Kim Y-J, Lee E-W, et al. Systematic Identification of a Nuclear Receptor-Enriched Predictive Signature for Erastin-Induced Ferroptosis. *Redox Biol* (2020) 37:101719. doi: 10.1016/j.redox.2020.101719
29. Deshmukh P, Unni S, Krishnappa G, Padmanabhan B. The Keap1–Nrf2 Pathway: Promising Therapeutic Target to Counteract ROS-Mediated Damage in Cancers and Neurodegenerative Diseases. *Biophys Rev* (2017) 9:41–56. doi: 10.1007/s12551-016-0244-4
30. Koppula P, Olszewski K, Zhang Y, Kondiparthi L, Liu X, Lei G, et al. KEAP1 Deficiency Drives Glucose Dependency and Sensitizes Lung Cancer Cells and Tumors to GLUT Inhibition. *Iscience* (2021) 24:102649. doi: 10.1016/j.celrep.2020.108444
31. Wohlhieter CA, Richards AL, Uddin F, Hulton CH, Quintanal-Villalonga À., Martin A, et al. Concurrent Mutations in STK11 and KEAP1 Promote Ferroptosis Protection and SCD1 Dependence in Lung Cancer. *Cell Rep* (2020) 33:108444. doi: 10.1016/j.celrep.2020.108444
32. Zhang J, Song F, Zhao X, Jiang H, Wu X, Wang B, et al. EGFR Modulates Monounsaturated Fatty Acid Synthesis Through Phosphorylation of SCD1 in Lung Cancer. *Mol Cancer* (2017) 16:1–15. doi: 10.1186/s12943-017-0704-x
33. Gao M, Yi J, Zhu J, Minikes AM, Monian P, Thompson CB, et al. Role of Mitochondria in Ferroptosis. *Mol Cell* (2019) 73:354–63. doi: 10.1016/j.molcel.2018.10.042
34. Liu P, Wu D, Duan J, Xiao H, Zhou Y, Zhao L, et al. NRF2 Regulates the Sensitivity of Human NSCLC Cells to Cystine Deprivation-Induced Ferroptosis *via* FOCAD-FAK Signaling Pathway. *Redox Biol* (2020) 37:101702. doi: 10.1016/j.redox.2020.101702
35. Kang YP, Mockabee-Macias A, Jiang C, Falzone A, Prieto-Farigua N, Stone E, et al. Non-Canonical Glutamate-Cysteine Ligase Activity Protects Against Ferroptosis. *Cell Metab* (2021) 33:174–89. doi: 10.1016/j.cmet.2020.12.007
36. Wang L, Chen Y, Mi Y, Qiao J, Jin H, Li J, et al. ATF2 Inhibits Ani-Tumor Effects of BET Inhibitor in a Negative Feedback Manner by Attenuating Ferroptosis. *Biochem Biophys Res Commun* (2021) 558:216–23. doi: 10.1016/j.bbrc.2020.08.113
37. Wang H, Huang Q, Xia J, Cheng S, Pei D, Zhang X, et al. The E3 Ligase MIB1 Promotes Proteasomal Degradation of NRF2 and Sensitizes Lung Cancer Cells to Ferroptosis. *Mol Cancer Res* (2021). doi: 10.1158/1541-7786.MCR-21-0342
38. Yuan Z, Liu T, Wang H, Xue L, Wang J. Fatty Acids Metabolism: The Bridge Between Ferroptosis and Ionizing Radiation. *Front Cell Dev Biol* (2021) 9:1691. doi: 10.3389/fcell.2021.675617
39. Li D, Li Y. The Interaction Between Ferroptosis and Lipid Metabolism in Cancer. *Signal Transduction Targeting Ther* (2020) 5:1–10. doi: 10.1038/s41392-019-0089-y
40. Bebber CM, Thomas ES, Stroh J, Chen Z, Androulidaki A, Schmitt A, et al. Ferroptosis Response Segregates Small Cell Lung Cancer (SCLC) Neuroendocrine Subtypes. *Nat Commun* (2021) 12:1–19. doi: 10.1038/s41467-021-22336-4
41. Zhang Y, Li S, Li F, Lv C, Yang Q. High-Fat Diet Impairs Ferroptosis and Promotes Cancer Invasiveness *via* Downregulating Tumor Suppressor ACSL4 in Lung Adenocarcinoma. *Biol Direct* (2021) 16:1–13. doi: 10.1186/s13062-020-00284-1
42. da Cunha Santos G, Shepherd FA, Tsao MS. EGFR Mutations and Lung Cancer. *Annu Rev Pathol Mech Dis* (2011) 6:49–69. doi: 10.1146/annurev-pathol-011110-130206
43. Poursaitidis I, Wang X, Crighton T, Labuschagne C, Mason D, Cramer SL, et al. Oncogene-Selective Sensitivity to Synchronous Cell Death Following Modulation of the Amino Acid Nutrient Cystine. *Cell Rep* (2017) 18:2547–56. doi: 10.1016/j.celrep.2017.02.054
44. Muz B, de la Puente P, Azab F, Azab AK. The Role of Hypoxia in Cancer Progression, Angiogenesis, Metastasis, and Resistance to Therapy. *Hypoxia* (2015) 3:83. doi: 10.2147/HP.S93413
45. Lee S-H, Koo KH, Park J-W, Kim H-J, Ye S-K, Park JB, et al. HIF-1 Is Induced *via* EGFR Activation and Mediates Resistance to Anoikis-Like Cell Death Under Lipid Rafts/Caveolae-Disrupting Stress. *Carcinogenesis* (2009) 30:1997–2004. doi: 10.1093/carcin/bgp233
46. Feng X, Wang S, Sun Z, Dong H, Yu H, Huang M, et al. Ferroptosis Enhanced Diabetic Renal Tubular Injury *via* HIF-1α/HO-1 Pathway in Db/Db Mice. *Front Endocrinol (Lausanne)* (2021) 12:21. doi: 10.3389/fendo.2021.626390
47. Fuhrmann DC, Mondorf A, Beifuß J, Jung M, Brüne B. Hypoxia Inhibits Ferritinophagy, Increases Mitochondrial Ferritin, and Protects From Ferroptosis. *Redox Biol* (2020) 36:101670. doi: 10.1016/j.redox.2020.101670
48. Jiang Y, Mao C, Yang R, Yan B, Shi Y, Liu X, et al. EGLN1/c-Myc Induced Lymphoid-Specific Helicase Inhibits Ferroptosis Through Lipid Metabolic Gene Expression Changes. *Theranostics* (2017) 7:3293. doi: 10.7150/thno.19988
49. Jiang Y, He Y, Liu S, Tao Y. Chromatin Remodeling Factor Lymphoid-Specific Helicase Inhibits Ferroptosis Through Lipid Metabolic Genes in Lung Cancer Progression. *Chin J Cancer* (2017) 36:1–3. doi: 10.1186/s40880-017-0248-x
50. Kang R, Kroemer G, Tang D. The Tumor Suppressor Protein P53 and the Ferroptosis Network. *Free Radic Biol Med* (2019) 133:162–8. doi: 10.1016/j.freeradbiomed.2018.05.074
51. Ou Y, Wang S-J, Li D, Chu B, Gu W. Activation of SAT1 Engages Polyamine Metabolism With P53-Mediated Ferroptotic Responses. *Proc Natl Acad Sci* (2016) 113:E6806–12. doi: 10.1073/pnas.1607152113
52. Shostak K, Jiang Z, Charloteaux B, Mayer A, Habraken Y, Tharun L, et al. The X-Linked Trichothiodystrophy-Causing Gene RNF113A Links the Spliceosome to Cell Survival Upon DNA Damage. *Nat Commun* (2020) 11:1–21. doi: 10.1038/s41467-020-15003-7
53. Wang GX, Tu H-C, Dong Y, Skanderup AJ, Wang Y, Takeda S, et al. Δnp63 Inhibits Oxidative Stress-Induced Cell Death, Including Ferroptosis, and Cooperates With the BCL-2 Family to Promote Clonogenic Survival. *Cell Rep* (2017) 21:2926–39. doi: 10.1016/j.celrep.2017.11.030
54. Wang X, Wang Y, Li Z, Qin J, Wang P. Regulation of Ferroptosis Pathway by Ubiquitination. *Front Cell Dev Biol* (2021) 9. doi: 10.3389/fcell.2021.699304
55. Tang Z, Jiang W, Mao M, Zhao J, Chen J, Cheng N. Deubiquitinase USP35 Modulates Ferroptosis in Lung Cancer *via* Targeting Ferroportin. *Clin Transl Med* (2021) 11:e390. doi: 10.1002/ctm2.390
56. Meng C, Zhan J, Chen D, Shao G, Zhang H, Gu W, et al. The Deubiquitinase USP11 Regulates Cell Proliferation and Ferroptotic Cell Death *via* Stabilization of NRF2 USP11 Deubiquitinates and Stabilizes NRF2. *Oncogene* (2021) 40:1706–20. doi: 10.1038/s41388-021-01660-5
57. Villalpando-Rodriguez GE, Blankstein AR, Konzelman C, Gibson SB. Lysosomal Destabilizing Drug Siramesine and the Dual Tyrosine Kinase Inhibitor Lapatinib Induce a Synergistic Ferroptosis Through Reduced Heme Oxygenase-1 (HO-1) Levels, Oxid. *Med Cell Longev* (2019) 2019:1–14. doi: 10.1155/2019/9561281

58. Zhou B, Liu J, Kang R, Klionsky DJ, Kroemer G, Tang D. Ferroptosis Is a Type of Autophagy-Dependent Cell Death. In: *Semin. Cancer Biol*. Elsevier (2020). p. 89–100.
59. Liu J, Kuang F, Kroemer G, Klionsky DJ, Kang R, Tang D. Autophagy-Dependent Ferroptosis: Machinery and Regulation. *Cell Chem Biol* (2020) 27:420–35. doi: 10.1016/j.chembiol.2020.02.005
60. Tsai Y, Xia C, Sun Z. The Inhibitory Effect of 6-Gingerol on Ubiquitin-Specific Peptidase 14 Enhances Autophagy-Dependent Ferroptosis and Anti-Tumor *In Vivo* and *In Vitro*. *Front Pharmacol* (2020) 11. doi: 10.3389/fphar.2020.598555
61. Tang X, Ding H, Liang M, Chen X, Yan Y, Wan N, et al. Curcumin Induces Ferroptosis in Non-Small-Cell Lung Cancer *via* Activating Autophagy. *Thorac Cancer* (2021) 12:1219–30. doi: 10.1111/1759-7714.13904
62. Boopathy GTK, Hong W. Role of Hippo Pathway-YAP/TAZ Signaling in Angiogenesis. *Front Cell Dev Biol* (2019) 7:49. doi: 10.3389/fcell.2019.00049
63. Zhang X, Yu K, Ma L, Qian Z, Tian X, Miao Y, et al. Endogenous Glutamate Determines Ferroptosis Sensitivity *via* ADCY10-Dependent YAP Suppression in Lung Adenocarcinoma. *Theranostics* (2021) 11:5650. doi: 10.7150/thno.55482
64. Chen P, Wu Q, Feng J, Yan L, Sun Y, Liu S, et al. Erianin, a Novel Dibenzyl Compound in Dendrobium Extract, Inhibits Lung Cancer Cell Growth and Migration *via* Calcium/Calmodulin-Dependent Ferroptosis. *Signal Transduction Targeting Ther* (2020) 5:1–11. doi: 10.1038/s41392-020-0149-3
65. Palmer LD, Jordan AT, Maloney KN, Farrow MA, Gutierrez DB, Gant-Branum R, et al. Zinc Intoxication Induces Ferroptosis in A549 Human Lung Cells. *Metallomics* (2019) 11:982–93. doi: 10.1039/C8MT00360B
66. Liu Y, Wang Y, Liu J, Kang R, Tang D. Interplay Between MTOR and GPX4 Signaling Modulates Autophagy-Dependent Ferroptotic Cancer Cell Death. *Cancer Gene Ther* (2021) 28:55–63. doi: 10.1038/s41417-020-0182-y
67. Slaby O, Laga R, Sedlacek O. Therapeutic Targeting of Non-Coding RNAs in Cancer. *Biochem J* (2017) 474:4219–51. doi: 10.1042/BCJ20170079
68. Xie B, Guo Y. Molecular Mechanism of Cell Ferroptosis and Research Progress in Regulation of Ferroptosis by Noncoding RNAs in Tumor Cells. *Cell Death Discovery* (2021) 7:1–10. doi: 10.1038/s41420-021-00483-3
69. Uddin A, Chakraborty S. Role of miRNAs in Lung Cancer. *J Cell Physiol* (2018), 1–10. doi: 10.1002/jcp.26607
70. Wei D, Ke Y-Q, Duan P, Zhou L, Wang C-Y, Cao P. MicroRNA-302a-3p Induces Ferroptosis of Non-Small Cell Lung Cancer Cells *via* Targeting Ferroportin. *Free Radic Res* (2021) 55:1–10. doi: 10.1080/10715762.2021.1947503
71. Deng S, Wu D, Li L, Liu T, Zhang T, Li J, et al. miR-324-3p Reverses Cisplatin Resistance by Inducing GPX4-Mediated Ferroptosis in Lung Adenocarcinoma Cell Line A549, Biochem. *Biophys Res Commun* (2021) 549:54–60. doi: 10.1016/j.bbrc.2021.02.077
72. Song Z, Jia G, Ma P, Cang S. Exosomal miR-4443 Promotes Cisplatin Resistance in Non-Small Cell Lung Carcinoma by Regulating FSP1 M6a Modification-Mediated Ferroptosis. *Life Sci* (2021) 276:119399. doi: 10.1016/j.lfs.2021.119399
73. Wang X, Yin H, Zhang L, Zheng D, Yang Y, Zhang J, et al. The Construction and Analysis of the Aberrant lncRNA-miRNA-mRNA Network in Non-Small Cell Lung Cancer. *J Thorac Dis* (2019) 11:1772. doi: 10.21037/jtd.2019.05.69
74. Wang M, Mao C, Ouyang L, Liu Y, Lai W, Liu N, et al. Long Noncoding RNA LINC00336 Inhibits Ferroptosis in Lung Cancer by Functioning as a Competing Endogenous RNA. *Cell Death Differ* (2019) 26:2329–43. doi: 10.1038/s41418-019-0304-y
75. Mao C, Wang X, Liu Y, Wang M, Yan B, Jiang Y, et al. A G3BP1-Interacting lncRNA Promotes Ferroptosis and Apoptosis in Cancer *via* Nuclear Sequestration of P53. *Cancer Res* (2018) 78:3484–96. doi: 10.1158/0008-5472.CAN-17-3454
76. Wu H, Liu A. Long Non-Coding RNA NEAT1 Regulates Ferroptosis Sensitivity in Non-Small-Cell Lung Cancer. *J Int Med Res* (2021) 49:0300060521996183. doi: 10.1177/0300060521996183
77. Sui X, Hu N, Zhang Z, Wang Y, Wang P, Xiu G. ASMTL-AS1 Impedes the Malignant Progression of Lung Adenocarcinoma by Regulating SAT1 to Promote Ferroptosis. *Pathol Int* (2021) 71(11):741–51. doi: 10.1111/pin.13158
78. Gai C, Liu C, Wu X, Yu M, Zheng J, Zhang W, et al. MT1DP Loaded by Folate-Modified Liposomes Sensitizes Erastin-Induced Ferroptosis *via* Regulating miR-365a-3p/NRF2 Axis in Non-Small Cell Lung Cancer Cells. *Cell Death Dis* (2020) 11:1–11. doi: 10.1038/s41419-020-02939-3
79. Chen H-H, Zhang T-N, Wu Q-J, Huang X-M, Zhao Y-H. Circular RNAs in Lung Cancer: Recent Advances and Future Perspectives. *Front Oncol* (2021) 11:2616. doi: 10.3389/fonc.2021.664290
80. Shanshan W, Hongying M, Jingjing F, Yiming Y, Yu R, Rui Y. CircDTL Functions as an Oncogene and Regulates Both Apoptosis and Ferroptosis in Non-Small Cell Lung Cancer Cells. *Front Genet* (2021) 1681. doi: 10.3389/fgene.2021.743505
81. Ren Z, Hu M, Wang Z, Ge J, Zhou X, Zhang G, et al. Ferroptosis-Related Genes in Lung Adenocarcinoma: Prognostic Signature and Immune, Drug Resistance, Mutation Analysis. *Front Genet* (2021) 12. doi: 10.3389/fgene.2021.672904
82. Cai J, Li C, Li H, Wang X, Zhou Y. Establishment of a Ferroptosis-Related Gene Signature for Prognosis in Lung Adenocarcinoma Patients. *PeerJ* (2021) 9:e11931. doi: 10.7717/peerj.11931
83. Ma C, Li F, Luo H. Prognostic and Immune Implications of a Novel Ferroptosis-Related Ten-Gene Signature in Lung Adenocarcinoma. *Ann Transl Med* (2021) 9:1–26. doi: 10.21037/atm-20-7936
84. Wang Y, Chen W, Zhu M, Xian L. Ferroptosis-Related Gene Signature and Patterns of Immune Infiltration Predict the Overall Survival in Patients With Lung Adenocarcinoma. *Front Mol Biosci* (2021) 8. doi: 10.3389/fmolb.2021.692530
85. Tian Q, Zhou Y, Zhu L, Gao H, Yang J. Development and Validation of a Ferroptosis-Related Gene Signature for Overall Survival Prediction in Lung Adenocarcinoma. *Front Cell Dev Biol* (2021) 9. doi: 10.3389/fcell.2021.684259
86. Tu G, Peng W, Cai Q, Zhao Z, Peng X, He B, et al. Construction and Validation of a 15-Gene Ferroptosis Signature in Lung Adenocarcinoma. *PeerJ* (2021) 9:e11687. doi: 10.7717/peerj.11687
87. Li F, Ge D, Sun S. A Novel Ferroptosis-Related Genes Model for Prognosis Prediction of Lung Adenocarcinoma. *BMC Pulm Med* (2021) 21:229. doi: 10.1186/s12890-021-01588-2
88. Wang S, Wu C, Ma D, Hu Q. Identification of a Ferroptosis-Related Gene Signature (FRGS) for Predicting Clinical Outcome in Lung Adenocarcinoma. *PeerJ* (2021) 9:e11233. doi: 10.7717/peerj.11233
89. Sun S, Guo W, Lv F, Zhang G, Wang J, Li R, et al. Comprehensive Analysis of Ferroptosis Regulators in Lung Adenocarcinomas Identifies Prognostic and Immunotherapy-Related Biomarkers. *Front Mol Biosci* (2021) 8:107. doi: 10.3389/fmolb.2021.587436
90. Liu T, Luo H, Zhang J, Hu X, Zhang J. Molecular Identification of an Immunity- and Ferroptosis-Related Gene Signature in Non-Small Cell Lung Cancer. *BMC Cancer* (2021) 21:783. doi: 10.1186/s12885-021-08541-w
91. Zhang A, Yang J, Ma C, Li F, Luo H. Development and Validation of a Robust Ferroptosis-Related Prognostic Signature in Lung Adenocarcinoma. *Front Cell Dev Biol* (2021) 9:1632. doi: 10.3389/fcell.2021.616271
92. Jin J, Liu C, Yu S, Cai L, Sitrakiniaina A, Gu R, et al. A Novel Ferroptosis-Related Gene Signature for Prognostic Prediction of Patients With Lung Adenocarcinoma. *Aging (Albany NY)* (2021) 13:16144. doi: 10.18632/aging.203140
93. Zhu G, Huang H, Xu S, Shi R, Gao Z, Lei X, et al. Prognostic Value of Ferroptosis-Related Genes in Patients With Lung Adenocarcinoma. *Thorac Cancer* (2021) 12(12):1890–9. doi: 10.1111/1759-7714.13998
94. Zheng Z, Zhang Q, Wu W, Xue Y, Liu S, Chen Q, et al. Identification and Validation of a Ferroptosis-Related Long Non-Coding RNA Signature for Predicting the Outcome of Lung Adenocarcinoma. *Front Genet* (2021) 12. doi: 10.3389/fgene.2021.690509
95. Guo Y, Qu Z, Li D, Bai F, Xing J, Ding Q, et al. Identification of a Prognostic Ferroptosis-Related lncRNA Signature in the Tumor Microenvironment of Lung Adenocarcinoma. *Cell Death Discovery* (2021) 7:1–11. doi: 10.1038/s41421-020-00236-z
96. Yao J, Chen X, Liu X, Li R, Zhou X, Qu Y. Characterization of a Ferroptosis and Iron-Metabolism Related lncRNA Signature in Lung Adenocarcinoma. *Cancer Cell Int* (2021) 21:1–14. doi: 10.1186/s12935-021-02027-2
97. Lu L, Liu L-P, Zhao Q-Q, Gui R, Zhao Q-Y. Identification of a Ferroptosis-Related LncRNA Signature as a Novel Prognosis Model for Lung Adenocarcinoma. *Front Oncol* (2021) 11:2443. doi: 10.3389/fonc.2021.675545

98. Huang F, Zheng Y, Li X, Luo H, Luo L. Ferroptosis-Related Gene AKR1C1 Predicts the Prognosis of Non-Small Cell Lung Cancer. *Cancer Cell Int* (2021) 21:1–16. doi: 10.1186/s12935-021-02267-2
99. Huang C, Yang M, Deng J, Li P, Su W, Jiang R. Upregulation and Activation of P53 by Erastin–Induced Reactive Oxygen Species Contribute to Cytotoxic and Cytostatic Effects in A549 Lung Cancer Cells. *Oncol Rep* (2018) 40:2363–70. doi: 10.3892/or.2018.6585
100. Guo J, Xu B, Han Q, Zhou H, Xia Y, Gong C, et al. Ferroptosis: A Novel Anti-Tumor Action for Cisplatin. *Cancer Res Treat Off J Korean Cancer Assoc* (2018) 50:445. doi: 10.4143/crt.2016.572
101. Liang Z, Zhao W, Li X, Wang L, Meng L, Yu R. Cisplatin Synergizes With PRLX93936 to Induce Ferroptosis in Non-Small Cell Lung Cancer Cells, Biochem. *Biophys Res Commun* (2021) 569:79–85. doi: 10.1016/j.bbrc.2021.06.088
102. Zhang T, Sun B, Zhong C, Xu K, Wang Z, Hofman P, et al. Targeting Histone Deacetylase Enhances the Therapeutic Effect of Erastin-Induced Ferroptosis in EGFR-Activating Mutant Lung Adenocarcinoma. *Transl Lung Cancer Res* (2021) 10:1857. doi: 10.21037/tlcr-21-303
103. Gai C, Yu M, Li Z, Wang Y, Ding D, Zheng J, et al. Acetaminophen Sensitizing Erastin-Induced Ferroptosis *via* Modulation of Nrf2/heme Oxygenase-1 Signaling Pathway in Non-Small-Cell Lung Cancer. *J Cell Physiol* (2020) 235:3329–39. doi: 10.1002/jcp.29221
104. Li Y, Yan H, Xu X, Liu H, Wu C, Zhao L. Erastin/sorafenib Induces Cisplatin–Resistant Non–Small Cell Lung Cancer Cell Ferroptosis Through Inhibition of the Nrf2/xCT Pathway. *Oncol Lett* (2020) 19:323–33. doi: 10.3892/ol.2019.11066
105. Meng M, Huang M, Liu C, Wang J, Ren W, Cui S, et al. Local Anesthetic Levobupivacaine Induces Ferroptosis and Inhibits Progression by Up-Regulating P53 in Non-Small Cell Lung Cancer. *Aging (Albany NY)* (2021) 13:1–12. doi: 10.18632/aging.203138
106. Boullosa LF, Van Loenhout J, Flieswasser T, De Waele J, Hermans C, Lambrechts H, et al. Auranofin Reveals Therapeutic Anticancer Potential by Triggering Distinct Molecular Cell Death Mechanisms and Innate Immunity in Mutant P53 Non-Small Cell Lung Cancer. *Redox Biol* (2021) 42:101949. doi: 10.1016/j.redox.2021.101949
107. Zhang Q, Yi H, Yao H, Lu L, He G, Wu M, et al. Artemisinin Derivatives Inhibit Non-Small Cell Lung Cancer Cells Through Induction of ROS-Dependent Apoptosis/Ferroptosis. *J Cancer* (2021) 12:4075. doi: 10.7150/jca.57054
108. Wu C-Y, Yang Y-H, Lin Y-S, Chang G-H, Tsai M-S, Hsu C-M, et al. Dihydroisotanshinone I Induced Ferroptosis and Apoptosis of Lung Cancer Cells. *Biomed Pharmacother* (2021) 139:111585. doi: 10.1016/j.biopha.2021.111585
109. Li X, Li W, Yang P, Zhou H, Zhang W, Ma L. Anticancer Effects of Cryptotanshinone Against Lung Cancer Cells Through Ferroptosis. *Arab J Chem* (2021) 14:103177. doi: 10.1016/j.arabjc.2021.103177
110. Iida Y, Okamoto-ĸatsuyama M, Maruoka S, Mizumura K, Shimizu T, Shikano S, et al. Effective Ferroptotic Small-Cell Lung Cancer Cell Death From SLC7A11 Inhibition by Sulforaphane. *Oncol Lett* (2021) 21:1. doi: 10.3892/ol.2020.12332
111. Lou J-S, Zhao L-P, Huang Z-H, Chen X-Y, Xu J-T, Tai WC-S, et al. Ginkgetin Derived From Ginkgo Biloba Leaves Enhances the Therapeutic Effect of Cisplatin *via* Ferroptosis-Mediated Disruption of the Nrf2/HO-1 Axis in EGFR Wild-Type Non-Small-Cell Lung Cancer. *Phytomedicine* (2021) 80:153370. doi: 10.1016/j.phymed.2020.153370
112. Wu W, Geng Z, Bai H, Liu T, Zhang B. Ammonium Ferric Citrate Induced Ferroptosis in Non-Small-Cell Lung Carcinoma Through the Inhibition of GPX4-GSS/GSR-GGT Axis Activity. *Int J Med Sci* (2021) 18:1899. doi: 10.7150/ijms.54860
113. Hsieh C-H, Hsieh H-C, Shih F-S, Wang P-W, Yang L-X, Shieh D-B, et al. An Innovative NRF2 Nano-Modulator Induces Lung Cancer Ferroptosis and Elicits an Immunostimulatory Tumor Microenvironment. *Theranostics* (2021) 11:7072. doi: 10.7150/thno.57803
114. Yuan L-Q, Wang C, Lu D-F, Zhao X-D, Tan L-H, Chen X. Induction of Apoptosis and Ferroptosis by a Tumor Suppressing Magnetic Field Through ROS-Mediated DNA Damage. *Aging (Albany NY)* (2020) 12:3662. doi: 10.18632/aging.102836
115. Ye LF, Chaudhary KR, Zandkarimi F, Harken AD, Kinslow CJ, Upadhyayula PS, et al. Radiation-Induced Lipid Peroxidation Triggers Ferroptosis and Synergizes With Ferroptosis Inducers. *ACS Chem Biol* (2020) 15:469–84. doi: 10.1021/acschembio.9b00939
116. Pan X, Lin Z, Jiang D, Yu Y, Yang D, Zhou H, et al. Erastin Decreases Radioresistance of NSCLC Cells Partially by Inducing GPX4–Mediated Ferroptosis. *Oncol Lett* (2019) 17:3001–8. doi: 10.3892/ol.2019.9888
117. Wang S, Liao H, Li F, Ling D. A Mini-Review and Perspective on Ferroptosis-Inducing Strategies in Cancer Therapy. *Chin Chem Lett* (2019) 30:847–52. doi: 10.1016/j.cclet.2019.03.025

Conflict of Interest: The authors declare that the research was conducted in the absence of any commercial or financial relationships that could be construed as a potential conflict of interest.

Publisher's Note: All claims expressed in this article are solely those of the authors and do not necessarily represent those of their affiliated organizations, or those of the publisher, the editors and the reviewers. Any product that may be evaluated in this article, or claim that may be made by its manufacturer, is not guaranteed or endorsed by the publisher.

frontiers in Pharmacology

ORIGINAL RESEARCH
published: 07 December 2021
doi: 10.3389/fphar.2021.778698

FBXO22 Promotes Growth and Metastasis and Inhibits Autophagy in Epithelial Ovarian Cancers *via* the MAPK/ERK Pathway

Minle Li[1†], Xue Zhao[1,2†], Hongmei Yong[3†], Bingqing Shang[1], Weihua Lou[4,5,6], You Wang[4,5,6*] and Jin Bai[1,7*]*

[1]Cancer Institute, Xuzhou Medical University, Xuzhou, China, [2]Cancer Research Center, School of Medicine, Xiamen University, Xiamen, China, [3]Department of Oncology, The Affiliated Huai'an Hospital of Xuzhou Medical University and The Second People's Hospital of Huai'an, Huai'an, China, [4]Department of Obstetrics and Gynecology, Renji Hospital, School of Medicine, Shanghai Jiao Tong University, Shanghai, China, [5]Shanghai Key Laboratory of Gynecologic Oncology, Shanghai, China, [6]State Key Laboratory of Oncogenes and Related Genes, Shanghai Cancer Institute, Renji Hospital, School of Medicine, Shanghai Jiao Tong University, Shanghai, China, [7]Center of Clinical Oncology, Affiliated Hospital of Xuzhou Medical University, Xuzhou, China

OPEN ACCESS

Edited by:
Xu Chen,
Guilin Medical University, China

Reviewed by:
Zhiwei Wang,
Wenzhou Medical University, China
Dalin He,
Xi'an Jiaotong University, China

****Correspondence:***
Weihua Lou
louweihua@renji.com
You Wang
wanghh0163@163.com
Jin Bai
bj@xzhmu.edu.cn

[†]These authors have contributed equally to this work

Specialty section:
This article was submitted to Pharmacology of Anti-Cancer Drugs, a section of the journal Frontiers in Pharmacology

Received: *17 September 2021*
Accepted: *15 November 2021*
Published: *07 December 2021*

Citation:
Li M, Zhao X, Yong H, Shang B, Lou W, Wang Y and Bai J (2021) FBXO22 Promotes Growth and Metastasis and Inhibits Autophagy in Epithelial Ovarian Cancers via the MAPK/ERK Pathway. Front. Pharmacol. 12:778698. doi: 10.3389/fphar.2021.778698

E3 ubiquitin ligase F-box only protein 22 (FBXO22), which targets the key regulators of cellular activities for ubiquitylation and degradation, plays an important role in tumorigenesis and metastasis. However, the function of FBXO22 in epithelial ovarian cancers has not been reported. This study aims to explore the biological function of FBXO22 in epithelial ovarian cancers progression and metastasis and its specific regulation mechanism. Immunohistochemistry analysis of tissue microarray was performed to evaluate the expression of FBXO22 in epithelial ovarian cancers patients. The proliferative ability of epithelial ovarian cancers cells was examined by the CCK8. The metastasis ability was detected by the wound healing assay, migration and invasion assays. Western blot was used to verify the relationship between FBXO22 expression and mitogen-activated protein kinase related proteins. Autophagic flux was detected by electron microscopy, mRFP-GFP-LC3 adenovirus, lysosomal tracker and western blot. For *in vivo* experiments, the effect of FBXO22 on epithelial ovarian cancers resistance was observed in a xenograft tumor model and a metastatic mice model. We found that FBXO22 expression was significantly increased in epithelial ovarian cancers tissues and was closely correlated with clinical pathological factors. As a result, we found that FBXO22 promoted the growth and metastasis, as well as inhibited the autophagy flux. In addition, we identified that FBXO22 performed these functions *via* the MAPK/ERK pathway. Our results first reported the function of FBXO22 in epithelial ovarian cancer and the correlation between FBXO22 and autophagy, suggesting FBXO22 as a novel target of epithelial ovarian cancers assessment and treatment.

Keywords: FBXO22, epithelial ovarian cancers (EOCs), metastasis, autophagy, MAPK, ERK

Abbreviations: ATG5, autophagy related 5; Bcl-2, B cell lymphoma-2; BECN1, Beclin 1; BH3, BCL-2 homology 3; CQ, chloroquine; EOCs, epithelial ovarian cancers; FBXO22, F-box only protein 22; JNK, c-Jun-NH2-terminal kinases; MAPK, the mitogen-activated protein kinase; MMP-9, matrix metalloproteinase-9; MMPs, matrix metalloproteinases; NC, nonspecific control; ROS, reactive oxygen species; siRNA, small interfering RNA; TMA, tissue microarray; TRAF6, tumor necrosis factor receptor associated protein 6; Vps34, vacuolar protein sorting 34.

INTRODUCTION

Ovarian cancer is the seventh most common cancer among women, and the age-standardized rates in developed and developing countries are approximately 9.4 and 5.0 per 100,000 people, respectively (Siegel et al., 2016; Reid et al., 2017). Despite developments in drug discovery and management, ovarian cancer remains the leading cause of death due to gynecological cancer (Miller et al., 2016). As many as 240,000 women worldwide are diagnosed with ovarian cancer, and nearly half of the women die every year (Reid et al., 2017). About 85–90% of all ovarian cancers are epithelial in origin, and around 70% of all epithelial ovarian cancers (EOCs) are high-grade serous (HGS) adenocarcinoma (McLachlan et al., 2016).

Early diagnosis increases the chance of recovery, but due to the nonspecific symptoms of the disease in the early stage, recovery is hindered. Advanced ovarian cancer is aggressive, has rapid growth and spread and chemotherapy/radiotherapy resistance, and recurs. At present, cytoreductive surgery is clinically adopted, along with chemotherapy using cisplatin and paclitaxel, but the multidrug resistance of ovarian cancer cells has severely reduced the long-term efficacy of these treatments; the 5-year survival rate is only 30% (Coleman et al., 2013). Therefore, issues concerning the in-depth exploration of the mechanism of the occurrence, development, invasion, and metastasis of ovarian cancer cells and in the search for effective targeted treatment approaches need to be resolved urgently.

Autophagy is a lysosome-dependent degradation pathway that widely occurs in eukaryotic cells. Under normal physiological conditions, autophagy facilitates the maintenance of cell homeostasis and promotes cell survival; however, excessive autophagy can cause cell death through a process called "autophagic cell death," along with apoptosis and necrosis (Hippert et al., 2006). This "double-edged sword" effect in the regulation cell fate is manifested in the relationships among autophagy, tumorigenesis, and development, and depends on the different stages of disease progression, changes in the surrounding environment of cells, and different therapeutic interventions. Autophagy is a tumor suppressor mechanism, and decline in autophagy may be beneficial to tumor development. Tumor cells have a lower degree of autophagy ability than normal cells. The autophagy ability of normal cells first eliminates organelles (mainly mitochondria) damaged by chemical carcinogens, radiation, and oxidative stress to prevent genetic instability due to the damage caused by reactive oxygen species (ROS) to DNA, thereby hindering the proliferation of tumor cells. Autophagy can degrade the endoplasmic reticulum, Golgi apparatus, other organelles, and long-lived proteins, causing premalignant cells to be in a negative protein balance and inhibiting their uncontrolled proliferation (Hait et al., 2006).

The mitogen-activated protein kinase (MAPK) family, which includes ERK2/ERK1 (also known as p42/p44MAPK), p38 MAPK, ERK5, and c-Jun-NH2-terminal kinases (JNK1/2/3), plays a crucial role in nearly all cell functions (Ramos, 2008). Depending on duration, magnitude, and subcellular localization, ERK activation controls various cell responses, such as proliferation, migration, differentiation, and death (Murphy and Blenis, 2006). ERK increases cell survival by promoting the activities of antiapoptotic proteins, such as B cell lymphoma (Bcl)-2 and Bcl-XL. ERK-dependent autophagic activity is associated with the classical markers of autophagy, such as the induction of LC3, conversion of LC3-I to LC3-II (Ogier-Denis et al., 2000; Cheng et al., 2008; Sivaprasad and Basu, 2008; Oh and Lim, 2009), and induction of Beclin 1 (BECN1) (Cheng et al., 2008). Remarkably, Bcl-2 inhibits autophagy by binding to the BCL-2 homology 3 (BH3) domain of BECN1, which block the binding between BECN1 and vacuolar protein sorting 34 (Vps 34).

FBXO22 is a member of the F-box protein family (Tan et al., 2011; Dikopoltsev et al., 2014). The SCF F-box complex have pivotal roles in multiple cellular processes and tumorigenesis through ubiquitylation and subsequent degradation of target proteins (Wang et al., 2014), including proteins related to cell cycle progression, signal transduction, and transcription (Nakayama and Nakayama, 2006; Sarikas et al., 2008; Sarikas et al., 2011). Several biological functions of FBXO22 in tumorigenesis have been determined in recent years. According to the different degradation target proteins of the FBXO22 complex, it plays a corresponding function in cells (Cheng et al., 2020). FBXO22 promotes tumorigenesis by degrading nuclear PTEN (Ge et al., 2020), promotes lung cancer by mediating the polyubiquitination with the inactivation of LKB1 (Zhu et al., 2019) and Bach1 (Lignitto et al., 2019), and promotes the development of hepatocellular carcinoma by regulating the ubiquitination and degradation of p21 (Zhang et al., 2019). Our previous research shown that FBXO22 targets HDM2 for degradation and modulates breast cancer cell invasion and metastasis (Bai et al., 2019), and it suppresses metastasis in human renal cell carcinoma by inhibiting matrix metalloproteinase (MMP)-9-mediated migration and invasion and VEGF-mediated angiogenesis (Guo et al., 2019). Moreover, FBXO22 knockdown inhibits melanoma cell migration, invasion, and angiogenesis via the HIF-1α/VEGF pathway (Zheng et al., 2020). By contrast, the function of FBXO22 in epithelial ovarian cancers is unclear.

In this study, we demonstrated the expression of FBXO22 in patients. We investigated the biological functions of FBXO22 *in vitro* and *in vivo*. Furthermore, we explore the mechanism and prospected the potential and profound significance of FBXO22 in epithelial ovarian cancers assessment and treatment.

MATERIALS AND METHODS

Patients and Samples

A tissue microarray (TMA) containing 251 EOCs tissues and 10 matched normal tissues were constructed by Jiangsu Cancer Biotherapy Institute (Xuzhou, China). The tissues, which were embedded in paraffin blocks, were collected from the Pathology Department of Affiliated Hospital of Xuzhou Medical University (Xuzhou, China). All the patients underwent definitive diagnosis of epithelial ovarian cancers and then radical surgery at the above

hospital. Detailed clinical information of each specimen was recorded accurately and completely. All the tissue specimens were obtained from the patient, all of whom provided informed consent, and the use of human specimens was approved by the Review Board of the Affiliated Hospital of Xuzhou Medical College.

Tissue Microarray Immunohistochemistry

TMA immunohistochemistry was implemented according to the streptavidin–peroxidase (Sp) method. A standard PV-9001 kit (Beijing Zhongshan Golden Bridge Biotechnology, Beijing, China) was used. Before immunostaining, TMA slides were dewaxed at 60°C for 2 h, then deparaffinized with xylene and hydrated with graded ethanol and distilled water. Endogenous peroxidases were inhibited with 3% H_2O_2 for 30 min. Antigen retrieval was performed by heating the TMA slides immersed in a retrieval solution (10 mM sodium citrate buffer, pH 6.0) at 95°C for 30 min in a pressure boiler. After 1 h of blocking with 5% normal goat serum, the sections were incubated with polyclonal rabbit anti-FBXO22 antibody (1:100 dilution, Proteintech) overnight at 4 °C. The slides were immersed in a response enhancer for 20 min and biotin-labeled secondary antibody (PV-9001 kit, Beijing Zhongshan Golden Bridge Biotechnology, Beijing, China) for 20 min at room temperature and then with avidin–peroxidase reagent and 3,3′-diaminobenzidine (Beijing Zhongshan Golden Bridge Biotechnology, Beijing, China) substrate. After hematoxylin counterstaining and dehydration, the sections were sealed with cover slips.

Evaluation of Immunostaining

Two pathologists separately examined the TMAs under blinded experimental conditions. The staining scores of FBXO22 were evaluated according to the intensity and percentage of cells with positive staining. The staining intensity of FBXO22 was scored 0, 1, 2, or 3 (0, negative; 1, weak; 2, moderate; 3, strong); the percentage of the FBXO22-positive stained cells was graded as 0 (<5%), 1 (5–25%), 2 (25–50%), 3 (50–75%), or 4 (75–100%). The immunoreactive score (IRS) of each section was calculated by multiplying the scores of staining intensity and the percentage of positive cells. On the basis of the IRS, staining patterns were divided into two classes: negative (IRS: 0–6) and positive (IRS: 7–12) expression.

Cell Lines and Cell Culture

Human epithelial ovarian cancers cell lines (OVCAR3, HO8910, and A2780) and human ovarian epithelium cells (IOSE) were obtained from the Type Culture Collection of the Chinese Academy of Sciences (Shanghai, China). The OVCAR3 cells were cultured in an RPMI 1640 medium supplemented with 20% fetal bovine serum (FBS) and 0.1 mg/ml insulin. The HO8910, A2780, and IOSE cell lines were cultured in an RPMI 1640 medium supplemented with 10% FBS. Then, 100 U/ml streptomycin/penicillin was added to the RPMI 1640 medium. All the cells were cultured in an incubator at 37°C with 5% CO_2.

Immunofluorescence

Cells were seeded on coverslips, fixed in 4% paraformaldehyde at room temperature for 15 min, rinsed in PBS for three times, permeabilized in 0.3% Triton X-100 for 15 min, rinsed in PBS for three times, and blocked in 2% bovine serum albumin at room temperature for 1 h. Then, coverslips were incubated with primary antibodies 1:100 diluted in staining buffer (1% bovine serum albumin in 0.3% Triton X-100/PBS) overnight at 4°C in a humid chamber. After washing three times, secondary antibodies (Alexa Fluor 595; Abcam) were applied in a 1:200 dilution in staining buffer for 1 h at 37°C in a humid chamber in the dark. After washing, coverslips were mounted with Vectorshield with 4′,6-diamidino-2-phenylindole (DAPI; Beyotime Biotechnology, Nanjing, China). Fluorescent signals were captured with a confocal laser scanning microscope (ZEISS LSM880, Germany).

FBXO22 Small Interfering RNA or Overexpression Plasmid Transfection

Small interfering RNA (siRNA) specific for FBXO2 (siFBXO22#1, siFBXO22#2, and siFBXO22#3), autophagy related 5 (ATG5, si-ATG5), and nonspecific control (NC) were purchased from Gene-Pharma (Shanghai, China) and transfected with siLentFect lipid reagent (Bio-Rad Laboratories, Inc.) according to the manufacturer's protocol when the epithelial ovarian cancers cells grew to 30–40% confluency. Approximately 6 h after transfection, the medium containing transfection reagents was replaced with a fresh medium. The siRNA sequences were as follows:

NC: sense, 5′-UUCUCCGAACGUGUCACGUTT-3′;
antisense, 5′-ACGUGACACGUUCGGAGATT-3′.
siFBXO22#1: sense, 5′-GGUGGGAGCCAGUAAUUAUTT-3′;
antisense, 5′-AUAAUUACUGGCUCCCACCTT-3′.
siFBXO22#2: sense, 5′-GUUCGCAUCUUACCACAUATT-3′;
antisense, 5′-UAUGUGGUAAGAUGCGAACTT-3′.
siFBXO22#3: sense, 5′-GCACCUUCGUGUUGAGUAATT-3′;
antisense, 5′-UUACUCAACACGAAGGUGCTT-3′.
siATG5: sense, 5′-CAGUUUGGCACAAUCAAUATT -3′;
antisense, 5′-UAUUGAUUGUGCCAAACUGTT-3′.

Overexpression plasmid (HA-FBXO22) and nonspecific control (pcDNA3.1-Ctrl) were purchased from You Bio (Hunan, China) and transfected with Lipo2000 (Invitrogen, Shanghai, China) according to the manufacturer's protocol when the epithelial ovarian cancers cells grew to 80–90% confluency. Approximately 6 h after transfection, the medium containing transfection reagents was replaced with a fresh medium.

Plasmid Construction

shFBXO22-LV3, Ctrl-LV3, Flag-FBXO22-LV5, and Ctrl-LV5 lentivirus (Gene-Pharma) were used for the stable suppression and overexpression of FBXO22. After 48 h of infection on HO8910 cells with the lentivirus, stable cells were extracted using 2 μg/ml puromycin for 14 days.

Antibodies and Western Blot Analysis

This procedure was completed using the following primary antibodies raised against: FBXO22, GAPDH, P62, BECN1 and ATG5 (Proteintech Group); MMP-2, ERK, p-ERK, P38, p-P38, p-90RSK, RAC1 and BCL-2 (Cell Signaling Technology), and LC3 I/II (Abcam). The secondary antibodies were goat anti-rabbit and goat anti-mouse corresponding HRP (Beijing Biodragon Immunotechnologies Co., Ltd., Beijing, China). The protein bands were determined using a Tanon 5200 automated chemiluminescent imaging analysis system with ECL reagents (Tanon, Shanghai, China).

Cell Proliferation Assay

After knock down or overexpression of FBXO22 in HO8910 and OVCAR3 cells, cell proliferation was monitored by the cell counting kit-8 (CCK-8; Beyotime Biotechnology, Nanjing, China). After knockdown or overexpression of FBXO22 in HO8910 and OVCAR3 cells, 5×10^3 cells were seeded in a 96-well culture plate and then incubated at 37°C in a humidified atmosphere containing 5% CO_2 for 24 h. Then, 10 μl of CCK-8 solution was added 24, 48, 72, and 96 h after plating, and the cells were incubated at 37°C for another 1 h. Absorbance was determined at 450 nm.

Wound Healing Assays

In the wound healing assays, cells were planted in six-well plates and cultured to 80% confluence. Then, a sterile 10 μl pipette tip was used in making artificial scratches in each well. Suspended cells were washed away with PBS, then the cells were cultured in a medium with 1% FBS. Cell migration distance was photographed at 0 and 24 h under an inverted light microscope.

Cell Migration and Invasion Assays

Assays on cell migration and invasion were performed using Transwell filter inserts (8.0 μm pore size with polycarbonate membranes) precoated with Matrigel (BD Biosciences, NJ, United States) and those that were not. The cells underwent serum starvation overnight, and 2×10^5 cells were seeded into the upper chamber for the migration assay kit. In the same chamber, 4×10^5 cells were seeded into a medium without serum for the invasion assay. The lower chamber was filled with RPMI 1640 supplemented with 20% FBS. After 24 and 48 h of incubation at 37°C in 5% CO_2, the cells were fixed in the membrane with methanol (90%) and then stained with crystal violet. The cells in the upper chamber were removed gently. Afterward, the traversed cells were dried and counted.

Electron Microscopy

shFBXO22–LV3, Ctrl–LV3, Flag–FBXO22–LV5, and Ctrl–LV5 cells (1×10^7) were pre-fixed in 2.5% glutaraldehyde and 1% osmium tetroxide and then incubated with 1% OsO_4 for 3 h at 4°C, dehydrated in a graded series of ethanol, and flat-embedded in epoxy resin. Ultrathin sections were stained with uranyl acetate and lead citrate and observed under a transmission electron microscope (Tecnai G2 Spirit Twin/*Tecnai G2 Spirit Twin).

Quantitation of Autophagy With mRFP-GFP-LC3 Adenovirus

After si-Ctrl, si-FBXO22, pcDNA3.1, and HA-FBXO22–pcDNA3.1 were transfected into the HO8910 cells, mRFP-GFP-LC3 adenoviral particles (50 MOI, Hanbio Biotechnology Co., Ltd. Shanghai, China) were infected for 24 h. Fluorescent signals were captured with a confocal laser scanning microscope (ZEISS LSM880, Germany). The number of autolysosomes and autophagosomes was determined by counting the red puncta or yellow puncta, respectively. Thirty randomly selected cells per experimental group were analyzed.

Lysosomal Tracker

A lysosomal tracker (Beyotime, Shanghai, China) was diluted with HBSS (1:10,000) and then incubated at 37°C under a humidified atmosphere containing 5% CO_2 for 1 h. Fluorescent signals were captured with a confocal laser scanning microscope (ZEISS LSM880, Germany).

Xenograft Mice Model *In Vivo*

Eight six-week-old BALB/c nude mice were used. Stable HO8910 cell lines constructed with Ctrl-LV3 and shFBXO22-LV3 were injected into the left and right backs successively with the number of 5×10^6. Five weeks after injection, the mice were sacrificed, and their subcutaneous tumors were excised and fixed in 10% buffered formalin for the detection of FBXO22 and Ki67expression levels through IHC analysis.

Metastatic Mice Model *In Vivo*

Sixteen six-week-old BALB/c nude mice were divided into two groups and injected i.p., with Ctrl-LV3 and shFBXO22-LV3 cells (5×10^6) respectively. Fourty days after injection, the mice were sacrificed, and their organs including colon, lung, kidney, liver, spleen and heart were excised and made into paraffin sections for analysis of metastasis by HE staining.

Statistical Analysis

Quantitative data are expressed as the means ± SD of at least three independent experiments. All experimental values were evaluated using GraphPad Prism 8.3.0 (GraphPad software). Differences between two groups were analyzed with Student's t test, whereas differences among more than two groups were evaluated by one-way ANOVA for independent samples or ANOVA for repeated measurements followed by Tukey post-hoc test. In all cases, $p < 0.05$ was considered statistically significant.

RESULTS

The Expression of FBXO22 Is Associated With Clinical Pathological Factors in Epithelial Ovarian Cancers

To evaluate whether the FBXO22 protein expression is related to EOCs, we performed immunohistochemistry experiments across an entire TMA containing 251 EOCs tissues and 10 matched

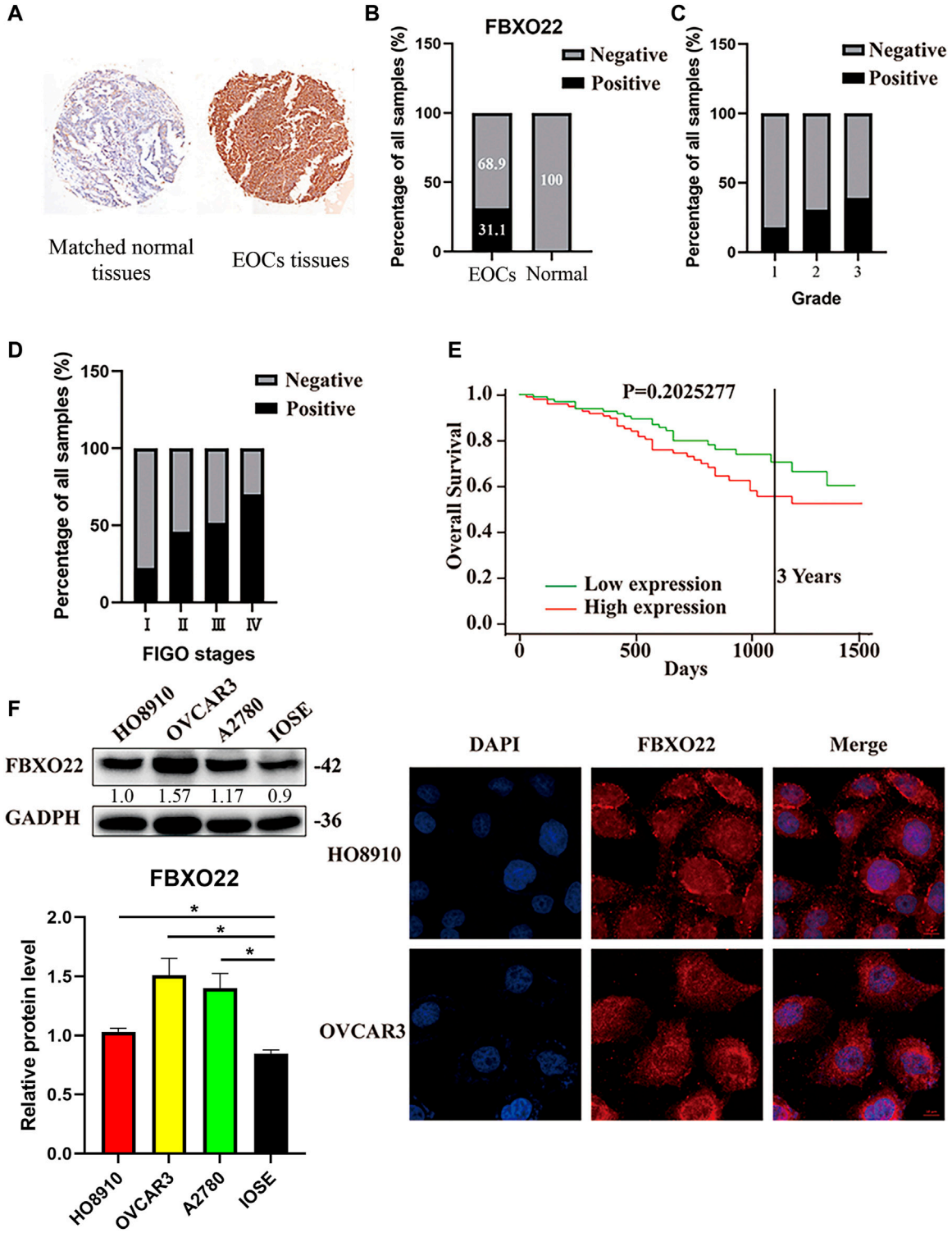

FIGURE 1 | The high expression of FBXO22 is associated with clinical pathological factors in EOCs. **(A)** IHC staining of FBXO22 in TMA containing 251 EOCs tissues and 10 matched normal tissues (×20). **(B)** Analysis of FBXO22 expression in EOCs and matched normal tissues. **(C)** Analysis between FBXO22 expression and pathological grade. **(D)** Analysis between FBXO22 expression and FIGO stages. **(E)** Survival analysis of ovarian cancers in TCGA. **(F)** Western blot results of FBXO22 expression in epithelial ovarian cancers cell lines (HO8910, OVCAR3, A2780) and ovarian epithelial cells (IOSE). Independent samples *t*-test was used for statistics and the results were expressed as mean ± SD, *, $p < 0.05$; ***, $p < 0.001$ ($N = 3$). **(G)** Immunofluorescence of FBXO22 in HO8910 and OVCAR3 cells (×100).

TABLE 1 | Expression of FBXO22 and clinicopathological factors of ovarian cancer patients.

Features	Total	Expression of FBXO22		χ^2 value	*p* Value
		Negative (%)	Positive (%)		
Age (years)				0.191	0.662
<49	121	85 (70.2)	36 (29.8)		
≥49	130	88 (67.7)	42 (32.3)		
FIGO stages				22.993	<0.001
I	175	136 (77.7)	39 (22.3)		
II	35	19 (54.3)	16 (45.7)		
III	31	15 (48.4)	16 (51.6)		
IV	10	3 (30.0)	7 (70.0)		
Grade				8.464	0.015
1	62	51 (82.3)	11 (17.7)		
2	79	55 (69.6)	24 (30.4)		
3	110	67 (60.9)	43 (39.1)		

normal tissues. The resulting FBXO22 staining intensity was quantified using IRS. Samples with IRS in the range of 0–6 or 7–12 were classified as negative or positive FBXO22 expression, respectively (**Figure 1A**). The statistic results show that negative or positive FBXO22 expression accounted for 68.9% or 31.1% of the 251 tumor samples analyzed, respectively (**Figure 1B**). The expression of FBXO22 in the all 10 matched normal tissues were negative (**Figure 1B**).

Moreover, the FBXO22 expression was positively correlated with clinical FIGO stages ($p < 0.001$) and pathological grades ($p = 0.015$) (**Figures 1C,D**; **Table 1**). No significant difference between FBXO22 expression and age was observed (**Table 1**, $p = 0.662$). Analysis of the epithelial ovarian cancer patients in TCGA shown that there was no significant difference in survival (**Figure 1E**, $p = 0.203$). These results shown that EOCs patients have higher expression of FBXO22 and the expression of FBXO22 is associated with clinical pathological factors.

Consistently, increased FBXO22 expression was also detected in three EOC cell lines (HO8910, OVCAR3 and A2780) as compared with normal ovarian epithelial cell line IOSE (**Figure 1F**). Moreover, the subcellular location of FBXO22 in HO8910 and OVCAR3 cells was determined by immunofluorescence, showing that FBXO22 was both nuclear and cytoplasmic (**Figure 1G**).

FBXO22 Promotes the Growth of Epithelial Ovarian Cancers *In Vitro* and *In Vivo*

To investigate the biological function of FBXO22 in epithelial ovarian cancers cell proliferation, we transfected HO8910 and OVCAR3 cells with negative control siRNA (NC) and siRNAs targeting FBXO22 (si#1, si#2 and si#3) successively (**Figure 2A**). Then, CCK-8 cell proliferation assays were performed. The knockdown of FBXO22 inhibited the growth of epithelial ovarian cancers cells (**Figure 2C**). Conversely, the proliferation of epithelial ovarian cancers cells was drastically increased in both cell lines overexpressing FBXO22 compared with the control groups (**Figures 2B,D**).

Furthermore, we established Ctrl-LV3 (NC) and shFBXO22-LV3 (sh-FBXO22) stable cell lines to verify the function of FBXO22 in the regulation of epithelial ovarian cancers cell *in vivo*. The cells were subcutaneously injected into BALB/c nude mice. The mice were sacrificed 5 weeks after the implementation, and the tumors were exposed (**Figure 3A**). Differences in tumor volume and weight between the two groups were statistically analyzed (**Figures 3B–D**). The results shown that knockdown of FBXO22 inhibited the growth of epithelial ovarian cancers *in vivo*. HE and IHC staining indicated that FBXO22 deficiency reduced the growth of epithelial ovarian cancers (**Figures 3E–G**). The results revealed that FBXO22 promotes cell proliferation in epithelial ovarian cancers.

FBXO22 Promoted Metastasis of Epithelial Ovarian Cancers *In Vitro* and *In Vivo*

The effect of FBXO22 on migration and invasion of EOCs were also explored. Knockdown of FBXO22 significantly inhibited the migration ability of HO8910 and OVCAR3 cells when compared with control cells (**Figure 4A**), as evidenced by wounding healing assay (**Figures 4C,D**). In contrast, FBXO22 overexpression promoted the migration ability of HO8910 and OVCAR3 cells (**Figures 4A,C,D**). In addition, Transwell matrige invasion assays also shown that FBXO22 knockdown reduced the invasion ability and overexpression FBXO22 enhanced the invasion ability, respectively (**Figure 4B**).

To further detect the role of FBXO22 in the peritoneal metastasis of EOCs, we used an intraperitoneal injection mice model. In brief, 2×10^6 HO8910 NC/sh-FBXO22 cells were injected to 7-week-old nude mice, and the peritoneal metastasis status was analyzed 8 weeks later. Compared with the NC group, sh-FBXO22 cells formed fewer metastatic foci in colon, lung, kidney, liver and spleen (**Figures 5A–E**). We analyze the incidence of metastasis (**Figure 5F**) and the number of metastatic organs (**Figure 5G**), as well as the incidence of metastasis in every organ (**Figure 5H**).

In conclusion, our results shown that FBXO22 promoted metastasis of EOCs both *in vitro* and *in vivo*.

FBXO22 Promotes the Growth and Metastasis of Epithelial Ovarian Cancers Cells *via* the MMP2 and Mitogen-Activated Protein Kinase Pathways

To explore the mechanism by which FBXO22 promotes the metastasis of epithelial ovarian cancers cells, we identified some related pathways and proteins. Matrix metalloproteinases (MMPs), as important enzymes that degrade the extracellular matrix, play an important role in mediating tumor angiogenesis, metastasis, and invasion. MMP-2 is an important MMP (Malemud, 2006). We detected the content of MMP-2 in epithelial ovarian cancers cells with interfered and overexpressed FBXO22. The results shown that MMP2 expression was decreased after interfering with FBXO22 and increased after the overexpression of FBXO22 (**Figures 6A,B**).

MAPKs constitute a group of serine threonine protein kinases that can be activated by a series of extracellular stimulus signals and mediate signal transduction from the

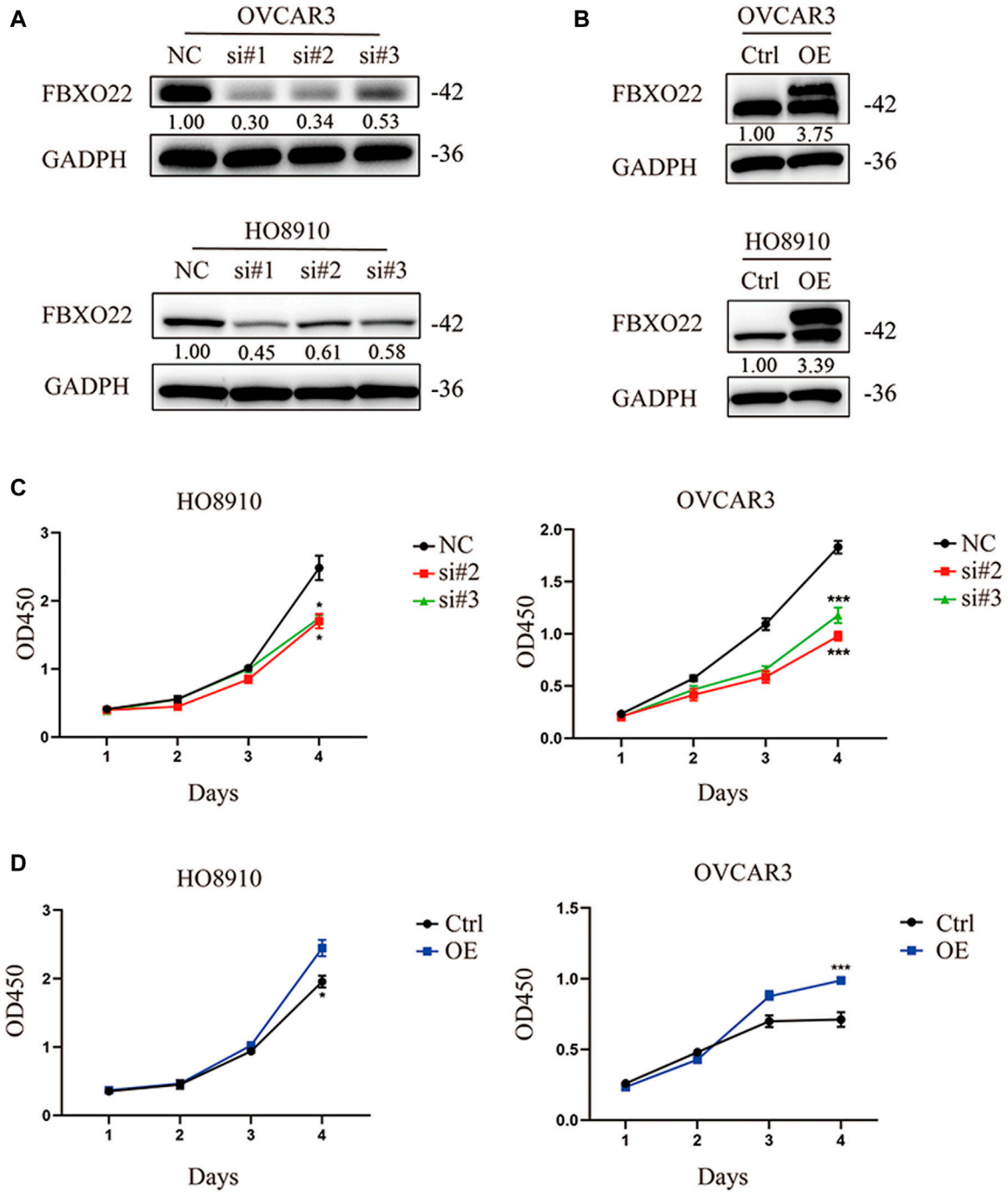

FIGURE 2 | FBXO22 promotes the growth of EOCs *in vitro*. **(A)** Knockdown of FBXO22 were confirmed at the protein level in OVCAR3 and HO8910 cells by western blot. **(B)** Overexpression of FBXO22 were confirmed at the protein level in OVCAR3 and HO8910 cells by western blot. **(C)** Cell proliferation of FBXO22 knockdown HO8910 and OVCAR3 cells by CCK8 assay. **(D)** Cell proliferation of FBXO22 overexpression HO8910 and OVCAR3 cells by CCK8 assay. Independent samples *t*-test was used for statistics and the results were expressed as mean ± SD, *, $p < 0.05$; **, $p < 0.01$; ***, $p < 0.001$ ($N = 6$).

cell membrane to the nucleus. They regulate many physiological activities, such as inflammation, apoptosis, carcinogenesis, invasion, and metastasis, particularly those of tumor cells. ERK1/2 and P38 are the two important members of MAPK (Fan and Chambers, 2001). We detected the levels of ERK1/2, P38, p-ERK1/2, and p-P38. The results shown that FBXO22 can promote the activation of ERK1/2 and P38 (**Figures 6A,B**). Subsequently, we verified some relevant proteins. Tumor necrosis factor receptor associated protein 6 (TRAF6) was reported to regulate

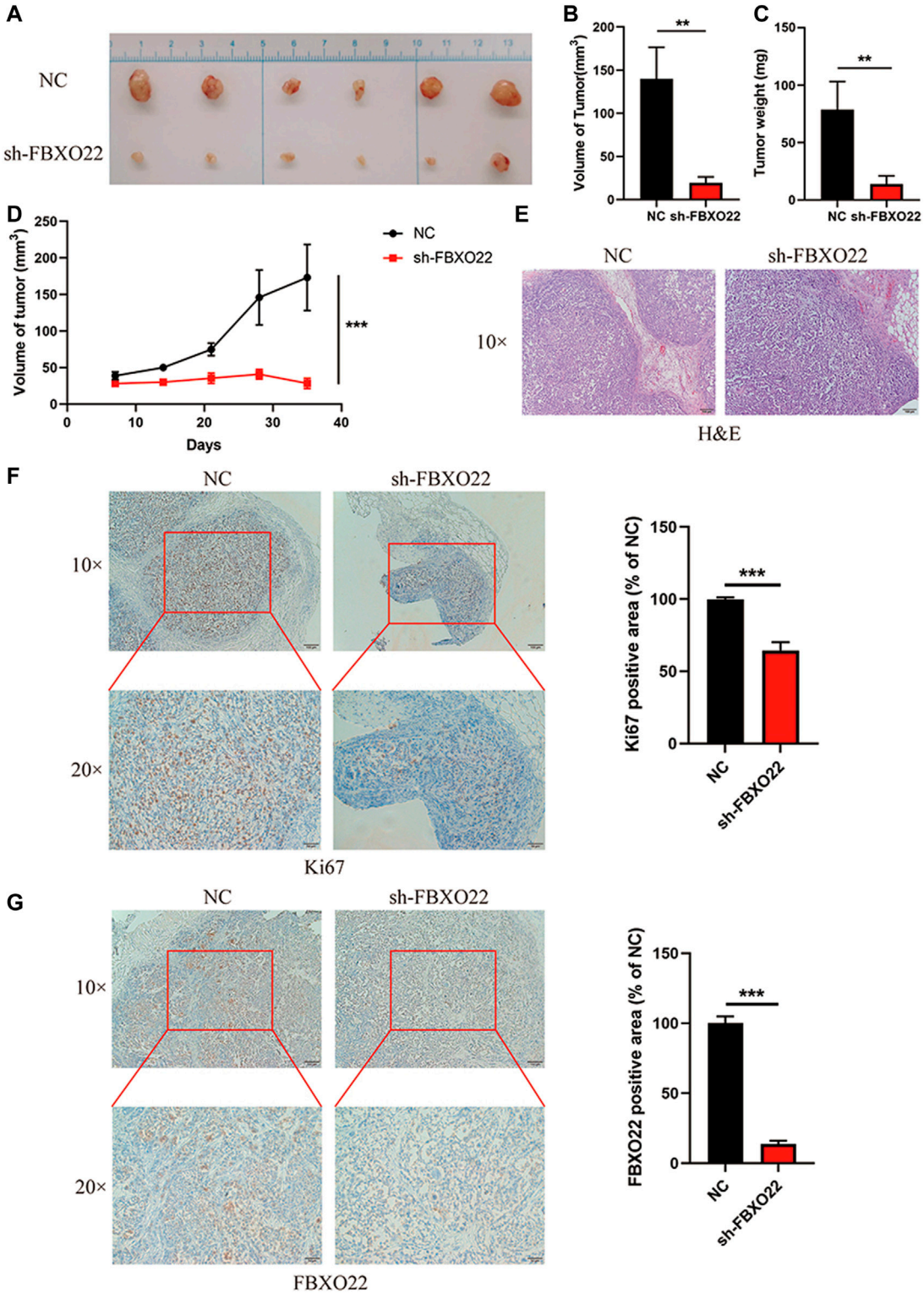

FIGURE 3 | FBXO22 promotes the growth of EOCs *in vivo*. **(A)** Images of subcutaneous tumors resected from the mice after 5 weeks of growth *in vivo*. **(B–D)** Analysis of volume and weight of tumors. Data were presented as mean ± SD, **, $p < 0.01$; ***, $p < 0.001$ ($N = 6$). **(E)** HE staining of the subcutaneous tumors. **(F,G)** Immunostaining of KI67 and FBXO22 were performed in the subcutaneous tumors (×10 and ×20). Independent samples *t*-test was used for statistics and the results were expressed as mean ± SD, ***, $p < 0.001$ ($N = 6$).

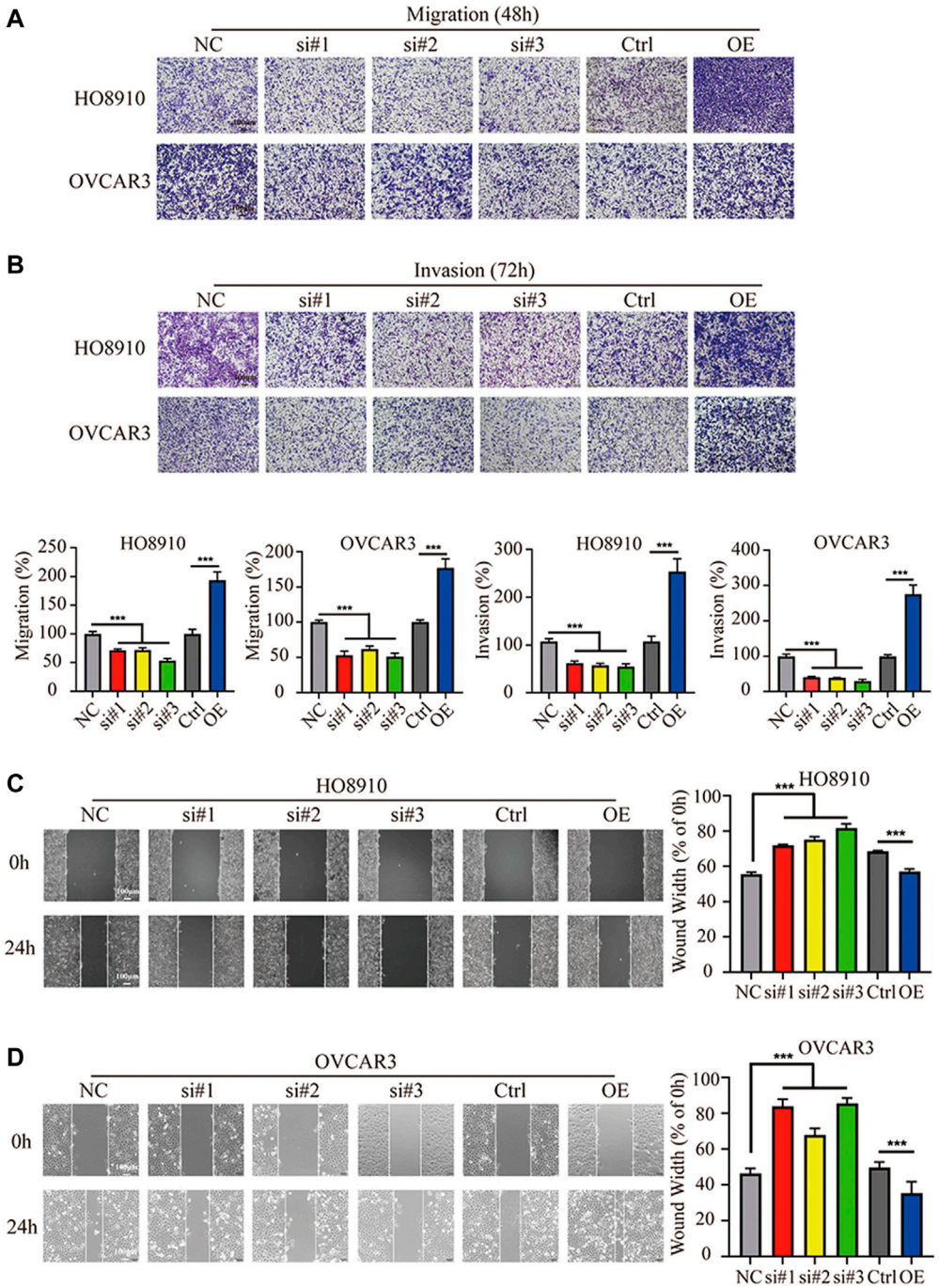

FIGURE 4 | FBXO22 promotes the metastasis of EOCs cells *in vitro*. **(A,B)** Cell wound healing assays in HO8910 and OVCAR3 cells after FBXO22 after treatment with siFBXO22 or overexpression plasmid (×10). Independent sample *t* test was used for statistics between Ctrl and OE, One-way ANOVA was used for NC vs si#1/si#2/si#3, the statistical results were expressed as mean ± standard deviation, ***, $p < 0.001$ ($N = 5$). **(C,D)** The knockdown of FBXO22 inhibits while the overexpression of FBXO22 promotes the migration and invasion of epithelial ovarian cancers cells (×10). Independent sample *t* test was used for statistics between Ctrl and OE, One-way ANOVA was used for NC vs si#1/si#2/si#3, the statistical results were expressed as mean ± SD, ***, $p < 0.001$ (N = 5).

MAPK pathway (Liu et al., 2017; Rasheed et al., 2019; Ahmedy et al., 2020). We found that the expression levels of TRAF6, as well as downstream proteins RAC1, p-P90RSK and BCL-2 changed respectively (**Figures 6C,D**). In conclusion, FBXO22 promotes the growth and metastasis of epithelial ovarian cancers cells via the MMP-2 and MAPK pathways.

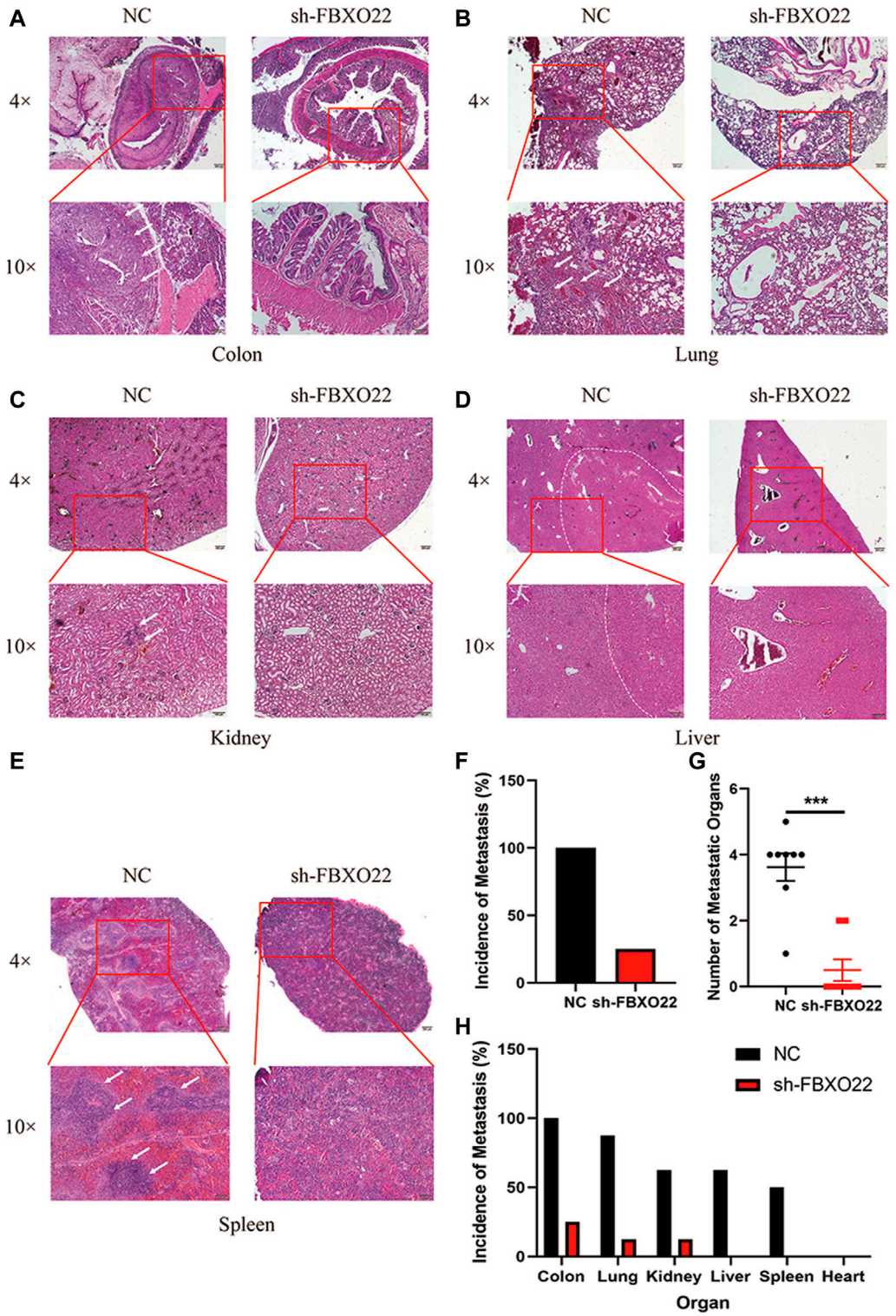

FIGURE 5 | FBXO22 promotes the metastasis of EOCs *in vivo*. HE staining of the NC and sh-FBXO22 mice organs: **(A)** colon; **(B)** lung; **(C)** kidney; **(D)** liver; **(E)** spleen; **(F)** Analysis of metastasis incidence in NC and sh-FBXO22 mice; **(G)** Analysis of metastatic organs number; **(H)** Analysis of metastasis incidence in organs. Independent samples *t*-test was used for statistics and the results were expressed as mean ± SD, ***, $p < 0.001$ ($N = 6$).

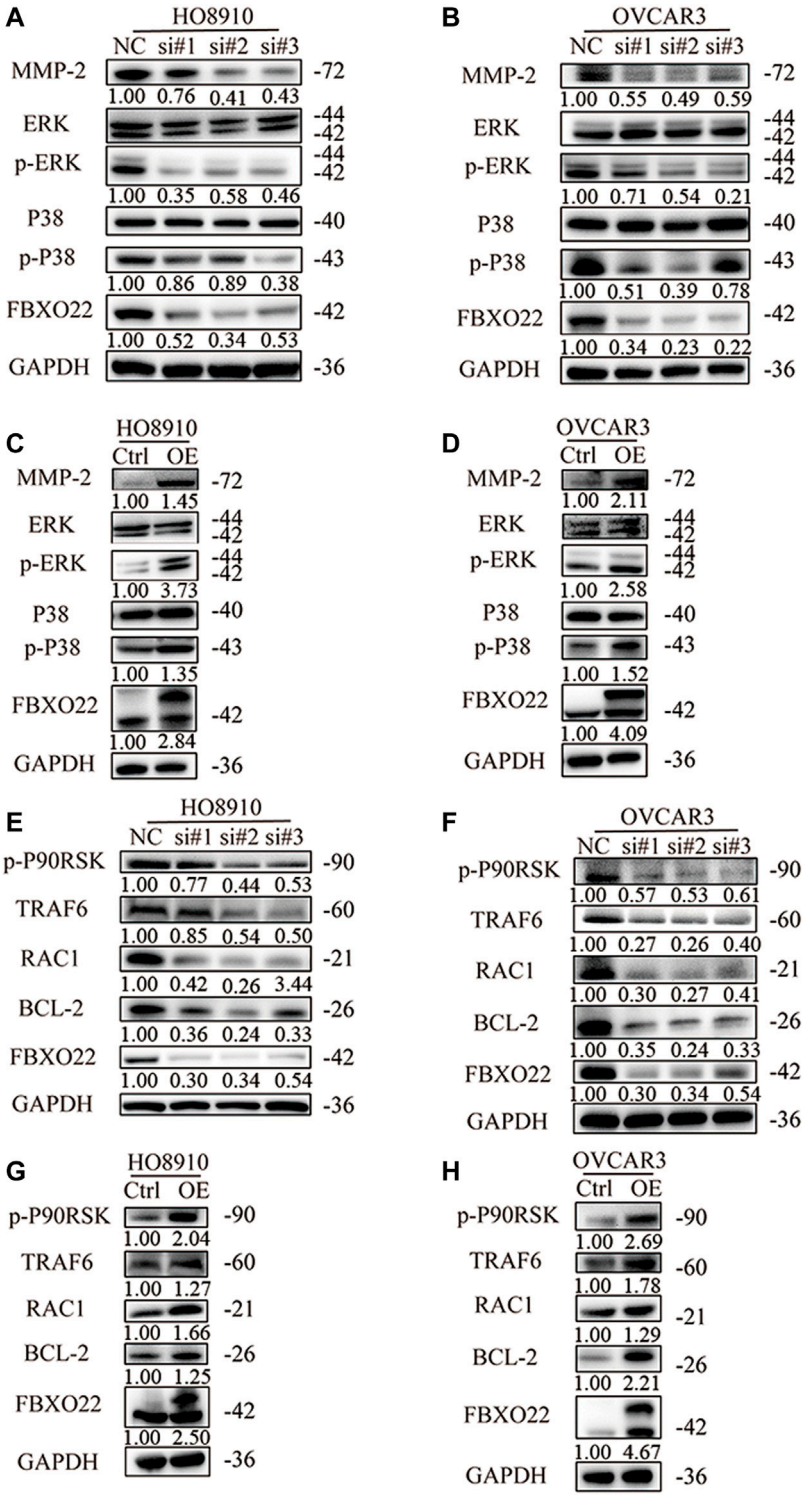

FIGURE 6 | FBXO22 promotes the growth and metastasis of EOCs cells via MMP2 and MAPK pathway. Western blot analysis was performed to measure the expression of MMP-2 and MAPK pathway related proteins in HO8910 and OVCAR3 cells after treatment with siFBXO22 **(A)**, and those in FBXO22 overexpressed HO8910 and OVCAR3 cells **(B)**. Western blot analysis was performed to measure the expression of TRAF6, RAC1, p-P90RSK and BCL-2 in FBXO22 interfered HO8910 and OVCAR3 cells **(C)**, and those in FBXO22 overexpressed HO8910 and OVCAR3 cells **(D)**.

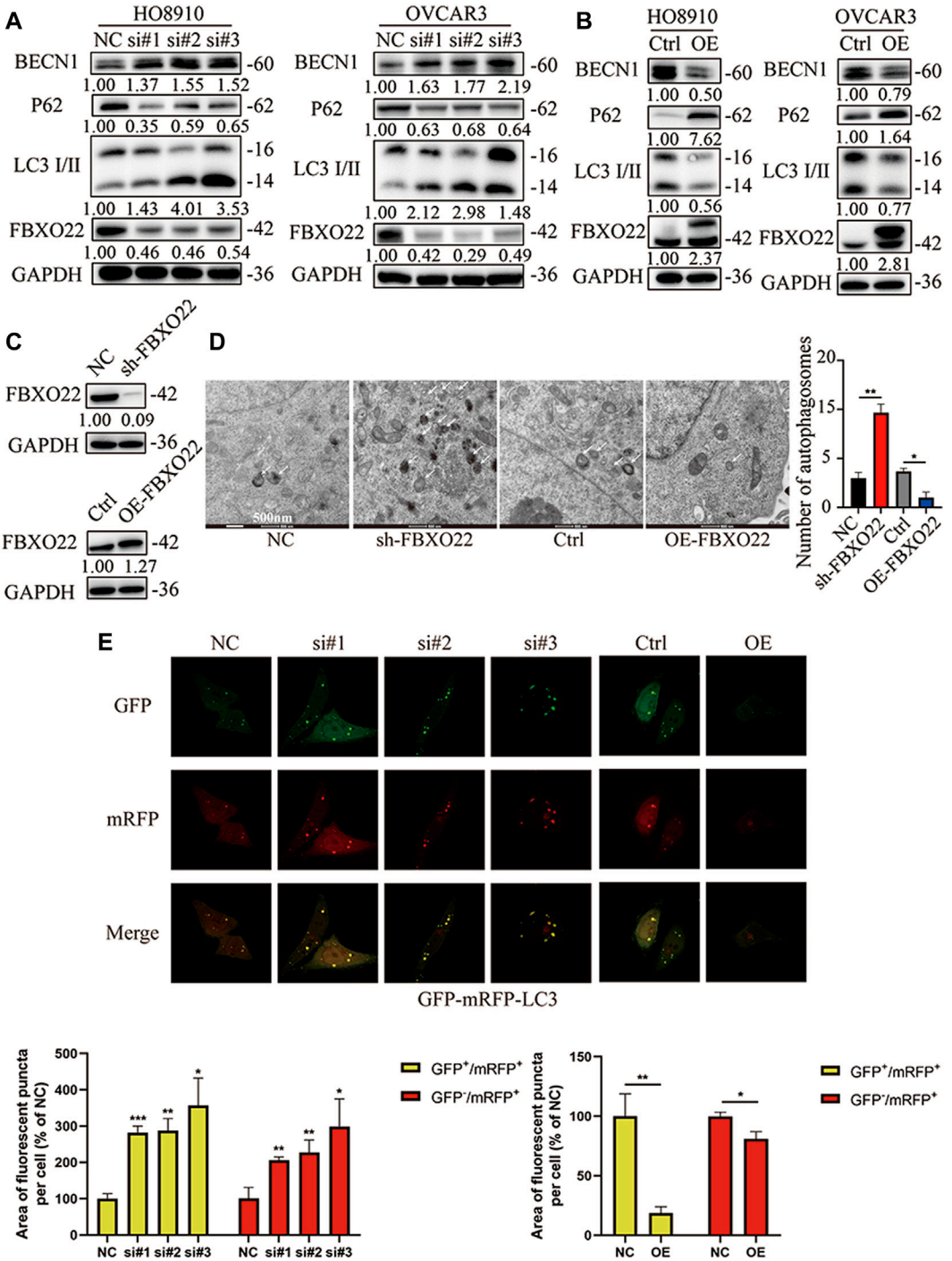

FIGURE 7 | FBXO22 inhibits autophagy of EOCs cells. Western blot shows the expression of P62 and LC3 I/II proteins in FBXO22 interfered HO8910 and OVCAR3 cells **(A)**, and those in FBXO22 overexpressed HO8910 and OVCAR3 cells **(B)**. s.t: short time exposure, l.t: long time exposure; **(C)** Expression of FBXO22 in stable cell lines was confirmed by western blot. **(D)** Autophagosomes observed by electron microscopy (×8,000). **(E)** mRFP-GFP-LC3 shows the change of autophagy flux in HO8910 cells by confocal (×100). Independent samples *t*-test was used for statistics and the results were expressed as mean ± SD, *, $p < 0.05$; **, $p < 0.01$; ***, $p < 0.001$ ($N = 5$).

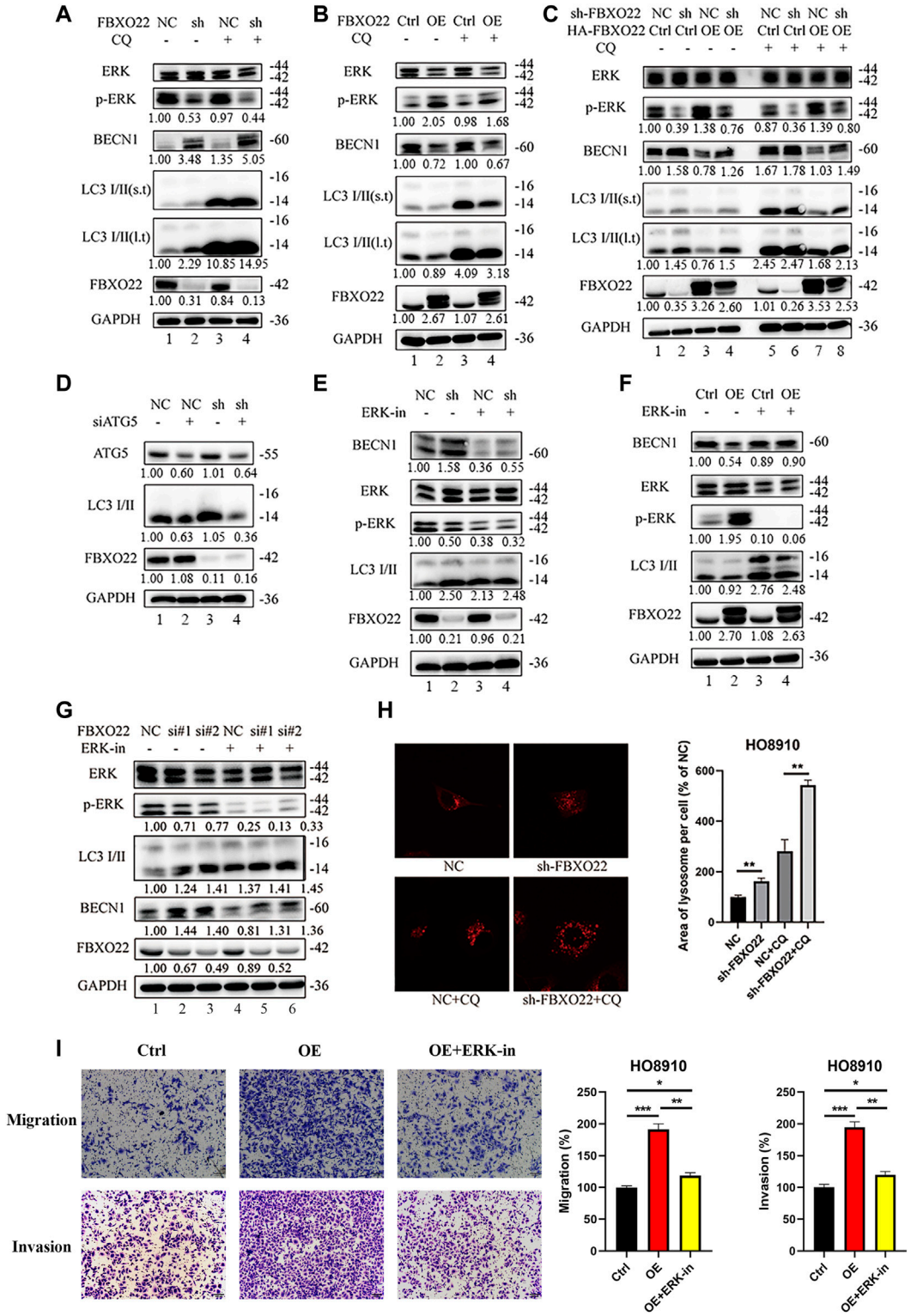

FIGURE 8 | The inhibition in autophagy of FBXO22 is p-ERK depended. **(A)** Western blot results of ERK, p-ERK, BECN1, LC3 I/II, FBXO22 and GAPDH in the stable NC and sh-FBXO22 HO8910 cells. **(B)** HO8910 cell were transfected with pcDNA3.1-Ctrl (Ctrl) or HA-FBXO22 plasmid (OE), then treated with CQ. **(C)** The stable NC and sh-FBXO22 HO8910 cells were transfected with pcDNA3.1-Ctrl (Ctrl) or HA-FBXO22 plasmid (OE), then treated with CQ. **(D)** The stable NC and sh-FBXO22 HO8910 cells were transfected with NC and siATG5. **(E)** The stable NC and sh-FBXO22 HO8910 cells were treated with ERK inhibitor. **(F)** HO8910 cell were transfected with pcDNA3.1-Ctrl (Ctrl) or HA-FBXO22 plasmid (OE), then treated with ERK inhibitor. **(G)** HO8910 cell were transfected with Negative Control siRNA (NC)

(*Continued*)

FIGURE 8 | or siRNAs of FBXO22 (si#1, si#2 and si#3), then treated with ERK inhibitor. Protein levels were demonstrated by Western blot. **(H)** The lysosomal tracker was transfected in the stable NC and sh-FBXO22 HO8910 cells. **(I)** Migration and invasion assay in HO8910 cells treated with Ctrl plasmid **(left)**, OE plasmid **(middle)** and OE plasmid as well as ERK1/2 inhibitor **(right)**. Independent samples *t*-test was used for statistics and the results were expressed as mean ± SD, *, $p < 0.05$; **, $p < 0.01$; ***, $p < 0.001$ ($N = 5$).

FBXO22 Inhibits the Autophagy of Epithelial Ovarian Cancers

Significantly, TRAF6 and BCL-2, which were proved correlated with FBXO22 in former study, reported to regulate autophagy (Shi and Kehrl, 2010; Fernández et al., 2018; Min et al., 2018). Thus, we hypothesized that FBXO22 could affect autophagy. LC3 I/II is one of the most important autophagy markers. The transformation from LC3 I to LC3 II reflects the process of autophagy, and P62 is the substrate of autophagy. The results shown that the rate of transformation from LC3 I to LC3 II increased and the substrate P62 decreased after FBXO22 interference, indicating that autophagy was enhanced (**Figure 7A**). By contrast, after the overexpression of FBXO22, the rate of transformation from LC3 I to LC3 II decreased, and the substrate p62 increased, indicating that autophagy was reduced (**Figure 7B**). BECN1, which plays a central role in autophagy, increased after FBXO22 knockout and decreased after FBXO22 overexpression (**Figures 7A,B**).

Then, stable cell lines were established (**Figure 7C**). Autophagosomes were observed through electron microscope, and the results confirmed that FBXO22 inhibits the autophagy flux of epithelial ovarian cancers cells (**Figure 7D**). To observe the autophagy flux directly, we infected the cells with the autophagy dual fluorescent virus mRFP-GFP-LC3. The results shown that FBXO22 knockdown increased the number of yellow autophagosomes, indicating that the induced production of autophagosomes increased. Meanwhile, the number of produced autophagosomes was reduced after FBXO22 was overexpressed (**Figure 7E**).

The Regulation of Autophagy by FBXO22 Depends on p-ERK

Chloroquine (CQ), an inhibitor of LC3B degradation in autolysosomes, was used to verify autophagy flux. Autophagy flux increased after FBXO22 knockout but decreased after FBXO22 overexpression, and was negatively correlated with p-ERK (**Figures 8A,B** lane 1 and 2). The result was validated again after CQ was added that FBXO22 inhibits the p-ERK correlated autophagy flux (**Figures 8A,B** lane 3 and 4). Furthermore, the increase in autophagy flux mediated by FBXO22 knockout was suppressed after FBXO22 was re-overexpressed (**Figure 8C** lane 3,4 vs. 1,2). The result was validated again after CQ was added (**Figure 8C** lane 7,8). ATG5 involved in autophagic vesicle formation and is a key protein in the process of autophagosome production. We then inhibited the formation of autophagosomes by knocking down ATG5 with siRNA and found that the increased autophagy flux was suppressed (**Figure 8D**).

To validate the essential functions of p-ERK, ERK1/2 inhibitor 1, a potent orally bioavailable ERK1/2 inhibitor, was used. The results shown that the level of p-ERK was decreased by the ERK inhibitor, which enhanced autophagy flux in HO8910 cells with FBXO22 knockdown or overexpression (**Figures 8E–G**). Moreover, lysosomal tracker was used. FBXO22 knockout increased the lysosomes (**Figure 8H**). In addition, the rescue Transwell matrige migration and invasion assays were carried out. As we can see, the migration and invasion percentage were declined in FBXO22 overexpression cells after using ERK1/2 inhibitor (**Figure 8I**).

In conclusion, FBXO22 inhibits the autophagy of EOCs, and the inhibition function is p-ERK dependent.

DISCUSSION

There is tremendous amount of research and focus on EOC as it presents in advanced stages and is the most fatal of the gynecologic malignancies. Since EOC does not have symptoms specific to cancer, there are no early screening and detection modalities (Kim et al., 2012; Lokadasan et al., 2016). Thus, around 75% of women are diagnosed in advanced stage disease (FIGO IIIc or IV) (Kim et al., 2012; Lokadasan et al., 2016). Moreover, clinical treatments for epithelial ovarian cancers have bottlenecks, and the molecular targets of epithelial ovarian cancers are extremely difficult to find, and thus the molecular mechanism of epithelial ovarian cancers remains a major research topic. Our study found that FBXO22 expression increased, and the increase was correlated with clinicopathological factors in patients with epithelial ovarian cancers. These results shown that FBXO22 has an inducing effect *in vivo* and *in vitro*, showing that FBXO22 is a potential target for the clinical diagnosis and treatment of epithelial ovarian cancers.

E3 ligase is the core component of the ubiquitination cascade. It controls the specificity of a substrate and directly binds to the substrate. Hundreds of E3 ubiquitin ligases are found in humans (Skaar et al., 2013). Among them, SKP1-cullin 1 (CUL1)-F-box (SCF) E3 ligase complex is by far the most characteristic E3 ligase family. The SCF complex is composed of four subunits, namely, the adaptor protein SKP1, the ring finger protein RBX1/2, the scaffold protein CUL1, and the variable F-box protein that recognizes a specific substrate (Frescas and Pagano, 2008). Although not all F-box proteins have good characteristics, many F-box proteins, such as SKP2, FBXW7, FBXO4, and FBXO32, are related to the cancer development and progression and cancer cachexia (Sukari et al., 2016). FBXO22, as a member of the F-box protein family, targets and degrades different proteins, such as PTEN, LKB1, P21, and HDM2. Our research shown that FBXO22 promotes growth and metastasis and inhibits autophagy via the MAPK/ERK pathway. However, the molecule that binds to FBXO22 directly is still unknown.

The results obtained generally supported the antitumor effect of autophagy in the early stage of tumorigenesis. Autophagy facilitates the removal of abnormal and damaged structures or harmful substances from normal cells. If not removed, these structures and substances can promote mutations and other cancer features. Some studies shown that BECN1 is a haploid-deficient tumor suppressor gene and supported the theory that autophagy can inhibit tumor formation as a tumor suppressor gene. A pioneering study of autophagy depletion by knocking out BECN1 (encoding Beclin-1) shown that spontaneous tumors occur in BECN1$^{+/-}$ mice (Aita et al., 1999; Liang et al., 1999; Qu et al., 2003; Yue et al., 2003; Shen et al., 2008).

Some core proteins engage in crosstalk between apoptosis and autophagy, including BCL-2 family members. Anti-apoptotic BCL-2 members inhibit autophagy by binding to BECN1, which contains a functional BH3 domain that inserts into the hydrophobic groove of anti-apoptotic BCL-2 members to regulate autophagy (Kang et al., 2011). Post-translational modifications of BECN1 or BCL-2 contribute to their interaction and autophagy induction. Thr108 phosphorylation of BECN1 promotes BCL-2–BECN1 interaction (Maejima et al., 2013). Anti-apoptotic BCL-2 members are globular proteins formed by nine α-helices with a hydrophobic cleft known as BH3 binding-groove at the surface; this cleft can accommodate the BH3 domains of pro-apoptotic or BH3-only members (Czabotar et al., 2014). Thus, anti-apoptotic BCL-2 members can interact with monomeric BAX or BAK to prevent their oligomerization or to antagonize BH3-only members by interacting with their BH3 domains (Willis et al., 2005; Llambi et al., 2011). Our results shown that FBXO22 increases the expression of BCL-2 and decreases the expression of BECN1. However, whether FBXO22 inhibits the apoptosis in epithelial ovarian cancers remains unclear.

Epithelial ovarian cancer is recognized as a heterogeneous disease and is classified according to histologic subtype: high-grade serous, low-grade serous, clear cell, endometrioid, and mucinous (Gilks and Prat, 2009). The mitogen-activated protein kinase pathway plays a prominent role in the pathogenesis of low-grade serous carcinoma of the ovary, and provides an attractive target for novel therapeutic agents. Mutations in KRAS or BRAF have been reported; the rates vary across studies (KRAS 19–35% and BRAF 2–33%) (Singer et al., 2003; Wong et al., 2010). Downstream inhibition of the MAPK pathway is therefore an attractive target for novel therapeutic agents in low-grade serous carcinoma. Selumetinib, a MEK1/2 inhibitor, demonstrates promising efficacy in women with relapsed low-grade serous carcinoma, and further trials of MEK-inhibition are underway (McLachlan et al., 2016). Our study demonstrated the correlation between FBXO22 and MAPK/ERK, which may provide new ideas for the treatment of epithelial ovarian cancer. However, the deep connection and therapeutic efficacy of combination therapy between FBXO22 and ERK/MEK inhibitor remain to be explored.

In summary, our study is the first to report that FBXO22 promotes growth and metastasis and inhibits autophagy in epithelial ovarian cancers, and these functions depend on the MAPK/ERK pathway. These findings suggest FBXO22 as a novel target of epithelial ovarian cancers assessment and treatment.

DATA AVAILABILITY STATEMENT

The original contributions presented in the study are included in the article/Supplementary Material, further inquiries can be directed to the corresponding authors.

ETHICS STATEMENT

The animal study was reviewed and approved by The ethics approval statements for animal work were provided by the Institutional Animal Care and Use Committee of Xuzhou Medical University.

AUTHOR CONTRIBUTIONS

WL, YW, and JB provided study concept and design. ML, XZ, and HY collected and analyzed the data. XZ, HY, and BS performed the experiments. ML and XZ wrote the manuscript. All authors approved the final version of manuscript.

FUNDING

This work was supported by grants from the National Natural Science Foundation of China (No. 82172918, 82072649), the Outstanding Youth Foundation of Jiangsu Province (BK20200046), the Postdoctoral Science Foundation of China (2019M651813) and the Shanghai Municipal Commission of Health (201940284).

ACKNOWLEDGMENTS

We sincerely appreciate researchers who worked for this experiment. The transmission electron microscope experiment in this article were completed in Public Experimental Research Center of Xuzhou Medical University, and thanks the teacher Biyu Zhang for her support and help during the experiment.

REFERENCES

Ahmedy, O. A., Ibrahim, S. M., Salem, H. H., and Kandil, E. A. (2020). Antiulcerogenic Effect of Melittin via Mitigating TLR4/TRAF6 Mediated NF-κB and p38MAPK Pathways in Acetic Acid-Induced Ulcerative Colitis in Mice. *Chem. Biol. Interact.* 331, 109276. doi:10.1016/j.cbi.2020.109276

Aita, V. M., Liang, X. H., Murty, V. V., Pincus, D. L., Yu, W., Cayanis, E., et al. (1999). Cloning and Genomic Organization of Beclin 1, a Candidate Tumor Suppressor Gene on Chromosome 17q21. *Genomics* 59, 59–65. doi:10.1006/geno.1999.5851

Bai, J., Wu, K., Cao, M. H., Yang, Y., Pan, Y., Liu, H., et al. (2019). SCFFBXO22 Targets HDM2 for Degradation and Modulates Breast Cancer Cell Invasion and Metastasis. *Proc. Natl. Acad. Sci. U S A.* 116, 11754–11763. doi:10.1073/pnas.1820990116

Cheng, J., Lin, M., Chu, M., Gong, L., Bi, Y., and Zhao, Y. (2020). Emerging Role of FBXO22 in Carcinogenesis. *Cell Death Discov.* 6, 66. doi:10.1038/s41420-020-00303-0

Cheng, Y., Qiu, F., Tashiro, S., Onodera, S., and Ikejima, T. (2008). ERK and JNK Mediate TNFalpha-Induced P53 Activation in Apoptotic and Autophagic L929 Cell Death. *Biochem. Biophys. Res. Commun.* 376, 483–488. doi:10.1016/j.bbrc.2008.09.018

Coleman, R. L., Monk, B. J., Sood, A. K., and Herzog, T. J. (2013). Latest Research and Treatment of Advanced-Stage Epithelial Ovarian Cancer. *Nat. Rev. Clin. Oncol.* 10, 211–224. doi:10.1038/nrclinonc.2013.5

Czabotar, P. E., Lessene, G., Strasser, A., and Adams, J. M. (2014). Control of Apoptosis by the BCL-2 Protein Family: Implications for Physiology and Therapy. *Nat. Rev. Mol. Cel Biol.* 15, 49–63. doi:10.1038/nrm3722

Dikopoltsev, E., Foltyn, V. N., Zehl, M., Jensen, O. N., Mori, H., Radzishevsky, I., et al. (2014). FBXO22 Protein Is Required for Optimal Synthesis of the N-Methyl-D-Aspartate (NMDA) Receptor Coagonist D-Serine. *J. Biol. Chem.* 289, 33904–33915. doi:10.1074/jbc.M114.618405

Fan, M., and Chambers, T. C. (2001). Role of Mitogen-Activated Protein Kinases in the Response of Tumor Cells to Chemotherapy. *Drug Resist. Updat.* 4, 253–267. doi:10.1054/drup.2001.0214

Fernández, Á. F., Sebti, S., Wei, Y., Zou, Z., Shi, M., McMillan, K. L., et al. (2018). Disruption of the Beclin 1-BCL2 Autophagy Regulatory Complex Promotes Longevity in Mice. *Nature* 558, 136–140. doi:10.1038/s41586-018-0162-7

Frescas, D., and Pagano, M. (2008). Deregulated Proteolysis by the F-Box Proteins SKP2 and Beta-TrCP: Tipping the Scales of Cancer. *Nat. Rev. Cancer* 8, 438–449. doi:10.1038/nrc2396

Ge, M. K., Zhang, N., Xia, L., Zhang, C., Dong, S. S., Li, Z. M., et al. (2020). FBXO22 Degrades Nuclear PTEN to Promote Tumorigenesis. *Nat. Commun.* 11, 1720. doi:10.1038/s41467-020-15578-1

Gilks, C. B., and Prat, J. (2009). Ovarian Carcinoma Pathology and Genetics: Recent Advances. *Hum. Pathol.* 40, 1213–1223. doi:10.1016/j.humpath.2009.04.017

Guo, F., Liu, J., Han, X., Zhang, X., Lin, T., Wang, Y., et al. (2019). FBXO22 Suppresses Metastasis in Human Renal Cell Carcinoma via Inhibiting MMP-9-Mediated Migration and Invasion and VEGF-Mediated Angiogenesis. *Int. J. Biol. Sci.* 15, 647–656. doi:10.7150/ijbs.31293

Hait, W. N., Jin, S., and Yang, J. M. (2006). A Matter of Life or Death (Or Both): Understanding Autophagy in Cancer. *Clin. Cancer Res.* 12, 1961–1965. doi:10.1158/1078-0432.CCR-06-0011

Hippert, M. M., O'Toole, P. S., and Thorburn, A. (2006). Autophagy in Cancer: Good, Bad, or Both? *Cancer Res.* 66, 9349–9351. doi:10.1158/0008-5472.CAN-06-1597

Kang, R., Zeh, H. J., Lotze, M. T., and Tang, D. (2011). The Beclin 1 Network Regulates Autophagy and Apoptosis. *Cell Death Differ.* 18, 571–580. doi:10.1038/cdd.2010.191

Kim, A., Ueda, Y., Naka, T., and Enomoto, T. (2012). Therapeutic Strategies in Epithelial Ovarian Cancer. *J. Exp. Clin. Cancer Res.* 31, 14. doi:10.1186/1756-9966-31-14

Liang, X. H., Jackson, S., Seaman, M., Brown, K., Kempkes, B., Hibshoosh, H., et al. (1999). Induction of Autophagy and Inhibition of Tumorigenesis by Beclin 1. *Nature* 402, 672–676. doi:10.1038/45257

Lignitto, L., LeBoeuf, S. E., Homer, H., Jiang, S., Askenazi, M., Karakousi, T. R., et al. (2019). Nrf2 Activation Promotes Lung Cancer Metastasis by Inhibiting the Degradation of Bach1. *Cell* 178, 316. doi:10.1016/j.cell.2019.06.003

Liu, X., Cao, H., Li, J., Wang, B., Zhang, P., Dong Zhang, X., et al. (2017). Autophagy Induced by DAMPs Facilitates the Inflammation Response in Lungs Undergoing Ischemia-Reperfusion Injury through Promoting TRAF6 Ubiquitination. *Cel Death Differ.* 24, 683–693. doi:10.1038/cdd.2017.1

Llambi, F., Moldoveanu, T., Tait, S. W., Bouchier-Hayes, L., Temirov, J., McCormick, L. L., et al. (2011). A Unified Model of Mammalian BCL-2 Protein Family Interactions at the Mitochondria. *Mol. Cel* 44, 517–531. doi:10.1016/j.molcel.2011.10.001

Lokadasan, R., James, F. V., Narayanan, G., and Prabhakaran, P. K. (2016). Targeted Agents in Epithelial Ovarian Cancer: Review on Emerging Therapies and Future Developments. *Ecancermedicalscience* 10, 626. doi:10.3332/ecancer.2016.626

Maejima, Y., Kyoi, S., Zhai, P., Liu, T., Li, H., Ivessa, A., et al. (2013). Mst1 Inhibits Autophagy by Promoting the Interaction between Beclin1 and Bcl-2. *Nat. Med.* 19, 1478–1488. doi:10.1038/nm.3322

Malemud, C. J. (2006). Matrix Metalloproteinases (MMPs) in Health and Disease: an Overview. *Front. Biosci.* 11, 1696–1701. doi:10.2741/1915

McLachlan, J., Lima, J. P., Dumas, L., and Banerjee, S. (2016). Targeted Agents and Combinations in Ovarian Cancer: where Are We Now? *Expert Rev. Anticancer Ther.* 16, 441–454. doi:10.1586/14737140.2016.1162101

Miller, K. D., Siegel, R. L., Lin, C. C., Mariotto, A. B., Kramer, J. L., Rowland, J. H., et al. (2016). Cancer Treatment and Survivorship Statistics, 2016. *CA Cancer J. Clin.* 66, 271–289. doi:10.3322/caac.21349

Min, Y., Kim, M. J., Lee, S., Chun, E., and Lee, K. Y. (2018). Inhibition of TRAF6 Ubiquitin-Ligase Activity by PRDX1 Leads to Inhibition of NFKB Activation and Autophagy Activation. *Autophagy* 14, 1347–1358. doi:10.1080/15548627.2018.1474995

Murphy, L. O., and Blenis, J. (2006). MAPK Signal Specificity: the Right Place at the Right Time. *Trends Biochem. Sci.* 31, 268–275. doi:10.1016/j.tibs.2006.03.009

Nakayama, K. I., and Nakayama, K. (2006). Ubiquitin Ligases: Cell-Cycle Control and Cancer. *Nat. Rev. Cancer* 6, 369–381. doi:10.1038/nrc1881

Ogier-Denis, E., Pattingre, S., El Benna, J., and Codogno, P. (2000). Erk1/2-dependent Phosphorylation of Galpha-Interacting Protein Stimulates its GTPase Accelerating Activity and Autophagy in Human colon Cancer Cells. *J. Biol. Chem.* 275, 39090–39095. doi:10.1074/jbc.M006198200

Oh, S. H., and Lim, S. C. (2009). Endoplasmic Reticulum Stress-Mediated Autophagy/apoptosis Induced by Capsaicin (8-Methyl-N-Vanillyl-6-Nonenamide) and Dihydrocapsaicin Is Regulated by the Extent of C-Jun NH2-terminal Kinase/extracellular Signal-Regulated Kinase Activation in WI38 Lung Epithelial Fibroblast Cells. *J. Pharmacol. Exp. Ther.* 329, 112–122. doi:10.1124/jpet.108.144113

Qu, X., Yu, J., Bhagat, G., Furuya, N., Hibshoosh, H., Troxel, A., et al. (2003). Promotion of Tumorigenesis by Heterozygous Disruption of the Beclin 1 Autophagy Gene. *J. Clin. Invest.* 112, 1809–1820. doi:10.1172/JCI20039

Ramos, J. W. (2008). The Regulation of Extracellular Signal-Regulated Kinase (ERK) in Mammalian Cells. *Int. J. Biochem. Cel Biol.* 40, 2707–2719. doi:10.1016/j.biocel.2008.04.009

Rasheed, Z., Rasheed, N., Abdulmonem, W. A., and Khan, M. I. (2019). MicroRNA-125b-5p Regulates IL-1β Induced Inflammatory Genes via Targeting TRAF6-Mediated MAPKs and NF-κB Signaling in Human Osteoarthritic Chondrocytes. *Sci. Rep.* 9, 6882. doi:10.1038/s41598-019-42601-3

Reid, B. M., Permuth, J. B., and Sellers, T. A. (2017). Epidemiology of Ovarian Cancer: a Review. *Cancer Biol. Med.* 14, 9–32. doi:10.20892/j.issn.2095-3941.2016.0084

Sarikas, A., Hartmann, T., and Pan, Z. Q. (2011). The Cullin Protein Family. *Genome Biol.* 12, 220. doi:10.1186/gb-2011-12-4-220

Sarikas, A., Xu, X., Field, L. J., and Pan, Z. Q. (2008). The Cullin7 E3 Ubiquitin Ligase: a Novel Player in Growth Control. *Cell Cycle* 7, 3154–3161. doi:10.4161/cc.7.20.6922

Shen, Y., Li, D. D., Wang, L. L., Deng, R., and Zhu, X. F. (2008). Decreased Expression of Autophagy-Related Proteins in Malignant Epithelial Ovarian Cancer. *Autophagy* 4, 1067–1068. doi:10.4161/auto.6827

Shi, C. S., and Kehrl, J. H. (2010). TRAF6 and A20 Regulate Lysine 63-linked Ubiquitination of Beclin-1 to Control TLR4-Induced Autophagy. *Sci. Signal.* 3, ra42. doi:10.1126/scisignal.2000751

Siegel, R. L., Miller, K. D., and Jemal, A. (2016). Cancer Statistics, 2016. *CA Cancer J. Clin.* 66, 7–30. doi:10.3322/caac.21332

Singer, G., Oldt, R., 3rd, Cohen, Y., Wang, B. G., Sidransky, D., Kurman, R. J., et al. (2003). Mutations in BRAF and KRAS Characterize the Development of Low-Grade Ovarian Serous Carcinoma. *J. Natl. Cancer Inst.* 95, 484–486. doi:10.1093/jnci/95.6.484

Sivaprasad, U., and Basu, A. (2008). Inhibition of ERK Attenuates Autophagy and Potentiates Tumour Necrosis Factor-Alpha-Induced Cell Death in MCF-7 Cells. *J. Cel Mol. Med.* 12, 1265–1271. doi:10.1111/j.1582-4934.2008.00282.x

Skaar, J. R., Pagan, J. K., and Pagano, M. (2013). Mechanisms and Function of Substrate Recruitment by F-Box Proteins. *Nat. Rev. Mol. Cel Biol.* 14, 369–381. doi:10.1038/nrm3582

Sukari, A., Muqbil, I., Mohammad, R. M., Philip, P. A., and Azmi, A. S. (2016). F-BOX Proteins in Cancer Cachexia and Muscle Wasting: Emerging Regulators and Therapeutic Opportunities. *Semin. Cancer Biol.* 36, 95–104. doi:10.1016/j.semcancer.2016.01.002

Tan, M. K., Lim, H. J., and Harper, J. W. (2011). SCF(FBXO22) Regulates Histone H3 Lysine 9 and 36 Methylation Levels by Targeting Histone Demethylase

KDM4A for Ubiquitin-Mediated Proteasomal Degradation. *Mol. Cel Biol.* 31, 3687–3699. doi:10.1128/MCB.05746-11

Wang, Z., Liu, P., Inuzuka, H., and Wei, W. (2014). Roles of F-Box Proteins in Cancer. *Nat. Rev. Cancer* 14, 233–247. doi:10.1038/nrc3700

Willis, S. N., Chen, L., Dewson, G., Wei, A., Naik, E., Fletcher, J. I., et al. (2005). Proapoptotic Bak Is Sequestered by Mcl-1 and Bcl-xL, but Not Bcl-2, until Displaced by BH3-Only Proteins. *Genes Dev.* 19, 1294–1305. doi:10.1101/gad.1304105

Wong, K. K., Tsang, Y. T., Deavers, M. T., Mok, S. C., Zu, Z., Sun, C., et al. (2010). BRAF Mutation Is Rare in Advanced-Stage Low-Grade Ovarian Serous Carcinomas. *Am. J. Pathol.* 177, 1611–1617. doi:10.2353/ajpath.2010.100212

Yue, Z., Jin, S., Yang, C., Levine, A. J., and Heintz, N. (2003). Beclin 1, an Autophagy Gene Essential for Early Embryonic Development, Is a Haploinsufficient Tumor Suppressor. *Proc. Natl. Acad. Sci. U S A.* 100, 15077–15082. doi:10.1073/pnas.2436255100

Zhang, L., Chen, J., Ning, D., Liu, Q., Wang, C., Zhang, Z., et al. (2019). FBXO22 Promotes the Development of Hepatocellular Carcinoma by Regulating the Ubiquitination and Degradation of P21. *J. Exp. Clin. Cancer Res.* 38, 101. doi:10.1186/s13046-019-1058-6

Zheng, Y., Chen, H., Zhao, Y., Zhang, X., Liu, J., Pan, Y., et al. (2020). Knockdown of FBXO22 Inhibits Melanoma Cell Migration, Invasion and Angiogenesis via the HIF-1α/VEGF Pathway. *Invest. New Drugs* 38, 20–28. doi:10.1007/s10637-019-00761-z

Zhu, X. N., He, P., Zhang, L., Yang, S., Zhang, H. L., Zhu, D., et al. (2019). FBXO22 Mediates Polyubiquitination and Inactivation of LKB1 to Promote Lung Cancer Cell Growth. *Cell Death Dis.* 10, 486. doi:10.1038/s41419-019-1732-9

Conflict of Interest: The authors declare that the research was conducted in the absence of any commercial or financial relationships that could be construed as a potential conflict of interest.

Publisher's Note: All claims expressed in this article are solely those of the authors and do not necessarily represent those of their affiliated organizations, or those of the publisher, the editors and the reviewers. Any product that may be evaluated in this article, or claim that may be made by its manufacturer, is not guaranteed or endorsed by the publisher.

frontiers in Pharmacology

MINI REVIEW
published: 10 December 2021
doi: 10.3389/fphar.2021.773909

The Art of War: Ferroptosis and Pancreatic Cancer

Jiao Liu[1]*, *Rui Kang*[2] and *Daolin Tang*[2]*

[1]The Third Affiliated Hospital of Guangzhou Medical University, Guangzhou, China, [2]Department of Surgery, UT Southwestern Medical Center, Dallas, TX, United States

Pancreatic cancer is a devastating gastrointestinal cancer, characterized by late diagnosis, low treatment success rate, and poor survival prognosis. The most common pathological type of pancreatic cancer is pancreatic ductal adenocarcinoma (PDAC), which is mainly driven by the K-Ras oncogene. Ferroptosis was originally described as Ras-dependent cell death, but is now defined as lipid peroxidation-mediated regulated necrosis, accompanied by excessive activation of the autophagy degradation pathway and limited membrane repair capacity. The impaired ferroptotic pathway is involved in many types of cancer, including PDAC. On the one hand, the chronic inflammation caused by ferroptotic damage contributes to the formation of K-Ras-driven PDAC. On the other hand, drug-induced ferroptosis is an emerging strategy to suppress tumor growth in established PDAC. In this mini-review, we outline the core process of ferroptosis, discuss the regulatory mechanism of ferroptosis in PDAC, and highlight some of the challenges of targeting ferroptosis in PDAC therapy.

Keywords: autophagy, ferroptosis, pancreatic cancer, tumorigenesis, targeted therapy

OPEN ACCESS

Edited by:
Olivier Feron,
Université catholique de Louvain, Belgium

Reviewed by:
Yongguang Tao,
Central South University, China
Sung Eun Kim,
Korea University, South Korea

***Correspondence:**
Jiao Liu
2018683073@gzhmu.edu.cn
Daolin Tang
daolin.tang@utsouthwestern.edu

Specialty section:
This article was submitted to Pharmacology of Anti-Cancer Drugs, a section of the journal Frontiers in Pharmacology

Received: *10 September 2021*
Accepted: *29 November 2021*
Published: *10 December 2021*

Citation:
Liu J, Kang R and Tang D (2021) The Art of War: Ferroptosis and Pancreatic Cancer. Front. Pharmacol. 12:773909. doi: 10.3389/fphar.2021.773909

INTRODUCTION

Pancreatic ductal adenocarcinoma (PDAC) is the most common pathological type of pancreatic cancer, accounting for more than 90% of all pancreatic malignancies (Kleeff et al., 2016). The *KRAS* gene is mutated in approximately 85–90% of PDAC and is the main driver of pancreatic tumorigenesis (Buscail et al., 2020). Despite improvements in surgical techniques, chemotherapy regimens, and the introduction of neoadjuvant chemoradiotherapy or chemoimmunotherapy, PDAC still accounts for 3% of all cancers and 7% of all cancer deaths in the United States (Siegel et al., 2021). Due to modifiable lifestyle factors, such as high-fat diets, the incidence of PDAC is increasing (Heinen et al., 2009). The American Cancer Society estimates that by 2021, there will be 60,430 pancreatic cancer diagnoses and 48,220 deaths in the United States (Siegel et al., 2021). From 2014 to 2021, the general 5-years survival rate of patients with PDAC slowly increased from 6 to 10%. The poor outcomes of PDAC are mainly due to the late diagnosis of the disease and its resistance to treatments involving cell death. Thus, it is essential to understand the cell death machinery of PDAC and to develop new treatment strategies (Chen et al., 2021a). Recent studies have shown that inducing ferroptotic cell death may be an attractive therapy for various types of cancer, including PDAC (Su et al., 2020; Chen et al., 2021b; Shi et al., 2021).

THE CORE MECHANISM OF FERROPTOSIS

The term "ferroptosis" was first proposed to describe a type of iron-dependent non-apoptotic cell death in cancer cells with RAS mutations (Dixon et al., 2012). Today, the core molecular mechanism

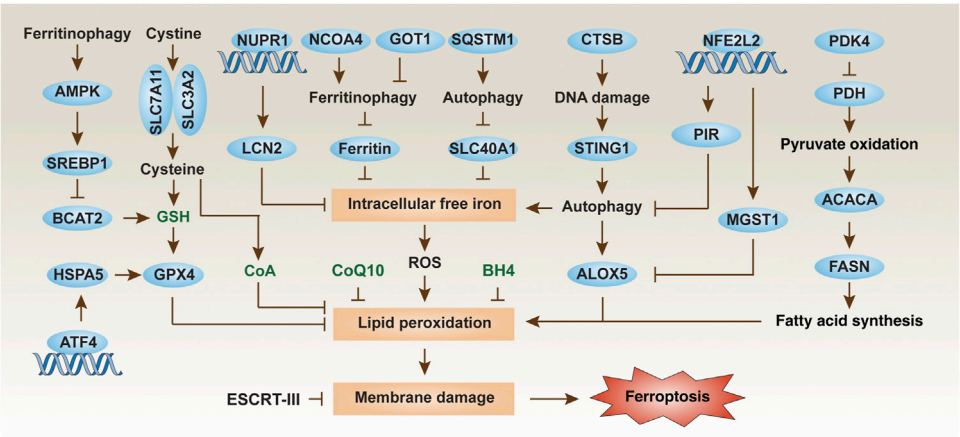

FIGURE 1 | Regulation mechanisms and signaling pathways of ferroptosis in PDAC cells. Ferroptosis is an iron-dependent cell death driven by lipid peroxidation and subsequent membrane damage. The level of ferroptosis in PDAC cells can be regulated in multiple ways, including through autophagic degradation, transcription factors, and metabolic pathways.

of ferroptosis is involved in the production of lipid peroxidation and subsequent plasma membrane damage (Stockwell et al., 2017; Tang et al., 2020a). During ferroptosis, reactive oxygen species (ROS) can be obtained from the iron-dependent Fenton reaction, a mitochondrial electron transport chain-mediated reaction, or a membrane NADPH oxidase (NOX)-mediated reaction (Xie et al., 2016). However, the connection between the multiple sources of ROS production during ferroptosis remains obscure. Three antioxidant systems [glutathione (GSH), coenzyme Q10 (CoQ10), and tetrahydrobiopterin (BH4)] have been shown to inhibit ferroptosis caused by oxidative damage (Dixon et al., 2012; Bersuker et al., 2019a; Kraft et al., 2020; Dai et al., 2020a). Among them, the system xc^--GSH-glutathione peroxidase 4 (GPX4) axis plays a major role in blocking lipid peroxidation during ferroptosis (**Figure 1**). System xc^-, a transmembrane protein complex composed of two subunits, namely solute carrier family 7 member 11 (SLC7A11) and solute carrier family 3 member 2 (SLC3A2), mediates the entry of cystine into cells to exchange glutamate. Once cystine enters cells, it is quickly reduced to cysteine, which is required for GSH synthesis. GSH is a substrate for the antioxidant GPX4 to prevent the accumulation of toxic lipids. GPX4 and SLC7A11 also regulate other types of non-ferroptotic death, indicating that it may not be possible to distinguish them based on a single molecular event (Ran et al., 2006; Canli et al., 2016; Kang et al., 2018; Chen et al., 2021c). Alternatively, apoptosis inducing factor mitochondria associated 2 (AIFM2) plays a GPX4-independent role in limiting ferroptosis by sustaining the production of reduced GSH (Bersuker et al., 2019b; Doll et al., 2019) or increasing membrane repair (Dai et al., 2020a).

Polyunsaturated fatty acids (PUFAs) are the main peroxidation substrates for ferroptosis in cell membranes. Consequently, increasing PUFA synthesis can increase the sensitivity to ferroptosis, which is positively regulated by acyl-coenzyme A (CoA) synthetase long-chain family member 4 (ACSL4) (Dixon et al., 2015; Yuan et al., 2016; Doll et al., 2017; Kagan et al., 2017). Apart from this, the biosynthesis of plasmalogens from peroxisomes also contributes to ferroptosis (Zou et al., 2020a). PUFAs are found in most foods, but are highest in fatty fish, seeds, and nuts. It is possible to adjust the sensitivity to ferroptosis by changing the content and type of dietary fat. Finally, two families of lipid peroxidases [lipoxygenase (ALOX) and cytochrome P450 oxidoreductase (POR)] play a context-dependent role in mediating toxic lipid production during ferroptosis (Yang et al., 2016; Wenzel et al., 2017; Chu et al., 2019; Li et al., 2020; Zou et al., 2020b; Yan et al., 2021). However, the molecular effectors of ferroptosis have not yet been identified. As a conservative membrane repair mechanism, the calcium-dependent endosomal sorting complexes required for transport (ESCRT)-III pathway can be activated to separate damaged membranes in various cancer cells (including PDAC) during ferroptosis (Dai et al., 2020b).

FERROPTOSIS IN PANCREATIC TUMORIGENESIS

The inflammatory process has become a key mediator of the development and progression of pancreatic cancer. Consistent with this notion, ferroptotic damage can release damage-associated molecular pattern molecules (DAMPs), thereby creating an inflammatory tumor microenvironment for tumor growth and development (Bianchi, 2007). For example, the conditional depletion of *Gpx4* in the pancreas or a high-iron diet accelerates the development of $Kras^{G12D}$-driven pancreatic tumors in mice (Dai et al., 2020c). This process is mediated by the release of nuclear DAMP 8-hydroxydeoxyguanosine (8-OH-dG) by ferroptotic cells. The released 8-OH-dG activates the stimulator of interferon response CGAMP interactor 1 (STING1, also known as TMEM173) pathway in surrounding macrophages, thereby inducing the release of cytokines (e.g., interleukin 6) to maintain the chronic inflammatory

TABLE 1 | Main regulators of ferroptosis in PDAC.

Name	Function	Mechanism	Refs.
NCOA4	Promoter of ferroptosis	Induce autophagic degradation of ferritin	Hou et al. (2016)
SQSTM1	Promoter of ferroptosis	Induce autophagic degradation of SLC40A1	Li et al. (2021a)
STING1	Promoter of ferroptosis	Induce autophagy-dependent ferroptosis	Li et al. (2020)
ALOX5	Promoter of ferroptosis	Induce lipid ROS production	Li et al. (2020)
CTSB	Promoter of ferroptosis	Induce DNA damage and lysosomal dysfunction	Kuang et al. (2020), Nagakannan et al. (2021)
ACACA	Promoter of ferroptosis	Increase fatty acid synthesis	Song et al. (2021)
FASN	Promoter of ferroptosis	Increase fatty acid synthesis	Song et al. (2021)
PDH	Promoter of ferroptosis	Increase pyruvate oxidation	Song et al. (2021)
AMPK	Promoter of ferroptosis	Inhibit BACT2 expression	Wang et al. (2020)
SREBP1	Promoter of ferroptosis	Inhibit BACT2 expression	Wang et al. (2020)
SLC7A11	Repressor of ferroptosis	Increase GSH or CoA synthesis	Badgley et al. (2020), Zhang et al. (2019), Badgley et al. (2020)
GOT1	Repressor of ferroptosis	Inhibit autophagic degradation of ferritin	Kremer et al. (2021)
SLC40A1	Repressor of ferroptosis	Promote iron export	Li et al. (2021a)
Ferritin	Repressor of ferroptosis	Promote iron storage	Hou et al. (2016)
ATF4	Repressor of ferroptosis	Induce HSPA5 expression	Zhu et al. (2017)
HSPA5	Repressor of ferroptosis	Inhibit GPX4 degradation	Zhu et al. (2017)
GPX4	Repressor of ferroptosis	Inhibit lipid ROS production	Zhu et al. (2017), Liu et al. (2021a)
PDK4	Repressor of ferroptosis	Inhibit pyruvate oxidation	Song et al. (2021)
BCAT2	Repressor of ferroptosis	Increase GSH synthesis	Wang et al. (2020)
MTOR	Repressor of ferroptosis	Inhibit autophagy-dependent ferroptosis	Liu et al. (2021a)
NFE2L2	Repressor of ferroptosis	Inhibit expression of antioxidant gene	Kuang et al. (2021), Hu et al. (2021)
MGST1	Repressor of ferroptosis	Inhibit oxidative stress	Kuang et al. (2021)
PIR	Repressor of ferroptosis	Inhibit oxidative DNA damage	Kuang et al. (2021)
POLG	Repressor of ferroptosis	Inhibit mitochondrial DNA damage-dependent autophagy	Li et al. (2020)
TFAM	Repressor of ferroptosis	Inhibit mitochondrial DNA damage-dependent autophagy	Li et al. (2020)
NUPR1	Repressor of ferroptosis	Increase LCN2 expression	Liu et al. (2021b)
LCN2	Repressor of ferroptosis	Promote iron export	Liu et al. (2021b)
ESCRT-III	Repressor of ferroptosis	Inhibit membrane repair	Dai et al. (2020b)

microenvironment of pancreatic tumorigenesis driven by $Kras^{G12D}$ (Dai et al., 2020c). These results explain the basic aspects of the inflammatory tumor microenvironment mediated by ferroptotic death in PDAC. Ferroptotic PDAC cells can also release $KRAS^{G12D}$ protein into the extracellular space, and macrophages take up $KRAS^{G12D}$ protein through advanced glycosylation end-product specific receptor (AGER, best known as RAGE), which eventually leads to macrophage polarization for tumor growth (Dai et al., 2020d). In contrast, the conditional deletion of *Slc7a11* in the pancreas inhibits $Kras^{G12D}$/$Tp53^{R172H}$ mutation-driven pancreatic tumors in mice (Badgley et al., 2020), suggesting that additional *Tp53* mutations may transform the carcinogenic effects of ferroptotic damage into anticancer effects in $Kras^{G12D}$-driven PDAC. In general, these animal studies show that ferroptosis plays a dual role in pancreatic tumorigenesis, depending on gene deletions and mutations. It remains questionable whether genomic instability can produce genetic diversity in driving ferroptosis. It also needs to examine whether *Gpx4* depletion has a similar effect in promoting mutant KRAS-driven tumorigenesis in other cancers, such as colorectal cancer and non-small cell lung cancer.

REGULATION OF FERROPTOSIS IN PDAC

The regulator of PDAC is involved in multiple molecules (**Table 1**). We discussed them from the following three perspectives, although this classification is rough considering the observed diversity of molecular mechanisms of ferroptosis.

DEGRADATION SYSTEMS

Macroautophagy (hereafter autophagy) and the ubiquitin-proteasome system are the two degradation systems responsible for regulating cellular homeostasis (Li et al., 2021b). Depending on the substrate being degraded, autophagic pathways play a significant role in pancreatic ferroptosis. A significant recent advance is that the autophagic degradation of the iron storage protein ferritin (a process also called ferritinophagy) (Hou et al., 2016) or the iron transporter solute carrier family 40 member 1 (SLC40A1, also known as ferroportin-1) (Li et al., 2021a) can increase the accumulation of free iron in cells, thereby inducing the Fenton reaction to produce ROS for ferroptosis in PDAC cells (**Figure 1**). More recently, glutamic-oxaloacetic transaminase 1 (GOT1) inhibition promotes ferroptosis in PDAC by inducing ferritinophagy to initiate iron-dependent oxidative damage (Kremer et al., 2021). Nuclear receptor coactivator 4 (NCOA4) (Hou et al., 2016) and sequestosome 1 (SQSTM1) (Li et al., 2021a) function as autophagy receptors to recognize and degrade ferritin or SLC40A1, respectively, during ferroptosis. However, identifying specific autophagy cargo receptors for ferroptosis remains a challenge.

In addition to the classic ferroptosis activators (erastin and RSL3), zalcitabine (a drug used to treat human immunodeficiency virus infection) can cause mitochondrial damage, thereby activating STING1-dependent autophagy pathway and inducing ALOX5-related ferroptotic death in human PDAC cells (Li et al., 2020). The activation and release of cystatin B (CSTB, a lysosomal cysteine protease) can partially act as a mediator of ferroptosis by amplifying the STING1 pathway in human PDAC cells, arguing that ferroptosis is a form of autophagy-dependent lysosomal cell death coupled with a DNA sensor pathway (Kuang et al., 2020; Nagakannan et al., 2021).

In addition to autophagy, other degradation pathways also regulate ferroptosis by affecting the stability of GPX4 protein. For example, transcription factor 4 (ATF4)-mediated heat shock protein family A (Hsp70) member 5 (HSPA5) expression related to endoplasmic reticulum stress can prevent the degradation of GPX4, thereby increasing the ferroptosis resistance of PDAC cells (Zhu et al., 2017). In contrast, high-dose rapamycin can induce ferroptosis by promoting the degradation of GPX4 (Liu et al., 2021a). Because autophagy is generally used as a pro-survival pathway in PDAC, the induction of autophagy-dependent ferroptosis may provide a way to kill established PDAC cells (Görgülü et al., 2020). Nevertheless, clinically available autophagy inhibitors (e.g., chloroquine) may weaken the anticancer activity of ferroptosis activators (Li et al., 2021a).

METABOLIC PATHWAYS

In the 1920s, Otto Warburg discovered that even in the presence of oxygen (aerobic glycolysis), cultured tumor cells had a high rate of glucose uptake and glycolysis (Vander Heiden et al., 2009). This Warburg effect triggers metabolic abnormalities, thereby promoting tumor growth or causing treatment resistance to transitional drugs (e.g., gemcitabine). Indeed, hyperglycemia occurs frequently in most patients with pancreatic cancer and is associated with a poor prognosis. Unexpectedly, ferroptosis in PDAC cells induced by system xc^- inhibitors (erastin and sulfasalazine), but not GPX4 inhibitors (RSL3 and FIN56), requires high-glucose conditions (Song et al., 2021). In contrast, high-glucose limits staurosporine-induced cell death (Song et al., 2021). These results imply that glucose selectively confers susceptibility to ferroptosis, rather than apoptosis. In line with this notion, diabetes induced by a high-fat diet in mice also increased the anti-PDAC activity of ferroptosis inducers (Song et al., 2021).

Subsequent studies of metabolic mechanisms showed that pyruvate oxidation, but not pyruvate reduction, in mitochondria promotes ferroptosis in PDAC cells by activating acetyl-CoA carboxylase alpha (ACACA) and fatty acid synthase (FASN)-mediated fatty acid synthesis and subsequent ALOX5-dependent lipid peroxidation (**Figure 1**) (Song et al., 2021). This pro-ferroptosis process caused by glucose is negatively regulated by pyruvate dehydrogenase kinase 4 (PDK4), a repressor of pyruvate oxidation in mitochondria by blocking pyruvate dehydrogenase (PDH) (Song et al., 2021). An integrated metabolic reprogramming pathway may drive the production of fatty acid for ferroptosis.

In addition to glucose and lipids, amino acids also affect ferroptosis. For example, branched chain amino acid aminotransferase 2 (BCAT2) can inhibit ferroptosis in PDAC cells that is induced by system xc^- inhibitors (erastin, sorafenib, and sulfasalazine) by producing sulfur amino acid for GSH synthesis (Wang et al., 2020). Moreover, system xc^--mediated cystine input is beneficial to the biosynthesis of CoA, which plays a GSH-independent role in preventing IKE-induced ferroptosis in PDAC cells (Badgley et al., 2020). These findings provide a feedback mechanism for controlling ferroptosis through amino acid metabolism. Although the role of AMP-activated protein kinase (AMPK)-sterol regulatory element binding transcription factor 1 (SREBP1) pathway in ferroptosis is related to the type of cancer, the activation of this signaling pathway by ferritinophagy limits the expression of BCAT2 in PDAC cells (Wang et al., 2020). Since AMPK is an important kinase in various metabolic pathways, targeting the AMPK pathway combined with ferroptosis induction may be a strategy worthy of further exploration (Song et al., 2018; Lee et al., 2020). Recently, the endogenous metabolite itaconate induces iron death in PDAC cells by activating ferritinophagy (Qu et al., 2021), highlighting the new metabolic pathway of ferroptosis.

STRESS SENSORS

Another important research direction is to identify and study redox sensors in ferroptosis. Nuclear factor, erythroid 2-like 2 (NFE2L2, best known as NRF2) is a transcription factor that is sensitive to the redox state of cells under various cell death stimuli. NFE2L2 is negatively regulated by Kelch-like ECH-associated protein 1 (KEAP1), which targets NFE2L2 for protein degradation by the ubiquitin-proteasome system. In response to the stimulation of ferroptosis, autophagy receptor SQSTM1 binds and inhibits KEAP1, thereby promoting the activation of NFE2L2 and increasing the expression of antioxidant genes (Anandhan et al., 2020). Specifically, the NFE2L2-targeted genes microsomal glutathione S-transferase 1 (MGST1) (Kuang et al., 2021) and pirin (PIR) (Hu et al., 2021) have recently been identified as redox-sensitive repressors of ferroptosis in PDAC cells by binding ALOX5 or limiting the oxidative damage of DNA-mediated autophagy, respectively (**Figure 1**). These studies provide new insight into the complex mechanisms of NFE2L2-dependent redox signaling in PDAC. A key unanswered question is whether certain types of cell death are particularly associated with dysregulated NFE2L2 signaling.

In addition to NFE2L2, other stress-related transcription factors are also involved in the defense of ferroptosis. Nuclear protein 1, transcriptional regulator (NUPR1) is upregulated in the pancreas during various stresses, including ferroptotic damage (Liu et al., 2021b). As a pro-survival response, NUPR1-mediated expression of the iron exporter lipocalin 2 (LCN2) can prevent iron accumulation, thereby limiting oxidative damage and

ferroptosis in PDAC cells (**Figure 1**) (Liu et al., 2021b). In a xenograft mouse model, the NUPR1 inhibitor ZZW-115 enhances the tumor suppressor effect of the ferroptosis activator IKE (Liu et al., 2021b). Together, targeting antioxidant transcription factors can enhance ferroptosis-mediated therapy in PDAC, although downstream effectors may be diverse.

OPPORTUNITIES AND CHALLENGES

The past few years have witnessed a rapid explosion of studies on ferroptosis and various cancers, including PDAC. Because PDAC responds weakly to all current treatment regimens, targeting the ferroptotic pathway may provide an alternative approach for this lethal disease. Exciting preclinical studies have shown that several drugs [artesunate (Eling et al., 2015) and zalcitabine (Li et al., 2020)] can suppress PDAC by inducing ferroptosis, although they may have off-target effects. Several therapy regimens related to ferroptosis (e.g., gemcitabine + sulfasalazine, sorafenib + sulfasalazine) have also been explored in PDAC in animal models. The ultimate goal of research is to develop clinically available drugs for the modulation of the ferroptosis pathway that can kill PDAC alone or in combination with other drugs. The challenge in developing effective drugs that induce ferroptosis is not to cause unnecessary side effects and to target specific sites in ferroptotic pathway. Under treatment selection pressure, resistance to treatment may appear due to the expansion of pre-existing subclonal populations or the evolution of drug-resistant cells (Yang et al., 2014; Hangauer et al., 2017; Viswanathan et al., 2017). Although there are currently no clinical trials of ferroptosis-dependent treatment strategies, it is still necessary to establish the relationship between molecular characteristics and response to specific drugs in preclinical studies.

In addition to understanding the processes and functions of ferroptosis in the context of the ever-evolving complex cell death network, we need to develop powerful ferroptotic biomarkers in humans (Chen et al., 2021d). Since inflammation is a double-edged sword, overcoming the immune side effects of ferroptotic damage may require a deeper understanding of the interaction between tumor cell death and immune cells. Several studies in other cancers have shown that DAMP released during erastin-induced ferroptosis may activate adaptive tumor immunity to inhibit tumor growth (Efimova et al., 2020; Tang et al., 2020b). However, the occurrence of ferroptosis in dendritic cells or $CD8^+$ T cells can impair their anti-tumor function (Han et al., 2021; Ma et al., 2021). In the next few years, the impact of genetic mutations, degradation pathways, and metabolic plasticity on susceptibility to ferroptosis in the different component cells of the tumor microenvironment will be an active area of research (Chen et al., 2021e; Chen et al., 2021f; Tang et al., 2021).

AUTHOR CONTRIBUTIONS

All authors listed have made a substantial, direct, and intellectual contribution to the work, and approved it for publication.

ACKNOWLEDGMENTS

We thank Dave Primm (Department of Surgery, University of Texas Southwestern Medical Center) for his critical reading of the manuscript.

REFERENCES

Anandhan, A., Dodson, M., Schmidlin, C. J., Liu, P., and Zhang, D. D. (2020). Breakdown of an Ironclad Defense System: The Critical Role of NRF2 in Mediating Ferroptosis. *Cell Chem Biol* 27, 436–447. doi:10.1016/j.chembiol.2020.03.011

Badgley, M. A., Kremer, D. M., Maurer, H. C., DelGiorno, K. E., Lee, H. J., Purohit, V., et al. (2020). Cysteine Depletion Induces Pancreatic Tumor Ferroptosis in Mice. *Science* 368, 85–89. doi:10.1126/science.aaw9872

Bersuker, K., Hendricks, J. M., Li, Z., Magtanong, L., Ford, B., Tang, P. H., et al. (2019). The CoQ Oxidoreductase FSP1 Acts Parallel to GPX4 to Inhibit Ferroptosis. *Nature* 575, 688–692. doi:10.1038/s41586-019-1705-2

Bersuker, K., Hendricks, J. M., Li, Z., Magtanong, L., Ford, B., Tang, P. H., et al. (2019). The CoQ Oxidoreductase FSP1 Acts Parallel to GPX4 to Inhibit Ferroptosis. *Nature* 575, 688–692. doi:10.1038/s41586-019-1705-2

Bianchi, M. E. (2007). DAMPs, PAMPs and Alarmins: All We Need to Know about Danger. *J. Leukoc. Biol.* 81, 1–5. doi:10.1189/jlb.0306164

Buscail, L., Bournet, B., and Cordelier, P. (2020). Role of Oncogenic KRAS in the Diagnosis, Prognosis and Treatment of Pancreatic Cancer. *Nat. Rev. Gastroenterol. Hepatol.* 17, 153–168. doi:10.1038/s41575-019-0245-4

Canli, Ö., Alankuş, Y. B., Grootjans, S., Vegi, N., Hültner, L., Hoppe, P. S., et al. (2016). Glutathione Peroxidase 4 Prevents Necroptosis in Mouse Erythroid Precursors. *Blood* 127, 139–148. doi:10.1182/blood-2015-06-654194

Chen, X., Comish, P. B., Tang, D., and Kang, R. (2021). Characteristics and Biomarkers of Ferroptosis. *Front Cel Dev Biol* 9, 637162. doi:10.3389/fcell.2021.637162

Chen, X., Kang, R., Kroemer, G., and Tang, D. (2021). Broadening Horizons: the Role of Ferroptosis in Cancer. *Nat. Rev. Clin. Oncol.* 18, 280. doi:10.1038/s41571-020-00462-0

Chen, X., Kang, R., Kroemer, G., and Tang, D. (2021). Ferroptosis in Infection, Inflammation, and Immunity. *J. Exp. Med.* 218, 218. doi:10.1084/jem.20210518

Chen, X., Kang, R., Kroemer, G., and Tang, D. (2021f). Targeting Ferroptosis in Pancreatic Cancer: A Double-Edged Sword. *Trends Cancer.* 7, 891–901. doi:10.1016/j.trecan.2021.04.005

Chen, X., Li, J., Kang, R., Klionsky, D. J., and Tang, D. (2021e). Ferroptosis: Machinery and Regulation. *Autophagy* 17, 2054–2081. doi:10.1080/15548627.2020.1810918

Chen, X., Zeh, H. J., Kang, R., Kroemer, G., and Tang, D. (2021). Cell Death in Pancreatic Cancer: from Pathogenesis to Therapy. *Nat. Rev. Gastroenterol. Hepatol.* 18, 804–823. doi:10.1038/s41575-021-00486-6

Chu, B., Kon, N., Chen, D., Li, T., Liu, T., Jiang, L., et al. (2019). ALOX12 Is Required for P53-Mediated Tumour Suppression through a Distinct Ferroptosis Pathway. *Nat. Cel Biol* 21, 579–591. doi:10.1038/s41556-019-0305-6

Dai, E., Han, L., Liu, J., Xie, Y., Kroemer, G., Klionsky, D. J., et al. (2020). Autophagy-dependent Ferroptosis Drives Tumor-Associated Macrophage Polarization via Release and Uptake of Oncogenic KRAS Protein. *Autophagy* 16, 2069–2083. doi:10.1080/15548627.2020.1714209

Dai, E., Han, L., Liu, J., Xie, Y., Zeh, H. J., Kang, R., et al. (2020). Ferroptotic Damage Promotes Pancreatic Tumorigenesis through a TMEM173/STING-dependent DNA Sensor Pathway. *Nat. Commun.* 11, 6339. doi:10.1038/s41467-020-20154-8

Dai, E., Meng, L., Kang, R., Wang, X., and Tang, D. (2020). ESCRT-III-dependent Membrane Repair Blocks Ferroptosis. *Biochem. Biophys. Res. Commun.* 522, 415–421. doi:10.1016/j.bbrc.2019.11.110

Dai, E., Zhang, W., Cong, D., Kang, R., Wang, J., and Tang, D. (2020). AIFM2 Blocks Ferroptosis Independent of Ubiquinol Metabolism. *Biochem. Biophys. Res. Commun.* 523, 966. doi:10.1016/j.bbrc.2020.01.066

Dixon, S. J., Lemberg, K. M., Lamprecht, M. R., Skouta, R., Zaitsev, E. M., Gleason, C. E., et al. (2012). Ferroptosis: an Iron-dependent Form of Nonapoptotic Cell Death. *Cell* 149, 1060–1072. doi:10.1016/j.cell.2012.03.042

Dixon, S. J., Winter, G. E., Musavi, L. S., Lee, E. D., Snijder, B., Rebsamen, M., et al. (2015). Human Haploid Cell Genetics Reveals Roles for Lipid Metabolism Genes in Nonapoptotic Cell Death. *ACS Chem. Biol.* 10, 1604–1609. doi:10.1021/acschembio.5b00245

Doll, S., Freitas, F. P., Shah, R., Aldrovandi, M., da Silva, M. C., Ingold, I., et al. (2019). FSP1 Is a Glutathione-independent Ferroptosis Suppressor. *Nature* 575, 693–698. doi:10.1038/s41586-019-1707-0

Doll, S., Proneth, B., Tyurina, Y. Y., Panzilius, E., Kobayashi, S., Ingold, I., et al. (2017). ACSL4 Dictates Ferroptosis Sensitivity by Shaping Cellular Lipid Composition. *Nat. Chem. Biol.* 13, 91–98. doi:10.1038/nchembio.2239

Efimova, I., Catanzaro, E., Van der Meeren, L., Turubanova, V. D., Hammad, H., Mishchenko, T. A., et al. (2020). Vaccination with Early Ferroptotic Cancer Cells Induces Efficient Antitumor Immunity. *J. Immunother. Cancer* 8, 8. doi:10.1136/jitc-2020-001369

Eling, N., Reuter, L., Hazin, J., Hamacher-Brady, A., and Brady, N. R. (2015). Identification of Artesunate as a Specific Activator of Ferroptosis in Pancreatic Cancer Cells. *Oncoscience* 2, 517–532. doi:10.18632/oncoscience.160

Görgülü, K., Diakopoulos, K. N., Kaya-Aksoy, E., Ciecielski, K. J., Ai, J., Lesina, M., et al. (2020). The Role of Autophagy in Pancreatic Cancer: From Bench to the Dark Bedside. *Cells* 99, 1063. doi:10.3390/cells9041063

Han, L., Bai, L., Qu, C., Dai, E., Liu, J., Kang, R., et al. (2021). PPARG-mediated Ferroptosis in Dendritic Cells Limits Antitumor Immunity. *Biochem. Biophys. Res. Commun.* 576, 33–39. doi:10.1016/j.bbrc.2021.08.082

Hangauer, M. J., Viswanathan, V. S., Ryan, M. J., Bole, D., Eaton, J. K., Matov, A., et al. (2017). Drug-tolerant Persister Cancer Cells Are Vulnerable to GPX4 Inhibition. *Nature* 551, 247–250. doi:10.1038/nature24297

Heinen, M. M., Verhage, B. A., Goldbohm, R. A., and van den Brandt, P. A. (2009). Meat and Fat Intake and Pancreatic Cancer Risk in the Netherlands Cohort Study. *Int. J. Cancer* 125, 1118–1126. doi:10.1002/ijc.24387

Hou, W., Xie, Y., Song, X., Sun, X., Lotze, M. T., Zeh, H. J., 3rd, et al. (2016). Autophagy Promotes Ferroptosis by Degradation of Ferritin. *Autophagy* 12, 1425–1428. doi:10.1080/15548627.2016.1187366

Hu, N., Bai, L., Dai, E., Han, L., Kang, R., Li, H., et al. (2021). Pirin Is a Nuclear Redox-Sensitive Modulator of Autophagy-dependent Ferroptosis. *Biochem. Biophys. Res. Commun.* 536, 100–106. doi:10.1016/j.bbrc.2020.12.066

Kagan, V. E., Mao, G., Qu, F., Angeli, J. P., Doll, S., Croix, C. S., et al. (2017). Oxidized Arachidonic and Adrenic PEs Navigate Cells to Ferroptosis. *Nat. Chem. Biol.* 13, 81–90. doi:10.1038/nchembio.2238

Kang, R., Zeng, L., Zhu, S., Xie, Y., Liu, J., Wen, Q., et al. (2018). Lipid Peroxidation Drives Gasdermin D-Mediated Pyroptosis in Lethal Polymicrobial Sepsis. *Cell Host Microbe* 24, 97–e4. doi:10.1016/j.chom.2018.05.009

Kleeff, J., Korc, M., Apte, M., La Vecchia, C., Johnson, C. D., Biankin, A. V., et al. (2016). Pancreatic Cancer. *Nat. Rev. Dis. Primers* 2, 16022. doi:10.1038/nrdp.2016.22

Kraft, V. A. N., Bezjian, C. T., Pfeiffer, S., Ringelstetter, L., Müller, C., Zandkarimi, F., et al. (2020). GTP Cyclohydrolase 1/Tetrahydrobiopterin Counteract Ferroptosis through Lipid Remodeling. *ACS Cent. Sci.* 6, 41–53. doi:10.1021/acscentsci.9b01063

Kremer, D. M., Nelson, B. S., Lin, L., Yarosz, E. L., Halbrook, C. J., Kerk, S. A., et al. (2021). GOT1 Inhibition Promotes Pancreatic Cancer Cell Death by Ferroptosis. *Nat. Commun.* 12, 4860. doi:10.1038/s41467-021-24859-2

Kuang, F., Liu, J., Li, C., Kang, R., and Tang, D. (2020). Cathepsin B Is a Mediator of Organelle-specific Initiation of Ferroptosis. *Biochem. Biophys. Res. Commun.* 533, 1464–1469. doi:10.1016/j.bbrc.2020.10.035

Kuang, F., Liu, J., Xie, Y., Tang, D., and Kang, R. (2021). MGST1 Is a Redox-Sensitive Repressor of Ferroptosis in Pancreatic Cancer Cells. *Cel Chem Biol* 28, 765. doi:10.1016/j.chembiol.2021.01.006

Lee, H., Zandkarimi, F., Zhang, Y., Meena, J. K., Kim, J., Zhuang, L., et al. (2020). Energy-stress-mediated AMPK Activation Inhibits Ferroptosis. *Nat. Cel Biol* 22, 225–234. doi:10.1038/s41556-020-0461-8

Li, C., Zhang, Y., Liu, J., Kang, R., Klionsky, D. J., and Tang, D. (2020). Mitochondrial DNA Stress Triggers Autophagy-dependent Ferroptotic Death. *Autophagy* 17, 948–960. doi:10.1080/15548627.2020.1739447

Li, C., Chen, X., Kang, R., Zeh, H., Klionsky, D. J., and Tang, D. (2021b). Regulation and Function of Autophagy in Pancreatic Cancer. *Autophagy* 17, 3275–3296. doi:10.1080/15548627.2020.1847462

Li, J., Liu, J., Xu, Y., Wu, R., Chen, X., Song, X., et al. (2021a). Tumor Heterogeneity in Autophagy-dependent Ferroptosis. *Autophagy* 17, 3361–3374. doi:10.1080/15548627.2021.1872241

Liu, J., Song, X., Kuang, F., Zhang, Q., Xie, Y., Kang, R., et al. (2021). NUPR1 Is a Critical Repressor of Ferroptosis. *Nat. Commun.* 12, 647. doi:10.1038/s41467-021-20904-2

Liu, Y., Wang, Y., Liu, J., Kang, R., and Tang, D. (2021). Interplay between MTOR and GPX4 Signaling Modulates Autophagy-dependent Ferroptotic Cancer Cell Death. *Cancer Gene Ther.* 28, 55–63. doi:10.1038/s41417-020-0182-y

Ma, X., Xiao, L., Liu, L., Ye, L., Su, P., Bi, E., et al. (2021). CD36-mediated Ferroptosis Dampens Intratumoral CD8+ T Cell Effector Function and Impairs Their Antitumor Ability. *Cell Metab* 33, 1001–e5. doi:10.1016/j.cmet.2021.02.015

Nagakannan, P., Islam, M. I., Conrad, M., and Eftekharpour, E. (2021). Cathepsin B Is an Executioner of Ferroptosis. *Biochim. Biophys. Acta Mol. Cel Res* 1868, 118928. doi:10.1016/j.bbamcr.2020.118928

Ran, Q., Gu, M., Van Remmen, H., Strong, R., Roberts, J. L., and Richardson, A. (2006). Glutathione Peroxidase 4 Protects Cortical Neurons from Oxidative Injury and Amyloid Toxicity. *J. Neurosci. Res.* 84, 202–208. doi:10.1002/jnr.20868

Qu, C., Dai, E., Lai, T., Cao, G., Liu, J., Kang, R., et al. (2021). Itaconic Acid Induces Ferroptosis by Activating Ferritinophagy. *Biochem. Biophys. Res. Commun.* 583, 56–62. doi:10.1016/j.bbrc.2021.10.054

Shi, Z., Zhang, L., Zheng, J., Sun, H., and Shao, C. (2021). Ferroptosis: Biochemistry and Biology in Cancers. *Front. Oncol.* 11, 579286. doi:10.3389/fonc.2021.579286

Siegel, R. L., Miller, K. D., Fuchs, H. E., and Jemal, A. (2021). Cancer Statistics, 2021. *CA A. Cancer J. Clin.* 71, 7–33. doi:10.3322/caac.21654

Song, X., Liu, J., Kuang, F., Chen, X., Zeh, H. J., 3rd, Kang, R., et al. (2021). PDK4 Dictates Metabolic Resistance to Ferroptosis by Suppressing Pyruvate Oxidation and Fatty Acid Synthesis. *Cell Rep* 34, 108767. doi:10.1016/j.celrep.2021.108767

Song, X., Zhu, S., Chen, P., Hou, W., Wen, Q., Liu, J., et al. (2018). AMPK-mediated BECN1 Phosphorylation Promotes Ferroptosis by Directly Blocking System Xc- Activity. *Curr. Biol.* 28, 2388–e5. doi:10.1016/j.cub.2018.05.094

Stockwell, B. R., Friedmann Angeli, J. P., Bayir, H., Bush, A. I., Conrad, M., Dixon, S. J., et al. (2017). Ferroptosis: A Regulated Cell Death Nexus Linking Metabolism, Redox Biology, and Disease. *Cell* 171, 273–285. doi:10.1016/j.cell.2017.09.021

Su, Y., Zhao, B., Zhou, L., Zhang, Z., Shen, Y., Lv, H., et al. (2020). Ferroptosis, a Novel Pharmacological Mechanism of Anti-cancer Drugs. *Cancer Lett.* 483, 127–136. doi:10.1016/j.canlet.2020.02.015

Tang, D., Chen, X., Kang, R., and Kroemer, G. (2021). Ferroptosis: Molecular Mechanisms and Health Implications. *Cell Res.* 31, 107–125. doi:10.1038/s41422-020-00441-1

Tang, D., Kepp, O., and Kroemer, G. (2020b). Ferroptosis Becomes Immunogenic: Implications for Anticancer Treatments. *Oncoimmunology* 10, 1862949. doi:10.1080/2162402X.2020.1862949

Tang, D., and Kroemer, G. (2020a). Ferroptosis. *Curr. Biol.* 30, R1292–R1297. doi:10.1016/j.cub.2020.09.068

Vander Heiden, M. G., Cantley, L. C., and Thompson, C. B. (2009). Understanding the Warburg Effect: the Metabolic Requirements of Cell Proliferation. *Science* 324, 1029–1033. doi:10.1126/science.1160809

Viswanathan, V. S., Ryan, M. J., Dhruv, H. D., Gill, S., Eichhoff, O. M., Seashore-Ludlow, B., et al. (2017). Dependency of a Therapy-Resistant State of Cancer Cells on a Lipid Peroxidase Pathway. *Nature* 547, 453–457. doi:10.1038/nature23007

Wang, K., Zhang, Z., Tsai, H.-i., Liu, Y., Gao, J., Wang, M., et al. (2020). Branched-chain Amino Acid Aminotransferase 2 Regulates Ferroptotic Cell

Death in Cancer Cells. *Cell Death Differ* 28, 1222–1236. doi:10.1038/s41418-020-00644-4

Wenzel, S. E., Tyurina, Y. Y., Zhao, J., St Croix, C. M., Dar, H. H., Mao, G., et al. (2017). PEBP1 Wardens Ferroptosis by Enabling Lipoxygenase Generation of Lipid Death Signals. *Cell* 171, 628–e26. doi:10.1016/j.cell.2017.09.044

Xie, Y., Hou, W., Song, X., Yu, Y., Huang, J., Sun, X., et al. (2016). Ferroptosis: Process and Function. *Cel Death Differ* 23, 369–379. doi:10.1038/cdd.2015.158

Yan, B., Ai, Y., Sun, Q., Ma, Y., Cao, Y., Wang, J., et al. (2021). Membrane Damage during Ferroptosis Is Caused by Oxidation of Phospholipids Catalyzed by the Oxidoreductases POR and CYB5R1. *Mol. Cel* 81, 355–369. doi:10.1016/j.molcel.2020.11.024

Yang, W. S., Kim, K. J., Gaschler, M. M., Patel, M., Shchepinov, M. S., and Stockwell, B. R. (2016). Peroxidation of Polyunsaturated Fatty Acids by Lipoxygenases Drives Ferroptosis. *Proc. Natl. Acad. Sci. U S A.* 113, E4966–E4975. doi:10.1073/pnas.1603244113

Yang, W. S., SriRamaratnam, R., Welsch, M. E., Shimada, K., Skouta, R., Viswanathan, V. S., et al. (2014). Regulation of Ferroptotic Cancer Cell Death by GPX4. *Cell* 156, 317–331. doi:10.1016/j.cell.2013.12.010

Yuan, H., Li, X., Zhang, X., Kang, R., and Tang, D. (2016). Identification of ACSL4 as a Biomarker and Contributor of Ferroptosis. *Biochem. Biophys. Res. Commun.* 478, 1338–1343. doi:10.1016/j.bbrc.2016.08.124

Zhang, Y., Tan, H., Daniels, J. D., Zandkarimi, F., Liu, H., Brown, L. M., et al. (2019). Imidazole Ketone Erastin Induces Ferroptosis and Slows Tumor Growth in a Mouse Lymphoma Model. *Cel Chem Biol* 26, 623–e9. doi:10.1016/j.chembiol.2019.01.008

Zhu, S., Zhang, Q., Sun, X., Zeh, H. J., 3rd, Lotze, M. T., Kang, R., et al. (2017). HSPA5 Regulates Ferroptotic Cell Death in Cancer Cells. *Cancer Res.* 77, 2064–2077. doi:10.1158/0008-5472.CAN-16-1979

Zou, Y., Henry, W. S., Ricq, E. L., Graham, E. T., Phadnis, V. V., Maretich, P., et al. (2020). Plasticity of Ether Lipids Promotes Ferroptosis Susceptibility and Evasion. *Nature* 585, 603–608. doi:10.1038/s41586-020-2732-8

Zou, Y., Li, H., Graham, E. T., Deik, A. A., Eaton, J. K., Wang, W., et al. (2020). Cytochrome P450 Oxidoreductase Contributes to Phospholipid Peroxidation in Ferroptosis. *Nat. Chem. Biol.* 16, 302–309. doi:10.1038/s41589-020-0472-6

Conflict of Interest: The authors declare that the research was conducted in the absence of any commercial or financial relationships that could be construed as a potential conflict of interest.

Publisher's Note: All claims expressed in this article are solely those of the authors and do not necessarily represent those of their affiliated organizations, or those of the publisher, the editors and the reviewers. Any product that may be evaluated in this article, or claim that may be made by its manufacturer, is not guaranteed or endorsed by the publisher.

frontiers in Pharmacology

ORIGINAL RESEARCH
published: 10 January 2022
doi: 10.3389/fphar.2021.781623

NVP-BEZ235 Inhibits Renal Cell Carcinoma by Targeting TAK1 and PI3K/Akt/mTOR Pathways

Bihui Li[1,2†], *Xing Zhang*[1†], *Qianyao Ren*[1], *Li Gao*[3*] and *Jing Tian*[1*]

[1]Guangxi Health Commission Key Laboratory of Tumor Immunology and Receptor-Targeted Drug Basic Research, Guilin Medical University, Guilin, China, [2]Department of Oncology, The Second Affiliated Hospital of Guilin Medical University, Guilin, China, [3]Department of Urinary Surgery, The First Affiliated Hospital of Guilin Medical University, Guilin, China

In spite of the promising *in vitro* and preclinical results, dual PI3K/Akt/mTOR inhibitor NVP-BEZ235, and ATP-competitive mTOR inhibitor PP242 both failed to confirm their inhibitory efficacy against renal cell carcinoma (RCC) in clinical settings. Therefore, a better understanding of the molecular mechanism is essential so as to provide possibilities for their use in combination with other agents. In present study, RCC cell lines (UMRC6, 786-0 and UOK121) were treated with NVP-BEZ235, PP242 or Rapamycin, an mTOR complex 1 (mTORC1)-specific inhibitor. They all suppressed cell proliferation and invasion, induced apoptosis and cell cycle arrest, and the effects were in the order of NVP-BEZ235 > PP242 > Rapamycin. Accordingly, the marked and sustained decrease in speckle-type POZ protein (SPOP) expression and phosphorylation of Akt and mTOR kinases was observed in RCC cells treated with NVP-BEZ235 and PP242, whereas only potent inhibition of mTOR activity was induced in Rapamycin-treated cells. In considering the overactivation of c-Jun and IκB-α in human renal tumor tissue, we next investigated the role of JNK and IKK pathways in the response of RCC cells to these compounds. First of all, transforming growth factor β activated kinase 1 (TAK1)-dependent activation of JNK/(activator protein-1) AP-1 axis in RCC cells was proved by the repression of AP-1 activity with TAK1 or JNK inhibitor. Second, the profound inhibition of TAK1/JNK/AP-1 pathway was demonstrated in RCC cells treated with NVP-BEZ235 or PP242 but not Rapamycin, which is manifested as a reduction in activity of TAK1, c-Jun and AP-1. Meanwhile, subsequent to TAK1 inactivation, the activation of IκB-α was also reduced by NVP-BEZ235 and PP242. Likewise, *in vivo*, treatment with NVP-BEZ235 and PP242 suppressed the growth of xenografts generated from 786-0 and A498 cells, along with decreased expression of phospho-TAK1, phospho-c-Jun, and phospho-IκB-α. In contrast, Rapamycin elicited no significant inhibitory effects on tumor growth and phosphorylation of TAK1, c-Jun and IκB-α. We conclude that besides PI3K/Akt/mTOR signaling, NVP-BEZ235, and PP242 simultaneously target TAK1-dependent pathways in RCC cells. Notably, these effects were more marked in the presence of NVP-BEZ235 than PP242, indicating the potential application of NVP-BEZ235 in combination therapy for RCC.

Keywords: renal cancer, NVP-BEZ235, PI3K, mTOR, TAK1

OPEN ACCESS

Edited by:
Jiaoti Huang,
Duke University, United States

Reviewed by:
Luis E. Arias-Romero,
National Autonomous University of Mexico, Mexico
Xiaodong Sun,
Affiliated Hospital of Weifang Medical University, China

***Correspondence:**
Li Gao
40407864@qq.com
Jing Tian
jingtian117@126.com

†These authors have contributed equally to this work and share first authorship

Specialty section:
This article was submitted to Pharmacology of Anti-Cancer Drugs, a section of the journal Frontiers in Pharmacology

Received: *23 September 2021*
Accepted: *07 December 2021*
Published: *10 January 2022*

Citation:
Li B, Zhang X, Ren Q, Gao L and Tian J (2022) NVP-BEZ235 Inhibits Renal Cell Carcinoma by Targeting TAK1 and PI3K/Akt/mTOR Pathways. Front. Pharmacol. 12:781623. doi: 10.3389/fphar.2021.781623

INTRODUCTION

Renal cell carcinomas (RCC) is the most frequent type of cancer originating from the kidney parenchyma (Inamura, 2017; Pietropaolo et al., 2019). Every year, approximately more than 200,000 individuals are newly diagnosed with RCC worldwide (Bray et al., 2018). Unfortunately, RCC is largely resistant to traditional chemotherapy, radiation, or hormonal therapy, leading to over 100,000 deaths per year (Linehan and Ricketts, 2017). Based on the growing understanding of the underlying molecular pathways in RCC, the drugs targeting the PI3K/Akt/mammalian target of rapamycin (mTOR) have been discovered and evaluated in clinical trials, but their clinical efficacy is limited by resistance, toxicity, and poor tolerability (Guo et al., 2015). To overcome these limitations, the combination with other therapeutic drugs has been attracting the attention of researchers. This requires further elucidation of the mechanism of these PI3K/AKT/mTOR inhibitors.

As is known, activated PI3K/Akt/mTOR signaling pathway is critical for many important cellular processes including proliferation, growth and survival (Chiarini et al., 2015; Kaur and Sharma, 2017). Rapamycin and its analogs are the first generation of mTOR inhibitors that selectively inhibit the activity of mTOR complex 1 (mTORC1), a multiprotein complex containing mTOR (Xu et al., 2016). Although Rapamycin raised the possibility of developing antitumor agent targeting PI3K/Akt/mTOR pathway, results have demonstrated that inhibiting mTORC1 induces feedback activation of the upstream PI3K/Akt pathway and thereby counteracts the anticancer efficacy (Osawa et al., 2019; Roskoski, 2019). Then new generations of agents targeting both mTORC1 and mTOR complex 2 (mTORC2) have been developed, for example PP242 and NVP-BEZ235. They both displayed anti-cancer activity against various types of cancer cells including RCC cells (Yang et al., 2013). What is more, besides inhibiting mTOR, NVP-BEZ235 could bind directly to the ATP-binding domain of PI3K and block PI3K-dependent Akt activation (Alqurashi et al., 2018). It may be hypothesized that dual PI3K/mTOR inhibitor NVP-BEZ235 is a more potent antitumor agent against RCC than the mTOR kinase inhibitor PP242 and selective mTORC1 inhibitor Rapamycin. Nevertheless, to our knowledge, there has been no study comparing the anticancer effects of NVP-BEZ235, PP242, and Rapamycin, not to mention deep investigation of the exact mechanism behind their difference.

Notably, emerging evidence proved that PI3K/Akt/mTOR pathway correlates with a new form of nonapoptotic cell death, ferroptosis, that is distinct from known forms of cell death such as apoptosis, necroptosis, and necrosis (Yi et al., 2020). Ferroptosis is caused by an imbalance in redox homeostasis due to glutathione (GSH) depletion or inactivation of glutathione peroxidase 4 (GPX4) (Hirschhorn and Stockwell, 2019). The dysregulation of ferroptosis has been linked to various cancers (Mou et al., 2019). It was found that inhibition of mTORC1 could trigger the degradation of GPX4 protein, and finally promote ferroptosis in cancer cells (Lei et al., 2021). Accordingly, mTORC1 is also considered as a key ferroptosis modulator. Consequently, the specific inhibition of mTORC1 *via* Rapamycin was demonstrated to induce ferroptotic cancer cell death and inhibit tumorigenesis. Hence, exploring the relationship between mTOR inhibitors and ferroptosis may offer a new perspective for the mechanisms of mTOR inhibitors in RCC.

In this study, as expected, it was demonstrated that NVP-BEZ235 inhibits RCC cells growth *in vitro* and *in vivo*, better than PP242 and Rapamycin. In addition to PI3K/Akt/mTOR signaling pathway, NVP-BEZ235, and PP242 also suppressed the activation of TGF-β-associated kinase 1 (TAK1) and its downstream effectors including c-Jun and IκB-α. Moreover, the inhibition was more remarkable in NVP-BEZ235-treated RCC cells. These results indicated that the dual suppression of PI3K/Akt/mTOR and TAK1 pathways by NVP-BEZ235 and PP242 may link to their greater anticancer activity, and NVP-BEZ235 may be an optimal candidate as mTOR inhibitor for combination therapy in RCC.

MATERIALS AND METHODS

Cell Lines and Reagents

Three human renal cell carcinoma cell lines, UMRC6 (from B Zbar, National Cancer Institute, Bethesda, MD, United States), 786-0 (from W Kaelin, Dana Farber Cancer Institute, Boston, MA, United States), and UOK121 cells (from J. Gnarra, Louisiana State University, Baton Rouge, LA, United States) have been described previously (An et al., 2013). HEK-293 cells were purchased from Shanghai cell bank of the Chinese Academy of Sciences (Shanghai, China). Cells were maintained in Dulbecco's modified Eagle's medium (DMEM; Invitrogen, Carlsbad, CA, United States) supplemented with 10% FBS and 1% penicillin-streptomycin at 37°C in a humidified atmosphere of 5% CO_2. NVP-BEZ235 (Novartis Pharmaceuticals, Basel, Switzerland), PP242 (Sigma-Aldrich, St Louis, MO, United States), and Rapamycin (Santa Cruz Biotechnology, Santa Cruz, CA, United States) were solubilized in DMSO (*in vitro* assays) or a solution of 2% DMSO, 30% PEG 300, 5% Tween 80, and ddH2O (*in vivo* assays). Antibodies against Akt, phospho-Akt, TAK1, phospho-TAK1, IκB-α, phospho-IκB-α, c-Jun, and phospho-c-Jun were all purchased from Cell Signaling Technology (Beverly, MA, United States). Antibodies against phospho-mTOR, speckle-type POZ protein (SPOP), and β-actin were from Santa Cruz Biotechnology.

Clinical Materials

The two RCC tissue microarrays were purchased from Fanpu Biotech, Inc. (Guilin, Guangxi, China). One chip consisted of 87 patients with RCC (65 cases of clear cell RCC and 22 cases of papillary RCC) and samples of normal tissues from 8 patients. The other one included 60 patients with RCC (47 cases of clear cell RCC and 13 cases of papillary RCC) and samples of normal tissues from 5 patients. The chips were heated at 60°C to melt the paraffin, washed in xylene, and hydrated through graded ethanols (100–70%). For antigen retrieval, the chips were heated in Tris-

EDTA for 20 min, and then blocked with 10% goat serum. Phospho-c-Jun and phospho-IκB-α staining was performed by incubation with rabbit anti-phospho-c-Jun antibody (1:100) and rabbit anti-phospho-IκB-α antibody (1:250) at 4°C overnight, followed by incubation of secondary antibody for 1 h at room temperature. Finally, the chips were stained with DAB chromogen solution and counterstained with hematoxylin.

Cell Viability Assays

The three RCC cell lines and HEK-293 cells were seeded in 96-well plates at a density of 1.5×10^3 or 3.0×10^3 per well. Cells were then treated with increasing doses (10, 100, 1,000 nM) of NVP-BEZ235, PP242, and Rapamycin for 48 h, or the equivalent amounts of DMSO as control. MTT (Sigma-Aldrich) was added to each well (1 mg/ml final concentration) and incubated at 37°C for 4 h. Then the plates were incubated with 100 μL of 10% SDS/0.01 N HCl. After incubation overnight, absorbance at 490 nM for each well was determined using a microplate reader (Bio-Rad, Sunnyvale, CA, United States). For colony formation assay, 786-0 and UOK121 cells were seeded in six-well plates with 500 cells per well, and cultured with 200 nM NVP-BEZ235, Rapamycin and PP242, or equivalent amounts of DMSO. Colonies were counted after 10–14 days of incubation.

Flow Cytometry Assay

Cell poptosis was analyzed using FITC Annexin V Apoptosis Detection Kit (BD Biosciences, San Jose, CA, United States). Briefly, after exposure to 100 nM of NVP-BEZ235, PP242, or Rapamycin for 72 h, cells were harvested, washed twice with cold PBS and resuspended in binding buffer at a density of 1×10^6 cells/ml. About 1×10^5 cells were stained with annexin V-FITC and propidium iodide (PI) for 15 min at room temperature in the dark and analyzed using a Beckman FC-500 flow cytometer (Beckman Coulter, CA, United States). For cell cycle assay, cells were respectively treated with different doses (100 and 500 nM) of NVP-BEZ235, PP242, and Rapamycin for 48 h, or equivalent amounts of DMSO. Then cells were fixed with 70% alcohol at 4°C overnight and stained with PI (5 ng/ml) for 20 min at room temperature. The cell distribution at various cell cycle phases were determined by flow cytometry.

Transwell Assay

First, the chamber membranes were coated using Matrigel (50 μg/ml). 2×10^5 cells were added in the upper chambers with medium containing 1% FBS. The lower chamber was filled with DMEM containing 10% FBS with or without 200 nM of NVP-BEZ235, PP242, Rapamycin. After incubating for 48 h, cells invaded to the lower chamber were stained with 0.5% crystal violet, and counted using a microscope at 200 × magnification.

Western Blot Assay

For time-dependent studies, cells were treated with 200 nM of NVP-BEZ235, PP242 and Rapamycin, or the equivalent amounts of DMSO as control. At different time points post-treatment, cells were harvested and lysed by incubation in lysis solution containing protease inhibitors. Equal amounts of total protein (20 or 40 μg) were separated by sodium dodecyl sulfate-polyacrylamide gel electrophoresis (SDS-PAGE), and transferred to polyvinylidene difluoride (PVDF) membrane (Millipore, Billerica, MA, United States). Membranes were probed with following primary antibodies: phospho- and total Akt, phospho-mTOR, SPOP, phospho- and total TAK1, phospho- and total c-Jun, phospho- and total IκB-α, β-actin. Band intensities were determined using ImageJ software (version 1.48; National Institutes of Health, Bethesda, MD, United States). For dose-dependent studies, cells were treated with increasing doses (10, 100, 500, 1,000 nM) of NVP-BEZ235, PP242, Rapamycin for 48 h. Protein was prepared and measured as described above. Data were expressed as ratio of phosphorylated component/total protein, p-mTOR/β-actin, or SPOP/β-actin.

Luciferase Reporter Assay

For luciferase assay, RCC cell lines were transfected with the AP-1 or IκB-α reporter vector and a Renilla luciferase plasmid (Promega, Madison, WI, United States) as a control for transfection efficiency. To study whether AP-1 activation is regulated by TAK1/JNK pathway in RCC cells, the transfected cells were pretreated with TAK1-inhibitor 5Z-7-oxozeaenol (0, 50, 100, 200 nM) (Tocris Bioscience, Ellisville, MO, United States) or JNK-inhibitor II SP600125 (0, 2.5, 5, 10 μM) (Calbiochem, San Diego, CA, United States) for 1 h. Furthermore, to study the possible role of AP-1 and IκB-α in anticancer activities of NVP-BEZ235, PP242, and Rapamycin, the transfected cells were treated with these compounds (10, 100, 1,000 nM) for 24 h, or the equivalent amounts of DMSO as control. Luciferase activity was measured using a Dual-Glo® Luciferase Assay System (Promega) according to the manufacturer's protocol.

Xenograft Model and Immunohistochemical Staining

Four-week old female BALB/c nude mice were purchased from the Animal Experiment Center of Guilin Medical University (Guilin, Guangxi, China). 786-0 and A498 cells were chosen for *in vivo* study. A498 cells were purchased from Institute of Biochemistry and Cell Biology of the Chinese Academy of Sciences (Shanghai, China). 1×10^7 786-0 or A498 cells were injected subcutaneously into nude mice. When the tumor xenografts reached around 300 mm^3, mice were randomized into different groups (n = 6/group), and given NVP-BEZ235, PP242 or Rapamycin (15 mg/kg) every 2 days *via* oral gavage. Tumor size and mice weight were measured every other day. Mice were sacrificed after 28 days of treatment, and then the tumors were excised for histological examination. Tumor samples were fixed and embedded in paraffin. Then 5 μm tissues sections were deparaffinized and immunolabeled with antibodies against phospho-TAK1, phospho-IκB-α, and phospho-c-Jun. The intensity of staining versus background staining was visually determined under a light microscope. For the animal experiments, all procedures were approved by the Animal Research Ethics Committee of Guilin Medical University.

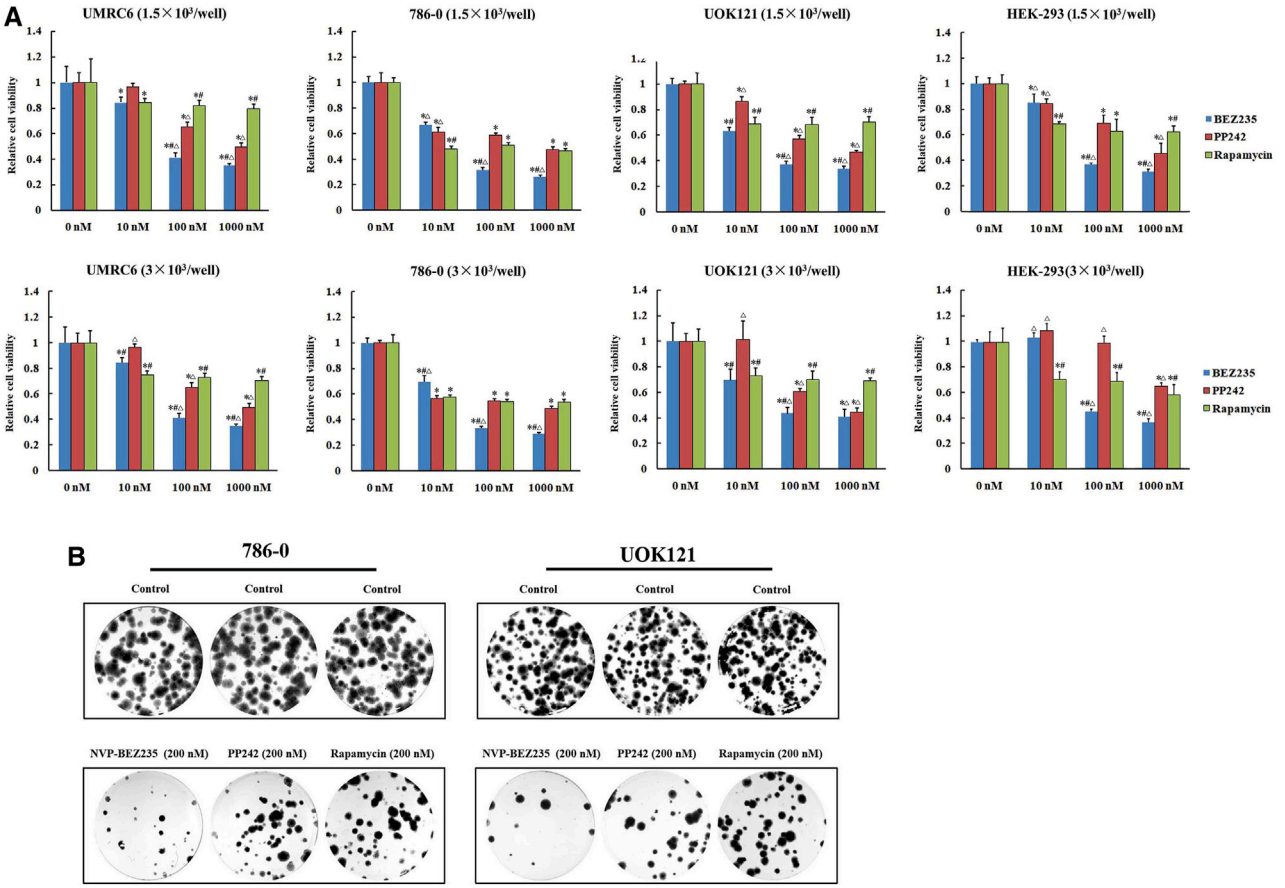

FIGURE 1 | Suppression of RCC cells proliferation by NVP-BEZ235, PP242, and Rapamycin *in vitro*. **(A)** 1.5 × 10^3 or 3.0 × 10^3 RCC cells (UMRC6, 786-0, and UOK121) and HEK-293 cells were treated with increasing concentrations of NVP-BEZ235, PP242, and Rapamycin for 48 h. Cell viability was measured with MTT. DMSO-treated cells served as control (0 nM). All value are means ± SD of three replicates. *$p < 0.05$, versus the corresponding control (0 nM) group; #$p < 0.05$, versus the corresponding PP242 group; Δ$p < 0.05$, versus the corresponding Rapamycin group. **(B)** For colony formation assay, 500 cells of 786-0 and UOK121 were cultured in six-well plate, and cultured with 200 nM of NVP-BEZ235, PP242, and Rapamycin. After 10-14 days of incubation, colonies were stained with Giemsa stain, and counted. Results are representative of three independent experiments.

Statistical Analysis

All data were expressed as mean ± standard deviation (SD). Statistical significance was determined using a one-way ANOVA followed by Tukey's post hoc test using the SPSS statistical program (version 12.0; SPSS, Chicago, IL). A value of $p < 0.05$ was considered significant.

RESULTS

Comparison of the Inhibitory Effects of NVP-BEZ235, PP242, and Rapamycin in RCC Cell Lines

We here used three human renal cancer cell lines, UMRC6, 786-0, and UOK121, to access and compare the anticancer activities of NVP-BEZ235, PP242, and Rapamycin. It was found that the proliferation of all cell lines was significantly reduced by each compound (**Figure 1A**). Moreover, treatment with NVP-BEZ235 produced the greatest reduction in cell viability, followed by PP242 and Rapamycin. As control, the normal human embryonic kidney HEK-293 cells were also treated with NVP-BEZ235, PP242, and Rapamycin. Similar proliferation inhibition was induced by treatment with high concentrations of the three compounds, but not by 10 nM NVP-BEZ235 and PP242. It is indicated that at appropriate concentrations, NVP-BEZ235 and PP242 could exert anti-proliferative effects on RCC cells with less profound effect on normal cells. Likewise, the most marked decrease in numbers of colonies was observed in 786-0 and UOK121 cells treated with NVP-BEZ235 (**Figure 1B**).

Additional studies were done to address the antiproliferative mechanism of NVP-BEZ235, PP242, and Rapamycin. Flow cytometric analysis of the cell cycle distribution of RCC cells showed that the cells were partially blocked in the G1 phase in all cultures, especially in NVP-BEZ235-treated cell lines (**Figure 2**). Cells at the G1 phase increased from 54.54% in control group to 69.03%

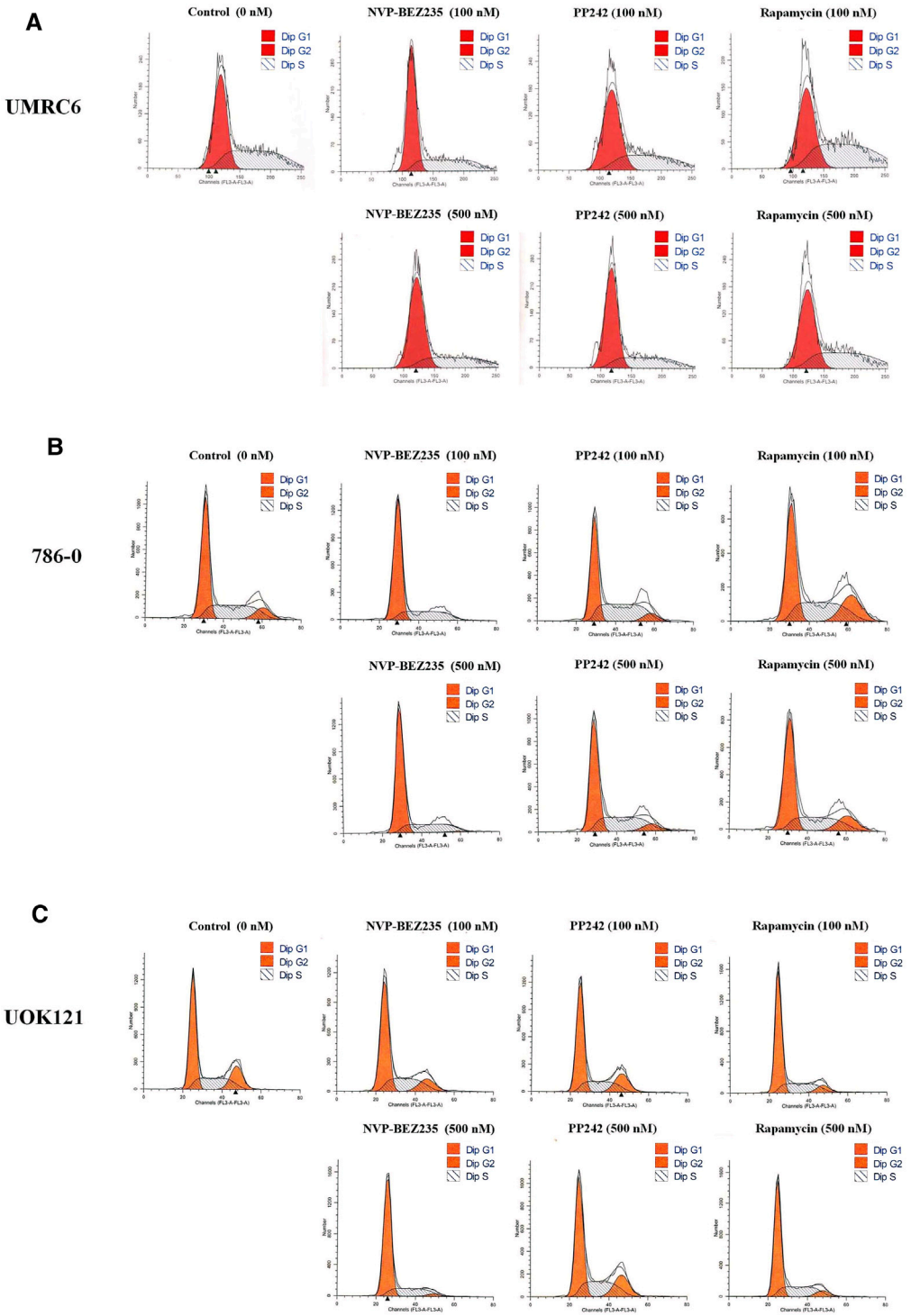

FIGURE 2 | Treatment with NVP-BEZ235, PP242, and Rapamycin induced cell cycle arrest in RCC cells. **(A)** UMRC6, **(B)** 786-0, and **(C)** UOK121 cells were incubated with indicated concentrations of NVP-BEZ235, PP242, and Rapamycin for 72 h. DMSO-treated cells served as control (0 nM). The proportion of cells in different phases of the cell cycle was determined by flow cytometry.

(500 nM NVP-BEZ235) in UMRC6 cells, from 54.76 to 71.79% in 786-0 cells, from 51.79 to 73.30% in UOK121 cells. Meanwhile, we observed that the percentage of apoptotic cells increased significantly in RCC cells when treated with the three compounds (**Figure 3A**). Also, NVP-BEZ235 possessed higher pro-apoptotic activity than PP242 and

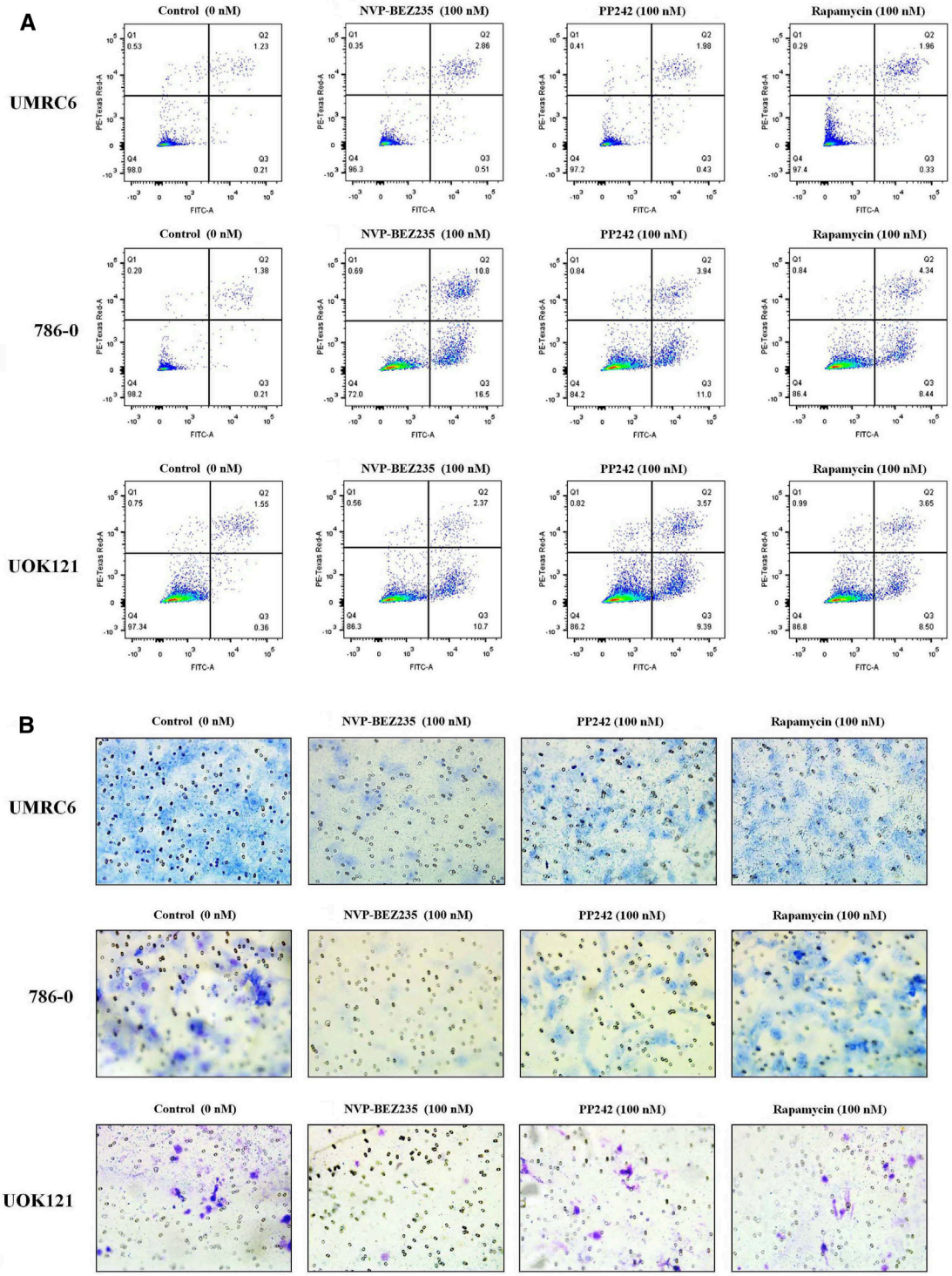

FIGURE 3 | Treatment with NVP-BEZ235, PP242, and Rapamycin increased apoptosis and reduced tumor cell invasion in RCC cells. UMRC6, 786-0, and UOK121 cells were respectively incubated with 100 nM NVP-BEZ235, PP242, and Rapamycin for 48 h or 72 h. DMSO-treated cells served as control (0 nM). **(A)** The apoptotic cell death was quantified by flow cytometry with Annexin V-FITC and PI staining. **(B)** A transwell invasion assay was performed on RCC cells with NVP-BEZ235, PP242, or Rapamycin. After 48 h, the invasive cells were stained with crystal violet and counted (final magnification, 200×). Results are representative of three independent experiments.

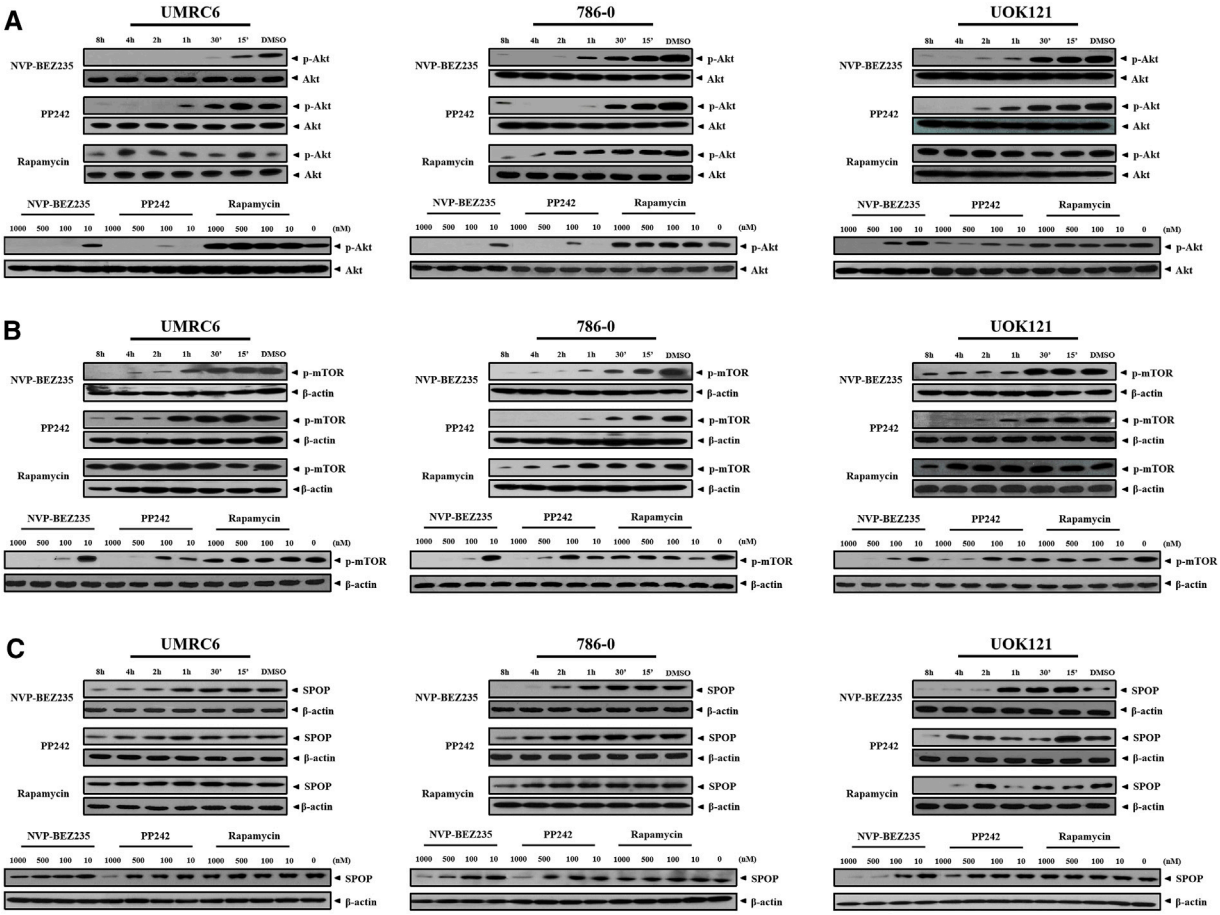

FIGURE 4 | Dose- and time-dependent regulation of PI3K/Akt/mTOR pathway by NVP-BEZ235, PP242, and Rapamycin. RCC cells (UMRC6, 786-0, and UOK121) were exposed to increasing concentrations (10, 100, 500, and 1,000 nM) of NVP-BEZ235, PP242, and Rapamycin for 48 h, or 200 nM of these compounds for different time periods as indicated, after which the alteration of phosphorylation of **(A)** Akt, **(B)** mTOR, and **(C)** SPOP expression was examined by Western blot respectively. The relative amounts of p-Akt normalized to total Akt, p-mTOR, and SPOP normalized to β-actin, are shown. Cells harvested at 0 h or DMSO-treated cells (0 nM) served as control. Results are representative of three independent experiments.

Rapamycin. These findings indicate that apoptosis induction and cell cycle arrest contribute to the growth inhibition of RCC cells by NVP-BEZ235, PP242, and Rapamycin. At the same time, these compounds significantly reduced cell migration in the order NVP-BEZ235 > PP242 > Rapamycin (**Figure 3B**).

Inhibition of PI3K/Akt/mTOR Pathway Signaling in RCC Cell Lines by NVP-BEZ235, PP242, and Rapamycin

NVP-BEZ235, PP242, and Rapamycin are inhibitors of PI3K/Akt/mTOR pathway. Consistent with previous studies, it was shown that NVP-BEZ235 and PP242 inhibited phosphorylation of Akt and mTOR in UMRC6, 786-0, and UOK121 cells, but Rapamycin only decreased p-mTOR expression in the three cell lines (**Figures 4A,B**; **Supplementary Figure S1**). On the contrary, Rapamycin induced feedback activation of Akt in UMRC6 cells, in coincidence with previous report (Osawa et al., 2019). Nevertheless, in UOK121 and 786-0 cells, Rapamycin produced no significant change in Akt phosphorylation, though there was an obvious decrease in p-Akt levels within the first 8 h after exposure in 786-0 cells. In view of the relationship between SPOP mutations and activation of PI3K pathway in cancers, we next detected the alteration of SPOP in RCC cells. NVP-BEZ235 and PP242 suppressed SPOP protein expression in RCC cell lines in a dose- and time-dependent manner, coincident with reduced Akt phosphorylation, whereas no obvious change was observed in Rapamycin-treated cells after 48 h of exposure (**Figure 4C**; **Supplementary Figure S2A**). Furthermore, in comparison with PP242, NVP-BEZ235 had a superior effect on reduction of SPOP expression and inactivation of PI3K/Akt/mTOR

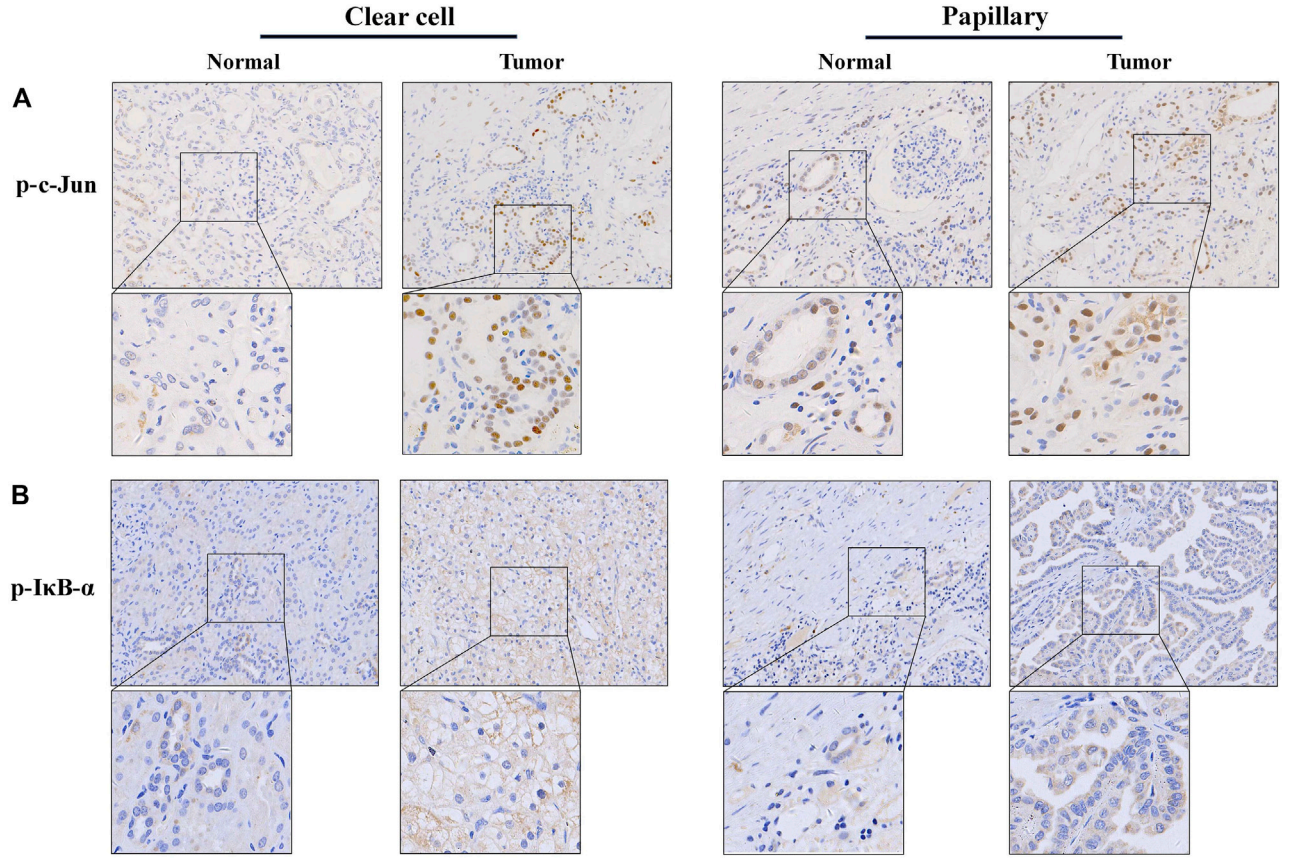

FIGURE 5 | Immunohistochemistry analysis of phospho-c-Jun and phospho-IκB-α expression in RCC tissue. A total of 147 RCC tissue samples were analyzed for stain localization and intensity. Immunohistochemistry was performed using polyclonal antibodies specific for p-c-Jun or p-IκB-α. **(A)** phosphorylated c-Jun and **(B)** phosphorylated IκB-α staining were mainly localized in the nucleus or cytoplasm, respectively. Their expression was both faint in the of normal renal tissue, and more conspicuous in the RCC tissue. (original magnification 200×, inset 400×).

pathway, and this effect was more pronounced in 786-0 and UOK121 cells.

Inhibition of TAK1/JNK/AP-1 and TAK1/IκB Kinase Pathways in RCC Cell Lines by NVP-BEZ235 and PP242 Rather Than Rapamycin

In present study, the elevated phosphorylation levels of c-Jun and IκB-α were found in RCC tissue samples, including both clear cell and papillary renal cell carcinomas, confirming the participation of JNK and IKK activation in the development and progression of renal carcinoma (**Figure 5**). Thus, we here focused on TAK1, a member of the mitogen-activated protein kinase kinase kinase (MAPKKK) family that can function in the JNK and IKK pathways (An et al., 2013). Exposure of RCC cell lines to NVP-BEZ235 and PP242 reduced phosphorylation of TAK1 in a time- and dose-dependent manner (**Figure 6D**). Additionally, the specific inhibitors of TAK1 and JNK both dose-dependently provoked a reduction of AP-1 activity, confirming that AP-1 acts as downstream of TAK1, and JNK in RCC cells (**Figure 6A**). Correspondingly, the inhibition on TAK1 and JNK by NVP-BEZ235 and PP242 was accompanied with reduced AP-1 activity and inhibition of c-Jun phosphorylation (**Figures 6B,E**; **Supplementary Figures S2B, S3A**). On the other hand, although Rapamycin suppressed AP-1 activation in 786-0 and UOK121 cells, it failed to significantly inhibit phosphorylation of TAK1 and c-Jun in RCC cell lines, except for a temporary down-regulation of p-TAK1 and p-c-Jun expression. IκB-α is another downstream molecule of TAK1, and its phosphorylation is mainly mediated by IKK. Subsequent to decreased TAK1 phosphorylation, the activation of IκB-α was steadily and significantly inhibited by NVP-BEZ235 and PP242 rather than Rapamycin in RCC cells (**Figures 6C,F**; **Supplementary Figure S3B**). The decline trend of c-Jun/AP-1 activity, Akt, and IκB-α phosphorylation was much more marked in RCC cells treated with NVP-BEZ235. These results demonstrated that TAK1-dependent JNK and IKK signaling is involved in anti-cancer mechanism of NVP-

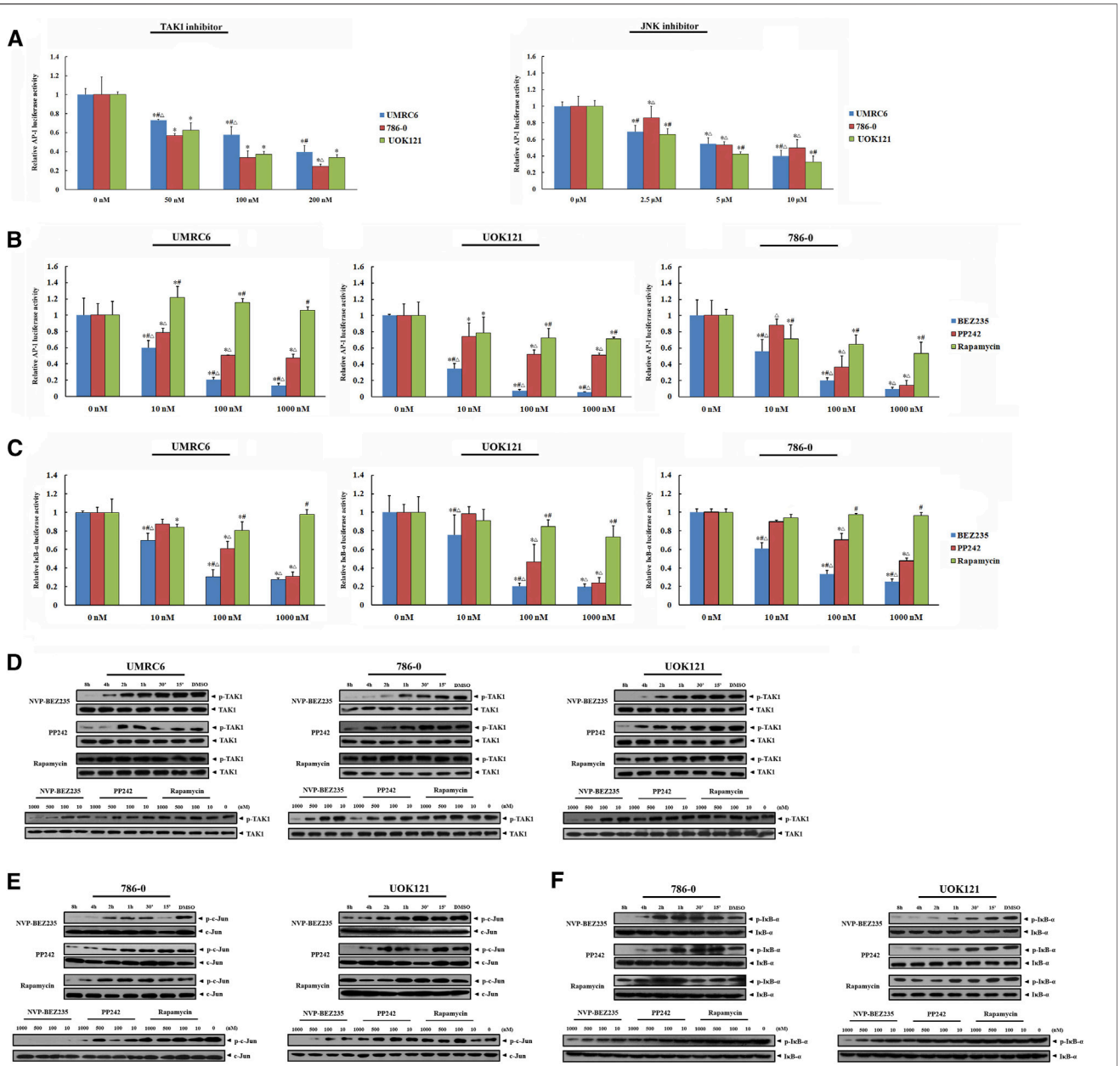

FIGURE 6 | Inhibition of JNK/AP-1 and IKK pathways *via* TAK1 in RCC cell lines by NVP-BEZ235 and PP242. **(A)** Effect of JNK or TAK1 inhibition on AP-1 transcriptional activity in RCC cells assessed by luciferase reporter assay. UMRC6, 786-0, and UOK121 cells were transfected with AP-1 reporter plasmid and a Renilla-luciferase control plasmid, followed by incubation with TAK1-inhibitor or JNK-inhibitor for 24 h. Untreated cells served as control (0 μM). The AP-1-dependent. firefly luciferase activity was normalized to the Renilla luciferase activity as a transfection control. Next, the transfected RCC cells were incubated with various concentrations (10, 100, 1,000 nM) of NVP-BEZ235, PP242, or Rapamycin for 24 h. The **(B)** AP-1 activity and **(C)** IκB-α activity were measured by the ratio of firefly luciferase activity to Renilla luciferase activity. DMSO-treated cells (0 nM) served as control. All value are means ± SD of three replicates. $^{*}p < 0.05$, versus the corresponding control (0 nM) group; #$p < 0.05$, versus the corresponding PP242 group; Δ$p < 0.05$, versus the corresponding Rapamycin group. Western blot assay further confirmed the inhibition of **(D)** TAK1, **(E)** JNK, and **(F)** IKK activation. RCC cells were incubated with 10, 100, 500, 1,000 nM of NVP-BEZ235, PP242 and Rapamycin for 48h, or 200 nm of these compounds for the time courses as indicated. The relative phosphorylation levels of TAK1, c-Jun and IκB-α were calculated and normalized to total protein. Cells harvested at 0 h or DMSO-treated cells (0 nM) served as control. Results are representative of three independent experiments.

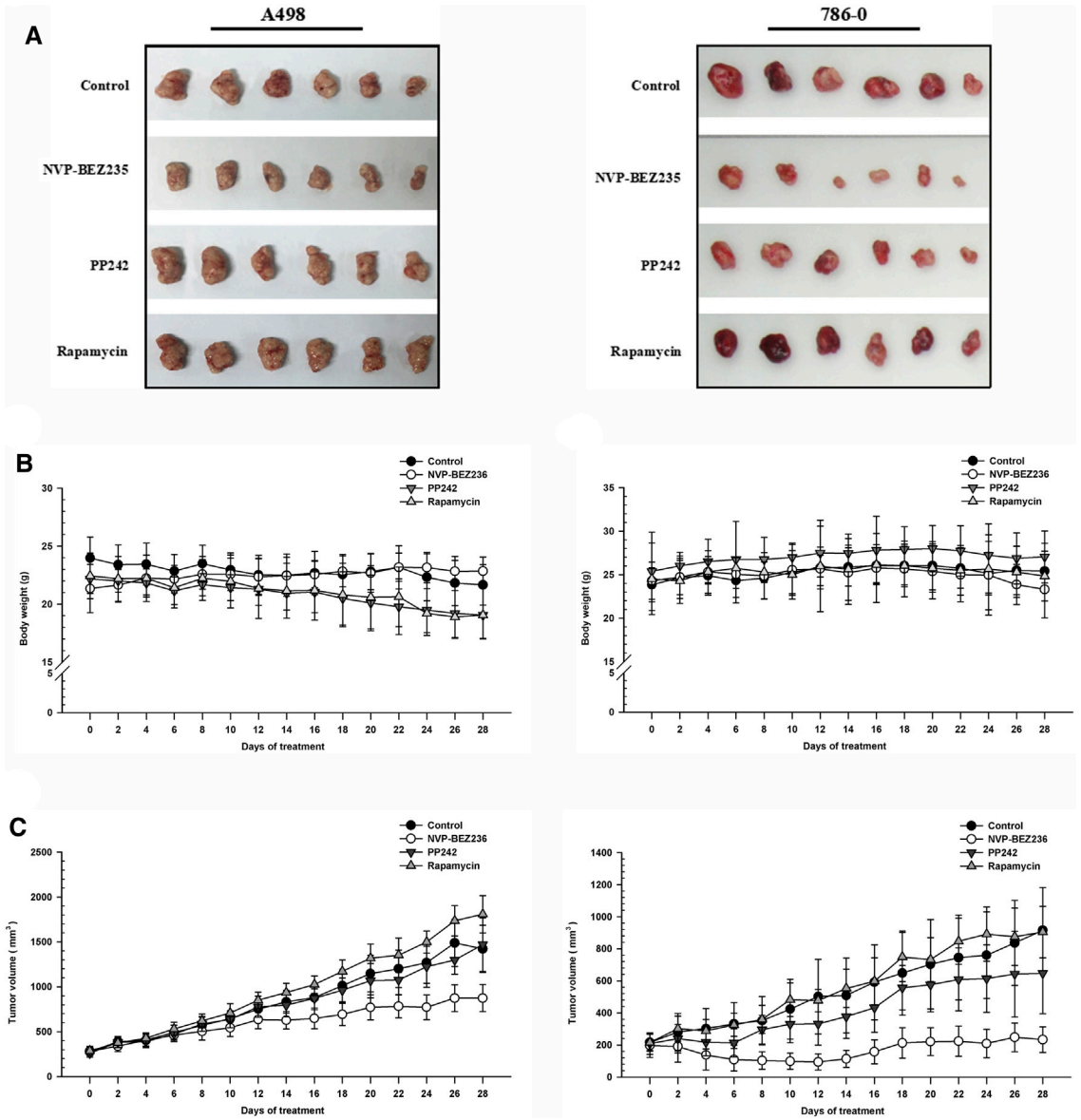

FIGURE 7 | Suppression of tumor growth by NVP-BEZ235, PP242 and Rapamycin *in vivo*. Subcutaneous RCC tumors were established by injection of 786-0 or A498 cells into nude mice. The treatment with NVP-BEZ235, PP242, and Rapamycin (15 mg/kg) started after the tumor size reached around 300 mm^3. All mice were sacrificed 28 days post injection. **(A)** Tumors were excised from the flank of these mice (n = 6/group). **(B)** Body weight and **(C)** tumor volume of A498 and 786-0 xenografts were measured periodically. A group of untreated mice served as control. Results are means ± SD of 6 different mice.

BEZ235 and PP242 in renal cell carcinoma, which may be a new possible explanation to the different response of RCC cells to these compounds.

Comparison of the Antitumor Activity of NVP-BEZ235, PP242, and Rapamycin in RCC Xenograft Models

To determine the *in vivo* efficacy of NVP-BEZ235, PP242 and Rapamycin against human renal cancer, nude mice bearing 786-0 or A498 tumor xenograft were treated daily with these compounds as described in Methods. As shown in **Figure 7B**, no significant change was observed in body weight in 786-0 xenograft model within each group, while the mice administrated with PP242 and Rapamycin showed decreased body weights as compared with the weights of the controls in A498 xenograft mouse model. In general, the tumors induced by 786-0 or A498 cells injection were both most sensitive to treatment with NVP-BEZ235, followed by PP242 (**Figures 7A,C**). At the end of the experiment, the tumor volumes of the nude mice bearing 786-0 and A498 cells were respectively reduced by 75 and 44.6% with treatment of NVP-BEZ235, while PP242 treatment reduced

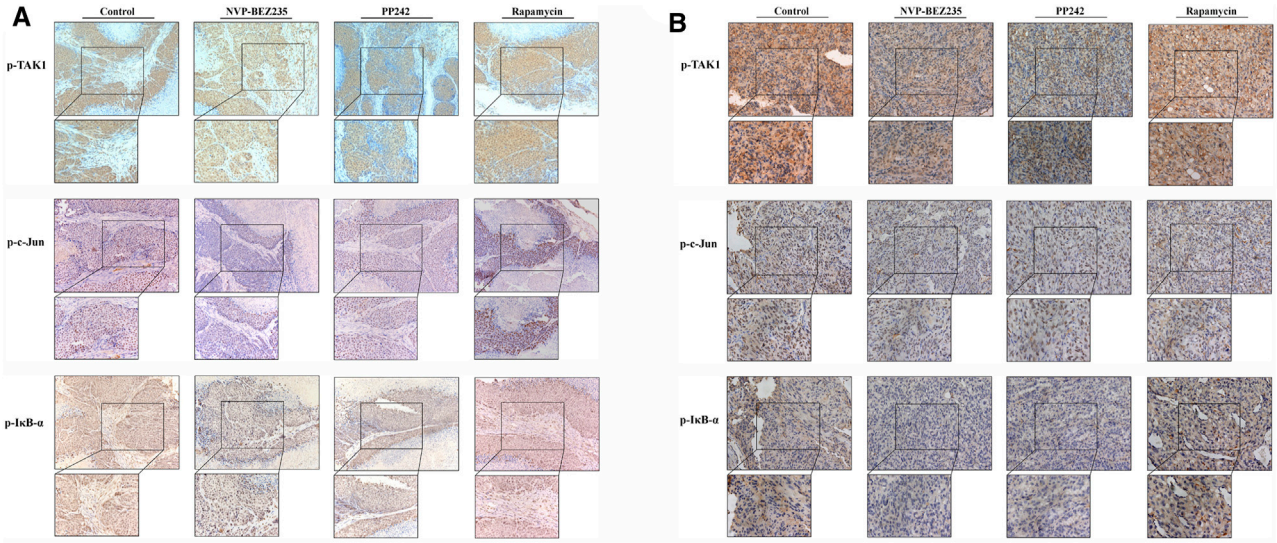

FIGURE 8 | Inhibition of the activity of TAK1, c-Jun, and IκB-α in RCC xenografts in response to treatment by NVP-BEZ235, PP242, and Rapamycin. Sections of all xenograft tumor tissues formed by **(A)** 786-0 and **(B)** A498 renal cancer cells were examined by immunohistochemical staining using anti-p-TAK1, anti-p-c-Jun, and anti-p-IκB-α antibodies. Representative images were taken at a magnification 200× (inset 400×). A group of untreated mice served as control.

tumor volumes by only 31% in 786-0 xenografts and 10.5% in A498 xenografts. Instead, Rapamycin displayed modest anti-cancer properties *in vivo* or, unexpectedly, even slightly promoted tumor growth at the late stage in mice bearing A498 tumor xenograft. By immunohistochemical staining, we demonstrated that NVP-BEZ235, and PP242 caused decrease in phosphorylation of TAK1, c-Jun and IκB-α in tumor tissues, indicating that the *in vivo* anticancer activity of NVP-BEZ235 and PP242 against RCC also depends on TAK1/JNK and TAK1/IKK signaling pathways (**Figure 8**). In agreement with the *in vitro* results, these decrease was more pronounced in NVP-BEZ235-treated xenograft model, while Rapamycin showed no inhibitory effects on phosphorylation of these molecules.

DISCUSSION

A major reason that highlights the importance of targeting mTOR in RCC relies on the observation that mTOR signaling pathway is activated in RCC, contributing to cancer development (Porta et al., 2014). Rapamycin is the first identified highly selective mTORC1 inhibitor. By binding to the FKBP12/rapamycin-binding (FRB) domain of mTORC1, Rapamycin induces the dissociation of Raptor from mTORC1, and subsequent a loss of contact between mTORC1 and its substrates (Xiong et al., 2016; Costa et al., 2018). However, the clinical outcomes of Rapamycin have been poor in RCC patients due to the reactivation of PI3K/Akt via S6K1-dependent feedback loops (Saxton and Sabatini, 2017). Then some selective ATP-competitive mTOR kinase inhibitors were developed as alternatives to the Rapamycin-based therapies. These inhibitors such as PP242 can bind to the active sites of both mTORC1 and mTORC2, and then inhibit phosphorylation of their substrate S6K1 and Akt, thereby achieving the dual target of mTOR function and Akt feedback activation (Zhang et al., 2016). Sure enough, PP242 showed better anticancer effects than Rapamycin in renal cell carcinoma (Maru et al., 2013). Meanwhile, based on the high sequence homology within the catalytic domains between PI3K and mTOR, another generation of dual PI3K/mTOR inhibitors were developed. These drugs could directly block not only mTORC1 and mTORC2, but also PI3K activity (Yang et al., 2019). This class of drugs also has been shown to yield better results than Rapamycin. As a major member of dual PI3K/mTOR inhibitors, NVP-BEZ235 has undergone Phase I/II trials for the treatment of some malignancies including renal carcinoma (Mayer and Arteaga, 2016).

In present study, we evaluated and compared the anticancer activity of Rapamycin, PP242, and NVP-BEZ235 in renal cell lines *in vivo* and *in vitro*. It was demonstrated that Rapamycin, PP242, and NVP-BEZ235 all suppressed cell proliferation and invasion, and induced apoptosis in RCC cell lines. Moreover, the inhibitory effects of these compounds basically decreased in the order of NVP-BEZ235 > PP242 > Rapamycin. Likewise, the reduction in tumor size was most prominent in NVP-BEZ235-treated xenograft mice, while Rapamycin unexpectedly failed to inhibit tumor growth. In addition, our data indicate that the three compounds induced G1 cell cycle arrest in RCC cells, consistent with previous studies (Calero et al., 2017). It can be inferred that the growth-suppressive effects of NVP-BEZ235, PP242, and Rapamycin is due to the apoptosis and cell cycle arrest.

In view of the involvement of PI3K/Akt/mTOR pathway in the inhibitory action of Rapamycin, PP242, and NVP-BEZ235, we investigated the phosphorylation of two key molecules (Akt and mTOR) in this pathway. As expected, NVP-BEZ235 simultaneously blocked Akt phosphorylation and mTOR activation in all three RCC cell lines, while PP242 directly

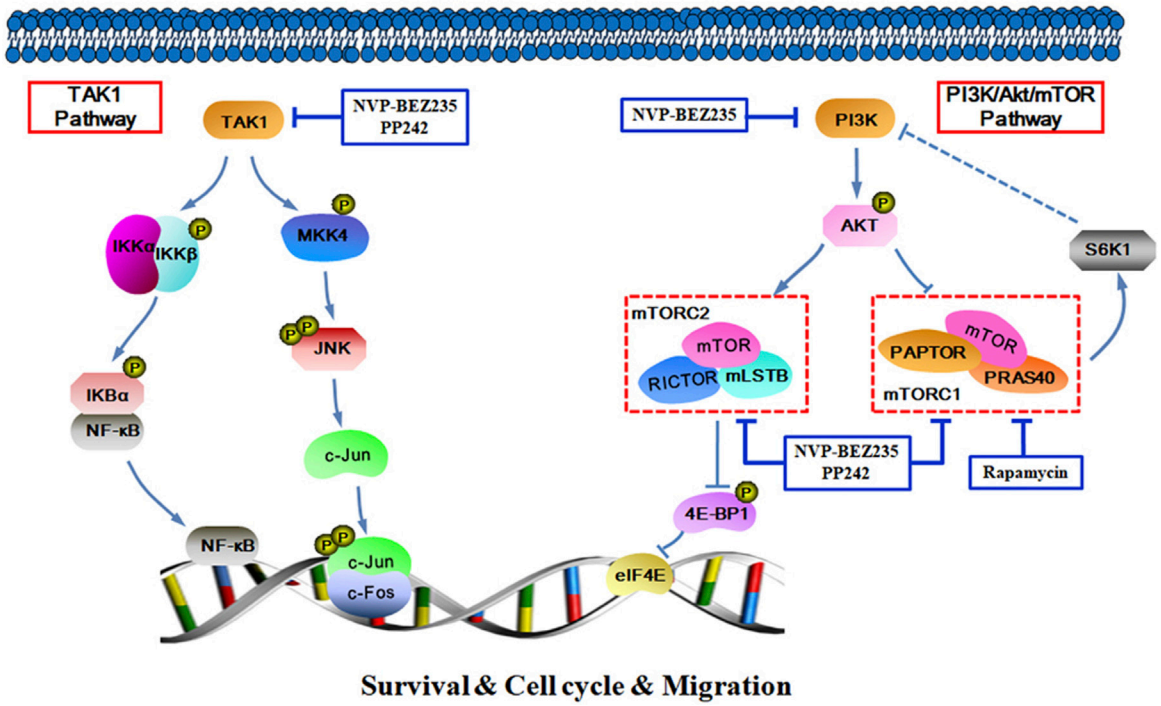

FIGURE 9 | Schematic figure of biochemical pathway whereby NVP-BEZ235, PP242, and Rapamycin lead to inhibition of RCC cell proliferation, survival, and invasion.

inhibited mTOR activity and subsequently prevented activation of Akt. Nevertheless, only reduced levels of phospho-mTOR were present in Rapamycin-treated RCC cells. Rapamycin had no stable effects on the down-regulation of phospho-Akt in 786-0 and UOK121 cells, and even induced feedback activation of Akt in UMRC6 cells.

In an attempt to elucidate the regulation of PI3K/Akt/mTOR signaling in RCC, we examined the activation of SPOP (also known as E3 ubiquitin ligase adaptor), the mutation of which has been shown to be positively associated with activation of PI3K/Akt/mTOR in human cancers such as prostate and colorectal cancers (Blattner et al., 2017; Xu et al., 2015). In three RCC cell lines treated with NVP-BEZ235 and PP242, the attenuated SPOP expression occurred in parallel with inactivation of Akt and mTOR, while Rapamycin had only modest effects on SPOP expression in spite of a transient lowering. In total, these findings support the view that the distinct inhibition of PI3K/Akt/mTOR signaling by Rapamycin, PP242, and NVP-BEZ235 was partially responsible for their varying inhibitory effects in human renal cancer cells. Furthermore, SPOP-mediated PI3K/Akt/mTOR signaling pathway was more significantly altered by NVP-BEZ235 than PP242.

Despite clear evidence that activation of PI3K/Akt/mTOR pathway contributes to RCC development and progression, inhibition of mTOR and/or PI3K did not provide effective and long-lasting anticancer benefits (Alzahrani, 2019). In this context, combination therapies with other anticancer agents might be an effective strategy to improve the clinical outcome of these mTOR inhibitors in RCC patients. For instance, the combination of NVP-BEZ235 and cisplatin produced synergistic antitumor effects on drug-resistant non-small cell lung cancer cells (Zhu et al., 2020). Therefore, it is important to understand the precise mechanism of these mTOR inhibitors, so as to optimize the combination therapy.

As one MAPK family member, JNK has been identified as a pro-tumorigenic factor in many cancer types. Its activity is mainly dependent on the phosphorylation of AP-1 family members, which was confirmed here in RCC cells by repression of AP-1 activity in the presence of JNK inhibitor (Oh et al., 2017). The AP-1 family, composed of c-Fos and c-Jun proteins, is characterized as inducible transcription factors in signal transduction processes. Activated JNK (p-JNK) triggers phosphorylation of c-Jun at sites in the N-terminal domain, which induces homodimerization of c-Jun. Subsequently, c-Jun/AP-1 binds to TPA-response elements (TRE) elements in the presence of co-factors, and activates transcription of genes responsible for cell proliferation, differentiation, apoptosis and migration (Papavassiliou and Musti, 2020). Previous study has shown that JNK/AP-1 pathway is activated in RCCs (An et al., 2013). Consistently, we here observed that phosphorylation of c-Jun was significantly overexpressed in RCC tissues. Moreover, both NVP-BEZ235 and PP242 inhibited c-Jun phosphorylation and AP-1 activity in RCC cell lines, while Rapamycin only inhibited AP-1 activity but not induced stable inactivation of c-Jun in 786-0 and UOK121 cells. These findings demonstrated the involvement of JNK/AP-1

signaling in the antitumor action of NVP-BEZ235 and PP242 rather than Rapamycin. The possible mechanism is that NVP-BEZ235 and PP242 suppress JNK activity, decrease c-Jun phospholation, block AP-1-DNA binding formation and finally induce alteration of gene expression, which needs further study.

TAK1 is a serine/threonine protein kinase of the MAP3K family. Several lines of evidence suggest that TAK1 possesses the ability to activate the downstream JNK/AP-1 and IKK/NK-κB pathways, leading to RCC progression (Hui et al., 2018; Aashaq et al., 2019). Consequently, in present study, AP-1 activity was also successfully blocked with the specific TAK1 inhibitor in RCC cells. Furthermore, NVP-BEZ235 and PP242 elicited a sustained decrease in TAK1 phosphorylation in RCC cell lines, along with inactivation of IκB-α in 786-0, and UOK121 cells. Of note, we similarly proved the elevated expression of phospho-IκB-α in RCC tissues. Based on these findings, it could be speculated that besides PI3K/Akt/mTOR pathway, TAK1-dependent inactivation of JNK/AP-1, and IKK signaling may be also responsible for the inhibitory effects of NVP-BEZ235 and PP242 against renal cell carcinoma but not Rapamycin. This possibly provided another anticancer mechanism of these compounds. Support for this idea comes from the *in vivo* experiment, where treatment of 786-0 and A498 cells xenograft-bearing mice with NVP-BEZ235 and PP242 resulted in significant inhibition of TAK1, c-Jun, and IκB-α activities. As expected, these inhibitory effects by Rapamycin were modest and transient. Meanwhile, we here demonstrated the distinct regulation of PI3K/Akt/mTOR and TAK1 signaling between UMRC6 and the other RCC cell lines, which might be explained by the cell type specificity and require further research.

It is worthy of note that the JNK and NF-κB signaling pathways are also involved in ferroptotic cell death (Ye et al., 2019; Schmitt et al., 2021). Ferroptosis has been recently proved to be critical in the modulation of tumor growth and progression in some cancer types among which renal cell carcinoma is particularly susceptible to ferroptosis. It is known that the ferroptosis process involves accumulation of reactive oxygen species (ROS) from lipid peroxidation within the cell. Furthermore, there is increasing understanding that ROS-mediated signaling cascades include MAPKs and NF-κB (An et al., 2019). Thus, we speculated that the inhibition of JNK/AP-1 and IKK signaling by NVP-BEZ235 and PP242 may induce ROS-dependent ferroptosis, thereby contributing to their anti-tumour effect on RCC cells. Li et al. constructed a nanoparticle carrying Rapamycin and ferroptosis-inducer erastin, which elicited robust ferroptosis-induced cytotoxicity *in vivo* (Li et al., 2019). They proved that Rapamycin played an important role in strengthening the ferroptotic cell death. Considering the high sensitivity of urinary tract tumors to programmed cell death including ferroptosis, we believe that combination of ferroptosis-inducer with ATP-competitive mTOR kinase (such as PP242) or dual mTOR/PI3K (such as NVP-BEZ235) may be a new strategy for treating RCC. Therefore, there is need for further investigation into the correlation between ferroptosis and anti-cancer mechanism of these mTOR inhibitors.

In summary, the data presented here demonstrate that NVP-BEZ235, PP242, and Rapamycin all exhibited anti-proliferative, pro-apoptotic and anti-invasive effects against RCC cells, and the inhibitory activity decreased in an order of NVP-BEZ235 > PP242 > Rapamycin. Furthermore, in addition to PI3K/Akt/mTOR signaling pathway, TAK1-dependent JNK/AP-1 and IKK pathways may also be important in the anticancer action of NVP-BEZ235 and PP242 against RCC (**Figure 9**). These findings revealed a new mechanism for the superior anticancer efficacy of NVP-BEZ235 compared to PP242 and Rapamycin in RCC, providing experimental basis for its clinical application.

DATA AVAILABILITY STATEMENT

The original contributions presented in the study are included in the article/**Supplementary Material**, further inquiries can be directed to the corresponding authors.

ETHICS STATEMENT

The studies involving human participants were reviewed and approved by the Hospital Ethics Committee of Guilin Medical University. The patients/participants provided their written informed consent to participate in this study. The animal study was reviewed and approved by the Animal Research Ethics Committee of Guilin Medical University.

AUTHOR CONTRIBUTIONS

JT and LG conceived of the study and participated in its design, conduct and coordination. JT drafted the article. BL and XZ performed the experiments shown in this work. QR checked and analyzed the data. All authors read and approved the final article.

FUNDING

This work was supported by grants from National Natural Science Foundation of China (81960530 and 82060736), Natural Science Foundation of Guangxi Province (2018GXNSFAA281037 and 2019GXNSFAA185034), and Central Government Guiding Local Scientific and Technological Development Fund Project (ZY201980022).

SUPPLEMENTARY MATERIAL

The Supplementary Material for this article can be found online at: https://www.frontiersin.org/articles/10.3389/fphar.2021.781623/full#supplementary-material

Supplementary Figure 1 | The alteration of Akt and mTOR phosphorylation detected by Western blot from the **Figures 4A,B** were quantified by densitometric analysis and corrected by using data of total Akt and β-actin protein content. All value are means ± SD of three replicates. $^{*}p < 0.05$, $^{**}p < 0.01$ versus the corresponding control (DMSO or 0 nM) group.

Supplementary Figure 2 | The alteration of SPOP expression and TAK1 phosphorylation detected by Western blot from the **Figures 4C**, **6D** were quantified by densitometric analysis and corrected by using data of β-actin and total TAK1 protein content. All value are means ± SD of three replicates. $^{*}p < 0.05$, $^{**}p < 0.01$, versus the corresponding control (DMSO or 0 nM) group.

Supplementary Figure 3 | The alteration of c-Jun and IκB-α phosphorylation detected by Western blot from the **Figures 6E,F** were quantified by densitometric analysis and corrected by using data of total protein content. All value are means ± SD of three replicates. $^{*}p < 0.05$, $^{**}p < 0.01$ versus the corresponding control (DMSO or 0 nM) group.

REFERENCES

Aashaq, S., Batool, A., and Andrabi, K. I. (2019). TAK1 Mediates Convergence of Cellular Signals for Death and Survival. *Apoptosis* 24 (1-2), 3–20. doi:10.1007/s10495-018-1490-7

Alqurashi, N., Hashimi, S. M., Alowaidi, F., Ivanovski, S., and Wei, M. Q. (2018). Dual mTOR/PI3K Inhibitor NVP-BEZ235 A-rrests C-olorectal C-ancer C-ell G-rowth and D-isplays D-ifferential I-nhibition of 4E-BP1. *Oncol. Rep.* 40 (2), 1083–1092. doi:10.3892/or.2018.6457

Alzahrani, A. S. (2019). PI3K/Akt/mTOR Inhibitors in Cancer: At the Bench and Bedside. *Semin. Cancer Biol.* 59, 125–132. doi:10.1016/j.semcancer.2019.07.009

An, J., Liu, H., Magyar, C. E., Guo, Y., Veena, M. S., Srivatsan, E. S., et al. (2013). Hyperactivated JNK Is a Therapeutic Target in pVHL-Deficient Renal Cell Carcinoma. *Cancer Res.* 73 (4), 1374–1385. doi:10.1158/0008-5472.CAN-12-2362

An, Y., Zhang, H., Wang, C., Jiao, F., Xu, H., Wang, X., et al. (2019). Activation of ROS/MAPKs/NF-κB/NLRP3 and Inhibition of Efferocytosis in Osteoclast-Mediated Diabetic Osteoporosis. *FASEB J.* 33 (11), 12515–12527. doi:10.1096/fj.201802805RR

Blattner, M., Liu, D., Robinson, B. D., Huang, D., Poliakov, A., Gao, D., et al. (2017). SPOP Mutation Drives Prostate Tumorigenesis *In Vivo* through Coordinate Regulation of PI3K/mTOR and AR Signaling. *Cancer Cell* 31 (3), 436–451. doi:10.1016/j.ccell.2017.02.004

Bray, F., Ferlay, J., Soerjomataram, I., Siegel, R. L., Torre, L. A., and Jemal, A. (2018). Global Cancer Statistics 2018: GLOBOCAN Estimates of Incidence and Mortality Worldwide for 36 Cancers in 185 Countries. *CA Cancer J. Clin.* 68 (6), 394–424. doi:10.3322/caac.21492

Calero, R., Morchon, E., Martinez-Argudo, I., and Serrano, R. (2017). Synergistic Anti-tumor Effect of 17AAG with the PI3K/mTOR Inhibitor NVP-BEZ235 on Human Melanoma. *Cancer Lett.* 406, 1–11. doi:10.1016/j.canlet.2017.07.021

Chiarini, F., Evangelisti, C., McCubrey, J. A., and Martelli, A. M. (2015). Current Treatment Strategies for Inhibiting mTOR in Cancer. *Trends Pharmacol. Sci.* 36 (2), 124–135. doi:10.1016/j.tips.2014.11.004

Costa, R. L. B., Han, H. S., and Gradishar, W. J. (2018). Targeting the PI3K/AKT/mTOR Pathway in Triple-Negative Breast Cancer: a Review. *Breast Cancer Res. Treat.* 169 (3), 397–406. doi:10.1007/s10549-018-4697-y

Guo, H., German, P., Bai, S., Barnes, S., Guo, W., Qi, X., et al. (2015). The PI3K/AKT Pathway and Renal Cell Carcinoma. *J. Genet. Genomics* 42 (7), 343–353. doi:10.1016/j.jgg.2015.03.003

Hirschhorn, T., and Stockwell, B. R. (2019). The Development of the Concept of Ferroptosis. *Free Radic. Biol. Med.* 133, 130–143. doi:10.1016/j.freeradbiomed.2018.09.043

Hui, B., Zhang, L., Zhou, Q., and Hui, L. (2018). Pristimerin Inhibits LPS-Triggered Neurotoxicity in BV-2 Microglia Cells through Modulating IRAK1/TRAF6/TAK1-Mediated NF-κB and AP-1 Signaling Pathways *In Vitro*. *Neurotox. Res.* 33 (2), 268–283. doi:10.1007/s12640-017-9837-3

Inamura, K. (2017). Renal Cell Tumors: Understanding Their Molecular Pathological Epidemiology and the 2016 WHO Classification. *Ijms* 18 (10), 2195. doi:10.3390/ijms18102195

Kaur, A., and Sharma, S. (2017). Mammalian Target of Rapamycin (mTOR) as a Potential Therapeutic Target in Various Diseases. *Inflammopharmacology* 25 (3), 293–312. doi:10.1007/s10787-017-0336-116

Lei, G., Zhuang, L., and Gan, B. (2021). mTORC1 and Ferroptosis: Regulatory Mechanisms and Therapeutic Potential. *Bioessays* 43 (8), 2100093. doi:10.1002/bies.202100093

Li, Y., Wang, X., Yan, J., Liu, Y., Yang, R., Pan, D., et al. (2019). Nanoparticle Ferritin-Bound Erastin and Rapamycin: a Nanodrug Combining Autophagy and Ferroptosis for Anticancer Therapy. *Biomater. Sci.* 7 (9), 3779–3787. doi:10.1039/c9bm00653b

Linehan, W. M., and Ricketts, C. J. (2017). Kidney Cancer in 2016: RCC - Advances in Targeted Therapeutics and Genomics. *Nat. Rev. Urol.* 14 (2), 76–78. doi:10.1038/nrurol.2016.260

Maru, S., Ishigaki, Y., Shinohara, N., Takata, T., Tomosugi, N., and Nonomura, K. (2013). Inhibition of mTORC2 but Not mTORC1 Up-Regulates E-Cadherin Expression and Inhibits Cell Motility by Blocking HIF-2α Expression in Human Renal Cell Carcinoma. *J. Urol.* 189 (5), 1921–1929. doi:10.1016/j.juro.2012.11.010

Mayer, I. A., and Arteaga, C. L. (2016). The PI3K/AKT Pathway as a Target for Cancer Treatment. *Annu. Rev. Med.* 67, 11–28. doi:10.1146/annurev-med-062913-051343

Mou, Y., Wang, J., Wu, J., He, D., Zhang, C., Duan, C., et al. (2019). Ferroptosis, a New Form of Cell Death: Opportunities and Challenges in Cancer. *J. Hematol. Oncol.* 12 (1), 34. doi:10.1186/s13045-019-0720-y

Oh, Y. T., Yue, P., and Sun, S. Y. (2017). DR5 Suppression Induces Sphingosine-1-phosphate-dependent TRAF2 Polyubiquitination, Leading to Activation of JNK/AP-1 and Promotion of Cancer Cell Invasion. *Cell Commun. Signal.* 15 (1), 18. doi:10.1186/s12964-017-0174-1

Osawa, T., Takeuchi, A., Kojima, T., Shinohara, N., Eto, M., and Nishiyama, H. (2019). Overview of Current and Future Systemic Therapy for Metastatic Renal Cell Carcinoma. *Jpn. J. Clin. Oncol.* 49 (5), 395–403. doi:10.1093/jjco/hyz013

Papavassiliou, A. G., and Musti, A. M. (2020). The Multifaceted Output of C-Jun Biological Activity: Focus at the junction of CD8 T Cell Activation and Exhaustion. *Cells* 9 (11), 2470. doi:10.3390/cells9112470

Pietropaolo, A., Jones, P., Aboumarzouk, O. M., Rai, B. P., Lockyer, C. R. W., Hayes, M. C., et al. (2019). Trends in Surgical and Ablative Treatment of Localised Renal Cell Carcinoma: A Review of Publication Trends over 16 Years (2000-2015). *Arab J. Urol.* 17 (2), 120–124. doi:10.1080/2090598X.2019.1590516

Porta, C., Paglino, C., and Mosca, A. (2014). Targeting PI3K/Akt/mTOR Signaling in Cancer. *Front. Oncol.* 4, 64. doi:10.3389/fonc.2014.00064

Roskoski, R., Jr. (2019). Properties of FDA-Approved Small Molecule Protein Kinase Inhibitors. *Pharmacol. Res.* 144, 19–50. doi:10.1016/j.phrs.2019.03.006

Saxton, R. A., and Sabatini, D. M. (2017). mTOR Signaling in Growth, Metabolism, and Disease. *Cell* 168 (2), 960–976. doi:10.1016/j.cell.2017.03.03510.1016/j.cell.2017.02.004

Schmitt, A., Xu, W., Bucher, P., Grimm, M., Konantz, M., Horn, H., et al. (2021). Dimethyl Fumarate Induces Ferroptosis and Impairs NF-κB/STAT3 Signaling in DLBCL. *Blood* 138 (10), 871–884. doi:10.1182/blood.2020009404

Xiong, F., Dong, P., Liu, M., Xie, G., Wang, K., Zhuo, F., et al. (2016). Tomato FK506 Binding Protein 12KD (FKBP12) Mediates the Interaction between Rapamycin and Target of Rapamycin (TOR). *Front. Plant Sci.* 7, 1746. doi:10.3389/fpls.2016.01746

Xu, J., Pham, C. G., Albanese, S. K., Dong, Y., Oyama, T., Lee, C. H., et al. (2016). Mechanistically Distinct Cancer-Associated mTOR Activation Clusters Predict Sensitivity to Rapamycin. *J. Clin. Invest.* 126 (9), 3526–3540. doi:10.1172/JCI86120

Xu, J., Wang, F., Jiang, H., Jiang, Y., Chen, J., and Qin, J. (2015). Properties and Clinical Relevance of Speckle-type POZ Protein in Human Colorectal Cancer. *J. Gastrointest. Surg.* 19 (8), 1484–1496. doi:10.1007/s11605-015-2767-6

Yang, H., Rudge, D. G., Koos, J. D., Vaidialingam, B., Yang, H. J., and Pavletich, N. P. (2013). mTOR Kinase Structure, Mechanism and Regulation. *Nature* 497 (7448), 217–223. doi:10.1038/nature12122

Yang, J., Nie, J., Ma, X., Wei, Y., Peng, Y., and Wei, X. (2019). Targeting PI3K in Cancer: Mechanisms and Advances in Clinical Trials. *Mol. Cancer* 18 (1), 26. doi:10.1186/s12943-019-0954-x

Ye, F., Chai, W., Xie, M., Yang, M., Yu, Y., Cao, L., et al. (2019). HMGB1 Regulates Erastin-Induced Ferroptosis via RAS-JNK/p38 Signaling in HL-60/NRAS^{Q61L} Cells. *Am. J. Cancer Res.* 9 (4), 730–739.

Yi, J., Zhu, J., Wu, J., Thompson, C. B., and Jiang, X. (2020). Oncogenic Activation of PI3K-AKT-mTOR Signaling Suppresses Ferroptosis via SREBP-Mediated Lipogenesis. *Proc. Natl. Acad. Sci. U S A.* 117 (49), 31189–31197. doi:10.1073/pnas.2017152117

Zhang, Z., Zhang, G., Kong, C., and Gong, D. (2016). PP242 Suppresses Bladder Cancer Cell Proliferation and Migration through Deactivating the Mammalian Target of Rapamycin Complex 2/AKT1 Signaling Pathway. *Mol. Med. Rep.* 13 (1), 333–338. doi:10.3892/mmr.2015.4528

Zhu, H., Shi, Y., Jiao, X., Yang, G., Wang, R., and Yuan, Y. (2020). Synergistic Antitumor Effect of Dual PI3K and mTOR Inhibitor NVP-BEZ235 in Combination with Cisplatin on Drug-Resistant Non-small Cell Lung Cancer Cell. *Oncol. Lett.* 20 (6), 326. doi:10.3892/ol.2020.12189

Conflict of Interest: The authors declare that the research was conducted in the absence of any commercial or financial relationships that could be construed as a potential conflict of interest.

Publisher's Note: All claims expressed in this article are solely those of the authors and do not necessarily represent those of their affiliated organizations, or those of the publisher, the editors and the reviewers. Any product that may be evaluated in this article, or claim that may be made by its manufacturer, is not guaranteed or endorsed by the publisher.

frontiers in Oncology

MINI REVIEW
published: 31 January 2022
doi: 10.3389/fonc.2022.771870

Epigenetic Regulation of Ferroptosis-Associated Genes and Its Implication in Cancer Therapy

Yanzi Pei[1], *Yujie Qian*[1], *Hao Wang*[2]* *and Li Tan*[1]*

[1] Center for Medical Research and Innovation, Shanghai Pudong Hospital, Fudan University Pudong Medical Center, and Shanghai Key Laboratory of Medical Epigenetics, Institutes of Biomedical Sciences, Fudan University, Shanghai, China, [2] Department of Anesthesiology, Zhongshan Hospital, Fudan University, Shanghai, China

Ferroptosis is an evolutionarily conserved form of regulated cell death triggered by iron-dependent phospholipid peroxidation. Ferroptosis contributes to the maintenance of tissue homeostasis under physiological conditions while its aberration is tightly connected with lots of pathophysiological processes such as acute tissue injury, chronic degenerative disease, and tumorigenesis. Epigenetic regulation controls chromatin structure and gene expression by writing/reading/erasing the covalent modifications on DNA, histone, and RNA, without altering the DNA sequence. Accumulating evidences suggest that epigenetic regulation is involved in the determination of cellular vulnerability to ferroptosis. Here, we summarize the recent advances on the epigenetic mechanisms that control the expression of ferroptosis-associated genes and thereby the ferroptosis process. Moreover, the potential value of epigenetic drugs in targeting or synergizing ferroptosis during cancer therapy is also discussed.

Keywords: ferroptosis, epigenetic regulation, cancer, DNA methylation, histone modifications, RNA methylation

OPEN ACCESS

Edited by:
Jian Chen,
Guilin Medical University, China

Reviewed by:
Shuai Jiang,
Fudan University, China
Alessandro Sacco,
University of Catanzaro, Italy

***Correspondence:**
Li Tan
litan@fudan.edu.cn
Hao Wang
wang.hao2@zs-hospital.sh.cn

Specialty section:
This article was submitted to Pharmacology of Anti-Cancer Drugs, a section of the journal Frontiers in Oncology

Received: *07 September 2021*
Accepted: *10 January 2022*
Published: *31 January 2022*

Citation:
Pei Y, Qian Y, Wang H and Tan L (2022) Epigenetic Regulation of Ferroptosis-Associated Genes and Its Implication in Cancer Therapy. Front. Oncol. 12:771870. doi: 10.3389/fonc.2022.771870

INTRODUCTION

Ferroptosis, which was first proposed by Dixon et al. in 2012, is a novel programmed cell death driven by iron-dependent accumulation of lipid peroxidation (1–7). As an evolutionally-conserved cell death form, ferroptosis plays a critical role in diverse physiological and pathological processes (8). Apparently, understanding the comprehensive molecular mechanisms of ferroptosis has great biological importance and clinical significance. Epigenetic regulation controls gene expression by writing/reading/erasing the covalent modifications on DNA, histone, and RNA, without altering the DNA sequence (9). Accumulating evidence suggests that epigenetic regulation modulates the expression dosages of ferroptosis-associated genes and consequently contributes to the determination of cell sensitivity to ferroptosis. Here we summarize current knowledge on the role of epigenetic regulation in ferroptosis and its implication in cancer therapy.

THE REGULATORY CIRCUITS OF FERROPTOSIS

Biochemistry of Ferroptosis

Since the ferroptosis was first defined in 2012, the core biochemical components of ferroptosis have been rapidly identified in the past decade.

Lipid Peroxidation

Polyunsaturated fatty acids are susceptible to lipid peroxidation and essential for the ferroptosis process (10). The abundance and localization of polyunsaturated fatty acids determine the level of intracellular lipid peroxidation and furtherly decide the sensitivity of cells to ferroptosis (11). Phosphatidylethanolamines (PEs) containing arachidonic acid are the major phospholipid that peroxides and promotes ferroptosis (7, 12). Further on, the PE-Coenzyme-A derivatives form and insert into phospholipid, which was defined as a necessary step of pro-ferroptotic signal production (7). In 2015, through the haploid genetic screening, Dixon et al. identified 9 lipid metabolism-associated genes, including the lipid remodeling gene *LPCAT3* and fat acid metabolism gene *ACSL4*, that play essential roles in ferroptosis (5). Doll et al. convincingly proved that ACSL4 is involved in the generation of pro-ferroptotic state (7).

Intracellular Iron

Iron complexes or loosely bound iron structure are essential for the formation of reactive oxygen (13). In eukaryotic cells, the uncoordinated redox-active Fe^{2+} that was temporally released in the plasma is generally referred as "The Labile Iron Pool" or "free Fe^{2+}" (14). Technically, free Fe^{2+} catalyzes the formation of hydroxyl radical and hydroxide from H_2O_2 through "Fenton reaction". Consistent to the name of "ferroptosis", both Fenton reaction and iron-dependent enzymes are the formation of reactive oxygen, which causes severe oxidative damage to neighbor cell structure, are key players in ferroptosis (15, 16). Conversely, treatment with iron chelators such as could inhibit ferroptosis. Under normal physiological condition, the level of iron is well regulated by transferrin (extracellular environment) and ferritin (intracellular environment). Apparently, the signaling pathways that alter iron metabolism have potential effect on the regulation of ferroptosis.

Glutathione and GPX4

Glutathione (GSH) metabolism was identified as the first pathway regulating the ferroptosis process. The hydro-sulfuryl structure makes GSH as a commonly considered antioxidant and free radical scavenger in the intracellular environment (17). In 1986, the glutamate-cystine transportation system X_c^- was identified by Bannai et al. (18). The transporter is composed by one light chain subunit and one heavy chain subunit, which were respectively encoded by *SLC7A11* and *SLC3A2*. System X_c^- transfers glutamate out of cells and cystine into cells at a ratio of 1:1, and then cystine is reduced into cysteine which participates in the synthesis of GSH (**Figure 1**) (19). High concentration of extracellular glutamate inhibits cystine uptake through inhibition of Xc^- leading to glutathione decrease and oxidative cell death (20, 21). Indeed, the first ferroptosis inducer, erastin, mainly targets on system X_c^- (1).

The glutathione peroxidases (GPXs) are series of peroxide-degrading enzymes. GPX4 uses GSH as an essential cofactor to prevent lipid peroxide and maintain redox homeostasis (22). In 2008, Seiler et al. identified lipid peroxidation as the key mediator of cell death in glutathione peroxidase 4 (GPX4) knockout cells (23). Thus, people began to consider this type of cell death different from either apoptosis or necrosis. Several small molecule compounds were screened out as ferroptosis inducer (24–27). Among them, RSL3 targets on GPX4 (25).

The FSP1-CoQ10 Pathway

Independent of GPX4 regulatory pathway, the FSP1-CoQ pathway is a novel ferroptosis pathway identified by Doll et al. through an expression cloning approach to identify genes in human cancer cells that are able to complement the loss of GPX4 (6).

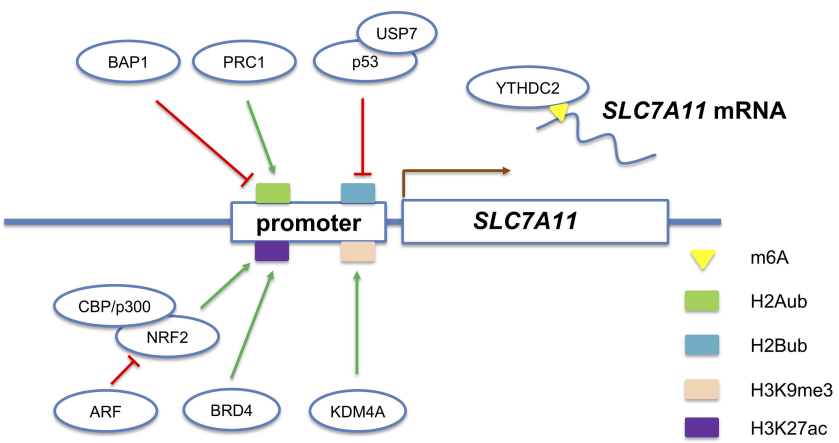

FIGURE 1 | Multiple epigenetic mechanisms regulate the expression of *SLC7A11* gene, a representative ferroptosis-associated gene.

Doll et al. revealed that apoptosis-inducing factor mitochondria-associated 2 (AIFM2, renamed as FSP1) overexpression can largely abrogate GPX4 inhibition-induced ferroptosis. A previous study showed that FSP1 functions as a NADP dependent coenzyme Q (CoQ) oxidoreductase *in vitro* (28). CoQ_{10} is a mobile lipophilic electron carrier that endogenously synthesizes lipid-soluble antioxidants and acts as a lipophilic free radical-trapping agents (RTAs) in the plasma membrane (29). Intriguingly, FSP1 overexpression fails to suppress ferroptosis in both CoQ_2 knockout cells and in cells treated with the CoQ_2 inhibitor (6, 30). CoQ_2 is the enzyme that catalyzes the first step in CoQ_{10} biosynthesis, and the soluble analog of CoQ_{10} is sufficient for suppressing ferroptosis and lipid peroxidation (6, 30). These two latest studies clearly suggest that FSP1 acts parallel to GPX4 to inhibit ferroptosis by regulating the nonmitochondrial CoQ_{10} antioxidant system.

The DHODH-$CoQH_2$ Pathway

Dihydroorotate dehydrogenase (DHODH), an enzyme essential for the *de novo* biosynthesis of pyrimidine-based nucleotides, is a known therapeutic target for multiple diseases (31). Furthermore, DHODH inhibitors, including brequinar, leflunomide, and teriflunomide, have been clinically evaluated but failed to receive FDA approval for the treatment of cancer (32–34). Mao et al. identified DHODH as the third anti-ferroptosis pathway, independent of GPX4 and FSP1 (35). Mechanistically, DHODH in the mitochondrial inner membrane regulates the production of $CoQH_2$, a radical-trapping antioxidant in mitochondrial. Importantly, DHODH inhibitor brequinar selectively suppresses GPX4-low tumor growth by inducing ferroptosis, whereas combined treatment with brequinar and sulfasalazine synergistically induces ferroptosis and suppresses GPX4-high tumor growth.

The GCH1-BH4 Pathway

Tetrahydrobiopterin (BH4) is a redox-active cofactor involved in the production of nitric oxide, neurotransmitters, and aromatic amino acids (36). The GCH1-PTS-SPR pathway catalyzes GTP to BH4, and GCH1 is a rate-limiting enzyme in the synthesis of BH4 (37, 38).

Kraft et al. found that the overexpression of GCH1 provide protection to against ferroptosis by abolishing lipid peroxidation (36). GCH1 overexpression exhibits robust protection against RSL3- and imidazole ketone erastin (IKE)-induced ferroptosis and genetic ablation of *GPX4*-induced ferroptosis but does not protect cells against inducers of apoptosis and is only marginally effective against necroptosis. Those results indicate that GCH1 selectively inhibits ferroptotic cell death (36).

Intriguingly, BH4 loss in cells leads the accumulation of coenzyme A, NADP, and oxidized GSH (GSSG) in cells. Further, the elevation of reduced CoQ_{10} in cells with GCH1 overexpression have been detected (38). Thus, these results indicate that the GCH1-BH4 pathway acts as an endogenous antioxidant pathway to inhibit ferroptosis through a mechanism independent of the GPX4 signal pathway.

The Signal Pathways of Ferroptosis

Several canonical oncogenic and tumor suppressive pathways have been reported to converge to the ferroptosis process. In general, these pathways alter the ferroptosis sensitivity through modulating the expression levels and enzymatic activities of core ferroptosis executors.

The p53 Pathway

The p53 pathway inhibits cystine uptake and sensitize cells to ferroptosis through repressing SLC7A11 expression (39). Notably, the acetylation–defective mutant $p53^{KR}$ loses the function of inducing cell-cycle arrest but still retains the ability to regulate SLC7A11. Moreover, the spermidine/spermine N1-acetyltransferase 1 (*SAT1*) gene, which encodes a rate-limiting enzyme in polyamine catabolism, was identified as a transcription target of p53 and promote ferroptosis through conversing spermidine and spermine back to putrescine (40). However, there were also some controversial reports on the function of p53 pathway in ferroptosis. For instance, the dipeptidyl-peptidase-4 (DPP4) can be blocked by p53, resulting in resistance to ferroptosis (41). Alternatively, the wild-type p53 stabilization can delay the induction of ferroptosis in cancer cells upon system X_c^- inhibition (42). These findings indicate a content-dependent role of p53 in the regulation of ferroptosis.

The KEAP1-NRF2 Pathway

It has been well-established that nuclear factor erythroid 2-related factor 2 (NRF2) pathway plays an essential role in antioxidant response. The correlation between NRF2 pathway and ferroptosis has also been studied (43, 44). NRF2 upregulates system X_c^- and thereby protects brain tumor cells from ferroptosis (45). Since the NRF2 pathway is commonly activated in diverse malignant tumors, it is likely that aberrant NRF2 activation contributes to protect tumor cells against ferroptosis. A recent work revealed that 3D organoid culture causes ferroptosis and insufficient NRF2 activation leads to the failure of establishment of organoids (46). In addition, the tumor suppressor ARF (CDKN2A) has recently been identified as a binding partner for NRF2 and impacts ferroptosis sensitivity (47). Mechanistically, ARF represses NRF2-induced transcriptional upregulation of SLC7A11 and other antioxidant genes.

The Hippo Pathway

Hippo pathway controls organ size by regulating cell proliferation, apoptosis, and stem cell self-renewal (48). Wu et al. observed that high cell density protects many types of cells against ferroptosis during the *in vitro* cell culture. Furthermore, they revealed that the cell density-dependent acquisition of ferroptosis resistance is triggered by E-cadherin-mediated activation of intracellular NF2 (also known as merlin) and Hippo signaling pathway (49, 50). Antagonizing this signaling allows the nuclear translocation of proto-oncogenic transcriptional co-activator YAP and promotes ferroptosis by upregulating several ferroptosis modulators, including ACSL4 and TFRC (50). The identification of E-Cad/Hippo/YAP/ACSL4 axis may explain a long term-observed

phenotype that mesenchymal cells are more sensitive to ferroptosis than epithelial cells (50). Similarly, epithelial-mesenchymal transition (EMT) increases the vulnerability of cells to ferroptosis, which may be partially attributed to the inactivation of Hippo pathway during EMT (51).

Besides the above three well-established signaling pathways, other canonical development and disease-associated pathways such as RAS-RAF-MAPK and PI3K/Akt also have intersection with the core regulatory circuity of ferroptosis and participate in the regulation of ferroptosis process.

EPIGENETIC MECHANISMS UNDERLYING FERROPTOSIS

DNA Modification

DNA methylation is the most common epigenetic modification that has been studied in gene regulation. Homocysteine treatment induced DNA methylation of *GPX4* gene in nucleus pulposus, leading to ferroptosis sensitivity (52). DNA hypermethylation of *CDH1* gene promoter in head and neck cancer cells repressed E-cadherin (encoding by *CDH1*) expression and increased ferroptosis susceptibility (51). These two cases clearly demonstrate that DNA methylation is involved in the epigenetic silencing of ferroptosis-associated genes. However, whether other ferroptosis-associated genes are also affected by DNA methylation requires further study. Moreover, TET (ten-eleven translocation) proteins could catalyze 5mC oxidation, which in turn initiates the active or passive DNA demethylation (53). It is still unclear whether TET proteins-mediated DNA demethylation also plays a role in the regulation of ferroptosis.

Histone Modifications

Histones form the framework of DNA entangling (54). The tails of four core histones (H2A, H2B, H3 and H4) are proved to undergo chemical modifications, including lysine methylation/acetylation, arginine methylation/citrullination and serine/threonine/tyrosine phosphorylation (55). These chemical modifications alter the interaction between histones and other nuclear proteins including the transcriptional machine, thereby changing the expression of targeted genes.

Histone acetylation marks are written by histone acetyltransferases (HATs), read by bromodomains (BRDs), and erased by histone deacetylases (HDACs). NRF2 activates the transcription of *SLC7A11* gene partially through recruiting HATs (CBP and p300) (47, 56). Moreover, the expression of many ferroptosis-associated genes (*GPX4, SLC7A11*, and *SLC3A2*) were down-regulated in breast and lung cancer cell lines upon BRD4 knockdown (57). The inhibition of BRD4 also enhances the expression of a histone deacetylase called sirtuin 1 (SIRT1) (57). Additionally, SIRT1 causes epigenetic reprogramming of epithelial-mesenchymal transition (EMT) thus promotes ferroptosis in head and neck cancer (51).

H2A ubiquitination/de-ubiquitination play a critical role in the regulation of *SLC7A11* expression and erastin-induced ferroptosis (**Figure 1**). PRC1 complex, the best-known ubiquitin ligase of H2Aub, is responsible for the establishment of H2A ubiquitination on *SLC7A11* promoter (58). In contrast, a nuclear deubiquitinating enzyme named BRCA1-associated protein 1 (BAP1) could decrease the H2A ubiquitination occupancy on the *SLC7A11* promoter (59). Interestingly, although H2Aub is generally correlated with gene repression, both BAP1 and PRC1 represses *SLC7A11* expression. The weird results indicate that BAP1 and PRC1 coordinately repress *SLC7A11* expression through dynamic regulation of H2Aub levels on the *SLC7A11* promoter. However, the exact role of H2Aub in *SLC7A11* gene expression requires further research. In addition to H2A, mono-ubiquitination of histone H2B on lysine 120 is an epigenetic active marker associated with *SLC7A11* expression. Wang et al. revealed that P53-mediated repression of SLC7A11 is dependent on USP7-mediated H2B de-ubiquitination (60).

The di- or tri-methylation of H3K9 are well-established epigenetic marks of heterochromatin and associated with transcriptional silencing (61). Inhibition of SUV39H1 (one of histone H3K9me3 methyltransferases) by small chemical molecules or siRNA upregulates *DPP4* expression through reducing the H3K9me3, thereby inducing iron accumulation, lipid peroxidation, and ferroptosis (62). In contrast, KDM3B, a histone H3 lysine 9 demethylase, was reported to prevent erastin-induced ferroptosis of HT-1080 cells (63). Mechanistically, KDM3B knockdown did not change the H3K9 methylation level on the *SLC7A11* promoter, while KDM3B cooperates with transcription factor ATF4 to upregulate the expression of *SLC7A11*. Also, KDM4A, a histone demethylase, was revealed to regulate *SLC7A11* transcription by controlling H3K9me3 demethylation in the promoter of *SLC7A11* (**Figure 1**) (64). Besides H3K9, multiple lysine and arginine residues of histones (such as H3R2, H3K4, H3K27, H3K79, H4R3, H4K20, and H2BK5) also undergo methylation/demethylation dynamics and exhibit pleiotropic roles in gene transcription (65). Therefore, it is of great interest to determine whether the histone methylation of other sites and their writers, readers, and erasers also participate in the regulation of ferroptosis-associated genes.

RNA Modifications

N6-methyladenosine (m6A) RNA modification emerges in recent years as a new layer of regulatory mechanism controlling gene expression in eukaryotes (66). The m6A RNA modification is a reversible epigenetic modification that targets on mRNA and noncoding RNAs. The m6A modification regulates gene expression by affecting the fate of the modified RNA molecules (67). Intriguingly, m6A modification has been observed to play a regulatory function in ferroptosis. The m6A reader YTH domain containing 2 (YTHDC2) can bind to *SLC7A11* mRNA and thereafter promotes its decay (**Figure 1**) (68). The main death type of tissue ischemic reperfusion injury has been proved to be ferroptosis (11). Xu et al. revealed that m6A methylase methyltransferase like 14 (METTL14) promotes renal ischemic reperfusion injury (69). Mechanistically, they identified *YAP1* mRNA as a target of METTL14 and the

translation of m6A-modified *YAP1* mRNA was inhibited. However, a recent study revealed that YAP1 activates *ACSCL4* gene transcription and thereby promotes ferroptosis (69). These paradoxical results suggest that the role of YAP1 in ferroptosis might be context-dependent and tissue or cell-type specific.

Non-Coding RNAs

The microRNA (miRNA) is a series of single strand noncoding small RNA, which is made up of 20-22 nucleotides. The miRNA can targets the 3'-UTR region of mRNA, triggering mRNA decay or translational inhibition (70). Plenty of miRNAs have been identified to participate in the regulation of the key genes of ferroptosis. For instance, miRNA-17-92 can protect cells from erastin-induced ferroptosis through targeting the ACSL4 axis and down regulating the *ACSL4* expression (71). miRNA-4715-3p induces ferroptosis by inhibiting *GPX4* expression (72). miRNA-137 targets *SLC1A5* to suppress glutamine transportation and induce ferroptosis (73).

The role of long noncoding RNA (lncRNA) in gene regulation is gradually focused during the recent years (74). lncRNA is defined as transcripts of more than 200 nucleotides that are not translated into proteins (75). lncRNAs including HOX transcript antisense RNA and metastasis–associated lung adenocarcinoma transcript 1 are identified in the mechanism of ferroptosis suppress induced by XAV939 treatment (76). The lncRNA P53RRA induces ferroptosis by interacting with Ras GTPase-activating protein-binding protein 1 (G3BP1) and activating p53 pathway, then induce ferroptosis by affecting transcription of several metabolic genes (77). Wang et al. found lncRNA LINC00336 combines with ELAVL1 and inhibit ferroptosis by decreasing intracellular iron and lipid ROS level (78).

Circular RNA (cirRNA) is a type of single-stranded RNA which, unlike linear RNA, forms a covalently closed continuous loop. Circular RNA can regulate gene regulation by directly conjugating mRNA or indirectly transporting miRNAs in the cell (79, 80). In addition, cirRNAs are appealed to involve the ferroptosis regulation. Circular RNA cIARS regulates ferroptosis in HCC cells through interacting with RNA binding protein alkB homolog 5 (ALKBH5) (81). CircABCB10 silencing inhibits the cell ferroptosis and apoptosis by regulating the miR-326/CCL5 axis in rectal cancer (82). Circ_0008035 contributes to cell proliferation and inhibits apoptosis and ferroptosis in gastric cancer *via* miR-599/EIF4A1 axis (83).

Collectively, these findings demonstrate that epigenetic mechanisms contribute to the regulation of ferroptosis-associated genes (**Table 1**). However, whether, when, and how those key regulator genes as well as many newly found genes are epigenetically modulated are poorly understood. Therefore, systematic identification of the epigenetic regulatory network underlying ferroptosis is required in future study.

TARGETING EPIGENETIC REGULATION: A NEW STRATEGY IN THE PREVENTION AND THERAPY OF FERROPTOSIS-ASSOCIATED DISEASES

As aforementioned, epigenetic mechanisms play a critical role in the regulation of ferroptosis-associated genes, thereby finetuning the cellular response to ferroptotic stress. Therefore, targeting epigenetic regulation represents a promising strategy to enhance or inhibit ferroptosis and has potential application in the prevention and therapy of ferroptosis-associated diseases. Indeed, many epigenetic drugs have been reported to display exciting results in cancer therapy through modulating ferroptosis (**Table 2**).

TABLE 1 | Epigenetic regulation of ferroptosis-associated genes.

Type	Molecular mechanism	Consequence on ferroptosis	Reference
DNA modification	Homocysteine treatment inhibits *GPX4* expression through increasing the promoter DNA methylation level	Promotion	(52)
	DNA hypermethylation of *CDH1* increases its expression	Inhibition	(51)
Histone modification	KDM4A induces H3K9me3 demethylation at the promoter region of *SLC7A11* and promotes its transcription	Inhibition	(64)
	BAP1 decreases the H2A ubiquitination level at *SLC7A11* promoter and suppresses its expression	Promotion	(59)
	PRC1 increases the H2A ubiquitination level at *SLC7A11* promoter and suppresses its expression	Promotion	(58)
	USP7 decreases H2Bub1 level at *SLC7A11* promoter and represses its expression	Promotion	(60)
	SUV39H1 modulates the H3K9me3 status of *DPP4* gene promoter and down-regulates its expression	Promotion	(62)
RNA modification	YTHDC2 binds on the mRNA of *SLC7A11* and promotes its decay	Promotion	(68)
	METTL14 deposits m6A on *YAP1* mRNA and inhibits its translation	Promotion	(69)
Noncoding RNAs	miRNA-17-92 down-regulates *ACSL4* expression	Inhibition	(71)
	miRNA-4715-3p inhibits *GPX4* expression	Promotion	(72)
	miRNA-137 suppresses *SLC1A5* expression	Promotion	(73)
	lncRNA P53RRA activates p53 pathways	Promotion	(77)
	lncRNA LINC00336 interacts with *ELAVL1* to decrease the intracellular iron and lipid ROS level	Inhibition	(78)
	cIARS interacts with *ALKBH5*	Promotion	(81)
	CircABCB10 regulates miR-326/CCL5 axis	Inhibition	(82)
	Circ_0008035 regulates miR-599/EIF4A1 axis	Inhibition	(83)

TABLE 2 | Epigenetic drugs that modulate ferroptosis in cancer therapy.

Drug type	Name	Molecular mechanism	Consequence on ferroptosis	Cancer types	Reference
DNMT inhibitors	5-Aza-cd	Inhibition of DNMT by 5-Aza-cd increases the expression of *E-cadherin* and *GPX4*	Inhibition	Head and neck cancer	(51, 52)
BET inhibitors	JQ-1	Inhibition of BRD4 by JQ-1 downregulates the expression of *GPX4, SLC7A11* and *SLCA2*	Promotion	Breast cancer; Lung Adenocarcinoma	(57)
HDAC inhibitors	EX-527	Inhibition of SIRT1 by EX-527 increases EMT	Promotion	Head and neck cancer	(51)
	Vorinostat	Unknown	Promotion	Small cell lung cancer; *IDH1/2* mutant brain tumors	(84)

DNMT Inhibitors

DNMT inhibitors have been successfully used in the treatment of certain hematopoietic malignancies (85). Moreover, recent work showed that DNMT inhibitors could enhance the efficiency of immune checkpoint inhibitors (ICI) in cancer immunotherapy (86). As aforementioned, 5-Aza-cd treatment could release the DNA methylation-mediated epigenetic silencing of *GPX4* and *CDH1* genes, restoring the resistance of cells to ferroptosis (51, 52). Given that DNMT inhibitors have very broad effect on gene expression and genomic stability, it should be careful to distinguish whether their effect on ferroptosis is achieved through the direct regulation of specific ferroptosis-associated gene or the indirect activation of certain signaling pathways due to epigenetic reprogramming.

BET Inhibitors

Bromodomain and extra terminal protein (BET) inhibitors are a class of drugs that prevent the interaction between BET proteins and acetylated histones (87–89). Sui et al. revealed that ferroptosis is involved in JQ1-induced cell death of BRCA and LUAD (57). Moreover, treatment with JQ1 and ferroptosis inducers (RSL3, erastin, or sorafenib) produced a satisfactory anticancer effect, suggesting that the combination of BET inhibitors with ferroptosis inducers may become a new therapeutic modality.

HDAC Inhibitors

Pharmacological inhibition of SIRT1 by EX-527 increases ferroptosis susceptibility by suppressing EMT, while SIRT1 agonists, resveratrol and SRT1720, promote ferroptosis (51). A recent drug screening also identified a class I HDAC inhibitor, Vorinostat, as an inducer of ferroptosis in small cell lung cancer (SCLC) and isocitrate dehydrogenase (*IDH1/2*)-mutant brain tumors, suggesting an unique vulnerability that is regulated by histone or non-histone acetylation (84).

DISCUSSION

As a new concept introduced in 2012, ferroptosis has attracted tremendous attention in biomedical fields. The existing work about the epigenetic regulation of ferroptosis mainly focused on several key ferroptosis genes. Whether the epigenetic mechanisms affect multiple ferroptosis genes and how these different epigenetic mechanisms corporate with diverse signaling pathways to determine the responsiveness of cells to ferroptosis stimuli remain unknown. Therefore, a systematic study on the epigenetic regulatory network of ferroptosis process is still a blank in this field and requires extensive investigation.

Given that ferroptosis plays a role of surveillance in tumorigenesis and also contributes to the efficiency of multiple cancer therapies [chemotherapy, radiotherapy (90), and immunotherapy (91)], it is rationale to speculate that targeting the epigenetic machines alone or in combination with the traditional therapies will be promising strategies for cancer therapy. Since ferroptosis is closely related to neurodegenerative diseases, ischemia-reperfusion injury of organ, neurotoxicity, and others (11, 92–95), it is also of great interest to explore the epigenetic mechanisms underlying the altered ferroptosis sensitivity under different pathological processes. The advances in this cross-disciplinary research field may shed light on the treatment of diseases mentioned above by modulating ferroptosis.

AUTHOR CONTRIBUTIONS

Conceptualization, YP, HW, and LT. Writing—original draft preparation, YP and LT. Writing—review and editing, YQ, HW, and LT. Funding acquisition, LT. All authors have read and agreed to the published version of the manuscript.

FUNDING

This review was supported by the National Natural Science Foundation of China (81672785, 31871291, and 82073113) and the National Key R&D Project of China (2016YFA0101800). LT was also supported by the innovative research team of high-level local university in Shanghai.

ACKNOWLEDGMENTS

We thank Dr Pingzhao Zhang for providing us critical advice.

REFERENCES

1. Dixon SJ, Lemberg KM, Lamprecht MR, Skouta R, Zaitsev EM, Gleason CE, et al. Ferroptosis: An Iron-Dependent Form of Nonapoptotic Cell Death. *Cell* (2012) 149:1060–72. doi: 10.1016/j.cell.2012.03.042
2. Friedmann Angeli JP, Schneider M, Proneth B, Tyurina YY, Tyurin VA, Hammond VJ, et al. Inactivation of the Ferroptosis Regulator Gpx4 Triggers Acute Renal Failure in Mice. *Nat Cell Biol* (2014) 16:1180–91. doi: 10.1038/ncb3064
3. Yang WS, SriRamaratnam R, Welsch ME, Shimada K, Skouta R, Viswanathan VS, et al. Regulation of Ferroptotic Cancer Cell Death by GPX4. *Cell* (2014) 156:317–31. doi: 10.1016/j.cell.2013.12.010
4. Li Y, Feng D, Wang Z, Zhao Y, Sun R, Tian D, et al. Ischemia-Induced ACSL4 Activation Contributes to Ferroptosis-Mediated Tissue Injury in Intestinal Ischemia/Reperfusion. *Cell Death Differ* (2019) 26:2284–99. doi: 10.1038/s41418-019-0299-4
5. Dixon SJ, Winter GE, Musavi LS, Lee ED, Snijder B, Rebsamen M, et al. Human Haploid Cell Genetics Reveals Roles for Lipid Metabolism Genes in Nonapoptotic Cell Death. *ACS Chem Biol* (2015) 10:1604–9. doi: 10.1021/acschembio.5b00245
6. Doll S, Freitas FP, Shah R, Aldrovandi M, da Silva MC, Ingold I, et al. FSP1 Is a Glutathione-Independent Ferroptosis Suppressor. *Nature* (2019) 575:693–8. doi: 10.1038/s41586-019-1707-0
7. Doll S, Proneth B, Tyurina YY, Panzilius E, Kobayashi S, Ingold I, et al. ACSL4 Dictates Ferroptosis Sensitivity by Shaping Cellular Lipid Composition. *Nat Chem Biol* (2017) 13:91–8. doi: 10.1038/nchembio.2239
8. Jiang X, Stockwell BR, Conrad M. Ferroptosis: Mechanisms, Biology and Role in Disease. *Nat Rev Mol Cell Biol* (2021) 22:266–82. doi: 10.1038/s41580-020-00324-8
9. Dawson MA, Kouzarides T. Cancer Epigenetics: From Mechanism to Therapy. *Cell* (2012) 150:12–27. doi: 10.1016/j.cell.2012.06.013
10. Yang WS, Stockwell BR. Ferroptosis: Death by Lipid Peroxidation. *Trends Cell Biol* (2016) 26:165–76. doi: 10.1016/j.tcb.2015.10.014
11. Stockwell BR, Friedmann Angeli JP, Bayir H, Bush AI, Conrad M, Dixon SJ, et al. Ferroptosis: A Regulated Cell Death Nexus Linking Metabolism, Redox Biology, and Disease. *Cell* (2017) 171:273–85. doi: 10.1016/j.cell.2017.09.021
12. Kagan VE, Mao G, Qu F, Angeli JPF, Doll S, Croix CS, et al. Oxidized Arachidonic and Adrenic PEs Navigate Cells to Ferroptosis. *Nat Chem Biol* (2017) 13:81–90. doi: 10.1038/nchembio.2238
13. Halliwell B, Cross CE. Oxygen-Derived Species: Their Relation to Human Disease and Environmental Stress. *Environ Health Perspect* (1994) 102 Suppl:10. doi: 10.1289/ehp.94102s105
14. Kakhlon O, Cabantchik ZI. The Labile Iron Pool: Characterization, Measurement, and Participation in Cellular Processes(1). *Free Radical Biol Med* (2002) 33:1037–46. doi: 10.1016/S0891-5849(02)01006-7
15. Dixon SJ, Stockwell BR. The Role of Iron and Reactive Oxygen Species in Cell Death. *Nat Chem Biol 10* (2014) 10:9–17. doi: 10.1038/nchembio.1416
16. Doll S, Conrad M. Iron and Ferroptosis: A Still Ill-Defined Liaison. *IUBMB Life* (2017) 69:423–34. doi: 10.1002/iub.1616
17. Paul BD, Sbodio JI, Snyder SH. Cysteine Metabolism in Neuronal Redox Homeostasis. *Trends Pharmacol Sci* (2018) 39:513–24. doi: 10.1016/j.tips.2018.02.007
18. Bannai S. Exchange of Cystine and Glutamate Across Plasma Membrane of Human Fibroblasts. *J Biol Chem* (1986) 261:2256–63. doi: 10.1016/S0021-9258(17)35926-4
19. Koppula P, Zhuang L, Gan B. Cystine Transporter SLC7A11/xCT in Cancer: Ferroptosis, Nutrient Dependency, and Cancer Therapy. *Protein Cell* (2020) 12:599–620. doi: 10.1007/s13238-020-00789-5
20. Tan S, Wood M, Maher P. Oxidative Stress Induces a Form of Programmed Cell Death With Characteristics of Both Apoptosis and Necrosis in Neuronal Cells. *J Neurochem* (1998) 71:95–105. doi: 10.1046/j.1471-4159.1998.71010095.x
21. Murphy TH, Miyamoto M, Sastre A, Schnaar RL, Coyle JT. Glutamate Toxicity in a Neuronal Cell Line Involves Inhibition of Cystine Transport Leading to Oxidative Stress. *Neuron* (1989) 2:1547–58. doi: 10.1016/0896-6273(89)90043-3
22. Ekoue DN, He C, Diamond AM, Bonini MG. Manganese Superoxide Dismutase and Glutathione Peroxidase-1 Contribute to the Rise and Fall of Mitochondrial Reactive Oxygen Species Which Drive Oncogenesis. *Biochim Biophys Acta Bioenerg* (2017) 1858:628–32. doi: 10.1016/j.bbabio.2017.01.006
23. Seiler A, Schneider M, Förster H, Roth S, Wirth EK, Culmsee C, et al. Glutathione Peroxidase 4 Senses and Translates Oxidative Stress Into 12/15-Lipoxygenase Dependent- and AIF-Mediated Cell Death. *Cell Metab* (2008) 8:237–48. doi: 10.1016/j.cmet.2008.07.005
24. Dolma S, Lessnick SL, Hahn WC, Stockwell BR. Identification of Genotype-Selective Antitumor Agents Using Synthetic Lethal Chemical Screening in Engineered Human Tumor Cells. *Cancer Cell* (2003) 3:285–96. doi: 10.1016/S1535-6108(03)00050-3
25. Yang WS, Stockwell BR. Synthetic Lethal Screening Identifies Compounds Activating Iron-Dependent, Nonapoptotic Cell Death in Oncogenic-RAS-Harboring Cancer Cells. *Chem Biol* (2008) 15:234–45. doi: 10.1016/j.chembiol.2008.02.010
26. Ko P-J, Woodrow C, Dubreuil MM, Martin BR, Skouta R, Bassik MC, et al. A ZDHHC5-GOLGA7 Protein Acyltransferase Complex Promotes Nonapoptotic Cell Death. *Cell Chem Biol* (2019) 26:1716–24. doi: 10.1016/j.chembiol.2019.09.014
27. Yang WS, Shimada K, Delva D, Patel M, Ode E, Skouta R, et al. Identification of Simple Compounds With Microtubule-Binding Activity That Inhibit Cancer Cell Growth With High Potency. *ACS Med Chem Lett* (2012) 3:35–8. doi: 10.1021/ml200195s
28. Marshall KR, Gong M, Wodke L, Lamb JH, Jones DJL, Farmer PB, et al. The Human Apoptosis-Inducing Protein AMID Is an Oxidoreductase With a Modified Flavin Cofactor and DNA Binding Activity. *J Biol Chem* (2005) 280:30735–40. doi: 10.1074/jbc.M414018200
29. Crane FL. Discovery of Ubiquinone (Coenzyme Q) and an Overview of Function. *Mitochondrion* (2007) 7 Suppl:S2–7. doi: 10.1016/j.mito.2007.02.011
30. Bersuker K, Hendricks JM, Li Z, Magtanong L, Ford B, Tang PH, et al. The CoQ Oxidoreductase FSP1 Acts Parallel to GPX4 to Inhibit Ferroptosis. *Nature* (2019) 575:688–92. doi: 10.1038/s41586-019-1705-2
31. Madak JT, Bankhead A, Cuthbertson CR, Showalter HD, Neamati N. Revisiting the Role of Dihydroorotate Dehydrogenase as a Therapeutic Target for Cancer. *Pharmacol Ther* (2019) 195:111–31. doi: 10.1016/j.pharmthera.2018.10.012
32. Fu H, Zhang Z, Dai Y, Liu S, Fu E. Brequinar Inhibits Enterovirus Replication by Targeting Biosynthesis Pathway of Pyrimidines. *Am J Transl Res* (2020) 12:8247–55.
33. Boyd AS. Leflunomide in Dermatology. *J Am Acad Dermatol* (2012) 66:673–9. doi: 10.1016/j.jaad.2011.08.025
34. Bar-Or A, Pachner A, Menguy-Vacheron F, Kaplan J, Wiendl H. Teriflunomide and Its Mechanism of Action in Multiple Sclerosis. *Drugs* (2014) 74:659–74. doi: 10.1007/s40265-014-0212-x
35. Mao C, Liu X, Zhang Y, Lei G, Yan Y, Lee H, et al. DHODH-Mediated Ferroptosis Defence Is a Targetable Vulnerability in Cancer. *Nature* (2021) 593:586–90. doi: 10.1038/s41586-021-03539-7
36. Kraft VAN, Bezjian CT, Pfeiffer S, Ringelstetter L, Müller C, Zandkarimi F, et al. GTP Cyclohydrolase 1/Tetrahydrobiopterin Counteract Ferroptosis Through Lipid Remodeling. *ACS Cent Sci* (2020) 6:41–53. doi: 10.1021/acscentsci.9b01063
37. Xu J, Wu Y, Song P, Zhang M, Wang S, Zou M-H. Proteasome-Dependent Degradation of Guanosine 5'-Triphosphate Cyclohydrolase I Causes Tetrahydrobiopterin Deficiency in Diabetes Mellitus. *Circulation* (2007) 116:944–53. doi: 10.1161/CIRCULATIONAHA.106.684795
38. Soula M, Weber RA, Zilka O, Alwaseem H, La K, Yen F, et al. Metabolic Determinants of Cancer Cell Sensitivity to Canonical Ferroptosis Inducers. *Nat Chem Biol* (2020) 16:1351–60. doi: 10.1038/s41589-020-0613-y
39. Jiang L, Kon N, Li T, Wang S-J, Su T, Hibshoosh H, et al. Ferroptosis as a P53-Mediated Activity During Tumour Suppression. *Nature* (2015) 520:57–62. doi: 10.1038/nature14344
40. Ou Y, Wang S-J, Li D, Chu B, Gu W. Activation of SAT1 Engages Polyamine Metabolism With P53-Mediated Ferroptotic Responses. *Proc Natl Acad Sci USA* (2016) 113:E6806–12. doi: 10.1073/pnas.1607152113
41. Xie Y, Zhu S, Song X, Sun X, Fan Y, Liu J, et al. The Tumor Suppressor P53 Limits Ferroptosis by Blocking DPP4 Activity. *Cell Rep* (2017) 20:1692–704. doi: 10.1016/j.celrep.2017.07.055
42. Tarangelo A, Magtanong L, Bieging-Rolett KT, Li Y, Ye J, Attardi LD, et al. P53 Suppresses Metabolic Stress-Induced Ferroptosis in Cancer Cells. *Cell Rep* (2018) 22:569–75. doi: 10.1016/j.celrep.2017.12.077

43. Song X, Long D. Nrf2 and Ferroptosis: A New Research Direction for Neurodegenerative Diseases. *Front Neurosci* (2020) 14:267. doi: 10.3389/fnins.2020.00267
44. Dodson M, Castro-Portuguez R, Zhang DD. NRF2 Plays a Critical Role in Mitigating Lipid Peroxidation and Ferroptosis. *Redox Biol* (2019) 23:101107. doi: 10.1016/j.redox.2019.101107
45. Fan Z, Wirth AK, Chen D, Wruck CJ, Rauh M, Buchfelder M, et al. Nrf2-Keap1 Pathway Promotes Cell Proliferation and Diminishes Ferroptosis. *Oncogenesis* (2017) 6:e371. doi: 10.1038/oncsis.2017.65
46. Takahashi N, Cho P, Selfors LM, Kuiken HJ, Kaul R, Fujiwara T, et al. 3d Culture Models With CRISPR Screens Reveal Hyperactive NRF2 as a Prerequisite for Spheroid Formation *via* Regulation of Proliferation and Ferroptosis. *Mol Cell* (2020) 80:828–44.e6. doi: 10.1016/j.molcel.2020.10.010
47. Chen D, Tavana O, Chu B, Erber L, Chen Y, Baer R, et al. NRF2 Is a Major Target of ARF in P53-Independent Tumor Suppression. *Mol Cell* (2017) 68:224–32.e4. doi: 10.1016/j.molcel.2017.09.009
48. Meng Z, Moroishi T, Guan K-L. Mechanisms of Hippo Pathway Regulation. *Genes Dev* (2016) 30:1–17. doi: 10.1101/gad.274027.115
49. Yang W-H, Ding C-KC, Sun T, Rupprecht G, Lin C-C, Hsu D, et al. The Hippo Pathway Effector TAZ Regulates Ferroptosis in Renal Cell Carcinoma. *Cell Rep* (2019) 28:2501–8.e4. doi: 10.2139/ssrn.3316797
50. Wu J, Minikes AM, Gao M, Bian H, Li Y, Stockwell BR, et al. Intercellular Interaction Dictates Cancer Cell Ferroptosis *via* NF2-YAP Signalling. *Nature* (2019) 572:402–6. doi: 10.1038/s41586-019-1426-6
51. Lee J, You JH, Kim M-S, Roh J-L. Epigenetic Reprogramming of Epithelial-Mesenchymal Transition Promotes Ferroptosis of Head and Neck Cancer. *Redox Biol* (2020) 37:101697. doi: 10.1016/j.redox.2020.101697
52. Zhang X, Huang Z, Xie Z, Chen Y, Zheng Z, X.a. Wei B, et al. Homocysteine Induces Oxidative Stress and Ferroptosis of Nucleus Pulposus *via* Enhancing Methylation of GPX4. *Free Radical Biol Med* (2020) 160:552–65. doi: 10.1016/j.freeradbiomed.2020.08.029
53. Tan L, Shi YG. Tet Family Proteins and 5-Hydroxymethylcytosine in Development and Disease. *Dev (Cambridge England)* (2012) 139:1895–902. doi: 10.1242/dev.070771
54. Bannister AJ, Schneider R, Kouzarides T. Histone Methylation: Dynamic or Static? *Cell* (2002) 109:801–6. doi: 10.1016/S0092-8674(02)00798-5
55. Rodríguez-Paredes M, Esteller M. Cancer Epigenetics Reaches Mainstream Oncology. *Nat Med* (2011) 17:330–9. doi: 10.1038/nm.2305
56. Sun Z, Chin YE, Zhang DD. Acetylation of Nrf2 by P300/CBP Augments Promoter-Specific DNA Binding of Nrf2 During the Antioxidant Response. *Mol Cell Biol* (2009) 29:2658–72. doi: 10.1128/MCB.01639-08
57. Sui S, Zhang J, Xu S, Wang Q, Wang P, Pang D. Ferritinophagy Is Required for the Induction of Ferroptosis by the Bromodomain Protein BRD4 Inhibitor (+)-JQ1 in Cancer Cells. *Cell Death Dis* (2019) 10:331. doi: 10.1038/s41419-019-1564-7
58. Zhang Y, Koppula P, Gan B. Regulation of H2A Ubiquitination and SLC7A11 Expression by BAP1 and PRC1. *Cell Cycle (Georgetown Tex)* (2019) 18:773–83. doi: 10.1080/15384101.2019.1597506
59. Zhang Y, Shi J, Liu X, Feng L, Gong Z, Koppula P, et al. BAP1 Links Metabolic Regulation of Ferroptosis to Tumour Suppression. *Nat Cell Biol* (2018) 20:1181–92. doi: 10.1038/s41556-018-0178-0
60. Wang Y, Yang L, Zhang X, Cui W, Liu Y, Sun QR, et al. Epigenetic Regulation of Ferroptosis by H2B Monoubiquitination and P53. *EMBO Rep* (2019) 20:e47563. doi: 10.15252/embr.201847563
61. Becker JS, Nicetto D, Zaret KS. H3K9me3-Dependent Heterochromatin: Barrier to Cell Fate Changes. *Trends Genet* (2016) 32:29–41. doi: 10.1016/j.tig.2015.11.001
62. Wang J, Yin X, He W, Xue W, Zhang J, Huang Y. SUV39H1 Deficiency Suppresses Clear Cell Renal Cell Carcinoma Growth by Inducing Ferroptosis. *Acta Pharm Sinica B* (2021) 11:406–19. doi: 10.1016/j.apsb.2020.09.015
63. Wang Y, Zhao Y, Wang H, Zhang C, Wang M, Yang Y, et al. Histone Demethylase KDM3B Protects Against Ferroptosis by Upregulating SLC7A11. *FEBS Open Bio* (2020) 10:637–43. doi: 10.1002/2211-5463.12823
64. Chen M, Jiang Y, Sun Y. KDM4A-Mediated Histone Demethylation of SLC7A11 Inhibits Cell Ferroptosis in Osteosarcoma. *Biochem Biophys Res Commun* (2021) 550:77–83. doi: 10.1016/j.bbrc.2021.02.137
65. Jambhekar A, Dhall A, Shi Y. Roles and Regulation of Histone Methylation in Animal Development. *Nat Rev Mol Cell Biol* (2019) 20:625–41. doi: 10.1038/s41580-019-0151-1
66. Chen X-Y, Zhang J, Zhu J-S. The Role of mA RNA Methylation in Human Cancer. *Mol Cancer* (2019) 18:103. doi: 10.1186/s12943-019-1033-z
67. Huang H, Weng H, Chen J. mA Modification in Coding and Non-Coding RNAs: Roles and Therapeutic Implications in Cancer. *Cancer Cell* (2020) 37:270–88. doi: 10.1016/j.ccell.2020.02.004
68. Ma L, Chen T, Zhang X, Miao Y, Tian X, Yu K, et al. The M6a Reader YTHDC2 Inhibits Lung Adenocarcinoma Tumorigenesis by Suppressing SLC7A11-Dependent Antioxidant Function. *Redox Biol* (2021) 38:101801. doi: 10.1016/j.redox.2020.101801
69. Xu Y, Yuan XD, Wu JJ, Chen RY, Xia L, Zhang M, et al. The N6-Methyladenosine mRNA Methylase METTL14 Promotes Renal Ischemic Reperfusion Injury *via* Suppressing YAP1. *J Cell Biochem* (2020) 121:524–33. doi: 10.1002/jcb.29258
70. Lu TX, Rothenberg ME. MicroRNA. *J Allergy Clin Immunol* (2018) 141:1202–7. doi: 10.1016/j.jaci.2017.08.034
71. Xiao F-J, Zhang D, Wu Y, Jia Q-H, Zhang L, Li Y-X, et al. miRNA-17-92 Protects Endothelial Cells From Erastin-Induced Ferroptosis Through Targeting the A20-ACSL4 Axis. *Biochem Biophys Res Commun* (2019) 515:448–54. doi: 10.1016/j.bbrc.2019.05.147
72. Gomaa A, Peng D, Chen Z, Soutto M, Abouelezz K, Corvalan A, et al. Epigenetic Regulation of AURKA by miR-4715-3p in Upper Gastrointestinal Cancers. *Sci Rep* (2019) 9:16970. doi: 10.1038/s41598-019-53174-6
73. Luo M, Wu L, Zhang K, Wang H, Zhang T, Gutierrez L, et al. miR-137 Regulates Ferroptosis by Targeting Glutamine Transporter SLC1A5 in Melanoma. *Cell Death Differ* (2018) 25:1457–72. doi: 10.1038/s41418-017-0053-8
74. Ulitsky I, Bartel DP. lincRNAs: Genomics, Evolution, and Mechanisms. *Cell* (2013) 154:26–46. doi: 10.1016/j.cell.2013.06.020
75. Kopp F, Mendell JT. Functional Classification and Experimental Dissection of Long Noncoding RNAs. *Cell* (2018) 172:393–407. doi: 10.1016/j.cell.2018.01.011
76. Yu H, Han Z, Xu Z, An C, Xu L, Xin H. RNA Sequencing Uncovers the Key Long Non-Coding RNAs and Potential Molecular Mechanism Contributing to XAV939-Mediated Inhibition of Non-Small Cell Lung Cancer. *Oncol Lett* (2019) 17:4994–5004. doi: 10.3892/ol.2019.10191
77. Mao C, Wang X, Liu Y, Wang M, Yan B, Jiang Y, et al. A G3BP1-Interacting lncRNA Promotes Ferroptosis and Apoptosis in Cancer *via* Nuclear Sequestration of P53. *Cancer Res* (2018) 78:3484–96. doi: 10.1158/0008-5472.CAN-17-3454
78. Wang M, Mao C, Ouyang L, Liu Y, Lai W, Liu N, et al. Long Noncoding RNA LINC00336 Inhibits Ferroptosis in Lung Cancer by Functioning as a Competing Endogenous RNA. *Cell Death Differ* (2019) 26:2329–43. doi: 10.1038/s41418-019-0304-y
79. Hentze MW, Preiss T. Circular RNAs: Splicing's Enigma Variations. *EMBO J* (2013) 32:923–5. doi: 10.1038/emboj.2013.53
80. Memczak S, Jens M, Elefsinioti A, Torti F, Krueger J, Rybak A, et al. Circular RNAs Are a Large Class of Animal RNAs With Regulatory Potency. *Nature* (2013) 495:333–8. doi: 10.1038/nature11928
81. Liu Z, Wang Q, Wang X, Xu Z, Wei X, Li J. Circular RNA Regulates Ferroptosis in HCC Cells Through Interacting With RNA Binding Protein ALKBH5. *Cell Death Discov* (2020) 6:72. doi: 10.1038/s41420-020-00306-x
82. Xian ZY, Hu B, Wang T, Cai JL, Zeng JY, Zou Q, et al. CircABCB10 Silencing Inhibits the Cell Ferroptosis and Apoptosis by Regulating the miR-326/CCL5 Axis in Rectal Cancer. *Neoplasma* (2020) 67:1063–73. doi: 10.4149/neo_2020_191024N1084
83. Li C, Tian Y, Liang Y, Li Q. Circ_0008035 Contributes to Cell Proliferation and Inhibits Apoptosis and Ferroptosis in Gastric Cancer *via* miR-599/EIF4A1 Axis. *Cancer Cell Int* (2020) 20:84. doi: 10.1186/s12935-020-01168-0
84. Yang H, Zhao L, Gao Y, Yao F, Marti TM, Schmid RA, et al. Pharmacotranscriptomic Analysis Reveals Novel Drugs and Gene Networks Regulating Ferroptosis in Cancer. *Cancers* (2020) 12:3273. doi: 10.3390/cancers12113273
85. Claus R, Lübbert M. Epigenetic Targets in Hematopoietic Malignancies. *Oncogene* (2003) 22:6489–96. doi: 10.1038/sj.onc.1206814

86. Perrier A, Didelot A, Laurent-Puig P, Blons H, Garinet S. Epigenetic Mechanisms of Resistance to Immune Checkpoint Inhibitors. *Biomolecules* (2020) 10:1061. doi: 10.3390/biom10071061
87. Garnier J-M, Sharp PP, Burns CJ. BET Bromodomain Inhibitors: A Patent Review. *Expert Opin Ther Patents* (2014) 24:185–99. doi: 10.1517/13543776.2014.859244
88. Shi J, Vakoc CR. The Mechanisms Behind the Therapeutic Activity of BET Bromodomain Inhibition. *Mol Cell* (2014) 54:728–36. doi: 10.1016/j.molcel.2014.05.016
89. Bowry A, Piberger AL, Rojas P, Saponaro M, Petermann E. BET Inhibition Induces HEXIM1- and RAD51-Dependent Conflicts Between Transcription and Replication. *Cell Rep* (2018) 25:2061–9.e4. doi: 10.1101/374660
90. Lei G, Zhang Y, Koppula P, Liu X, Zhang J, Lin SH, et al. The Role of Ferroptosis in Ionizing Radiation-Induced Cell Death and Tumor Suppression. *Cell Res* (2020) 30:146–62. doi: 10.1038/s41422-019-0263-3
91. Wang W, Green M, Choi JE, Gijón M, Kennedy PD, Johnson JK, et al. CD8+ T Cells Regulate Tumour Ferroptosis During Cancer Immunotherapy. *Nature* (2019) 569:270–4. doi: 10.1038/s41586-019-1170-y
92. Devos D, Moreau C, Devedjian JC, Kluza J, Petrault M, Laloux C, et al. Targeting Chelatable Iron as a Therapeutic Modality in Parkinson's Disease. *Antioxid Redox Signaling* (2014) 21:195–210. doi: 10.1089/ars.2013.5593
93. Moreau C, Duce JA, Rascol O, Devedjian J-C, Berg D, Dexter D, et al. Iron as a Therapeutic Target for Parkinson's Disease. *Mov Disord Off J Mov Disord Soc* (2018) 33:568–74. doi: 10.1002/mds.27275
94. Bulk M, Kenkhuis B, van der Graaf LM, Goeman JJ, Natté R, van der Weerd L. Postmortem T2*- Weighted MRI Imaging of Cortical Iron Reflects Severity of Alzheimer's Disease. *J Alzheimer's Dis JAD* (2018) 65:1125–37. doi: 10.3233/JAD-180317
95. Gong N-J, Dibb R, Bulk M, van der Weerd L, Liu C. Imaging Beta Amyloid Aggregation and Iron Accumulation in Alzheimer's Disease Using Quantitative Susceptibility Mapping MRI. *NeuroImage* (2019) 191:176–85. doi: 10.1016/j.neuroimage.2019.02.019

Conflict of Interest: The authors declare that the research was conducted in the absence of any commercial or financial relationships that could be construed as a potential conflict of interest.

The reviewer, SJ, declared a shared parent affiliation with the authors to the handling editor at the time of the review.

Publisher's Note: All claims expressed in this article are solely those of the authors and do not necessarily represent those of their affiliated organizations, or those of the publisher, the editors and the reviewers. Any product that may be evaluated in this article, or claim that may be made by its manufacturer, is not guaranteed or endorsed by the publisher.

frontiers in Oncology

ORIGINAL RESEARCH
published: 14 February 2022
doi: 10.3389/fonc.2022.820059

Network Pharmacology Study and Experimental Validation of Yiqi Huayu Decoction Inducing Ferroptosis in Gastric Cancer

*Siyuan Song[1,2,3], Fang Wen[2], Suping Gu[2], Peixin Gu[2], Wenjie Huang[1,2,3], Shuai Ruan[1,2,3], Xiaoxue Chen[1,2,3], Jiayu Zhou[1,2,3], Ye Li[1,2,3], Jiatong Liu[2] and Peng Shu[1,2,3]**

[1] Department of Medical Oncology, Affiliated Hospital of Nanjing University of Chinese Medicine, Nanjing, China, [2] The First College for Clinical Medicine, Nanjing University of Chinese Medicine, Nanjing, China, [3] Department of Medical Oncology, Jiangsu Provincial Hospital of Chinese Medicine, Nanjing, China

OPEN ACCESS

Edited by:
Jian Chen,
Guilin Medical University, China

Reviewed by:
Hongguang Ding,
Guangdong Provincial People's Hospital, China
Ali Hafez El-Far,
Damanhour University, Egypt
Bichun Li,
Yangzhou University, China

***Correspondence:**
Peng Shu
shupengsp@njucm.edu.cn

Specialty section:
This article was submitted to Pharmacology of Anti-Cancer Drugs, a section of the journal Frontiers in Oncology

Received: *06 December 2021*
Accepted: *17 January 2022*
Published: *14 February 2022*

Citation:
Song S, Wen F, Gu S, Gu P, Huang W, Ruan S, Chen X, Zhou J, Li Y, Liu J and Shu P (2022) Network Pharmacology Study and Experimental Validation of Yiqi Huayu Decoction Inducing Ferroptosis in Gastric Cancer. Front. Oncol. 12:820059. doi: 10.3389/fonc.2022.820059

Objective: This study aimed to identify the mechanism of Yiqi Huayu Decoction (YQHY) induced ferroptosis in gastric cancer (GC) by using network pharmacology and experimental validation.

Methods: The targets of YQHY, ferroptosis-related targets, and targets related to GC were derived from databases. Following the protein–protein interaction (PPI) network, the hub targets for YQHY induced ferroptosis in GC were identified. Furthermore, gene ontology (GO) and Kyoto Encyclopedia of Genes and Genomes (KEGG) enrichment were used to analyze the hub targets from a macro perspective. We verified the hub targets by molecular docking, GEPIA, HPA, and the cBioPortal database. Finally, we performed cell viability assays, quantitative real-time polymerase chain reaction (qRT-PCR), western blotting, lipid peroxidation, and GSH assays to explore the mechanism of YQHY induced ferroptosis in GC.

Results: We identified the main active compounds and hub targets: Quercetin, DIBP, DBP, Mipax, Phaseol and TP53, ATM, SMAD4, PTGS2, and ACSL4. KEGG enrichment analyses indicated that the JAK2-STAT3 signaling pathway may be a significant pathway. Molecular docking results showed that the main active compounds had a good binding activity with the hub targets. The experimental results proved that YQHY could induce ferroptosis in AGS by increasing the MDA content and reducing the GSH content. qRT–PCR and Western blot results showed that YQHY can induce ferroptosis in GC by affecting the JAK2-STAT3 pathway and the expression of ACSL4.

Conclusions: This study indicated that YQHY can induce ferroptosis in GC by affecting the JAK2–STAT3 pathway and the expression of ACSL4, and induction of ferroptosis may be one of the possible mechanisms of YQHY's anti-recurrence and metastasis of GC.

Keywords: ferroptosis, GC, network pharmacology, molecular docking, bioinformatics, Yiqi Huayu decoction

1 INTRODUCTION

The incidence of GC in China accounts for nearly half of the world (1, 2). At present, surgery is considered the only radical cure method (3). Early GC has a high cure rate, whereas advanced GC is characterized by a high metastasis rate, a high mortality rate, a low curative resection rate, and a poor five-year survival rate (4). The occurrence and development of cancer are closely related to cell death. One of the important characteristics of cancer cells is avoiding death. Thus, it is necessary to explore a new strategy to treat GC by inducing tumor cell death.

Ferroptosis is a new cell death mode discovered in recent years, which is different from autophagy, necrosis, and scorch death. It is the result of ferroptosis-dependent accumulation of lipid peroxides to lethal levels (5). The ferroptosis signature is mainly characterized by the accumulation of iron and lipid reactive oxygen species and inhibition of the cystine/glutamate antiporter (system XC), leading to reduced cystine uptake and reduced glutathione (GSH) synthesis (6). Studies have shown that ferroptosis plays an important role in the development of various cancers (7). There is a close relationship between ferroptosis and GC, as ferroptosis is significantly suppressed in GC, resulting in reduced tumor growth and sensitivity to cisplatin versus paclitaxel (8). The expression of ultralong-chain fatty acid protein 5 and fatty acid desaturase 1 in mesenchymal GC cells is upregulated, leading to ferroptosis sensitization (9). Erastin, a typical ferroptosis inducer, can induce ferroptosis in GC cells. Silencing CDO1 *in vitro* and *in vivo* can restore intracellular glutathione levels and prevent ROS production, thus inhibiting ferroptosis in GC cells induced by erastin (10, 11). Therefore, inducing GC cells to undergo ferroptosis could be a potential direction for GC treatment (12).

The pathogenesis of postoperative patients with GC can be summarized as "Qi deficiency and blood stasis and toxin", with deficiency of vital qi as the foundation and blood stasis and toxin as the standard. YQHY was pioneered by Professor Shen Lin Liu of a nationwide Chinese medicine and is based on Invigorating Qi and invigorating spleen and removing blood stasis as therapeutic points for GC, which is widely used in the clinical treatment of GC. Our previous studies have proven that YQHY can reduce the risk of recurrence and metastasis of patients with GC after stage II and III operations. Compared with chemotherapy alone, the risk of recurrence and metastasis is decreased by 32.8% (P = 0.0042). Especially for patients with stage III disease, the percentage of recurrence and metastasis risk is decreased to 34.7% (P = 0.0072) (13). Traditional Chinese medicine (TCM) has "multicomponent, multitarget, and multipathway" advantages for treating diseases (14). However, the mechanism of YQHY in reducing the risk of recurrence and metastasis of GC is still unclear. Therefore, in this paper, we combined the results of the network pharmacology study and verified them through experiments *in vitro*, which can provide new ideas for clarifying the pathogenesis of GC and for clinical intervention and treatment. The protocol of our study procedures is shown in **Figure 1**.

Abbreviations: GC, gastric cancer; YQHY, Yiqi Huayu Decoction; TCMSP, Traditional Chinese Medicine Systems Pharmacology Database and Analysis Platform; OB, Oral bioavailability; DL, Drug-likeness; GO, Gene Ontology; BP, Biological process; CC, Cellular component; MF, Molecular function; FDR, Error Detection Rate; KEGG, Kyoto Encyclopedia of Genes and Genomes; PPI, Protein–protein interaction; OS, Overall Survival; qRT-PCR, Quantitative Real-Time Polymerase Chain Reaction.

2 METHODS

2.1 Network Pharmacology Analysis

2.1.1 Screening the Main Active Compounds of YQHY

The active compounds of YQHY were derived from the TCMSP database (TCMSP, http://lsp.nwu.edu.cn/tcmsp.php). To better screen the active compounds of YQHY, OB ≥30% (15) and DL ≥0.05 (16) were used as screening conditions in this article. After that, a total of 360 active compounds were finally obtained.

2.1.2 Collection of Targets

Through the PubChem database (https://pubchem.ncbi.nlm.nih.gov/), the screened active compounds were transformed into the SMILES structural formula, and the SMILES structural formula was imported into the Swiss Target Prediction website, setting *Homo sapiens*, to predict all potential targets of the active compounds in YQHY. The relevant targets in GC were obtained by using the DisGeNET, GeneCards, and OMIM databases. We screened targets related to ferroptosis from the FerrDB (http://www.zhounan.org/ferrdb/) database (17). All potential targets and corresponding active compounds of YQHY were input into Cytoscape to construct the "YQHY active compound-target" network.

2.1.3 Screening of Hub Targets for YQHY Induced Ferroptosis in GC

Taking the intersection of the whole decoction targets, GC targets, and ferroptosis targets, we obtained the targets of YQHY induced ferroptosis in GC. The targets were imported into the STRING database to construct a PPI network and visualized using Cytoscape, of which the CytoNCA plug-in was used to calculate the parameters, and the hub targets for YQHY induced ferroptosis in GC were obtained according to BC, CC, and Degree.

2.1.4 GO and KEGG Enrichment Analysis

The targets of YQHY induced ferroptosis in GC were imported into the DAVID database for GO and KEGG enrichment analysis. The final analysis results included

Biological Process (BP), Cellular Component (CC), and Molecular Function (MF). GO enrichment analysis was performed according to P <0.05 and FDR <0.05, and KEGG enrichment analysis was performed according to P <0.01 as the filtering criterion. Top20 were plotted into bubble charts using R language.

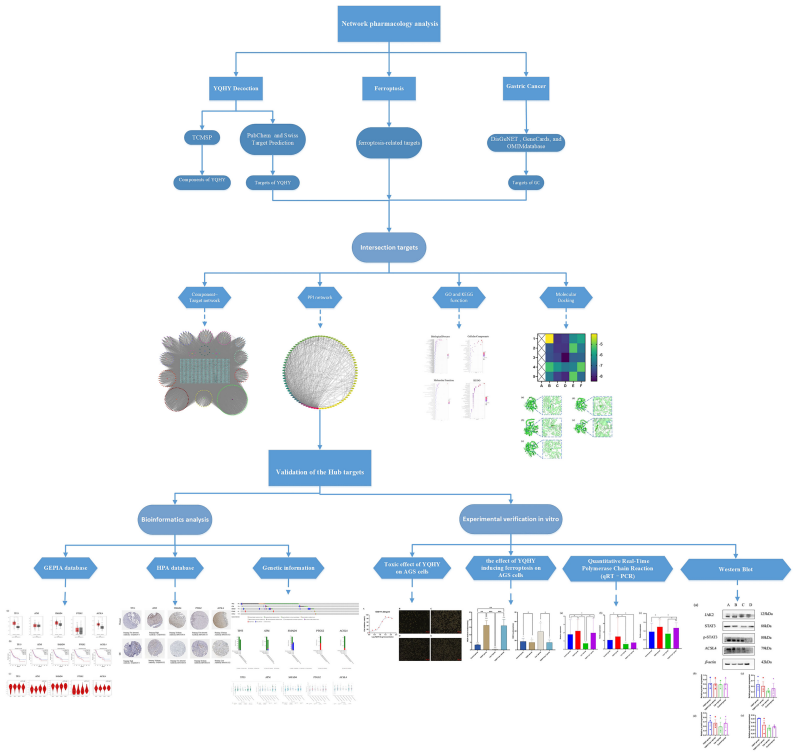

FIGURE 1 | The protocol of our study procedures. (*P < 0.05, ** P < 0.01, *** P < 0.001).

2.1.5 Molecular Docking

Molecular docking is mainly used for structural docking of small molecules with target proteins and evaluating their binding affinities with defined binding sites (18). A negative docking binding energy suggests efficient autonomous binding of the small molecule to the target protein. It is generally believed that the lower the energy the conformation in which a ligand binds to a receptor is stabilized, the more likely the effect will be. In this study, the main active compounds and hub targets of YQHY induced ferroptosis in GC were molecularly docked. The TCMSP database was used to download the structure diagram of the main active compounds, which were saved in SDF format. Open Babel GUL software was used to convert the SDF format into the PDB format. We used the PDB database to download the 3D structure diagram of hub targets, and saved it in PDB format, then imported them into AutoDock software for molecular docking. Docking results were visualized using PyMol software.

2.2 Bioinformatics Analysis

The hub targets were input into the online tool GEPIA (http://gepia.cancer-pku.cn/index.html) (19) to verify their mRNA expression level, pathological stages, and overall survival (OS) in TCGA-STAD. The protein expression of hub targets was investigated in the HPA database (https://www.proteinatlas.org/) (20). The cBioPortal tool (http://www.cbioportal.org/) (21) was used to discover the genetic information and the correlation between mRNA expression of hub targets.

2.3 Experimental Validation *In Vitro*

2.3.1 Preparation of YQHY Freeze-Dried Powder

The YQHY decoction consists of Huangqi, Dangshen, Chenpi, Banxia, Baizhu, Baishao, Danggui, Sanleng, Ezhu, Sheshecao, Shijianchuan, Fulin, Muxiang, Sharen, and Gancao. YQHY medicine was dried for 24 h, pulverized, and sieved with an 80 mesh sieve. The decoction was mixed, filtered, and concentrated to 250 ml. The concentrated solution was added to a special freeze-drying bottle, quickly frozen with liquid nitrogen, and dried at −50°C in FreezeDryers. The lyophilized powder was removed at 48 h and stored under cryogenic drying after crushing.

2.3.2 Cell Viability Assay

Different concentrations of YQHY were added to the experimental group, and F12K culture medium was added to the zeroing group and control group. The reaction was carried out at 37°C and 5% carbon dioxide for 24 h. After CCK8 solution was added to each well to react for 1 h, the OD of each sample was measured by setting up the microplate reader at 490 nm. IC50 was calculated using GraphPad Prism software.

2.3.3 Lipid Peroxidation and GSH Assays

The MDA and GSH contents in cell lysates were assessed using lipid peroxidation and GSH assay kits, respectively, according to the manufacturer's (Abcam) instructions.

2.3.4 Quantitative Real-Time Polymerase Chain Reaction (qRT-PCR)

According to the results of network pharmacology, we selected ACSL4, JAK2, and STAT3 to explore the mechanism by which YQHY induces ferroptosis in GC. Total RNA was extracted from cultured cells using TRIzol and phenol–chloroform phase separation according to the manufacturer's instructions and then reverse transcribed using the RevertAid RT Reverse Transcription Kit (Invitrogen, K1691). The primer sequences used for qRT-PCR are listed in **Table 1**. qRT–PCR was performed using a StepOne Real-Time PCR system (Applied Biosystems).

2.3.5 Western Blot

The protein expression of JAK2, STAT3, p-STAT3, and ACSL4 was detected by Western blot. Total proteins were obtained using RIPA buffer, and protein concentrations were measured using a BCA protein assay kit. The protein samples were blotted onto PVDF membranes. Next, the membranes were incubated at 4°C overnight with primary antibodies against JAK2, STAT3, p-STAT3, ACSL4, and β-actin, followed by HRP-conjugated secondary antibodies. The grayscale values were quantified by Image Lab software.

2.3.6 Statistical Analysis

The experimental results were statistically analyzed by GraphPad Prism software. Single-factor ANOVA was used to compare the differences in experimental data among groups. A P-value less than 0.05 was considered significant.

3 RESULTS

3.1 Network Pharmacology Analysis

3.1.1 Screening the Main Active Compounds of YQHY

Through the screening of the TCMSP database, a total of 360 active compounds were obtained, namely, 23 Huangqi, 27 Dangshen, 10 Chenpi, 20 Banxia,16 Baizhu, 17 Baishao, 22 Danggui, 10 Sanleng, 21 Ezhu, 7 Sheshecao, 4 Shijianchuan, 16 Fulin, 30 Muxiang, 54 Sharen, and 83 Gancao.

3.1.2 Collection of Targets and Construction of the "YQHY compound-target" Network

After the prediction of the database and deletion of duplicate values, a total of 1,373 potential targets of active compounds, 15,842 targets of GC, and 205 targets of ferroptosis were obtained. A total of 87 common targets were obtained by combining the three target sets. At the same time, a "YQHY compound-target" network was constructed (**Figure 2**), in which quercetin, DIBP, DBP, Mipax, and Phaseol were considered the main active components for YQHY induced ferroptosis in GC. Then the PPI network was constructed according to the degree value (**Figure 3**).

TABLE 1 | Real-Time polymerase chain reaction primers.

Gene	Sequence (5′-3′)
JAK2-F	CGAATGGTGTTTCTGATGTACC
JAK2-R	GTCTCCTACTTCTCTTCGTACG
STAT3-F	TTGTGTGTATGCGTCGGCTTCAG
STAT3-R	GCGGCTATACTGCTGGTCAATCTC
ACSL4-F	TCTCTTGCCTCAGCCTCCTTAGTAG
ACSL4-R	CGAGACCAGCCTGACCAACATG
β-ACTIN-F	CAGATGTGGATCAGCAAGCAGGA
β-ACTIN-R	CGCAACTAAGTCATAGTCCGCCTA

3.1.3 Screening of Hub Targets for YQHY Induced Ferroptosis in GC

According to the ranking of BC, CC, and degree calculated by the CytoNCA plug-in, TP53, ATM, SMAD4, PTGS2, and ACSL4 were identified as the hub targets of YQHY induced ferroptosis in GC. Meanwhile, a PPI network diagram of hub targets was constructed.

3.1.4 GO and KEGG Enrichment Analysis

GO enrichment analysis showed that the biological functions mainly involved positive regulation of transcription from the RNA polymerase II promoter, negative regulation of apoptotic processes, and oxidation–reduction processes. Cell components mainly included the cytoplasm, cytosol, and nucleus. Molecular functions mainly included protein binding, identical protein binding, and DNA binding. KEGG functional enrichment analysis showed that the hub targets were mainly enriched in microRNAs in cancer and the JAK2-STAT3 signaling pathway (**Figure 4**), suggesting that the JAK2-STAT3 pathway is one of the main potential signaling pathways of YQHY induced ferroptosis in GC.

3.1.5 Molecular Docking

A binding energy <−5 kcal mol^{-1} indicates good binding activity. The results of molecular docking were plotted as a heatmap (**Figure 5**). It can be seen from the figure that DIBP, DBP, Phaseol with TP53, SMAD4, and ACSL4 all had good binding activities. We selected the molecular docking results of ACSL4 with the main active compounds, and visual analysis was carried out by PyMol software (**Figure 6**).

3.2 Bioinformatics Analysis

The results of the GEPIA database showed that the mRNA levels of TP53 and ACSL4 were significantly highly expressed in GC tissues (**Figure 7A**). Survival analysis of the hub targets (**Figure 7B**) showed that the prognostic value of PTGS2 was significantly different (P <0.05). We analyzed the relationship between hub target mRNA levels and the pathological stage of GC. The results showed that the levels of ATM changed significantly with pathological stage and increased significantly in stage IV (**Figure 7C**).

The HPA database results showed that the hub targets were expressed to different degrees in normal gastric tissues. Compared with normal gastric tissues, the expression levels of TP53 and PTGS2 were increased in GC tissues, while the expression of ATM, SMAD4, and ACSL4 was decreased in GC tissues (**Figure 8**).

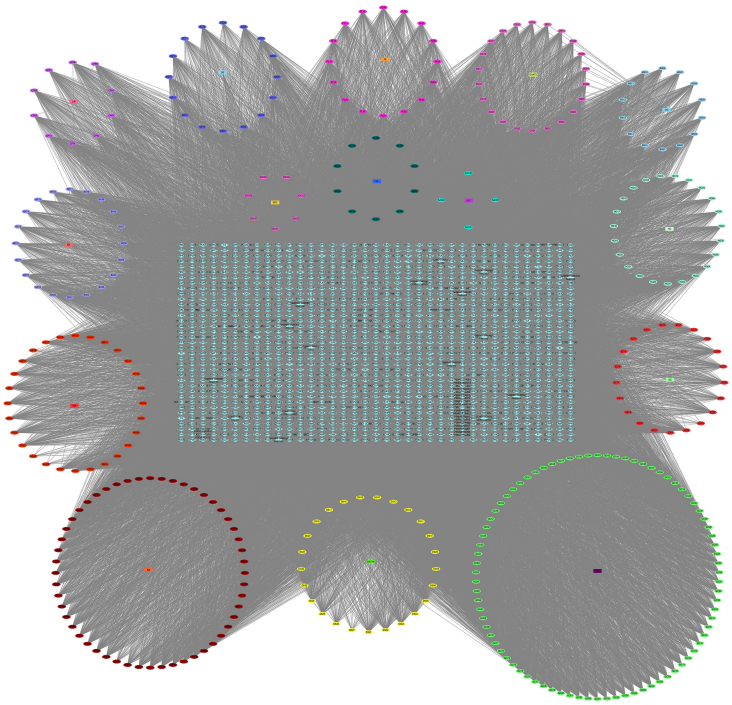

FIGURE 2 | YQHY Compound-Target Network. The circle represents the YQHY active compound, the rectangle represents the herb, and the blue diamond represents the target.

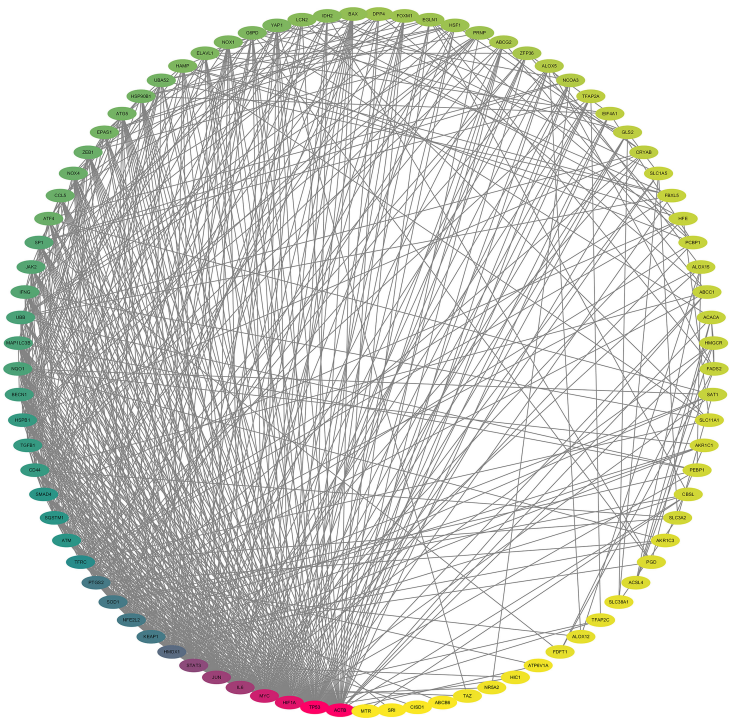

FIGURE 3 | Protein–protein interaction Network. The darker the color, the greater the Degree value. The lighter the yellow color, the smaller the degree value.

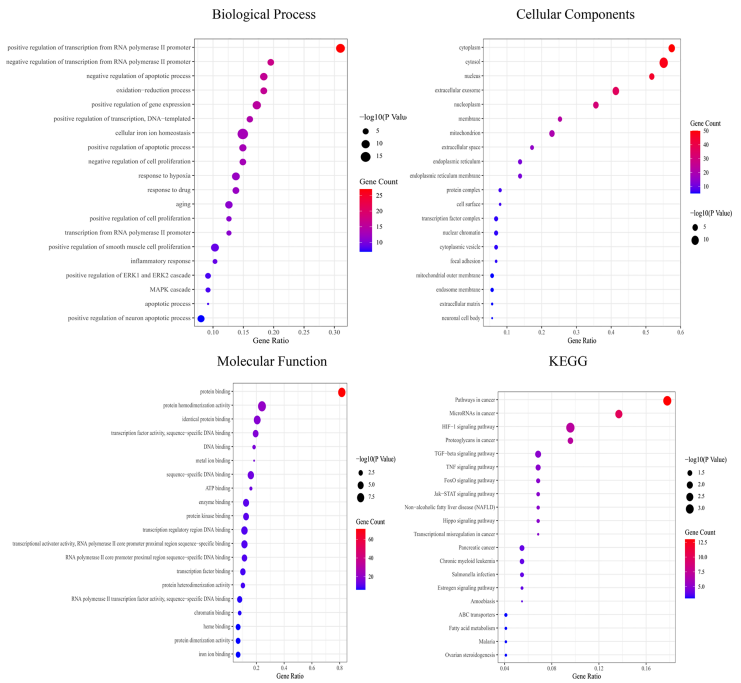

FIGURE 4 | Bubble diagram for GO and KEGG enrichment analysis. The bubble size represents the number of enriched genes, and the bubble color difference represents the significant magnitude of target gene enrichment.

The cBioPortal tool showed that 278 of 434 patients (64%) had genetic mutations in these five targets (**Figure 9A**). An overview of the genetic variation of five targets was also analyzed (**Figure 9B**). **Figure 9C** shows the number of gene mutations in different types of GC.

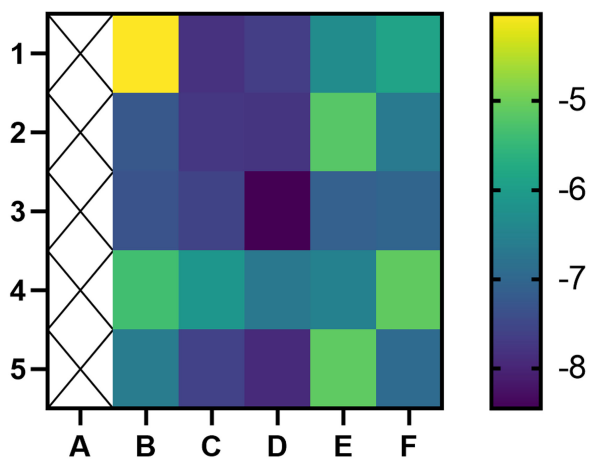

FIGURE 5 | Heatmap of binding between main active components and hub targets. The darker the color, the better the binding activity. **(A)** represent blank, **(B–F)** represent TP53, ATM, SMAD4, PTGS2, and ACSL4, respectively, while 1, 2, 3, 4, and 5 represent Quercetin, DIBP, DBP, Mipax, and Phaseol, respectively.

3.3 Experimental Validation *In Vitro*

3.3.1 Cell Viability Assay

It can be concluded that with increasing concentrations of YQHY, the toxic effect on AGS gradually intensified, and the inhibition rate of AGS showed a gradually increasing trend (**Figure 10**). According to the curve in the figure, we found that the IC50 of YQHY on AGS was 11.20 mg/ml, which means that approximately 50% of AGS was inhibited after exposure to 11.20 mg/ml YQHY for 24 h. This result suggested that YQHY had a toxic effect on AGS, and we chose this concentration at half inhibition rate for subsequent experiments.

3.3.2 Lipid Peroxidation and GSH Assays

The MDA content in the YQHY group was the highest compared with the other three groups ($P < 0.05$) (**Figure 11A**), and YQHY reversed the ferroptosis inhibition induced by the ferroptosis inhibitor liproxstatin-1. The GSH content in the YQHY group was the lowest compared with the other three groups ($P < 0.05$) (**Figure 11B**), and the GSH content in the YQHY + liproxstatin-1 group was lower than that in the control group, indicating that YQHY can reduce the intracellular GSH content and induce ferroptosis in AGS and that YQHY can reverse ferroptosis due to liproxstatin-1 inhibition.

3.3.3 Quantitative Real-Time Polymerase Chain Reaction (qRT-PCR)

We used qRT-PCR to measure the effect of YQHY, liproxstatin-1, and YQHY + liproxstatin-1 on the mRNA expression of JAK2,

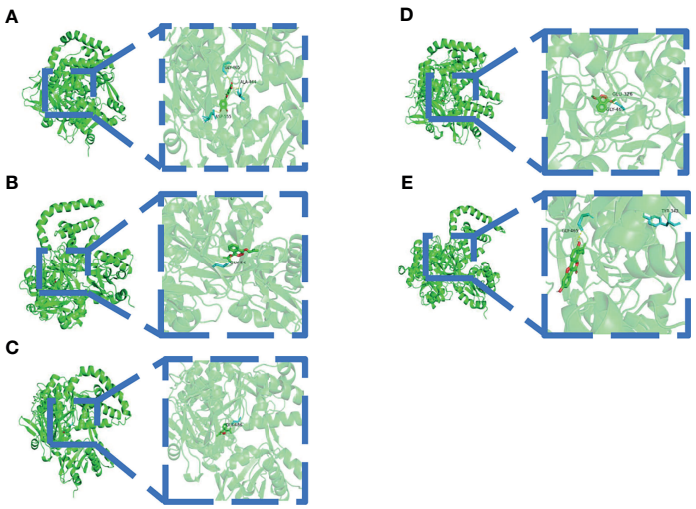

FIGURE 6 | Schematic diagram of docking between active compounds and ACSL4. **(A–E)** represent the molecular binding of ACSL4 with Quercetin, DIBP, DBP, Mipax, and Phaseol, respectively.

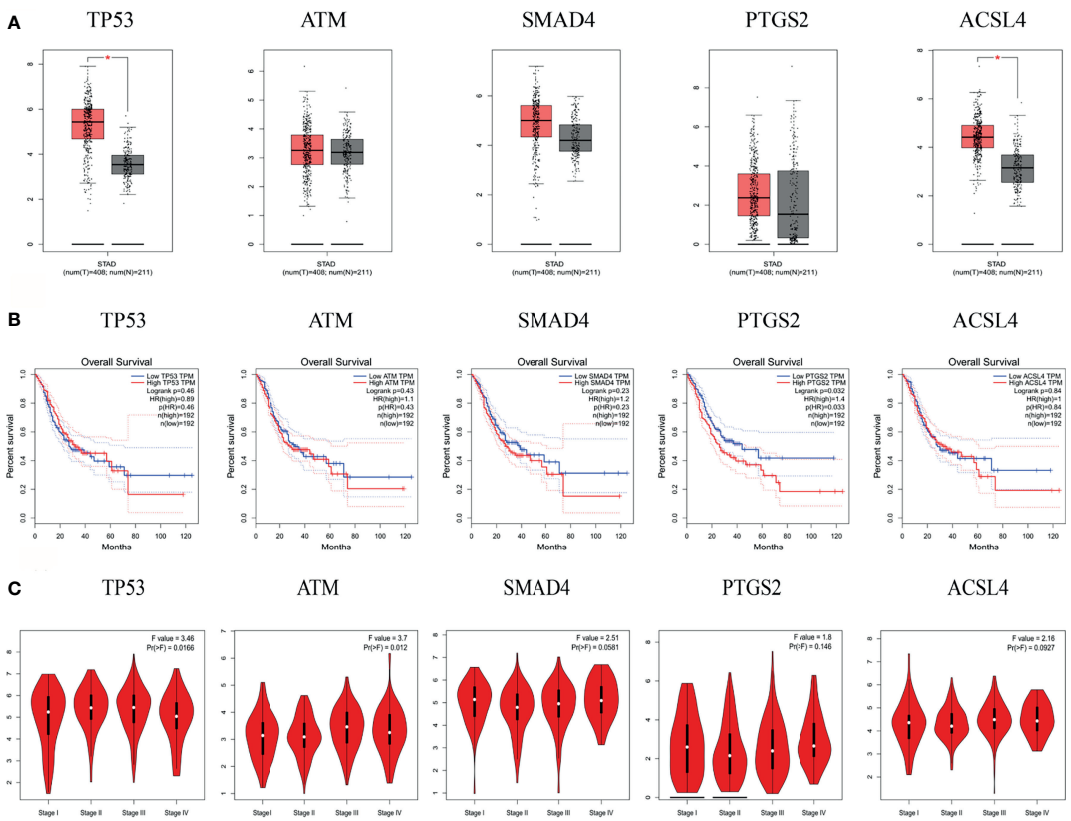

FIGURE 7 | mRNA expression level, pathological stage and OS in the GEPIA database. **(A)** Box plots showing the mRNA expression levels of TP53, ATM, SMAD4, PTGS2, and ACSL4. Red represents Tumor, Gray represents normal. **(B)** The line charts show the OS of hub genes in GEPIA. The survival curve comparing the patients with high (red) and low (blue) expression in GC. **(C)** The violin diagram shows the stage plot of mRNA expression level and pathological stage in the GEPIA database.

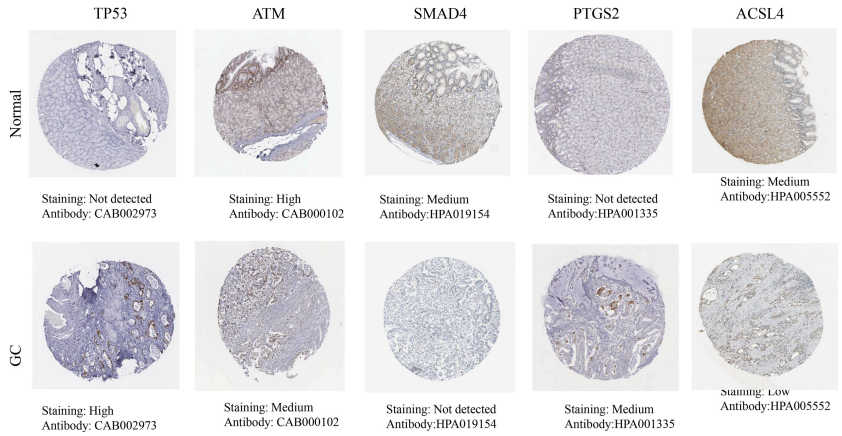

FIGURE 8 | The protein expression levels in the HPA database.

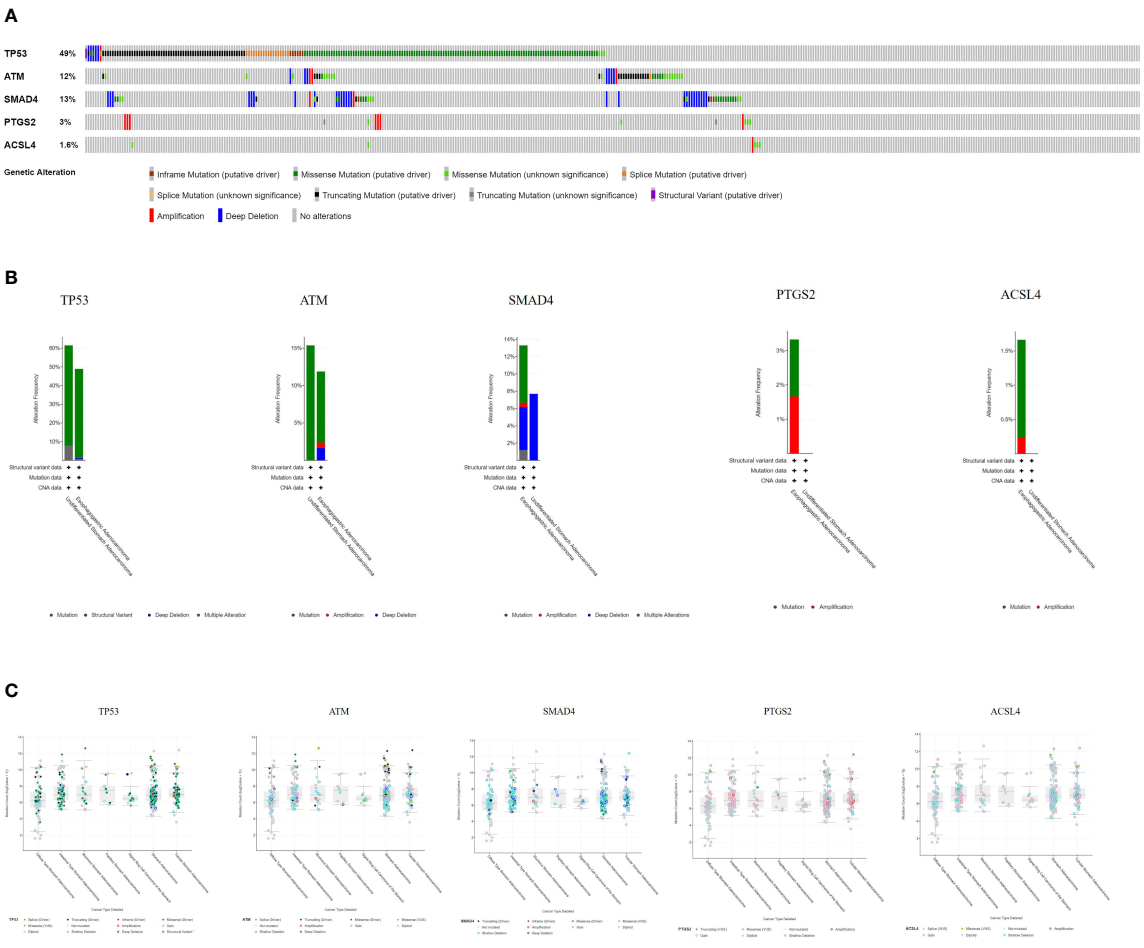

FIGURE 9 | Genetic information of hub targets. **(A)** Data from TCGA of gastric adenocarcinoma showed that 278 of 434 patients (64%) had genetic mutations in these five targets. **(B)** The diagram shows the genetic variation of five targets. **(C)** The diagram shows the number of gene mutations in different types of GC.

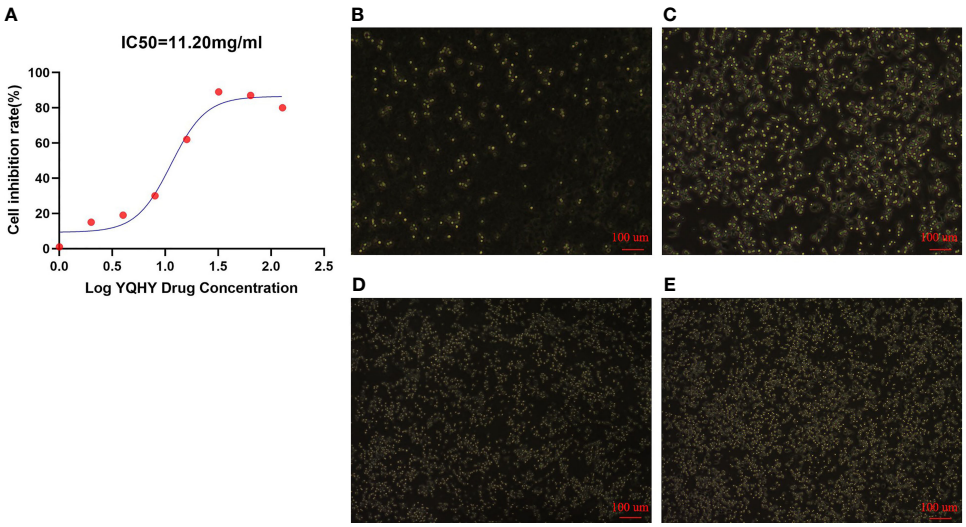

FIGURE 10 | The graph of YQHY inhibiting AGS growth. **(A)** The IC50 of YQHY on AGS cells was 11.20 mg/ml, which means that approximately 50% of AGS cells were inhibited after exposure to 11.20 mg/ml YQHY for 24 h. **(B–E)** show the growth state of AGS cells in different groups after 24 h of dose. Among them, **(B)** represents the YQHY group, **(C)** represents the YQHY + liproxstatin-1 group, **(D)** represents the control group, and **(E)** represents the liproxstatin-1 group.

STAT3, and ACSL4. The results showed that the mRNA expression levels of JAK2, STAT3, and ACSL4 were higher in the YQHY group than in the control group (P <0.05). After the addition of liproxstatin-1, the mRNA expression of JAK2, STAT3, and ACSL4 was decreased compared with that in the YQHY group (P <0.05). The mRNA expression of JAK2, STAT3 and ACSL4 in the liproxstatin-1 group was significantly decreased relative to the control group (P <0.05) (**Figure 12**).

3.3.4 Western Blot

Compared with the control group, the protein expression of JAK2, STAT3, p-STAT3, and ACSL4 in the YQHY group was higher than those in the other three groups, while the expression level of each protein in the liproxstatin-1 group was lower. It could be concluded that YQHY can induce ferroptosis in AGS by regulating the JAK2-STAT3 pathway and the expression of ACSL4 (**Figure 13**).

4 DISCUSSION

Recently, the incidence and mortality of GC have gradually increased, which is related to diet, lifestyle, genetics, and other factors. Due to distant metastasis and recurrence, most patients have a poor prognosis (22). According to clinical studies, YQHY has a clear antirecurrence and metastasis effect in GC (23). Our team wanted to further investigate whether this is achieved by

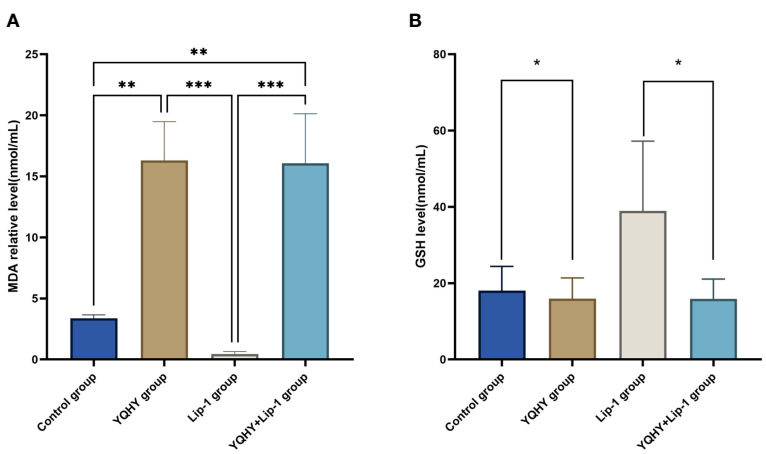

FIGURE 11 | Effect of YQHY on MDA and GSH content in AGS cells (*P <0.05), ** P < 0.01, *** P < 0.001

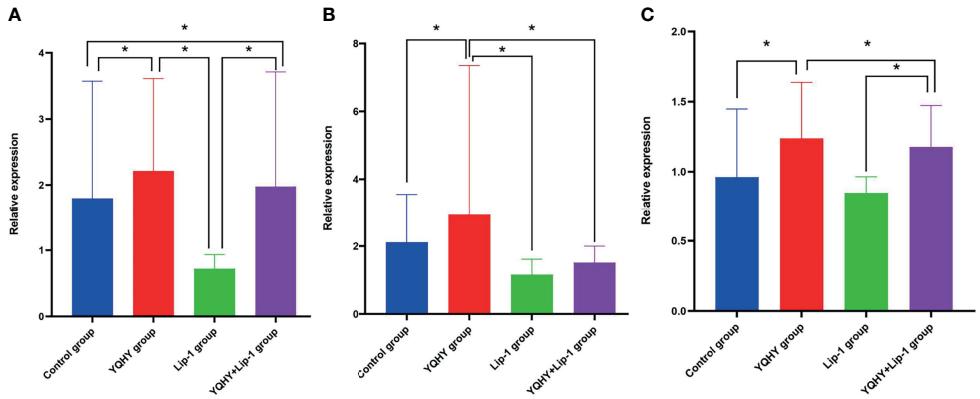

FIGURE 12 | Effect of YQHY on JAK2, STAT3, and ACSL4 mRNA. **(A)** represents the relative mRNA expression of JAK2, **(B)** represents the relative mRNA expression of STAT3, and **(C)** represents the relative mRNA expression of ACSL4. (*P < 0.05).

inducing ferroptosis in GC and whether the influence of the JAK2–STAT3 signaling pathway and ACSL4 expression is one of the mechanisms of YQHY-induced ferroptosis in GC.

Through the network pharmacology study, Quercetin, DIBP, DBP, Mipax, and Phaseol were identified as the main active compounds of YQHY-induced ferroptosis in GC. Quercetin is a flavonoid, which exists in many edible and medicinal plants (24). It has various pharmacological activities, such as antioxidant, anti-inflammatory, and antitumor activities. Quercetin can be used as an antioxidant activity ROS scavenger and metal chelating agent to protect gastric epithelial cells from oxidative damage (25, 26). Many studies have shown that quercetin has antiproliferative and antiangiogenic effects in various cancers (27), such as lung cancer (28), breast cancer (29), colon cancer (30), and GC (31). Quercetin was found to arrest cell division by inducing cell cycle arrest at G0/G1 or G2/M phase in BGC-823 gastric cancer cells through protein analysis of Bax, Bcl-2, and caspases (32). Phasol is rich in flavonol glycosides and coumarin. Coumarin can induce apoptosis of Jurkat cells by inducing mitochondrial depolarization, which may contribute to cell death by inducing cell cycle arrest at the G1 phase, reducing BCL2 levels, and increasing PARP-1 cleavage (33), but there have been no reports on its association with GC. DIBP, DBP, and Mipax were the main compounds we identified for the treatment of GC, but there is no related report.

We analyzed the biological functions and signaling pathways of YQHY and found that TP53, ATM, SMAD4, PTGS2, and ACSL4 were the hub targets of YQHY induced ferroptosis in GC. TP53 is a

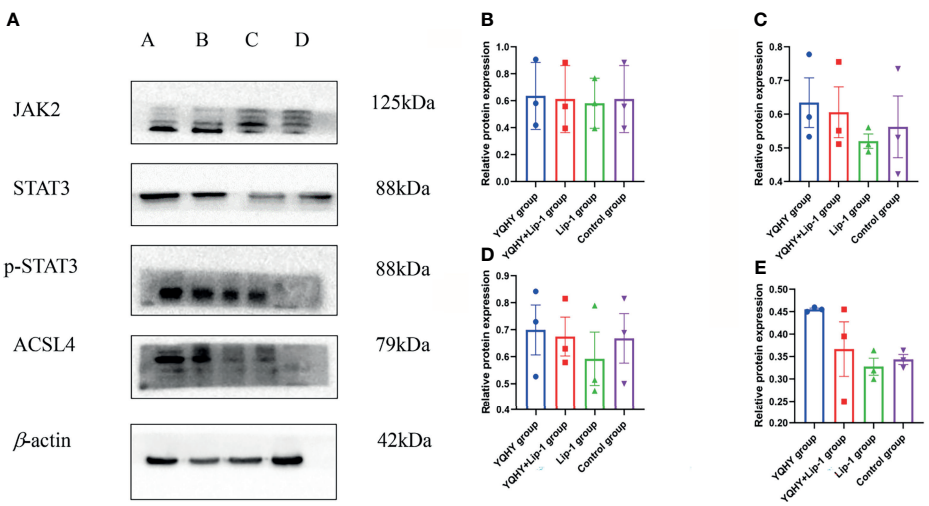

FIGURE 13 | Effect of YQHY on JAK2, STAT3, p-STAT3, and ACSL4 protein. **(A)** A represents the YQHY group, B represents the YQHY + liproxstatin-1 group, C represents the liproxstatin-1 group, and D represents the control group. **(B)** represents the relative protein expression of JAK2, **(C)** represents the relative protein expression of STAT3, **(D)** represents the relative protein expression of p-STAT3, and **(E)** represents the relative protein expression of ACSL4.

tumor suppressor gene that has attracted wide attention at present. Mutant TP53 has an influence on the proliferation, migration, survival, and invasion of tumors and the drug resistance of chemotherapy drugs (34). When TP53 is mutated, the original tumor suppressor function is affected, which further increases the apoptosis process of gastric mucosa cells and impairs the damage repair function of the cells, thus inducing the transition of normal cells to cancer cells and increasing the incidence of GC (35). ATM is a cell housekeeping gene encoding ATM protein kinase, which plays a key role in the early signal transduction of cell cycle checkpoints (36, 37). ATM is a potential marker for GC (38), and previous studies (39) have confirmed that HP infection can cause upregulated expression of ATM. SMAD4 is a tumor suppressor gene discovered in recent years. Patients with GC often have mutations or loss of expression of SMAD4 (40). Reduced expression of SMAD4 in GC is one of the main reasons for its abnormal proliferation and migration (41). PTGS2 is closely related to apoptosis and promotes tumor progression (42). Lin (43) demonstrated that PTGS2 mediated cisplatin-induced BCL2 expression and subsequent apoptosis resistance through a PGE2/EP4/MAPK (ERK1/2, P38)-dependent mechanism. The ACSL family mainly catalyzes fatty acids with 12–20 carbon chains (44). Evidence has shown that ACSLs are enzymes crucial for the body's response to fatty acid metabolism (45). Mammalian ACSLs have five different isozymes, namely, ACSL1, ACSL3, ACSL4, ACSL5, and ACSL6, which are different in intracellular functions in their tissue expression specificity (46). Studies have shown that ACSL4 is involved in various biological processes, such as proliferation, apoptosis, migration, and invasion of tumor cells. It is also a biomarker and contributor of ferroptosis (47). Ferroptosis contributes to the antitumor function of several tumor suppressors, such as p53, BAP1, and fumarase (48). ACSL4 was differentially expressed in tumor tissues compared with adjacent carcinoma normal tissues. For example, an increase in ACSL4 expression is related to the differentiation of colon adenocarcinoma (49). One of these reports indicated that ACSL4 is part of the mechanism responsible for the promotion of breast cancer cell proliferation, invasion, and migration (50). However, ACSL4 is underexpressed in GC tissue and represents an undifferentiated or poorly differentiated malignant phenotype (51). Therefore, the expression of ACSL4 can inhibit the migration and invasion of GC, which illustrates that ACSL4 can be a potential therapeutic target as a tumor suppressor in GC.

The enrichment analysis of the KEGG suggested that the JAK2–STAT3 pathway was one of the main potential signaling pathways of YQHY induced ferroptosis in GC. The JAK2–STAT3 signaling pathway is a typical oncogenic signaling pathway (52). JAK2 serves as a signaling hub that integrates extracellular signals from interleukin receptors and oncogenic receptor tyrosine kinases into STAT3, which phosphorylates STAT3 at Y705 and homodimerizes with p-STAT3 to induce its nuclear translocation and transcriptional activity through interaction with its phosphorylated Y705 site and SH2 domain (53, 54). STAT3 binds to the promoters of its target genes to induce tumor cell migration, growth, and differentiation and plays an important role in the development of a variety of tumors (55).

Molecular docking results showed that the main active compounds of YQHY had good binding activity with the hub targets, and then we identified the hub targets in different databases. We found that the mRNA levels of TP53 and ACSL4 were significantly expressed in GC tissues, and the prognostic value of PTGS2 was significantly different (P b<0.05). The levels of ATM changed significantly with pathological stage and increased significantly in stage IV. The cBioPortal tool showed that 278 of 434 patients (64%) had genetic mutations in these five targets. The results of the above analysis were mostly consistent with previous literature reports.

To further clarify the relationship between YQHY and ferroptosis, we selected ACSL4, which is closely related to ferroptosis, as the target of this topic, and the JAK2–STAT3 pathway as the pathway of this topic to explore whether YQHY could induce ferroptosis in GC by influencing the expression of ACSL4, JAK2, and STAT3. The results showed that YQHY had a toxic effect on AGS, and with increasing concentration, the inhibition rate of AGS showed a gradually increasing trend. The increase in MDA and the decrease in GSH synthesis are the main characteristics of ferroptosis. We found that the MDA content in the YQHY group was the highest compared with the other three groups (P <0.05), and YQHY reversed the ferroptosis inhibition induced by the ferroptosis inhibitor liproxstatin-1. The GSH content in the YQHY group was the lowest compared with the other three groups (P <0.05), and the GSH content in the YQHY + liproxstatin-1 group was lower than that in the control group, indicating that YQHY can reduce the intracellular GSH content and induce ferroptosis in AGS and that YQHY can reverse ferroptosis due to liproxstatin-1 inhibition.

The qRT-PCR results showed that the mRNA expression levels of JAK2, STAT3, and ACSL4 were higher in the YQHY group than in the control group. After the addition of liproxstatin-1, the mRNA expression of JAK2, STAT3, and ACSL4 was decreased compared with that in the YQHY group. The mRNA expression of JAK2, STAT3 and ACSL4 in the liproxstatin-1 group was significantly decreased relative to the control group.Western blot analysis confirmed that compared with the control group, the expression of JAK2, STAT3, p-STAT3, and ACSL4 protein in the YQHY group was higher than those in the other three groups, while the expression level of each protein in the liproxstatin-1 group was lower. It could be concluded that YQHY can induce ferroptosis in AGS by regulating the JAK2-STAT3 pathway and the expression of ACSL4. This illustrates that influencing the JAK2-STAT3 signaling pathway and expression of ACSL4 is one of the mechanisms of inducing ferroptosis in GC, and induction of ferroptosis may be one of the possible mechanisms of YQHY's anti-recurrence and metastasis of GC.

5 CONCLUSION

The material basis of YQHY induced ferroptosis in GC is based on active compounds such as Quercetin, DIBP, DBP, Mipax, and

Phaseol. The related mechanism was characterized by multiple targets and pathways. YQHY can induce ferroptosis in GC by affecting the JAK2–STAT3 pathway and the expression of ACSL4, and induction offerroptosis may be one of the possible mechanisms of YQHY's anti-recurrence and metastasis of GC.

DATA AVAILABILITY STATEMENT

The original contributions presented in the study are included in the article/**Supplementary Material**. Further inquiries can be directed to the corresponding author.

AUTHOR CONTRIBUTIONS

PS designed the research. SS analyzed the data and wrote the paper. FW, SG, WH, JL, JZ, PG, SR, XC, and YL selected the materials. All authors read and approved the submitted version.

FUNDING

This work was funded by the National Natural Science Foundation of China (nos. 81673918). Pilot GC project of clinical collaboration of traditional Chinese medicine and Western medicine on major difficult diseases in the state administration of traditional Chinese medicine; the 2019" Construction Project of Evidence-based Capacity for Traditional Chinese Medicine" (2019XZZX-ZL003) in state administration of traditional Chinese medicine; the Open Program of the Third Phase of the Program of Traditional Chinese Medicine (TCM) Advantageous Subjects (ZYX03KF020); and the Science and Technology Project of Jiangsu Provincial Administration of Traditional Chinese Medicine (ZD201803).

SUPPLEMENTARY MATERIAL

The Supplementary Material for this article can be found online at: https://www.frontiersin.org/articles/10.3389/fonc.2022.820059/full#supplementary-material

REFERENCES

1. Bray F, Ferlay J, Soerjomataram I, Siegel RL, Torre LA, Jemal A. Global Cancer Statistics 2018: GLOBOCAN Estimates of Incidence and Mortality Worldwide for 36 Cancers in 185 Countries. *CA Cancer J Clin* (2018) 68 (6):394–424. doi: 10.3322/caac.21492
2. Zhang T, Chen H, Yin X, He Q, Man J, Yang X, et al. Changing Trends of Disease Burden of Gastric Cancer in China From 1990 to 2019 and Its Predictions: Findings From Global Burden of Disease Study. *Chin J Cancer Res* (2021) 33(1):11–26. doi: 10.21147/j.issn.1000-9604.2021.01.02
3. Yusefi AR, Bagheri Lankarani K, Bastani P, Radinmanesh M, Kavosi Z. Risk Factors for Gastric Cancer: A Systematic Review. *Asian Pac J Cancer Prev* (2018) 19(3):591–603. doi: 10.22034/APJCP.2018.19.3.591
4. Nie S, Yang G, Lu H. Current Molecular Targeted Agents for Advanced Gastric Cancer. *Onco Targets Ther* (2020) 13:4075–88. doi: 10.2147/OTT.S246412
5. Liang C, Zhang X, Yang M, Dong X. Recent Progress in Ferroptosis Inducers for Cancer Therapy. *Adv Mater* (2019) 31(51):e1904197. doi: 10.1002/adma.201904197
6. Liu Z, Zhao Q, Zuo ZX, Yuan SQ, Yu K, Zhang Q, et al. Systematic Analysis of the Aberrances and Functional Implications of Ferroptosis in Cancer. *iScience* (2020) 23(7):101302. doi: 10.1016/j.isci.2020.101302
7. Mou Y, Wang J, Wu J, He D, Zhang C, Duan C, et al. Ferroptosis, a New Form of Cell Death: Opportunities and Challenges in Cancer. *J Hematol Oncol* (2019) 12(1):34. doi: 10.1186/s13045-019-0720-y
8. Zhang H, Deng T, Liu R, Ning T, Yang H, Liu D, et al. CAF Secreted miR-522 Suppresses Ferroptosis and Promotes Acquired Chemo-Resistance in Gastric Cancer. *Mol Cancer* (2020) 19(1):43. doi: 10.1186/s12943-020-01168-8
9. Lee JY, Nam M, Son HY, Hyun K, Jang SY, Kim JW, et al. Polyunsaturated Fatty Acid Biosynthesis Pathway Determines Ferroptosis Sensitivity in Gastric Cancer. *Proc Natl Acad Sci U.S.A.* (2020) 117(51):32433–42. doi: 10.1073/pnas.2006828117
10. Hao S, Yu J, He W, Huang Q, Zhao Y, Liang B, et al. Cysteine Dioxygenase 1 Mediates Erastin-Induced Ferroptosis in Human Gastric Cancer Cells. *Neoplasia* (2017) 19(12):1022–32. doi: 10.1016/j.neo.2017.10.005
11. Sha W, Hu F, Xi Y, Chu Y, Bu S. Mechanism of Ferroptosis and Its Role in Type 2 Diabetes Mellitus. *J Diabetes Res* (2021) 2021:9999612. doi: 10.1155/2021/9999612
12. Alvarez SW, Sviderskiy VO, Terzi EM, Papagiannakopoulos T, Moreira AL, Adams S, et al. NFS1 Undergoes Positive Selection in Lung Tumours and Protects Cells From Ferroptosis. *Nature* (2017) 551(7682):639–43. doi: 10.1038/nature24637
13. Shu P, Tang H, Zhou B, Wang R, Xu Y, Shao J, et al. Effect of Yiqi Huayu Jiedu Decoction on Stages II and III Gastric Cancer: A Multicenter, Prospective, Cohort Study. *Med (Baltimore)* (2019) 98(47):e17875. doi: 10.1097/MD.0000000000017875
14. Zhang R, Zhu X, Bai H, Ning K. Network Pharmacology Databases for Traditional Chinese Medicine: Review and Assessment. *Front Pharmacol* (2019) 10:123. doi: 10.3389/fphar.2019.00123
15. Xu X, Zhang W, Huang C, Li Y, Yu H, Wang Y, et al. A Novel Chemometric Method for the Prediction of Human Oral Bioavailability. *Int J Mol Sci* (2012) 13(6):6964–82. doi: 10.3390/ijms13066964
16. Li J, Zhao P, Li Y, Tian Y, Wang Y. Systems Pharmacology-Based Dissection of Mechanisms of Chinese Medicinal Formula Bufei Yishen as an Effective Treatment for Chronic Obstructive Pulmonary Disease. *Sci Rep* (2015) 5:15290. doi: 10.1038/srep15290
17. Zhou N, Bao J. FerrDb: A Manually Curated Resource for Regulators and Markers of Ferroptosis and Ferroptosis-Disease Associations. *Database (Oxford)* (2020) 2020:80. doi: 10.1093/database/baaa021
18. Pinzi L, Rastelli G. Molecular Docking: Shifting Paradigms in Drug Discovery. *Int J Mol Sci* (2019) 20(18):11–3. doi: 10.3390/ijms20184331
19. Tang Z, Li C, Kang B, Gao G, Li C, Zhang Z. GEPIA: A Web Server for Cancer and Normal Gene Expression Profiling and Interactive Analyses. *Nucleic Acids Res* (2017) 45(W1):W98–W102. doi: 10.1093/nar/gkx247
20. Digre A, Lindskog C. The Human Protein Atlas-Spatial Localization of the Human Proteome in Health and Disease. *Protein Sci* (2021) 30(1):218–33. doi: 10.1002/pro.3987
21. Gao J, Aksoy BA, Dogrusoz U, Dresdner G, Gross B, Sumer SO, et al. Integrative Analysis of Complex Cancer Genomics and Clinical Profiles Using the Cbioportal. *Sci Signal* (2013) 6(269):pl1. doi: 10.1126/scisignal.2004088
22. Machlowska J, Baj J, Sitarz M, Maciejewski R, Sitarz R. Gastric Cancer: Epidemiology, Risk Factors, Classification, Genomic Characteristics and Treatment Strategies. *Int J Mol Sci* (2020) 21(11):57. doi: 10.3390/ijms21114012
23. Huang W, Tang H, Wen F, Lu X, Li Q, Shu P. Jianpi-Yangwei Decoction Inhibits DNA Damage Repair in the Drug Resistance of Gastric Cancer by Reducing FEN1 Expression. *BMC Complement Med Ther* (2020) 20(1):196. doi: 10.1186/s12906-020-02983-8
24. Reyes-Farias M, Carrasco-Pozo C. The Anti-Cancer Effect of Quercetin: Molecular Implications in Cancer Metabolism. *Int J Mol Sci* (2019) 20 (13):34. doi: 10.3390/ijms20133177

25. Massi A, Bortolini O, Ragno D, Bernardi T, Sacchetti G, Tacchini M, et al. Research Progress in the Modification of Quercetin Leading to Anticancer Agents. *Molecules* (2017) 22(8):121. doi: 10.3390/molecules22081270
26. Tang SM, Deng XT, Zhou J, Li QP, Ge XX, Miao L. Pharmacological Basis and New Insights of Quercetin Action in Respect to its Anti-Cancer Effects. *BioMed Pharmacother* (2020) 121:109604. doi: 10.1016/j.biopha.2019.109604
27. Almatroodi SA, Alsahli MA, Almatroudi A, Verma AK, Aloliqi A, Allemailem KS, et al. Potential Therapeutic Targets of Quercetin, a Plant Flavonol, and Its Role in the Therapy of Various Types of Cancer Through the Modulation of Various Cell Signaling Pathways. *Molecules* (2021) 26(5):69. doi: 10.3390/molecules26051315
28. Wang Q, Chen Y, Lu H, Wang H, Feng H, Xu J, et al. Quercetin Radiosensitizes non-Small Cell Lung Cancer Cells Through the Regulation of miR-16-5p/WEE1 Axis. *IUBMB Life* (2020) 72(5):1012–22. doi: 10.1002/iub.2242
29. Ezzati M, Yousefi B, Velaei K, Safa A. A Review on Anti-Cancer Properties of Quercetin in Breast Cancer. *Life Sci* (2020) 248:117463. doi: 10.1016/j.lfs.2020.117463
30. Li Y, Wang Z, Jin J, Zhu SX, He GQ, Li SH, et al. Quercetin Pretreatment Enhances the Radiosensitivity of Colon Cancer Cells by Targeting Notch-1 Pathway. *Biochem Biophys Res Commun* (2020) 523(4):947–53. doi: 10.1016/j.bbrc.2020.01.048
31. Lei CS, Hou YC, Pai MH, Lin MT, Yeh SL. Effects of Quercetin Combined With Anticancer Drugs on Metastasis-Associated Factors of Gastric Cancer Cells: *In Vitro* and *In Vivo* Studies. *J Nutr Biochem* (2018) 51:105–13. doi: 10.1016/j.jnutbio.2017.09.011
32. Yang X, Zhang W, Zhao Z, Li N, Mou Z, Sun D, et al. Quercetin Loading CdSe/ZnS Nanoparticles as Efficient Antibacterial and Anticancer Materials. *J Inorg Biochem* (2017) 167:36–48. doi: 10.1016/j.jinorgbio.2016.11.023
33. Thuy NTT, Lee JE, Yoo HM, Cho N. Antiproliferative Pterocarpans and Coumestans From Lespedeza Bicolor. *J Nat Prod* (2019) 82(11):3025–32. doi: 10.1021/acs.jnatprod.9b00567
34. Donehower LA, Soussi T, Korkut A, Liu Y, Schultz A, Cardenas M, et al. Integrated Analysis of TP53 Gene and Pathway Alterations in The Cancer Genome Atlas. *Cell Rep* (2019) 28(5):1370–1384 e1375. doi: 10.1016/j.celrep.2019.08.061
35. Stoehr R, Weisser R, Wendler O, Giedl J, Daifalla K, Gaisa NT, et al. P53 Codon 72 Polymorphism and Risk for Squamous Cell Carcinoma of the Penis: A Caucasian Case-Control Study. *J Cancer* (2018) 9(22):4234–41. doi: 10.7150/jca.26050
36. Rimkus SA, Wassarman DA. A Pharmacological Screen for Compounds That Rescue the Developmental Lethality of a Drosophila ATM Mutant. *PloS One* (2018) 13(1):e0190821. doi: 10.1371/journal.pone.0190821
37. Zheng C, Zhou Y, Huang Y, Chen B, Wu M, Xie Y, et al. Effect of ATM on Inflammatory Response and Autophagy in Renal Tubular Epithelial Cells in LPS-Induced Septic AKI. *Exp Ther Med* (2019) 18(6):4707–17. doi: 10.3892/etm.2019.8115
38. Nie K, Zheng Z, Wen Y, Shi L, Xu S, Wang X, et al. Construction and Validation of a TP53-Associated Immune Prognostic Model for Gastric Cancer. *Genomics* (2020) 112(6):4788–95. doi: 10.1016/j.ygeno.2020.08.026
39. Santos JC, Gambeloni RZ, Roque AT, Oeck S, Ribeiro ML. Epigenetic Mechanisms of ATM Activation After Helicobacter Pylori Infection. *Am J Pathol* (2018) 188(2):329–35. doi: 10.1016/j.ajpath.2017.10.005
40. Ma C, Wang X, Yang F, Zang Y, Liu J, Wang X, et al. Circular RNA Hsa_Circ_0004872 Inhibits Gastric Cancer Progression *via* the miR-224/Smad4/ADAR1 Successive Regulatory Circuit. *Mol Cancer* (2020) 19(1):157. doi: 10.1186/s12943-020-01268-5
41. Ruoming W, Zhen Y, Tengteng Z, Jisheng H. Tumor Suppressor microRNA-31 Inhibits Gastric Carcinogenesis by Targeting Smad4 and SGPP2. *Cancer Gene Ther* (2015) 22(12):564–72. doi: 10.1038/cgt.2015.41
42. Desai SJ, Prickril B, Rasooly A. Mechanisms of Phytonutrient Modulation of Cyclooxygenase-2 (COX-2) and Inflammation Related to Cancer. *Nutr Cancer* (2018) 70(3):350–75. doi: 10.1080/01635581.2018.1446091
43. Lin XM, Li S, Zhou C, Li RZ, Wang H, Luo W, et al. Cisplatin Induces Chemoresistance Through the PTGS2-Mediated Anti-Apoptosis in Gastric Cancer. *Int J Biochem Cell Biol* (2019) 116:105610. doi: 10.1016/j.biocel.2019.105610
44. Quan J, Bode AM, Luo X. ACSL Family: The Regulatory Mechanisms and Therapeutic Implications in Cancer. *Eur J Pharmacol* (2021) 909:174397. doi: 10.1016/j.ejphar.2021.174397
45. Cruz-Gil S, Sanchez-Martinez R, Gomez de Cedron M, Martin-Hernandez R, Vargas T, Molina S, et al. Targeting the Lipid Metabolic Axis ACSL/SCD in Colorectal Cancer Progression by Therapeutic miRNAs: miR-19b-1 Role. *J Lipid Res* (2018) 59(1):14–24. doi: 10.1194/jlr.M076752
46. Tang Y, Zhou J, Hooi SC, Jiang YM, Lu GD. Fatty Acid Activation in Carcinogenesis and Cancer Development: Essential Roles of Long-Chain Acyl-CoA Synthetases. *Oncol Lett* (2018) 16(2):1390–6. doi: 10.3892/ol.2018.8843
47. Yuan H, Li X, Zhang X, Kang R, Tang D. Identification of ACSL4 as a Biomarker and Contributor of Ferroptosis. *Biochem Biophys Res Commun* (2016) 478(3):1338–43. doi: 10.1016/j.bbrc.2016.08.124
48. Wu J, Minikes AM, Gao M, Bian H, Li Y, Stockwell BR, et al. Intercellular Interaction Dictates Cancer Cell Ferroptosis *via* NF2-YAP Signalling. *Nature* (2019) 572(7769):402–6. doi: 10.1038/s41586-019-1426-6
49. Sanchez-Martinez R, Cruz-Gil S, Garcia-Alvarez MS, Reglero G, Ramirez de Molina A. Complementary ACSL Isoforms Contribute to a non-Warburg Advantageous Energetic Status Characterizing Invasive Colon Cancer Cells. *Sci Rep* (2017) 7(1):11143. doi: 10.1038/s41598-017-11612-3
50. Sha R, Xu Y, Yuan C, Sheng X, Wu Z, Peng J, et al. Predictive and Prognostic Impact of Ferroptosis-Related Genes ACSL4 and GPX4 on Breast Cancer Treated With Neoadjuvant Chemotherapy. *EBioMedicine* (2021) 71:103560. doi: 10.1016/j.ebiom.2021.103560
51. Ye X, Zhang Y, Wang X, Li Y, Gao Y. Tumor-Suppressive Functions of Long-Chain Acyl-CoA Synthetase 4 in Gastric Cancer. *IUBMB Life* (2016) 68(4):320–7. doi: 10.1002/iub.1486
52. Yuan K, Ye J, Liu Z, Ren Y, He W, Xu J, et al. Complement C3 Overexpression Activates JAK2/STAT3 Pathway and Correlates With Gastric Cancer Progression. *J Exp Clin Cancer Res* (2020) 39(1):9. doi: 10.1186/s13046-019-1514-3
53. Liang L, Hui K, Hu C, Wen Y, Yang S, Zhu P, et al. Autophagy Inhibition Potentiates the Anti-Angiogenic Property of Multikinase Inhibitor Anlotinib Through JAK2/STAT3/VEGFA Signaling in non-Small Cell Lung Cancer Cells. *J Exp Clin Cancer Res* (2019) 38(1):71. doi: 10.1186/s13046-019-1093-3
54. Park SY, Lee CJ, Choi JH, Kim JH, Kim JW, Kim JY, et al. The JAK2/STAT3/CCND2 Axis Promotes Colorectal Cancer Stem Cell Persistence and Radioresistance. *J Exp Clin Cancer Res* (2019) 38(1):399. doi: 10.1186/s13046-019-1405-7
55. Jaskiewicz A, Domoradzki T, Pajak B. Targeting the JAK2/STAT3 Pathway-Can We Compare It to the Two Faces of the God Janus? *Int J Mol Sci* (2020) 21(21):20–2. doi: 10.3390/ijms21218261

Conflict of Interest: The authors declare that the research was conducted in the absence of any commercial or financial relationships that could be construed as a potential conflict of interest.

Publisher's Note: All claims expressed in this article are solely those of the authors and do not necessarily represent those of their affiliated organizations, or those of the publisher, the editors and the reviewers. Any product that may be evaluated in this article, or claim that may be made by its manufacturer, is not guaranteed or endorsed by the publisher.

frontiers in Pharmacology

ORIGINAL RESEARCH
published: 14 March 2022
doi: 10.3389/fphar.2022.851540

Network Pharmacology Identifies Therapeutic Targets and the Mechanisms of Glutathione Action in Ferroptosis Occurring in Oral Cancer

Chen Huang[1*†] *and Lei Zhan*[2†]

[1]The Center for Data Science in Health and Medicine, Business School, Qingdao University, Qingdao, China, [2]Department of Ophthalmology, The Second People's Hospital of Guilin, Guilin, China

Oral cancer (OC) is one of the most pernicious cancers with increasing incidence and mortality worldwide. Surgery is the primary approach for the treatment of early-stage OC, which reduces the quality of life of the patients. Therefore, there is an urgent need to discover novel treatments for OC. Targeting ferroptosis to induce cell death through the modulation of lipid oxidation has been used as a new approach to treat many cancers. Glutathione (GSH) is a coenzyme factor of GSH peroxidase 4, and it carries potential applicability in treating OC. By using network pharmacology and molecular docking followed by systematic bioinformatic analysis, we aimed to study GSH-targeting ferroptosis to treat OC. We identified 14 core molecular targets, namely, EGFR, PTGS2, HIF1A, VEGFA, TFRC, SLC2A1, CAV1, CDKN2A, SLC3A2, IFNG, NOX4, DDIT4, CA9, and DUSP1, involved in ferroptosis that were targeted by GSH for OC treatment. Functional characterization of these molecular targets showed their importance in the control of cell apoptosis, cell proliferation, and immune responses through various kinase activities such as the mitogen-activated protein kinase activity (e.g., ERK1 and ERK2 cascades) and modulation of TOR signaling (e.g., the HIF-1 signaling pathway). Molecular docking further revealed the direct binding of GSH with EGFR, PTGS2, and HIF1A proteins. These findings provide a novel insight into the targets of GSH in ferroptosis as well as possible molecular mechanisms involved, suggesting the possible use of GSH as a combined therapy for treating OC.

Keywords: oral cancer, GSH, ferroptosis, network pharmacology, targets

OPEN ACCESS

Edited by:
Jiaoti Huang,
Duke University, United States

Reviewed by:
Li Li,
Sichuan University, China
Yiying Wu,
Chengdu Medical College, China

****Correspondence:***
Chen Huang
chenh0608@126.com

†These authors have contributed equally to this work.

Specialty section:
This article was submitted to Pharmacology of Anti-Cancer Drugs, a section of the journal Frontiers in Pharmacology

Received: *10 January 2022*
Accepted: *23 February 2022*
Published: *14 March 2022*

Citation:
Huang C and Zhan L (2022) Network Pharmacology Identifies Therapeutic Targets and the Mechanisms of Glutathione Action in Ferroptosis Occurring in Oral Cancer. Front. Pharmacol. 13:851540. doi: 10.3389/fphar.2022.851540

INTRODUCTION

Oral cancer (OC) is a type of malignant tumor that occurs in the oral cavity; it includes tongue cancer, gum cancer, palate cancer, oropharyngeal cancer, and lip cancer (Wong and Wiesenfeld 2018). OC is one of the most pernicious cancers reported in the world, accounting for around 2% of all new cases (Sung et al., 2021). In recent decades, the incidence and mortality of OC have shown markedly increasing trends (Chen et al., 2016). Potential risk factors for OC include smoking, drinking, poor oral hygiene, malnutrition, environmental impact, genetic factors, and infectious diseases (Shield et al., 2017). Tumor formation in OC results from abnormal activation patterns of proto- and anti-oncogenes and epigenetic modification (Osan et al., 2021). Early clinical detection of OC may be difficult to achieve because of insidious conditions and anatomical characteristics prior to

initial treatment (Dhanuthai et al., 2018). Clinically, surgery is prioritized for early-stage OC with better treatment effects (D'Souza and Kumar 2020). However, chemotherapy is a palliative regimen, and its efficacy is not yet satisfactory for patients with advanced OC (Mohan et al., 2021). Therefore, markers for early detection of oral malignancies and alternative treatment agents are necessary. Ferroptosis, a type of programmed cell death dependent on iron and activated by lipid peroxidation, is closely related to cancer development (Nie et al., 2022). Initiation and induction of ferroptosis can cause abnormal function of mitochondria and peroxidation-based lipotoxicity, resulting in regulation of tumor formation (Wu et al., 2020). It is reported that malignant tumor cells contain high levels of iron elements for anarchic cell proliferation and tumor growth (Tang et al., 2021a). Therefore, targeting ferroptosis may be a promising approach for OC treatment. Glutathione (GSH) is a bioactive substance involved in cellular metabolism that physiologically functions to protect the body against lesions induced by reducing agents (Forman et al., 2009). GSH is a coenzyme factor of GSH peroxidase 4 (GPx4), an essential reaction substrate for the degradation of lipid peroxides. As a key enzyme regulating ferroptosis, GPx4 can inhibit the occurrence of ferroptosis by catalyzing the reduction of lipid peroxides (Xuan et al., 2021). Patients with OC have markedly low levels of superoxide dismutase, GSH peroxidase, and GSH transferase (Sushma et al., 2021). An *in vitro* study demonstrated that enhanced intracellular GSH activity induced by natural compounds might have anti-oral cancer action by modulating oxidative stress, autophagy, and cell death (Contant et al., 2021). Although the physiological function of GSH in OC and underlying molecular mechanisms are well-reported, pharmacological mechanisms of GSH against OC remain unclear, especially ferroptosis-associated signaling pathways. Recently, network pharmacology-based discovery of individual compounds that act against dysregulated disorders, including malignant cancer (Li et al., 2021a), has been demonstrated (Li et al., 2020). Using a network pharmacology screening approach, our previous study demonstrated the core targets and therapeutic mechanisms of the GSH action against the cleft lip (Li et al., 2021b). In this study, available bioinformatic data of GSH were processed and studied for the potential efficacy against OC *via* multi-step network pharmacology and molecular docking approach, revealing ferroptosis-associated biotargets and signaling mechanisms.

MATERIAL AND METHODS

Identification of Common Oral Cancer-, Ferroptosis-, and Glutathione-Associated Genes

The Cancer Genome Atlas (TCGA) database (https://portal.gdc.cancer.gov/) was used to determine OC-associated genes. Using the limma package of R in the Bioconductor software, genes with FDR <0.05 and |log2 fold change| > 1 were considered as OC-associated genes (Ritchie et al., 2015). The FerrDb database was then used to search for ferroptosis-associated genes (Zhou and Bao 2020). For GSH-associated genes, the chemical structure of GSH, C (CC(=O)NC(CS)C (=O)NCC(=O)O)C(C(=O)O)N, was obtained from the traditional Chinese medicine system pharmacology database (Ru et al., 2014) and used to determine the pharmacological targets of GSH using various online tools and databases including SwissTargetPrediction (Daina et al., 2019), SuperPred (Nickel et al., 2014), TargetNet (Yao et al., 2016), Batman (Liu et al., 2016), DrugBank (Wishart et al., 2018), and BindingDB (Liu et al., 2007). The target genes were subjected to UniProt for human database correction. Subsequently, all targets of OC, ferroptosis, and GSH were overlapped to obtain the common targets.

Protein Network Involved in Glutathione Action Against Oral Cancer Through Ferroptosis

The common targets were subjected to a protein–protein interaction (PPI) network analysis by using the STRING (Version 11.0) database (Szklarczyk et al., 2019). The network analyzer in Cytoscape v3.7.2 was set under median or maximum degrees of freedom; the core targets were obtained under the upper limit of the screening range with a maximum degree value of the topology data, and the lower limit was twice the median degree of freedom (Shannon et al., 2003).

Gene Ontology and Pathway Enrichment Analysis of CA028 Action Against Oral Cancer

The common targets were subjected to Bioconductor packages in the R-language software for Gene Ontology (GO) and Kyoto Encyclopedia of Genes and Genomes (KEGG) enrichment analysis. Then, the Cytoscape software was used to visualize the biological processes and signaling pathways involved in the GSH action against OC through ferroptosis (Shannon et al., 2003).

Molecular Docking Analysis

The binding of GSH to its core targets including the epidermal growth factor receptor (EGFR), prostaglandin-endoperoxide synthase 2 (PTGS2), and hypoxia inducible factor 1 subunit alpha (HIF1A) was studied by molecular docking. The protein structures of EGFR, PTGS2, and HIF1A were obtained from the PDB database. Then, MGLTools 1.5.6 of AutoDock Vina and the ChemBio3D Draw tool were used to conduct the docking analysis (Morris et al., 2009; Trott and Olson 2010). The docking parameter setting was assessed according to the root mean square deviation (RMSD) of the ligand molecule. RMSD ≤ 4Å was the permissive threshold for the conformation of the ligand molecule.

RESULTS

Identification of Glutathione Targets for Treating Oral Cancer Through Ferroptosis

By searching the FerrDb and GeneCards databases, 259 ferroptosis-associated targets were identified (**Figure 1A**).

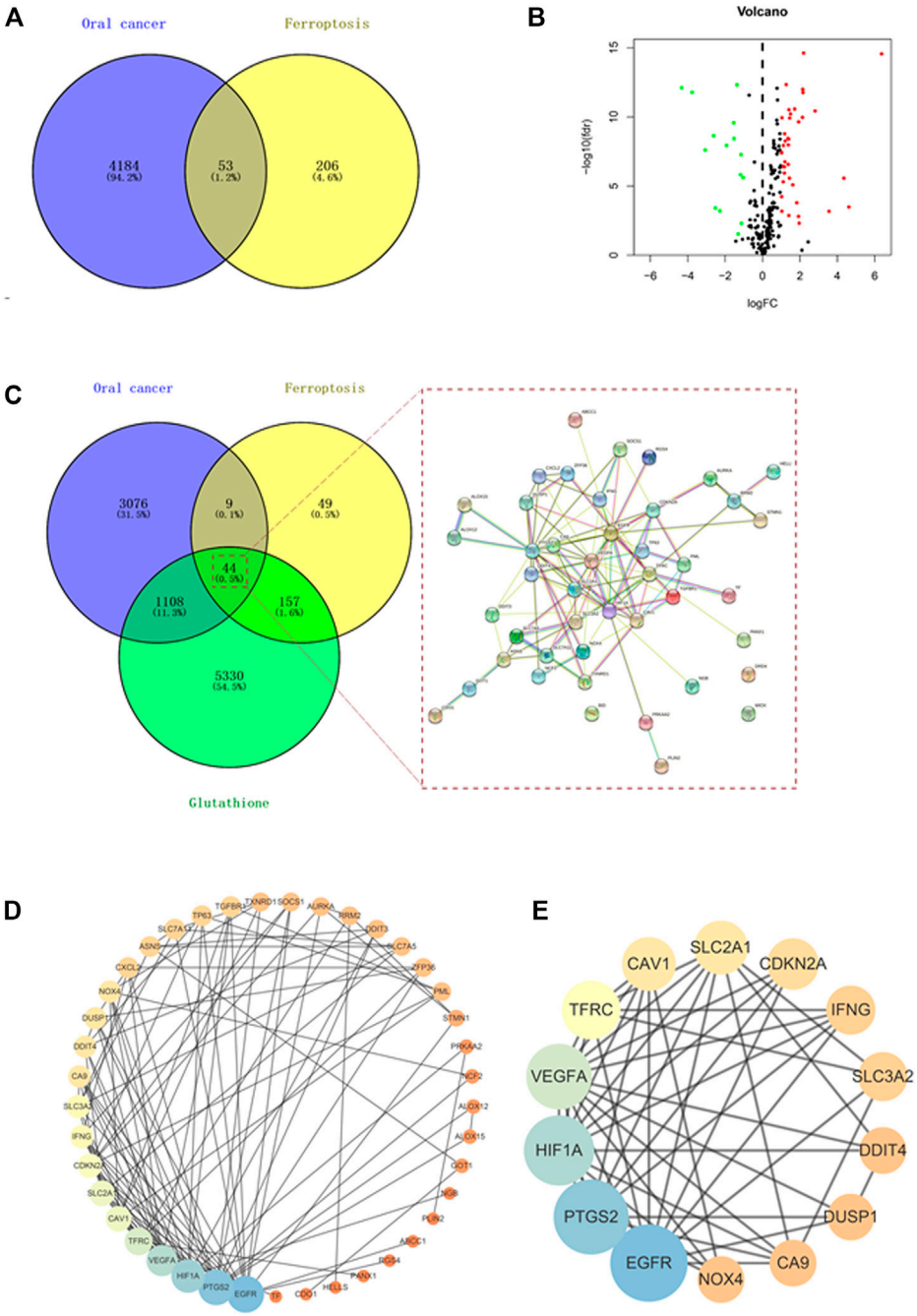

FIGURE 1 | Network pharmacology identified the anti-oral cancer genes involved in targeting ferroptosis by glutathione (GSH). **(A)** Venn diagram showing the interacting genes associated with oral cancer (OC) and ferroptosis. **(B)** Volcano plot showing the differential expression of ferroptosis-associated genes in OC. The genes with FDR <0.05 and |log2 fold change| > 1 were considered as differentially expressed genes. Green dots represent downregulated genes, and red dots represent upregulated genes. **(C)** Venn diagram showing the interacting genes associated with OC, ferroptosis, and GSH. **(D)** Protein–protein interaction (PPI) of OC-, ferroptosis-, and GSH-associated genes. **(E)** Cytoscape analysis identified 14 core targets of GSH for treating OC by targeting ferroptosis.

Additionally, using TCGA database, the comparison of gene sequences from 32 normal adults and 330 patients with OC identified 4,237 differentially expressed genes (DEGs) (**Figure 1A**). Among these, 53 DEGs including 38 upregulated genes and 15 downregulated genes overlapped with ferroptosis-associated targets (**Figure 1B**). Furthermore, 6639 GSH-associated target genes were identified by searching different databases, and 44 of them were found to be shared with OC- and ferroptosis-associated targets (**Figure 1C**). Then, the common targets were subjected to the STRING analysis to

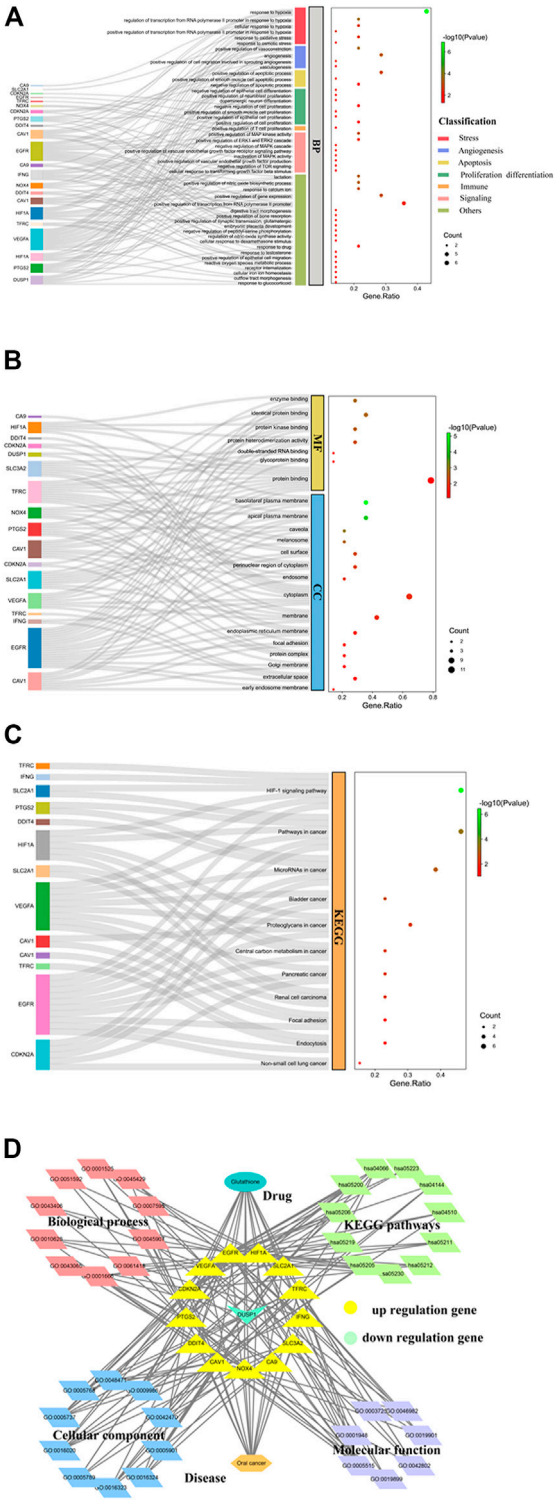

FIGURE 2 | Functional characterization of glutathione (GSH)-targeting ferroptosis genes in oral cancer (OC). **(A)** Gene Ontology (GO) enrichment analysis highlighting the biological roles of GSH-targeting ferroptosis genes in stress responses, angiogenesis, apoptosis, cell proliferation, cell differentiation, immune responses, and cell signaling for treating OC. **(B)** GO enrichment analysis highlighting the molecular functions and cellular

(*Continued*)

FIGURE 2 | components of GSH-targeting ferroptosis genes for treating OC. **(C)** Kyoto Encyclopedia of Genes and Genomes (KEGG) pathway analysis showed the importance of target genes of GSH action in cell signaling pathways involved in OC. The size of the dots represents the number of genes, whereas the color of the dots represents the significance of the terms. **(D)** Complex network analysis using Cytoscape to visualize the biological processes and signaling pathways involved in the mechanism of GSH action against OC through ferroptosis.

delineate the PPI involved in the GSH action against OC through ferroptosis (**Figure 1D**). By using the Cytoscape tool, 14 core targets, namely, PTGS2, EGFR, HIF1A, cyclin-dependent kinase inhibitor 2A (CDKN2A), vascular endothelial growth factor A (VEGFA), interferon gamma (IFNG), dual specificity phosphatase 1 (DUSP1), NADPH oxidase 4 (NOX4), solute carrier family 3 member 2 (SLC3A2), solute carrier family 2 member 1 (SLC2A1), caveolin 1 (CAV1), carbonic anhydrase 9 (CA9), transferrin receptor (TFRC), and DNA damage-inducible transcript 4 (DDIT4) were obtained. The median degree of freedom was 5.37, whereas the maximum degree of freedom was 19 (**Figure 1E** and **Table 1**).

Glutathione Targeted Ferroptosis to Control Stress Responses and Cell Apoptosis of Oral Cancer

GO enrichment analysis of the 14 core targets highlighted the biological processes related to stress responses such as oxidative stress and hypoxic stress (**Figure 2A**). Besides, altered angiogenesis through vasoconstriction and vasculogenesis was observed (**Figure 2A**). Furthermore, this could lead to the control of cell apoptosis, cell proliferation, and immune responses through many kinase activities and pathways, such as the mitogen-activated protein kinase (MAPK) activity, the extracellular signal-regulated kinase (ERK)1 and ERK2 cascades, and TOR signaling (**Figure 2A**). Molecular functional analysis of GO showed the involvement of the core targets in many binding activities such as enzyme binding, protein binding, protein kinase binding, glycoprotein binding, double-stranded RNA binding, and protein heterodimerization

TABLE 1 | Information of GSH anti-oral cancer genes.

Gene name	Gene symbol	UniProt ID
Prostaglandin-endoperoxide synthase 2	PTGS2	P35354
Epidermal growth factor receptor	EGFR	P00533
Hypoxia inducible factor 1 subunit alpha	HIF1A	Q16665
Cyclin-dependent kinase inhibitor 2A	CDKN2A	P42771
Vascular endothelial growth factor A	VEGFA	P15692
Interferon gamma	IFNG	P01579
Dual specificity phosphatase 1	DUSP1	P28562
NADPH oxidase 4	NOX4	Q9NPH5
Solute carrier family 3 member 2	SLC3A2	P08195
Solute carrier family 2 member 1	SLC2A1	P11166
Caveolin 1	CAV1	Q03135
Carbonic anhydrase 9	CA9	Q16790
Transferrin receptor	TFRC	P02786
DNA damage inducible transcript 4	DDIT4	Q9NX09

activity (**Figure 2B**). GO analysis also highlighted the contribution of core targets to different cellular components such as the endosome, cytoplasm membrane, Golgi membrane, and extracellular space (**Figure 2B**). KEGG pathway analysis revealed the control of cell signaling pathways such as the HIF-1 signaling pathway by GSH targets (**Figure 2C**). In addition, many cancer-related signaling pathways, including mRNAs in cancer, bladder cancer, proteoglycans in cancer, central carbon metabolism in cancer, pancreatic cancer, renal cell carcinoma, and non-small cell lung cancer, were highlighted in our analysis (**Figure 2C**). Taken together, our results show the importance of GSH against ferroptosis in OC through the regulation of many cancer-related biological processes and signaling pathways (**Figure 2D**).

Direct Binding of Glutathione to Oral Cancer- and Ferroptosis-Associated Genes

Molecular docking analysis was conducted to investigate the possible direct binding of GSH to its target proteins. The results showed that GSH had a high binding affinity to EGFR, PTGS2, and HIF1A (**Figure 3**). The protein structures of EGFR, PTGS2, and HIF1A were obtained from the PDB database. Furthermore, the AutoDock Vina program was used to determine the binding affinity between these proteins and GSH. The results demonstrated that GSH formed hydrogen bonds with amino acid residues CYS-797 (1.9 Å), MET-793 (2.5 Å), and LYS-716 (2.5 Å) of EGFR (PDB ID: 5UGC) of EGFR, and the free binding energy was −5.1 kcal/mol. For PTGS2 protein (PDB ID: 5IKR), GSH formed hydrogen bonds with amino acid residues TYR-355 (2.6 Å), ARG-120 (2.3 Å), and VAL-523 (2.4 Å) of PTGS2 (**Figure 3B**), and the free binding energy was -5.12 kcal/mol. Similar bonds were observed between GSH and amino acid residues ARG-238 (2.5 Å) and GLN-239 (1.8 Å) of HIF1A (PDB ID: 1H2M) (**Figure 3C**), with a free binding energy of −5.32 kcal/mol. Collectively, our data suggested direct binding of GSH to its target proteins EGFR, PTGS2, and HIF1A.

DISCUSSION

In the present study, we investigated the possible use of GSH in treating OC by targeting ferroptosis. Ferroptosis, a newly discovered type of cell death mediated by iron-dependent lipid peroxidation (Chen S. et al., 2021), is reported to be a promising approach in cancer therapy (Tang et al., 2021b). Oral squamous cell carcinoma was shown to have a ferroptosis-specific gene-expression signature, suggesting ferroptosis regulation may be clinically relevant for combination therapies (Gu et al., 2021). We hypothesized that GSH can be a potential drug for combination therapies of OC as it is a key player in cellular oxidation–reduction homeostasis and is closely associated with ferroptosis in various cancers (Elakkad et al., 2021; Liu et al., 2021; Xu et al., 2021).

By using network pharmacology, we identified 14 core targets of GSH action against OC by targeting ferroptosis. Bioinformatic analysis of these 14 targets suggested the role of GSH in cell apoptosis, cell proliferation, and immune responses through the regulation of MAPK, ERK, and TOR signaling pathways. MAPK

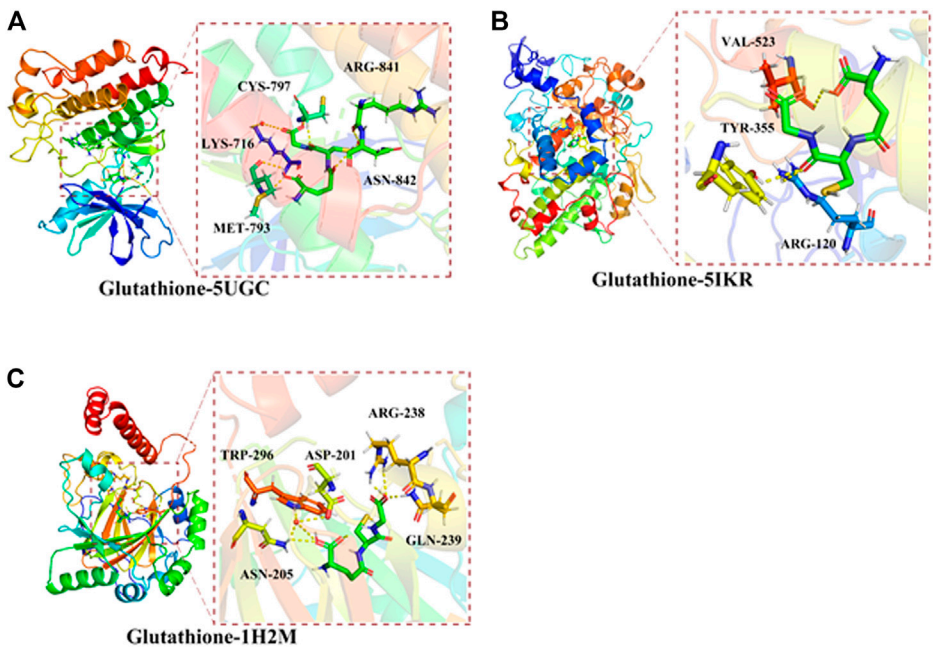

FIGURE 3 | Direct binding of glutathione (GSH) to its targets against oral cancer through ferroptosis. Molecular docking analysis predicted the preferred orientation of hydrogen bonds between GSH and amino acid residues **(A)** CYS-797, MET-793, and LYS-716 of EGFR (PDB ID:5UGC) **(B)** TYR-355, ARG-120, and VAL-523 of PTGS2 (PDB ID: 5IKR) **(C)** ARG-238 and GLN-239 of HIF1A (PDB ID: 1H2M).

was found to be involved in ferroptosis regulation in many human body functions (Nguyen et al., 2020). Activation of MAPK signaling induced ferroptosis in human pancreatic islet-cell clusters (Li and Leung 2020). In contrast, inhibition of MAPK signaling suppressed inflammation and oxidative stress of acute respiratory distress syndrome caused by ferroptosis (Wang et al., 2022). In other studies, MAPK signaling was found to control ferroptosis in various cancers including nasopharyngeal carcinoma, hepatocellular carcinoma, osteosarcoma, and non-small cell lung cancer through redox balance (Poursaitidis et al., 2017; Lv et al., 2020; Chang et al., 2021; He et al., 2021). More importantly, MAPK signaling was linked to many other cell signaling pathways mediating the carcinogenicity of OC. For instance, MAPK signaling regulated the viability of OC *via* the response gene FOS as a subunit of the AP-1 complex (Greer et al., 2022). Also, inhibition of the MAPK pathway diminished invasion and the migration ability in OC through the regulation of matrix metalloproteinase-2 activity (Pramanik and Mishra 2022). Besides the MAPK signaling, our results highlighted the involvement of ERK signaling in ferroptosis targeted by GSH. ERK signaling is associated with ferroptosis in many cancers, including multiple myeloma (Chen J. et al., 2021), endometrial carcinoma (Qin et al., 2021), hepatocellular carcinoma (Fei et al., 2021), and pancreatic cancer (Ye et al., 2020). Specifically, the ERK signaling pathway has been linked with ferroptosis and associated with the prognosis of OC (Chen R. et al., 2021). For TOR signaling, only limited studies have demonstrated its direct link to ferroptosis. A study by Ni et al. demonstrated that inhibition of mTOR overcame anticancer drug resistance by promoting ferroptosis in lung cancer cells (Ni et al., 2021). Another study on xenograft mouse models suggested that the combination of mTORC1 inhibition with ferroptosis induction resulted in tumor regression in PI3K-mutated breast cancer and PTEN-defective prostate cancer (Yi et al., 2020). Therefore, the use of GSH to target ferroptosis could be a promising combination therapy for treating OC.

In addition to network pharmacology, we applied molecular docking to investigate the possible direct binding of GSH to its target proteins involved in ferroptosis. Our results showed a strong binding affinity of GSH to EGFR, PTGS2, and HIFIA.

EGFR, a receptor tyrosine kinase, is a major regulator of cancer development (Ni et al., 2021). It coordinates with mTOR and MAPK signaling to regulate ferroptosis in cancer. For example, EGFR was associated with the mTOR pathway to mediate ferroptosis and apoptosis of ovarian cancer (Li et al., 2022). In addition, the EGFR tyrosine kinase inhibitor lapatinib regulated mTOR to promote ferroptosis in lung cancer cells (Ni et al., 2021). Another study of non-small cell lung cancer demonstrated that the blockade of EGFR or MAPK signaling protected the lung cancer cells from ferroptosis (Poursaitidis et al., 2017). Furthermore, it has been shown that ferroptosis can be targeted to treat EGFR-mutant lung cancer (Zhang et al., 2021). Additionally, driving EGFR could induce ferroptosis in hepatocellular carcinoma and glioblastoma (Kadioglu et al., 2021; Sun et al., 2021). PTGS2 is responsible for the prostanoid biosynthesis involved in inflammation and mitogenesis (Gómez-Valenzuela et al., 2021). It was reported that upregulation of PTGS2 induces the ferroptosis of colorectal cancer cells (Zhao and Chen 2021); thus, PTGS2 is considered as a marker of ferroptosis. The PTGS2 expression was associated with increased lipid peroxidation in gastric cancer cells (Guan et al., 2020). In another study, the PTGS2 expression modulated esophageal squamous cell carcinoma radiosensitivity by inhibiting ferroptosis (Feng et al., 2021). In addition, HIF1A was associated with increased tumor immunity and aggressive phenotypes in human cancers (Chen et al., 2020). Ferroptosis-related genes associated with the overall survival in patients with diffuse large B-cell lymphoma have also been reported (Chen H. et al., 2021).

In conclusion, we identified the targets of GSH in ferroptosis associated with OC, providing new mechanistic insights that may be clinically relevant for combination therapies of OC. However, the findings of the present study are mainly based on network pharmacology and bioinformatics analysis; therefore, further preclinical investigation is needed to verify the results.

DATA AVAILABILITY STATEMENT

The datasets presented in this study can be found in online repositories. The names of the repository/repositories and accession number(s) can be found in the article/supplementary material.

AUTHOR CONTRIBUTIONS

CH and LZ contributed to the conception and design of the manuscript. CH and LZ contributed to the acquisition, analysis, and interpretation of data in this manuscript. CH and LZ drafted this manuscript. CH and LZ revised this manuscript.

REFERENCES

Chang, W. T., Bow, Y. D., Fu, P. J., Li, C. Y., Wu, C. Y., Chang, Y. H., et al. (2021). A Marine Terpenoid, Heteronemin, Induces Both the Apoptosis and Ferroptosis of Hepatocellular Carcinoma Cells and Involves the ROS and MAPK Pathways. *Oxid Med. Cel Longev* 2021, 7689045. PMID: 33488943; PMCID: PMC7803406. doi:10.1155/2021/7689045

Chen, B., Li, L., Li, M., and Wang, X. (2020). HIF1A Expression Correlates with Increased Tumor Immune and Stromal Signatures and Aggressive Phenotypes in Human Cancers. *Cel Oncol (Dordr)* 43 (5), 877–888. Epub 2020 Jun 1. PMID: 32488852. doi:10.1007/s13402-020-00534-4

Chen, H., He, Y., Pan, T., Zeng, R., Li, Y., Chen, S., et al. (2021). Ferroptosis-Related Gene Signature: A New Method for Personalized Risk Assessment in Patients with Diffuse Large B-Cell Lymphoma. *Pharmgenomics Pers Med.* 14, 609–619. PMID: 34079336; PMCID: PMC8165657. doi:10.2147/PGPM.S309846

Chen, J., Zaal, E. A., Berkers, C. R., Ruijtenbeek, R., Garssen, J., and Redegeld, F. A. (2021). Omega-3 Fatty Acids DHA and EPA Reduce Bortezomib Resistance in Multiple Myeloma Cells by Promoting Glutathione Degradation. *Cells* 10 (9), 2287. PMID: 34571936; PMCID: PMC8465636. doi:10.3390/cells10092287

Chen, R., Cao, J., Jiang, W., Wang, S., and Cheng, J. (2021). Upregulated Expression of CYBRD1 Predicts Poor Prognosis of Patients with Ovarian Cancer. *J. Oncol.* 2021, 7548406. PMID: 34594380; PMCID: PMC8478559. doi:10.1155/2021/7548406

Chen, S., Zhu, J. Y., Zang, X., and Zhai, Y. Z. (2021). The Emerging Role of Ferroptosis in Liver Diseases. *Front Cel Dev Biol* 9, 801365. doi:10.3389/fcell.2021.801365

Chen, W., Zheng, R., Baade, P. D., Zhang, S., Zeng, H., Bray, F., et al. (2016). Cancer Statistics in China, 2015. *CA Cancer J. Clin.* 66, 115–132. doi:10.3322/caac.21338

Contant, C., Rouabhia, M., Loubaki, L., Chandad, F., and Semlali, A. (2021). Anethole Induces Anti-oral Cancer Activity by Triggering Apoptosis, Autophagy and Oxidative Stress and by Modulation of Multiple Signaling Pathways. *Sci. Rep.* 11, 13087. doi:10.1038/s41598-021-92456-w

D'Souza, W., and Kumar, A. (2020). microRNAs in Oral Cancer: Moving from Bench to Bed as Next Generation Medicine. *Oral Oncol.* 111, 104916. doi:10.1016/j.oraloncology.2020.104916

Daina, A., Michielin, O., and Zoete, V. (2019). SwissTargetPrediction: Updated Data and New Features for Efficient Prediction of Protein Targets of Small Molecules. *Nucleic Acids Res.* 47, W357–W364. doi:10.1093/nar/gkz382

Dhanuthai, K., Rojanawatsirivej, S., Thosaporn, W., Kintarak, S., Subarnbhesaj, A., Darling, M., et al. (2018). Oral Cancer: A Multicenter Study. *Med. Oral Patol Oral Cir Bucal* 23, e23–29. doi:10.4317/medoral.21999

Elakkad, Y. E., Mohamed, S. N. S., and Abuelezz, N. Z. (2021). Potentiating the Cytotoxic Activity of a Novel Simvastatin-Loaded Cubosome against Breast Cancer Cells: Insights on Dual Cell Death via Ferroptosis and Apoptosis. *Breast Cancer (Dove Med. Press.* 13, 675–689. PMID: 34934357; PMCID: PMC8684378. doi:10.2147/BCTT.S336712

Fei, Z., Lijuan, Y., Jing, Z., Xi, Y., Yuefen, P., and Shuwen, H. (2021). Molecular Characteristics Associated with Ferroptosis in Hepatocellular Carcinoma Progression. *Hum. Cel* 34 (1), 177–186. Epub 2020 Sep 16. PMID: 32936424. doi:10.1007/s13577-020-00431-w

Feng, L., Zhao, K., Sun, L., Yin, X., Zhang, J., Liu, C., et al. (2021). SLC7A11 Regulated by NRF2 Modulates Esophageal Squamous Cell Carcinoma Radiosensitivity by Inhibiting Ferroptosis. *J. Transl Med.* 19 (1), 367. PMID: 34446045; PMCID: PMC8393811. doi:10.1186/s12967-021-03042-7

Forman, H. J., Zhang, H., and Rinna, A. (2009). Glutathione: Overview of its Protective Roles, Measurement, and Biosynthesis. *Mol. Aspects Med.* 30, 1–12. doi:10.1016/j.mam.2008.08.006

Gómez-Valenzuela, F., Escobar, E., Pérez-Tomás, R., and Montecinos, V. P. (2021). The Inflammatory Profile of the Tumor Microenvironment, Orchestrated by Cyclooxygenase-2, Promotes Epithelial-Mesenchymal Transition. *Front. Oncol.* 11, 686792. PMID: 34178680; PMCID: PMC8222670. doi:10.3389/fonc.2021.686792

Greer, P. F. C., Rich, A., and Coates, D. E. (2022). Effects of Galectin-1 Inhibitor OTX008 on Oral Squamous Cell Carcinoma Cells *In Vitro* and the Role of AP-1 and the MAPK/ERK Pathway. *Arch. Oral Biol.* 134, 105335. Epub ahead of print. PMID: 34891102. doi:10.1016/j.archoralbio.2021.105335

Gu, W., Kim, M., Wang, L., Yang, Z., Nakajima, T., and Tsushima, Y. (2021). Multi-omics Analysis of Ferroptosis Regulation Patterns and Characterization of Tumor Microenvironment in Patients with Oral Squamous Cell Carcinoma. *Int. J. Biol. Sci.* 17 (13), 3476–3492. PMID: 34512160; PMCID: PMC8416738. doi:10.7150/ijbs.61441

Guan, Z., Chen, J., Li, X., and Dong, N. (2020). Tanshinone IIA Induces Ferroptosis in Gastric Cancer Cells through P53-Mediated SLC7A11 Down-Regulation. *Biosci. Rep.* 40 (8), BSR20201807. PMID: 32776119; PMCID: PMC7953492. doi:10.1042/BSR20201807

He, X., Yao, Q., Fan, D., Duan, L., You, Y., Liang, W., et al. (2021). Cephalosporin Antibiotics Specifically and Selectively Target Nasopharyngeal Carcinoma through HMOX1-Induced Ferroptosis. *Life Sci.* 277, 119457. Epub 2021 Apr 5. PMID: 33831425. doi:10.1016/j.lfs.2021.119457

Kadioglu, O., Saeed, M. E. M., Mahmoud, N., Azawi, S., Mrasek, K., Liehr, T., et al. (2021). Identification of Novel Drug Resistance Mechanisms by Genomic and Transcriptomic Profiling of Glioblastoma Cells with Mutation-Activated EGFR. *Life Sci.* 284, 119601. Epub 2021 May 13. PMID: 33991550. doi:10.1016/j.lfs.2021.119601

Li, H. W., Liu, M. B., Jiang, X., Song, T., Feng, S. X., Wu, J. Y., et al. (2022). GALNT14 Regulates Ferroptosis and Apoptosis of Ovarian Cancer through the EGFR/mTOR Pathway. *Future Oncol.* 18 (2), 149–161. Epub 2021 Oct 13. PMID: 34643088. doi:10.2217/fon-2021-0883

Li, R., Guo, C., Li, Y., Liang, X., Yang, L., and Huang, W. (2020). Therapeutic Target and Molecular Mechanism of Vitamin C-Treated Pneumonia: a Systematic Study of Network Pharmacology. *Food Funct.* 11, 4765–4772. doi:10.1039/d0fo00421a

Li, R., Li, Y., Liang, X., Yang, L., Su, M., and Lai, K. P. (2021a). Network Pharmacology and Bioinformatics Analyses Identify Intersection Genes of Niacin and COVID-19 as Potential Therapeutic Targets. *Brief Bioinform* 22, 1279–1290. doi:10.1093/bib/bbaa300

Li, R., Huang, C., Ho, J. C. H., Leung, C. C. T., Kong, R. Y. C., Li, Y., et al. (2021b). The Use of Glutathione to Reduce Oxidative Stress Status and its Potential for Modifying the Extracellular Matrix Organization in Cleft Lip. *Free Radic. Biol. Med.* 164, 130–138. doi:10.1016/j.freeradbiomed.2020.12.455

Li, X. Y., and Leung, P. S. (2020). Erastin-induced Ferroptosis Is a Regulator for the Growth and Function of Human Pancreatic Islet-like Cell Clusters. *Cell Regen* 9 (1), 16. PMID: 32893325; PMCID: PMC7475162. doi:10.1186/s13619-020-00055-3

Liu, J., Wen, Q., Zhou, B., Yuan, C., Du, S., Li, L., et al. (2021). "Clickable" ZIF-8 for Cell-type-specific Delivery of Functional Proteins. *ACS Chem. Biol.* 17, 32–38. Epub ahead of print. PMID: 34936351. doi:10.1021/acschembio.1c00872

Liu, T., Lin, Y., Wen, X., Jorissen, R. N., and Gilson, M. K. (2007). BindingDB: a Web-Accessible Database of Experimentally Determined Protein-Ligand Binding Affinities. *Nucleic Acids Res.* 35 (Database issue), D198–D201. doi:10.1093/nar/gkl999

Liu, Z., Guo, F., Wang, Y., Li, C., Zhang, X., Li, H., et al. (2016). BATMAN-TCM: a Bioinformatics Analysis Tool for Molecular mechANism of Traditional Chinese Medicine. *Sci. Rep.* 6, 21146. doi:10.1038/srep21146

Lv, H., Zhen, C., Liu, J., and Shang, P. (2020). β-Phenethyl Isothiocyanate Induces Cell Death in Human Osteosarcoma through Altering Iron Metabolism, Disturbing the Redox Balance, and Activating the MAPK Signaling Pathway. *Oxid Med. Cel Longev* 2020, 5021983. PMID: 32322335; PMCID: PMC7160723. doi:10.1155/2020/5021983

Mohan, S., Popli, G., and Aggarwal, K. (2021). Oral Oncology and Reconstructive Surgery Fellowship Training Programs in India-A Trainee Perspective. *South. Asian J. Cancer* 10, 267–268. doi:10.1055/s-0041-1731582

Morris, G. M., Huey, R., Lindstrom, W., Sanner, M. F., Belew, R. K., Goodsell, D. S., et al. (2009). AutoDock4 and AutoDockTools4: Automated Docking with Selective Receptor Flexibility. *J. Comput. Chem.* 30 (16), 2785–2791. doi:10.1002/jcc.21256

Nguyen, T. H. P., Mahalakshmi, B., and Velmurugan, B. K. (2020). Functional Role of Ferroptosis on Cancers, Activation and Deactivation by Various Therapeutic Candidates-An Update. *Chem. Biol. Interact* 317, 108930. Epub 2019 Dec 19. PMID: 31866335. doi:10.1016/j.cbi.2019.108930

Ni, J., Chen, K., Zhang, J., and Zhang, X. (2021). Inhibition of GPX4 or mTOR Overcomes Resistance to Lapatinib via Promoting Ferroptosis in NSCLC Cells. *Biochem. Biophys. Res. Commun.* 567, 154–160. Epub 2021 Jun 20. PMID: 34157442. doi:10.1016/j.bbrc.2021.06.051

Nickel, J., Gohlke, B. O., Erehman, J., Banerjee, P., Rong, W. W., Goede, A., et al. (2014). SuperPred: Update on Drug Classification and Target Prediction. *Nucleic Acids Res.* 42, W26–W31. doi:10.1093/nar/gku477

Nie, Q., Hu, Y., Yu, X., Li, X., and Fang, X. (2022). Induction and Application of Ferroptosis in Cancer Therapy. *Cancer Cel Int* 22, 12. doi:10.1186/s12935-021-02366-0

Osan, C., Chira, S., Nutu, A. M., Braicu, C., Baciut, M., Korban, S. S., et al. (2021). The Connection between MicroRNAs and Oral Cancer Pathogenesis: Emerging Biomarkers in Oral Cancer Management. *Genes (Basel)* 12, 1989. doi:10.3390/genes12121989

Poursaitidis, I., Wang, X., Crighton, T., Labuschagne, C., Mason, D., Cramer, S. L., et al. (2017). Oncogene-Selective Sensitivity to Synchronous Cell Death Following Modulation of the Amino Acid Nutrient Cystine. *Cell Rep* 18 (11), 2547–2556. PMID: 28297659; PMCID: PMC5368412. doi:10.1016/j.celrep.2017.02.054

Pramanik, K. K., and Mishra, R. (2022). ERK-mediated Upregulation of Matrix Metalloproteinase-2 Promotes the Invasiveness in Human Oral Squamous Cell Carcinoma (OSCC). *Exp. Cel Res* 411 (1), 112984. Epub ahead of print. PMID: 34951997. doi:10.1016/j.yexcr.2021.112984

Qin, J., Shao, X., Wu, L., and Du, H. (2021). Identification of the Ferroptosis-Associated Gene Signature to Predict the Prognostic Status of Endometrial Carcinoma Patients. *Comput. Math. Methods Med.* 2021, 9954370. PMID: 34531924; PMCID: PMC8440105. doi:10.1155/2021/9954370

Ritchie, M. E., Phipson, B., Wu, D., Hu, Y., Law, C. W., Shi, W., et al. (2015). Limma powers Differential Expression Analyses for RNA-Sequencing and Microarray Studies. *Nucleic Acids Res.* 43 (7), e47. doi:10.1093/nar/gkv007

Ru, J., Li, P., Wang, J., Zhou, W., Li, B., Huang, C., et al. (2014). TCMSP: a Database of Systems Pharmacology for Drug Discovery from Herbal Medicines. *J. Cheminform* 6, 13. doi:10.1186/1758-2946-6-13

Shannon, P., Markiel, A., Ozier, O., Baliga, N. S., Wang, J. T., Ramage, D., et al. (2003). Cytoscape: a Software Environment for Integrated Models of Biomolecular Interaction Networks. *Genome Res.* 13, 2498–2504. doi:10.1101/gr.1239303

Shield, K. D., Ferlay, J., Jemal, A., Sankaranarayanan, R., Chaturvedi, A. K., Bray, F., et al. (2017). The Global Incidence of Lip, Oral Cavity, and Pharyngeal Cancers by Subsite in 2012. *CA Cancer J. Clin.* 67, 51–64. doi:10.3322/caac.21384

Sun, J., Zhou, C., Zhao, Y., Zhang, X., Chen, W., Zhou, Q., et al. (2021). Quiescin Sulfhydryl Oxidase 1 Promotes Sorafenib-Induced Ferroptosis in Hepatocellular Carcinoma by Driving EGFR Endosomal Trafficking and Inhibiting NRF2 Activation. *Redox Biol.* 41, 101942. Epub 2021 Mar 13. PMID: 33770521; PMCID: PMC8024711. doi:10.1016/j.redox.2021.101942

Sung, H., Ferlay, J., Siegel, R. L., Laversanne, M., Soerjomataram, I., Jemal, A., et al. (2021). Global Cancer Statistics 2020: GLOBOCAN Estimates of Incidence and Mortality Worldwide for 36 Cancers in 185 Countries. *CA Cancer J. Clin.* 71, 209–249. doi:10.3322/caac.21660

Sushma, P. S., Jamil, K., Udaykumar, P., Aldakheel, F. M., Alduraywish, S. A., Alali, B. H., et al. (2021). Analysis of CCND1 Protein and Circulatory Antioxidant Enzyme Activity Association in Oral Squamous Cell Carcinoma. *Saudi J. Biol. Sci.* 28, 6987–6991. doi:10.1016/j.sjbs.2021.07.085

Szklarczyk, D., Gable, A. L., Lyon, D., Junge, A., Wyder, S., Huerta-Cepas, J., et al. (2019). STRING V11: Protein-Protein Association Networks with Increased Coverage, Supporting Functional Discovery in Genome-wide Experimental Datasets. *Nucleic Acids Res.* 47 (D1), D607–D613. doi:10.1093/nar/gky1131

Tang, Z., Huang, Z., Huang, Y., Chen, Y., Huang, M., Liu, H., et al. (2021). Ferroptosis: The Silver Lining of Cancer Therapy. *Front. Cel Dev Biol* 9, 765859. doi:10.3389/fcell.2021.765859

Tang, Z., Huang, Z., Huang, Y., Chen, Y., Huang, M., Liu, H., et al. (2021). Ferroptosis: The Silver Lining of Cancer Therapy. *Front. Cel Dev Biol*, 9. 765859PMC8667274. PMCID, PMID: 34912804. doi:10.3389/fcell.2021.765859

Trott, O., and Olson, A. J. (2010). AutoDock Vina: Improving the Speed and Accuracy of Docking with a New Scoring Function, Efficient Optimization, and Multithreading. *J. Comput. Chem.* 31 (2), 455–461. doi:10.1002/jcc.21334

Wang, X., Zhang, C., Zou, N., Chen, Q., Wang, C., Zhou, X., et al. (2022). Lipocalin-2 Silencing Suppresses Inflammation and Oxidative Stress of Acute Respiratory Distress Syndrome by Ferroptosis via Inhibition of MAPK/ERK Pathway in Neonatal Mice. *Bioengineered* 13 (1), 508–520. PMID: 34969358. doi:10.1080/21655979.2021.2009970

Wishart, D. S., Feunang, Y. D., Guo, A. C., Lo, E. J., Marcu, A., Grant, J. R., et al. (2018). DrugBank 5.0: a Major Update to the DrugBank Database for 2018. *Nucleic Acids Res.* 46, D1074–D1082. doi:10.1093/nar/gkx1037

Wong, T., and Wiesenfeld, D. (2018). Oral Cancer. *Aust. Dent J.* 63 Suppl 1, S91–S99. doi:10.1111/adj.12594

Wu, Y., Yu, C., Luo, M., Cen, C., Qiu, J., Zhang, S., et al. (2020). Ferroptosis in Cancer Treatment: Another Way to Rome. *Front. Oncol.* 10, 571127. doi:10.3389/fonc.2020.571127

Xu, X. L., Zhang, N. N., Shu, G. F., Liu, D., Qi, J., Jin, F. Y., et al. (2021). A Luminol-Based Self-Illuminating Nanocage as a Reactive Oxygen Species Amplifier to Enhance Deep Tumor Penetration and Synergistic Therapy. *ACS Nano* 15 (12), 19394–19408. Epub 2021 Nov 22. PMID: 34806870. doi:10.1021/acsnano.1c05891

Xuan, Z., Zhang, Y., Pan, Z., Zheng, X., and Huang, P. (2021). Natural Medicinal Ingredients Induce Tumor Ferroptosis and Related Mechanisms. *J. Zhejiang Univ. (Med Sci.* 50, 601–606. doi:10.3724/zdxbyxb-2021-0198

Yao, Z. J., Dong, J., Che, Y. J., Zhu, M. F., Wen, M., Wang, N. N., et al. (2016). TargetNet: a Web Service for Predicting Potential Drug-Target Interaction Profiling via Multi-Target SAR Models. *J. Comput. Aided Mol. Des.* 30, 413–424. doi:10.1007/s10822-016-9915-2

Ye, Z., Hu, Q., Zhuo, Q., Zhu, Y., Fan, G., Liu, M., et al. (2020). Abrogation of ARF6 Promotes RSL3-Induced Ferroptosis and Mitigates Gemcitabine Resistance in Pancreatic Cancer Cells. *Am. J. Cancer Res.* 10 (4), 1182–1193. PMID: 32368394; PMCID: PMC7191101.

Yi, J., Zhu, J., Wu, J., Thompson, C. B., and Jiang, X. (2020). Oncogenic Activation of PI3K-AKT-mTOR Signaling Suppresses Ferroptosis via SREBP-Mediated Lipogenesis. *Proc. Natl. Acad. Sci. U S A.* 117 (49), 31189–31197. Epub 2020 Nov 23. PMID: 33229547; PMCID: PMC7733797. doi:10.1073/pnas.2017152117

Zhang, T., Sun, B., Zhong, C., Xu, K., Wang, Z., Hofman, P., et al. (2021). Targeting Histone Deacetylase Enhances the Therapeutic Effect of Erastin-Induced Ferroptosis in EGFR-Activating Mutant Lung Adenocarcinoma. *Transl Lung Cancer Res.* 10 (4), 1857–1872. PMID: 34012798; PMCID: PMC8107764. doi:10.21037/tlcr-21-303

Zhao, X., and Chen, F. (2021). Propofol Induces the Ferroptosis of Colorectal Cancer Cells by Downregulating STAT3 Expression. *Oncol. Lett.* 22 (5), 767. Epub 2021 Sep 8. PMID: 34589146; PMCID: PMC8442167. doi:10.3892/ol.2021.13028

Zhou, N., and Bao, J. (2020). FerrDb: a Manually Curated Resource for Regulators and Markers of Ferroptosis and Ferroptosis-Disease Associations. *Database (Oxford)* 2020, baaa021. doi:10.1093/database/baaa021

Conflict of Interest: The authors declare that the research was conducted in the absence of any commercial or financial relationships that could be construed as a potential conflict of interest.

Publisher's Note: All claims expressed in this article are solely those of the authors and do not necessarily represent those of their affiliated organizations, or those of the publisher, the editors, and the reviewers. Any product that may be evaluated in this article, or claim that may be made by its manufacturer, is not guaranteed or endorsed by the publisher.

frontiers in Oncology

ORIGINAL RESEARCH
published: 22 March 2022
doi: 10.3389/fonc.2022.852095

FNDC5 Causes Resistance to Sorafenib by Activating the PI3K/Akt/Nrf2 Pathway in Hepatocellular Carcinoma Cells

Huayuan Liu[1], Lei Zhao[2], Mengya Wang[3], Kexin Yang[4], Zhipeng Jin[1], Chengjian Zhao[1] and Guangjun Shi[1]**

[1] Department of Hepatobiliary Surgery, The Affiliated Qingdao Municipal Hospital of Qingdao University, Qingdao, China, [2] Department of Infection Management, The Affiliated Qingdao Municipal Hospital of Qingdao University, Qingdao, China, [3] Department of Physiology, School of Basic Medicine, Institute of Brain Science and Disorders, Qingdao University, Qingdao, China, [4] Department of Gynecology, The Affiliated Qingdao Municipal Hospital of Qingdao University, Qingdao, China

OPEN ACCESS

Edited by:
Xu Chen,
Guilin Medical University, China

Reviewed by:
Evin Iscan,
Dokuz Eylül University, Turkey
Jiang Chen,
Zhejiang University, China

***Correspondence:**
Chengjian Zhao
17685552070@163.com
Guangjun Shi
sgjzp@hotmail.com

Specialty section:
This article was submitted to Pharmacology of Anti-Cancer Drugs, a section of the journal Frontiers in Oncology

Received: 10 January 2022
Accepted: 28 February 2022
Published: 22 March 2022

Citation:
Liu H, Zhao L, Wang M, Yang K, Jin Z, Zhao C and Shi G (2022) FNDC5 Causes Resistance to Sorafenib by Activating the PI3K/Akt/Nrf2 Pathway in Hepatocellular Carcinoma Cells. Front. Oncol. 12:852095. doi: 10.3389/fonc.2022.852095

In this study, we aimed to reveal the resistance mechanism of hepatocellular carcinoma (HCC) cells to sorafenib by exploring the effect of FNDC5 on sorafenib-induced ferroptosis in HCC cells. We compared the expression level of FNDC5 between sorafenib-resistant and sorafenib-sensitive HCC cell lines and the level of ferroptosis between the groups after treatment with sorafenib. We knocked down FNDC5 in drug-resistant cell lines and overexpressed it in sorafenib-sensitive HCC cell lines to further demonstrate the role of FNDC5 in sorafenib-induced ferroptosis. Using PI3K inhibitors, we revealed the specific mechanism by which FNDC5 functions. In addition, we verified our findings obtained in *in vitro* experiments using a subcutaneous tumorigenic nude mouse model. The findings revealed that FNDC5 inhibits sorafenib-induced ferroptosis in HCC cells. In addition, FNDC5 activated the PI3K/Akt pathway, which in turn promoted the nuclear translocation of Nrf2 and increased the intracellular antioxidant response, thereby conferring resistance to ferroptosis. Our study provides novel insights for improving the efficacy of sorafenib.

Keywords: fibronectin type III domain containing 5, ferroptosis, hepatocellular carcinoma, PI3K/Akt/Nrf2 pathway, sorafenib

INTRODUCTION

Hepatocellular carcinoma (HCC) has become a serious threat to human health because of its high malignancy and occurrence worldwide (1). Despite recent advances in the exploration of treatments and mechanisms of occurrence, the overall prognosis of HCC remains poor owing to factors such as insidious onset and susceptibility to drug resistance (2).

Currently, sorafenib is used as a first-line agent for the treatment of advanced HCC; it mainly acts through the modulation of the RAF/MEK/ERK pathway and vascular endothelial growth factor receptor (VEGF), thereby inhibiting tumor growth (3). Recent studies have shown that sorafenib-treated HCC cells undergo specific ferroptosis-related manifestations, such as lipid peroxidation, glutathione depletion, and iron accumulation (4–6). These events lead to HCC cell death; thus,

induction of ferroptosis could improve the anticancer effect of sorafenib and might be a new therapeutic strategy for HCC (7).

Nuclear factor E2-related factor 2 (Nrf2), which mainly regulates the transcription of intracellular antioxidant enzymes, can improve the antioxidant capacity of cancer cells, thereby inhibiting the occurrence of ferroptosis in HCC cells (8). Moreover, it is a key factor in the resistance of cancer cells to sorafenib. Studies have found that Nrf2 is activated by the PI3K/Akt pathway (9, 10), and abnormal activation of the PI3K/Akt pathway is also an important factor leading to resistance to sorafenib in HCC (11, 12).

Fibronectin type III domain containing 5 (FNDC5) is a recently identified factor associated with electron transport in mitochondrial oxidative respiration, which converts white adipose tissue to brown adipose tissue (13, 14). Several inflammation-related studies have revealed that FNDC5 might affect the activation of Nrf2 (15–17). Furthermore, in a previous study, we found that FNDC5 activates the PI3K/Akt pathway in HCC cells (18). However, the specific mechanism of FNDC5 in hepatocarcinogenesis needs further exploration. In the present study, we aimed to reveal the antioxidant role of FNDC5 in the treatment of HCC with sorafenib. We found that FNDC5 might activate Nrf2 through the PI3K/Akt pathway, leading to the development of ferroptosis resistance in HCC cells, and thus resistance to sorafenib.

MATERIALS AND METHODS

Ethical Statement

Tumor tissue specimens from patients were obtained in strict accordance with the regulations of the research ethics committee of Qingdao Municipal Hospital. In addition, all immunohistochemistry experiments were performed under the supervision of personnel of the research ethics committee. Animal experiment protocols were designed in strict accordance with the ARRIVE guidelines and reviewed and approved by the research ethics committee of Qingdao Municipal Hospital. All experimental procedures were recorded, reviewed, and completed under the supervision and guidance of the research ethics committee (ethics approval number: 104).

Immunohistochemistry

Immunohistochemistry was performed as previously described (19). Tumor and adjacent noncancerous (normal) liver tissues (60 pairs in total) were obtained from patients with liver cancer, fixed with 4.0% paraformaldehyde, paraffin-embedded, and cut into 4-μm-thick sections. The sections were treated with 3.0% hydrogen peroxide and blocked with 5.0% bovine serum, and then incubated with FNDC5 (1:200, ab181884; Abcam, Cambridge, MA, USA) and Nrf2 (1:200, 16396-1-AP, Proteintech, Beijing, China) antibodies overnight at 4°C. After washing with PBS, the sections were incubated with secondary antibodies conjugated with species-specific horseradish peroxidase (HRP) for 1 h at 25°C, and finally stained with diaminobenzidine (DAB) and hematoxylin. Images were taken using an AxioVision Rel.4.6 computerized image analysis system (Carl Zeiss). The degree of staining was assessed based on the staining area and intensity, using to the following formula: degree of staining = area × intensity. Staining area was scored as follows: 0 (staining area close to 0%), 1 (staining area less than 10%), 2 (staining area between 10% and 35%), 3 (staining area between 35% and 75%), and 4 (staining area between 76% and 100%). Staining intensity was scored as follows: 0 (no staining), 1 (weak staining), 3 (moderate staining), and 4 (strong staining). The final expression level of the target protein is expressed as the SI score, which was calculated using the following formula: SI = staining area score × staining intensity score, with SI ≥ 8 indicating high expression, whereas SI < 8 indicating low expression.

Cell Culture

HepG-2 and Huh7 human HCC cell lines were provided by the Chinese Academy of Sciences Cell Bank (Shanghai, China). The cells were cultured in Dulbecco's modified Eagle's medium (DMEM; HyClone, USA) containing 10% fetal bovine serum (FBS; Excellbio, USA) and 1% penicillin–streptomycin (HyClone, USA). All cells were incubated at 37°C under 5% CO_2.

Culture of Drug-Resistant Cell Lines

The HCC cells were incubated in 96-well plates with different concentrations of sorafenib, and the half-inhibitory concentration (IC_{50}) was determined. The HCC cells were then cultured in six-well plates at a density of 10^4 cells per well and treated with sorafenib at concentrations slightly below the IC_{50} value. The concentration of sorafenib was increased by 0.25 μmol/L every week until the maximum tolerated concentration of 10 μM was reached; at this point, the HepG2-SR- and Huh7-SR-resistant cell lines were obtained and cultured continuously in a medium with sorafenib at 1 μM to ensure the persistence of drug resistance.

Cell Viability Assay

The HCC cells were inoculated in 96-well plates at a density of 5×10^3 cells/well and incubated for 12 h, and then treatment with different concentrations (1, 2, 4, 8, 16, 32, 64, and 128 μM) of sorafenib for 24 h. The medium was replaced with fresh medium; there were six replicates per group. The Cell Counting Kit-8 (CCK8) reagent (APExBIO, K1018, USA) was added into the wells according to the manufacturer's instructions. After incubating the plates for 1 h in the dark, the absorbance of the samples was measured at 450 nm using a microplate reader (Bio-Tek, VT, USA). Cell survival was calculated using the following formula: Cell survival (%) = (test group OD − negative control value)/(control group OD − negative control OD) × 100. The IC_{50} was calculated using GraphPad Prism 7.0 software.

Detection of Apoptosis Using Annexin-V-FITC/PI Staining

The cells cultured in six-well plates were collected, washed twice with PBS, and resuspended using the binding buffer available in the Annexin-V-FITC/PI kit; then, 5 μL of Annexin V-FITC and 5 μL of PI were successively added. The cells were stained in the

dark for 15 min, and then immediately analyzed using flow cytometry.

EdU Assay

Cell proliferation was determined using the BeyoClick EdU-594 kit (Beyotime, Shanghai, China). The cultured HCC cells were washed with PBS, and then 10 μM EdU and fresh medium were added; the cells were incubated at 37°C for 2 h. Subsequently, the cells were washed twice with PBS, fixed with 4% paraformaldehyde for 15 min, washed with PBS, and finally stained with DAPI for 5 min before washing with PBS. Images were acquired under a fluorescence microscope (IX70; Olympus, Tokyo, Japan).

Knockdown and Overexpression of FNDC5

Human *FNDC5* cDNA was constructed by Gene Chem (Shanghai, China), packaged in a lentiviral plasmid vector, and used for cell transfection. The experimental group overexpressing *FNDC5* and negative control were named FNDC5-OE and FNDC5-NC2, respectively. siRNAs for knocking down *FNDC5* were constructed by RIBOBIO with the following sequences (5'-3'): 1. GGAGGATACGGA GTACATA; 2. AGAAGATGGCCTCCAAGAA; 3. GCTTCA TCCAGGAGGTGAA. The first and second siRNAs exhibiting better knockdown effects were selected, and plasmids were constructed and packaged into lentiviral plasmid vectors by Gene Chem, using the component sequence hU6-MCS-CBh-gcGFP-IRES-puromycin. The experimental groups with *FNDC5* knockdown and negative control were named FNDC5-KD1, FNDC5-KD2, and FNDC5-NC1, respectively.

Following the culture of HepG-2 and Huh7 HCC cells and drug-resistant cell lines in six-well plates to reach 40% fusion, 10 μL of viral solution and 40 μL of infection enhancing solution were added, and the cells were transfected for 24 h. The complete medium was then replaced, and the culture was continued for 24 h. Finally, successfully transfected cells were screened using 1 μg/mL puromycin and used in the subsequent experiments.

Transmission Electron Microscopy

The HCC cells were fixed with 2.5% glutaraldehyde for 1 h, washed three times with PBS, and fixed in 2% sodium tetroxide for 1 h. Thereafter, ethanol dehydration was performed, followed by sectioning and staining after embedding of the samples. Finally, the sections were observed using a Hitachi-7500 transmission electron microscope (Hitachi, Tokyo, Japan).

Mitochondrial Membrane Potential Assay

JC-1 is a fluorescent probe that detects the ΔΨm mitochondrial membrane potential. When mitochondrial membrane potential decreases, JC-1 is converted from red fluorescent polymers (J-aggregates) to green fluorescent monomers (J-monomers). The HCC cells were incubated with JC-1 (Beyotime, Shanghai, China) in the dark at 37°C for 20 min, and then washed twice with staining buffer before analysis using a flow cytometer (Accuri C6, BD Biosciences, USA).

Reactive Oxygen Species and Malondialdehyde Assays

The levels of reactive oxygen species (ROS) in HCC cells cultured in six-well plates were measured using the oxidation-sensitive fluorescent probe DCFH-DA (#D6883; Sigma) and analyzed using flow cytometry. After cell lysis, the concentration of malondialdehyde (MDA) was determined using the lipid peroxidation malondialdehyde assay kit (S0131S; Beyotime), according to the manufacturer's instructions.

Western Blotting

Total protein was extracted from HCC cells using the RIPA lysis buffer (Beyotime). Nuclei and cytoplasmic proteins were extracted using the nuclei and cytoplasmic protein extraction kit (Beyotime). Protein concentration was determined using a BCA protein quantification kit (Beyotime). The samples were then boiled for 10 min, followed by electrophoresis on 10% SDS-polyacrylamide gels, and the separated proteins were transferred on to polyvinylidene fluoride (PVDF) membranes (Millipore, Bedford, MA, USA). The membranes were then blocked with 5% skimmed milk and incubated at 25°C for 2 h. The membranes were then incubated with primary antibodies (1:1000, Proteintech) at 4°C overnight. Antibodies used included SLC7A11 (26864-1-AP), GPX4 (67763-1-Ig), DMT1 (20507-1-AP), PI3K (20584-1-AP), Akt (60203-2-Ig), p-Akt (66535-1-Ig), and Nrf2 (16396-1-AP), whereas β-actin (1:5000, #4967, Cell Signaling Technology, USA), and lamin B1 (1:2000, 12987-1-AP, Proteintech) were used as the internal references. The membranes were then washed thrice with TBST buffer and incubated with diluted HRP-coupled secondary antibodies for 2 h under 25°C. Finally, protein blots were detected using an ECL reagent (Millipore). Three independent replicate experiments were performed, and the intensity of protein blots was analyzed using ImageJ software.

Xenograft Mouse Model

NOD-SCID (NOD CB17-Prkdcscid/NcrCrl) 5-week-old male mice were purchased from Beijing Life River Laboratory Animal Technology Company (Beijing, China). The mice were housed in a 12-h light/dark cycling environment. The temperature was 25°C ± 1°C, humidity was maintained at 56%, and the mice were provided adequate food and water. Mice weighing between 20 and 23 g were selected and 5×10^6 Hep-G2 cells were subcutaneously injected into their backs. The mice were subsequently divided into the following four groups: control (n = 5), FNDC5 overexpressing (n = 5), FNDC5 overexpressing followed by treatment with the PI3K inhibitor LY294002 (MCE, China), and FNDC5 knockdown (n = 5). Seven days after cell injection, sorafenib (30 mg/kg) was administered to all mice *via* intraperitoneal injection every alternate day for 4 weeks. The mice in the third group were intraperitoneally injected with LY294002 (25 mg/kg) diluted with DMSO twice a week for 4 weeks. Tumor volumes were measured every 4 days, and the mice were sacrificed on day 28 using the cervical dislocation method. Tumor tissues were dissected out and processed into homogenates, lysed, and centrifuged, and the expression level of the target proteins was

detected using western blotting. The levels of MDA in tumor tissues were detected using the MDA kit.

Data Analysis

GraphPad 7 (GraphPad Software Inc., CA, USA) was used for data analysis. All experimental results represent data from at least three independent replicate experiments, and the results are expressed as mean ± SD. A *t*-test was used to compare the differences between groups. A one-way ANOVA was used to compare differences among multiple experimental groups. Results with p value < 0.05 were considered statistically significant.

RESULTS

Expression of FNDC5 Was Elevated in Sorafenib-Resistant HCC Cells

In our previous study, we found that FNDC5 was highly expressed in HCC tissues, promoting cancer progression (18). Our present immunohistochemical results also showed that among the 60 pairs of HCC and paraneoplastic tissues, the expression of FNDC5 was high in 48 HCC tissues, whereas its expression was low in 12 HCC and all paracancerous tissues (**Figure 1A**). To investigate whether the level of expression of FNDC5 was altered in sorafenib-resistant HCC cells, we treated HCC cell lines with increasing concentrations of sorafenib for 24 h. Following the CCK8 assay, we calculated the 24 h half-inhibitory concentration (IC_{50}) of sorafenib in HepG2 and Huh7 cell lines, and by gradually increasing the concentration of sorafenib, we established sorafenib-resistant cell lines. We also examined the IC_{50} of the obtained resistant cell lines. We found that the IC_{50} of sorafenib for HepG2-SR and Huh7-SR cells was 2–3 times higher than that for sorafenib-sensitive HCC cells (**Figure 1B**). Following treatment of HCC cells with different concentrations of sorafenib for 24 h, we found that the viability of drug-resistant cells was significantly higher than that of the sorafenib-sensitive HCC cells (**Figure 1B**). After confirming the successful development of sorafenib-resistant HCC cells, we examined the expression of FNDC5 in HCC sorafenib-resistant and sorafenib-sensitive HCC cells using western blotting. We found that the expression of FNDC5 was significantly higher in resistant cells than in sorafenib-sensitive HCC cells (**Figure 1C**).

Changes in the Expression of FNDC5 Caused Alterations in the Levels of Sorafenib-Induced Ferroptosis

To further investigate whether the resistance of HepG2-SR and Huh7-SR cells to sorafenib was caused by changes in the expression of FNDC5, we knocked down *FNDC5* in HCC resistant cells (**Figure 2A**). The cells were then treated sorafenib-sensitive, drug-resistant, and *FNDC5*-knockdown drug-resistant cell lines using the same concentration of sorafenib, followed by staining with EdU and

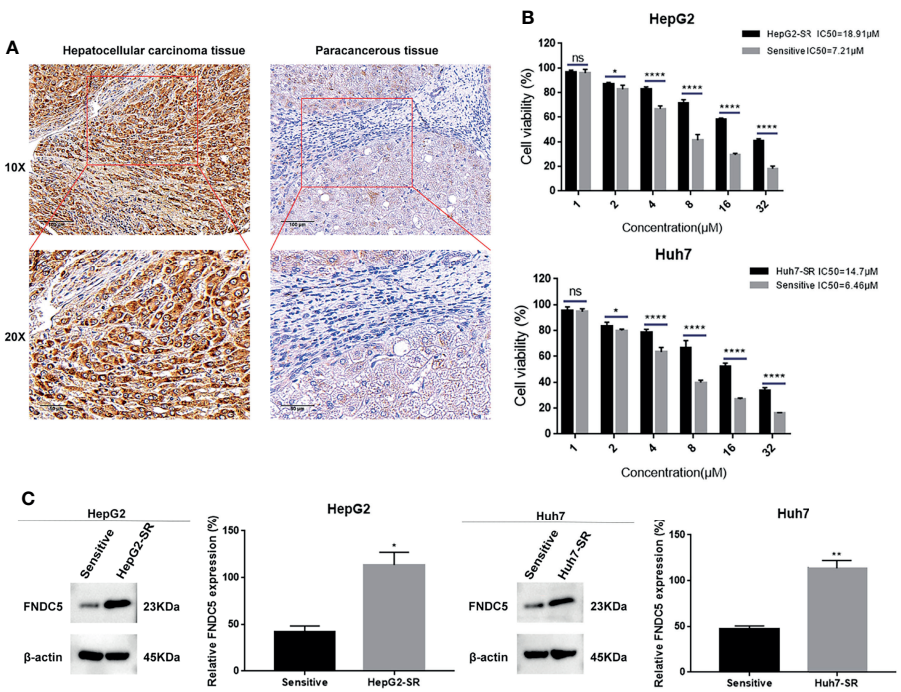

FIGURE 1 | Elevated levels of FNDC5 in sorafenib-resistant HCC cells. **(A)** FNDC5 is overexpressed in HCC tissues. **(B)** IC_{50} values of sorafenib-sensitive and -resistant HCC cells were calculated using the CCK8 method after treating HCC cells with increasing concentrations of sorafenib for 24 h, and cell survival rates were measured. **(C)** Western blotting to detect differences in the expression of FNDC5 between sorafenib-sensitive and -resistant HCC cells. *Compared with the sorafenib-sensitive HCC cells, *p < 0.05, **p < 0.01, ****p < 0.0001. ns, no significant difference.

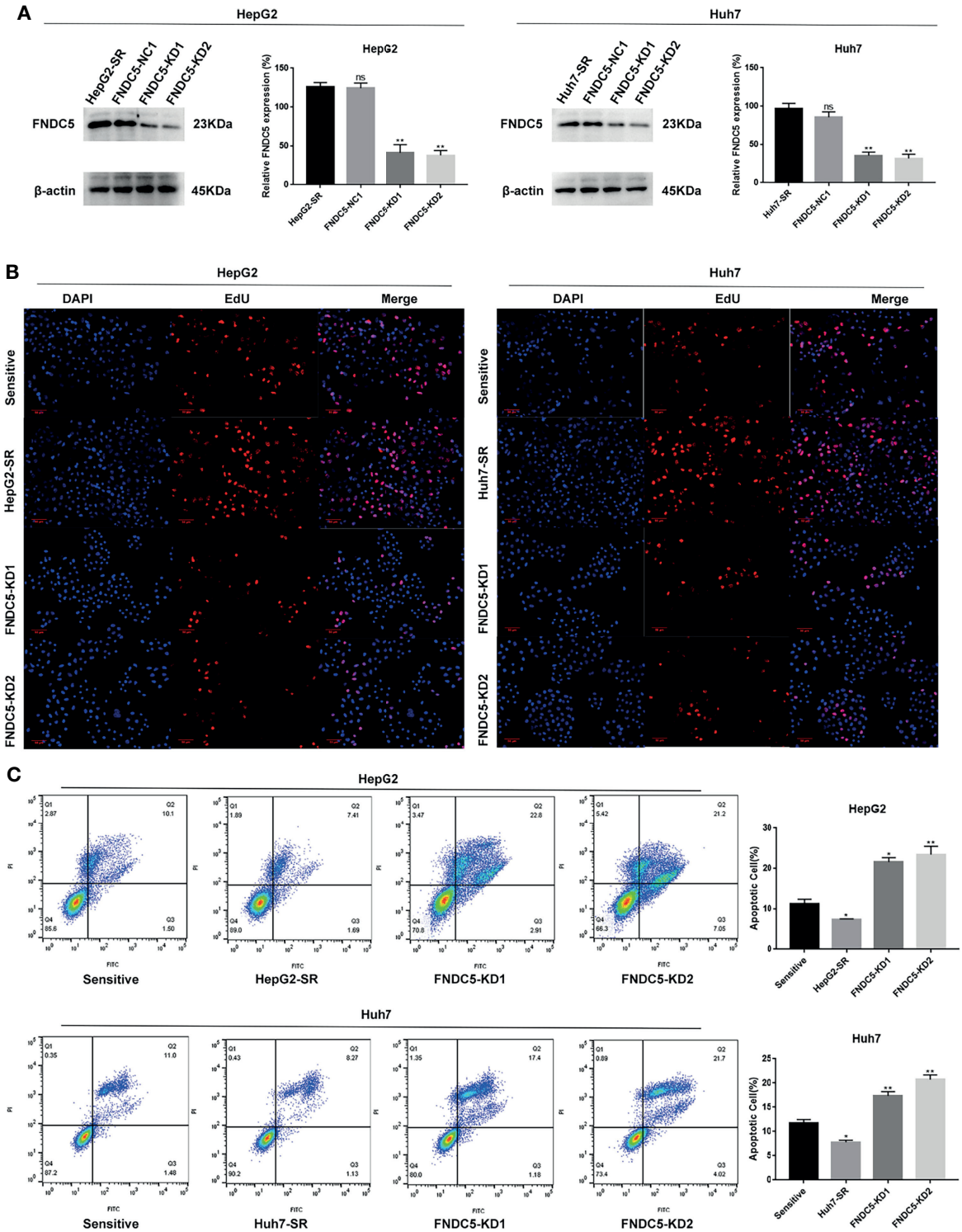

FIGURE 2 | Knockdown of FNDC5 decreases drug resistance in sorafenib-resistant HCC cells. **(A)** A lentiviral plasmid vector was used to knockdown FNDC5 in drug-resistant cell lines; the knockdown effect was verified using western blotting. *Compared with the drug-resistant cell lines, *p < 0.05, **p < 0.01. Sorafenib (10 μM) was administered to sorafenib-sensitive HCC, drug-resistant, and FNDC5-knockdown drug-resistant cell lines for 24 h. **(B)** EdU staining was used to detect viability in each group of cells. **(C)** Annexin-V-FITC/PI staining was used to determine the inhibitory ability of sorafenib in each group of cells. *Compared with the sorafenib-sensitive HCC cells, *p < 0.05, **p < 0.01. ns, no significant difference.

Annexin-V-FITC/PI to detect the inhibitory effect of sorafenib on each group (**Figures 2B, C**). We observed a higher rate of apoptosis in sorafenib-sensitive HCC cells, whereas drug-resistant HCC cells were obviously insensitive to sorafenib. However, we noticed that resistance to sorafenib was reversed after knocking down *FNDC5* in drug-resistant HCC cells. We then examined the alterations in the level of ferroptosis in each group of HCC cells through the evaluation of the levels of ROS and MDA (**Figures 3A, B**), JC-1 detection of mitochondrial membrane potential (**Figure 3C**), electron microscopic observation of mitochondria (**Figure 3D**), and detection of the changes in ferroptosis markers in each subgroup using western blotting (**Figure 3E**). We found that the sorafenib-induced level of ferroptosis was lower in sorafenib-resistant cells with high expression of FNDC5 than in sorafenib-sensitive HCC cells, whereas the level of ferroptosis was elevated in *FNDC5*-knockdown sorafenib-resistant cells.

FNDC5 Inhibited Sorafenib-Induced Ferroptosis in Hepatocellular Carcinoma Cells Through the PI3K/Akt/Nrf2 Pathway

Based on previous findings, we hypothesized that FNDC5 affects the expression of Nrf2 in HCC tissues. After selecting HCC tissues with different levels of expression of FNDC5 *via* immunohistochemical detection, we found that the expression of Nrf2 was also elevated in HCC tissues with high expression of FNDC5 (**Figure 4A**). As the PI3K/Akt pathway regulates the expression of Nrf2, and as we previously found that FNDC5 affects the PI3K/Akt pathway, we evaluated the changes in the expression of PI3K, Akt, and Nrf2 in sorafenib-sensitive HCC, sorafenib-resistant, and *FNDC5*-knockdown resistant cell lines following treatment with the same concentration of sorafenib (**Figure 4B**). Our western blotting results showed that the levels of PI3K, pAkt, and Nrf2 in the nucleus were elevated in the drug-resistant cells compared with sorafenib-sensitive HCC, whereas the activation of the PI3K pathway was diminished and the level of Nrf2 in the nucleus was reduced after the knockdown of FNDC5. To further verify the effect of FNDC5 on the levels of Nrf2 *via* the PI3K/Akt pathway, we treated HCC sorafenib-resistant cells with a PI3K inhibitor for 1 h, and then added sorafenib to detect the levels of Nrf2 and ferroptosis marker proteins. Compared with those in the resistant cells not treated with the PI3K inhibitor, the level of Nrf2 in the nucleus of HCC sorafenib-resistant cells decreased, whereas the level of ferroptosis increased after the administration of the PI3K inhibitor (**Figure 5A**). We further confirmed that the addition of the PI3K inhibitor led to increased levels of ferroptosis in sorafenib-resistant cells as indicated by the levels of ROS and MDA and mitochondrial membrane potential (**Figures 5B–D**). Furthermore, we demonstrated that the PI3K inhibitor reversed the resistance of sorafenib-resistant cells as indicated by the flow cytometry detection of apoptotic rate (**Figure 5E**).

Overexpression of FNDC5 in Hepatocellular Carcinoma Cells Inhibited Sorafenib-Induced Ferroptosis

To further demonstrate that high expression of FNDC5 leads to the resistance of HCC cells to sorafenib, we overexpressed FNDC5 in sorafenib-sensitive HCC cell lines (**Figure 6A**). Annexin-V-FITC/PI staining indicated that the overexpression of FNDC5 in HCC cells led to increased resistance to sorafenib (**Figure 6B**). Furthermore, analyses of the levels of ROS and MDA and mitochondrial membrane potential further confirmed the level of ferroptosis was decreased in sorafenib-sensitive HCC cells with overexpression of FNDC5 compared with sorafenib-sensitive HCC cells (**Figures 6C, D**). Finally, western blotting showed that after the overexpression of FNDC5, the PI3K/Akt pathway was activated, the level of Nrf2 in the nucleus was increased, the levels of GPX4 and SLC7721 were increased, whereas the levels of DMT1 and ferroptosis were reduced (**Figure 6E**).

Alterations in the Level of Expression of FNDC5 Affected the Inhibitory Effect of Sorafenib on Hepatocellular Carcinoma *In Vivo*

We subcutaneously injected HCC cells with different levels of expression of FNDC5 into mice to further investigate whether the changes in the levels of expression of FNDC5 in HCC cells continued to affect the efficacy of sorafenib *in vivo* (**Figures 7A–C**). At the same concentration of sorafenib, HCC cells with high expression of FNDC5 exhibited an increased rate of proliferation under the skin of mice and low levels of ferroptosis, whereas *FNDC5*-knockdown HCC cells grew slowly and presented elevated levels of ferroptosis as indicated by western blotting and MDA assays. In addition, we found that treatment with a combination of sorafenib and PI3K inhibitors slowed the growth of HCC cells with high expression of FNDC5 and increased the level of ferroptosis (**Figures 7D, E**).

DISCUSSION

Recent studies have revealed that FNDC5 protects cells from oxidative damage in myocardial inflammation and neurological diseases (20, 21) and reduces the production of ROS, inhibiting the occurrence of ferroptosis in cells (22). As the role of FNDC5 has also been gradually revealed in tumors (23, 24) and in the progression of HCC, FNDC5 has been suggested to play a role in promoting the proliferation of cancer cells. In our previous study, we found that the expression of FNDC5 was higher in cancer than in normal tissues (18, 19). In the present study, we found that the expression of FNDC5 was elevated in sorafenib-resistant cells and that drug-resistant cells with high expression of FNDC5 were not sensitive to treatment with sorafenib, whereas *FNDC5*-knockdown HCC cells were readily killed by sorafenib as observed using the EdU and CCK8 assays. These results suggested that FNDC5 might be one of the factors promoting the development of resistance to sorafenib in HCC.

We also found a substantial decrease in the level of ferroptosis induced by sorafenib in HCC resistant cells with high expression of FNDC5 in *in-vitro* experiments, whereas the level of ferroptosis was elevated in *FNDC5*-knockdown drug-resistant cells. Ferroptosis is a newly identified nonprogrammed apoptotic cell death process (25). It is triggered by the accumulation of iron in cells with decreased levels of glutathione peroxidase (GPX4) (26, 27), increased levels of ROS, and membrane lipid

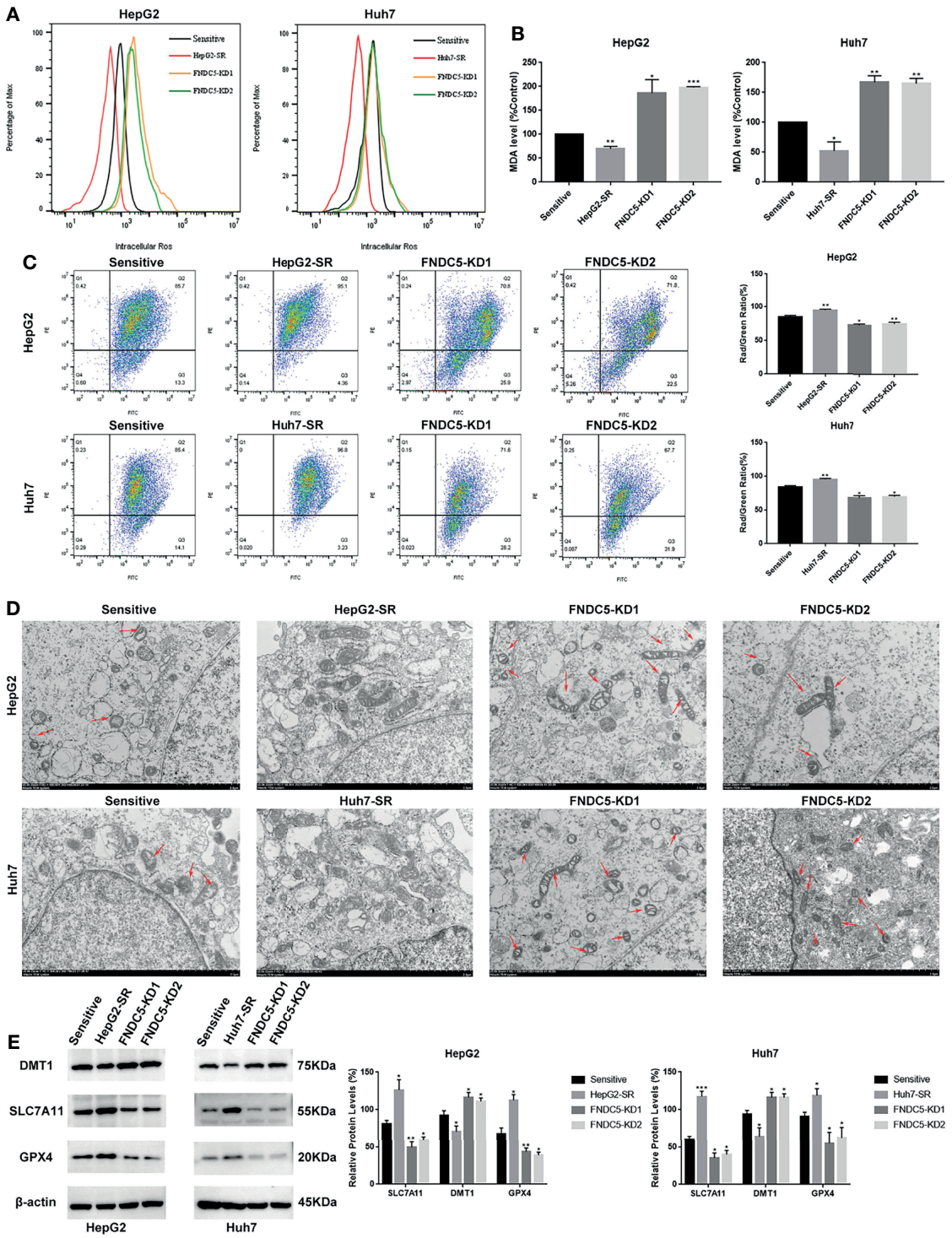

FIGURE 3 | Effect of alterations in the expression level of FNDC5 on sorafenib-induced levels of ferroptosis in HCC cells. **(A, B)**. After 24 h of treatment of sorafenib-sensitive HCC cells, drug-resistant, and FNDC5-knockdown drug-resistant cells with sorafenib (10 μM), the levels of ROS and MDA were measured to assess the level of ferroptosis in each group of cells. **(C)**. Flow cytometry was used to detect changes in mitochondrial membrane potential in each group of cells. **(D)** The mitochondrial morphology in each group of cells was observed under an electron microscope, with red arrows indicating mitochondria with altered membrane potential. **(E)** Western blotting for detecting the level of ferroptosis markers in each group of cells. *Compared with the sorafenib-sensitive HCC cells, *$p < 0.05$, **$p < 0.01$, ***$p < 0.001$.

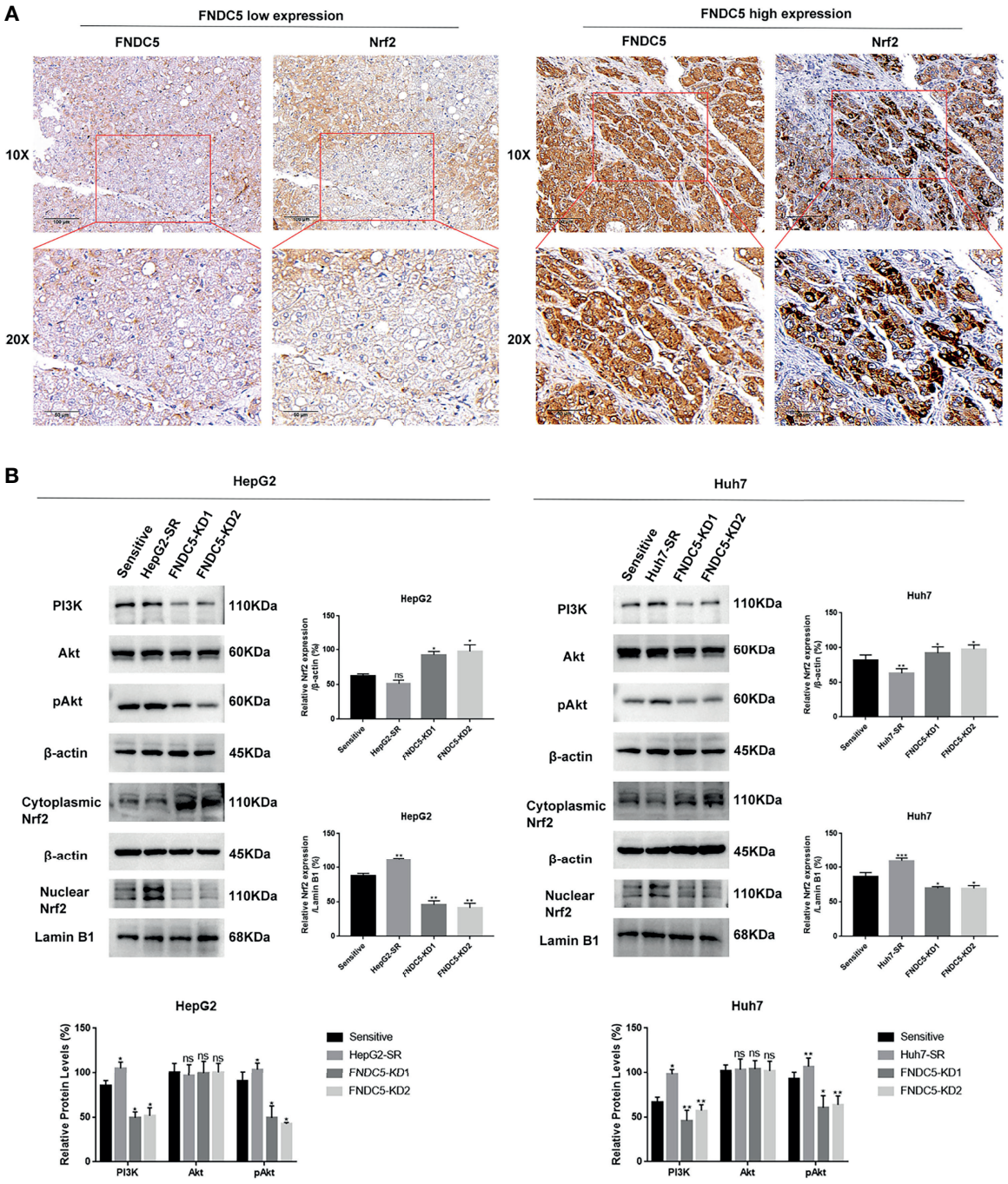

FIGURE 4 | Changes in the expression level of FNDC5 affect the expression level of Nrf2. **(A)** Nrf2 expression was elevated in hepatocellular carcinoma tissues with high FNDC5 expression. **(B)** sorafenib-sensitive HCC cells, drug-resistant, and FNDC5-knockdown resistant cells were treated with sorafenib (10 μM) for 24 h, and the levels of PI3K/Akt/Nrf2 pathway proteins were detected in each group of cells using western blotting. *Compared with the sorafenib-sensitive HCC cells, *p < 0.05, **p < 0.01, ***p < 0.001. ns, no significant difference.

peroxidation reactions that damage cell and mitochondrial membranes (28, 29), leading to cancer cell death (30). Ferroptosis has been shown to promote cancer cell death and exert anticancer effects in a variety of cancers (31). In addition, ferroptosis is an important mode for sorafenib to exert its efficacy during treatment of HCC with sorafenib (6). Using western blotting, we found that after treatment with the same concentration of sorafenib, the levels of xCT and GPX4 were increased, whereas the levels of DMT1 were decreased in drug-resistant HCC cells or *FNDC5*-overexpressing HCC cells

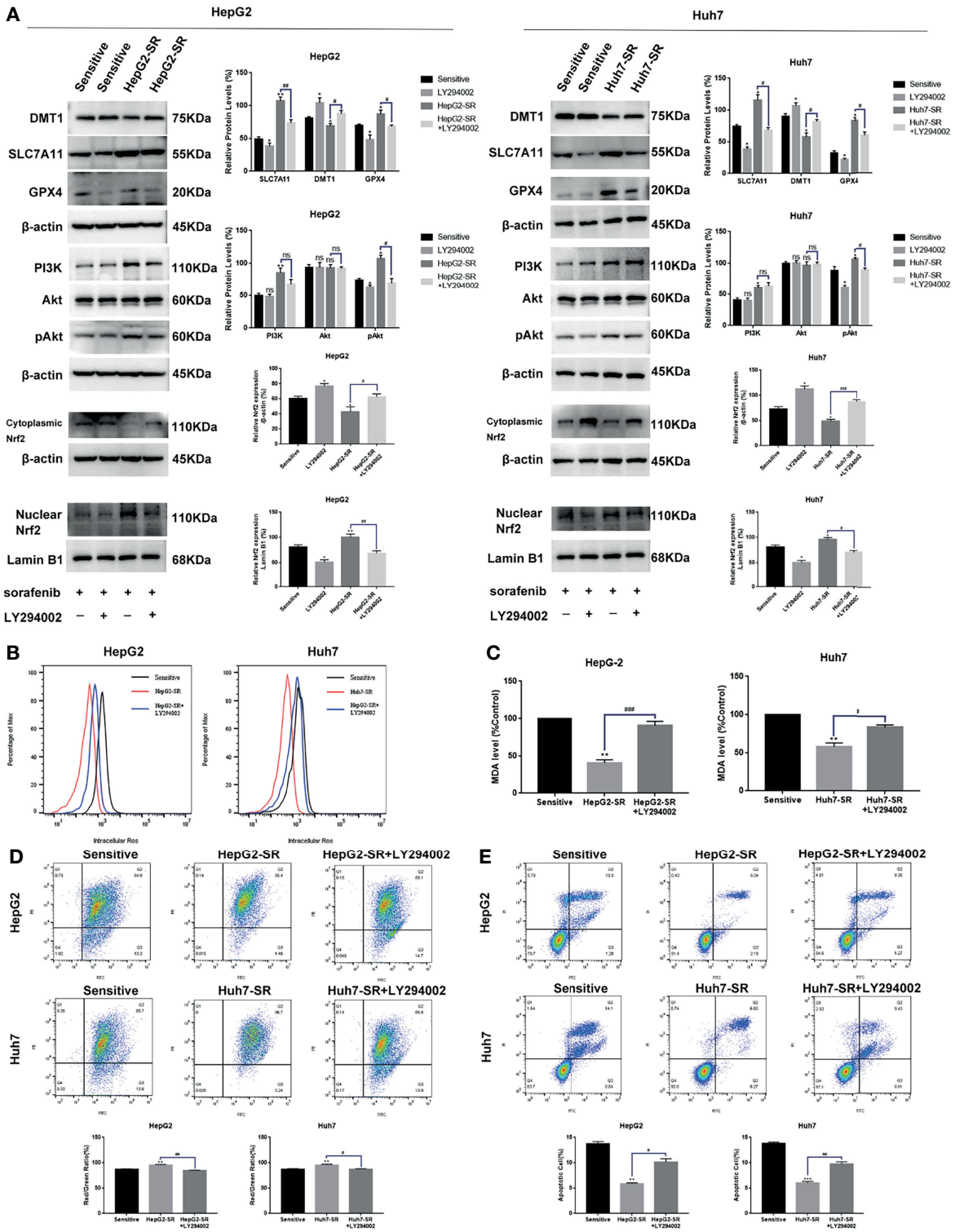

FIGURE 5 | FNDC5 inhibits sorafenib-induced ferroptosis in HCC cells by activating the PI3K/Akt/Nrf2 pathway. Sorafenib (10 μM) was added to the medium of LY294002 (5 μM)-treated resistant, untreated resistant, and sorafenib-sensitive HCC cells and incubated for 24 h. **(A)** Western blotting of ferroptosis markers and PI3K/Akt/Nrf2 pathway proteins in each group of cells. **(B, C)**. Detection of levels of ROS and MDA. **(D)**. JC-1 staining for detecting mitochondrial membrane potential in each group of cells. **(E)**. Annexin-V-FITC/PI staining for detecting apoptosis rate in each group of cells. *Compared with the sorafenib-sensitive HCC cells, *$p < 0.05$, **$p < 0.01$, ***$p < 0.001$. #Compared with HepG2-SR+LY294002 or Huh7-SR+LY294002, #$p < 0.05$, ##$p < 0.01$, ###$p < 0.001$. ns, no significant difference.

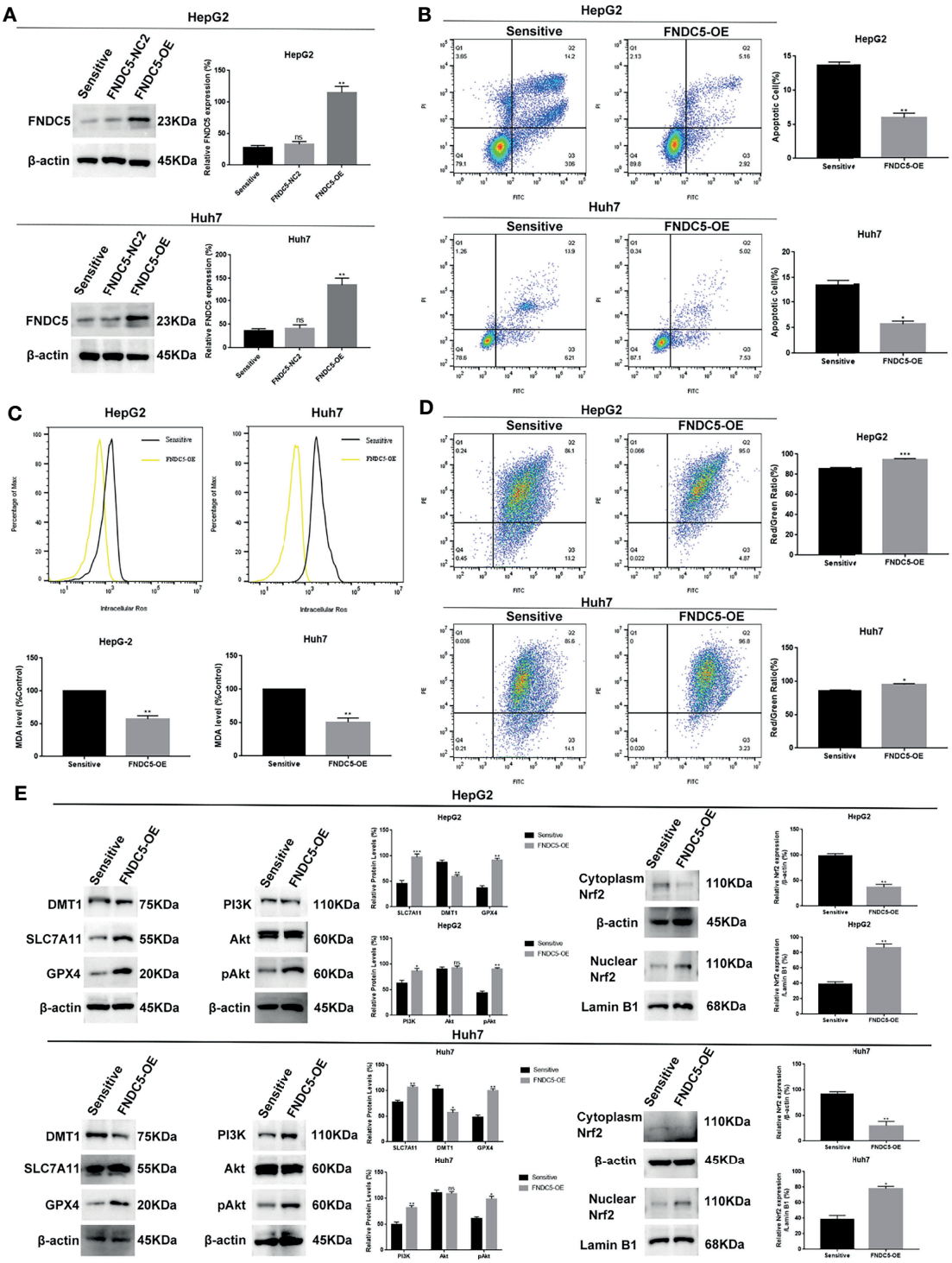

FIGURE 6 | Overexpression of FNDC5 reduces the sensitivity of HCC cells to sorafenib. **(A)** A lentiviral vector was used to overexpress FNDC5; western blotting was performed to verify the overexpression effect. **(B)** After treatment of sorafenib-sensitive HCC and FNDC5-overexpressing HCC cell lines with sorafenib (10 μM) for 24 h, flow cytometry was used to detect the apoptotic rates in both groups. **(C)** ROS and MDA assays were performed to compare the level of ferroptosis between the groups. **(D)** Flow cytometry analysis of alterations in mitochondrial membrane potential in both groups. **(E)** Western blotting for detecting the expression levels of ferroptosis markers and Nrf2-associated pathway proteins in both groups of cells. *Compared with the sorafenib-sensitive HCC cells, *p < 0.05, **p < 0.01, ***p < 0.001. ns, no significant difference.

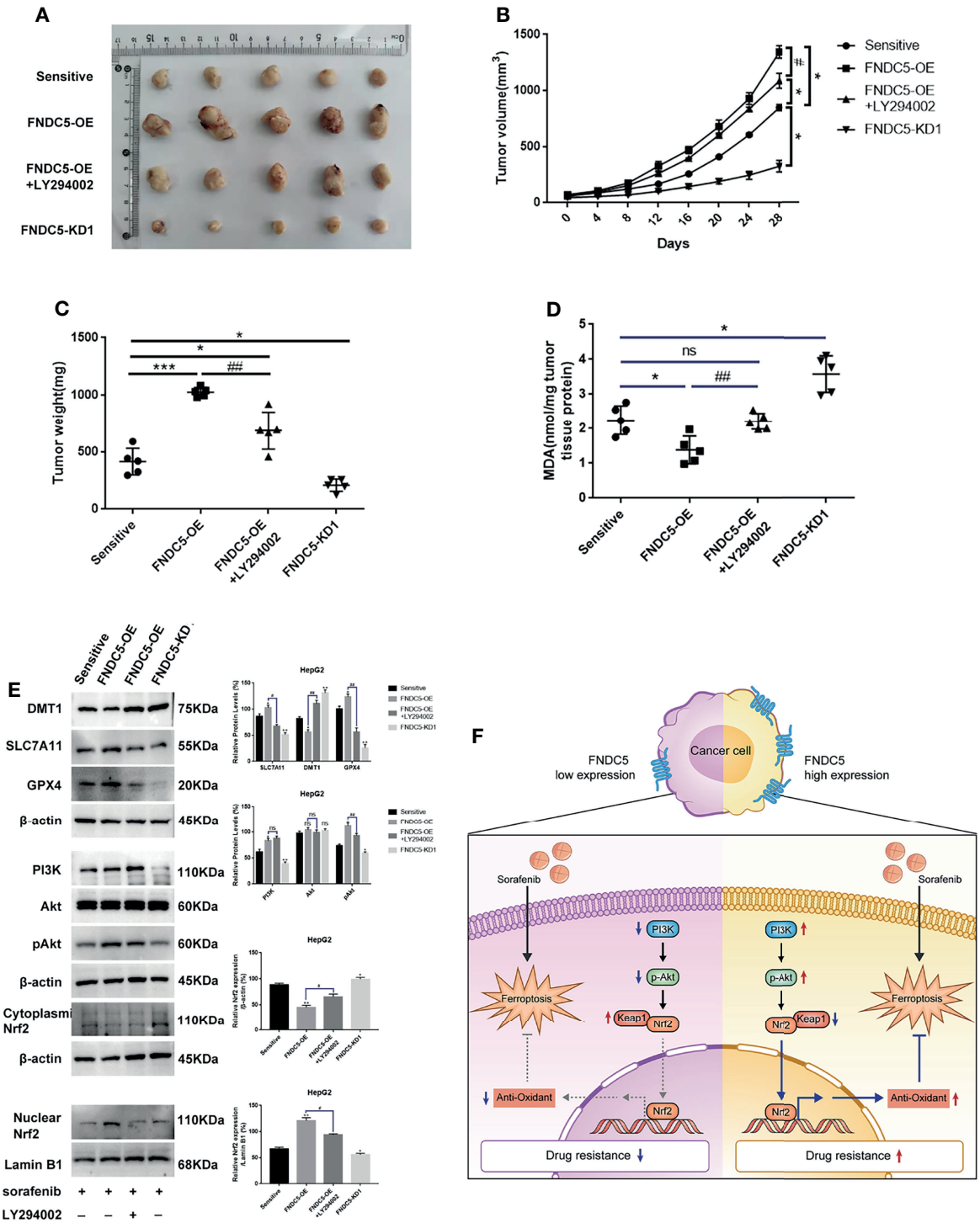

FIGURE 7 | Alterations in the levels of expression of FNDC5 can affect sorafenib-induced ferroptosis in HCC cells *in vivo*. Animals were divided into four groups according to the expression level of FNDC5 and whether or not they were treated with LY294002; all groups were treated with sorafenib. **(A–C)**. Tumor volume in each group was measured every 4 days and final tumor weight was measured. **(D)** The level of MDA in tumor tissues in each group was measured. **(E)** Western blotting for detecting the expression level of ferroptosis markers and Nrf2-associated pathway proteins in tumor tissues in each group. **(F)** Illustration of the mechanistic pathway by which FNDC5 overexpression leads to the resistance of HCC cells to sorafenib. *Compared with the sorafenib-sensitive HCC cells, *p < 0.05, **p < 0.01, ***p < 0.001. #Compared with FNDC5-OE+LY294002, #p < 0.05, ##p < 0.01. ns, no significant difference.

compared with those in sorafenib-sensitive HCC cells. However, the opposite results were obtained after the knockdown of FNDC5, indicating that sorafenib-induced ferroptosis was inhibited by the overexpression of FNDC5.

Nrf2 is a major intracellular regulator of oxidative stress, which is generally expressed at low levels in the cytoplasm, and regulated by ubiquitinated degradation mediated by Kelch-like ECH-associated protein 1 (Keap1) (32). When initiating oxidative stress, Nrf2 translocates into the nucleus and binds to the antioxidant response element (ARE), thereby initiating the transcription of antioxidant enzymes (33). Thus, Nrf2 also serves as a factor that inhibits ferroptosis. It has been demonstrated that the activation of Nrf2 reduces the killing effect of sorafenib on HCC cells by inhibiting ferroptosis (34, 35). The PI3K/Akt pathway is an important pathway that regulates the proliferation of tumor cells, and its aberrant activation is one of the mechanisms underlying the progression of many tumors (36–38). Recent studies have shown that Nrf2 is activated by the PI3K/Akt pathway and is involved in regulating tumor growth and the resistance of cancer cells to chemotherapeutic agents (39, 40). In this study, we used immunohistochemistry to investigate whether the expression of Nrf2 was altered in HCC tissues with different levels of expression of FNDC5. Our results showed that Nrf2 was highly expressed in HCC tissues with high expression of FNDC5. Next, we explored the mechanism by which FNDC5 affects the resistance of cells to sorafenib under conditions of co-culturing sorafenib-sensitive HCC, drug-resistant, and FNDC5-knockdown drug-resistant cells with sorafenib. Western blotting showed that, compared with sorafenib-sensitive HCC cells, sorafenib-resistant cells with high expression of FNDC5 presented elevated expression of PI3K, increased levels of downstream pAkt, and elevated levels of Nrf2 in the nucleus. In contrast, in *FNDC5*-knockdown drug-resistant cells, the levels of PI3K and pAkt were reduced, and the level of Nrf2 in the nucleus was also reduced. In resistant cells, we found that PI3K inhibitors decreased the levels of phosphorylated Akt and Nrf2 entering the nucleus but increased the level of ferroptosis. Subsequent validation of the overexpression of FNDC5 further demonstrated that the overexpression of FNDC5 promoted the activation of the PI3K/Akt pathway, increased the level of Nrf2 in the nucleus, and lowered the level of ferroptosis. Finally, *in vivo* experiments also confirmed that FNDC5 inhibited sorafenib-induced ferroptosis by activating the PI3K/Akt/Nrf2 pathway (**Figure 7F**).

CONCLUSION

In conclusion, we confirmed that FNDC5 promotes the nuclear translocation of Nrf2 through the activation of the PI3K/Akt pathway, leading to enhanced intracellular antioxidant capacity and ultimately reducing sorafenib-induced ferroptosis. This discovery could contribute to the improvement in the efficacy of sorafenib.

DATA AVAILABILITY STATEMENT

The original contributions presented in the study are included in the article/supplementary material. Further inquiries can be directed to the corresponding authors.

ETHICS STATEMENT

The studies involving human participants were reviewed and approved by Qingdao Municipal Hospital Ethics Committee. The patients/participants provided their written informed consent to participate in this study. The animal study was reviewed and approved by Qingdao Municipal Hospital Ethics Committee.

AUTHOR CONTRIBUTIONS

HL: investigation, formal analysis, and writing – original draft. LZ: methodology and resources. MW: resources and writing – review and editing. KY: resources. ZJ: resources. CZ: writing – review and editing and funding acquisition. GS: conceptualization and project administration, writing review and editing, and funding acquisition. All authors contributed to the article and approved the submitted version.

FUNDING

This work was supported by research grants from the National Natural Science Foundation of China (NO. 81601617); Shandong Province Key Research and Development Project (NO. 2018G SF118057).

ACKNOWLEDGMENTS

We would like to thank Editage (www.editage.cn) for English language editing.

REFERENCES

1. Bray F, Ferlay J, Soerjomataram I, Siegel RL, Torre LA, Jemal A. Global Cancer Statistics 2018: GLOBOCAN Estimates of Incidence and Mortality Worldwide for 36 Cancers in 185 Countries. *CA Cancer J Clin* (2018) 68 (6):394–424. doi: 10.3322/caac.21492
2. Testino G, Leone S, Patussi V, Scafato E, Borro P. Hepatocellular Carcinoma: Diagnosis and Proposal of Treatment. *Minerva Med* (2016) 107(6):413–26.
3. Llovet JM, Ricci S, Mazzaferro V, Hilgard P, Gane E, Blanc JF, et al. Sorafenib in Advanced Hepatocellular Carcinoma. *N Engl J Med* (2008) 359(4):378–90. doi: 10.1056/NEJMoa0708857
4. Sun X, Niu X, Chen R, He W, Chen D, Kang R, et al. Metallothionein-1G Facilitates Sorafenib Resistance Through Inhibition of Ferroptosis. *Hepatology* (2016) 64(2):488–500. doi: 10.1002/hep.28574
5. Xie Y, Hou W, Song X, Yu Y, Huang J, Sun X, et al. Ferroptosis: Process and Function. *Cell Death Differ* (2016) 23(3):369–79. doi: 10.1038/cdd.2015.158

6. Li Y, Xia J, Shao F, Zhou Y, Yu J, Wu H, et al. Sorafenib Induces Mitochondrial Dysfunction and Exhibits Synergistic Effect With Cysteine Depletion by Promoting HCC Cells Ferroptosis. *Biochem Biophys Res Commun* (2021) 534:877–84. doi: 10.1016/j.bbrc.2020.10.083
7. Chen S, Zhu JY, Zang X, Zhai YZ. The Emerging Role of Ferroptosis in Liver Diseases. *Front Cell Dev Biol* (2021) 9:801365. doi: 10.3389/fcell.2021.801365
8. Sun X, Ou Z, Chen R, Niu X, Chen D, Kang R, et al. Activation of the P62-Keap1-NRF2 Pathway Protects Against Ferroptosis in Hepatocellular Carcinoma Cells. *Hepatology* (2016) 63(1):173–84. doi: 10.1002/hep.28251
9. Yu C, Xiao JH. The Keap1-Nrf2 System: A Mediator Between Oxidative Stress and Aging. *Oxid Med Cell Longev* (2021) 2021:6635460. doi: 10.1155/2021/6635460
10. Rojo AI, Medina-Campos ON, Rada P, Zuniga-Toala A, Lopez-Gazcon A, Espada S, et al. Signaling Pathways Activated by the Phytochemical Nordihydroguaiaretic Acid Contribute to a Keap1-Independent Regulation of Nrf2 Stability: Role of Glycogen Synthase Kinase-3. *Free Radic Biol Med* (2012) 52(2):473–87. doi: 10.1016/j.freeradbiomed.2011.11.003
11. Zhai B, Hu F, Jiang X, Xu J, Zhao D, Liu B, et al. Inhibition of Akt Reverses the Acquired Resistance to Sorafenib by Switching Protective Autophagy to Autophagic Cell Death in Hepatocellular Carcinoma. *Mol Cancer Ther* (2014) 13(6):1589–98. doi: 10.1158/1535-7163.MCT-13-1043
12. Zhu YJ, Zheng B, Wang HY, Chen L. New Knowledge of the Mechanisms of Sorafenib Resistance in Liver Cancer. *Acta Pharmacol Sin* (2017) 38(5):614–22. doi: 10.1038/aps.2017.5
13. Lourenco MV, Frozza RL, de Freitas GB, Zhang H, Kincheski GC, Ribeiro FC, et al. Exercise-Linked FNDC5/irisin Rescues Synaptic Plasticity and Memory Defects in Alzheimer's Models. *Nat Med* (2019) 25(1):165–75. doi: 10.1038/s41591-018-0275-4
14. Cao RY, Zheng H, Redfearn D, Yang J. FNDC5: A Novel Player in Metabolism and Metabolic Syndrome. *Biochimie* (2019) 158:111–6. doi: 10.1016/j.biochi.2019.01.001
15. Mazur-Bialy AI, Kozlowska K, Pochec E, Bilski J, Brzozowski T. Myokine Irisin-Induced Protection Against Oxidative Stress *In Vitro*. Involvement of Heme Oxygenase-1 and Antioxidazing Enzymes Superoxide Dismutase-2 and Glutathione Peroxidase. *J Physiol Pharmacol* (2018) 69(1):117–25. doi: 10.26402/jpp.2018.1.13
16. Cao G, Yang C, Jin Z, Wei H, Xin C, Zheng C, et al. FNDC5/irisin Reduces Ferroptosis and Improves Mitochondrial Dysfunction in Hypoxic Cardiomyocytes by Nrf2/HO-1 Axis. *Cell Biol Int* (2022). doi: 10.1002/cbin.11763
17. Ning H, Chen H, Deng J, Xiao C, Xu M, Shan L, et al. Exosomes Secreted by FNDC5-BMMSCs Protect Myocardial Infarction by Anti-Inflammation and Macrophage Polarization *via* NF-kappaB Signaling Pathway and Nrf2/HO-1 Axis. *Stem Cell Res Ther* (2021) 12(1):519. doi: 10.1186/s13287-021-02591-4
18. Shi G, Tang N, Qiu J, Zhang D, Huang F, Cheng Y, et al. Irisin Stimulates Cell Proliferation and Invasion by Targeting the PI3K/AKT Pathway in Human Hepatocellular Carcinoma. *Biochem Biophys Res Commun* (2017) 493(1):585–91. doi: 10.1016/j.bbrc.2017.08.148
19. Liu H, Wang M, Jin Z, Sun D, Zhu T, Liu X, et al. FNDC5 Induces M2 Macrophage Polarization and Promotes Hepatocellular Carcinoma Cell Growth by Affecting the PPARgamma/NF-Kappab/NLRP3 Pathway. *Biochem Biophys Res Commun* (2021) 582:77–85. doi: 10.1016/j.bbrc.2021.10.041
20. Zhang X, Hu C, Kong CY, Song P, Wu HM, Xu SC, et al. FNDC5 Alleviates Oxidative Stress and Cardiomyocyte Apoptosis in Doxorubicin-Induced Cardiotoxicity *via* Activating AKT. *Cell Death Differ* (2020) 27(2):540–55. doi: 10.1038/s41418-019-0372-z
21. Pignataro P, Dicarlo M, Zerlotin R, Zecca C, Dell'Abate MT, Buccoliero C, et al. FNDC5/Irisin System in Neuroinflammation and Neurodegenerative Diseases: Update and Novel Perspective. *Int J Mol Sci* (2021) 22(4):1605. doi: 10.3390/ijms22041605
22. Zhang J, Bi J, Ren Y, Du Z, Li T, Wang T, et al. Involvement of GPX4 in Irisin's Protection Against Ischemia Reperfusion-Induced Acute Kidney Injury. *J Cell Physiol* (2021) 236(2):931–45. doi: 10.1002/jcp.29903
23. Zhang D, Tan X, Tang N, Huang F, Chen Z, Shi G. Review of Research on the Role of Irisin in Tumors. *Onco Targets Ther* (2020) 13:4423–30. doi: 10.2147/OTT.S245178
24. Pinkowska A, Podhorska-Okolow M, Dziegiel P, Nowinska K. The Role of Irisin in Cancer Disease. *Cells* (2021) 10(6):1479. doi: 10.3390/cells10061479
25. Dixon SJ, Lemberg KM, Lamprecht MR, Skouta R, Zaitsev EM, Gleason CE, et al. Ferroptosis: An Iron-Dependent Form of Nonapoptotic Cell Death. *Cell* (2012) 149(5):1060–72. doi: 10.1016/j.cell.2012.03.042
26. Stockwell BR, Friedmann Angeli JP, Bayir H, Bush AI, Conrad M, Dixon SJ, et al. Ferroptosis: A Regulated Cell Death Nexus Linking Metabolism, Redox Biology, and Disease. *Cell* (2017) 171(2):273–85. doi: 10.1016/j.cell.2017.09.021
27. Jiang X, Stockwell BR, Conrad M. Ferroptosis: Mechanisms, Biology and Role in Disease. *Nat Rev Mol Cell Biol* (2021) 22(4):266–82. doi: 10.1038/s41580-020-00324-8
28. Cao JY, Dixon SJ. Mechanisms of Ferroptosis. *Cell Mol Life Sci* (2016) 73(11-12):2195–209. doi: 10.1007/s00018-016-2194-1
29. Liu J, Kang R, Tang D. Signaling Pathways and Defense Mechanisms of Ferroptosis. *FEBS J* (2021). doi: 10.1111/febs.16059
30. Xia X, Fan X, Zhao M, Zhu P. The Relationship Between Ferroptosis and Tumors: A Novel Landscape for Therapeutic Approach. *Curr Gene Ther* (2019) 19(2):117–24. doi: 10.2174/1566523219666190628152137
31. Wang Y, Wei Z, Pan K, Li J, Chen Q. The Function and Mechanism of Ferroptosis in Cancer. *Apoptosis* (2020) 25(11-12):786–98. doi: 10.1007/s10495-020-01638-w
32. Pillai R, Hayashi M, Zavitsanou AM, Papagiannakopoulos T. NRF2: KEAPing Tumors Protected. *Cancer Discov* (2022) 12(3):625-63. doi: 10.1158/2159-8290.CD-21-0922
33. Suzuki T, Motohashi H, Yamamoto M. Toward Clinical Application of the Keap1-Nrf2 Pathway. *Trends Pharmacol Sci* (2013) 34(6):340–6. doi: 10.1016/j.tips.2013.04.005
34. Sun J, Zhou C, Zhao Y, Zhang X, Chen W, Zhou Q, et al. Quiescin Sulfhydryl Oxidase 1 Promotes Sorafenib-Induced Ferroptosis in Hepatocellular Carcinoma by Driving EGFR Endosomal Trafficking and Inhibiting NRF2 Activation. *Redox Biol* (2021) 41:101942. doi: 10.1016/j.redox.2021.101942
35. Wang Q, Bin C, Xue Q, Gao Q, Huang A, Wang K, et al. GSTZ1 Sensitizes Hepatocellular Carcinoma Cells to Sorafenib-Induced Ferroptosis *via* Inhibition of NRF2/GPX4 Axis. *Cell Death Dis* (2021) 12(5):426. doi: 10.1038/s41419-021-03718-4
36. Yang Q, Jiang W, Hou P. Emerging Role of PI3K/AKT in Tumor-Related Epigenetic Regulation. *Semin Cancer Biol* (2019) 59:112–24. doi: 10.1016/j.semcancer.2019.04.001
37. Wu Y, Zhang Y, Qin X, Geng H, Zuo D, Zhao Q. PI3K/AKT/mTOR Pathway-Related Long Non-Coding RNAs: Roles and Mechanisms in Hepatocellular Carcinoma. *Pharmacol Res* (2020) 160:105195. doi: 10.1016/j.phrs.2020.105195
38. Akbarzadeh M, Mihanfar A, Akbarzadeh S, Yousefi B, Majidinia M. Crosstalk Between miRNA and PI3K/AKT/mTOR Signaling Pathway in Cancer. *Life Sci* (2021) 285:119984. doi: 10.1016/j.lfs.2021.119984
39. Tsai CH, Shen YC, Chen HW, Liu KL, Chang JW, Chen PY, et al. Docosahexaenoic Acid Increases the Expression of Oxidative Stress-Induced Growth Inhibitor 1 Through the PI3K/Akt/Nrf2 Signaling Pathway in Breast Cancer Cells. *Food Chem Toxicol* (2017) 108(Pt A):276–88. doi: 10.1016/j.fct.2017.08.010
40. Gao AM, Ke ZP, Wang JN, Yang JY, Chen SY, Chen H. Apigenin Sensitizes Doxorubicin-Resistant Hepatocellular Carcinoma BEL-7402/ADM Cells to Doxorubicin *via* Inhibiting PI3K/Akt/Nrf2 Pathway. *Carcinogenesis* (2013) 34(8):1806–14. doi: 10.1093/carcin/bgt108

Conflict of Interest: The authors declare that the research was conducted in the absence of any commercial or financial relationships that could be construed as a potential conflict of interest.

frontiers | Frontiers in Pharmacology

REVIEW
published: 20 May 2022
doi: 10.3389/fphar.2022.879317

Ferroptosis and Tumor Drug Resistance: Current Status and Major Challenges

Zhenyu Nie[1], Mei Chen[1], Yuanhui Gao[1], Denggao Huang[1], Hui Cao[1], Yanling Peng[1], Na Guo[1], Fei Wang[2] and Shufang Zhang[1]**

[1]Central Laboratory, Affiliated Haikou Hospital of Xiangya Medical College, Central South University, Haikou, China, [2]Department of Urology, Hainan General Hospital, Affiliated Hainan Hospital of Hainan Medical University, Haikou, China

Ferroptosis is a novel type of regulated cell death, whose unique metabolic characteristics are commonly used to evaluate the conditions of various diseases especially in tumors. Accumulating evidence supports that ferroptosis can regulate tumor development, metastasis, and therapeutic responses. Considering to the important role of chemotherapy in tumor treatment, drug resistance has become the most serious challenge. Revealing the molecular mechanism of ferroptosis is expected to solve tumor drug resistance and find new therapies to treat cancers. In this review, we discuss the relationship between ferroptosis and tumor drug resistance, summarize the abnormal ferroptosis in tissues of different cancer types and current research progress and challenges in overcoming treatment resistance, and explore the concept of targeting ferroptosis to improve tumor treatment outcomes.

Keywords: ferroptosis, tumor drug resistance, chemotherapy, target therapy, immunotherapy

OPEN ACCESS

Edited by:
Xu Chen,
Guilin Medical University, China

Reviewed by:
Xiawei Cheng,
East China University of Science and Technology, China
Darius John Rowland Lane,
University of Melbourne, Australia

****Correspondence:***
Shufang Zhang
zsf66189665@126.com
Fei Wang
hnsywangfei@163.com

Specialty section:
This article was submitted to Pharmacology of Anti-Cancer Drugs, a section of the journal Frontiers in Pharmacology

Received: *19 February 2022*
Accepted: *19 April 2022*
Published: *20 May 2022*

Citation:
Nie Z, Chen M, Gao Y, Huang D, Cao H, Peng Y, Guo N, Wang F and Zhang S (2022) Ferroptosis and Tumor Drug Resistance: Current Status and Major Challenges. Front. Pharmacol. 13:879317. doi: 10.3389/fphar.2022.879317

INTRODUCTION

Malignant tumors are the second leading cause of death worldwide, following cardiovascular disease (Siegel et al., 2020). With the development of the global economy and the extension of human life expectancy, the prevention and treatment of cancer have become a global health, economic and social issue. In 2020, the number of estimated new cases of cancer and death around the world reached 1,92,92,789 and 99,58,133, respectively (Cao et al., 2021). This is equivalent to about 36.7 people being diagnosed with cancer every minute and 19 people dying from cancer. In the United States, a total of 18,06,590 new cancer cases and 6,06,520 deaths estimated to occur in 2020 (Siegel et al., 2020). The most common tumor in males is prostate cancer (21%) while that in female is breast cancer (30%). The second and third most common tumors in both sexes are lung and bronchus cancer (13% for males, 12% for females) and colon and rectum cancer (9% for males, 8% for females). Lung and bronchus cancer has the highest mortality rate in both sexes (23% for males, 22% for females) whereas colon and rectum cancer has the third highest mortality rate (9% for both); meanwhile, prostate cancer and breast cancer have the second highest mortality rate in males (10%) and females (15%), respectively (Siegel et al., 2020). China is the largest developing country. The rapid economic development has made the improvement of people's living standards and extended the life expectancy. Cancers have become the main factor threatening the health of Chinese people. In 2020, 45,68,754 new cases of cancer were recorded in China, accounting for 48.07% of all new cases in Asia that year, and 30,02,899 deaths were noted, accounting for 51.69% in Asia (Cao et al., 2021). Drug therapy is the most important component of cancer treatment. These drugs include chemotherapeutic drugs, targeted drugs, and immune checkpoint inhibitors (ICIs). In particular,

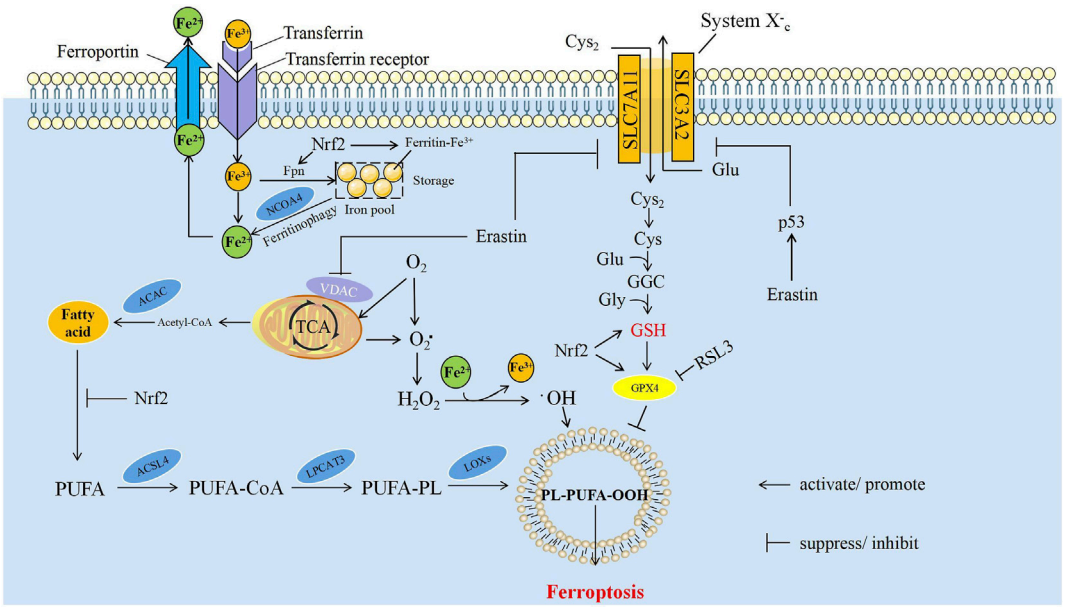

FIGURE 1 | The mechanism of ferroptosis. The core mechanisms affecting ferroptosis are mainly iron metabolism, lipid peroxidation and amino acid metabolism. ACAC, acetyl CoA carboxylase; ACSL4, acyl-CoA synthetase long-chain member 4; Cys, cysteine; Cys2, cystine; Fe2+, ferrous ion; Fe3+, ferric ion; Fpn, ferroportin; Glu, glutamate; Gly, glycine; GPX4, glutathione peroxidase 4; GSH, glutathione; H2O2, hydrogen peroxide; LPCAT3, lysophosphatidylcholine acyl-transferase 3; LOXs, lipoxygenases; NCOA4, nuclear receptor coactivator 4; Nrf2, nuclear factor erythroid 2-related factor 2; O2, oxygen; O2, Oxygen free radicals, PUFA, polyunsaturated fatty acids; PUFA-CoA, polyunsaturated fatty acids-CoA; PUFA-PL, polyunsaturated fatty acids-phospholipids; PL-PUFA-OOH, phospholipids-polyunsaturated fatty acids-peroxide; SLC3A2, solute carrier family 3 member 2; SLC7A11, solute carrier family 7 member 11; TCA, tricarboxylic acid cycle.

the emergence of new targeted drugs and ICIs has greatly extended the survival time of cancer patients. However, the ensuing drug resistance has become a new challenge (Balaban et al., 2004). Research on tumor drug resistance, found that many factors lead to drug resistance. Reverse or anti-drug resistance has attracted more attention in tumor research.

Ferroptosis is a kind of regulated cell death (RCD). Abnormal iron metabolism and lipid peroxidation are the two most typical characteristics in ferroptosis. Because ferroptosis is affected by the metabolism of iron ions, lipids, amino acids and other substances, a variety of ferroptosis inducers or inhibitors have been found, and the regulation of ferroptosis has been achieved *in vivo* and *in vitro*. Accumulating studies have found that the regulation of ferroptosis can affect the drug sensitivity of tumors and sensitized tumors and even reverse drug resistance. Although this discovery still requires a lot of preliminary work before clinical application, it provides new opportunities for refractory or recurring tumors. Therefore, this review summarizes the research progress of tumor drug resistance and ferroptosis to provide some ideas for either basic and clinical researchers.

FERROPTOSIS

In 2003, erastin was found to induce the death of tumor cells with RAS mutations (Dolma et al., 2003). In 2008, RSL3 and RSL5 were also found to have similar efficacy to erastin, and this process can be inhibited by iron chelators or antioxidants, depending on the concentration of intracellular iron and reactive oxygen species (ROS) (Wan and Stockwell, 2008). In 2012, the term ferroptosis was to describe this cell death dependent on the accumulation of iron and lipid peroxides (Dixon et al., 2012). After nearly a decade of research, ferroptosis has been confirmed to be related to various diseases such as organ ischemia–reperfusion injury and stroke injury (Wang et al., 2019). In addition, studies have found that immunotherapy can promote ferroptosis by increasing the accumulation of lipid peroxide and iron in tumor cells, and improve the efficacy of immunotherapy (Xie et al., 2016). Ferroptosis can also affect the resistance of tumors to anti-tumor drugs, specifically through the regulation of iron and lipids.

Mechanism of Ferroptosis

The mechanism of ferroptosis mainly relies on intracellular dynamically balanced biochemical processes: the production and elimination of lipid peroxides. In these processes, iron and polyunsaturated fatty acids (PUFAs) are used as raw materials for lipid peroxidation to promote ferroptosis. Glutathione peroxidase 4 (GPX4) uses glutathione (GSH) as a substrate to reverse the regulation of ferroptosis. When cells cannot remove excess ROS, ferroptosis is induced. Iron, lipid, and amino acid metabolism are the most important factors in the regulation of ferroptosis (**Figure 1**).

Iron Metabolism

The participation of Fe^{2+}/Fe^{3+} in the formation of ROS is one of the critical factors of ferroptosis. Iron from food is absorbed

through duodenal epithelial cells. The ferric reductase in the intestinal epithelium can reduce Fe^{3+} to Fe^{2+}, and then it is transported to the cells through divalent metal transporter 1 (Fleming and Bacon, 2005; Cao and Dixon, 2016). Extracellular iron can be transferred into cells by binding to transferrin and then act as a ligand for the transferrin receptor; ferroportin can transfer iron inside of cells to the outside, and then into the circulatory system (Hentze et al., 2010). Iron can be stored in ferritin which is called iron pool (IP), and it is non-toxic to the cell. Free Fe^{2+} formed labile iron pool within the cell, which is much less than the IP (Kwon et al., 2015). Free Fe^{2+} has strong reducibility and easily reacts with hydrogen peroxide (H_2O_2) in the cell to produce hydroxyl free radicals that can cause oxidative damage to DNA, protein, and membrane lipids; promote lipid peroxidation; and cause damage to the cell membranes, leading to cell death (Maines, 1988). The process of ferritin degradation to release Fe^{2+} is called ferritinophagy, and nuclear receptor coactivator 4 (NCOA4) acts as a linker protein to mediate this process (Mancias et al., 2014). The overexpression of NCOA4 can promote ferritinophagy, increase the concentration of free Fe^{2+} in cells, and promote ferroptosis; on the contrary, knocking down the expression of NCOA4 can inhibit the degradation of ferritin and reduce the sensitivity of cells to oxidative damage. The iron responsive element binding protein can inhibit the occurrence of ferroptosis by increasing the expression of ferritin (Dixon et al., 2012). Iron is a direct factor affecting the production of ROS. Heme oxygenase-1 catalyzes the degradation of heme and produces free Fe^{2+}. The overexpression of heme oxygenase-1 can accelerate the ferroptosis induced by erastin (McKie et al., 2001; Rouault, 2005). RAS increases the intracellular iron concentration by upregulating transferrin receptor and downregulating ferritin, resulting in the occurrence of ferroptosis. RAS mutations increase the ability of cellular resistance to ferroptosis (Yang and Stockwell, 2008; Schott et al., 2015).

Lipid Metabolism and Lipid Peroxides

PUFAs are important components of the phospholipid bilayer in the cell membrane and maintain the fluidity. Fe^{2+} can oxidize excess PUFAs into hydroxyl free radicals through Fenton reaction, produce a large amount of lipid peroxides, and induce ferroptosis in cells (Lin et al., 2018). As a member of intracellular ROS, lipid peroxide can strongly induce ferroptosis. ROS is a class of molecules including peroxides, superoxides, singlet oxygen, and free radicals. They can cause cell death by damaging DNA, RNA and lipid molecules (Wan and Stockwell, 2015). During ferroptosis, the accumulation of lipid peroxides, especially phospholipid peroxides, is considered to be a landmark event of ferroptosis and also a prerequisite for ferroptosis (D'Herde and Krysko, 2017). Phosphatidylethanolamine (PE) is a kind of glycerophospholipid in the cell membrane. The PE content in the inner mitochondrial membrane accounts for about 40% of the total phospholipids, and it accounts for about 15%–25% in other organelle membranes (Feng and Stockwell, 2018). PE is also involved in ferroptosis induced by arachidonic acid (AA) and its derivatives (Dixon et al., 2015; Kagan et al., 2017). For example, acyl-CoA synthetase long-chain member 4 (ACSL4) can activate AA and its derivative adrenic acid into arachidene acyl-CoA and adrenal-CoA, respectively. Lysophosphatidylcholine acyl transferase 3 (LPCAT3) binds them to PE on the inner membrane, and mediates the peroxidation of membrane phospholipids through lipoxygenases (LOXs) to promote ferroptosis (**Figure 1**) (Sato et al., 1999; Dixon et al., 2015; Doll et al., 2016). Knockout of LOXs helps protect cells from ferroptosis induced by erastin (Yang et al., 2016).

Lipid peroxides can damage cells in many ways. First, lipid peroxides can be decomposed into ROS to amplify the lipid peroxidation process. Second, lipid peroxides can be released by changing the physical structure of the membrane, such as the thickness and degree of curvature of the membrane; perforating the membrane; releasing cytokines and disrupting the metabolism of cells. Finally, the by-products in the process of lipid peroxidation, such as malondialdehyde and 4-hydroxynonenal, can directly damage cells (Gaschler and Stockwell, 2017; van der Veen et al., 2017).

Amino Acid Metabolism

GSH is an important antioxidant. It can not only reduce H_2O_2 to H_2O directly and maintain the balance of intracellular free radical content, but also act as a substrate of GPX4 to participate in the intracellular antioxidant system and repair cell membranes. Therefore, the activity of GSH and GPX4 is a key factor of ferroptosis (Bridges et al., 2012). Cystine/glutamate antiporter (system Xc-) is a transporter necessary for GSH synthesis. System Xc- is a heterodimer, formed by glycosylated solute carrier family 3 member 2 (SLC3A2) and non-glycosylated solute carrier family 7 member 11 (SLC7A11) linked by disulfide bonds (Gao et al., 2015). System Xc- can mediate the entry of cystine into the cell and the exchange of glutamate. Cystine can be reduced to cysteine after entering the cell, and then GSH is synthesized by the sequential activities of glutamate cysteine ligase (GCL) and glutathione synthetase (GSS) to regulate the downstream lipid peroxidation process. The imbalance of amino acid metabolism by inhibiting System Xc- can induce ferroptosis. The high concentration of extracellular glutamate can also inhibit System Xc- and induce ferroptosis. This may be one of the reasons for the cytotoxicity of glutamate in the brain (Dixon et al., 2012). Glutamine is one of the sources of glutamate. Inhibiting the decomposition of glutamine greatly improves the cell survival rate and inhibits ferroptosis in the absence of cystine (Maiorino et al., 2018). Cysteine can directly limit the biosynthesis of GSH. Therefore, cysteine can be directly transported into the cell through the alanine serine cysteine (ASC) system to inhibit ferroptosis (Doll and Conrad, 2017). Drugs, such as RSL3 (Wan and Stockwell, 2008) or hexamethylmelamine (altretamine) (Woo et al., 2015), can inhibit the expression and activity of GPX4, leading to ferroptosis (Yang et al., 2014). The content of GSH was significantly reduced in erastin-treated cells is due to the fact that erastin directly reduces uptake of cystine by inhibiting the activity of xCT (Dixon et al., 2012; Huang et al., 2018), which causes a decrease in GSH synthesis (Skouta et al., 2014; Reina and De Pinto, 2017). Therefore, the antioxidant capacity of erastin-treated cells was reduced (Reina and De Pinto, 2017).

Other Factors of Ferroptosis

P53 is the most widely known tumor suppressor. Under different conditions, the expression of p53 may promote, inhibit, or limit the occurrence of ferroptosis, and p53 can regulate ferroptosis from two pathways: cell-specific or environment-dependent. For example, p53 activation can inhibit the uptake of cystine by inhibiting the transcription of SLC7A11, promote the accumulation of ROS, and induce ferroptosis (Bersuker et al., 2019). The expression of the long non-coding RNA (LncRNA)-p53RRA is low in tumors. It can release p53 from the G3BP1 complex, causing the accumulation of p53 in the nucleus and ultimately inducing ferroptosis (Doll et al., 2019). It has been shown that erastin can also enhance ferroptosis by activating p53, upregulate its transcriptional product and cause an increase in ROS (Yang et al., 2014). SAT1 (spermidine/Spermine N1-acetyltransferase 1) is an important regulator in polyamine metabolism (Hu et al., 2010). In cancer cells, overexpression of SAT1 results in rapid depletion of cellular spermidine and spermine, which can inhibit cell growth and induce apoptosis (Mandal et al., 2015). It has reported that SAT1 is a transcriptional target of p53 in some cancer cell lines. Depletion of SAT1 also negatively feedback inhibits p53-induced ferroptosis in cancer cells (Ou et al., 2016). Mechanistically, SAT1 induction correlates with the expression levels of ALOX15 (arachidonate 15-lipoxygenase), and ALOX15 is a downstream effector of p53-induced SAT1 expression in ferroptosis (Ou et al., 2016). However, the deeper mechanism of p53-SAT1-ALOX15 has not yet been fully elucidated. GSL2 has been identified as a transcriptional target of p53 too, which expression is responsible for p53-mediated oxygen consumption, mitochondrial respiration, and ATP generation in cancer cells (Tarangelo et al., 2018). Since GSL2 can increase cellular antioxidant function by promoting GSH production in cancer cells, it is considered to be a negative regulator of ferroptosis (Tarangelo et al., 2018). Although p53 can induce ferroptosis through various mechanisms, surprisingly, p53 also protects cancer cells against ferroptosis through DPP4 or p21. For example, p53 can limit erastin-induced ferroptosis by blocking dipeptidyl peptidase 4 (DPP4) activity in a transcription-independent manner. Loss of p53 prevents nuclear accumulation of DPP4, thereby promoting plasma membrane-associated DPP4-dependent lipid peroxidation, ultimately leading to ferroptosis (Thomas and Thomas, 2003). The tumor suppressor p21, also known as cyclin dependent kinase inhibitor 1A (CDKN1A), is a cell cycle regulator. It has been reported that p53-mediated expression of p21 can delay the onset of ferroptosis and is associated with reduced intracellular glutathione depletion and ROS accumulation. Therefore, the p53-p21 axis may help cancer cells cope with the metabolic stress caused by cystine deprivation by delaying the onset of ferroptosis (Xie et al., 2017). In general, p53 plays an extremely important and complex role in the process of ferroptosis, and affects the occurrence and progression of ferroptosis through different signaling pathways or regulatory factors, thereby affecting tumorigenesis. A better understanding of the mechanism by which p53 controls tumor ferroptosis will help researchers discover more targets in tumor therapy.

The RAS protein plays an important role in human tumors, and its common mutation forms include KRAS, NRAS, and HRAS. Tumors with RAS mutations are sensitive to ferroptosis induced by erastin and RSL3, but the specific mechanism is unclear at present (Dolma et al., 2003; Wan and Stockwell, 2008). KRAS, which is the first reported oncogene, can regulate intracellular ROS levels through a variety of mechanisms. However, according to the erastin sensitivity analysis of 117 cancer cell lines, RAS mutations and the sensitivity of ferroptosis inducer are not significantly related compared with those in wild-type cells. This finding suggests that RAS mutations may not be sufficient as evidence of sensitivity to ferroptosis (Yang et al., 2014).

Apoptosis-inducing factor mitochondria-associated 2 (AIFM2) is also known as ferroptosis suppressor protein 1 (FSP1). It can reduce Coenzyme Q10 (CoQ10) to CoQ10H2, the latter of which acts as a radical trapping antioxidant (RTA) to quench lipid peroxyl radicals and provide protection from ferroptosis. In addition, CoQ10H2, the reduced form of CoQ10, exerts an antioxidant effect from capturing free radicals, preventing lipid peroxidation and avoiding ferroptosis (Mao et al., 2018; Shi et al., 2019).

Heat shock proteins (HSPs) are a class of highly conserved molecular chaperones that can change their expression levels in response to environmental stress, and help cells resist various types of death. Among them, HSPB1 can inhibit ferroptosis by reducing iron uptake (Sun et al., 2015). HSPA5 can bind and stabilize GPX4, avoiding the damage of lipid peroxide from ferroptosis indirectly (Yagoda et al., 2007).

Mitochondria are also involved in the occurrence of ferroptosis. CDGSH iron-sulfur domain 1 is a type of mitochondrial iron transport protein that inhibits ferroptosis by preventing the accumulation of iron in the mitochondria and the production of ROS (Yuan et al., 2016). The other is voltage-dependent anion channels (VDAC), which is a channel in the outer mitochondrial membrane that control the flow of metabolites across the membrane (Agyeman et al., 2012). Its role is to maintain mitochondrial membrane potential ($\Delta\Psi$) and to generate adenosine triphosphate (ATP). In the open state, VDAC allows the entry of the substrates of respiratory chain, adenosine diphosphate (ADP), and phosphate (Pi) into the mitochondria. Mitochondria is closed while the VDAC closed (Caterino et al., 2017). The dynamic "open-closed" state of the VDAC will have a significant impact on mitochondrial metabolism and cellular bioenergetics. Proliferating tumor cells usually have much higher levels of free tubulin (Lemasters, 2017). Low doses of tubulin can make VDAC closed and reduce $\Delta\Psi$, inhibiting the entry of respiratory substrates through VDAC into mitochondria (Maldonado et al., 2010; Maldonado, 2017). However, erastin could block the inhibitory effect of free tubulin on VDAC and promote the increase of $\Delta\Psi$ and the production of mitochondrial ROS (Yagoda et al., 2007; Rostovtseva et al., 2008; Maldonado et al., 2013), and induce ferroptosis finally (Dixon et al., 2012).

The transcription factor nuclear factor erythroid 2-related factor 2 (NRF2) is an important antioxidant defense system and plays a predominantly negative role in the regulation of ferroptosis. Nrf2 acts as a transcription factor that regulates a variety of genes related to iron metabolism, lipid peroxidation and ferroptosis, such as ferritin, transferrin receptor 1 (TfR1), ferroportin (Fpn/SLC40A1), ferrochelatase (FECH), ATP-binding cassette subfamily B member 6 (ABCB6), SLC7A11, GSS, GPX4 and so on (Dodson et al., 2019). Therefore, Nrf2 can prevent ferroptosis by regulating the expression of different genes. For example, Nrf2 can reduce the unstable free iron content by upregulating the expression of ferritin (Harada et al., 2011), because both ferritin and Fpn, a key protein for iron storage, are regulated by Nrf2 (Krishnamurthy et al., 2006; Kerins and Ooi, 2018). Both ABCB6 located in the outer mitochondrial membrane and FECH in the inner membrane are positively regulated by Nrf2, which can chelate excess iron in mitochondria by promoting the synthesis of heme, reducing mitochondrial iron overload (Wu et al., 2001; Mazure, 2017). The GSH-GPX system is an important component of anti-lipid peroxidation (Yagoda et al., 2007), and Nrf2 is not only a transcription factor for GSH reductase and GPX4, but also promotes GSH biosynthesis, and prevents ferroptosis (Dodson et al., 2019). Nrf2 can also regulate the transcription of aldehyde-ketone reductase 1C1-3 and acetaldehyde dehydrogenase 3A1 (Zakharova et al., 2018), degrade the products of lipid peroxidation, and prevent the occurrence of ferroptosis (Dodson et al., 2019).

TUMOR DRUG RESISTANCE

In the past few decades, the treatment of tumors has been greatly advanced. From the earliest surgery or chemotherapy, it has gradually evolved into "polytherapy" which includes surgery, chemotherapy, immunotherapy, and molecular targeted therapy. With the proposal and wide application of polytherapy, the survival of patients has remarkably increased. Unfortunately, tumor drug resistance greatly limits the long-term survival of patients (Balaban et al., 2004).

The concept of drug resistance first came from the resistance of bacteria to antibiotics (Blakely et al., 2015; Fisher et al., 2017; Chatterjee and Bivona, 2019). In oncology, drug resistance refers to the heritable ability of cells to survive exposure to the high concentrations of a drug. "Tolerance and persistence" are concepts used to describe the sensitivity and resistance of cells to drug treatments. "Tolerance" is the ability of cells to survive ephemeral exposure to therapeutic concentrations of drugs, and "persistence" is the ability of a sub-population of cell clones to survive in a treatment (Holohan et al., 2013; Holden, 2015).

Tumor resistance to therapeutic drugs is divided into primary resistance and acquired resistance. Primary resistance refers to the phenomenon of resistance to drugs in the initial treatment, and without tumor shrinkage or remission after receiving the treatment. It is usually due to the genetic mutation or abnormal cell status in the tumor or is caused by the rapid adaptation of the cell to the drug (Konieczkowski et al., 2014; Lee et al., 2014). Compared with primary resistance, acquired resistance is more prevalent. It refers to resistance developed during treatment. At present, there are two main speculations about the mechanism of acquired resistance: pre-existing and re-evolutionary. The pre-existing hypothesis believes that there are multiple potential clonal heterogeneities in the tumor, and the rare subclones may be resistant to drugs before treatment begins. After receiving drug treatment, these resistant subclones continue to expand, eventually resulting in drug-driven tumor recurrence (Nikolaou et al., 2018; Yoda et al., 2019). The re-evolution hypothesis refers to the cell survival through epigenetic adaptation in the initial treatment, so that phenotypes such as drug resistance and cell cycle delay are developed before permanent drug resistance. This part of the cells can turn into the state of "persistence" to escape the efficacy of drugs and serve as "seeds" from which drug-resistant clones evolve (Kobayashi et al., 2005; Pao et al., 2005; Bean et al., 2007; Yun et al., 2008; Wang et al., 2015; Flinders et al., 2016; Hata et al., 2016; Li et al., 2016). It also reveals the mechanism of minimal residual disease causing tumor recurrence. The tumor microenvironment (TME) can also promote acquired resistance: the growth factors secreted by tumor cells or tumor-resident stromal cells can maintain tumor cell survival in the initial treatment (Straussman et al., 2014; Wilson et al., 2014; Obenauf et al., 2015).

Mechanism of Tumor Drug Resistance

Tumor Heterogeneity

The mechanism of tumor resistance is diverse and complex. As tumors are generally considered to be genetic diseases with genetic diversity and selective evolution, drug resistance is usually also caused by genetic changes. Hence, drug resistance, whether primary or acquired, is a definite and irreversible phenomenon (Stratton et al., 2009; Greaves and Maley, 2012; Velculescu et al., 2013). Even in the same kind of tumor, the phenotype of the tumor is different due to the different genotypes of its internal cells. This phenomenon is called tumor heterogeneity. Tumor heterogeneity is the most common factor that promotes tumor resistance (Concannon et al., 2015; Kobayashi et al., 2016; Vinogradova et al., 2016). Tumor heterogeneity also changes with the progress of tumor treatment. Studies comparing the primary tumor and metastasis found changes in heterogeneity. This phenomenon indicates that the heterogeneity of the tumor has time and spatial specificity, and it also plays a key role in tumor drug resistance (Gerlinger and Swanton, 2010). Tumor heterogeneity results from genetic or epigenetic changes in tumor cells or cells in the TME (Gorre et al., 2001; Stratton et al., 2009). Chromosomal instability, genetic missense mutations, or epigenetic changes, such as DNA methylation or histone modification, can all lead to changes in tumor heterogeneity (**Figure 2**) (Gorre et al., 2001; Stratton et al., 2009; Negrini et al., 2010). In chronic myeloid leukemia (CML), heterogeneity has been confirmed to cause drug resistance. BCR-ABL translocation is an established driver mutation in CML. The subclone of leukemia cells carrying imatinib-resistant mutations in the kinase domain of BCR-ABL can cause CML patients to relapse after receiving imatinib treatment (Charles, 2012; Wilting and Dannenberg,

FIGURE 2 | The Mechanisms of tumor drug resistance. Tumor heterogeneity is usually caused by chromosomal instability, mutations and epigenetics changes. Cancer stem cells can resist drugs by increasing the expression of ABC, dormant by arresting cell cycle, improving repair ability, and creating a hypoxic niche; The components of TME, including cells and cytokines, can cause tumor cells to resist drugs. Last but not least, tumors can resist drugs by reducing absorption, changing activity, affecting metabolism and increasing excretion. ABC, adenosine-triphosphate binding cassette; CSCs, cancer stem cells; TME, tumor micro environment.

2012). Tumor heterogeneity also promotes the resistance of lung cancer to epidermal growth factor receptor (EGFR) tyrosine kinase inhibitors (TKIs). More than 75% of non-small cell lung cancer (NSCLC) patients have multiple subclonal driver mutations, which affect the response of high-grade lung cancer to EGFR treatment (Blakely et al., 2017; Jamal-Hanjani et al., 2017). In addition, the EGFR T790M subclone can not only resist first- and second-generation EGFR inhibitors, but also promote resistance to EGFR inhibitors in NSCLC patients who are treated for the first time (Piotrowska et al., 2015).

Cancer Stem Cells (CSCs)

CSCs are cell subclones that have the ability to self-renew in tumor tissues and produce a series of heterogeneous tumor cells (Al-Hajj et al., 2003). CSCs are also considered to be the source of tumor heterogeneity (Bonnet and Dick, 1997). CSCs have strong abilities of proliferation and differentiation, which are similar to stem cells. In addition, CSCs have similar characteristics to side population (SP) cells. SP cells are a group of cells that deviate from the main peak in the flow cytometer scatter diagram because they are less stained by Hoechst 33,342 (Cao et al., 2011). CSCs and SP cells can excrete chemotherapeutic drugs out of cells by highly expressing adenosine triphosphate-binding cassette (ABC) G2 (Clarke et al., 2006). CSCs have stronger tumor-forming ability in *in vitro* and *in vivo* experiments; for example, about 500–1,000 CSCs cells are needed to form tumors (Jang et al., 2012; Teshima et al., 2014; Peiris-Pagès et al., 2016).

The development of drug resistance is closely related to the biological characteristics of CSCs. PAXC-002 and PAXC-003 are two colon cancer cell lines established from a primary human xenograft model. Compared with PAXC-003, PAXC-002 shows significant resistance to gemcitabine and also has strong abilities to clone and express cluster of differentiation 133 (Cioffi et al., 2015). Breast cancer MCF-7 cells pretreated with paclitaxel can obtain a stronger ability to form cell spheres, indicating that paclitaxel has a certain enrichment effect on breast CSCs (Jang et al., 2012).

The specific mechanisms of drug resistance caused by CSCs be initiated as follows (**Figure 2**): 1) CSCs generally highly express ABC, which can transport drugs outside the cell, reduce the intracellular drug concentration, and reduce the cytotoxic effect of the drug. Inhibiting the expression of ABC transport protein or knocking out ABC G2 gene can improve the sensitivity of CSCs to chemotherapeutics (Mare et al., 2013). 2) CSCs are mostly dormant: Given that tumor cells are usually in an active state of proliferation, irreversible damage can be inflicted on dividing cells by interfering with or inhibiting DNA or RNA synthesis, inserting alkylation, or inhibiting key enzymes required for DNA synthesis. However, most CSCs. are in the G0 phase; they are not sensitive to the efficacy of these drugs. Instead, the drug

eliminates tumor cells and enriches CSCs. In pancreatic CSCs, the cyclin-dependent kinase inhibitor P21 and tumor factor P53 are highly expressed, while the expression of cyclin D1 is reduced. The cell cycle is arrested in the G0/G1 phase, and the sensitivity to chemotherapeutic agents is significantly reduced (Meng et al., 2014). In ovarian cancer, CSCs with positive acetaldehyde dehydrogenase 1 (ALDH1) expression are significantly resistant to chemotherapeutic agents. This is because ALDH can oxidize aldehydes into carboxylic acids and resist the cytotoxic effects of alkylating agents. ALDH1 can also make more cells stagnate in the G0 phase by regulating the cell cycle (Hu et al., 2012). 3) CSCs show strong repair ability in the process of coping with damage. CSCs will activate p53, ataxia-telangiectasia mutated-cell cycle checkpoint kinase 2, and other damage repair pathways, causing cell cycle arrest and providing sufficient time and opportunity for damaged cells to complete self-repair (Karran, 2001). Compared with ordinary tumor cells, CSCs highly express endonucleases, DNA polymerases, and DNA ligases related to DNA repair and have stronger enzymatic activity (Shiotani et al., 2006). 4) The special hypoxia niche in which CSCs are located helps to avoid the efficacy of drugs. Using trastuzumab to treat breast cancer can enrich breast CSCs. The interleukin-6 (IL-6) secreted by breast CSCs is about 100 times higher than that in parental cell. The inflammatory niche activated by IL-6 is the key for $HER2^+$ cells to resist trastuzumab. This suggests that the cytokine of the TME also plays an important role in tumor drug resistance (Bhowmick et al., 2004).

Tumor Micro Environment

The TME is the environment in which tumor cells grow; it is usually composed of tumor cells, immune and inflammatory cells, tumor-associated fibroblasts, blood vessels, extracellular matrix, and various cytokines (Dobbs et al., 2016; Ireland et al., 2016). The metabolism of tumor tissue affects the changes of TME. At the same time, the TME can also reshape tumors, such as affecting tumor proliferation, invasion, metastasis, or apoptosis. Similarly, many components in the TME can also affect the sensitivity of tumor cells to drugs (**Figure 2**). IL-10 secreted by tumor-associated macrophages (TAMs) causes breast cancer to resist paclitaxel through the signal transducer and activator of transcription 3/B-cell lymphoma-2 pathway (Korkaya et al., 2012). In addition, TAMs can activate insulin-like growth factor (IGF) receptors on pancreatic cancer cells by secreting IGF-1 and 2, causing pancreatic cancer to resist gemcitabine (Shiao et al., 2011). The fat cells in the TME can increase the resistance of breast cancer to chemotherapy by releasing IL-6 (Yang et al., 2015). Various cytokines in the TME can activate signal pathways that maintain survival and make tumor cells resistant to chemotherapy and molecular targeted therapies. For example, in Burkitt's lymphoma, the use of doxorubicin treatment can cause the thymus to release IL-6 and tissue inhibitor of metalloproteinase 1 (TIMP1), causing the remaining lymphoma tissue to resist the drug, which leads to the recurrence of lymphoma (Gilbert and Hemann, 2010). Hypoxia is the most common feature in the TME (Kumar and Vaidya, 2016). Hypoxia can cause cell cycle arrest in tumor cells, and can also induce an increase in P27 expression, arrest cell division in the G1/S phase, and make tumor cells resistant to chemotherapy drugs (Mazumdar et al., 2009). In cholangiocarcinoma, hypoxia can promote the expression of procollagen lysine-2-ketoglutarate 5-dioxygenase, a kind of collagen-modifying enzyme that can cause resistance to gemcitabine and promote epithelial mesenchymal transition (EMT) (Yeo et al., 2017).

Interactions Between Cancer and Drugs

Tumor cells can resist chemotherapy drugs by changing the activity, reducing absorption, increasing efflux, or influencing metabolism (**Figure 2**). For example, cytarabine needs to be phosphorylated to be converted into cytarabine triphosphate to exert anti-tumor effects. The downregulation or mutation of enzymes involved in this pathway can reduce the efficacy of cytarabine, leading to tumor cell resistance to cytarabine (Kort et al., 2015). P-protein is a multi-drug membrane transporter that can transport a variety of chemotherapeutic drugs such as doxorubicin, vincristine, or paclitaxel from the cell to the outside, thereby reducing the intracellular drug concentrations and reducing the therapeutic effect (Cros et al., 2009). Mutations in the folate carrier gene in patients with acute lymphoblastic leukemia can reduce the binding of methotrexate to transporters and cause resistance to methotrexate (De Andres and Llerena, 2016). The mechanism of chemotherapy drugs mainly depends on the metabolism of enzymes to exert anti-cancer effects, so enzymes are the most important factor in determining drug concentration. In pharmacology, drug metabolism reactions are mainly divided into phase Ⅰ and phase Ⅱ reactions. Phase Ⅰ reaction includes oxidation, reduction, and hydrolysis reactions, and phase Ⅱ reaction is a combination reaction (Guengerich, 1997). In breast cancer, increasing the activity of P450 can enhance the cell metabolism and inactivate docetaxel. Therefore, reducing the activity of cytochrome P450 can improve the therapeutic effect (Hentrich and Barta, 2016). In phase Ⅱ reaction, the drug can combine with GSH to reduce drug activity and electrophilicity and increase GSH and glutathione transferase activity, reducing anti-tumor effects of alkylating or platinum-containing chemotherapeutic agents (Liu et al., 2006).

The treatment of tumors has evolved from chemotherapy or radiotherapy to polytherapy including surgery, chemotherapy, radiotherapy, targeted therapy, immunotherapy, and other methods. Therefore, the mechanisms of tumor drug resistance are constantly being developed and improved. For example, immunotherapy is a novel remedy of treating tumors. ICI therapy uses the abnormal characteristics of tumors to find suitable targets and accurately destroy tumor cells. Drugs such as programmed cell death protein-1 (PD-1) monoclonal antibody and cytotoxic T lymphocyte-associated antigen-4 monoclonal antibody have been developed (Amaral et al., 2017). However, with the widespread application of immunotherapy, the number of patients with acquired resistance to ICIs has gradually increased. This phenomenon is related to the loss of function of T cells, the inability to form new antigens, genetic and epigenetic changes in presentation and processing, changes in the pathways of cell signaling that disrupt the action of cytotoxic

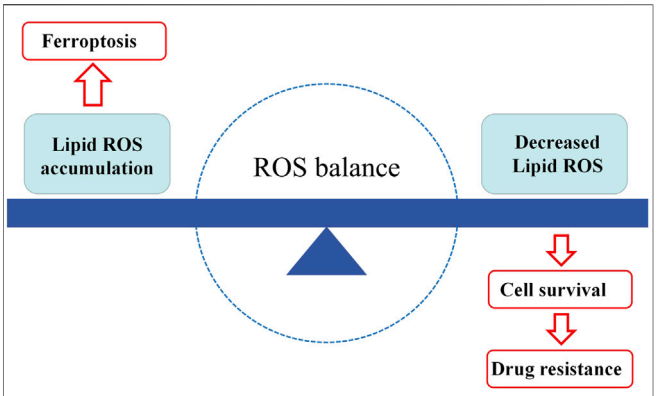

FIGURE 3 | The balance of ferroptosis and drug resistance. When lipid peroxides accumulate in the cells, hence ferroptosis occurs. When lipid peroxides are decreased in the cells, the cells will have more opportunities to survive, in the result of tumor drug resistance. ROS, reactive oxygen species.

T cells, and the formation of tumor immune escape cell lines (Gajewski et al., 2013; Jenkins et al., 2018). Under the selection of drugs, tumors can evolve innate and adaptive abilities in order to escape the immune system, thereby resisting the therapeutic effects of ICIs (Perrier et al., 2020). The drug resistance mechanism of tumor cells is very complicated, and this concept is constantly developing. A profound understanding of the mechanism of tumor resistance can enhance the therapeutic efficacy and benefit the survival of tumor patients. In terms of pathology, oncology is developing rapidly at present, and finding more accurate drug targets has become a new direction for the treatment of tumor drug resistance. Accumulated evidence show that the regulation of ferroptosis can promote cell death or maintain cell survival. This suggests that the regulation of ferroptosis can improve tumor drug resistance, and it will bring novel development opportunities for tumor treatment.

CROSSTALK BETWEEN FERROPTOSIS AND TUMOR DRUG RESISTANCE

Tumor drug resistance is related to a variety of mechanisms, among which the destruction of redox homeostasis is one of the key factors leading to it. Tumor cells can enhance their tolerance to oxidative stress by inhibiting their own ROS generation, and develop acquired drug resistance (Yang et al.). Ferroptosis is closely related to the production of oxidative stress and ROS. The regulation of oxidative stress can cause changes in ferroptosis, thereby affecting the sensitivity of tumor cells to drugs. The relationship seems to be placed on two ends of a balance: on the one hand, lipid peroxidation and ROS accumulation cause ferroptosis in tumor cells, which limits tumor proliferation. On the other hand, if lipid peroxidation and ROS are reduced, tumor cells will survive and develop resistance to anti-tumor drugs. The central point is the dynamic balance between the generation and removal of ROS (**Figure 3**).

Crosstalk Between Ferroptosis-Related Oxidative Stress and Tumor Drug Resistance

Increasing evidence show that abnormal iron metabolism, especially iron overload, is closely related to tumors. On the one hand, iron overload in tumor cells can catalyze the production of ROS, which can meet the needs of their proliferation to a certain extent; on the other hand, when tumor cells are exposed to drugs, they induce large amounts of ROS production, and the excessive accumulation of ROS brings great challenges for the survival of tumor cells. Once tumor cells activate a certain mechanism to change their metabolic microenvironment and inhibit the formation of ROS, drug resistance is developed (Chen et al., 2016). For example, the treatment of cervical cancer cells with deferoxamine (DFO) can enhance their sensitivity to oxaliplatin, indicating that iron overload is also a factor that regulates tumor resistance (Galadari et al., 2017). The production of ROS and ferroptosis caused by iron-triggered oxidative damage are closely related to the drug resistance of tumors (Watson, 2013). For example, oxidative stress related to ferroptosis is also an important factor in the resistance of pancreatic cancer to gemcitabine. In view of the core position of gemcitabine in the treatment of pancreatic cancer, many scholars have made efforts in this field. Nrf2 is commonly believed to play a key role in this process (Yang et al., 2021b).

Nrf2 is an important antioxidant defense system, and it plays a negative role in the regulation of ferroptosis. In liver cancer, the p62–Keap1–Nrf2 signaling pathway can inhibit ferroptosis induced by erastin and sorafenib (Sun et al., 2016b). Similarly, in NSCLC, the activation of the Keap1–Nrf2 signaling pathway can comprehensively improve the resistance of tumor cells to radiotherapy, chemotherapy, and TKIs, and is significantly associated with a shorter overall survival in patients (Dempke and Reck, 2021). Inhibiting the Keap1–Nrf2 pathway can promote ferroptosis of head and neck tumor cells and reverse the phenomenon of cisplatin resistance (Roh et al., 2017). The resistance of head and neck tumors to GPX4 inhibitors is due to the activation of the Nrf2 signaling pathway (Shin et al., 2018). iASPP is a P53 inhibitor that suppresses the ubiquitination and degradation of Nrf2, increases its accumulation, and reduces the production of ROS. It has been shown to promote tumor proliferation and increase tumor resistance to drugs *in vitro* and *in vivo* (Chen et al., 2017). ARF is an alternative reading frame product of the CDKN2A locus, which can inhibit tumors by inhibiting the negative regulators of MDM2 and ARF-BP1 (HUWE1), E3 ubiquitin ligase, and TP53 (Sherr, 2006). In addition, ARF can activate the expression of SLC7A11 by inhibiting the transcription of Nrf2, promote ferroptosis by regulating the sensitivity of tumor cells to oxidative stress, and suppress the resistance to drugs (Ge et al., 2017). In liver cancer, the expression level of Nrf2 determines the sensitivity to ferroptosis-targeted therapy (Sun et al., 2016a). Sorafenib, which is widely used to treat liver cancer, is a strong inducer of ferroptosis. The activation of the Nrf2 pathway in hepatocellular carcinoma can up-regulate the expression of

metallothinonein-1G, and promote the resistance to sorafenib by inhibiting ferroptosis (Xie et al., 2016). In fact, the overexpression of Nrf2 can produce resistance to all major classes of chemotherapeutic drugs, such as anthracyclines, mitomycin, platin, antitubulin agents, vinca alkaloids, and cyclophosphamide, and even sexual hormone drugs. This phenomenon is related to the positive regulation of human aldo-keto reductases (AKRs) by Nrf2. AKRs directly participate in drug metabolism or eliminate the cell stress caused by drugs, especially ROS and lipid peroxidation, and promote tumor resistance to these drugs (Penning et al., 2021).

Influencing Tumor Resistance by Regulating the Sensitivity to Ferroptosis

Given that ferroptosis is closely related to a variety of biochemical processes, the sensitivity of tumor cells to ferroptosis can be regulated by intervening in these key processes. For example, erastin significantly enhances the anti-tumor activity of cytarabine and doxorubicin in acute myeloid leukemia (AML) (Conrad et al., 2016). The drug resistance of AML cells can be reversed by inducing ferroptosis (Lu et al., 2017). Kidney cancer, B-cell lymphoma and triple-negative breast cancer are strongly dependent on the expression of GPX4 and xCT (Yu et al., 2015). The tumor suppressor effect of P53 is related to the inhibition of xCT on the cell membrane and induction of ferroptosis in tumors. According to the classic tumor suppressor effect of P53, ferroptosis may play a key role in the occurrence of tumors (Drayton et al., 2014).

Many ncRNAs are also involved in the regulation of ferroptosis. For example, the aforementioned lncRNA P53RRA participates in ferroptosis by regulating the expression of P53, mediating tumor resistance to drugs (Doll et al., 2019). MiR-27a reverses the resistance of bladder cancer cells to cisplatin through targeted regulation of SLC7A11 (Jiang et al., 2015). In oral squamous cell carcinoma, miR-375 can inhibit SLC7A11 transcription and regulate tumor resistance (Wu et al., 2017).

Ferroptosis and Tumor Resistance to Cisplatin

After treatment of a variety of tumor cells with cisplatin, apoptosis and ferroptosis could occur at the same time. The currently known mechanisms of drug resistance can all affect cisplatin-induced apoptosis, but no effect has been found on cisplatin-induced ferroptosis (Guo et al., 2018). Hence, ferroptosis is different from apoptosis, which provides a new idea for solving the problem of cisplatin resistance. After pretreatment of cisplatin-resistant ovarian cancer cells with erastin, the sensitivity to cisplatin is increased, and it shows a good synergistic effect between erastin and cisplatin (Sato et al., 2018; Cheng et al., 2021). In cisplatin-resistant gastric cancer, the high expression of ATF3 can cooperate with erastin to inhibit the Keap1–Nrf2–xCT pathway, promote the ferroptosis of cancer cells, and reverse cisplatin resistance (Fu et al., 2021). However, cisplatin is not always sensitive to ferroptosis inducers in cancer cell lines. Usually, RAS mutations cause iron overload, making cells more sensitive to ferroptosis inducers (Steuer et al., 2016). About 20% of human tumors have activating mutations in RAS, and they are usually associated with drug resistance (Yang and Stockwell, 2008; Young et al., 2013). Studies have found that transient exposure of cells to low erastin concentrations can produce strong and long-lasting inhibition of xCT, leading to GSH depletion. Importantly, short-term exposure of tumor cells to erastin strongly enhances the cytotoxicity of cisplatin, thereby effectively eradicating tumor cells, which may provide guidance for cisplatin combined with erastin to treat tumors (Sato et al., 2018). Considering that cisplatin exhibits good anti-tumor efficacy in a variety of tumors, the therapeutic method of cisplatin combined with induction of ferroptosis has great potential. Moreover, it can be used to develop new ways in reversing drug resistance and expanding the application of classic therapy.

Ferroptosis and Resistance to Targeted and Immunotherapy

The prevalence and effectiveness of molecular targeted therapy have been widely recognized. Evidence shows that ferroptosis can prevent acquired resistance to multiple targeted therapies, such as: lapatinib, erlotinib, trametinib, dabrafenib, and vemurafenib (Hangauer et al., 2017; Viswanathan et al., 2017; Tsoi et al., 2018). These targeted drug-resistant tumor cell lines express EMT markers and become more sensitive to ferroptosis (Hangauer et al., 2017; Viswanathan et al., 2017; Tsoi et al., 2018). EMT means that epithelial cells lose their characteristic polarity and adhesion ability, and acquire the ability of migration and invasion related to the mesenchymal phenotype (Yang et al., 2021a). EMT has been proven to make tumor cells resistant to drugs, which is stimulated by transcription factors, such as TWIST1 and ZEB1 (Yang et al., 2021a). For example, β-elemene can increase the sensitivity of KRAS mutant colorectal cancer cells to cetuximab by inducing ferroptosis and inhibiting EMT (Chen et al., 2020). Therefore, ferroptosis can not only regulate tumor resistance to targeted drugs, but may also be closely related to EMT.

PD-1 and PD-L1 targeted agents have been approved by the Food and Drug Administration for the treatment of a variety of tumors. Anti-PD-L1 antibody can promote lipid peroxide-dependent ferroptosis in tumor cells, and the use of ferroptosis inhibitors can inhibit the anti-tumor efficacy of anti-PD-L1 antibody. The combination of anti-PD-L1 antibody and ferroptosis inducers has been inferred to greatly inhibit tumor growth (Liu J. et al., 2018). The mechanism is related to the release of interferon-γ by cytotoxic T cells, which activate STAT1 and inhibits xCT expression, resulting in the promotion of ferroptosis (Liu J. et al., 2018). The use of ferroptosis inducers that activate STAT1 can effectively prevent tumor resistance to immunotherapy and provide a broad prospect for the clinical application of ferroptosis inducers and ICIs.

FUTURE PROSPECTS

Ferroptosis responds to a complex regulatory network, including epigenetic, pre-transcriptional, post-transcriptional, and post-

translational modification (Praticò and Sung, 2004). Because tumor cells are usually particularly sensitive to the signals that maintain survival or induce death, they are particularly susceptible to ferroptosis. Many factors that are conducive to tumor growth, such as iron accumulation, increased lipid synthesis, or EMT, can make tumor cells more sensitive to ferroptosis. A variety of chemotherapeutic agents also exert anti-tumor activity by inducing oxidative stress, interfering with the anabolism of genetic substances and other means, and exert a synergistic anti-cancer effect with ferroptosis. However, how to target tumor cells to induce ferroptosis is a tough problem at present. This is because excessive induction of ferroptosis usually causes certain damage to normal tissues. For example, iron deposition often occurs in the process of brain aging, mainly in the substantia nigra, globular nucleus, caudate nucleus, and cerebral cortex. Ferroptosis induced by deposited iron is often closely related to neurodegenerative diseases (Tang et al., 2021). Alzheimer's disease (AD) is the most common neurodegenerative disease that causes cognitive dysfunction. The pathological characteristics of AD are the accumulation of lipid peroxides and the imbalance of iron homeostasis (Wang et al., 2019). GPX4 gene-deficient mice have the biochemical characteristics of ferroptosis and the performance of AD, and AD performance can be alleviated by ferroptosis inhibitors (Ward et al., 2014). Except for neurological diseases, ferroptosis also plays an important role in ischemia–reperfusion injury (Hu et al., 2019). Ferroptosis inhibitors have been used to treat intestinal injury and rhabdomyolysis caused by ischemia–reperfusion (Martin-Sanchez et al., 2017; Li et al., 2019). In addition, inhibitors of ferroptosis have good renal protection effect in the model of acute kidney injury (Skouta et al., 2014; Yan et al., 2020). Targeting ferroptosis in tumor cells to avoid the occurrence in normal tissues is of great significance for the precise treatment of tumors, and it is also one of the urgent problems that need to be solved in the current research field of ferroptosis.

Nano-vehicle agents may provide a solution for targeting tumor cell ferroptosis. Compared with traditional drugs, nano-vehicle agents can greatly improve the ability to selectively kill tumors and increase tumor treatment effects (Hussain et al., 2021). By carrying ferroptosis inducers on nano-vehicles, the solubility, biocompatibility, and tumor targeting can be greatly improved (Kim et al., 2016). For example, ferroptosis inducers and chemotherapeutic agents have been loaded into silica nanoparticles. These nanoparticles can attract iron in the extracellular environment, increase the iron content in tumor cells, and express ferritin *in vivo*. Inhibiting the expression of GSH will increase the level of intracellular ROS and promote ferroptosis (Ma et al., 2017). Iron can also be directly loaded into nanoparticles, such as ferric oxide nanoparticles or platinum–iron nanoparticles. When these nanoparticles reach the tumor site, they will release iron and promote ferroptosis of cells (Yue et al., 2018; Zhang et al., 2019). According to the mechanism of ferroptosis, nanoparticles also have various designs, which can act on mechanisms such as iron, lipid, or amino acid metabolism. For example, because the catalytic effect of Fe^{2+} is better that of than Fe^{3+}, you can choose to directly increase the concentration of Fe^{2+} in the cell or carry Fe^{3+} and tannic acid at the same time, which can reduce Fe^{3+} to Fe^{2+}, so that the cell will be maintained in the process of ferroptosis (Lin et al., 2018; Liu T. et al., 2018). In addition, the substrate required to produce ROS can be carried in nanoparticles, which directly increases the level of intracellular ROS, thereby improving the efficacy of the drug (Zheng et al., 2017). The mechanism of nano-vehicles in targeting tumors is related not only to the specific antigen expressed on tumors, but also to the difference between normal tissue and TME (Dai et al., 2017). Therefore, the future design of nano-vehicle agents should also focus on targeting the TME, and promoting ferroptosis in tumor cells by reshaping the TME may be able to bring a new strategy for tumor treatment.

CONCLUSION

Ferroptosis is a novel type of RCD, and its mechanism and application are in a period of rapid development. The core mechanism is iron metabolism and lipid peroxides. The discovery of FSP1 as a negative regulator enriches the connotation of ferroptosis. The in-depth study of ferroptosis also provides more possible therapeutic targets for tumor treatment. New drugs and treatment methods for these targets are expected to be developed. At present, resistance to traditional chemotherapy, targeted therapy, or immunotherapy agents is the most critical factor for refractory tumor or recurrence. Due to the universality of the drug resistance mechanism, when tumor cells are resistant to a drug, they usually have different degrees of resistance to other drugs of the same type. A small number of tumor cells even appear multi-drug resistant, which greatly impairs the efficacy of the drug and shortens the survival time of patients. Many studies have confirmed that ferroptosis can promote tumor cell death through synergistic effects with anti-tumor drugs, improve drug efficacy, and even reverse drug resistance. It provides a new treatment strategy for patients with drug resistance. Compared with normal cells, the dependence of tumor cells on iron makes them more sensitive to iron load and ROS accumulation. Therefore, targeting iron ions is a feasible method that can improve the efficacy and reduce the side effects of treatment. Cross-field technologies can be combined. For example, the combination of nano-vehicle agents and ferroptosis may be more suitable for tumor treatment. However, before clinical application, many problems still need to be solved. For example, although many methods can be used to detect the level of ferroptosis *in vitro*, better methods for evaluating ferroptosis *in vivo* are still lacking. Without sensitive and accurate detection indicators, the drug's efficacy cannot be accurately detected leading to risks and injuries caused by treatment. Second, whether the compound targeted to the ferroptosis regulator can maintain a high degree of specificity and minimize side effects in preclinical or clinical applications must be clarified. Finally, which types or characteristics of tumors, such as tumors with certain gene mutations, are more susceptible to ferroptosis remains to be elucidated. However, it is undeniable that in-depth studies of the mechanism of ferroptosis and tumor drug resistance will surely create new opportunities for tumor diagnosis and treatment.

AUTHOR CONTRIBUTIONS

ZN and SZ conceived and designed the framework of the study. MC, YG, DH, HC, YP, and NG collected and reviewed the data. ZN wrote the manuscript. SZ and FW reviewed and edited the manuscript. All authors contributed to the article and approved the submitted version.

FUNDING

This work was supported by the National Nature Science Foundation of China (grant Nos 81760465, 82160531, and 82060461), the Finance Science and Technology Project of Hainan Province (grant numbers ZDYF2019163, ZDKJ2017007, and ZDYF2021SHFZ096).

REFERENCES

Agyeman, A. S., Chaerkady, R., Shaw, P. G., Davidson, N. E., Visvanathan, K., and Pandey, A. (2012). Transcriptomic and Proteomic Profiling of KEAP1 Disrupted and Sulforaphane-Treated Human Breast Epithelial Cells Reveals Common Expression Profiles. *Breast cancer Res. Treat.* 132 (1), 175–187. doi:10.1007/s10549-011-1536-9

Al-Hajj, M., Wicha, M. S., Benito-Hernandez, A., Morrison, S. J., and Clarke, M. F. (2003). Prospective Identification of Tumorigenic Breast Cancer Cells. *Proc. Natl. Acad. Sci.* 100 (7), 3983–3988. doi:10.1073/pnas.0530291100

Amaral, T., Meraz-Torres, F., and Garbe, C. (2017). Immunotherapy in Managing Metastatic Melanoma: Which Treatment when? *Expert Opin. Biol. Ther.* 17 (12), 1523–1538. doi:10.1080/14712598.2017.1378640

Balaban, N., Merrin, J., Chait, R., Kowalik, L., and Leibler, S. (2004). Bacterial Persistence as a Phenotypic Switch. *Science* 305 (5690), 1622–1625. doi:10.1126/science.1099390

Bean, J., Brennan, C., Shih, J. Y., Riely, G., Viale, A., Wang, L., et al. (2007). MET Amplification Occurs with or without T790M Mutations in EGFR Mutant Lung Tumors with Acquired Resistance to Gefitinib or Erlotinib. *Proc. Natl. Acad. Sci. U. S. A.* 104 (52), 20932–20937. doi:10.1073/pnas.0710370104

Bersuker, K., Hendricks, J., Li, Z., Magtanong, L., Ford, B., Tang, P., et al. (2019). The CoQ Oxidoreductase FSP1 Acts Parallel to GPX4 to Inhibit Ferroptosis. *Nature* 575 (7784), 688–692. doi:10.1038/s41586-019-1705-2

Bhowmick, N. A., Neilson, E. G., and Moses, H. L. (2004). Stromal Fibroblasts in Cancer Initiation and Progression. *Nature* 432 (7015), 332–337. doi:10.1038/nature03096

Blakely, C., Pazarentzos, E., Olivas, V., Asthana, S., Yan, J., Tan, I., et al. (2015). NF-κB-activating Complex Engaged in Response to EGFR Oncogene Inhibition Drives Tumor Cell Survival and Residual Disease in Lung Cancer. *Cell Rep.* 11 (1), 98–110. doi:10.1016/j.celrep.2015.03.012

Blakely, C., Watkins, T., Wu, W., Gini, B., Chabon, J., McCoach, C., et al. (2017). Evolution and Clinical Impact of Co-occurring Genetic Alterations in Advanced-Stage EGFR-Mutant Lung Cancers. *Nat. Genet.* 49 (12), 1693–1704. doi:10.1038/ng.3990

Bonnet, D., and Dick, J. E. (1997). Human Acute Myeloid Leukemia Is Organized as a Hierarchy that Originates from a Primitive Hematopoietic Cell. *Nat. Med.* 3 (7), 730–737. doi:10.1038/nm0797-730

Bridges, R., Natale, N., and Patel, S. (2012). System Xc^- Cystine/glutamate Antiporter: an Update on Molecular Pharmacology and Roles within the CNS. *Br. J. Pharmacol.* 165 (1), 20–34. doi:10.1111/j.1476-5381.2011.01480.x

Cao, J., and Dixon, S. (2016). Mechanisms of Ferroptosis. *Cell. Mol. life Sci. CMLS* 73, 2195–2209. doi:10.1007/s00018-016-2194-1

Cao, L., Zhou, Y., Zhai, B., Liao, J., Xu, W., Zhang, R., et al. (2011). Sphere-forming Cell Subpopulations with Cancer Stem Cell Properties in Human Hepatoma Cell Lines. *BMC Gastroenterol.* 11 (1), 71. doi:10.1186/1471-230X-11-71

Cao, W., Chen, H. D., Yu, Y. W., Li, N., and Chen, W. Q. (2021). Changing Profiles of Cancer Burden Worldwide and in China: a Secondary Analysis of the Global Cancer Statistics 2020. *Chin. Med. J.* 134 (7), 9. doi:10.1097/CM9.0000000000001474

Caterino, M., Ruoppolo, M., Mandola, A., Costanzo, M., Orrù, S., and Imperlini, E. (2017). Protein-protein Interaction Networks as a New Perspective to Evaluate Distinct Functional Roles of Voltage-dependent Anion Channel Isoforms. *Mol. Biosyst.* 13 (12), 2466–2476. doi:10.1039/c7mb00434f

Charles, S. (2012). Intratumor Heterogeneity: Evolution through Space and Time. *Cancer Res.* 72 (19), 4875–4882. doi:10.1158/0008-5472.can-12-2217

Chatterjee, N., and Bivona, T. (2019). Polytherapy and Targeted Cancer Drug Resistance. *Trends cancer* 5 (3), 170–182. doi:10.1016/j.trecan.2019.02.003

Chen, D., Tavana, O., Chu, B., Erber, L., Chen, Y., Baer, R., et al. (2017). NRF2 Is a Major Target of ARF in P53-independent Tumor Suppression. *Mol. Cell* 68 (1), 224–232. e224. doi:10.1016/j.molcel.2017.09.009

Chen, P., Li, X., Zhang, R., Liu, S., Xiang, Y., Zhang, M., et al. (2020). Combinative Treatment of β-elemene and Cetuximab Is Sensitive to KRAS Mutant Colorectal Cancer Cells by Inducing Ferroptosis and Inhibiting Epithelial-Mesenchymal Transformation. *Theranostics* 10 (11), 5107–5119. doi:10.7150/thno.44705

Chen, S., Kuo, C., Pan, H., Tsou, T., Yeh, S., and Chang, J. (2016). Desferal Regulates hCtr1 and Transferrin Receptor Expression through Sp1 and Exhibits Synergistic Cytotoxicity with Platinum Drugs in Oxaliplatin-Resistant Human Cervical Cancer Cells *In Vitro* and *In Vivo*. *Oncotarget* 7 (31), 49310–49321. doi:10.18632/oncotarget.10336

Cheng, Q., Bao, L., Li, M., Chang, K., and Yi, X. (2021). Erastin Synergizes with Cisplatin via Ferroptosis to Inhibit Ovarian Cancer Growth *In Vitro* and *In Vivo*. *J. obstetrics Gynaecol. Res.* 47 (7), 2481–2491. doi:10.1111/jog.14779

Cioffi, M., Trabulo, S. M., Sanchez-Ripoll, Y., Miranda-Lorenzo, I., Lonardo, E., Dorado, J., et al. (2015). The miR-17-92 Cluster Counteracts Quiescence and Chemoresistance in a Distinct Subpopulation of Pancreatic Cancer Stem Cells. *Gut* 64 (12), 1936–1948. doi:10.1136/gutjnl-2014-308470

Clarke, M. F., Dick, J. E., Dirks, P. B., Eaves, C. J., Jamieson, C., Jones, D. L., et al. (2006). Cancer Stem Cells—Perspectives on Current Status and Future Directions: AACR Workshop on Cancer Stem Cells. *Cancer Res.* 66 (19), 9339–9344. doi:10.1158/0008-5472.CAN-06-3126

Concannon, K., Faber, A. C., Rivera, M. N., Lockerman, E. L., Turke, A. B., Boulay, G., et al. (2015). Inhibition of Mutant EGFR in Lung Cancer Cells Triggers SOX2-FOXO6-dependent Survival Pathways. *eLife* 4, e06132. doi:10.7554/eLife.06132

Conrad, M., Angeli, J., Vandenabeele, P., and Stockwell, B. (2016). Regulated Necrosis: Disease Relevance and Therapeutic Opportunities. *Nat. Rev. Drug Discov.* 15 (5), 348–366. doi:10.1038/nrd.2015.6

Cros, E., Jordheim, L., Dumontet, C., and Galmarini, C. M. (2009). Problems Related to Resistance to Cytarabine in Acute Myeloid Leukemia. *Leukemia Lymphoma* 45 (6), 1123–1132. doi:10.1080/1042819032000159861

D'Herde, K., and Krysko, D. (2017). Ferroptosis: Oxidized PEs Trigger Death. *Nat. Chem. Biol.* 13 (1), 4–5. doi:10.1038/nchembio.2261

Dai, Y., Xu, C., Sun, X., and Chen, X. (2017). Nanoparticle Design Strategies for Enhanced Anticancer Therapy by Exploiting the Tumour Microenvironment. *Chem. Soc. Rev.* 46 (12), 3830–3852. doi:10.1039/c6cs00592f

De Andres, F., and Llerena, A. (2016). Simultaneous Determination of Cytochrome P450 Oxidation Capacity in Humans: A Review on the Phenotyping Cocktail Approach. *Curr. Pharm. Biotechnol.* 17 (13), 1159–1180. doi:10.2174/1389201017666160926150117

Dempke, W., and Reck, M. (2021). KEAP1/NRF2 (NFE2L2) Mutations in NSCLC - Fuel for a Superresistant Phenotype? *Lung cancer* 159, 10–17. (Amsterdam, Netherlands). doi:10.1016/j.lungcan.2021.07.006

Dixon, S. J., Winter, G. E., Musavi, L. S., Lee, E., Snijder, B., Rebsamen, M., et al. (2015). Human Haploid Cell Genetics Reveals Roles for Lipid Metabolism Genes in Nonapoptotic Cell Death. *ACS Chem. Biol.* 10 (7), 1604–1609. doi:10.1021/acschembio.5b00245

Dixon, S., Lemberg, K., Lamprecht, M., Skouta, R., Zaitsev, E., Gleason, C., et al. (2012). Ferroptosis: an Iron-dependent Form of Nonapoptotic Cell Death. *Cell* 149 (5), 1060–1072. doi:10.1016/j.cell.2012.03.042

Dobbs, J. L., Shin, D., Krishnamurthy, S., Kuerer, H., Yang, W., and Richards-Kortum, R. (2016). Confocal Fluorescence Microscopy to Evaluate Changes in Adipocytes in the Tumor Microenvironment Associated with Invasive Ductal Carcinoma and Ductal Carcinoma *In Situ*. *Int. J. Cancer* 139 (5), 1140–1149. doi:10.1002/ijc.30160

Dodson, M., Castro-Portuguez, R., and Zhang, D. (2019). NRF2 Plays a Critical Role in Mitigating Lipid Peroxidation and Ferroptosis. *Redox Biol.* 23, 101107. doi:10.1016/j.redox.2019.101107

Doll, S., and Conrad, M. (2017). Iron and Ferroptosis: A Still Ill-Defined Liaison. *IUBMB life* 69 (6), 423–434. doi:10.1002/iub.1616

Doll, S., Freitas, F., Shah, R., Aldrovandi, M., da Silva, M., Ingold, I., et al. (2019). FSP1 Is a Glutathione-independent Ferroptosis Suppressor. *Nature* 575 (7784), 693–698. doi:10.1038/s41586-019-1707-0

Doll, S., Proneth, B., Tyurina, Y. Y., Panzilius, E., Kobayashi, S., Ingold, I., et al. (2016). ACSL4 Dictates Ferroptosis Sensitivity by Shaping Cellular Lipid Composition. *Nat. Chem. Biol.* 13, 91–98. doi:10.1038/nchembio.2239

Dolma, S., Lessnick, S. L., Hahn, W. C., and Stockwell, B. R. (2003). Identification of Genotype-Selective Antitumor Agents Using Synthetic Lethal Chemical Screening in Engineered Human Tumor Cells - ScienceDirect. *Cancer Cell* 3 (3), 285–296. doi:10.1016/s1535-6108(03)00050-3

Drayton, R., Dudziec, E., Peter, S., Bertz, S., Hartmann, A., Bryant, H., et al. (2014). Reduced Expression of miRNA-27a Modulates Cisplatin Resistance in Bladder Cancer by Targeting the Cystine/glutamate Exchanger SLC7A11. *Clin. Cancer Res.* 20 (7), 1990–2000. doi:10.1158/1078-0432.Ccr-13-2805

Feng, H., and Stockwell, B. (2018). Unsolved Mysteries: How Does Lipid Peroxidation Cause Ferroptosis? *PLoS Biol.* 16 (5), e2006203. doi:10.1371/journal.pbio.2006203

Fisher, R., Gollan, B., and Helaine, S. (2017). Persistent Bacterial Infections and Persister Cells. *Nat. Rev. Microbiol.* 15 (8), 453–464. doi:10.1038/nrmicro.2017.42

Fleming, R., and Bacon, B. (2005). Orchestration of Iron Homeostasis. *N. Engl. J. Med.* 352 (17), 1741–1744. doi:10.1056/NEJMp048363

Flinders, C., Lam, L., Rubbi, L., Ferrari, R., Fitz-Gibbon, S., Chen, P. Y., et al. (2016). Epigenetic Changes Mediated by Polycomb Repressive Complex 2 and E2a Are Associated with Drug Resistance in a Mouse Model of Lymphoma. *Genome Med.* 8 (1), 54. doi:10.1186/s13073-016-0305-0

Fu, D., Wang, C., Yu, L., and Yu, R. (2021). Induction of Ferroptosis by ATF3 Elevation Alleviates Cisplatin Resistance in Gastric Cancer by Restraining Nrf2/Keap1/xCT Signaling. *Cell. Mol. Biol. Lett.* 26 (1), 26. doi:10.1186/s11658-021-00271-y

Gajewski, T. F., Schreiber, H., and Fu, Y. X. (2013). Innate and Adaptive Immune Cells in the Tumor Microenvironment. *Nat. Immunol.* 14 (10), 1014–1022. doi:10.1038/ni.2703

Galadari, S., Rahman, A., Pallichankandy, S., and Thayyullathil, F. (2017). Reactive Oxygen Species and Cancer Paradox: To Promote or to Suppress? *Free Radic. Biol. Med.* 104, 144–164. doi:10.1016/j.freeradbiomed.2017.01.004

Gao, M., Monian, P., Quadri, N., Ramasamy, R., and Jiang, X. (2015). Glutaminolysis and Transferrin Regulate Ferroptosis. *Mol. Cell* 59 (2), 298–308. doi:10.1016/j.molcel.2015.06.011

Gaschler, M., and Stockwell, B. (2017). Lipid Peroxidation in Cell Death. *Biochem. biophysical Res. Commun.* 482 (3), 419–425. doi:10.1016/j.bbrc.2016.10.086

Ge, W., Zhao, K., Wang, X., Li, H., Yu, M., He, M., et al. (2017). iASPP Is an Antioxidative Factor and Drives Cancer Growth and Drug Resistance by Competing with Nrf2 for Keap1 Binding. *Cancer Cell* 32 (5), 561–573. e566. doi:10.1016/j.ccell.2017.09.008

Gerlinger, M., and Swanton, C. (2010). How Darwinian Models Inform Therapeutic Failure Initiated by Clonal Heterogeneity in Cancer Medicine. *Br. J. Cancer* 103 (8), 1139–1143. doi:10.1038/sj.bjc.6605912

Gilbert, L., and Hemann, M. (2010). DNA Damage-Mediated Induction of a Chemoresistant Niche. *Cell* 143 (3), 355–366. doi:10.1016/j.cell.2010.09.043

Gorre, M. E., Mohammed, M., Ellwood, K., Hsu, N., Paquette, R., Rao, P. N., et al. (2001). Clinical Resistance to STI-571 Cancer Therapy Caused by BCR-ABL Gene Mutation or Amplification. *Science* 293 (5531), 876–880. doi:10.1126/science.1062538

Greaves, M., and Maley, C. C. (2012). Clonal Evolution in Cancer. *Nature* 481 (7381), 306–313. doi:10.1038/nature10762

Guengerich, F. P. (1997). Role of Cytochrome P450 Enzymes in Drug-Drug Interactions. *Adv. Pharmacol.* 43, 7–35. doi:10.1016/s1054-3589(08)60200-8

Guo, J., Xu, B., Han, Q., Zhou, H., Xia, Y., Gong, C., et al. (2018). Ferroptosis: A Novel Anti-tumor Action for Cisplatin. *Cancer Res. Treat.* 50 (2), 445–460. doi:10.4143/crt.2016.572

Hangauer, M., Viswanathan, V., Ryan, M., Bole, D., Eaton, J., Matov, A., et al. (2017). Drug-tolerant Persister Cancer Cells Are Vulnerable to GPX4 Inhibition. *Nature* 551 (7679), 247–250. doi:10.1038/nature24297

Harada, N., Kanayama, M., Maruyama, A., Yoshida, A., Tazumi, K., Hosoya, T., et al. (2011). Nrf2 Regulates Ferroportin 1-mediated Iron Efflux and Counteracts Lipopolysaccharide-Induced Ferroportin 1 mRNA Suppression in Macrophages. *Archives Biochem. biophysics* 508 (1), 101–109. doi:10.1016/j.abb.2011.02.001

Hata, A. N., Niederst, M. J., Archibald, H. L., Gomez-Caraballo, M., Siddiqui, F. M., Mulvey, H. E., et al. (2016). Tumor Cells Can Follow Distinct Evolutionary Paths to Become Resistant to Epidermal Growth Factor Receptor Inhibition. *Nat. Med.* 22 (3), 262–269. doi:10.1038/nm.4040

Hentrich, M., and Barta, S. K. (2016). HIV-associated Hematological Malignancies. *Anticancer Res.* 36 (4), 2046.

Hentze, M., Muckenthaler, M., Galy, B., and Camaschella, C. (2010). Two to Tango: Regulation of Mammalian Iron Metabolism. *Cell* 142 (1), 24–38. doi:10.1016/j.cell.2010.06.028

Holden, D. (2015). Microbiology. Persisters Unmasked. *Science* 347 (6217), 30–32. doi:10.1126/science.1262033

Holohan, C., Van Schaeybroeck, S., Longley, D., and Johnston, P. (2013). Cancer Drug Resistance: an Evolving Paradigm. *Nat. Rev. Cancer* 13 (10), 714–726. doi:10.1038/nrc3599

Hu, G, Li, F, Ouyang, K, Xie, F., Tang, X., Wang, K., et al. (2012). Intrinsic Gemcitabine Resistance in a Novel Pancreatic Cancer Cell Line Is Associated with Cancer Stem Cell-like Phenotype. *Int. J. Oncol.* 40 (3), 798–806. doi:10.3892/ijo.2011.1254

Hu, W., Zhang, C., Wu, R., Sun, Y., Levine, A., and Feng, Z. (2010). Glutaminase 2, a Novel P53 Target Gene Regulating Energy Metabolism and Antioxidant Function. *Proc. Natl. Acad. Sci. U. S. A.* 107 (16), 7455–7460. doi:10.1073/pnas.1001006107

Hu, Z., Zhang, H., Yang, S., Wu, X., He, D., Cao, K., et al. (2019). Emerging Role of Ferroptosis in Acute Kidney Injury. *Oxidative Med. Cell. Longev.* 2019, 8010614. doi:10.1155/2019/8010614

Huang, C., Yang, M., Deng, J., Li, P., Su, W., and Jiang, R. (2018). Upregulation and Activation of P53 by Erastin-Induced Reactive Oxygen Species Contribute to Cytotoxic and Cytostatic Effects in A549 Lung Cancer Cells. *Oncol. Rep.* 40 (4), 2363–2370. doi:10.3892/or.2018.6585

Hussain, Y., Mirzaei, S., Ashrafizadeh, M., Zarrabi, A., Hushmandi, K., Khan, H., et al. (2021). Quercetin and its Nano-Scale Delivery Systems in Prostate Cancer Therapy: Paving the Way for Cancer Elimination and Reversing Chemoresistance. *Cancers* 13 (7), 1602. doi:10.3390/cancers13071602

Ireland, L., Santos, A., Ahmed, M. S., Rainer, C., and Mielgo, A. (2016). Chemoresistance in Pancreatic Cancer Is Driven by Stroma-Derived Insulin-like Growth Factors. *Cancer Res.* 76 (23), 6851–6863. doi:10.1158/0008-5472.CAN-16-1201

Jamal-Hanjani, M., Wilson, G., McGranahan, N., Birkbak, N., Watkins, T., Veeriah, S., et al. (2017). Tracking the Evolution of Non-small-cell Lung Cancer. *N. Engl. J. Med.* 376 (22), 2109–2121. doi:10.1056/NEJMoa1616288

Jang, J. Y., Kim, M. K., Jeon, Y. K., Joung, Y. K., Park, K. D., and Kim, C. W. (2012). Adenovirus Adenine Nucleotide Translocator-2 shRNA Effectively Induces Apoptosis and Enhances Chemosensitivity by the Down-Regulation of ABCG2 in Breast Cancer Stem-like Cells. *Exp. Mol. Med.* 44 (4), 251–259. doi:10.3858/emm.2012.44.4.019

Jenkins, R. W., Barbie, D. A., and Flaherty, K. T. (2018). Mechanisms of Resistance to Immune Checkpoint Inhibitors. *Br. J. Cancer* 118 (1), 9–16. doi:10.1038/bjc.2017.434

Jiang, L., Kon, N., Li, T., Wang, S., Su, T., Hibshoosh, H., et al. (2015). Ferroptosis as a P53-Mediated Activity during Tumour Suppression. *Nature* 520 (7545), 57–62. doi:10.1038/nature14344

Kagan, V., Mao, G., Qu, F., Angeli, J., Doll, S., Croix, C., et al. (2017). Oxidized Arachidonic and Adrenic PEs Navigate Cells to Ferroptosis. *Nat. Chem. Biol.* 13 (1), 81–90. doi:10.1038/nchembio.2238

Karran, P. (2001). Mechanisms of Tolerance to DNA Damaging Therapeutic Drugs. *Carcinogenesis* 22 (12), 1931–1937. doi:10.1093/carcin/22.12.1931

Kerins, M., and Ooi, A. (2018). The Roles of NRF2 in Modulating Cellular Iron Homeostasis. *Antioxidants redox Signal.* 29 (17), 1756–1773. doi:10.1089/ars.2017.7176

Kim, S., Zhang, L., Ma, K., Riegman, M., Chen, F., Ingold, I., et al. (2016). Ultrasmall Nanoparticles Induce Ferroptosis in Nutrient-Deprived Cancer Cells and Suppress Tumour Growth. *Nat. Nanotechnol.* 11 (11), 977–985. doi:10.1038/nnano.2016.164

Kobayashi, I., Takahashi, F., Nurwidya, F., Nara, T., Hashimoto, M., Murakami, A., et al. (2016). Oct4 Plays a Crucial Role in the Maintenance of Gefitinib-Resistant Lung Cancer Stem Cells. *Biochem. Biophysical Res. Commun.* 473 (1), 125–132. doi:10.1016/j.bbrc.2016.03.064

Kobayashi, S., Boggon, T. J., Dayaram, T., Jnne, P. A., and Halmos, B. (2005). EGFR Mutation and Resistance of Non–small-cell Lung Cancer to Gefitinib. *N. Engl. J. Med.* 352 (8), 786–792. doi:10.1056/NEJMoa044238

Konieczkowski, D., Johannessen, C., Abudayyeh, O., Kim, J., Cooper, Z., Piris, A., et al. (2014). A Melanoma Cell State Distinction Influences Sensitivity to MAPK Pathway Inhibitors. *Cancer Discov.* 4 (7), 816–827. doi:10.1158/2159-8290.Cd-13-0424

Korkaya, H., Kim, G. I., Davis, A., Malik, F., and Wicha, M. S. (2012). Activation of an IL6 Inflammatory Loop Mediates Trastuzumab Resistance in HER2+ Breast Cancer by Expanding the Cancer Stem Cell Population. *Mol. Cell* 47 (4), 570–584. doi:10.1016/j.molcel.2012.06.014

Kort, A., Durmus, S., Sparidans, R. W., Wagenaar, E., Beijnen, J. H., and Schinkel, A. H. (2015). Brain and Testis Accumulation of Regorafenib Is Restricted by Breast Cancer Resistance Protein (BCRP/ABCG2) and P-Glycoprotein (P-GP/ABCB1). *Pharm. Res.* 32 (7), 2205–2216. doi:10.1007/s11095-014-1609-7

Krishnamurthy, P., Du, G., Fukuda, Y., Sun, D., Sampath, J., Mercer, K., et al. (2006). Identification of a Mammalian Mitochondrial Porphyrin Transporter. *Nature* 443 (7111), 586–589. doi:10.1038/nature05125

Kumar, S., and Vaidya, M. (2016). Hypoxia Inhibits Mesenchymal Stem Cell Proliferation through HIF1α-dependent Regulation of P27. *Mol. Cell. Biochem.* 415 (1-2), 29–38. doi:10.1007/s11010-016-2674-5

Kwon, M., Park, E., Lee, S., and Chung, S. (2015). Heme Oxygenase-1 Accelerates Erastin-Induced Ferroptotic Cell Death. *Oncotarget* 6 (27), 24393–24403. doi:10.18632/oncotarget.5162

Lee, H., Zhuang, G., Cao, Y., Du, P., Kim, H., and Settleman, J. (2014). Drug Resistance via Feedback Activation of Stat3 in Oncogene-Addicted Cancer Cells. *Cancer Cell* 26 (2), 207–221. doi:10.1016/j.ccr.2014.05.019

Lemasters, J. (2017). Evolution of Voltage-dependent Anion Channel Function: From Molecular Sieve to Governator to Actuator of Ferroptosis. *Front. Oncol.* 7, 303. doi:10.3389/fonc.2017.00303

Li, J., Alyamani, M., Ao, Z., Kai, H. C., Berk, M., Li, Z., et al. (2016). Aberrant Corticosteroid Metabolism in Tumor Cells Enables GR Takeover in Enzalutamide Resistant Prostate Cancer. *eLife* 6, e20183. doi:10.7554/eLife.20183

Li, Y., Feng, D., Wang, Z., Zhao, Y., Sun, R., Tian, D., et al. (2019). Ischemia-induced ACSL4 Activation Contributes to Ferroptosis-Mediated Tissue Injury in Intestinal Ischemia/reperfusion. *Cell death Differ.* 26 (11), 2284–2299. doi:10.1038/s41418-019-0299-4

Lin, L. S., Song, J., Song, L., Ke, K., Liu, Y., Zhou, Z., et al. (2018). Simultaneous Fenton-like Ion Delivery and Glutathione Depletion by MnO2-Based Nanoagent to Enhance Chemodynamic Therapy. *Angew. Chem. Int. Ed. Engl.* 57 (18), 4902–4906. doi:10.1002/anie.201712027

Liu, J., Fan, Y., Yang, Z., Wang, Z., and Guo, C. (2018). Iron and Alzheimer's Disease: From Pathogenesis to Therapeutic Implications. *Front. Neurosci.* 12, 632. doi:10.3389/fnins.2018.00632

Liu, M., Ge, Y., Payton, S. G., Aboukameel, A., Buck, S., Flatley, R. M., et al. (2006). Transcriptional Regulation of the Human Reduced Folate Carrier in Childhood Acute Lymphoblastic Leukemia Cells. *Clin. Cancer Res.* 12 (2), 608–616. doi:10.1158/1078-0432.CCR-05-1954

Liu, T., Liu, W., Zhang, M., Yu, W., Gao, F., Li, C., et al. (2018). Ferrous-Supply-Regeneration Nanoengineering for Cancer-cell-specific Ferroptosis in Combination with Imaging-Guided Photodynamic Therapy. *ACS Nano* 12 (12), 12181–12192. doi:10.1021/acsnano.8b05860

Lu, B., Chen, X., Ying, M., He, Q., Cao, J., and Yang, B. (2017). The Role of Ferroptosis in Cancer Development and Treatment Response. *Front. Pharmacol.* 8, 992. doi:10.3389/fphar.2017.00992

Ma, P., Xiao, H., Yu, C., Liu, J., Cheng, Z., Song, H., et al. (2017). Enhanced Cisplatin Chemotherapy by Iron Oxide Nanocarrier-Mediated Generation of Highly Toxic Reactive Oxygen Species. *Nano Lett.* 17 (2), 928–937. doi:10.1021/acs.nanolett.6b04269

Maines, M. (1988). Heme Oxygenase: Function, Multiplicity, Regulatory Mechanisms, and Clinical Applications. *FASEB J.* 2 (10), 2557–2568. doi:10.1096/fasebj.2.10.3290025

Maiorino, M., Conrad, M., and Ursini, F. (2018). GPx4, Lipid Peroxidation, and Cell Death: Discoveries, Rediscoveries, and Open Issues. *Antioxidants redox Signal.* 29 (1), 61–74. doi:10.1089/ars.2017.7115

Maldonado, E., Patnaik, J., Mullins, M., and Lemasters, J. (2010). Free Tubulin Modulates Mitochondrial Membrane Potential in Cancer Cells. *Cancer Res.* 70 (24), 10192–10201. doi:10.1158/0008-5472.Can-10-2429

Maldonado, E., Sheldon, K., DeHart, D., Patnaik, J., Manevich, Y., Townsend, D., et al. (2013). Voltage-dependent Anion Channels Modulate Mitochondrial Metabolism in Cancer Cells: Regulation by Free Tubulin and Erastin. *J. Biol. Chem.* 288 (17), 11920–11929. doi:10.1074/jbc.M112.433847

Maldonado, E. (2017). VDAC-tubulin, an Anti-warburg Pro-oxidant Switch. *Front. Oncol.* 7, 4. doi:10.3389/fonc.2017.00004

Mancias, J., Wang, X., Gygi, S., Harper, J., and Kimmelman, A. (2014). Quantitative Proteomics Identifies NCOA4 as the Cargo Receptor Mediating Ferritinophagy. *Nature* 509 (7498), 105–109. doi:10.1038/nature13148

Mandal, S., Mandal, A., and Park, M. (2015). Depletion of the Polyamines Spermidine and Spermine by Overexpression of Spermidine/spermine N^1-Acetyltransferase 1 (SAT1) Leads to Mitochondria-Mediated Apoptosis in Mammalian Cells. *Biochem. J.* 468 (3), 435–447. doi:10.1042/bj20150168

Mao, C., Wang, X., Liu, Y., Wang, M., Yan, B., Jiang, Y., et al. (2018). A G3BP1-Interacting lncRNA Promotes Ferroptosis and Apoptosis in Cancer via Nuclear Sequestration of P53. *Cancer Res.* 78 (13), 3484–3496. doi:10.1158/0008-5472.Can-17-3454

Mare, J. A. D. L., Sterrenberg, J. N., Sukhthankar, M. G., Chiwakata, M. T., and Edkins, A. L. (2013). Assessment of Potential Anti-cancer Stem Cell Activity of Marine Algal Compounds Using an *In Vitro* Mammosphere Assay. *Cancer Cell Int.* 13, 39. doi:10.1186/1475-2867-13-39

Martin-Sanchez, D., Ruiz-Andres, O., Poveda, J., Carrasco, S., Cannata-Ortiz, P., Sanchez-Niño, M., et al. (2017). Ferroptosis, but Not Necroptosis, Is Important in Nephrotoxic Folic Acid-Induced AKI. *J. Am. Soc. Nephrol.* 28 (1), 218–229. doi:10.1681/asn.2015121376

Mazumdar, J., Dondeti, V., and Simon, M. C. (2009). Hypoxia-inducible Factors, Stem Cells, and Cancer. *J. Cell. Mol. Med.* 13 (11-12), 4319–4328. doi:10.1111/j.1582-4934.2009.00963.x

Mazure, N. (2017). VDAC in Cancer. *Biochimica biophysica acta. Bioenergetics* 1858 (8), 665–673. doi:10.1016/j.bbabio.2017.03.002

McKie, A., Barrow, D., Latunde-Dada, G., Rolfs, A., Sager, G., Mudaly, E., et al. (2001). An Iron-Regulated Ferric Reductase Associated with the Absorption of Dietary Iron. *Science* 291 (5509), 1755–1759. doi:10.1126/science.1057206

Meng, E., Mitra, A., Tripathi, K., Finan, M. A., Scalici, J., Mcclellan, S., et al. (2014). ALDH1A1 Maintains Ovarian Cancer Stem Cell-like Properties by Altered Regulation of Cell Cycle Checkpoint and DNA Repair Network Signaling. *Plos One* 9, e107142. doi:10.1371/journal.pone.0107142

Negrini, S., Gorgoulis, V. G., and Halazonetis, T. D. (2010). Genomic Instability—An Evolving Hallmark of Cancer. *Nat. Rev. Mol. Cell Biol.* 11 (3), 220–228. doi:10.1038/nrm2858

Nikolaou, M., Pavlopoulou, A., Georgakilas, A., and Kyrodimos, E. (2018). The Challenge of Drug Resistance in Cancer Treatment: a Current Overview. *Clin. Exp. metastasis* 35 (4), 309–318. doi:10.1007/s10585-018-9903-0

Obenauf, A., Zou, Y., Ji, A., Vanharanta, S., Shu, W., Shi, H., et al. (2015). Therapy-induced Tumour Secretomes Promote Resistance and Tumour Progression. *Nature* 520 (7547), 368–372. doi:10.1038/nature14336

Ou, Y., Wang, S., Li, D., Chu, B., and Gu, W. (2016). Activation of SAT1 Engages Polyamine Metabolism with P53-Mediated Ferroptotic Responses. *Proc. Natl. Acad. Sci. U. S. A.* 113 (44), E6806–E6812. doi:10.1073/pnas.1607152113

Pao, W., Miller, V. A., Politi, K. A., Riely, G. J., Somwar, R., Zakowski, M. F., et al. (2005). Acquired Resistance of Lung Adenocarcinomas to Gefitinib or Erlotinib Is Associated with a Second Mutation in the EGFR Kinase Domain. *Plos Med.* 2 (3), e73. doi:10.1371/journal.pmed.0020073

Peiris-Pagès, M., Martinez-Outschoorn, U. E., Pestell, R. G., Sotgia, F., and Lisanti, M. P. (2016). Cancer Stem Cell Metabolism. *Breast Cancer Res.* 18 (1), 55. doi:10.1186/s13058-016-0712-6

Penning, T., Jonnalagadda, S., Trippier, P., and Rižner, T. (2021). Aldo-Keto Reductases and Cancer Drug Resistance. *Pharmacol. Rev.* 73 (3), 1150–1171. doi:10.1124/pharmrev.120.000122

Perrier, A., Didelot, A., Laurent-Puig, P., Blons, H., and Garinet, S. (2020). Epigenetic Mechanisms of Resistance to Immune Checkpoint Inhibitors. *Biomolecules* 10 (7), 1061. doi:10.3390/biom10071061

Piotrowska, Z., Niederst, M., Karlovich, C., Wakelee, H., Neal, J., Mino-Kenudson, M., et al. (2015). Heterogeneity Underlies the Emergence of EGFRT790 Wild-type Clones Following Treatment of T790M-Positive Cancers with a Third-Generation EGFR Inhibitor. *Cancer Discov.* 5 (7), 713–722. doi:10.1158/2159-8290.Cd-15-0399

Praticò, D., and Sung, S. (2004). Lipid Peroxidation and Oxidative Imbalance: Early Functional Events in Alzheimer's Disease. *J. Alzheimer's Dis.* 6 (2), 171–175. doi:10.3233/jad-2004-6209

Reina, S., and De Pinto, V. (2017). Anti-Cancer Compounds Targeted to VDAC: Potential and Perspectives. *Curr. Med. Chem.* 24 (40), 4447–4469. doi:10.2174/0929867324666170530074039

Roh, J., Kim, E., Jang, H., and Shin, D. (2017). Nrf2 Inhibition Reverses the Resistance of Cisplatin-Resistant Head and Neck Cancer Cells to Artesunate-Induced Ferroptosis. *Redox Biol.* 11, 254–262. doi:10.1016/j.redox.2016.12.010

Rostovtseva, T., Sheldon, K., Hassanzadeh, E., Monge, C., Saks, V., Bezrukov, S., et al. (2008). Tubulin Binding Blocks Mitochondrial Voltage-dependent Anion Channel and Regulates Respiration. *Proc. Natl. Acad. Sci. U. S. A.* 105 (48), 18746–18751. doi:10.1073/pnas.0806303105

Rouault, T. (2005). The Intestinal Heme Transporter Revealed. *Cell* 122 (5), 649–651. doi:10.1016/j.cell.2005.08.027

Sato, H., Tamba, M., Ishii, T., and Bannai, S. (1999). Cloning and Expression of a Plasma Membrane Cystine/Glutamate Exchange Transporter Composed of Two Distinct Proteins. *J. Biol. Chem.* 274 (17), 11455–11458. doi:10.1074/jbc.274.17.11455

Sato, M., Kusumi, R., Hamashima, S., Kobayashi, S., Sasaki, S., Komiyama, Y., et al. (2018). The Ferroptosis Inducer Erastin Irreversibly Inhibits System X- and Synergizes with Cisplatin to Increase Cisplatin's Cytotoxicity in Cancer Cells. *Sci. Rep.* 8 (1), 968. doi:10.1038/s41598-018-19213-4

Schott, C., Graab, U., Cuvelier, N., Hahn, H., and Fulda, S. (2015). Oncogenic RAS Mutants Confer Resistance of RMS13 Rhabdomyosarcoma Cells to Oxidative Stress-Induced Ferroptotic Cell Death. *Front. Oncol.* 5, 131. doi:10.3389/fonc.2015.00131

Sherr, C. (2006). Divorcing ARF and P53: an Unsettled Case. *Nat. Rev. Cancer* 6 (9), 663–673. doi:10.1038/nrc1954

Shi, Z., Fan, Z., Chen, Y., Xie, X., Jiang, W., Wang, W., et al. (2019). Ferroptosis in Carcinoma: Regulatory Mechanisms and New Method for Cancer Therapy. *OncoTargets Ther.* 12, 11291–11304. doi:10.2147/ott.S232852

Shiao, S. L., Ganesan, A. P., Rugo, H. S., and Coussens, L. M. (2011). Immune Microenvironments in Solid Tumors: New Targets for Therapy. *Genes & Dev.* 25 (24), 2559–2572. doi:10.1101/gad.169029.111

Shin, D., Kim, E., Lee, J., and Roh, J. (2018). Nrf2 Inhibition Reverses Resistance to GPX4 Inhibitor-Induced Ferroptosis in Head and Neck Cancer. *Free Radic. Biol. Med.* 129, 454–462. doi:10.1016/j.freeradbiomed.2018.10.426

Shiotani, B., Kobayashi, M., Watanabe, M., Yamamoto, K., Sugimura, T., and Wakabayashi, K. (2006). Involvement of the ATR- and ATM-dependent Checkpoint Responses in Cell Cycle Arrest Evoked by Pierisin-1. *Mol. cancer Res.* 4 (2), 125–133. doi:10.1158/1541-7786.Mcr-05-0104

Siegel, R., Miller, K., and Jemal, A. (2020). Cancer Statistics, 2020. *CA Cancer J. Clin.* 70 (1), 7–30. doi:10.3322/caac.2159010.3322/caac.21637

Skouta, R., Dixon, S., Wang, J., Dunn, D., Orman, M., Shimada, K., et al. (2014). Ferrostatins Inhibit Oxidative Lipid Damage and Cell Death in Diverse Disease Models. *J. Am. Chem. Soc.* 136 (12), 4551–4556. doi:10.1021/ja411006a

Steuer, C., Behera, M., Berry, L., Kim, S., Rossi, M., Sica, G., et al. (2016). Role of Race in Oncogenic Driver Prevalence and Outcomes in Lung Adenocarcinoma: Results from the Lung Cancer Mutation Consortium. *Cancer* 122 (5), 766–772. doi:10.1002/cncr.29812

Stratton, M. R., Campbell, P. J., and Futreal, P. A. (2009). The Cancer Genome. *Nature* 458 (7239), 719. doi:10.1038/nature07943

Straussman, R., Morikawa, T., Shee, K., Barzily-Rokni, M., and Du, J. Y. (2014). Tumour Micro-environment Elicits Innate Resistance to RAF Inhibitors through HGF Secretion. *eLife* 3, e04034. doi:10.7554/eLife.04034

Sun, X., Niu, X., Chen, R., He, W., Chen, D., Kang, R., et al. (2016a). Metallothionein-1G Facilitates Sorafenib Resistance through Inhibition of Ferroptosis. *Hepatology* 64 (2), 488–500. doi:10.1002/hep.28574

Sun, X., Ou, Z., Chen, R., Niu, X., Chen, D., Kang, R., et al. (2016b). Activation of the P62-Keap1-NRF2 Pathway Protects against Ferroptosis in Hepatocellular Carcinoma Cells. *Hepatology* 63 (1), 173–184. doi:10.1002/hep.28251

Sun, X., Ou, Z., Xie, M., Kang, R., Fan, Y., Niu, X., et al. (2015). HSPB1 as a Novel Regulator of Ferroptotic Cancer Cell Death. *Oncogene* 34 (45), 5617–5625. doi:10.1038/onc.2015.32

Tang, D., Chen, X., Kang, R., and Kroemer, G. (2021). Ferroptosis: Molecular Mechanisms and Health Implications. *Cell Res.* 31 (2), 107–125. doi:10.1038/s41422-020-00441-1

Tarangelo, A., Magtanong, L., Bieging-Rolett, K., Li, Y., Ye, J., Attardi, L., et al. (2018). p53 Suppresses Metabolic Stress-Induced Ferroptosis in Cancer Cells. *Cell Rep.* 22 (3), 569–575. doi:10.1016/j.celrep.2017.12.077

Teshima, K., Nara, M., Watanabe, A., Ito, M., Ikeda, S., Hatano, Y., et al. (2014). Dysregulation of BMI1 and microRNA-16 Collaborate to Enhance an Anti-apoptotic Potential in the Side Population of Refractory Mantle Cell Lymphoma. *Oncogene* 33 (17), 2191–2203. doi:10.1038/onc.2013.177

Thomas, T., and Thomas, T. (2003). Polyamine Metabolism and Cancer. *J. Cell. Mol. Med.* 7 (2), 113–126. doi:10.1111/j.1582-4934.2003.tb00210.x

Tsoi, J., Robert, L., Paraiso, K., Galvan, C., Sheu, K., Lay, J., et al. (2018). Multi-stage Differentiation Defines Melanoma Subtypes with Differential Vulnerability to Drug-Induced Iron-dependent Oxidative Stress. *Cancer Cell* 33 (5), 890–904. e895. doi:10.1016/j.ccell.2018.03.017

van der Veen, J., Kennelly, J., Wan, S., Vance, J., Vance, D., and Jacobs, R. (2017). The Critical Role of Phosphatidylcholine and Phosphatidylethanolamine Metabolism in Health and Disease. *Biochimica biophysica acta. Biomembr.* 1859, 1558–1572. doi:10.1016/j.bbamem.2017.04.006

Velculescu, V. E., Diaz, L. C., Kinzler, W. L., Zhou, S., Kinzler, K., Papadopoulos, N., et al. (2013). Cancer Genome Landscapes. *Science* 339 (6127), 1546–1558. doi:10.1126/science.1235122

Vinogradova, M., Gehling, V. S., Gustafson, A., Arora, S., Tindell, C. A., Wilson, C., et al. (2016). An Inhibitor of KDM5 Demethylases Reduces Survival of Drug-Tolerant Cancer Cells. *Nat. Chem. Biol.* 12 (7), 531–538. doi:10.1038/nchembio.2085

Viswanathan, V., Ryan, M., Dhruv, H., Gill, S., Eichhoff, O., Seashore-Ludlow, B., et al. (2017). Dependency of a Therapy-Resistant State of Cancer Cells on a Lipid Peroxidase Pathway. *Nature* 547 (7664), 453–457. doi:10.1038/nature23007

Wan, S. Y., and Stockwell, B. R. (2015). Ferroptosis: Death by Lipid Peroxidation. *Trends Cell Biol.* 26 (3), 165–176. doi:10.1016/j.tcb.2015.10.014

Wan, S. Y., and Stockwell, B. R. (2008). Synthetic Lethal Screening Identifies Compounds Activating Iron-dependent, Nonapoptotic Cell Death in Oncogenic-RAS-Harboring Cancer Cells. *Chem. Biol.* 15 (3), 234–245.

Wang, J., Huang, S. K., Marzese, D. M., Hsu, S. C., Kawas, N. P., Chong, K. K., et al. (2015). Epigenetic Changes of EGFR Have an Important Role in BRAF Inhibitor-Resistant Cutaneous Melanomas. *J. Investigative Dermatology* 135 (2), 532–541. doi:10.1038/jid.2014.418

Wang, W., Green, M., Choi, J., Gijón, M., Kennedy, P., Johnson, J., et al. (2019). CD8 T Cells Regulate Tumour Ferroptosis during Cancer Immunotherapy. *Nature* 569 (7755), 270–274. doi:10.1038/s41586-019-1170-y

Ward, R., Zucca, F., Duyn, J., Crichton, R., and Zecca, L. (2014). The Role of Iron in Brain Ageing and Neurodegenerative Disorders. *Lancet. Neurology* 13 (10), 1045–1060. doi:10.1016/s1474-4422(14)70117-6

Watson, J. (2013). Oxidants, Antioxidants and the Current Incurability of Metastatic Cancers. *Open Biol.* 3 (1), 120144. doi:10.1098/rsob.120144

Wilson, T. R., Fridlyand, J., Yan, Y., Penuel, E., and Settleman, J. (2014). Widespread Potential for Growth-Factor-Driven Resistance to Anticancer Kinase Inhibitors. *Elife* 3, e04037. doi:10.7554/eLife.04037

Wilting, R. H., and Dannenberg, J. H. (2012). Epigenetic Mechanisms in Tumorigenesis, Tumor Cell Heterogeneity and Drug Resistance. *Drug Resist Updat* 15 (1-2), 21–38. doi:10.1016/j.drup.2012.01.008

Woo, J., Shimoni, Y., Yang, W., Subramaniam, P., Iyer, A., Nicoletti, P., et al. (2015). Elucidating Compound Mechanism of Action by Network Perturbation Analysis. *Cell* 162 (2), 441–451. doi:10.1016/j.cell.2015.05.056

Wu, C., Dailey, H., Rose, J., Burden, A., Sellers, V., and Wang, B. (2001). The 2.0 A Structure of Human Ferrochelatase, the Terminal Enzyme of Heme Biosynthesis. *Nat. Struct. Biol.* 8 (2), 156–160. doi:10.1038/84152

Wu, Y., Sun, X., Song, B., Qiu, X., and Zhao, J. (2017). MiR-375/SLC7A11 axis Regulates Oral Squamous Cell Carcinoma Proliferation and Invasion. *Cancer Med.* 6 (7), 1686–1697. doi:10.1002/cam4.1110

Xie, Y., Hou, W., Song, X., Yu, Y., Huang, J., Sun, X., et al. (2016). Ferroptosis: Process and Function. *Cell death Differ.* 23 (3), 369–379. doi:10.1038/cdd.2015.158

Xie, Y., Zhu, S., Song, X., Sun, X., Fan, Y., Liu, J., et al. (2017). The Tumor Suppressor P53 Limits Ferroptosis by Blocking DPP4 Activity. *Cell Rep.* 20 (7), 1692–1704. doi:10.1016/j.celrep.2017.07.055

Yagoda, N., von Rechenberg, M., Zaganjor, E., Bauer, A., Yang, W., Fridman, D., et al. (2007). RAS-RAF-MEK-dependent Oxidative Cell Death Involving Voltage-dependent Anion Channels. *Nature* 447 (7146), 864–868. doi:10.1038/nature05859

Yan, H., Tuo, Q., Yin, Q., and Lei, P. (2020). The Pathological Role of Ferroptosis in Ischemia/reperfusion-Related Injury. *Zoological Res.* 41 (3), 220–230. doi:10.24272/j.issn.2095-8137.2020.042

Yang, C., He, L., He, P., Liu, Y., Wang, W., He, Y., et al. (2015). Increased Drug Resistance in Breast Cancer by Tumor-Associated Macrophages through IL-10/STAT3/bcl-2 Signaling Pathway. *Med. Oncol.* 32 (2), 14. doi:10.1007/s12032-014-0352-6

Yang, J., Antin, P., Berx, G., Blanpain, C., Brabletz, T., Bronner, M., et al. (2021a). Author Correction: Guidelines and Definitions for Research on Epithelial-Mesenchymal Transition. *Nat. Rev. Mol. Cell Biol.* 22 (12), 834. doi:10.1038/s41580-021-00428-9

Yang, J., Xu, J., Zhang, B., Tan, Z., Meng, Q., Hua, J., et al. (2021b). Ferroptosis: At the Crossroad of Gemcitabine Resistance and Tumorigenesis in Pancreatic Cancer. *Int. J. Mol. Sci.* 22 (20), 10944. doi:10.3390/ijms222010944

Yang, W. S., Kim, K. J., Gaschler, M. M., Patel, M., Shchepinov, M. S., and Stockwell, B. R. (2016). Peroxidation of Polyunsaturated Fatty Acids by Lipoxygenases Drives Ferroptosis. *Proc. Natl. Acad. Sci. U. S. A.* 113 (34), E4966. doi:10.1073/pnas.1603244113

Yang, W., SriRamaratnam, R., Welsch, M., Shimada, K., Skouta, R., Viswanathan, V., et al. (2014). Regulation of Ferroptotic Cancer Cell Death by GPX4. *Cell* 156, 317–331. doi:10.1016/j.cell.2013.12.010

Yang, W., and Stockwell, B. (2008). Synthetic Lethal Screening Identifies Compounds Activating Iron-dependent, Nonapoptotic Cell Death in Oncogenic-RAS-Harboring Cancer Cells. *Chem. Biol.* 15 (3), 234–245. doi:10.1016/j.chembiol.2008.02.010

Yeo, C. D., Kang, N., Choi, S. Y., Kim, B. N., and Kim, S. J. (2017). The Role of Hypoxia on the Acquisition of Epithelial-Mesenchymal Transition and Cancer Stemness: a Possible Link to Epigenetic Regulation. *Korean J. Intern Med.* 32 (4), 589–599. doi:10.3904/kjim.2016.302

Yoda, S., Dagogo-Jack, I., and Hata, A. (2019). Targeting Oncogenic Drivers in Lung Cancer: Recent Progress, Current Challenges and Future Opportunities. *Pharmacol. Ther.* 193, 20–30. doi:10.1016/j.pharmthera.2018.08.007

Young, A., Lou, D., and McCormick, F. (2013). Oncogenic and Wild-type Ras Play Divergent Roles in the Regulation of Mitogen-Activated Protein Kinase Signaling. *Cancer Discov.* 3 (1), 112–123. doi:10.1158/2159-8290.Cd-12-0231

Yu, Y., Xie, Y., Cao, L., Yang, L., Yang, M., Lotze, M., et al. (2015). The Ferroptosis Inducer Erastin Enhances Sensitivity of Acute Myeloid Leukemia Cells to Chemotherapeutic Agents. *Mol. Cell. Oncol.* 2 (4), e1054549. doi:10.1080/23723556.2015.1054549

Yuan, H., Li, X., Zhang, X., Kang, R., and Tang, D. (2016). CISD1 Inhibits Ferroptosis by Protection against Mitochondrial Lipid Peroxidation. *Biochem. biophysical Res. Commun.* 478 (2), 838–844. doi:10.1016/j.bbrc.2016.08.034

Yue, L., Dai, Z., Chen, X., Liu, C., Hu, Z., Song, B., et al. (2018). Development of a Novel FePt-Based Multifunctional Ferroptosis Agent for High-Efficiency Anticancer Therapy. *Nanoscale* 10 (37), 17858–17864. doi:10.1039/c8nr05150j

Yun, C. H., Mengwasser, K. E., Toms, A. V., Woo, M. S., and Eck, M. J. (2008). The T790M Mutation in EGFR Kinase Causes Drug Resistance by Increasing the Affinity for ATP. *Proc. Natl. Acad. Sci.* 105 (6), 2070–2075. doi:10.1073/pnas.0709662105

Zakharova, E., Sokolov, A., Pavlichenko, N., Kostevich, V., Abdurasulova, I., Chechushkov, A., et al. (2018). Erythropoietin and Nrf2: Key Factors in the Neuroprotection provided by Apo-Lactoferrin. *Biometals* 31 (3), 425–443. doi:10.1007/s10534-018-0111-9

Zhang, Y., Tan, H., Daniels, J., Zandkarimi, F., Liu, H., Brown, L., et al. (2019). Imidazole Ketone Erastin Induces Ferroptosis and Slows Tumor Growth in a Mouse Lymphoma Model. *Cell Chem. Biol.* 26 (5), 623–633. e629. doi:10.1016/j.chembiol.2019.01.008

Zheng, D., Lei, Q., Zhu, J., Fan, J., Li, C., Li, C., et al. (2017). Switching Apoptosis to Ferroptosis: Metal-Organic Network for High-Efficiency Anticancer Therapy. *Nano Lett.* 17 (1), 284–291. doi:10.1021/acs.nanolett.6b04060

Conflict of Interest: The authors declare that the research was conducted in the absence of any commercial or financial relationships that could be construed as a potential conflict of interest.

Publisher's Note: All claims expressed in this article are solely those of the authors and do not necessarily represent those of their affiliated organizations, or those of the publisher, the editors and the reviewers. Any product that may be evaluated in this article, or claim that may be made by its manufacturer, is not guaranteed or endorsed by the publisher.

frontiers | Frontiers in Pharmacology

REVIEW
published: 24 May 2022
doi: 10.3389/fphar.2022.908772

Post-Translational Modifications of p53 in Ferroptosis: Novel Pharmacological Targets for Cancer Therapy

Le Zhang[1,2†], Ningning Hou[1,2†], Bing Chen[3], Chengxia Kan[1,2], Fang Han[3], Jingwen Zhang[1,2] and Xiaodong Sun[1,2*]*

[1]Department of Endocrinology and Metabolism, Affiliated Hospital of Weifang Medical University, Weifang, China, [2]Clinical Research Center, Affiliated Hospital of Weifang Medical University, Weifang, China, [3]Department of Pathology, Affiliated Hospital of Weifang Medical University, Weifang, China

The tumor suppressor p53 is a well-known cellular guardian of genomic integrity that blocks cell cycle progression or induces apoptosis upon exposure to cellular stresses. However, it is unclear how the remaining activities of p53 are regulated after the abrogation of these routine activities. Ferroptosis is a form of iron- and lipid-peroxide-mediated cell death; it is particularly important in p53-mediated carcinogenesis and corresponding cancer prevention. Post-translational modifications have clear impacts on the tumor suppressor function of p53. Here, we review the roles of post-translational modifications in p53-mediated ferroptosis, which promotes the elimination of tumor cells. A thorough understanding of the p53 functional network will be extremely useful in future strategies to identify pharmacological targets for cancer therapy.

Keywords: ferroptosis, cancer, pharmacology, post-translational modifications, p53, cancer therapy

OPEN ACCESS

Edited by:
Xu Chen,
Guilin Medical University, China

Reviewed by:
Yin Lin Ge,
Qingdao University, China
Pengyu Chang,
First Affiliated Hospital of Jilin University, China

***Correspondence:**
Jingwen Zhang
fyjwzhang@wfmc.edu.cn
Xiaodong Sun
xiaodong.sun@wfmc.edu.cn

[†]These authors have contributed equally to this work and share first authorship

Specialty section:
This article was submitted to Pharmacology of Anti-Cancer Drugs, a section of the journal Frontiers in Pharmacology

Received: *31 March 2022*
Accepted: *10 May 2022*
Published: *24 May 2022*

Citation:
Zhang L, Hou N, Chen B, Kan C, Han F, Zhang J and Sun X (2022) Post-Translational Modifications of p53 in Ferroptosis: Novel Pharmacological Targets for Cancer Therapy. Front. Pharmacol. 13:908772. doi: 10.3389/fphar.2022.908772

1 INTRODUCTION

The tumor suppressor protein p53 is often regarded as the gatekeeper of the cell because it is essential for stabilizing the cellular genome (Levine, 1997; Blagih et al., 2020). p53 exerts a tumor-suppressive function when exposed to DNA damage and various endogenous/exogenous stresses (Pietsch et al., 2008). Routinely activated p53 regulates cell cycle arrest and induces apoptosis to suppress cancer growth (Kastenhuber and Lowe, 2017). In contrast, 50% of human cancer cases are caused by biallelic mutations or deletions in the human gene *TP53*, leading to inappropriate activity of wild-type p53 and unrestrained tumor progression (Olivier et al., 2002). Thus, the preservation of p53 function to induce cell death is considered essential for cancer therapy.

In the past, apoptosis was regarded as the primary cell death mechanism in conventional cancer treatments. However, multidrug insensitivity or acquired resistance to existing traditional chemotherapy remains a major challenge for oncology treatment. Ferroptosis is an iron-dependent cell death process, characterized by excessive lipid peroxidation and iron overload (Dixon et al., 2012). Recently, ferroptosis has demonstrated considerable advantages in cancer treatment. Cancer cells are sensitive to ferroptosis because of their vigorous division and robust oxidative metabolic activity (Badgley et al., 2020). Additionally, cancer cells contain many targets for ferroptosis induction (Datta et al., 2007). Furthermore, ferroptosis can be combined with classical cancer treatments to reduce the survival and progression of malignant cells (Matsushita et al., 2015; Lin et al., 2016; Xu et al., 2018). For example, the anti-tumor medicine cisplatin can induce

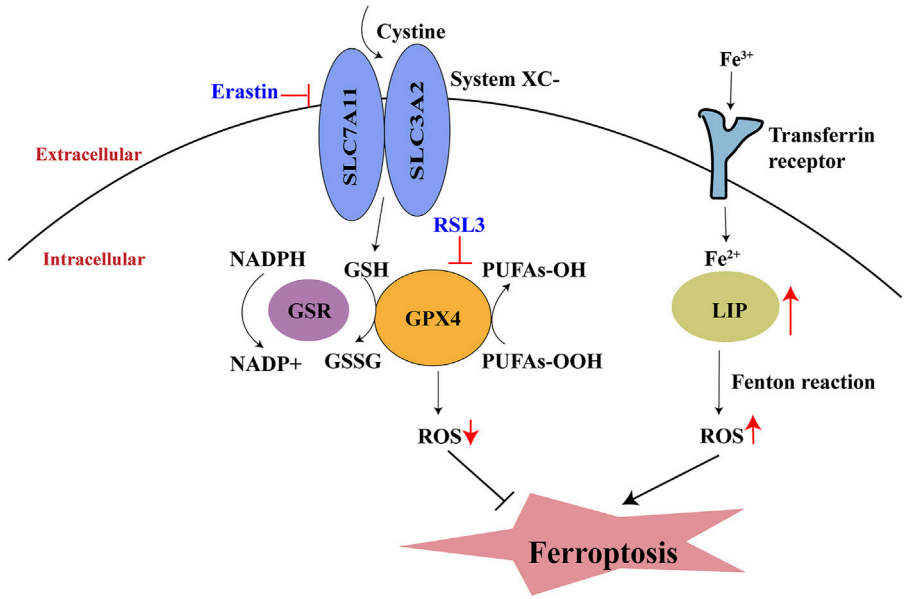

FIGURE 1 | Process of ferroptosis. System Xc-, cystine/glutamate antiporter system; GSH, glutathione; GPX4, glutathione peroxidase; GSSG, oxidative glutathione; LIP, labile iron pool; NADPH, Nicotinamide adenine dinucleotide phosphate; PUFA, polyunsaturated fatty acid.

ferroptosis and apoptosis in lung cancer. Simultaneous application of cisplatin and erastin synergistically induces ferroptosis in colon and lung cancer cells (Guo et al., 2018). Thus, cancer cells with resistance to conventional chemotherapy, as well as cancer cells with a high propensity for metastasis, may be particularly vulnerable to ferroptosis.

Recently, the role of p53 biology in ferroptosis has received increasing interest for novel cancer treatments (Jiang et al., 2015). p53 is closely associated with key metabolic processes involved in ferroptosis (Liu and Gu, 2021). For example, p53 promotes cell survival by inhibiting ferroptosis in the absence of cysteine, suggesting an association between p53 and cysteine metabolism in ferroptosis (Tarangelo et al., 2018). Furthermore, ferroptosis is associated with both cancer and non-cancer diseases. Therefore, the regulation of ferroptosis by treatments that target p53 is a novel approach to cancer therapy.

Among the known regulatory processes, reversible post-translational modifications (PTMs) are regarded as critical regulators that control cellular quiescence and proliferation (Chen et al., 2020). PTMs are the most complex and efficient patterns that dynamically regulate the stability, conformation, and functions of p53 (Liu et al., 2019). Under various conditions, p53 can induce or suppress ferroptosis through transcriptional regulation or PTMs (Pietsch et al., 2008; Kang et al., 2019). However, the primary functions of PTMs of p53 in tumorigenesis-related ferroptosis have not been thoroughly reviewed in published literature. This review focuses on recent advancements in understanding the various PTMs of p53, as well as their roles in ferroptosis; we expect that this thorough analysis will promote research into the implications of those PTMs in cancer treatment.

2 MOLECULAR MECHANISMS OF P53 IN FERROPTOSIS-BASED CANCER THERAPY

The term "ferroptosis" was initially used in 2012 by Dixon et al. (2012) to explain a new type of erastin-induced cell death that lacked features of apoptosis, necroptosis, and autophagy. The progression of ferroptosis is characterized by iron-dependent lipid peroxide injury in mitochondria; this injury involves inhibition of the cysteine/glutamate antiporter system (system Xc-), insufficient synthesis of glutathione (GSH), and depletion of glutathione peroxidase (GPX4) (Hassannia et al., 2019). The two key events in ferroptosis are dysregulation of lipid peroxidation and disruption of iron metabolism. Initially, cysteine is absorbed into the cytoplasm *via* system Xc-transporters; it then promotes GSH synthesis. GSH is then converted into oxidized glutathione (GSSG) *via* GPX4, thus reducing the amount of lipid-based reactive oxygen species (ROS) (Stockwell et al., 2017). Transferrin receptors import extracellular Fe^{3+} into cells; this Fe^{3+} is then converted to Fe^{2+} and transferred to the labile iron pool (Gkouvatsos et al., 2012). An increase in the labile iron pool leads to the accumulation of lipid ROS through the Fenton reaction; this eventually results in ferroptosis (Su et al., 2020) (**Figure 1**).

In 2015, Jiang et al. first identified a link between p53 and ferroptosis, such that p53 sensitized cells to ferroptosis (Jiang et al., 2015). Thus far, there have been numerous reports of p53-mediated ferroptosis. Generally, p53 is considered to be closely associated with cell cycle arrest, apoptosis, and senescence (Brady et al., 2011; Li et al., 2012; Valente et al., 2013). Usually, these processes are induced by p53 to repair DNA damage and prevent the development of malignant cells. Nonetheless, apoptosis evasion and enhanced resistance to apoptosis can impede

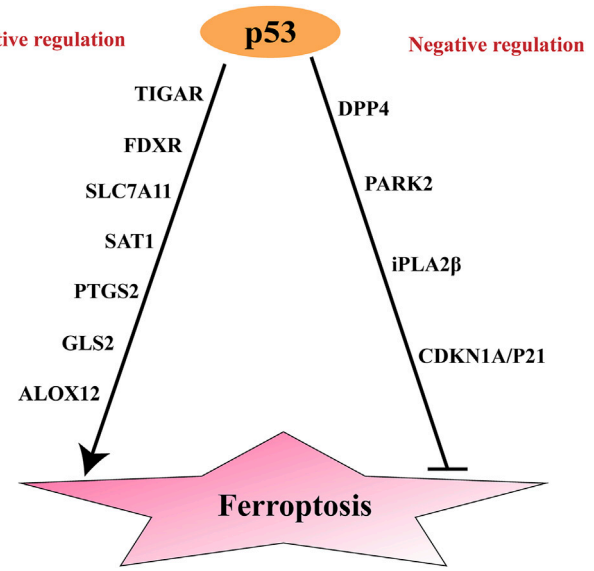

FIGURE 2 | Positive and negative regulation of p53 to ferroptosis. SAT1, Spermidine/spermine N1-acetyltransferase; ; ALOX15, Arachidonic acid 15 lipoxygenases; GLS2, Glutaminases; PTGS2, Prostaglandin-endoperoxide synthase 2; ALOX12, Arachidonic acid 12 lipoxygenases; TIGAR, TP53-induced glycolysis and apoptosis regulator; FDXR, Ferredoxin reductase; DPP4, dipeptidyl peptidase-4; CDKN1A, encoding p21: cyclin-dependent kinase inhibitor; PARK2, parkinson disease 2.

cancer treatment (Guo et al., 2018). The discovery of p53 involvement in ferroptosis solved this problem. There have been multiple reports of combined cancer treatments that use conventional approaches and p53-mediated ferroptosis. For example, Lei et al. showed that radiotherapy-induced ferroptosis was also influenced by p53, leading to radiosensitivity in cancer cells. Some drugs for other diseases also have positive effects on p53-mediated ferroptosis. Sinapine, an alkaloid with antioxidant and anti-inflammatory properties, upregulates transferrin receptors in a p53-dependent manner that leads to ferroptosis in non-small cell lung cancer (Shao et al., 2022).

In addition to the p53-mediated ferroptosis network, several other networks mediate the induction of ferroptosis; these include autophagy proteins 5 and 7, the nuclear receptor coactivator four pathway, nuclear factor erythroid 2-related factor (Nrf2) in iron metabolism, and acyl-CoA synthetase long-chain family member four in lipid metabolism (Capelletti et al., 2020). However, these p53-independent types of ferroptosis have some limitations. For example, while enhanced expression of Nrf2 can reduce ROS levels and decrease stress responses (Suzuki et al., 2013), the activation of Nrf2 minimizes cancer cell sensitivity to conventional cancer treatments (e.g., chemotherapy and radiation) (DeNicola et al., 2011). This reduced sensitivity limits the usefulness of Nrf2-mediated ferroptosis in cancer therapy.

Notably, p53 has two opposing effects on ferroptosis: it promotes and suppresses ferroptosis under specific conditions (Kang et al., 2019) (**Figure 2**). Under normal conditions, p53 can increase tumor cell sensitivity to ferroptosis and thus promote cell death. However, upon exposure to stresses such as cysteine deprivation, p53 delays ferroptosis (Friedmann Angeli et al., 2019). Differences in cell types and p53 mutation sites also influence the effects of p53 on ferroptosis in tumor cells. In the following sections, these opposing effects of p53 on ferroptosis will be clearly illustrated (**Table 1**).

2.1 Positive Regulation of Ferroptosis by p53

System X_C- includes the transport component SLC7A11 and the regulatory module SLC3A2. SLC7A11 negatively regulates ferroptosis progression (Mou et al., 2019) and is overexpressed in various human cancers (Jiang et al., 2015; Koppula et al., 2021). In 2015, p53 was reported to promote ferroptosis through the transrepression of SLC7A11 expression (Jiang et al., 2015). Jiang et al. (2015) found that when p53 was activated by nutlin-3 or exposed to DNA damage stress, the expression of SLC7A11 was reduced. p53 binds to the promoter region of SLC7A11 to inhibit its expression, thus regulating cysteine metabolism and sensitizing cancer cells to ferroptosis.

Spermidine/spermine N1-acetyltransferase (SAT1) is a regulatory enzyme of the polyamine catabolism process (Pegg, 2008); it can be activated by oxidative stress, inflammation, and heat shock (Mandal et al., 2015). Because SAT1 is a transcriptional target of p53, SAT1 deficiency blocks p53-mediated ferroptosis in cancer. Upon exposure to combined treatment with nutlin and ROS, SAT1 induces p53-mediated ferroptosis (Ou et al., 2016). Although the p53–SAT1 axis increases cancer cell sensitivity to ferroptosis, this axis is not associated with GPX4-mediated ferroptosis (Ou et al., 2016). Notably, SAT1 overexpression leads to upregulation of arachidonic acid 15 lipoxygenase (ALOX15), which oxidizes polyunsaturated fatty acids and increases lipid peroxidation; these activities induce mitochondrial apoptosis and inhibit cell proliferation (Liu J et al., 2020). Taken together, these findings suggest that ALOX15 is a mediator of p53–SAT1 axis-induced ferroptosis in cancer (Ou et al., 2016).

Glutaminase 2 (GLS2) participates in glutamine metabolism; this enzyme is essential for the regulation of ferroptosis because it decreases glutathione and increases cellular ROS levels (Hu et al., 2010). GLS2 reportedly exhibited tumor-suppressive functions in liver and brain carcinomas with reduced levels of GSL2 (Hu et al., 2010; Liu et al., 2014; Martín-Rufián et al., 2014). The ability of p53 to bind to the GSL2 response element under stressed or unstressed conditions suggests that GSL2 can affect p53 function. GSL2 expression is responsible for p53-mediated oxygen consumption, mitochondrial respiration, and adenosine triphosphate production in cancer cells (Hu et al., 2010; Suzuki et al., 2010; Ou et al., 2016). However, further investigation is needed to determine whether GLS2 is critical for p53-mediated ferroptosis.

Prostaglandin-endoperoxide synthase 2 (PTGS2) encodes the enzyme cyclooxygenase 2, which catalyzes lipid oxidation (Liu J et al., 2020). PTGS2 regulates cellular sensitivity to ferroptosis by regulating phospholipid P, a critical membrane component. Both

PTGS2 and SAT1 can affect the abundance and distribution of polyunsaturated fatty acids (essential substrates for ferroptosis), thus affecting lipid peroxidation and ferroptosis (Zheng and Conrad, 2020).

Arachidonic acid 12 lipoxygenase (ALOX12) is also closely associated with p53-mediated ferroptosis (Chu et al., 2019). ALOX12 inactivation abolishes p53-mediated ferroptosis in lymphoma. The potential mechanism is that, under ROS stress, p53 indirectly activates ALOX12 by transcriptional repression of SLC7A11 (Chu et al., 2019).

TP53-induced glycolysis and apoptosis regulator (TIGAR) is a target gene of p53 that inhibits cancer and has an antioxidant effect (Rajendran et al., 2013). Its possible role in ferroptosis is associated with its ability to maintain a lower level of cellular GSH. TIGAR promotes NADPH production through the pentose phosphate pathway, which has an important role in regulating subsequent NADPH-related ferroptosis (Ji et al., 2021).

p53 can also promote ferroptosis by influencing the function of ferredoxin reductase (FDXR) in iron metabolism (Ji et al., 2021). FDXR is a mitochondrial flavoprotein that transfers electrons to ferredoxin 1 (FDX1) and FDX2 (Brandt and Vickery, 1992); FDX1 is closely associated with steroidogenesis in mitochondria, while FDX2 is closely associated with cell survival. In the presence of FDX2 deficiency, mitochondrial iron overload occurs and p53 expression decreases, suggesting that FDX2 can transduce FDXR signals to regulate processes such as iron homeostasis, p53 expression, and tumor suppression (Zhang et al., 2017). p53 plays a role in iron homeostasis and mediates FDXR-dependent iron metabolism; the interaction between FDXR and p53 can also inhibit tumor initiation and progression. Notably, FDXR deficiency or overexpression combined with RSL3 and erastin led to the induction of ferroptosis, suggesting that FDXR is closely associated with the underlying induction mechanism. Additionally, FDXR-deficient mice are more likely to develop tumors (Zhang et al., 2017). These findings imply that the FDXR–p53 interaction inhibits tumorigenesis by maintaining iron homeostasis.

2.2 Negative Regulation of Ferroptosis by p53

In addition to its ferroptosis-promoting effects, p53 represses ferroptosis by inducing cyclin-dependent kinase inhibitor (CDKN1A, encoding p21), Parkinson disease 2 (PARK2) and iPLA2β, or by inhibiting dipeptidyl peptidase-4 (DPP4) (Kang et al., 2019) (**Figure 2**).

p53 targets CDKN1A/p21 in response to stress and senescence. p53-mediated CDKN1A/p21 expression hinders ferroptosis in response to cysteine deprivation (Tarangelo et al., 2018). In a recent study, p53-mediated CDKN1A expression delayed the onset of ferroptosis in response to subsequent cysteine deprivation in cancer cells (Tarangelo et al., 2018). This may be associated with reduced ROS production and attenuated GSH consumption (Ji et al., 2021). Importantly, that study was conducted in cells that had been pretreated with the p53 stabilizer nutlin-3; it remains unknown whether similar results can be achieved using other cells.

Furthermore, p53 targets PARK2 during mitophagy; PARK2 eliminates damaged mitochondria and attenuates sensitivity to ferroptosis in cancer (Zhang et al., 2011). Upon exposure to infrared radiation, p53-mediated expression of PARK2 is enhanced. p53 exerts its functions in mitochondrial respiration, oxygen consumption, and antioxidant defense by promoting PARK2 expression, suggesting that activation of the p53–PARK2 axis can limit cysteine deprivation-mediated ferroptosis. In PARK2-deficient mice, the tumor spectrum after exposure to infrared radiation was shorter than in wild-type mice, implying that PARK2 can serve as a tumor suppressor (Zhang et al., 2011). However, it is unclear whether p53 is involved in the inhibition of PARK2-mediated ferroptosis because p53 can also inhibit PARK2 activity (Hoshino et al., 2013; Gao et al., 2019).

In a recent paper, iPLA2β was reported to play a role in p53-mediated ferroptosis (Chen et al., 2021). Chen et al. (2021) found that iPLA2β could inhibit p53-mediated ferroptosis. When p53 was activated by nutlin or exposure to DNA damage, iPLA2β expression was increased. The loss of iPLA2β resulted in sensitivity to ferroptosis during ROS-induced stress in MCF7 cells and U2OS cells. This suppression mainly depended on the elimination of ALOX12-induced lipid peroxidation. In a xenograft mouse model, reduced expression of endogenous iPLA2β caused tumor cells to become sensitized to ferroptosis; thus, p53-mediated ferroptosis was enhanced. This finding suggested that iPLA2β could inhibit p53-driven ferroptosis.

The multifunctional protease DPP4 plays an essential role in cell death (Xie et al., 2017). In colorectal cancer, p53 regulates the cellular localization and activity of DPP4, rather than affecting its expression level (Xie et al., 2017). This effect is presumably because, in p53-deficient cells, DPP4 is located on the plasma membrane and binds to NADPH oxidase 1, thereby increasing lipid peroxidation and promoting ferroptosis. In colorectal cancer cells with high expression of DPP4, p53 binds and isolates DPP4 *via* ribozyme inactivation; this causes dissociation of NADPH oxidase one and nuclear translocation of DPP4, leading to diminished lipid peroxidation and abrogation of ferroptosis-promoting activity (Xie et al., 2017). However, this phenomenon has only been observed in colorectal cancer cells.

Thus, p53 is closely associated with the induction of ferroptosis. Regulation of p53 and its downstream genes (e.g., SLC7A11, iPLA2β, ALOX15, GLS2, TIGAR, PTGS2, FDR, DPP4, p21, and PARK2) may promote or inhibit the induction of ferroptosis. These are all known drug targets; however, new drugs can be designed for use in regulating ferroptosis and providing novel research insights.

3 EFFECTS OF P53 PTMS ON FERROPTOSIS

3.1 p53 Functional Domains, Stability, and Activity

p53 is a type of sequence-specific DNA-binding protein that is referred to as a quantum jump (Bargonetti et al., 1991). The p53 protein contains 393 amino acids and six structural domains: two

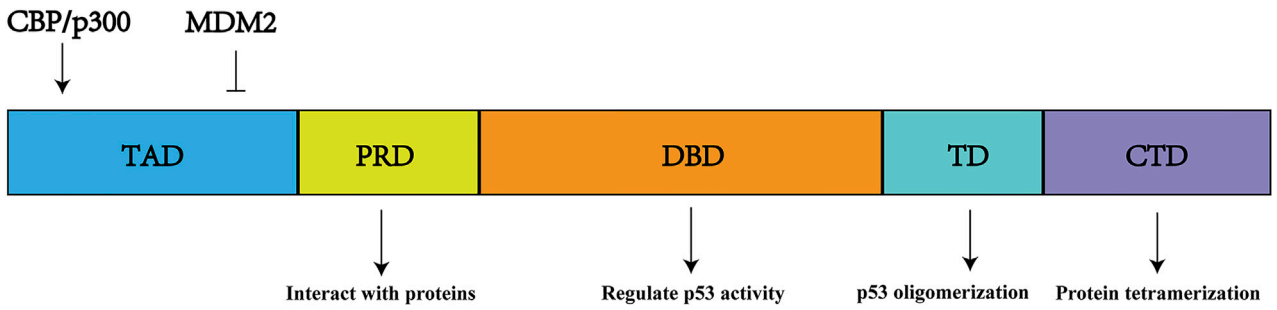

FIGURE 3 | p53 structure and function. It includes six protein domains. TAD, N-terminal transactivation domains (s); DBD, central DNA-binding domain; PRD, proline-rich domain; TD, a tetramerization domain; CTD, C-terminal domain.

N-terminal transactivation domains, a central DNA-binding domain, a proline-rich domain, a tetramerization domain, and a C-terminal domain (Joerger and Fersht, 2016) (**Figure 3**). CBP/p300 (described in **Section 3.2**) and murine double minute-2 (MDM2), respectively, are positive and negative regulators that bind to sites on the N-terminal region of p53 (Mavinahalli et al., 2010). The DNA-binding domain allows p53 to bind to response elements on its target genes; thus, it is essential for p53 activity (Ryan, 2011). *TP53* mutations frequently occur in the DNA-binding domain, thereby disrupting the function of the p53 protein and its downstream network (Hainaut and Hollstein, 2000). Additionally, the proline-rich domain contains five PXXP motifs, which participate in interactions between p53 and various proteins; this domain is primarily responsible for the regulation of apoptosis (Lacroix et al., 2006). Finally, the tetramerization domain regulates the oligomerization of p53, while the C-terminal domain is associated with tetramerization of p53 (Golubovskaya and Cance, 2013).

Under normal physiological conditions, p53 is a housekeeping protein with a short half-life (Liu et al., 2019). However, in the presence of various types and levels of stress, p53 can be activated and accumulated to coordinate cellular responses. The activation of p53 is associated with cancer prevention; it initiates DNA repair, promotes apoptosis, influences ferroptosis, and regulates energy metabolism (Kaiser and Attardi, 2018; Zhao et al., 2021). Although multiple mechanisms have been proposed to explain the unique tumor suppression effects of p53, the specific function necessary for these effects remains unknown.

3.2 Post-Translational Modifications of p53 and Their Impacts on p53-Mediated Ferroptosis

The paradigm shift concerning the role of p53 in ferroptosis prompted us to investigate how and when p53 promotes or suppresses ferroptosis. p53 activation is subject to a complex and diverse array of PTMs, which substantially influence the expression patterns of p53 target genes and related functional groups after the translation of p53 (Chen et al., 2020). PTMs of p53 can be rapidly reversed and constitute critical steps that greatly influence both carcinogenesis and cancer prevention (Gu and Zhu, 2012; Hassannia et al., 2019). PTMs of p53 mainly include phosphorylation, acetylation, ubiquitination, O-GlcNAcylation, SUMOylation, and methylation. This review focuses on the functional importance of the various PTMs in p53-mediated ferroptosis, specifically in the context of carcinogenesis and cancer prevention (**Figure 4**).

3.2.1 Phosphorylation

Phosphorylation is the most widely studied protein modification (**Figure 4A**). p53 is usually phosphorylated at Ser15, which is located in a homologous subdomain of the N-terminal transactivation domain. Several kinases can phosphorylate p53 at these sites, including ataxia-telangiectasia mutated (ATM) kinase, ATM- and Rad3-related (ATR) kinase, and checkpoint kinase 1/2(CHK1/2) (Appella and Anderson, 2001). Because of their shared Ser20 phosphorylation mechanism, both ATM kinase and ATR kinase mediate the stabilization of human p53 in response to infrared- and ultraviolet-induced DNA damage (Chehab et al., 1999). Phosphorylation at Ser15 frequently occurs in glucose-dependent cell cycle arrest; it is regulated by adenosine monophosphate-activated protein kinase (AMPK) (Shieh et al., 1997; Jones et al., 2005; Yang et al., 2019). Phosphorylation at Ser15 results in a conformational change in the tertiary structure of p53; phosphorylation at Ser20 involves the tetramerization domain of p53. Both types of phosphorylation reduce the ability of p53 to bind its negative regulator MDM2, thereby improving p53 stability and function (Shieh et al., 1997; Shieh et al., 1999, Shieh et al., 2000; Teufel et al., 2009).

Suppressor of cytokine signaling 1 (SOCS1) is essential for the activation of p53-mediated ferroptosis and regulation of cellular senescence (Calabrese et al., 2009; Mallette et al., 2010). Saint-Germain et al. (2017) found that, under moderate DNA damage stress, SOCS1 phosphorylates Ser15 by promoting the interaction of p53 and ATM. Under high DNA damage stress, phosphorylation at Ser15 was independent of SOCS1, although SOCS1 continued to stabilize p53. SOCS1-mediated phosphorylation at Ser15 led to ferroptosis-related downregulation of SLC7A11 and upregulation of SAT1.

Among the known PTMs, Ser46 is another major phosphorylation site of the transactivation domain (Liebl and Hofmann, 2019). Phosphorylation of p53 at Ser46 has been

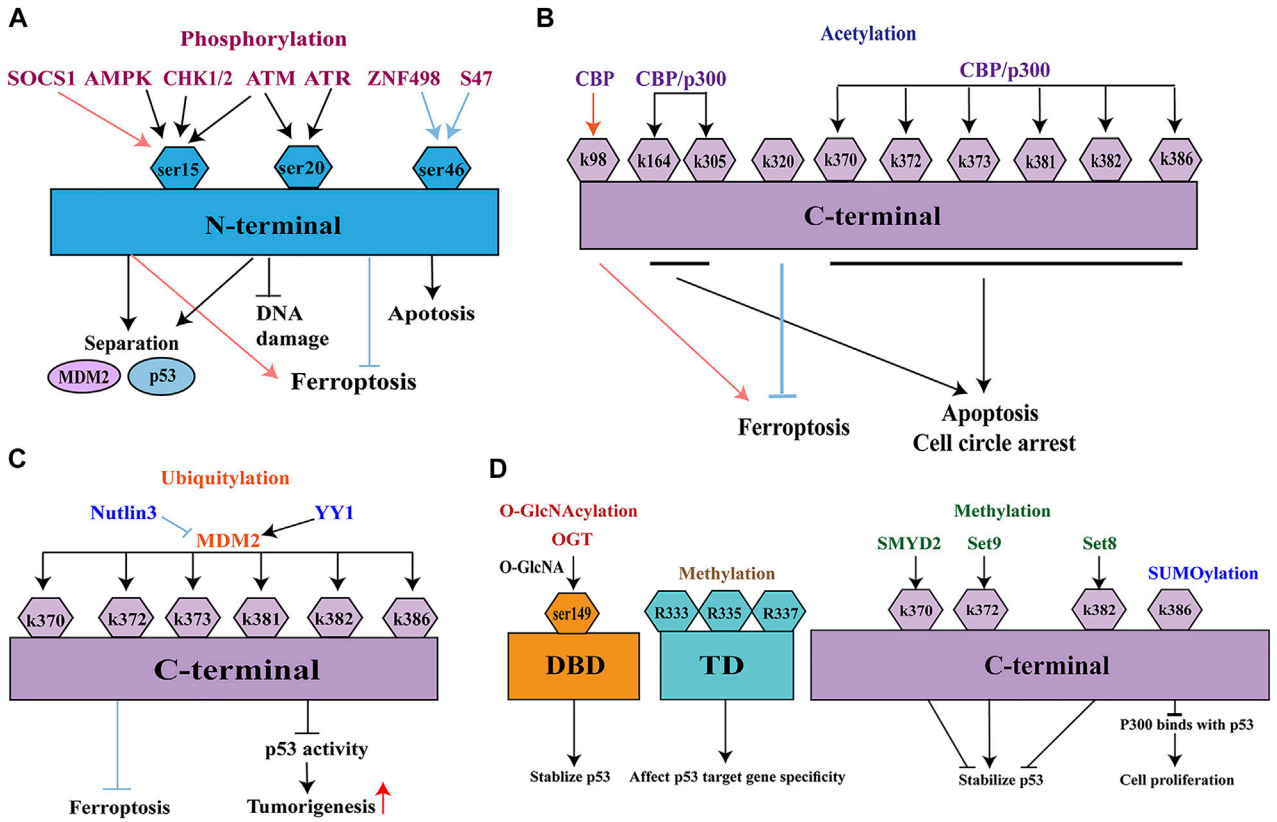

FIGURE 4 | Post-translational modifications of p53. **(A)** phosphorylation; **(B)** acetylation; **(C)** ubiquitination; **(D)** O-GlcNAcylation, SUMOylation, and methylation. MDM2, Murine double minute-2; ATM, ataxia-telangiectasia mutated kinase; ATR, ATM-and Rad3-related kinase; CHK1/2, checkpoint kinase 1/2; AMPK, adenosine monophosphate-activated protein kinase; CBP, CREB binding protein; EP300/p300, E1A binding protein P300; PCAF, p300/CBP-associated factor; KAT5/Tip60, lysine acetyltransferase 5; KAT8/MOF, lysine acetyltransferase 8; MOZ, monocytic leukemia zinc finger; YY1, Yin Yang 1.

implicated in p53 activation and its various pathophysiological effects. This type of phosphorylation induces apoptosis and ferroptosis in cells exposed to various stress (Zhang et al., 2022). An example is ZNF498, one of the Krüppel-associated box domain zinc-finger proteins. In ferroptosis-induced HepG2 cells, the overexpression of ZNF498 led to decreases in ROS production and GSL2 expression, as well as an increase in GSH production; these effects resulted in cell survival. Thus, overexpression of ZNF498 is presumably associated with tumor advancement and poor prognosis in hepatocellular carcinoma. A potential underlying mechanism involves attenuated phosphorylation of p53 at Ser46, which inhibits p53-mediated apoptosis and ferroptosis (Zhang et al., 2022). Another example is the Pro47Ser polymorphism (S47), which converts the proline residue adjacent to Ser46 in human p53 into serine (Lane, 2016). This change reduces ferroptosis by impairing p53-mediated downstream genes; it reduces apoptosis by decreasing the phosphorylation of Ser46 (Zhang et al., 2018). In a recent study, flubendazole (an anti-malarial drug) exhibited an anti-tumor effect by mediating the phosphorylation of p53; this promoted ferroptosis in castration-resistant prostate cancer. This process was associated with regulatory effects by SLC7A11 and GPX4 (Zhou et al., 2021). Further elucidation of the mechanisms that underlie p53 phosphorylation will yield new therapeutic strategies for ferroptosis-induced tumor suppression.

3.2.2 Acetylation

Acetylation is also a common PTM that involves the modification of lysine residues in p53 (**Figure 4B**). Acetylation increases the stability of p53 and is essential for its ability to repair DNA damage (Kruse and Gu, 2009). Six p53 acetyltransferases have been identified, all of which modify p53 at lysines mainly in the C-terminus. These acetyltransferases include CREB-binding protein (CBP), E1A-binding protein P300 (EP300/p300), p300/CBP-associated factor (PCAF), lysine acetyltransferase 5 (KAT5/Tip60), lysine acetyltransferase 8 (KAT8/MOF), and monocytic leukemia zinc finger (MOZ). CBP/p300 is a transcriptional coactivator protein with acetyltransferase activity. Mutations in CBP/p300 commonly occur in several types of cancers, where they enhance histone acetylation and transcription of genes that surround the target gene (Goodman and Smolik, 2000; Luo et al., 2004). The transcriptional activity of p53 is enhanced by CBP/p300 through acetylation at C-terminal lysines (K370, K372, K373, K381, K382, K386, K164, and K305); these instances of acetylation lead to growth arrest and/or apoptosis (Dai and Gu, 2010). In a recent study, CBP acetylated residue K98 in mouse

p53 (residue K101 in human p53) without disturbing p53 homeostasis, DNA-binding ability, or transcription activity (Wang et al., 2016). $p53^{3KR}$ has a complete tumor suppression system (Brady et al., 2011). In a xenograft tumor model, a mutant $p53^{3KR}$ (K117/161/162) that lacked acetylation capacity could not induce cell senescence and apoptosis; however, it repressed SLC7A11 expression and induced ferroptosis (Jiang et al., 2015). However, simultaneous mutation of K98 produced a new mutant ($p53^{4KR}$), which lacked the ability to repress SLC7A11 expression and thus could not suppress tumor formation. Therefore, acetylation of p53 at K98 is essential for p53-mediated ferroptosis (Pegg, 2008; Lei et al., 2019). Mechanistic analysis indicated that combined removal of acetylation at K117/161/162 and K98 impeded p53-mediated transcriptional regulation of TIGAR and GLS2, which are closely associated with ferroptosis (Wang et al., 2016).

In addition to its effects on SLC7A11 suppression, p53 acetylation can regulate ferroptosis by regulating its downstream genes. Acetylation of p53 at K320 activates CDKN1A/p21, thereby delaying ferroptosis (Abbas and Dutta, 2009; Ji et al., 2021); however, the underlying mechanism is unknown. According to one hypothesis, p21 acts on GSH, thereby increasing the synthesis of GSH and GPX4, decreasing lipid peroxide accumulation, and reducing cell sensitivity to ferroptosis. However, the absence of cysteine leads to insufficient GPX4 synthesis, increased expression of wild-type p53, and increased cell sensitivity to ferroptosis (Bretscher et al., 2015). p53-mediated regulation of ferroptosis is closely associated with the levels of GPX4 and toxic peroxides. Therefore, p53 will affect cell sensitivity to ferroptosis by acting on p21 to control intracellular GSH levels, or by inhibiting SLC7A11 transcription (thereby increasing intracellular cysteine) (Ji et al., 2021). However, extensive studies regarding the mechanistic importance of p53 acetylation in tumor suppression are needed to determine the contributions of these acetyltransferases to the control of p53-mediated ferroptosis.

3.2.3 Ubiquitination

Ubiquitination is a PTM of proteins that participates in the management of biological processes, immune responses, apoptosis, and cancer (Han et al., 2018) (**Figure 4C**). Ubiquitin-mediated proteasomal degradation tightly controls p53 activity at the cellular level. MDM2, a major E3 ubiquitin-protein ligase, is an oncoprotein overexpressed in many human cancers (Wade et al., 2013; Spiegelberg et al., 2018). It mainly targets six lysine residues in p53: K370, K372, K373, K381, K382, and K386 within the C-terminal domain (Rodriguez et al., 2000). Endogenous MDM2 is the major negative regulator of p53; it is highly specific for p53 ubiquitination. In the absence of stress, MDM2 maintains an appropriately low level of p53 by ubiquitinating the transactivation domain of p53 (Oliner et al., 1993; Zhu et al., 2018). Overexpression of MDM2 leads to inactive p53, resulting in the generation of infinitely replicating cells (Li et al., 2003). MDM2 interacts with the transcription factor Yin Yang1, which maintains binding between p53 and MDM2; this promotes p53 ubiquitination and represses p53 activity, thereby promoting tumorigenesis (Kruse and Gu, 2009). The relationship between p53 ubiquitination and ferroptosis differs according to cell type. Ferroptosis can be delayed by pretreatment with nutlin-3 (an inhibitor of MDM2), suggesting that stable and persistent p53 reduces the rate of ferroptosis (Ji et al., 2021). Nutlin-3-mediated activation of p53 significantly reduces the expression of SLC7A11 in HT-1080 human fibrosarcoma cells (Zhang et al., 2018). In addition to the above-mentioned roles, MDM2 and MDMX can induce ferroptosis in a p53-independent manner, which is associated with PPARα-mediated lipid regulation by the MDM2-MDMX complex (Venkatesh et al., 2020).

Additionally, MDM2-independent ubiquitination regulates p53 activity by influencing cell degradation and localization. A recent study reported dual regulatory effects of p62 on ferroptosis in glioblastoma (Yuan et al., 2022). In mutant p53 glioblastoma, p62 activates p53; it then promotes ferroptosis by inhibiting p53 ubiquitination and SLC7A11 expression. However, in p53 wild-type glioblastoma, p62 attenuates ferroptosis and promotes SLC7A11 expression.

Acetylation and ubiquitination are mutually exclusive because they both modify the same lysine residue in the C-terminus of p53. MDM2 binds to amino acids 17–28, while CBP/p300 binds to amino acids 22–26 (Golubovskaya and Cance, 2013). MDM2-mediated ubiquitination prevents p53 acetylation, thereby causing rapid proteasome-mediated degradation (Ito et al., 2001). Elucidation of the relationship between acetylation and ubiquitination could provide further insight into the biology of p53 and its tumor suppression effects.

3.2.4 SUMOylation

SUMOylation, a reversible PTM of p53, has attracted increasing attention because it occurs in almost all eukaryotes (**Figure 4D**). SUMOylation participates in cellular death processes, maintains genome integrity, and regulates biological processes (Han et al., 2018). This process involves a small ubiquitin-like modifier (SUMO), which is a ubiquitin-like protein that is conjugated to lysines on p53 through a mechanism similar to ubiquitination. Thus far, five SUMO isoforms (SUMO1–5) have been identified in mammalian cells. Both SUMO1 and SUMO2/3 can SUMOylate p53 at K386 (Sheng et al., 2021). This SUMOylation prevents p300 from accessing C-terminal lysines and represses transcriptional activation, thus promoting cell proliferation by inhibiting the antigrowth function (Chen et al., 2020). Furthermore, SUMOylation can regulate the p53–MDM2 interaction, inhibiting tumor cell proliferation or inducing death (Carter et al., 2007).

SUMOylation is also implicated in ferroptosis (Stockwell et al., 2017) and is hyperactive in many cancers (Sheng et al., 2021). For example, Nrf2 can reduce ferroptosis by SUMOylation at K110 (Guo et al., 2019; Liu P et al., 2020). In addition, GPX4 can be SUMOylated at K125, which enables it to participate in ferroptosis (Sheng et al., 2021). However, few studies have explored the relationship between SUMOylation of p53 and ferroptosis; further investigations are needed.

3.2.5 Methylation

Methylation is an important PTM of p53; it most commonly occurs on lysine and arginine (**Figure 4D**). It is an important

TABLE 1 | Regulation of p53 in ferroptosis network.

Downstream regulation of p53	Ferroptosis network alternations	Cancer type	Stress condition	Ways of regulation	References
SLC7A11	Regulate cystine metabolism	Human osteosarcoma U2OS cells	Nutlin-3 treatment; DNA damage	Positive regulation	Jiang et al. (2015) Saint-Germain et al. (2017) Yuan et al. (2022)
SAT1	Oxidize polyunsaturated fatty acids; increase lipid peroxidation	Melanoma cell line, A375	Nutlin and ROS treatment	Positive regulation	Ou et al. (2016) Saint-Germain et al. (2017)
GLS2	Reduce GSH; increase ROS	Human glioblastoma; HCC	Doxycycline existence; unstressed condition	Positive regulation	Hu et al. (2010) Wang et al. (2016) Jennis et al. (2016)
PTGS2	Regulate crucial membrane phospholipid; affect polyunsaturated fatty acids abundance and distribution	$P53^{3KR/3KR}$ $Mdm2^{-/-}$embryos	Not mentioned	Positive regulation	Jiang et al. (2015)
ALOX12	Activate lipoxygenase; induce ferroptosis	Human osteosarcoma cell	ROS stress	Positive regulation	Chu et al. (2019)
TIGAR	Maintain reduced state of GSH	Lung cancer cell	Adriamycin treatment	Positive regulation	Bensaad et al. (2006) Wang et al. (2016)
FDXR	Promote p53 expression; interact with p53; regulate iron metabolisms	Human colon cancer cells	Not mentioned	Positive regulation	Zhang et al. (2017)
PARK2	Eliminate damaged mitochondria; enhance GSH; reduce ROS	Lung cancer cells	Infrared radiation	Negative regulation	Zhang et al. (2011)
CDKN1A/p21	Consume intracellular GSH; reduce ROS level	Fibrosarcoma cells	Cystine deprivation; GPX4 inhibition	Negative regulation	Tarangelo et al. (2018)
iPLA2β	Downregulation of peroxidized membrane lipids	Melanoma cells	Nutlin; doxorubicin	Negative regulation	Chen et al. (2021)
DPP4	Diminish lipid peroxidation	Colorectal cancer	DPP4 inhibitor vildagliptin	Negative regulation	Xie et al. (2017)

ALOX12, Arachidonic acid 12 lipoxygenases; ALOX15, Arachidonic acid 15 lipoxygenases; CDKN1A/p21, Cyclin-dependent kinase inhibitor; DPP4, Dipeptidyl peptidase-4; FDXR, ferredoxin reductase; GLS2, glutaminases; PARK2, Parkinson disease 2; PTGS2, Prostaglandin-endoperoxide synthase 2; SAT1, Spermidine/spermine N1-acetyltransferase; TIGAR, TP53-induced glycolysis and apoptosis regulator.

epigenetic marker on lysines in histone tails, similar to acetylation. The first reported methylation of p53 was lysine methylation by Set9 methyltransferase at K372, which positively stabilizes p53 by stabilizing the chromatin-bound portion of p53 (Chuikov et al., 2004). p53 can also be methylated at K382 by Set8 or K370 by SMYD2, both of which negatively stabilize p53 (Huang et al., 2006; Shi et al., 2007). Thus, the activating or repressing effects of methylation on p53 function depend on the sites that are modified. p53 methylation may also occur at the arginine residues R333, R335, and R337; these affect p53 target gene specificity in response to DNA damage (Jansson et al., 2008). Methylation also interacts with other PTMs. Methylation at K372 suppresses inhibitory methylation at K370, while methylation at K382 competes with acetylation at the same site (Huang et al., 2006; Shi et al., 2007). A better understanding of the relationships among different PTMs under specific stress should provide important insights into the function of the p53 pathway in ferroptosis.

3.2.6 O-GlcNAcylation

O-GlcNAcylation is another type of PTM, which involves the addition of N-acetylglucosamine (GlcNAc) to Ser or Thr residues (**Figure 4D**). O-GlcNAcylation is associated with cancer metabolism because of the Warburg effect in cancer cells, which exhibit high glycolytic flux and glucose uptake (de Queiroz et al., 2016). O-GlcNAcylation is mainly regulated by O-GlcNAc transferase and O-GlcNAcase, which are responsible for the addition or removal of O-GlcNAc. O-GlcNAcylation communicating with other PTMs may reveal the tumor-suppressive potential of the remaining p53 pathway. p53 can be O-GlcNAcylated at Ser149, thereby reducing proteasome-induced p53 degradation and stabilizing p53 (Yang et al., 2006). However, other O-GlcNAcylated sites have not been identified because Ser149 mutations do not lead to reduced levels of O-GlcNAcylation on p53. Furthermore, O-GlcNAcylation is reportedly associated with decreased phosphorylation of Thr155 at p53, which leads to increased protein stability, rather than interaction with MDM2 and subsequent ubiquitination (Yang et al., 2006). Acute exposure of endothelial cells to hyperglycemic conditions increases acetylation of p53 and expression of p21, suggesting that O-GlcNAcylation leads to increased transcription of p53 target genes (Zhang et al., 2015). Because O-GlcNAcylation has considerable effects in cellular metabolism, an emerging key question is whether the O-GlcNAcylation of p53 participates in the ferroptosis pathway.

3.3 Pharmacological Targets of p53-Mediated Ferroptosis Network for Cancer Therapy

Numerous studies have explored the pharmacological targets in p53-meditated ferroptosis for cancer therapy. SLC7A11 and GPX4 may be the most valuable pharmacological targets in the ferroptosis network. This has been confirmed by several studies on traditional antitumors drugs such as olaparib (Hong et al., 2021), tanshinone IIA (Guan et al., 2020) and bavachin (Luo et al., 2021). The poly (ADP-ribose) polymerase olaparib has been demonstrated to promote ferroptosis in ovarian cancer cells by downregulating SLC7A11 expression (Hong et al., 2021). This is a new way completely different from classical DNA repair function. Tanshinone IIA, the active ingredient of Chinese herbal medicine Salvia miltiorrhiza Bunge, also promotes ferroptosis in gastric cancer cells *via* p53/SLC7A11 (Guan et al., 2020). Bavachin induces ferroptosis in osteosarcoma cells *via* repressing SLC7A11 (Luo et al., 2021). Interestingly, bavachin also increases intracellular labile iron levels (Luo et al., 2021). This reveals that some drugs may not only act on a single target but promote ferroptosis through multiple pathways.

Targeting the p53/SLC7A11/GPX4 axis has also been found in non-anti-tumor drugs. Flubendazole, an antimalarial drug, inhibits SLC7A11/GPX4, promoting ferroptosis in castration-resistant prostate cancer (Zhou et al., 2021). Levobupivacaine, distinct from its anesthetic effect, inhibits SLC7A11/GPX4 and promotes p53-mediated ferroptosis to exert an antitumor effect in non-small cell lung cancer (Meng et al., 2021). Besides, other targets can also be utilized. For example, an increased dose of N-acylsphingosine amidohydrolase (ASAH2) inhibitor NC06 promotes p53 and heme oxygenase-1 and thus causes ferroptosis in colon cancer *via* decreasing oxidized glutathione (Zhu et al., 2021). The pharmacological targets described above bring new ideas for future research.

4 TARGETING PTMS AS A PERSPECTIVE STRATEGY

Recently, a new generation of anticancer agents targeting PTMs has led to a revolutionary therapeutic approach that provides enhanced selectivity and context-specificity. Most anti-tumor small-molecule compounds are pan-inhibitors, which act on multiple proteins with similar modifications; thus, they cause unexpected side effects. p53 maintains a series of complex PTMs during its activation; for example, it exhibits different types of PTMs at specific lysine residues (acetylation, methylation, and ubiquitination). Thus, precision cancer treatment can be achieved by accurately targeting PTMs of p53 under specific conditions.

Several small-molecule inhibitors can block or promote the interplay between specific PTMs of p53 and corresponding upstream proteins; these inhibitors include aurora-A, ZNF498, and eupaformosanin (Hsueh et al., 2013; Wei et al., 2022; Zhang et al., 2022). For example, ZNF498 inhibits Ser46 phosphorylation to reduce p53 transcription in hepatocellular carcinoma (Zhang et al., 2022). This provides a novel perspective for the treatment of hepatocellular carcinoma by suppressing ZNF498. Eupaformosanin is a natural product that ubiquitinates p53 and can induce ferroptosis in triple-negative breast cancer (Wei et al., 2022). Additionally, some specific PTMs of p53 or its upstream proteins have been found play roles in ferroptosis. Ferroptosis can be regulated by CBP analogs or inhibitors such as C646 (Zhou et al., 2018). Among the various PTMs, acetylation of p53 might be the most powerful pharmacological target; however, this hypothesis requires further investigation.

5 CONCLUSION AND PERSPECTIVES

Dysfunction of the tumor suppressor p53 has a widespread impact during carcinogenesis. The multiple functions of p53 and its numerous PTMs make its biology particularly complex. This review described diverse PTMs of p53 in cancer, with a focus on how p53 and its PTMs participate in ferroptosis. The dual effects (positive or negative) of p53 on ferroptosis are closely related to cancer cell type. PTMs are important components in the p53 signaling pathway; they strictly control the functional diversity of p53. Among the various PTMs of p53, acetylation has the greatest effects on p53-mediated ferroptosis during tumorigenesis. More detailed studies of how O-GlcNAcylation, SUMOylation, and methylation affect ferroptosis, as well as the corresponding networks, are needed to fully elucidate the landscape of p53 function in cancer treatment. Additionally, the biological effects of some drugs that target PTMs of p53 should be investigated to bring new insights to clinical cancer treatment.

AUTHOR CONTRIBUTIONS

JZ, NH, and XS: Conceptualization, Writing—Review and Editing. LZ and BC: Methodology, Software, Visualization, Writing-Original Draft. FH and CK: Visualization, Writing—Review.

FUNDING

This work was supported by the National Natural Science Foundation of China (81870593, 82170865), Natural Science Foundation of Shandong Province of China (ZR2020MH106) and Clinical research of Affiliated Hospital of Weifang Medical University (2021wyfylcyj05).

REFERENCES

Abbas, T., and Dutta, A. (2009). p21 in Cancer: Intricate Networks and Multiple Activities. *Nat. Rev. Cancer* 9, 400–414. doi:10.1038/nrc2657

Appella, E., and Anderson, C. W. (2001). Post-translational Modifications and Activation of P53 by Genotoxic Stresses. *Eur. J. Biochem.* 268, 2764–2772. doi:10.1046/j.1432-1327.2001.02225.x

Badgley, M. A., Kremer, D. M., Maurer, H. C., DelGiorno, K. E., Lee, H. J., Purohit, V., et al. (2020). Cysteine Depletion Induces Pancreatic Tumor Ferroptosis in Mice. *Science* 368, 85–89. doi:10.1126/science.aaw9872

Bargonetti, J., Friedman, P. N., Kern, S. E., Vogelstein, B., and Prives, C. (1991). Wild-type but Not Mutant P53 Immunopurified Proteins Bind to Sequences Adjacent to the SV40 Origin of Replication. *Cell.* 65, 1083–1091. doi:10.1016/0092-8674(91)90560-l

Bensaad, K., Tsuruta, A., Selak, M. A., Vidal, M. N., Nakano, K., and Bartrons, R. (2006). TIGAR, A p53-Inducible Regulator of Glycolysis and Apoptosis. *Cell* 126, 107–120. doi:10.1016/j.cell.2006.05.036

Blagih, J., Buck, M. D., and Vousden, K. H. (2020). p53, Cancer and the Immune Response. *J. Cell. Sci.* 133, jcs237453. doi:10.1242/jcs.237453

Brady, C. A., Jiang, D., Mello, S. S., Johnson, T. M., Jarvis, L. A., Kozak, M. M., et al. (2011). Distinct P53 Transcriptional Programs Dictate Acute DNA-Damage Responses and Tumor Suppression. *Cell.* 145, 571–583. doi:10.1016/j.cell.2011.03.035

Brandt, M. E., and Vickery, L. E. (1992). Expression and Characterization of Human Mitochondrial Ferredoxin Reductase in *Escherichia coli*. *Arch. Biochem. Biophys.* 294, 735–740. doi:10.1016/0003-9861(92)90749-m

Bretscher, P., Egger, J., Shamshiev, A., Trötzmüller, M., Köfeler, H., Carreira, E. M., et al. (2015). Phospholipid Oxidation Generates Potent Anti-inflammatory Lipid Mediators that Mimic Structurally Related Pro-resolving Eicosanoids by Activating Nrf2. *EMBO Mol. Med.* 7, 593–607. doi:10.15252/emmm.201404702

Calabrese, V., Mallette, F. A., Deschênes-Simard, X., Ramanathan, S., Gagnon, J., Moores, A., et al. (2009). SOCS1 Links Cytokine Signaling to P53 and Senescence. *Mol. Cell.* 36, 754–767. doi:10.1016/j.molcel.2009.09.044

Capelletti, M. M., Manceau, H., Puy, H., and Peoc'h, K. (2020). Ferroptosis in Liver Diseases: An Overview. *Int. J. Mol. Sci.* 21, 4908. doi:10.3390/ijms21144908

Carter, S., Bischof, O., Dejean, A., and Vousden, K. H. (2007). C-terminal Modifications Regulate MDM2 Dissociation and Nuclear Export of P53. *Nat. Cell. Biol.* 9, 428–435. doi:10.1038/ncb1562

Chehab, N. H., Malikzay, A., Stavridi, E. S., and Halazonetis, T. D. (1999). Phosphorylation of Ser-20 Mediates Stabilization of Human P53 in Response to DNA Damage. *Proc. Natl. Acad. Sci. U. S. A.* 96, 13777–13782. doi:10.1073/pnas.96.24.13777

Chen, D., Chu, B., Yang, X., Liu, Z., Jin, Y., Kon, N., et al. (2021). iPLA2β-mediated Lipid Detoxification Controls P53-Driven Ferroptosis Independent of GPX4. *Nat. Commun.* 12, 3644. doi:10.1038/s41467-021-23902-6

Chen, L., Liu, S., and Tao, Y. (2020). Regulating Tumor Suppressor Genes: Post-translational Modifications. *Signal Transduct. Target Ther.* 5, 90. doi:10.1038/s41392-020-0196-9

Chu, B., Kon, N., Chen, D., Li, T., Liu, T., Jiang, L., et al. (2019). ALOX12 Is Required for P53-Mediated Tumour Suppression through a Distinct Ferroptosis Pathway. *Nat. Cell. Biol.* 21, 579–591. doi:10.1038/s41556-019-0305-6

Chuikov, S., Kurash, J. K., Wilson, J. R., Xiao, B., Justin, N., Ivanov, G. S., et al. (2004). Regulation of P53 Activity through Lysine Methylation. *Nature* 432, 353–360. doi:10.1038/nature03117

Dai, C., and Gu, W. (2010). p53 Post-translational Modification: Deregulated in Tumorigenesis. *Trends Mol. Med.* 16, 528–536. doi:10.1016/j.molmed.2010.09.002

Datta, J., Majumder, S., Kutay, H., Motiwala, T., Frankel, W., Costa, R., et al. (2007). Metallothionein Expression Is Suppressed in Primary Human Hepatocellular Carcinomas and Is Mediated through Inactivation of CCAAT/enhancer Binding Protein Alpha by Phosphatidylinositol 3-kinase Signaling Cascade. *Cancer Res.* 67, 2736–2746. doi:10.1158/0008-5472.CAN-06-4433

de Queiroz, R. M., Madan, R., Chien, J., Dias, W. B., and Slawson, C. (2016). Changes in O-Linked N-Acetylglucosamine (O-GlcNAc) Homeostasis Activate the P53 Pathway in Ovarian Cancer Cells. *J. Biol. Chem.* 291, 18897–18914. doi:10.1074/jbc.M116.734533

DeNicola, G. M., Karreth, F. A., Humpton, T. J., Gopinathan, A., Wei, C., Frese, K., et al. (2011). Oncogene-induced Nrf2 Transcription Promotes ROS Detoxification and Tumorigenesis. *Nature* 475, 106–109. doi:10.1038/nature10189

Dixon, S. J., Lemberg, K. M., Lamprecht, M. R., Skouta, R., Zaitsev, E. M., Gleason, C. E., et al. (2012). Ferroptosis: an Iron-dependent Form of Nonapoptotic Cell Death. *Cell.* 149, 1060–1072. doi:10.1016/j.cell.2012.03.042

Friedmann Angeli, J. P., Krysko, D. V., and Conrad, M. (2019). Ferroptosis at the Crossroads of Cancer-Acquired Drug Resistance and Immune Evasion. *Nat. Rev. Cancer* 19, 405–414. doi:10.1038/s41568-019-0149-1

Gao, M., Yi, J., Zhu, J., Minikes, A. M., Monian, P., Thompson, C. B., et al. (2019). Role of Mitochondria in Ferroptosis. *Mol. Cell.* 73, 354. doi:10.1016/j.molcel.2018.10.042

Gkouvatsos, K., Papanikolaou, G., and Pantopoulos, K. (2012). Regulation of Iron Transport and the Role of Transferrin. *Biochim. Biophys. Acta* 1820, 188–202. doi:10.1016/j.bbagen.2011.10.013

Golubovskaya, V. M., and Cance, W. G. (2013). Targeting the P53 Pathway. *Surg. Oncol. Clin. N. Am.* 22, 747–764. doi:10.1016/j.soc.2013.06.003

Goodman, R. H., and Smolik, S. (2000). CBP/p300 in Cell Growth, Transformation, and Development. *Genes. Dev.* 14, 1553–1577. doi:10.1101/gad.14.13.1553

Gu, B., and Zhu, W. G. (2012). Surf the Post-translational Modification Network of P53 Regulation. *Int. J. Biol. Sci.* 8, 672–684. doi:10.7150/ijbs.4283

Guan, Z., Chen, J., Li, X., and Dong, N. (2020). Tanshinone IIA Induces Ferroptosis in Gastric Cancer Cells through P53-Mediated SLC7A11 Down-Regulation. *Biosci. Rep.* 40, BSR20201807. doi:10.1042/BSR20201807

Guo, H., Xu, J., Zheng, Q., He, J., Zhou, W., Wang, K., et al. (2019). NRF2 SUMOylation Promotes De Novo Serine Synthesis and Maintains HCC Tumorigenesis. *Cancer Lett.* 466, 39–48. doi:10.1016/j.canlet.2019.09.010

Guo, J., Xu, B., Han, Q., Zhou, H., Xia, Y., Gong, C., et al. (2018). Ferroptosis: A Novel Anti-tumor Action for Cisplatin. *Cancer Res. Treat.* 50, 445–460. doi:10.4143/crt.2016.572

Hainaut, P., and Hollstein, M. (2000). p53 and Human Cancer: the First Ten Thousand Mutations. *Adv. Cancer Res.* 77, 81–137. doi:10.1016/s0065-230x(08)60785-x

Han, Z. J., Feng, Y. H., Gu, B. H., Li, Y. M., and Chen, H. (2018). The Post-translational Modification, SUMOylation, and Cancer (Review). *Int. J. Oncol.* 52, 1081–1094. doi:10.3892/ijo.2018.4280

Hassannia, B., Vandenabeele, P., and Vanden Berghe, T. (2019). Targeting Ferroptosis to Iron Out Cancer. *Cancer Cell.* 35, 830–849. doi:10.1016/j.ccell.2019.04.002

Hong, T., Lei, G., Chen, X., Li, H., Zhang, X., Wu, N., et al. (2021). PARP Inhibition Promotes Ferroptosis via Repressing SLC7A11 and Synergizes with Ferroptosis Inducers in BRCA-Proficient Ovarian Cancer. *Redox Biol.* 42, 101928. doi:10.1016/j.redox.2021.101928

Hoshino, A., Mita, Y., Okawa, Y., Ariyoshi, M., Iwai-Kanai, E., Ueyama, T., et al. (2013). Cytosolic P53 Inhibits Parkin-Mediated Mitophagy and Promotes Mitochondrial Dysfunction in the Mouse Heart. *Nat. Commun.* 4, 2308. doi:10.1038/ncomms3308

Hsueh, K. W., Fu, S. L., Chang, C. B., Chang, Y. L., and Lin, C. H. (2013). A Novel Aurora-A-mediated Phosphorylation of P53 Inhibits its Interaction with MDM2. *Biochim. Biophys. Acta* 1834, 508–515. doi:10.1016/j.bbapap.2012.11.005

Hu, W., Zhang, C., Wu, R., Sun, Y., Levine, A., and Feng, Z. (2010). Glutaminase 2, a Novel P53 Target Gene Regulating Energy Metabolism and Antioxidant Function. *Proc. Natl. Acad. Sci. U. S. A.* 107, 7455–7460. doi:10.1073/pnas.1001006107

Huang, J., Perez-Burgos, L., Placek, B. J., Sengupta, R., Richter, M., Dorsey, J. A., et al. (2006). Repression of P53 Activity by Smyd2-Mediated Methylation. *Nature* 444, 629–632. doi:10.1038/nature05287

Ito, A., Lai, C. H., Zhao, X., Saito, S., Hamilton, M. H., Appella, E., et al. (2001). p300/CBP-mediated P53 Acetylation Is Commonly Induced by P53-Activating Agents and Inhibited by MDM2. *EMBO J.* 20, 1331–1340. doi:10.1093/emboj/20.6.1331

Jansson, M., Durant, S. T., Cho, E. C., Sheahan, S., Edelmann, M., Kessler, B., et al. (2008). Arginine Methylation Regulates the P53 Response. *Nat. Cell. Biol.* 10, 1431–1439. doi:10.1038/ncb1802

Jennis, M., Kung, C. P., Basu, S., Budina-Kolomets, A., Leu, J. I., Khaku, S., et al. (2016). An African-Specific Polymorphism in the TP53 Gene Impairs p53 Tumor Suppressor Function in a Mouse Model. *Genes Dev.* 30, 918–930. doi:10.1101/gad.275891.115

Ji, H., Wang, W., Li, X., Han, X., Zhang, X., Wang, J., et al. (2022). p53: A Double-Edged Sword in Tumor Ferroptosis. *Pharmacol. Res.* 177, 106013. doi:10.1016/j.phrs.2021.106013

Jiang, L., Kon, N., Li, T., Wang, S. J., Su, T., Hibshoosh, H., et al. (2015). Ferroptosis as a P53-Mediated Activity during Tumour Suppression. *Nature* 520, 57–62. doi:10.1038/nature14344

Joerger, A. C., and Fersht, A. R. (2016). The P53 Pathway: Origins, Inactivation in Cancer, and Emerging Therapeutic Approaches. *Annu. Rev. Biochem.* 85, 375–404. doi:10.1146/annurev-biochem-060815-014710

Jones, R. G., Plas, D. R., Kubek, S., Buzzai, M., Mu, J., Xu, Y., et al. (2005). AMP-activated Protein Kinase Induces a P53-dependent Metabolic Checkpoint. *Mol. Cell.* 18, 283–293. doi:10.1016/j.molcel.2005.03.027

Kaiser, A. M., and Attardi, L. D. (2018). Deconstructing Networks of P53-Mediated Tumor Suppression *In Vivo*. *Cell. Death Differ.* 25, 93–103. doi:10.1038/cdd.2017.171

Kang, R., Kroemer, G., and Tang, D. (2019). The Tumor Suppressor Protein P53 and the Ferroptosis Network. *Free Radic. Biol. Med.* 133, 162–168. doi:10.1016/j.freeradbiomed.2018.05.074

Kastenhuber, E. R., and Lowe, S. W. (2017). Putting P53 in Context. *Cell.* 170, 1062–1078. doi:10.1016/j.cell.2017.08.028

Koppula, P., Zhuang, L., and Gan, B. (2021). Cystine Transporter SLC7A11/xCT in Cancer: Ferroptosis, Nutrient Dependency, and Cancer Therapy. *Protein Cell.* 12, 599–620. doi:10.1007/s13238-020-00789-5

Kruse, J. P., and Gu, W. (2009). Modes of P53 Regulation. *Cell.* 137, 609–622. doi:10.1016/j.cell.2009.04.050

Lacroix, M., Toillon, R. A., and Leclercq, G. (2006). p53 and Breast Cancer, an Update. *Endocr. Relat. Cancer* 13, 293–325. doi:10.1677/erc.1.01172

Lane, D. (2016). p53: Out of Africa. *Genes. Dev.* 30, 876–877. doi:10.1101/gad.281733.116

Lei, P., Bai, T., and Sun, Y. (2019). Mechanisms of Ferroptosis and Relations with Regulated Cell Death: A Review. *Front. Physiol.* 10, 139. doi:10.3389/fphys.2019.00139

Levine, A. J. (1997). p53, the Cellular Gatekeeper for Growth and Division. *Cell.* 88, 323–331. doi:10.1016/s0092-8674(00)81871-1

Li, M., Brooks, C. L., Wu-Baer, F., Chen, D., Baer, R., and Gu, W. (2003). Mono- versus Polyubiquitination: Differential Control of P53 Fate by Mdm2. *Science* 302, 1972–1975. doi:10.1126/science.1091362

Li, T., Kon, N., Jiang, L., Tan, M., Ludwig, T., Zhao, Y., et al. (2012). Tumor Suppression in the Absence of P53-Mediated Cell-Cycle Arrest, Apoptosis, and Senescence. *Cell.* 149, 1269–1283. doi:10.1016/j.cell.2012.04.026

Liebl, M. C., and Hofmann, T. G. (2019). Cell Fate Regulation upon DNA Damage: P53 Serine 46 Kinases Pave the Cell Death Road. *Bioessays* 41, e1900127. doi:10.1002/bies.201900127

Lin, R., Zhang, Z., Chen, L., Zhou, Y., Zou, P., Feng, C., et al. (2016). Dihydroartemisinin (DHA) Induces Ferroptosis and Causes Cell Cycle Arrest in Head and Neck Carcinoma Cells. *Cancer Lett.* 381, 165–175. doi:10.1016/j.canlet.2016.07.033

Liu, J., Zhang, C., Wang, J., Hu, W., and Feng, Z. (2020). The Regulation of Ferroptosis by Tumor Suppressor P53 and its Pathway. *Int. J. Mol. Sci.* 21, 8387. doi:10.3390/ijms21218387

Liu, J., Zhang, C., Lin, M., Zhu, W., Liang, Y., Hong, X., et al. (2014). Glutaminase 2 Negatively Regulates the PI3K/AKT Signaling and Shows Tumor Suppression Activity in Human Hepatocellular Carcinoma. *Oncotarget* 5, 2635–2647. doi:10.18632/oncotarget.1862

Liu, P., Wu, D., Duan, J., Xiao, H., Zhou, Y., Zhao, L., et al. (2020). NRF2 Regulates the Sensitivity of Human NSCLC Cells to Cystine Deprivation-Induced Ferroptosis via FOCAD-FAK Signaling Pathway. *Redox Biol.* 37, 101702. doi:10.1016/j.redox.2020.101702

Liu, Y., Tavana, O., and Gu, W. (2019). p53 Modifications: Exquisite Decorations of the Powerful Guardian. *J. Mol. Cell. Biol.* 11, 564–577. doi:10.1093/jmcb/mjz060

Liu, Y., and Gu, W. (2021). The Complexity of P53-Mediated Metabolic Regulation in Tumor Suppression. *Seminars Cancer Biol.* doi:10.1016/j.semcancer.2021.03.010

Luo, J., Li, M., Tang, Y., Laszkowska, M., Roeder, R. G., and Gu, W. (2004). Acetylation of P53 Augments its Site-specific DNA Binding Both *In Vitro* and *In Vivo*. *Proc. Natl. Acad. Sci. U. S. A.* 101, 2259–2264. doi:10.1073/pnas.0308762101

Luo, Y., Gao, X., Zou, L., Lei, M., Feng, J., and Hu, Z. (2021). Bavachin Induces Ferroptosis through the STAT3/P53/SLC7A11 Axis in Osteosarcoma Cells. *Oxid. Med. Cell. Longev.* 2021, 1783485. doi:10.1155/2021/1783485

Mallette, F. A., Calabrese, V., Ilangumaran, S., and Ferbeyre, G. (2010). SOCS1, a Novel Interaction Partner of P53 Controlling Oncogene-Induced Senescence. *Aging (Albany NY)* 2, 445–452. doi:10.18632/aging.100163

Mandal, S., Mandal, A., and Park, M. H. (2015). Depletion of the Polyamines Spermidine and Spermine by Overexpression of Spermidine/spermine N^1-acetyltransferase 1 (SAT1) Leads to Mitochondria-Mediated Apoptosis in Mammalian Cells. *Biochem. J.* 468, 435–447. doi:10.1042/BJ20150168

Martín-Rufián, M., Nascimento-Gomes, R., Higuero, A., Crisma, A. R., Campos-Sandoval, J. A., Gómez-García, M. C., et al. (2014). Both GLS Silencing and GLS2 Overexpression Synergize with Oxidative Stress against Proliferation of Glioma Cells. *J. Mol. Med. Berl.* 92, 277–290. doi:10.1007/s00109-013-1105-2

Matsushita, M., Freigang, S., Schneider, C., Conrad, M., Bornkamm, G. W., and Kopf, M. (2015). T Cell Lipid Peroxidation Induces Ferroptosis and Prevents Immunity to Infection. *J. Exp. Med.* 212, 555–568. doi:10.1084/jem.20140857

Mavinahalli, J. N., Madhumalar, A., Beuerman, R. W., Lane, D. P., and Verma, C. (2010). Differences in the Transactivation Domains of P53 Family Members: a Computational Study. *BMC Genomics* 11, S5. doi:10.1186/1471-2164-11-S1-S5

Meng, M., Huang, M., Liu, C., Wang, J., Ren, W., Cui, S., et al. (2021). Local Anesthetic Levobupivacaine Induces Ferroptosis and Inhibits Progression by Up-Regulating P53 in Non-small Cell Lung Cancer. *Aging (Albany NY)* 13. doi:10.18632/aging.203138

Mou, Y., Wang, J., Wu, J., He, D., Zhang, C., Duan, C., et al. (2019). Ferroptosis, a New Form of Cell Death: Opportunities and Challenges in Cancer. *J. Hematol. Oncol.* 12, 34. doi:10.1186/s13045-019-0720-y

Oliner, J. D., Pietenpol, J. A., Thiagalingam, S., Gyuris, J., Kinzler, K. W., and Vogelstein, B. (1993). Oncoprotein MDM2 Conceals the Activation Domain of Tumour Suppressor P53. *Nature* 362, 857–860. doi:10.1038/362857a0

Olivier, M., Eeles, R., Hollstein, M., Khan, M. A., Harris, C. C., and Hainaut, P. (2002). The IARC TP53 Database: New Online Mutation Analysis and Recommendations to Users. *Hum. Mutat.* 19, 607–614. doi:10.1002/humu.10081

Ou, Y., Wang, S. J., Li, D., Chu, B., and Gu, W. (2016). Activation of SAT1 Engages Polyamine Metabolism with P53-Mediated Ferroptotic Responses. *Proc. Natl. Acad. Sci. U. S. A.* 113, E6806–E6812. doi:10.1073/pnas.1607152113

Pegg, A. E. (2008). Spermidine/spermine-N(1)-acetyltransferase: a Key Metabolic Regulator. *Am. J. Physiol. Endocrinol. Metab.* 294, E995–E1010. doi:10.1152/ajpendo.90217.2008

Pietsch, E. C., Sykes, S. M., McMahon, S. B., and Murphy, M. E. (2008). The P53 Family and Programmed Cell Death. *Oncogene* 27, 6507–6521. doi:10.1038/onc.2008.315

Rajendran, R., Garva, R., Ashour, H., Leung, T., Stratford, I., Krstic-Demonacos, M., et al. (2013). Acetylation Mediated by the p300/CBP-Associated Factor Determines Cellular Energy Metabolic Pathways in Cancer. *Int. J. Oncol.* 42, 1961–1972. doi:10.3892/ijo.2013.1907

Rodriguez, M. S., Desterro, J. M., Lain, S., Lane, D. P., and Hay, R. T. (2000). Multiple C-Terminal Lysine Residues Target P53 for Ubiquitin-Proteasome-Mediated Degradation. *Mol. Cell. Biol.* 20, 8458–8467. doi:10.1128/MCB.20.22.8458-8467.2000

Ryan, K. M. (2011). p53 and Autophagy in Cancer: Guardian of the Genome Meets Guardian of the Proteome. *Eur. J. Cancer(Oxford, Engl. 1990)* 47, 44–50. doi:10.1016/j.ejca.2010.10.020

Saint-Germain, E., Mignacca, L., Vernier, M., Bobbala, D., Ilangumaran, S., and Ferbeyre, G. (2017). SOCS1 Regulates Senescence and Ferroptosis by Modulating the Expression of P53 Target Genes. *Aging (Albany NY)* 9, 2137–2162. doi:10.18632/aging.101306

Shao, M., Jiang, Q., Shen, C., Liu, Z., and Qiu, L. (2022). Sinapine Induced Ferroptosis in Non-small Cell Lung Cancer Cells by Upregulating

Transferrin/transferrin Receptor and Downregulating SLC7A11. *Gene* 827, 146460. doi:10.1016/j.gene.2022.146460

Sheng, Z., Zhu, J., Deng, Y. N., Gao, S., and Liang, S. (2021). SUMOylation Modification-Mediated Cell Death. *Open Biol.* 11, 210050. doi:10.1098/rsob.210050

Shi, X., Kachirskaia, I., Yamaguchi, H., West, L. E., Wen, H., Wang, E. W., et al. (2007). Modulation of P53 Function by SET8-Mediated Methylation at Lysine 382. *Mol. Cell.* 27, 636–646. doi:10.1016/j.molcel.2007.07.012

Shieh, S. Y., Ahn, J., Tamai, K., Taya, Y., and Prives, C. (2000). The Human Homologs of Checkpoint Kinases Chk1 and Cds1 (Chk2) Phosphorylate P53 at Multiple DNA Damage-Inducible Sites. *Genes. Dev.* 14, 289–300. doi:10.1101/gad.14.3.289

Shieh, S. Y., Ikeda, M., Taya, Y., and Prives, C. (1997). DNA Damage-Induced Phosphorylation of P53 Alleviates Inhibition by MDM2. *Cell.* 91, 325–334. doi:10.1016/s0092-8674(00)80416-x

Shieh, S. Y., Taya, Y., and Prives, C. (1999). DNA Damage-Inducible Phosphorylation of P53 at N-Terminal Sites Including a Novel Site, Ser20, Requires Tetramerization. *EMBO J.* 18, 1815–1823. doi:10.1093/emboj/18.7.1815

Spiegelberg, D., Mortensen, A. C., Lundsten, S., Brown, C. J., Lane, D. P., and Nestor, M. (2018). The MDM2/MDMX-P53 Antagonist PM2 Radiosensitizes Wild-type P53 Tumors. *Cancer Res.* 78, 5084–5093. doi:10.1158/0008-5472.CAN-18-0440

Stockwell, B. R., Friedmann Angeli, J. P., Bayir, H., Bush, A. I., Conrad, M., Dixon, S. J., et al. (2017). Ferroptosis: A Regulated Cell Death Nexus Linking Metabolism, Redox Biology, and Disease. *Cell.* 171, 273–285. doi:10.1016/j.cell.2017.09.021

Su, Y., Zhao, B., Zhou, L., Zhang, Z., Shen, Y., Lv, H., et al. (2020). Ferroptosis, a Novel Pharmacological Mechanism of Anti-cancer Drugs. *Cancer Lett.* 483, 127–136. doi:10.1016/j.canlet.2020.02.015

Suzuki, S., Tanaka, T., Poyurovsky, M. V., Nagano, H., Mayama, T., Ohkubo, S., et al. (2010). Phosphate-activated Glutaminase (GLS2), a P53-Inducible Regulator of Glutamine Metabolism and Reactive Oxygen Species. *Proc. Natl. Acad. Sci. U. S. A.* 107, 7461–7466. doi:10.1073/pnas.1002459107

Suzuki, T., Motohashi, H., and Yamamoto, M. (2013). Toward Clinical Application of the Keap1-Nrf2 Pathway. *Trends Pharmacol. Sci.* 34, 340–346. doi:10.1016/j.tips.2013.04.005

Tarangelo, A., Magtanong, L., Bieging-Rolett, K. T., Li, Y., Ye, J., Attardi, L. D., et al. (2018). p53 Suppresses Metabolic Stress-Induced Ferroptosis in Cancer Cells. *Cell. Rep.* 22, 569–575. doi:10.1016/j.celrep.2017.12.077

Teufel, D. P., Bycroft, M., and Fersht, A. R. (2009). Regulation by Phosphorylation of the Relative Affinities of the N-Terminal Transactivation Domains of P53 for P300 Domains and Mdm2. *Oncogene* 28, 2112–2118. doi:10.1038/onc.2009.71

Valente, L. J., Gray, D. H., Michalak, E. M., Pinon-Hofbauer, J., Egle, A., Scott, C. L., et al. (2013). p53 Efficiently Suppresses Tumor Development in the Complete Absence of its Cell-Cycle Inhibitory and Proapoptotic Effectors P21, Puma, and Noxa. *Cell. Rep.* 3, 1339–1345. doi:10.1016/j.celrep.2013.04.012

Venkatesh, D., O'Brien, N. A., Zandkarimi, F., Tong, D. R., Stokes, M. E., Dunn, D. E., et al. (2020). MDM2 and MDMX Promote Ferroptosis by PPARα-Mediated Lipid Remodeling. *Genes. Dev.* 34, 526–543. doi:10.1101/gad.334219.119

Wade, M., Li, Y. C., and Wahl, G. M. (2013). MDM2, MDMX and P53 in Oncogenesis and Cancer Therapy. *Nat. Rev. Cancer* 13, 83–96. doi:10.1038/nrc3430

Wang, S. J., Li, D., Ou, Y., Jiang, L., Chen, Y., Zhao, Y., et al. (2016). Acetylation Is Crucial for P53-Mediated Ferroptosis and Tumor Suppression. *Cell. Rep.* 17, 366–373. doi:10.1016/j.celrep.2016.09.022

Wei, Y., Zhu, Z., Hu, H., Guan, J., Yang, B., and Zhao, H. (2022). Eupaformosanin Induces Apoptosis and Ferroptosis through Ubiquitination of Mutant P53 in Triple-Negative Breast Cancer. *Eur. J. Pharmacol.* 924, 174970. doi:10.1016/j.ejphar.2022.174970

Xie, Y., Zhu, S., Song, X., Sun, X., Fan, Y., Liu, J., et al. (2017). The Tumor Suppressor P53 Limits Ferroptosis by Blocking DPP4 Activity. *Cell. Rep.* 20, 1692–1704. doi:10.1016/j.celrep.2017.07.055

Xu, W. H., Li, C. H., and Jiang, T. L. (2018). Ferroptosis Pathway and its Intervention Regulated by Chinese Materia Medica. *Zhongguo Zhong Yao Za Zhi* 43, 4019–4026. doi:10.19540/j.cnki.cjcmm.20180517.001

Yang, T., Choi, Y., Joh, J. W., Cho, S. K., Kim, D. S., and Park, S. G. (2019). Phosphorylation of P53 Serine 15 Is a Predictor of Survival for Patients with Hepatocellular Carcinoma. *Can. J. Gastroenterol. Hepatol.* 2019, 9015453. doi:10.1155/2019/9015453

Yang, W. H., Kim, J. E., Nam, H. W., Ju, J. W., Kim, H. S., Kim, Y. S., et al. (2006). Modification of P53 with O-Linked N-Acetylglucosamine Regulates P53 Activity and Stability. *Nat. Cell. Biol.* 8, 1074–1083. doi:10.1038/ncb1470

Yuan, F., Sun, Q., Zhang, S., Ye, L., Xu, Y., Deng, G., et al. (2022). The Dual Role of P62 in Ferroptosis of Glioblastoma According to P53 Status. *Cell. Biosci.* 12, 20. doi:10.1186/s13578-022-00764-z

Zhang, C., Lin, M., Wu, R., Wang, X., Yang, B., Levine, A. J., et al. (2011). Parkin, a P53 Target Gene, Mediates the Role of P53 in Glucose Metabolism and the Warburg Effect. *Proc. Natl. Acad. Sci. U. S. A.* 108, 16259–16264. doi:10.1073/pnas.1113884108

Zhang, E., Guo, Q., Gao, H., Xu, R., Teng, S., and Wu, Y. (2015). Metformin and Resveratrol Inhibited High Glucose-Induced Metabolic Memory of Endothelial Senescence through SIRT1/p300/p53/p21 Pathway. *PLoS ONE* 10, e0143814. doi:10.1371/journal.pone.0143814

Zhang, W., Gai, C., Ding, D., Wang, F., and Li, W. (2018). Targeted P53 on Small-Molecules-Induced Ferroptosis in Cancers. *Front. Oncol.* 8, 507. doi:10.3389/fonc.2018.00507

Zhang, X., Zheng, Q., Yue, X., Yuan, Z., Ling, J., Yuan, Y., et al. (2022). ZNF498 Promotes Hepatocellular Carcinogenesis by Suppressing P53-Mediated Apoptosis and Ferroptosis via the Attenuation of P53 Ser46 Phosphorylation. *J. Exp. Clin. Cancer Res.* 41, 79. doi:10.1186/s13046-022-02288-3

Zhang, Y., Qian, Y., Zhang, J., Yan, W., Jung, Y. S., Chen, M., et al. (2017). Ferredoxin Reductase Is Critical for P53-dependent Tumor Suppression via Iron Regulatory Protein 2. *Genes. Dev.* 31, 1243–1256. doi:10.1101/gad.299388.117

Zhao, X., Sun, W., Ren, Y., and Lu, Z. (2021). Therapeutic Potential of P53 Reactivation in Cervical Cancer. *Crit. Rev. Oncol. Hematol.* 157, 103182. doi:10.1016/j.critrevonc.2020.103182

Zheng, J., and Conrad, M. (2020). The Metabolic Underpinnings of Ferroptosis. *Cell. Metab.* 32, 920–937. doi:10.1016/j.cmet.2020.10.011

Zhou, X., Zou, L., Chen, W., Yang, T., Luo, J., Wu, K., et al. (2021). Flubendazole, FDA-Approved Anthelmintic, Elicits Valid Antitumor Effects by Targeting P53 and Promoting Ferroptosis in Castration-Resistant Prostate Cancer. *Pharmacol. Res.* 164, 105305. doi:10.1016/j.phrs.2020.105305

Zhou, Y., Que, K. T., Zhang, Z., Yi, Z. J., Zhao, P. X., You, Y., et al. (2018). Iron Overloaded Polarizes Macrophage to Proinflammation Phenotype through ROS/acetyl-p53 Pathway. *Cancer Med.* 7, 4012–4022. doi:10.1002/cam4.1670

Zhu, D., Osuka, S., Zhang, Z., Reichert, Z. R., Yang, L., Kanemura, Y., et al. (2018). Bai1 Suppresses Medulloblastoma Formation by Protecting P53 from Mdm2-Mediated Degradation. *Cancer Cell.* 33, 1004. doi:10.1016/j.ccell.2018.05.006

Zhu, H., Klement, J. D., Lu, C., Redd, P. S., Yang, D., Smith, A. D., et al. (2021). Asah2 Represses the P53-Hmox1 Axis to Protect Myeloid-Derived Suppressor Cells from Ferroptosis. *J.I. Baltim. Md* 206, 1395–1404. doi:10.4049/jimmunol.2000500

Conflict of Interest: The authors declare that the research was conducted in the absence of any commercial or financial relationships that could be construed as a potential conflict of interest.

Publisher's Note: All claims expressed in this article are solely those of the authors and do not necessarily represent those of their affiliated organizations, or those of the publisher, the editors and the reviewers. Any product that may be evaluated in this article, or claim that may be made by its manufacturer, is not guaranteed or endorsed by the publisher.

frontiers | Frontiers in Oncology

ORIGINAL RESEARCH
published: 09 June 2022
doi: 10.3389/fonc.2022.888699

Ferroptosis-Related Long Noncoding RNAs as Prognostic Biomarkers for Ovarian Cancer

Kaili Wang[1†], *Shanshan Mei*[1,2†], *Mengcheng Cai*[1†], *Dongxia Zhai*[1], *Danying Zhang*[1], *Jin Yu*[1,3*], *Zhexin Ni*[1*] and *Chaoqin Yu*[1,2*]

[1] Department of Traditional Chinese Gynecology, The First Affiliated Hospital of Naval Medical University, Shanghai, China,
[2] Department of Gynecology of Traditional Chinese Medicine, Shanghai University of Traditional Chinese Medicine, Shanghai, China,
[3] International Peace Maternity and Child Health Hospital, School of Medicine, Shanghai Jiao Tong University, Shanghai, China

OPEN ACCESS

Edited by:
Jian Chen,
Guilin Medical University, China

Reviewed by:
Yinu Wang,
Northwestern University, United States
Vijay Pandey,
Tsinghua University, China

***Correspondence:**
Jin Yu
395005545@163.com
Zhexin Ni
nizxzg@163.com
Chaoqin Yu
chqyu81@163.com

[†]These authors have contributed equally to this work and share first authorship

Specialty section:
This article was submitted to Pharmacology of Anti-Cancer Drugs, a section of the journal Frontiers in Oncology

Received: 03 March 2022
Accepted: 27 April 2022
Published: 09 June 2022

Citation:
Wang K, Mei S, Cai M, Zhai D, Zhang D, Yu J, Ni Z and Yu C (2022) Ferroptosis-Related Long Noncoding RNAs as Prognostic Biomarkers for Ovarian Cancer. Front. Oncol. 12:888699. doi: 10.3389/fonc.2022.888699

Ovarian cancer (OC) is a highly malignant gynecologic tumor with few treatments available and poor prognosis with the currently available diagnostic markers and interventions. More effective methods for diagnosis and treatment are urgently needed. Although the current evidence implicates ferroptosis in the development and therapeutic responses of various types of tumors, it is unclear to what extent ferroptosis affects OC. To explore the potential of ferroptosis-related genes as biomarkers and molecular targets for OC diagnosis and intervention, this study collected several datasets from The Cancer Genome Atlas-OC (TCGA-OC), analyzed and identified the coexpression profiles of 60 ferroptosis-related genes and two subtypes of OC with respect to ferroptosis and further examined and analyzed the differentially expressed genes between the two subtypes. The results indicated that the expression levels of ferroptosis genes were significantly correlated with prognosis in patients with OC. Single-factor Cox and LASSO analysis identified eight lncRNAs from the screened ferroptosis-related genes, including lncRNAs RP11-443B7.3, RP5-1028K7.2, TRAM2-AS1, AC073283.4, RP11-486G15.2, RP11-95H3.1, RP11-958F21.1, and AC006129.1. A risk scoring model was constructed from the ferroptosis-related lncRNAs and showed good performance in the evaluation of OC patient prognosis. The high- and low-risk groups based on tumor scores presented obvious differences in clinical characteristics, tumor mutation burden, and tumor immune cell infiltration, indicating that the risk score has a good ability to predict the benefit of immunotherapy and may provide data to support the implementation of precise immunotherapy for OC. Although *in vivo* tests and research are needed in the future, our bioinformatics analysis powerfully supported the effectiveness of the risk signature of ferroptosis-related lncRNAs for prognosis prediction in OC. The findings suggest that these eight identified lncRNAs have great potential for development as diagnostic markers and intervention targets for OC and that patients with high ferroptosis-related lncRNA expression will receive greater benefits from conventional chemotherapy or treatment with ferroptosis inducers.

Keywords: ferroptosis, long noncoding RNA, biomarkers, tumor immune, ovarian cancer

INTRODUCTION

Ovarian cancer (OC) is the seventh most common cancer of the female reproductive system and one of the most common gynecologic malignant tumors worldwide, and the 5-year survival rate of OC has remained between 30% and 50% for decades (1, 2). The female ovary is located deep in the pelvic cavity and has multiple histological characteristics, causing a series of clinical diagnostic problems for OC. Effective diagnostic methods for early OC remain lacking. According to its histopathological characteristics, OCs are categorized as epithelial OC tumors, germ cell tumors, or sex cord-stromal tumors, accounting for more than 90%, 2–3%, and 5–6% of cases, respectively (3). The preventive measures and treatments for OC, such as surgical treatment, systemic treatment, and targeted therapy, have made great progress (4). However, due to the lack of typical clinical symptoms in the early stage of onset, 75% of cases are diagnosed at stage III or IV, and 70–80% of patients relapse after early treatment (5). Most OC cases identified late in life initially respond well to chemotherapy treatment, but the development of resistance always leads to a poor long-term prognosis (6). Therefore, it is urgent to identify sensitive biomarkers to provide personalized diagnosis and accurate prognostic evaluation for the treatment of patients with OC (7, 8), as has occurred with the emergence of platinum resistance and new anticancer therapies, such as immunotherapy (7, 8).

Ferroptosis is a newly identified nonapoptotic, iron-dependent form of programmed cell death that is characterized by the accumulation of lipid peroxidation; it was originally found by Dixon et al. in 2012 (9). As accumulating reactive oxygen species (ROS) attack the polyunsaturated fatty acids (PUFAs) of phospholipid membranes with multiple unsaturated double bonds, they trigger nonenzymatic lipid peroxidation and produce end-products of lipid peroxidation, such as 4-hydroxy-2-nonenol and malondialdehyde (10), which have toxic effects on cells, thereby initiating iron ion-dependent cell death (11), that is, ferroptosis. Emerging evidence suggests that ferroptosis may be a critical adaptive process for eradicating carcinogenic cells (12; Wang et al., 2021). It may also play vital roles in the pathological development and clinical therapeutics of tumor cells and cancers relevant to ferroptosis, p53, noncoding RNAs (ncRNAs), and the tumor microenvironment (TME); moreover, a series of small molecules have been found to be able to induce ferroptosis in a wide range of cancer cells. However, whether ferroptosis and its related genes and proteins are involved in the formation and growth of OC is still unclear (13–15).

LncRNAs, which are RNA molecules with more than 200 nucleotides, have been demonstrated to have a potential role in regulating normal or cancerous cells: on the one hand, their dysregulation results in abnormalities in cell migration, proliferation, the cell cycle, apoptosis and autophagy, which are closely involved in different cancers; on the other hand, alterations in lncRNAs lead to the emergence of cancer (16, 17; Li and Ugalde et al., 2021; 18, 19). For instance, the lncRNAs NEAT1, SNHG3 and H19 can function in cancer proliferation and metastasis as upstream mediators of the STAT3 pathway (16); lncRNAs HANR, BORG, etc., drive DOX resistance by activating the NF-κB, PI3K/Akt, and Wnt pathways; and the lncRNA SOX2OT-V7 can activate protective autophagy in response to the stress caused by DOX (17, 18). In OC, it has been found that the lncRNAs ROR, HOTAIR, H19 and UCA1 can influence the progression of ovarian cancer by promoting EMT (20), while the upregulation of the lncRNA CCAT2 significantly accelerates the proliferation, migration and invasion of tumor cells in OC (21). In addition, it has been found that lncRNA SPRY4-IT1 can promote OC by affecting the cell cycle. Therefore, regulating the expression of lncRNAs is of significant importance in cancer therapy.

Multiple studies have shown that lncRNAs may regulate cancers through ferroptosis. For instance, the lncRNA NEAT1 can regulate ferroptosis sensitivity (22), LINC00336, as a competing endogenous RNA, can inhibit ferroptosis in lung cancer (Wang Z et al., 2021), and LINC00618 can reduce the expression of lymphoid-specific helicase, thus inhibiting ferroptosis (Wang et al., 2021). Mao et al. demonstrated that the cytoplasmic lncRNA P53RRA is downregulated and interacts with Ras-GTPase activating protein binding protein 1 (G3BP1) to transfer p53 from the G3BP1 complex, resulting in p53 retention in the nucleus, leading to ferroptosis (23). Furthermore, GABBB1 and its antisense lncRNA GAPB1-AS1 can interact in erastin-induced ferroptosis (24).

In addition, recent studies have shown that lncRNAs directly or indirectly regulate ferroptosis and its related signaling pathways (25) and play a key role in the processes of ferroptosis-regulated cancers (23, 24; Wang et al., 2020; 26). On the one hand, the expression of lncRNA TINCR increases in breast cancer, and lncRNA FTX promotes the proliferation and invasion of gastric cancer through miR-144/ZFX (27, 28). TINCR combines with STAU1 to guide STAU1 to regulate the stability of OAS1, and low levels of OAS1 aggravate tumor proliferation and migration (29). The lncRNA LINC00336 may increase the growth of lung cancer cells through the LSH/ELAVL1/LINC00336 axis, accelerate tumor formation, and inhibit ferroptosis pathways in lung cancer cells (30, 31).

On the other hand, lncRNAs are widely involved in p53-related signaling pathways. p53 promotes dipeptidylpeptidase-4 (DPP4) translocation into the tumor cell nucleus in a transcription-independent manner, forming a p53-DPP4 complex, and thus negatively regulates the ferroptosis of colorectal cancer cells by inhibiting the association of DPP4 and nicotinamide adenine dinucleotide phosphate oxidase 1 (NOX1) (32). Furthermore, lncRNAs inhibit the binding of miRNAs and mRNAs by competitively adsorbing miRNAs in response to the original, resulting in the silencing of target genes (33). The above studies have shown that lncRNAs may be key molecular regulators in tumor and ferroptosis pathways and participate in the occurrence and development of tumors. A recent study found that eight lncRNAs, including AC138904.1, AP005205.2 and UBXN10-AS1, which are associated with iron metabolism in OC, were strongly associated with the overall survival of patients (34). However, lncRNAs involved in regulating ferroptosis pathways have not been reported in the diagnosis, intervention or prognosis of OC; it is still unclear whether these ferroptosis-related lncRNAs play roles in OC.

To explore and verify whether ferroptosis-related lncRNAs are involved in the pathogenesis and disease processes of OC and further validate their significance in the diagnosis and prognosis evaluation of OC, the expression profile and clinical follow-up information data of patients with OC were obtained and analyzed in the TCGA database (**Figure 1**). Differentially expressed ferroptosis-related lncRNAs were screened, and the lncRNAs that were significantly coexpressed with ferroptosis-related genes were finally identified by single-factor Cox and least absolute shrinkage and selection operator (LASSO). Using the TCGA-OC data, a risk scoring model between the identified lncRNAs and OC was also constructed with multivariate Cox regression to assess and confirm the accuracy of patient diagnosis and prognosis prediction. TCGA-OC tumor samples were divided into two different groups on the basis of the risk score, and differences in clinical characteristics, tumor mutation burden, and tumor immune cell infiltration (ICI) were found. Moreover, the ability of the risk score to predict the benefit of immunotherapies for OC was further evaluated. These results (**Figure 1**) provide powerful support for the implementation of precise immunotherapy for OC and act as a reference for the early diagnosis and prognosis evaluation of patients with OC. Furthermore, these ferroptosis-related lncRNAs and genes may be vital regulatory molecules for OC treatment.

METHODS

Samples and Data Collection for Clinical Patients With OC

The gene expression profile data and clinical follow-up information of patients with OC (**Figure 1**) were collected by exploring and analyzing the TCGA database (https://portal.gdc.cancer.gov/). Then, the obtained samples and RNA-Seq data were analyzed and processed as follows: (1) samples without clinical follow-up information were removed; (2) samples with a certain survival time, less than 30 days of survival, or no survival status were removed; (3) the peaks of gene expression assays were converted to Gene Symbols; (4) probes that corresponded to multiple genes were removed; and (5) the expression of genes corresponding to multiple Gene Symbols was presented as the average value. In this study, data for a total of 357 tumor samples were acquired and confirmed from TCGA-OC. The clinical statistics of the samples are shown in **Table 1**.

Heterogeneous Clustering Analysis of Tumorous Gene Profiles Related to Ferroptosis

As ferroptosis is activated by excessive lipid peroxidation, accompanied by the accumulation of lipid peroxidation markers, the cell death caused by ferroptosis could be completely suppressed by the consumption of iron chelators, lipophilic antioxidants, lipid peroxidation inhibitors, and polyunsaturated fatty acids. Ferroptosis is reflected by metabolic dysfunction involving abnormal levels of ROS, iron, and PUFAs around tumors. Thus, in this study, various genes and pathways related to iron, energy metabolism, lipid synthesis, and oxidative stress were considered, as they may negatively affect the sensitivity of ferroptosis-related analyses.

Research papers on ferroptosis published in the past 3 years were collected, and then all of the ferroptosis-related genes in these research results were obtained. Using an impact factor (IF) above 10 as an inclusion criterion to select high-quality studies, a total of 60 ferroptosis-related genes were identified (10, 35–37). The expression profiles of these 60 screened genes were extracted from the TCGA database. Unsupervised clustering was performed on Consensus Cluster Plus-R packages *via* Euclid with the Ward's and PAM methods. The procedure was repeated 1000 times to ensure test stability.

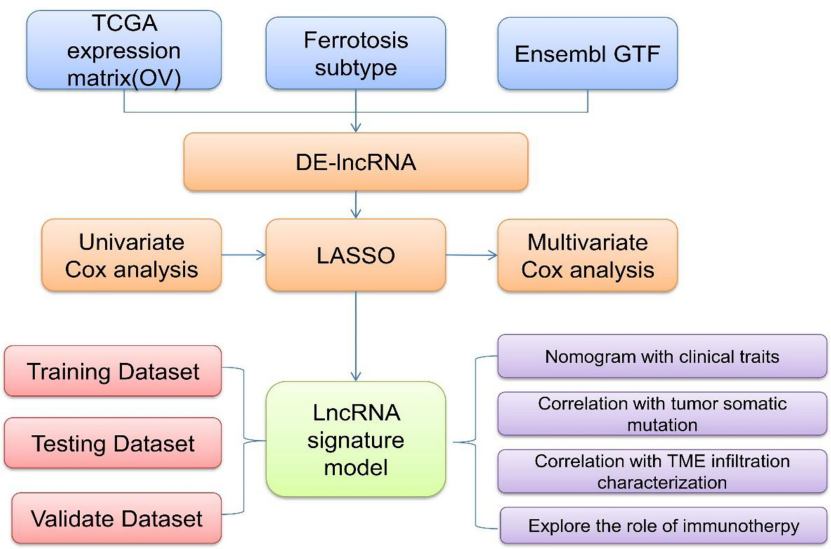

FIGURE 1 | A flowchart and analysis approaches of this study.

TABLE 1 | Profile data of gene expression and clinical follow-up information from TCGA-OC.

		TCGA-OC
Survial		
OS	Status_0	139
	Status_1	218
Age		
	Age>65	112
	Age<=65	245
Grade		
	G1	1
	G2	45
	G3	310
	G4	1
Stage		
	Stage_I	1
	Stage_II	21
	Stage_III	283
	Stage_IV	52

Differentially Expressed Genes Between the Two Subtypes

On the basis of the differentially expressed genes and clustering analysis results (**Figure 1**), tumorous samples from patients with OC were divided into two subtype groups (Fer-1 and Fer-2). Then, the differentially expressed genes between the two groups was compared and analyzed *via* the limma package of R software. After the filtering threshold of the differentially expressed gene was adjusted to $P < 0.05$ and $|\log2 \text{ (fold change)}| > 2/3$, the genome annotation file in Ensemble was used to extract the lncRNAs from the set of differentially expressed genes.

Feature Dimension and Risk Scoring Model for Ferroptosis-Related lncRNAs

On the basis of the two subtypes of lncRNAs, tumor risk scoring models were constructed for the screened ferroptosis-related LncRNAs (**Figure 1**). First, the single-factor Cox algorithm was used to reduce the size of the lncRNA gene sets related to ICI subtypes to reduce noise and eliminate redundant genes. Afterward, LASSO (Tibshirani) was used to screen variables to reduce the number of genes in the risk models. Finally, a multifactor Cox regression model was used to construct a risk scoring model for tumor ICI. The calculation formula was as follows:

$$\text{Risk}\_scores = \sum Coef(i) * Exp(i)$$

Gene Set Enrichment Analysis (GSEA)

GSEA is a gene enrichment analysis method that takes a knowledge-based approach to interpreting genome-wide expression profiles. One or more functional gene sets, stemming from the gene matrix transposition file formats, were sorted according to the correlation levels between the gene expression values and tumorous phenotypes, thus forming the different gene lists (**Figure 1**). They were then used to judge whether the genes of each gene set were enriched in the upper or lower part of the gene list to assess the influence of the coordinated phenotypic changes.

Statistical Analysis

Statistical analysis was performed in R software (3.6). R packages and tools used in the study were indicated. Statistical methods were described in the corresponding sections. $P < 0.05$ was considered as significant. ns, no significance. *$P < 0.05$, **$P < 0.01$, ***$P < 0.001$, ****$P < 0.0001$.

RESULTS

Classification of OC Based on Ferroptosis-Related Gene Sets

On the basis of the best density algorithm, 60 ferroptosis-related genes for OC were divided into high- and low-expression groups. The high-expression group included *AKR1C3, CD44, CISD1, GCLC, SLC7A11, PHKG2, HSBP1, KEAP1, NQO1, SLC1A5, G6PD*, and *PGD*. The low-expression group included *ACSL4, ALOX15, ALOX12, ATP5MC3, CBS, FANCD2, CRYAB, LPCAT3, STEAP3, ACACA, ZEB1, NOX1, ABCC1, IREB2, HMOX1*, and *ACSF2*. Both groups showed significant differences between the prognostic treatment survival curves of OC ($p<0.05$, **Figure 2** and **Supplementary Material F1**).

Subsequently, the analyzed results suggested that 96.79% of tumor samples in the TCGA-OC dataset had gene mutations. Among them, TP53 and TTN mutations were most prevalent, occurring in up to 88% and 34% of the samples, respectively (**Figure 3A**). Hypothesis tests were performed to further determine whether the gene mutations in TP53 and TTN affected the expression of 60 ferroptosis-related genes. The results showed that in the TP53-mutation group, the expression levels of CHAC1, FANCD2, PGD, and other genes were significantly higher than in the wild type, whereas the expression levels of ALOX5, DPP4, GLS2, and FTH1 were significantly lower (**Supplementary Material F2**). In the TTN-mutation group, the expression of CHAC1 and KEAP1 was significantly lower than in the wild type, while the expression of NCO4A and ACO1 was significantly higher (**Figure 3** and **Supplementary Material F2**). Furthermore, the expression levels showed mutual promotion effects and a high correlation of expression among the 60 ferroptosis-related genes (**Figure 4**)

Functional Annotations of Significant Genes for Ferroptosis Subtypes

On the basis of the expression values of the 60 screened ferroptosis-related genes, clustering analysis suggested that when the cluster k values were 2, 3, or 4 (**Figures 5A–C**), but especially 2, the difference between the two subtypes was significant, and the trend was proximate (**Figures 5A–D**). Meanwhile, analyses of survival rates indicated that when $k = 2$, survival was distinct between the two subtypes. Fer-2 predicted better prognosis than Fer-1, and Fer-1 was associated with poor prognosis. These results confirmed the two subtypes of OC with respect to ferroptosis, Fer-1 and Fer-2.

The R limma package was used to analyze the differences in the gene expression levels in the two subtypes of Fer-1 and Fer-2. When the gene expression threshold values were set to adjusted values of

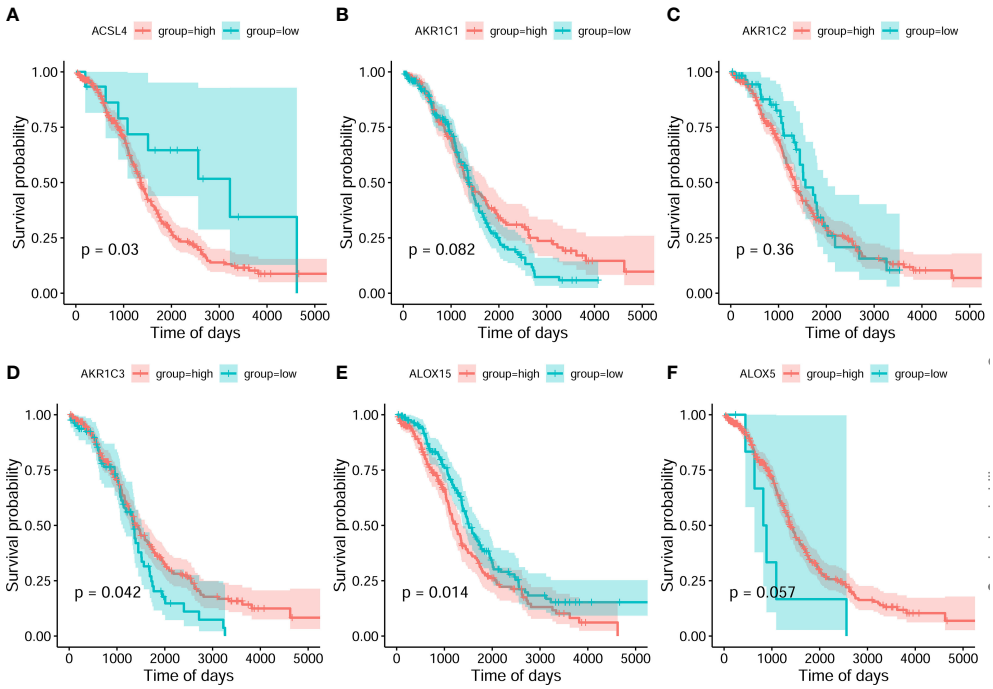

FIGURE 2 | Classification analysis for 6 ferroptosis-related gene expression and overall survival curve in the OC gene dataset of the Cancer Genome Atlas. **(A)** ACSL4 **(B)** AKR1C1 **(C)** AKR1C2 **(D)** AKR1C3 **(E)** ALOX15 **(F)** ALOX5.

$p < 0.05$ and $|\log2 \text{(fold change)}| > 0.58$, 207 differentially expressed genes were identified (**Table S1**). Of these, 78 genes had higher expression levels in Fer-1 than in Fer-2 (**Figure 6**), whereas 129 genes had lower expression levels. Functional enrichment analysis of GO annotations was used for the genes that were differentially expressed in Fer-1 and Fer-2 (**Figure 6B**). The Fer-1 genes may be principally engaged in the enrichment biological processes of mesenchyme morphogenesis, mesenchymal cell differentiation, and apoptotic process involved in morphogenesis. The Fer-2 genes may be related to the positive regulation of leukocyte migration, the T-cell receptor signaling pathway, and the positive regulation of leukocyte chemotaxis (**Figure 6C**).

In addition, enrichment analysis suggested that these differentially expressed genes were involved in the KEGG pathways shown in **Figure 6D**, including fatty acid metabolism, butanoate metabolism, pyruvate metabolism, glycolysis, gluconeogenesis, steroid biosynthesis, nicotinate and nicotinamide metabolism, PPAR signaling, and amino sugar and nucleotide sugar metabolism.

Principal component analysis (PCA) of the differentially expressed gene profiles indicated that the first principal component accounted for 25.18% of the difference between subtypes, and the Fer-1 and Fer-2 subtype samples were clearly separated (**Figure 6E**). The immune infiltrating cell amounts and ratios showed significant differences between the Fer-1 and Fer-2 groups, such as in central memory CD4+-T cells, activated CD4+-T cells, M0 macrophages, and M1 macrophages, indicating significant differences in the immune microenvironment between the two ferroptosis subtypes related to OC (**Figure 6F**). In summary, consistency could be observed between the gene expression and prognosis profile of the two ferroptosis subtypes in OC tumors, indicating that the classification method was sound and reasonable.

Risk Score of Ferroptosis-Related lncRNAs in OC

Pearson correlation analysis was used to identify the lncRNAs that were coexpressed with ferroptosis-related genes ($P < 0.001$ and $|R| > 0.4$) in OC to explore the expression of ferroptosis-related lncRNAs and their role in overall survival in OC. The results showed that 215 lncRNAs had significant coexpression with ferroptosis genes (**Table S2**).

A risk scoring model of tumor ICI was further established on the basis of the coexpressed lncRNAs. First, the overall TCGA-OC set (n = 368) was divided into a training set (n = 246) and a test set (n = 122). In the training set, single-factor Cox analysis was used to identify 215 candidate lncRNAs. When the significance threshold was set to $P < 0.05$, 16 lncRNAs were retained and confirmed (**Figure 7A** and **Table S3**).

To improve clinical application, LASSO Cox regression, as a compressed estimation method, was used to screen variables *via* the R package for glmnet (**Figures 7B, C**). With the gradual increase in lambda, the number of independent variable coefficients trending to zero gradually increased. Through 10-fold cross-validation, the optimal lambda of 0.06048449 was chosen for the model. Thus, 14 lncRNAs were retained as the target genes for the next step (**Table S4**).

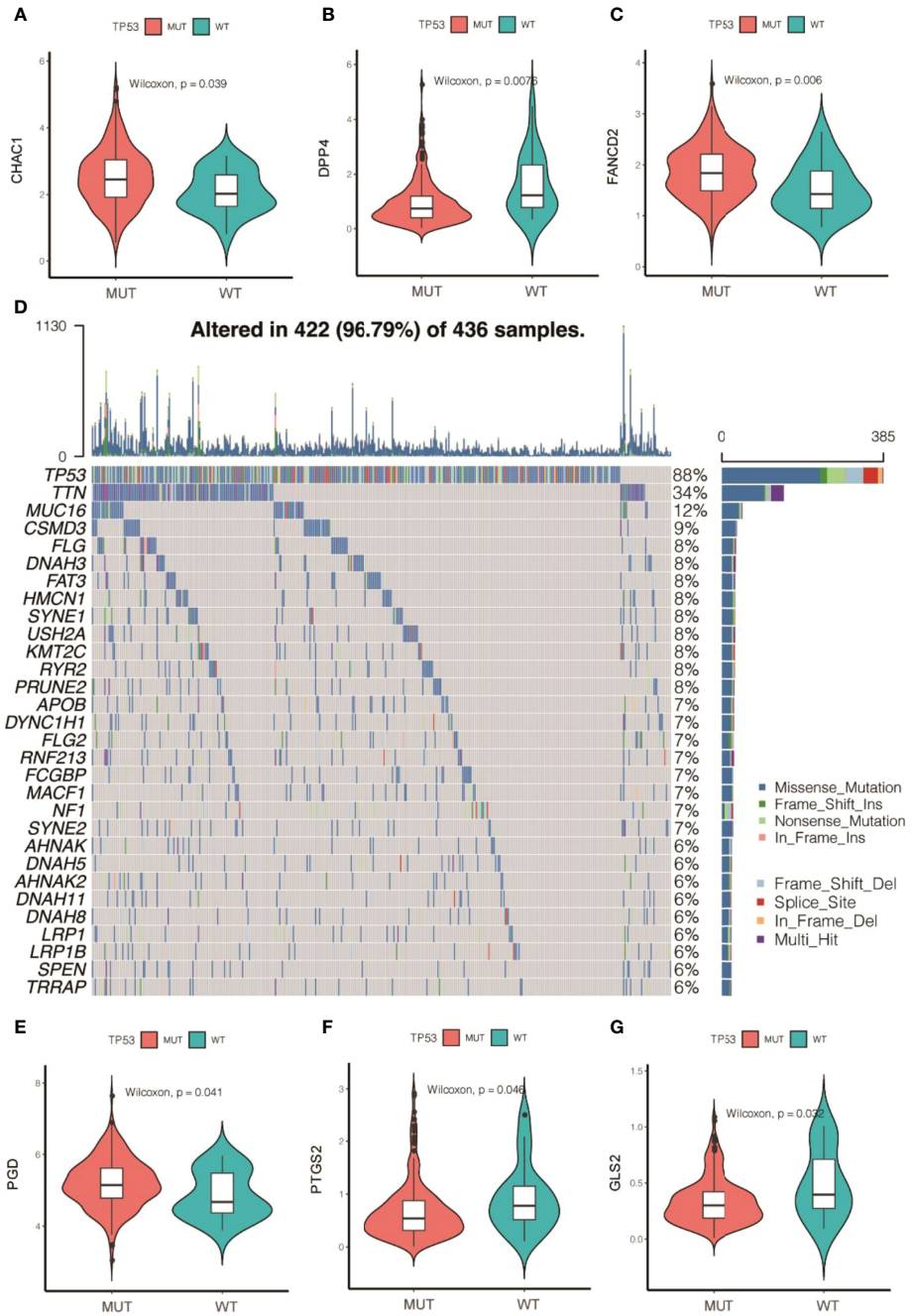

FIGURE 3 | Gene mutations of tumor samples in OC gene dataset of the Cancer Genome Atlas and its regulation on 60 ferroptosis-related genes. **(A)** Waterfall chart of genetic mutations; **(A–G)** effects of TP53 mutations on the expression of ferroptosis-related genes.

Finally, the Akaike information criterion (AIC) was used for further stepwise regression to obtain a sufficient degree of fitting with fewer parameters. The regression model finally reduced 14 lncRNA genes to eight, namely, lncRNAs RP11-443B7.3, RP5-1028K7.2, TRAM2-AS1, AC073283.4, RP11-486G15.2, RP11-95H3.1, RP11-958F21.1, and AC006129.1 (**Table S5**). Multivariate Cox regression was also used to construct a risk scoring model of the eight lncRNAs related to tumor ICI in OC as follows: risk score = (2.65865) * RP11-443B7.3 + (−1.82366) * RP5-1028K7.2 + (−0.43758) * TRAM2-AS1 + (1.01663) * AC073283.4 + (−0.49744) * RP11-486G15.2 + (1.34710) * RP11-95H3.1 + (1.97023) * RP11-958F21.1 + (1.44802) * AC006129.1.

The samples were divided into high-risk and low-risk groups on the basis of the algorithm of optimal density gradient to further assess the effects of the established risk score on overall survival (OS, **Figure 7D**). The results showed that the proportion

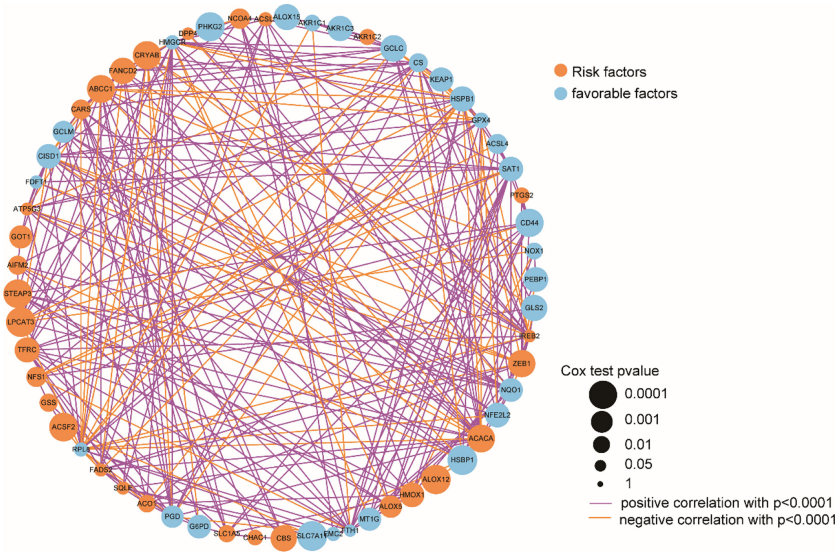

FIGURE 4 | Correlation of 60 ferroptosis-related gene expression.

of nonsurviving patients was higher in the high-risk group than in the low-risk group. The Kaplan–Meier analysis also showed that the OS of the high-risk group was significantly shorter than that of the low-risk group (**Figure 7E**), suggesting that the risk score possesses great potential for the prognosis of OS in the TCGA-OC sets. The AUC values of prognostic sensitivity at 1, 3, and 5 years were 0.735, 0.6873, and 0.7354, respectively. Similarly, the OS time of patients in the high-risk group was significantly lower (**Figure 7G**), and the AUC values at 1, 3, and 5 years were 0.6512, 0.6395, and 0.6695, respectively.

Relationships of Risk Score and Clinical Pathological Features for Patients

The age and tumor grades of clinical characteristics are important clinical diagnostic and treatment indicators for patients with OC. It is beneficial for OC diagnosis and intervention to assess and verify the relationships between the prognostic risk scores of the identified lncRNAs and the clinical characteristics. Univariate and multivariate Cox analyses of clinical variables showed that the risk score was an independent prognostic factor among patients stratified by age, OC stage, and grade (**Figures 8A, B**). Subsequently, multivariate Cox analysis was used to construct a nomogram between risk score and age for convenient use in the clinic (**Figure 8C**). Furthermore, the calibration curves of the nomograms showed that the risk score had prognostic stability for OC (**Figure 8D**).

ROC curves showed that the nomogram of the risk score had higher prognostic predictive performance (above 0.65) at 1, 3, and 5 years than other indicators (**Figures 9A–C**). DCA was carried out to further determine the accuracy of the nomograms. The net benefits of the nomogram at 1, 3, and 5 years were obviously and significantly higher than those of the other clinical variables (**Figures 9D–F**). All of these results confirmed that the tumor risk score was a relatively independent prognostic indicator for OC.

Relationships of Risk Score and Tumor Mutational Burden (TMB) for OC

Substantial clinical evidence suggests that TMB may partly determine individual responses to cancer immunotherapy. Thus, exploring the intrinsic links between TMB and risk score and elucidating the genetic characteristics of each ferroptosis subgroup are of great importance. The R package Survminer was used to further calculate and test the optimal density gradient threshold of TMB and survival. The obtained tumor samples were divided into high- and low-TMB score groups, and a significant difference in survival was found between the two groups (**Figure 10A**). Subsequently, correlation analysis showed that the risk score was negatively correlated with TMB ($R = -0.09$), as shown in **Figure 9B**. Patients with high TMB had a lower risk score, suggesting better treatment effects of immunotherapy on patients with OC with high TMB scores (**Figure 10B**).

In addition, to evaluate the somatic variant distributions associated with immunity, the top 20 genes with high-frequency variants in the OC-actuated genes were compared between the low- and high-risk score groups (**Figures 10C, D**). Analysis of mutation annotation files from the TCGA-OC sets revealed significant differences in the mutational spectrum between the low- and high-risk score groups. These results may provide new guidance for exploring the mechanisms of ferroptosis gene mutation-related immune checkpoints.

Correlation of Tumor Risk Score and ICI

GSEA was used to evaluate 28 kinds of ICIs in the TCGA-OC datasets to explore the relationships between the risk score constructed by tumorous ferroptosis-related lncRNAs and tumor

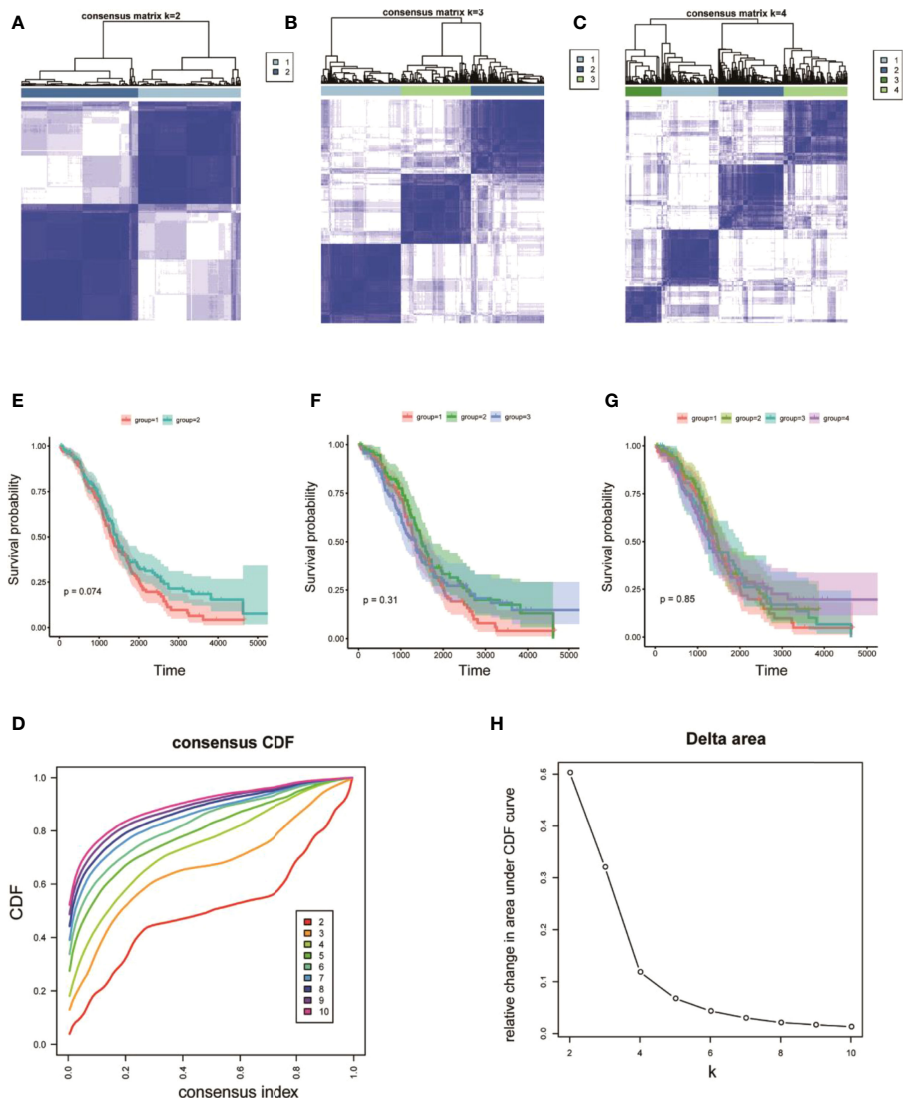

FIGURE 5 | Heterogeneous clustering analysis for 60 ferroptosis-related gene expression values. **(A–C)** Clustering results, with classification k values of 2, 3, and 4, respectively; **(D)** CDF curve distribution of consistent clustering; **(E–G)** survival analysis of OC samples, with classification k values of 2, 3, and 4, respectively; **(H)** distribution of AUC under the CDF curve of consistent clustering.

immune microenvironments (**Table S6**). Regarding the overall levels of tumor ICI, immune cells with high-level infiltration included $CD4^+$-central memory T cells, $CD56^+$-suspicious natural killer cells ($CD56^+$-NK cells), immature dendritic cells, myeloid suppressor cells (MDSCs), and $CD8^+$-central memory T cells (**Figure 11A**). Significance analysis showed that in the high-risk score group, the levels of infiltrating central memory $CD4^+$-T cells, $CD8^+$-T cells, and MDSCs significantly increased compared with those in the low-risk group. In contrast, the level of infiltrating activated $CD4^+$-T cells was significantly lower than that in the low-risk group (**Figure 11B**).

The immunotherapy cohort was evaluated and analyzed on the basis of the immunophenoscore (IPS) in TCGA-OC samples to further confirm the prediction performances and efficiency of the tumor risk score on the immunotherapy benefits of patients with OC. As shown in **Figures 10C–F**, four types of IPS, ips_ctla4_neg_pd1_neg, ips_ctla4_pos_pd1_neg, ips_ctla4_neg_pd1_pos, and ips_ctla4_pos_pd1_pos, were significantly higher in the low-risk score group than in the high-risk score group, indicating that patients in the low-risk score group were more likely to benefit from immunotherapies.

DISCUSSION

OC develops to advanced stages without producing symptoms, and it is characterized by extensive metastasis, chemoresistance, and poor prognosis. Currently, platinum and paclitaxel drugs are the

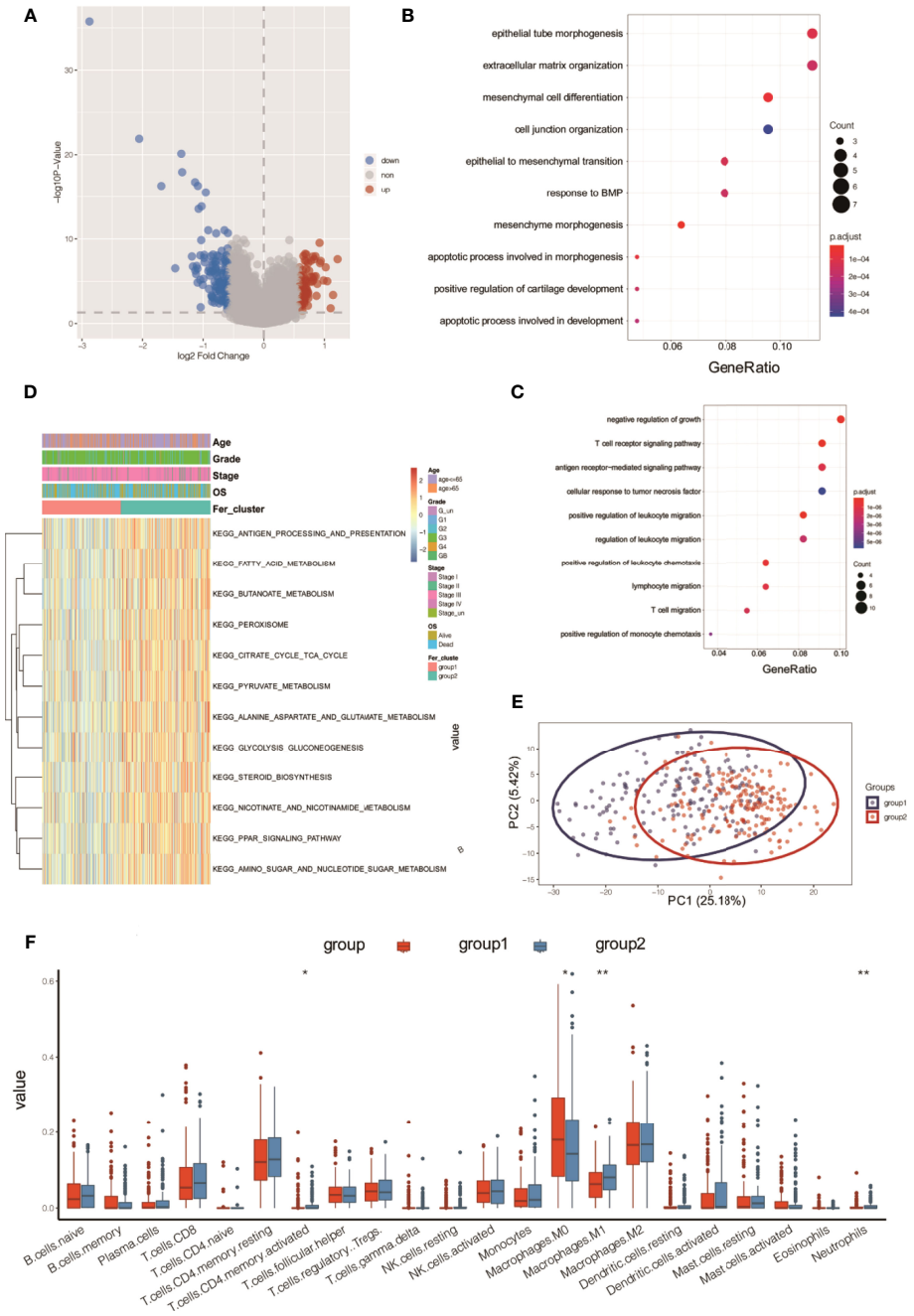

FIGURE 6 | Functional annotation analysis of differentially expressed genes beween two ferroptosis subtypes in OC tumors. **(A)** Volcano map of differentially expressed genes between two subtypes; **(B)** bubble chart of high-expression genes in Fer-1; **(C)** bubble chart of high-expression genes in Fer-2; **(D)** KEGG analysis; **(E)** PCA analysis; **(F)** tumor ICI values of the two groups. *P < 0.05, **P < 0.01.

main clinical chemotherapies for OC, but limited or little progress can be observed in the prognosis for advanced OC. Recent evidence has shown that because ferroptosis can be induced in cancer cells, the enhancement of cancer cell sensitivity to ferroptosis is obviously beneficial for cancer treatment (38–40). In this study, we obtained OC-related expression profile data and clinical follow-up information. A total of 60 ferroptosis-related genes were identified (**Figures 2**, **4**), and a heterogeneous cluster analysis was performed on the basis of the expression values of the 60 identified genes (**Figure 5**). Preclinical- and clinical-related research results indicate that ferroptosis is involved in the proliferation, migration, infection, and apoptosis of cancer cells

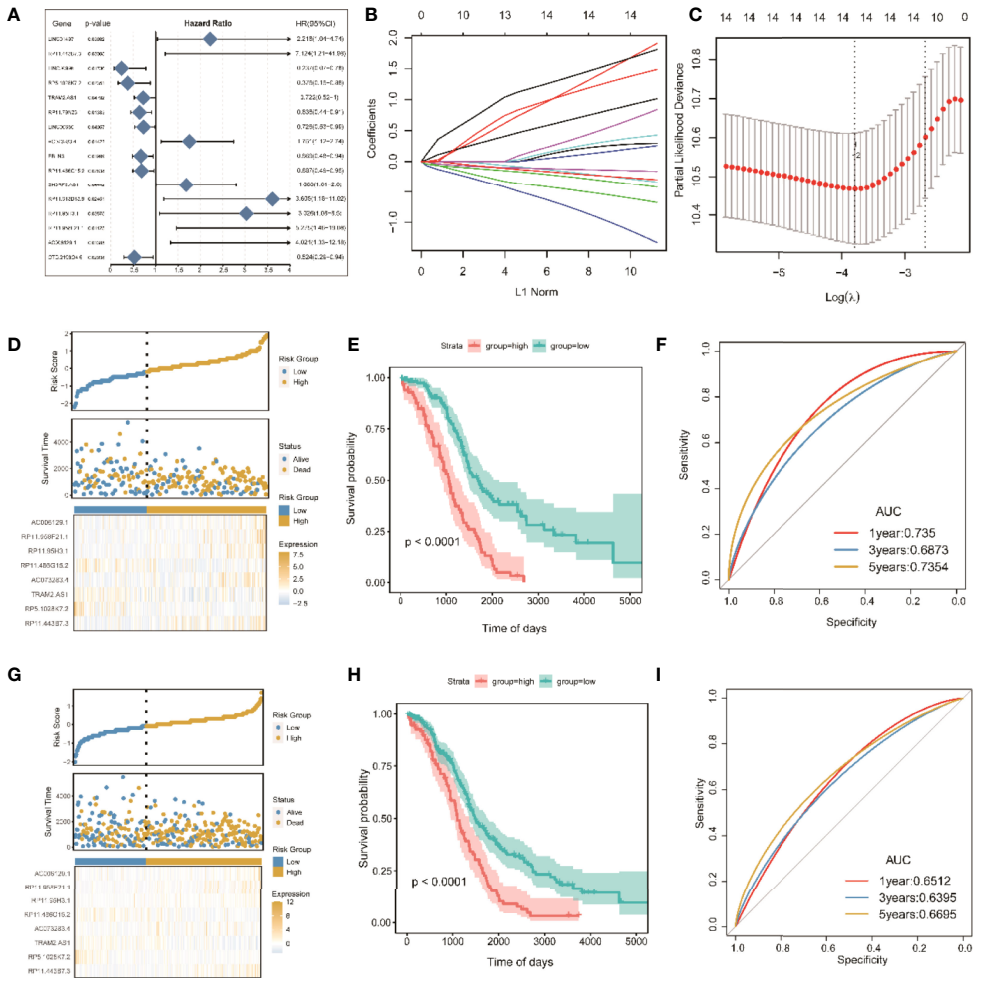

FIGURE 7 | Screening of significant LncRNAs in OC and construction of its risk score model. **(A)** Forest plots of single-factor Cox analysis; **(B)** change trajectory of each independent variable, the horizontal axis represents the log value of the independent variable lambda (the vertical axis represents the coefficient of the independent variable); **(C)** confidence interval under each lambda; **(D)** risk distribution map of the risk score in the training set; **(E)** survival curves of risk score in the training set; **(F)** ROC curves of risk score in the training set; **(G)** distribution map of risk score in all sets. **(H)** risk score survival curve in the total set; (I) ROC curve of risk score in total set.

(32, 41). Thus, the present study supported the speculation that ferroptosis-related genes or lncRNAs may play a vital role in the treatment and prognosis of OC. Moreover, the two molecular subtypes were found to have significant differences: the prognosis of Fer-2 was better than that of Fer-1, and Fer-1 showed poor prognosis (**Figure 5**).

Previous studies found that the overexpression of lncRNA RP11 inhibited the proliferation, migration, colony formation, and nuclear translocation of SOX2 in OC cells. The lncRNA RP11 also exerted inhibitory effects on tumor growth in nude mice and could exert tumor suppressor effects by regulating the RP11-PAK2-SOX2 axis in OC (42). Consistent with these previous results, our study screened and identified eight ferroptosis genes as potential biomarkers of OC diagnosis, treatment, or prognosis, namely, lncRNA RP11-443B7.3, RP5-1028K7.2, TRAM2-AS1, AC073283.4, RP11-486G15.2, RP11-95H3.1, RP11-958F21.1, and AC006129.1 (**Figure 6** and **Tables S3–S5**). This finding suggested that the present research has great clinical predictive value and application prospects and that lncRNAs may be used as potential treatment and prognostic biomarkers for OC.

In vitro cell experiments showed that the expression of lncRNA RP11 was negatively correlated with treatment time and the dose of cisplatin administered (43). Western blot analysis results indicated that cisplatin induced autophagy in OC cells in a time- and dose-dependent manner, and cisplatin combined with lncRNA RP11 markedly decreased the autophagy of OC cells, increased apoptosis, and inhibited their cellular activities. In addition, cisplatin could induce autophagy in OC cells (44, 45). Overexpression of the lncRNA RP11 improved the autophagy induced by cisplatin, thereby enhancing the effect of cisplatin on OC cells (43).

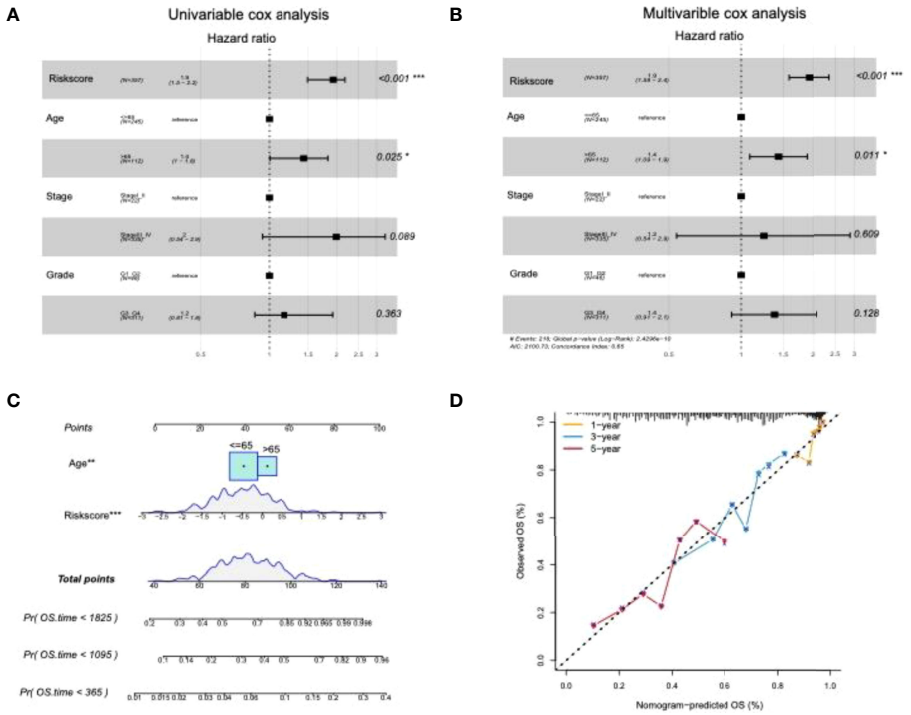

FIGURE 8 | Prognostic predictive assession of risk score and clinical pathological features for patients with OC. **(A, B)** Univariate and multivariate cox analysis of clinical variables and clinical pathological features; **(C)** nomogram between clinical features and risk score; **(D)** calibration chart of the nomogram at 1, 3, and 5 years. P < 0.05 was considered as significant. *P < 0.05, ***P < 0.001.

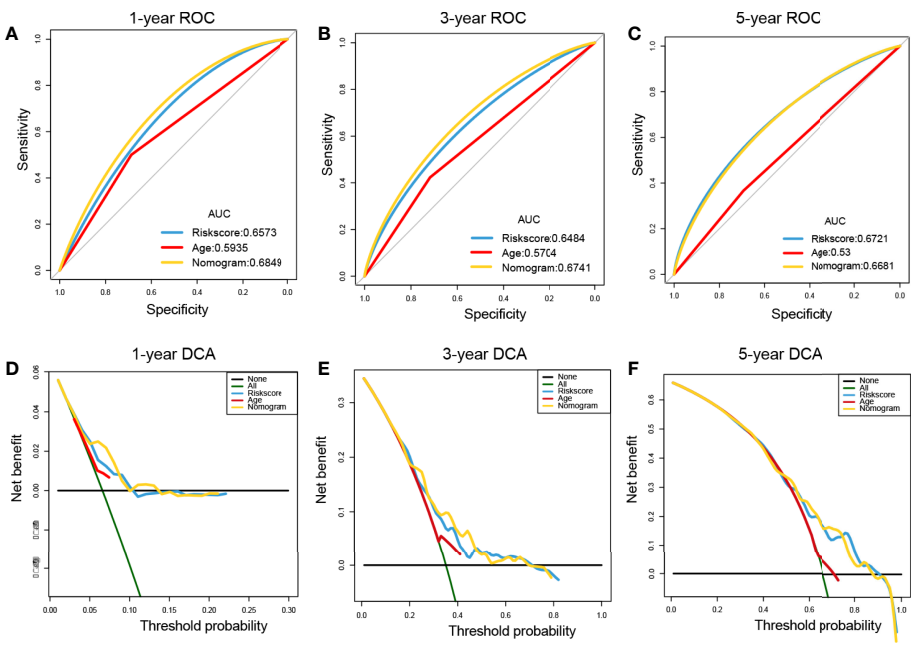

FIGURE 9 | Prognostic performance assessment of risk score. **(A–C)** ROC curves of risk score nomograms at 1, 3, and 5 years, respectively; **(D–F)** DCA distribution maps at 1, 3, and 5 years, respectively.

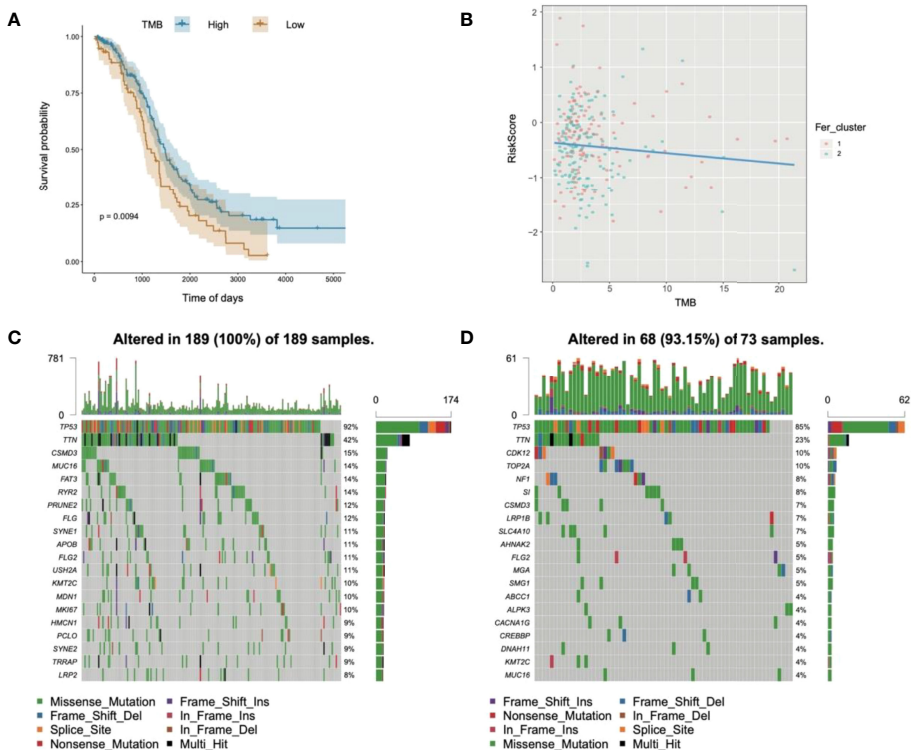

FIGURE 10 | Relationships of risk score and tumor mutational burden for OC. **(A)** Survival curves of high- and low-TMB groups; **(B)** correlation analysis in two groups; **(C)** waterfall chart of gene mutation in the high-risk score group; **(D)** waterfall chart of gene mutation in the low-risk score group.

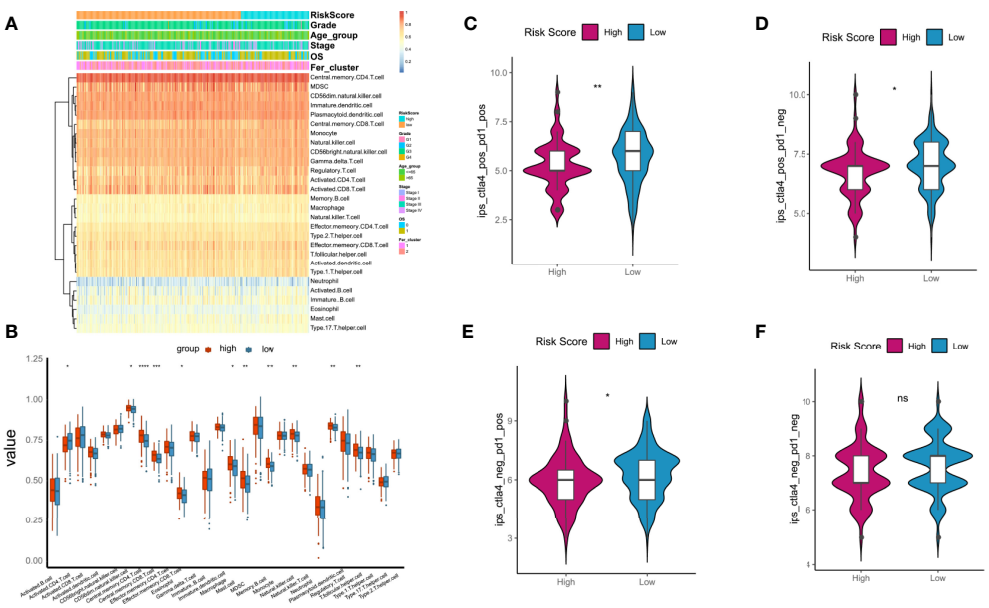

FIGURE 11 | Relationships between tumor risk score and immune cell infiltration (ICI). **(A)** Heatmap of distribution of ICI ratios; **(B)** boxplot of differences in ICI between high- and low-risk score groups; **(C–F)** relationships between tumor risk score and related immunophenoscore. P < 0.05 was considered as significant. ns, no significance. *P < 0.05, **P < 0.01, ***P < 0.001, ****P < 0.0001.

This was confirmed by our work, in which a tumor risk scoring model was constructed for ICI on the basis of the coexpressed lncRNAs with ferroptosis-related genes in OC (**Figure 7**). Thus, the lncRNA RP11 and the other lncRNAs coexpressed with ferroptosis-related genes identified through model analysis in the present study may be vital genes and potential regulatory targets for OC.

Clinical research data further confirmed the above results. Serum samples were collected from clinical patients with OC, those with benign ovarian disease, and controls. Then, the differential gene expression levels in the serum were detected using RT–PCR methods (46). The results showed that serum lncRNA RP5 expression was significantly upregulated in the malignant tumor group compared with the benign and control groups. The lncRNA RP5 expression was lower in malignant ovarian tissue and adjacent nontumor tissues from patients with OC than in normal tissues. Furthermore, the operator characteristic curves showed that the expression values of lncRNA RP5 obviously distinguished the patients with OC from patients with benign masses and control patients, with an accuracy rate of 96% (46). These results indicate that these new diagnostic biomarker RNAs could help diagnose OC and could be of great importance for the early detection and treatment of clinical tumors. The eight identified lncRNAs related to ferroptosis are likely to be key biomarkers for the diagnosis and prognosis of OC.

YAP is a transcriptional cofactor that binds to thousands of enhancer sites to stimulate tumor aggressiveness (47). Based on whole-genome chip analysis, TRAM2 was identified as the YAP-bound enhancer, and the target genes of the lncRNA TRAM2 had the strongest correlation with YAP-expression activities in almost all tumors. Interestingly, the lncRNA TRAM2 affected the cell proliferation, migration, and invasion phenotypes induced by YAP, and it was associated with low survival rates in patients with tumors. Therefore, the lncRNA TRAM2 may be a crucial mediator of YAP-induced tumorigenicity (Li et al., 2021).

Recent studies indicated that the lncRNA AC, as a competitive endogenous RNA (ceRNA), played a key role as a tumor suppressor gene in breast cancer tissues and exerted its anti-breast cancer effect by regulating the expression of miR-18b-5p and targeting the cell division factor DOCK4 (48–51). In breast cancer cells, the lncRNA AC was used as a ceRNA to regulate miR-18b-5p and inhibit its negative regulatory effects on the expression of targeted DOCK4 genes (48–51). In addition, lncRNA AC decreased the migration ability of breast cancer cells, inhibited cell cycle progression from G0/G1 phase to S phase, enhanced the apoptosis of breast cancer cells, and reversed the EMT phenotype (52). Therefore, abnormal changes in lncRNAs are closely related to the phenotypes of tumor cell proliferation, migration, and invasion, and they are important molecular targets for tumor regulation. In the pathological process of the induction and occurrence of OC, it is urgent to determine whether lncRNAs play a key role, and their relationship with ferroptosis remains unclear (53, 54). In contrast, a risk scoring model of the screened lncRNAs related to tumor ICI was used to solve the current problems (**Figure 7**). Kaplan–Meier analysis was implemented to analyze the difference in risk score between the two groups, and the OS of the high-risk group was found to be significantly lower than that of the low-risk group (**Figures 7E–G**). These results indicated that the risk score had high performance in predicting OS in the TCGA-OC dataset.

Moreover, univariate and multivariate Cox analyses were performed on the risk score and important clinical variables (**Figure 7**). The tumor samples in TCGA-OC were divided into high- and low-risk score groups on the basis of the risk score. The differences in clinical characteristics (**Figures 8**, **9**), tumor mutation burden (**Figure 10**), and tumor ICI (**Figure 11**) between the two risk groups in OC were deeply explored and illustrated, and the predictive ability of the risk score with respect to the benefits of immunotherapy were further evaluated, thus providing powerful support for the implementation of precise immunotherapy for OC.

In summary, multiple bioinformatics methods were used in this study to screen and identify ferroptosis-related genes and eight important lncRNAs in OC, namely, lncRNAs RP11-443B7.3, RP5-1028K7.2, TRAM2-AS1, AC073283.4, RP11-486G15.2, RP11-95H3.1, RP11-958F21.1, and AC006129.1 (**Table S5**). The modeling results confirmed that these lncRNAs were closely related to OC. These ferroptosis-related genes and important lncRNAs may serve as vital clinical biomarkers, and targeting them may be a potential approach for the diagnosis, clinical treatment, and prognostic evaluation of OC (55–57). Our work suggests that patients with high ferroptosis-related lncRNA expression will be benefit more from conventional chemotherapy or treatment with ferroptosis inducers. However, this study has some shortcomings and limitations. First, due to the limited number of OC samples in the database, more database information and patient data need to be included in future research to validate the current findings. Second, the eight screened ferroptosis genes were identified and confirmed only through bioinformatics analysis in the later stages. *In vivo* and *in vitro* OC models should be designed to further verify and clarify the clinical prognosis associated with these ferroptosis-related genes and molecules and their potential intervention effects in OC.

DATA AVAILABILITY STATEMENT

The original contributions presented in the study are included in the article/**Supplementary Material**. Further inquiries can be directed to the corresponding authors.

AUTHOR CONTRIBUTIONS

Conceptualization: ZN and CY; Visualization: KW, SM, and MC; Writing-original draft preparation: KW, JY, SM, and MC; Writing-review and editing: JY, ZN, DXZ, DYZ, and CY; Supervision: JY, ZN, and CY. All authors agree to be

accountable for the content of the work. All authors contributed to the article and approved the submitted version.

FUNDING

This work was funded by National Natural Science Foundation of China (82074206, 81973896), Shanghai 3-Year Action Plan for Traditional Chinese Medicine [ZY(2018-2020)-FWTX-1107], Leading Project of Traditional Chinese Medicine of Shanghai Science and Technology Committee (19401930200), and China Postdoctoral Science Foundation (2020M681337).

ACKNOWLEDGMENTS

Thanks to the researchers and clinicians in the field of OC for their data support.

SUPPLEMENTARY MATERIAL

The Supplementary Material for this article can be found online at: https://www.frontiersin.org/articles/10.3389/fonc.2022.888699/full#supplementary-material

REFERENCES

1. Lee JY, Kim S, Kim YT, Lim MC, Lee B, Jung KW, et al. Changes in Ovarian Cancer Survival During the 20 Years Before the Era of Targeted Therapy. *BMC Cancer* (2018) 18(1):601. doi: 10.1186/s12885-018-4498-z
2. Ormsby EL, Pavlik EJ, McGahan JP. Ultrasound Monitoring of Extant Adnexal Masses in the Era of Type 1 and Type 2 Ovarian Cancers: Lessons Learned From Ovarian Cancer Screening Trials. *Diagnos (Basel)* (2017) 7 (2):25. doi: 10.3390/diagnostics7020025
3. Brown J, Friedlander M, Backes FJ, Harter P, O'Connor DM, de la Motte Rouge T, et al. Gynecologic Cancer Intergroup (GCIG) Consensus Review for Ovarian Germ Cell Tumors. *Int J Gynecol Cancer* (2014) 24(9 Suppl 3):S48–54. doi: 10.1097/igc.0000000000000223
4. Teng PN, Bateman NW, Wang G, Litzi T, Blanton BE, Hood BL, et al. Establishment and Characterization of a Platinum- and Paclitaxel-Resistant High Grade Serous Ovarian Carcinoma Cell Line. *Hum Cell* (2017) 30 (3):226–36. doi: 10.1007/s13577-017-0162-1
5. Matulonis UA, Sood AK, Fallowfield L, Howitt BE, Sehouli J, Karlan BY. Ovarian Cancer. *Nat Rev Dis Primers* (2016) 2:16061. doi: 10.1038/nrdp.2016.61
6. Cummings M, Freer C, Orsi NM. Targeting the Tumour Microenvironment in Platinum-Resistant Ovarian Cancer. *Semin Cancer Biol* (2021) 77(3):3–28. doi: 10.1016/j.semcancer.2021.02.007
7. Makovec T. Cisplatin and Beyond: Molecular Mechanisms of Action and Drug Resistance Development in Cancer Chemotherapy. *Radiol Oncol* (2019) 53(2):148–58. doi: 10.2478/raon-2019-0018
8. Wang X, Fan S, Pan H, Chen W, Wang H. Cancer Immunotherapy for Metastasis: Past, Present and Future. *Brief Funct Genomics* (2019) 18(2):140–6. doi: 10.1093/bfgp/ely022
9. Dixon SJ, Lemberg KM, Lamprecht MR, Skouta R, Zaitsev EM, Gleason CE, et al. Ferroptosis: An Iron-Dependent Form of Nonapoptotic Cell Death. *Cell* (2012) 149(5):1060–72. doi: 10.1016/j.cell.2012.03.042
10. Stockwell BR, Friedmann Angeli JP, Bayir H, Bush AI, Conrad M, Dixon SJ, et al. Ferroptosis: A Regulated Cell Death Nexus Linking Metabolism, Redox Biology, and Disease. *Cell* (2017) 171(2):273–85. doi: 10.1016/j.cell.2017.09.021
11. Doll S, Conrad M. Iron and Ferroptosis: A Still Ill-Defined Liaison. *IUBMB Life* (2017) 69(6):423–34. doi: 10.1002/iub.1616
12. Hong T, Lei G, Chen X, Li H, Zhang X, Wu N, et al. PARP Inhibition Promotes Ferroptosis *via* Repressing SLC7A11 and Synergizes With Ferroptosis Inducers in BRCA-Proficient Ovarian Cancer. *Redox Biol* (2021) 42:101928. doi: 10.1016/j.redox.2021.101928
13. Bebber CM, Müller F, Prieto Clemente L, Weber J, von Karstedt S. Ferroptosis in Cancer Cell Biology. *Cancers (Basel)* (2020) 12(1):164. doi: 10.3390/cancers12010164
14. Fonseca-Nunes A, Jakszyn P, Agudo A. Iron and Cancer Risk–a Systematic Review and Meta-Analysis of the Epidemiological Evidence. *Cancer Epidemiol Biomarkers Prev* (2014) 23(1):12–31. doi: 10.1158/1055-9965.Epi-13-0733
15. Yang WH, Huang Z, Wu J, Ding CC, Murphy SK, Chi JT. A TAZ-ANGPTL4-NOX2 Axis Regulates Ferroptotic Cell Death and Chemoresistance in Epithelial Ovarian Cancer. *Mol Cancer Res* (2020) 18(1):79–90. doi: 10.1158/1541-7786.Mcr-19-0691
16. Ashrafizadeh M, Gholami MH, Mirzaei S, Zabolian A, Haddadi A, Farahani MV, et al. Dual Relationship Between Long Non-Coding RNAs and STAT3 Signaling in Different Cancers: New Insight to Proliferation and Metastasis. *Life Sci* (2021) 270:119006. doi: 10.1016/j.lfs.2020.119006
17. Ashrafizaveh S, Ashrafizadeh M, Zarrabi A, Husmandi K, Zabolian A, Shahinozzaman M, et al. Long Non-Coding RNAs in the Doxorubicin Resistance of Cancer Cells. *Cancer Lett* (2021) 104–14. doi: 10.1016/j.canlet.2021.03.018
18. Mirzaei S, Zarrabi A, Hashemi F, Zabolian A, Saleki H, Ranjbar A, et al. Regulation of Nuclear Factor-KappaB (NF-Kappab) Signaling Pathway by non-Coding RNAs in Cancer: Inhibiting or Promoting Carcinogenesis? *Cancer Lett* (2021) 509:63–80. doi: 10.1016/j.canlet.2021.03.025
19. Peng J, Hao Y, Rao B, Zhang Z. A Ferroptosis-Related lncRNA Signature Predicts Prognosis in Ovarian Cancer Patients. *Transl Cancer Res* (2021) 10 (11):4802–16. doi: 10.21037/tcr-21-1152
20. Bhardwaj V, Tan YQ, Wu MM, Ma L, Zhu T, Lobie PE, et al. Long non-Coding RNAs in Recurrent Ovarian Cancer: Theranostic Perspectives. *Cancer Lett* (2021) 502:97–107. doi: 10.1016/j.canlet.2020.12.042
21. Nandwani A, Rathore S, Datta M. LncRNAs in Cancer: Regulatory and Therapeutic Implications. *Cancer Lett* (2021) 501:162–71. doi: 10.1016/j.canlet.2020.11.048
22. Wu H, Liu A. Long Non-Coding RNA NEAT1 Regulates Ferroptosis Sensitivity in non-Small-Cell Lung Cancer. (2021), 49 (3), 0300060521996183. doi: 10.1177/0300060521996183
23. Mao C, Wang X, Liu Y, Wang M, Yan B, Jiang Y, et al. A G3BP1-Interacting LncRNA Promotes Ferroptosis and Apoptosis in Cancer *via* Nuclear Sequestration of P53. *Cancer Res* (2018) 78(13):3484–96. doi: 10.1158/0008-5472.Can-17-3454
24. Qi W, Li Z, Xia L, Dai J, Zhang Q, Wu C, et al. LncRNA GABPB1-AS1 and GABPB1 Regulate Oxidative Stress During Erastin-Induced Ferroptosis in HepG2 Hepatocellular Carcinoma Cells. *Sci Rep* (2019) 9(1):16185. doi: 10.1038/s41598-019-52837-8
25. Jathar S, Kumar V, Srivastava J, Tripathi V. Technological Developments in LncRNA Biology. *Adv Exp Med Biol* (2017) 1008:283–323. doi: 10.1007/978-981-10-5203-3_10
26. Yu H, Han Z, Xu Z, An C, Xu L, Xin H. RNA Sequencing Uncovers the Key Long non-Coding RNAs and Potential Molecular Mechanism Contributing to XAV939-Mediated Inhibition of Non-Small Cell Lung Cancer. *Oncol Lett* (2019) 17(6):4994–5004. doi: 10.3892/ol.2019.10191
27. Lee HY, Chen YJ, Chang WA, Li WM, Ke HL, Wu WJ, et al. Effects of Epigallocatechin Gallate (EGCG) on Urinary Bladder Urothelial Carcinoma-Next-Generation Sequencing and Bioinformatics Approaches. *Med (Kaunas)* (2019) 55(12):768. doi: 10.3390/medicina55120768
28. Li H, Yao G, Zhai J, Hu D, Fan Y. LncRNA FTX Promotes Proliferation and Invasion of Gastric Cancer *via* miR-144/ZFX Axis. *Onco Targets Ther* (2019) 12:11701–13. doi: 10.2147/ott.S220998
29. Lu D, Di S, Zhuo S, Zhou L, Bai R, Ma T, et al. The Long Noncoding RNA TINCR Promotes Breast Cancer Cell Proliferation and Migration by Regulating OAS1. *Cell Death Discov* (2021) 7(1):41. doi: 10.1038/s41420-021-00419-x

30. Gai C, Liu C, Wu X, Yu M, Zheng J, Zhang W, et al. MT1DP Loaded by Folate-Modified Liposomes Sensitizes Erastin-Induced Ferroptosis *via* Regulating miR-365a-3p/NRF2 Axis in Non-Small Cell Lung Cancer Cells. *Cell Death Dis* (2020) 11(9):751. doi: 10.1038/s41419-020-02939-3
31. Wang M, Mao C, Ouyang L, Liu Y, Lai W, Liu N, et al. Long Noncoding RNA LINC00336 Inhibits Ferroptosis in Lung Cancer by Functioning as a Competing Endogenous RNA. *Cell Death Diff* (2019) 26(11):2329–43. doi: 10.1038/s41418-019-0304-y
32. Xie Y, Zhu S, Song X, Sun X, Fan Y, Liu J, et al. The Tumor Suppressor P53 Limits Ferroptosis by Blocking DPP4 Activity. *Cell Rep* (2017) 20(7):1692–704. doi: 10.1016/j.celrep.2017.07.055
33. Ye G, Guo L, Xing Y, Sun W, Yuan M. Identification of Prognostic Biomarkers of Prostate Cancer With Long Non-Coding RNA-Mediated Competitive Endogenous RNA Network. *Exp Ther Med* (2019) 17(4):3035–40. doi: 10.3892/etm.2019.7277
34. Feng S, Yin H, Zhang K, Shan M, Ji X, Luo S, et al. Integrated Clinical Characteristics and Omics Analysis Identifies a Ferroptosis and Iron-Metabolism-Related lncRNA Signature for Predicting Prognosis and Therapeutic Responses in Ovarian Cancer. *J Ovarian Res* (2022) 15(1):10. doi: 10.1186/s13048-022-00944-y
35. Bersuker K, Hendricks JM, Li Z, Magtanong L, Ford B, Tang PH, et al. The CoQ Oxidoreductase FSP1 Acts Parallel to GPX4 to Inhibit Ferroptosis. *Nature* (2019) 575(7784):688–92. doi: 10.1038/s41586-019-1705-2
36. Doll S, Freitas FP, Shah R, Aldrovandi M, da Silva MC, Ingold I, et al. FSP1 is a Glutathione-Independent Ferroptosis Suppressor. *Nature* (2019) 575 (7784):693–8. doi: 10.1038/s41586-019-1707-0
37. Hassannia B, Vandenabeele P, Vanden Berghe T. Targeting Ferroptosis to Iron Out Cancer. *Cancer Cell* (2019) 35(6):830–49. doi: 10.1016/j.ccell.2019.04.002
38. Jiang M, Qiao M, Zhao C, Deng J, Li X, Zhou C. Targeting Ferroptosis for Cancer Therapy: Exploring Novel Strategies From its Mechanisms and Role in Cancers. *Transl Lung Cancer Res* (2020) 9(4):1569–84. doi: 10.21037/tlcr-20-341
39. Viswanathan VS, Ryan MJ, Dhruv HD, Gill S, Eichhoff OM, Seashore-Ludlow B, et al. Dependency of a Therapy-Resistant State of Cancer Cells on a Lipid Peroxidase Pathway. *Nature* (2017) 547(7664):453–7. doi: 10.1038/nature23007
40. Yang WS, SriRamaratnam R, Welsch ME, Shimada K, Skouta R, Viswanathan VS, et al. Regulation of Ferroptotic Cancer Cell Death by GPX4. *Cell* (2014) 156(1-2):317–31. doi: 10.1016/j.cell.2013.12.010
41. Cheng J, Fan YQ, Liu BH, Zhou H, Wang JM, Chen QX. ACSL4 Suppresses Glioma Cells Proliferation *via* Activating Ferroptosis. *Oncol Rep* (2020) 43 (1):147–58. doi: 10.3892/or.2019.7419
42. Yang J, Peng S, Zhang K. LncRNA RP11-499e18.1 Inhibits Proliferation, Migration, and Epithelial-Mesenchymal Transition Process of Ovarian Cancer Cells by Dissociating PAK2-SOX2 Interaction. *Front Cell Dev Biol* (2021) 9:697831. doi: 10.3389/fcell.2021.697831
43. Zou SH, Du X, Sun FD, Wang PC, Li M. Cisplatin Suppresses Tumor Proliferation by Inhibiting Autophagy in Ovarian Cancer *via* Long non-Coding RNA RP11-135l22.1. *Eur Rev Med Pharmacol Sci* (2018) 22(4):928–35. doi: 10.26355/eurrev_201802_14372
44. Liu N, Tai S, Ding B, Thor RK, Bhuta S, Sun Y, et al. Arsenic Trioxide Synergizes With Everolimus (Rad001) to Induce Cytotoxicity of Ovarian Cancer Cells Through Increased Autophagy and Apoptosis. *Endocr Relat Cancer* (2012) 19(5):711–23. doi: 10.1530/erc-12-0150
45. Wang J, Wu GS. Role of Autophagy in Cisplatin Resistance in Ovarian Cancer Cells. *J Biol Chem* (2014) 289(24):17163–73. doi: 10.1074/jbc.M114.558288
46. El-Shal AS, Matboli M, Abdelaziz AM, Morsy AA, Abdelbary EH. Role of a Novel Circulatory RNA-Based Biomarker Panel Expression in Ovarian Cancer. *IUBMB Life* (2019) 71(12):2031–47. doi: 10.1002/iub.2153
47. Verma NK, Gadi A, Maurizi G, Roy UB, Mansukhani A, Basilico C. Myeloid Zinc Finger 1 and GA Binding Protein Co-Operate With Sox2 in Regulating the Expression of Yes-Associated Protein 1 in Cancer Cells. *Stem Cells* (2017) 35(12):2340–50. doi: 10.1002/stem.2705
48. Shao Y, Ye M, Li Q, Sun W, Ye G, Zhang X, et al. LncRNA-RMRP Promotes Carcinogenesis by Acting as a miR-206 Sponge and Is Used as a Novel Biomarker for Gastric Cancer. *Oncotarget* (2016) 7(25):37812–24. doi: 10.18632/oncotarget.9336
49. Wang J, Liu X, Wu H, Ni P, Gu Z, Qiao Y, et al. CREB Up-Regulates Long Non-Coding RNA, HULC Expression Through Interaction With microRNA-372 in Liver Cancer. *Nucleic Acids Res* (2010) 38(16):5366–83. doi: 10.1093/nar/gkq285
50. Zhang EB, Kong R, Yin DD, You LH, Sun M, Han L, et al. Long Noncoding RNA ANRIL Indicates a Poor Prognosis of Gastric Cancer and Promotes Tumor Growth by Epigenetically Silencing of miR-99a/miR-449a. *Oncotarget* (2014) 5(8):2276–92. doi: 10.18632/oncotarget.1902
51. Zhang Y, Tang X, Shi M, Wen C, Shen B. MiR-216a Decreases MALAT1 Expression, Induces G2/M Arrest and Apoptosis in Pancreatic Cancer Cells. *Biochem Biophys Res Commun* (2017) 483(2):816–22. doi: 10.1016/j.bbrc.2016.12.167
52. Wang YY, Yan L, Yang S, Xu HN, Chen TT, Dong ZY, et al. Long Noncoding RNA AC073284.4 Suppresses Epithelial-Mesenchymal Transition by Sponging miR-18b-5p in Paclitaxel-Resistant Breast Cancer Cells. *J Cell Physiol* (2019) 234(12):23202–15. doi: 10.1002/jcp.28887
53. Li L, Ugalde AP, Scheele C, Dieter SM, Nagel R, Ma J, et al. A Comprehensive Enhancer Screen Identifies TRAM2 as a Key and Novel Mediator of YAP Oncogenesis. *Genome Biol* (2021) 22(1):54. doi: 10.1186/s13059-021-02272-8
54. Li L, Qiu C, Hou M, Wang X, Huang C, Zou J, et al. Ferroptosis in Ovarian Cancer: A Novel Therapeutic Strategy. *Front Oncol* (2021) 11:665945. doi: 10.3389/fonc.2021.665945
55. Wang Y, Zhao G, Condello S, Huang H, Cardenas H, Tanner EJ, et al. Frizzled-7 Identifies Platinum-Tolerant Ovarian Cancer Cells Susceptible to Ferroptosis. *Cancer Res* (2021) 81(2):384–99. doi: 10.1158/0008-5472.Can-20-1488
56. Wang Z, Chen X, Liu N, Shi Y, Liu Y, Ouyang L, et al. A Nuclear Long Non-Coding RNA LINC00618 Accelerates Ferroptosis in a Manner Dependent Upon Apoptosis. *Mol Ther* (2021) 29(1):263–74. doi: 10.1016/j.ymthe.2020.09.024
57. Worku T, Bhattarai D, Ayers D, Wang K, Wang C, Rehman ZU, et al. Long Non-Coding RNAs: The New Horizon of Gene Regulation in Ovarian Cancer. *Cell Physiol Biochem* (2017) 44(3):948–66. doi: 10.1159/000485395

Conflict of Interest: The authors declare that the research was conducted in the absence of any commercial or financial relationships that could be construed as a potential conflict of interest.

Publisher's Note: All claims expressed in this article are solely those of the authors and do not necessarily represent those of their affiliated organizations, or those of the publisher, the editors and the reviewers. Any product that may be evaluated in this article, or claim that may be made by its manufacturer, is not guaranteed or endorsed by the publisher.

frontiers | Frontiers in Oncology

ORIGINAL RESEARCH
published: 10 June 2022
doi: 10.3389/fonc.2022.897702

A Novel Prognostic Signature Based on Glioma Essential Ferroptosis-Related Genes Predicts Clinical Outcomes and Indicates Treatment in Glioma

Debo Yun[1,2,3†], Xuya Wang[1,2†], Wenbo Wang[1,2†], Xiao Ren[1,2†], Jiabo Li[1,2], Xisen Wang[1,2], Jianshen Liang[1,2], Jie Liu[1,2], Jikang Fan[1,2], Xiude Ren[1,2], Hao Zhang[1,2], Guanjie Shang[1,2], Jingzhang Sun[1,2], Lei Chen[1,2], Tao Li[1,2], Chen Zhang[2], Shengping Yu[1,2] and Xuejun Yang[1,2,4]*

[1] Department of Neurosurgery, Tianjin Medical University General Hospital, Tianjin, China, [2] Laboratory of Neuro-oncology, Tianjin Neurological Institute, Tianjin, China, [3] Department of Neurosurgery, Nanchong Central Hospital, Nanchong, China, [4] Department of Neurosurgery, Beijing Tsinghua Changgung Hospital, Beijing, China

OPEN ACCESS

Edited by:
Xu Chen,
Guilin Medical University, China

Reviewed by:
Jing Sun,
Shanghai Jiao Tong University, China
Jie Ding,
Stanford University, United States
Cheng Zhou,
West China Hospital of Si Chuan University, China

***Correspondence:**
Xuejun Yang
yxja03728@btch.edu.cn;
ydenny@126.com

[†]These authors have contributed equally to this work

Specialty section:
This article was submitted to Pharmacology of Anti-Cancer Drugs, a section of the journal Frontiers in Oncology

Received: 16 March 2022
Accepted: 05 May 2022
Published: 10 June 2022

Citation:
Yun D, Wang X, Wang W, Ren X, Li J, Wang X, Liang J, Liu J, Fan J, Ren X, Zhang H, Shang G, Sun J, Chen L, Li T, Zhang C, Yu S and Yang X (2022) A Novel Prognostic Signature Based on Glioma Essential Ferroptosis-Related Genes Predicts Clinical Outcomes and Indicates Treatment in Glioma. Front. Oncol. 12:897702. doi: 10.3389/fonc.2022.897702

Background: Ferroptosis is a form of programmed cell death (PCD) that has been implicated in cancer progression, although the specific mechanism is not known. Here, we used the latest DepMap release CRISPR data to identify the essential ferroptosis-related genes (FRGs) in glioma and their role in patient outcomes.

Methods: RNA-seq and clinical information on glioma cases were obtained from the Chinese Glioma Genome Atlas (CGGA) and The Cancer Genome Atlas (TCGA). FRGs were obtained from the FerrDb database. CRISPR-screened essential genes (CSEGs) in glioma cell lines were downloaded from the DepMap portal. A series of bioinformatic and machine learning approaches were combined to establish FRG signatures to predict overall survival (OS) in glioma patients. In addition, pathways analysis was used to identify the functional roles of FRGs. Somatic mutation, immune cell infiltration, and immune checkpoint gene expression were analyzed within the risk subgroups. Finally, compounds for reversing high-risk gene signatures were predicted using the GDSC and L1000 datasets.

Results: Seven FRGs (ISCU, NFS1, MTOR, EIF2S1, HSPA5, AURKA, RPL8) were included in the model and the model was found to have good prognostic value ($p < 0.001$) in both training and validation groups. The risk score was found to be an independent prognostic factor and the model had good efficacy. Subgroup analysis using clinical parameters demonstrated the general applicability of the model. The nomogram indicated that the model could effectively predict 12-, 36-, and 60-months OS and progression-free interval (PFI). The results showed the presence of more aggressive phenotypes (lower numbers of IDH mutations, higher numbers of EGFR and PTEN mutations, greater infiltration of immune suppressive cells, and higher expression of

immune checkpoint inhibitors) in the high-risk group. The signaling pathways enriched closely related to the cell cycle and DNA damage repair. Drug predictions showed that patients with higher risk scores may benefit from treatment with RTK pathway inhibitors, including compounds that inhibit RTKs directly or indirectly by targeting downstream PI3K or MAPK pathways.

Conclusion: In summary, the proposed cancer essential FRG signature predicts survival and treatment response in glioma.

Keywords: glioma, ferroptosis, cancer essential genes, LASSO analysis, risk model, clinical outcomes, drug screening

INTRODUCTION

Gliomas are common primary malignant tumors of the central nervous system (1), representing nearly half of all primary intracranial neoplasms (2) and 80% of all malignant brain tumors (3). At present, the main treatment strategy for gliomas throughout the world is surgery (4) followed by postoperative adjuvant radiotherapy and chemotherapy (5, 6). Despite therapeutic advances, glioma patients have a poor prognosis (7), especially those with high-grade tumors (8), due to high levels of tumor cell diversity, proliferation, and metastasis (9). It has been hoped that the use of molecular markers may improve glioma characterization and predict survival (10, 11) but, thus far, the results, including those of clinical trials, have been disappointing (12). The identification of markers and potential targets that can be used for prediction and treatment is thus important, not only for managing the cancer but also for drug discovery.

Ferroptosis is a recently identified form of programmed cell death that is dependent on iron (13, 14). It has been linked with the outcomes of several cancers, including hepatocellular carcinoma, breast cancer, renal cell carcinoma, lung squamous cell carcinoma, and pancreatic carcinoma (15–19). Invasive and metastatic tumor cells have been found to be susceptible to ferroptosis (20) suggesting that targeting the process may be useful for treating cancer. However, there is limited information on the feasibility of targeting FRGs in glioma. The use of CRISPR-Cas9 knockout screening can elucidate relationships between genotype and phenotype through ablation of gene expression on a genome-wide scale and the consequent phenotypic alterations, for the specific identification of genes that could be targeted for inducing tumor growth inhibition or death. Our aim was to combine the CRISPR data to construct a novel prognostic signature based on the identified glioma-essential ferroptosis-related genes to specifically predict clinical outcomes and, importantly, to suggest directions for gene-targeted therapy.

MATERIAL AND METHODS

Data Collection and Preprocessing

Clinical and RNA-seq transcripts per million reads (TPM) data were obtained from TCGA (https://xenabrowser.net) and CGGA-693 (http://www.cgga.org.cn). Patients with complete clinical data (age, sex, vital status, OS, PFI, IDH status, 1p-19q status, and WHO grade) were included. In all, 1170 patients were included, representing 551 in the training cohort and 619 in the validation cohort (**Table 1**). Ethical approval was waived as the study followed the TCGA and CGGA regulations for accessing data. Information on 388 FRGs was acquired from FerrDb (http://www.zhounan.org/ferrdb/) (**Table S1**) (21) and genome-wide CRISPR information on glioma cells was obtained from DepMap (https://depmap.org/portal/download/). The CERES algorithm (22) was used for the determination of dependency scores. First, genes with CERES scores below -1 in more than 75% of glioma cell lines were included. Many of these genes with known housekeeping functions that did not represent feasible targets were excluded, leaving 747 genes that were necessary for glioma cell survival *in vitro* (**Table S2**) and were termed glioma essential genes. Potentially targetable genes were identified as those falling into both FRG and CSEG categories. The flow chart of the study is illustrated in **Figure 1**.

Construction and Verification of Risk Models

Before establishing the model, multivariate regression analysis was performed to identify potential genes related to prognosis ($p < 0.05$).

TABLE 1 | The clinical features of TCGA cohort and CGGA cohort.

	TCGA cohort	CGGA cohort
Characteristic	N = 551	N = 619
Age		
Median	47.21	43.44
Gender		
Male	313	356
Female	238	263
Grade		
Grage 2	209	173
Grage 3	232	231
Grage 4	110	215
IDH-status		
IDH_WT	188	258
IDH_Mut	363	316
1p/19q co-deletion		
Non-codel	403	427
Codel	148	128
Vital status		
Alive	365	296
Dead	186	323

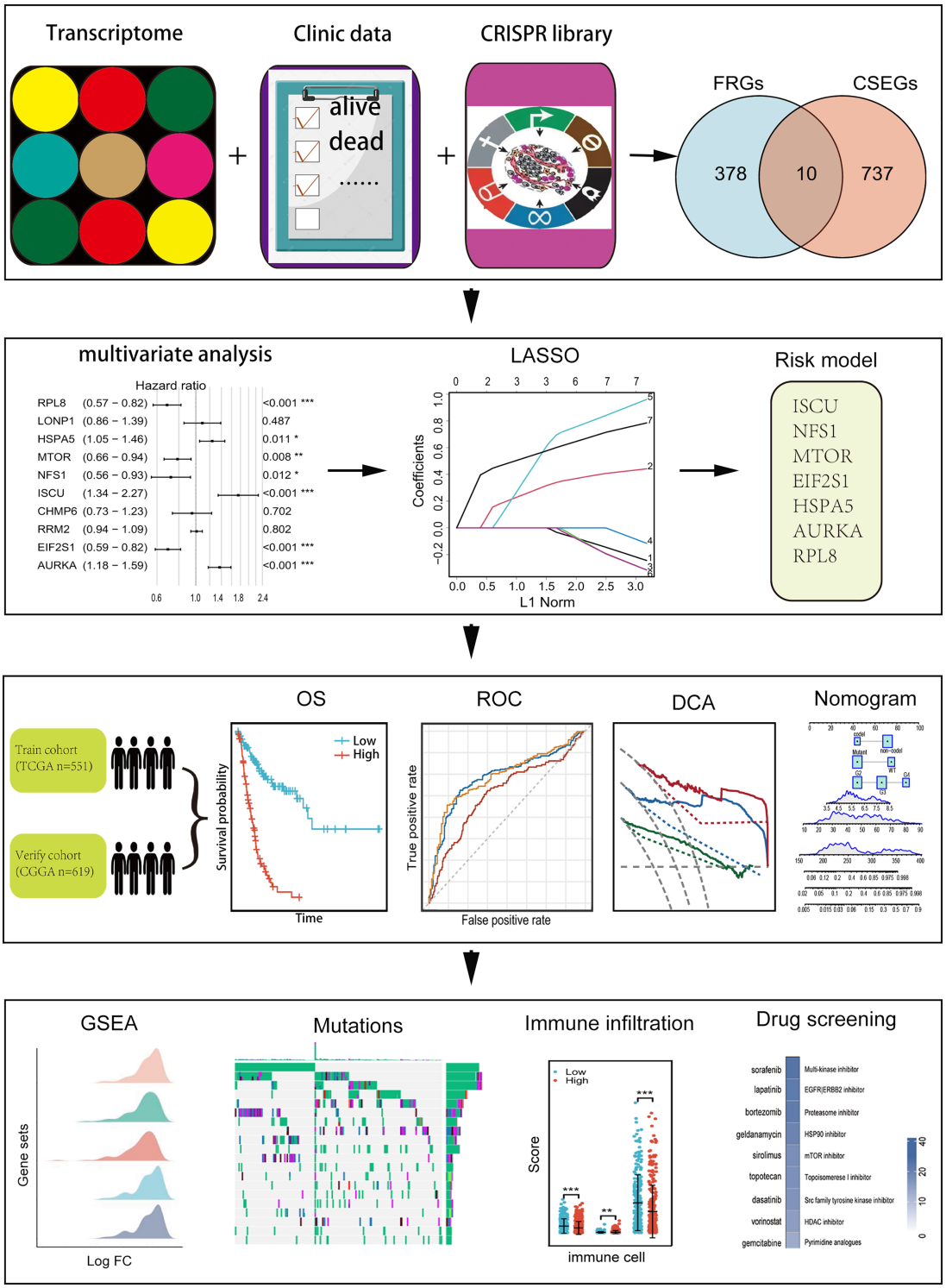

FIGURE 1 | Flow chart showing the design of the study.

Suitable candidate genes were identified as those with a minimal partial likelihood of deviance in LASSO regression and were used to construct the prognostic model (23). Risk scores were calculated as the sum of the products of regression coefficients and the expression of the individual genes. A cut-off value, represented by the median risk score, was used to separate both cohorts into high- and low-risk groups. The prognostic efficacy of the signature was assessed by analyzing survival. Time-dependent receiver operating characteristic (tROC) curves were used to calculate the area under the curve (AUC) for the 1-, 3-, and 5-year OS by using the R package "survivalROC" (24). Analysis of clinical correlates was performed between expression of cancer-essential FRGs and clinical characteristics using the R package "ggplot2" (25).

Somatic Mutation, Immune Microenvironment and Function Enrichment Analyses

Mutation data were downloaded and visualized using the "maftools" R package to determine the somatic mutation landscape of glioma patients in the TCGA database, identifying distinct ferroptosis-related subtypes (26). Immune infiltration scores of glioma patients in the TCGA were downloaded from TIMER2.0 (http://timer.cistrome.org/) (27) and the patients were divided into high- and low-risk groups. The R packages "ComplexHeatmap" (28) and "ggplot2" were used to analyze and visualize the CIBERSORT algorithm data. Differentially expressed genes (DEGs) were identified using the median risk score as a threshold and the expression of the DEGs was analyzed using the R package "DESeq2" (29). Gene Set Enrichment Analysis (GSEA) was conducted on the TCGA cohort to examine the biological functions and pathways of the cancer-essential FRGs using the "clusterProfiler4.0" package in R (30).

Nomogram Construction and Verification

The nomogram for glioma prognostic prediction was established using risk scores and clinical features (31). The accuracy and discriminative ability of the nomogram were assessed by calibration curves. Decision curve analysis (DCA) using the "ggDCA" and "stdca" packages (32) in R was performed to determine the survival net benefits at one, three, and five years for both OS and PFI (33).

Identification of Potential Compounds

Spearman correlation analysis was used to identify compounds negatively associated with the AUC values and glioma cell FRG scores using the GDSC1 and GDSC2 drug response datasets (https://www.cancerrxgene.org) (34) using Spearman's $r < -0.30$ and P-values < 0.05 for GDSC1 or <0.1 for GDSC2. DEG expression between the high- and low-risk groups was analyzed. The 150 most upregulated or downregulated genes in the high-risk group were used for further analysis. The relationships of 978 compounds with these 150 genes were examined in CLUE (summary connectivity score) (https://clue.io/repurposing) (35) and the genes were The 150 genes were then analyzed using iLINCS (http://www.ilincs.org/ilincs/) "Pharmacogenomics transcriptional signatures" (36) connectivity algorithms.

Statistical Analysis

R version 4.0.2 was used for all analyses. Differences in normally distributed data were analyzed by unpaired t-tests, and those in non-normally distributed data by the Wilcoxon test. P-values <0.05 were considered significant.

RESULTS

Construction and Verification of Risk Models

Ten genes (ISCU, NFS1, MTOR, EIF2S1, HSPA5, AURKA, RPL8, LONP1, RRM2, and CHMP6) that fell into both the FRG and CSEG categories were used for further study (**Figure 2A**). Multivariate Cox regression showed that seven cancer-essential FRGs (ISCU, NFS1, MTOR, EIF2S1, HSPA5, AURKA, and RPL8) were significantly associated ($p<0.05$) with OS (**Figure 2B**). LASSO was then applied to reduce the number of these genes. As the partial likelihood was minimal, all the genes were retained and used for the construction of the risk model (**Figures 2C, D**). The risk score of the training cohort was calculated as 0.4181306×expression of HSPA5-0.2335796×expression of MTOR-0.0372456 ×expression of NFS1 +0.8788312×expression of ISCU-0.2320588×expression of EIF2S1+ 0.7371187×expression of AURKA-0.1765609×expression of RPL8.

Prognostic Assessment Using the Risk Model

Patients in the training cohort were assigned to high- and low-risk groups according to the median risk score. Kaplan-Meier curves showed that members of the high-risk groups had significantly lower OS (p<0.001 in both cohorts) (**Figures 3A, B**). The AUCs for one-, three-, and five-year OS were 0.840, 0.906, and 0.833, respectively, in the training set (**Figure 3C**) and 0.638, 0.734, and 0.736, respectively, in the validation set (**Figure 3D**). The risk scores were then ranked in relation to OS and the levels of the seven cancer-essential FRGs were determined in the low- and high-risk groups, as shown in the heatmaps (**Figures 3E, F**). This indicated that a higher risk score was associated with lower OS for both groups, levels of the AURKA, EIF2S1, and HSPA5 genes were elevated in high-risk individuals in the training set, and all seven genes were strongly expressed in the high-risk category of the validation cohort.

Relationships Between Risk Model Gene Levels and Clinical Characteristics

m_sc_clean_body_s.tgaThe relationships between the levels of the seven signature genes and the clinical features of glioma patients from TCGA were investigated. The expression levels of these genes in tumor tissue were significantly different in comparison with those in normal tissues (**Figure 4C**). The levels of AURKA, EIF2S1, and HSPA5 were significantly associated with age (**Figure 4A**), grade (**Figure 4D**), the 1p/19q codeletion (**Figure 4E**), and isocitrate dehydrogenase (IDH) status (**Figure 4F**). The risk model genes were not related to sex (**Figure 4B**). In addition, immunohistochemical data on the risk model genes in normal and tumor specimens were downloaded from The Human Protein Atlas (https://www.proteinatlas.org/) for further verification (**Figure 4G**).

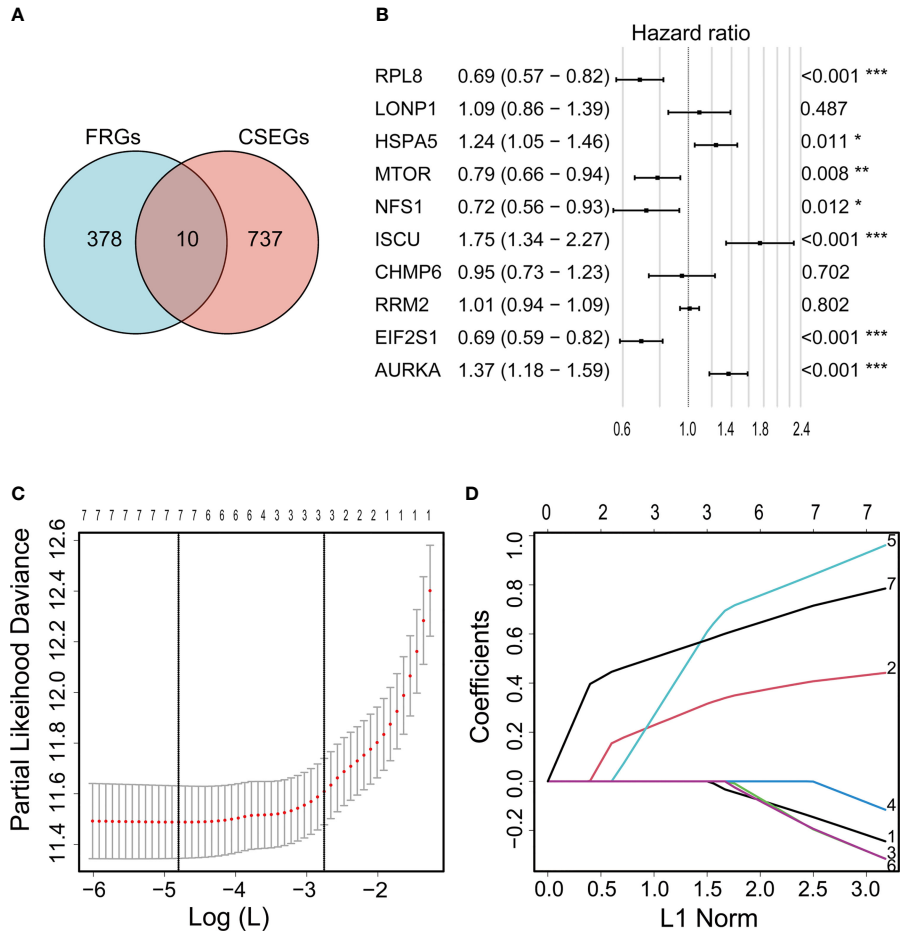

FIGURE 2 | Venn diagram showing overlap of 10 genes between the CSEGs and FRGs **(A)**. Top prognosis-associated candidate genes identified by Cox regression **(B)**. Re-filtering of genes in **(B)** by LASSO **(C, D)**. *p < 0.05, **p < 0.01, ***p < 0.001.

Prognostic Value of the Risk Model for Subgroups of Clinical Classifications

Patients in both the training and validation cohorts were divided into subgroups according to clinical features, including the age, sex, IDH status, 1p/19q con-deletion status, and WHO classification of the TCGA (**Figure 5A**) and the CGGA (**Figure 5B**) patients, as well as the primary/recurrent tumor types of the CGGA patients (**Figure 5B**). The subgroups were assessed in terms of median risk scores and survival curves were compiled for each of the clinical features. The results showed that the risk model was effective for these factors, except for patients with IDH-mut in the training cohort (**Figure 5A**) and those with the 1p/19q con-deletion and WHO IV in both the training and validation groups (**Figures 5A, B**).

Comprehensive Analyses of Somatic Mutations, Immune Cell Infiltration, and Immune Checkpoint Expression in the Different Risk Groups

Intuitively, the landscapes of somatic genetic alterations provided the 20 most frequently mutated genes in each risk cohort of TCGA samples. The results showed that 91.6% of patients in the low-risk group had IDH mutations, in contrast to only 38.5% in the high-risk group (**Figures 6A, B**), while PTEN and EGFR had higher rates of mutation in the high-risk group (**Figure 6B**). The immune cell infiltration scores of each sample were estimated using the CIBERSORT algorithm. Notably, the levels of regulatory T cells (Tregs) and M2 macrophages were higher in the high-risk group (**Figures 6C, D**) and the expression of immune checkpoint genes (CD274, CTLA4, CEACAM1, LAG3, TIGIT, PDCD1, and BTLA) were also higher in the high-risk group (**Figure 6E**). These results indicated that high-risk patients may be sensitive to PTEN or EGFR inhibition or the blocking of immune checkpoint gene expression.

Construction and Verification of Nomogram

Univariate and multivariate analyses demonstrated that the risk score and clinical characteristics (age, grade, IDH status, and 1p/19q status) were risk factors linked to glioma prognosis in

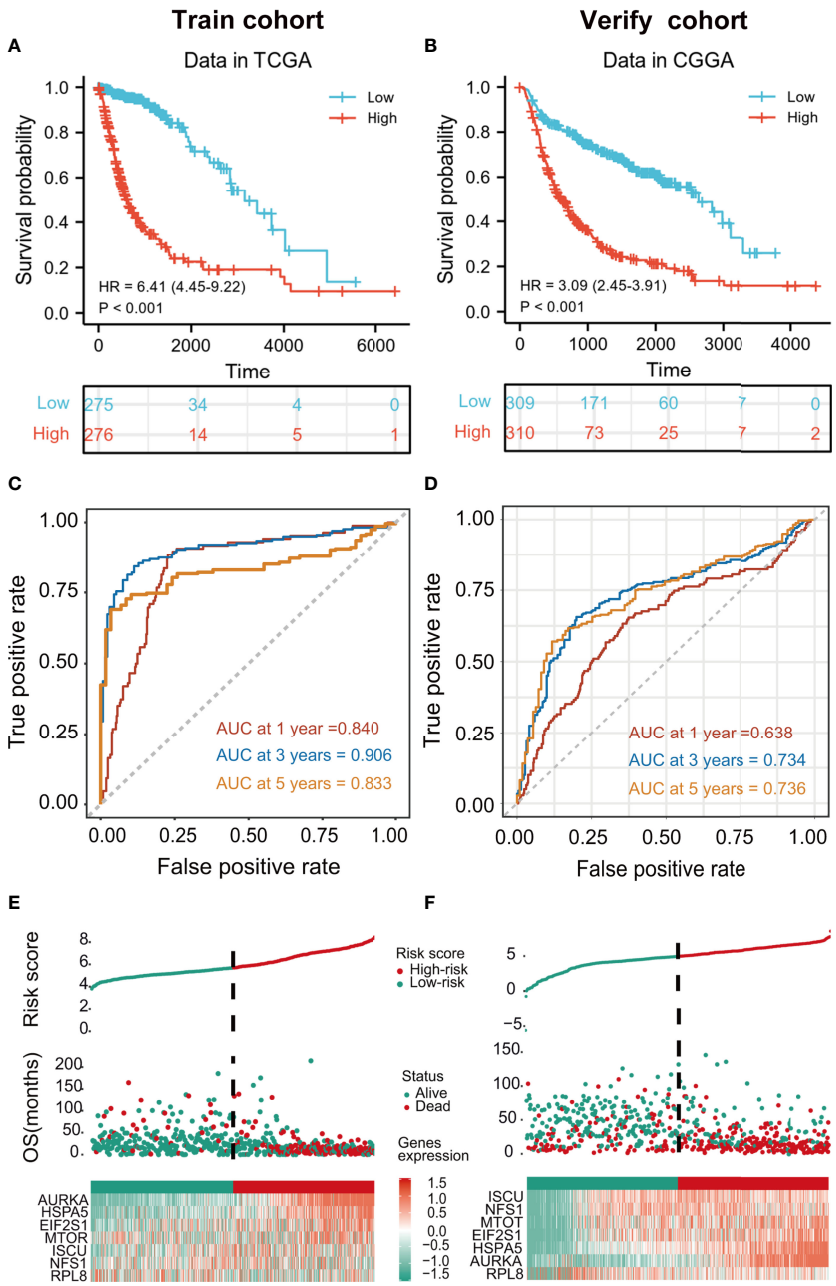

FIGURE 3 | Kaplan-Meier curves showing risk scores of FRG signature genes in both training and validation cohorts ($p < 0.001$) **(A, B)**. tROC curves for one-, three- and five-year survival **(C, D)**. Heatmaps of risk score rankings, survival, and levels of cancer-essential FRGs in the training and validation cohorts **(E, F)**.

TCGA.(**Figures 7A, B**). The risk score was added to the nomogram prediction model for accurately predicting 12-, 36- and 60-months OS (**Figure 7C**) and PFI (**Figures 7D**). The calibration plots showed that the predicted and actual one- three- and five-year OS and PFI approximated well, indicating the good performance of the nomogram in comparison with an ideal model (**Figures 7E, F**). The clinical value of the nomogram was confirmed by DCA (**Figures 7G, H**).

Gene Set Enrichment Analysis to Reveal the Functional Roles of Essential FRGs in Glioma

The expression of the DEGs in the high- and low-risk groups in the TCGA cohort was examined to investigate their functions in glioma. Further functional analysis was performed by GSEA using the HALLMARK (**Figure 8A**), KEGG (**Figure 8B**), and Reactome (**Figure 8C**) databases.

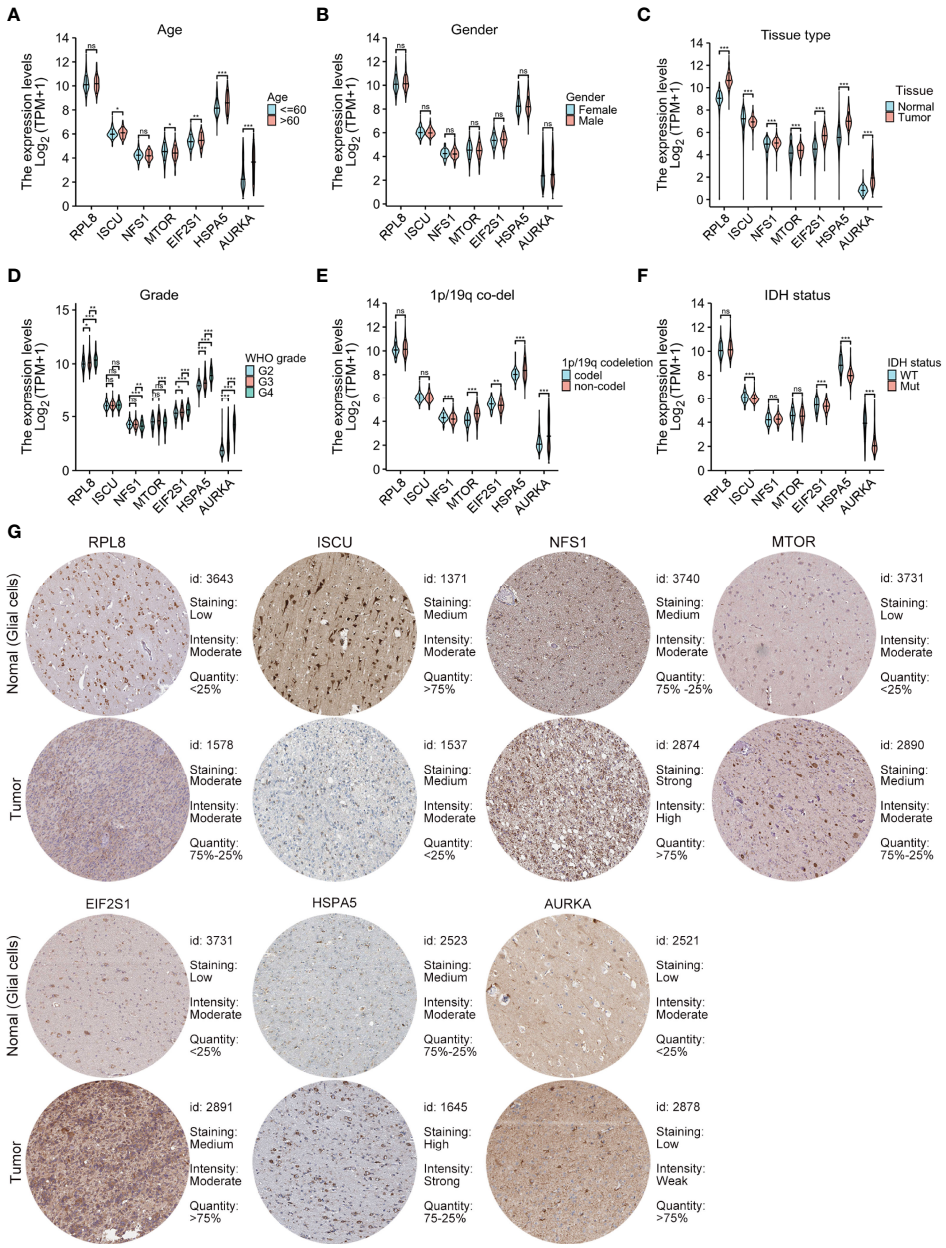

FIGURE 4 | Relationships between the levels of the seven cancer-essential FRGs and clinical features. Age **(A)**, sex **(B)**, normal versus tumor tissue **(C)**, WHO grade **(D)**, 1p/19q co-deletion status **(E)**, and IDH status **(F)**. Immunohistochemistry showing the protein expression of risk model genes in normal and tumor specimens of The Human Protein Atlas **(G)**. ns, p≥0.05, *p < 0.05, **p < 0.01, ***p < 0.001.

Examination of the top 30 pathways showed that the TP53 signaling pathway was enriched in all three databases. Many of the enriched signaling pathways in the three databases were closely related to the cell cycle and DNA damage repair. Other enriched pathways were associated with tumor progression, including the IL6/JAK/STAT3, KRAS, and PI3K/AKT/mTOR signaling pathways, which corresponded to the higher mutation rate of EGFR and PTEN in high-risk patients mentioned above.

Identification of an RTK Pathway Inhibitor With Significant Inhibitory Activity in High-Risk Patients

Correlation analysis identified six GDSC1-derived compounds, namely, voxtalisib, rucaparib, trametinib, LL.Z1640.2, KU.57788, and SB.505124.1, and five GDSC2-derived compounds, namely, MIM.1, epirubicin, AZD4547, GSK1904529A, and AZD5363 (**Figures 9 D, E**). Although these candidate compounds showed high drug sensitivities in

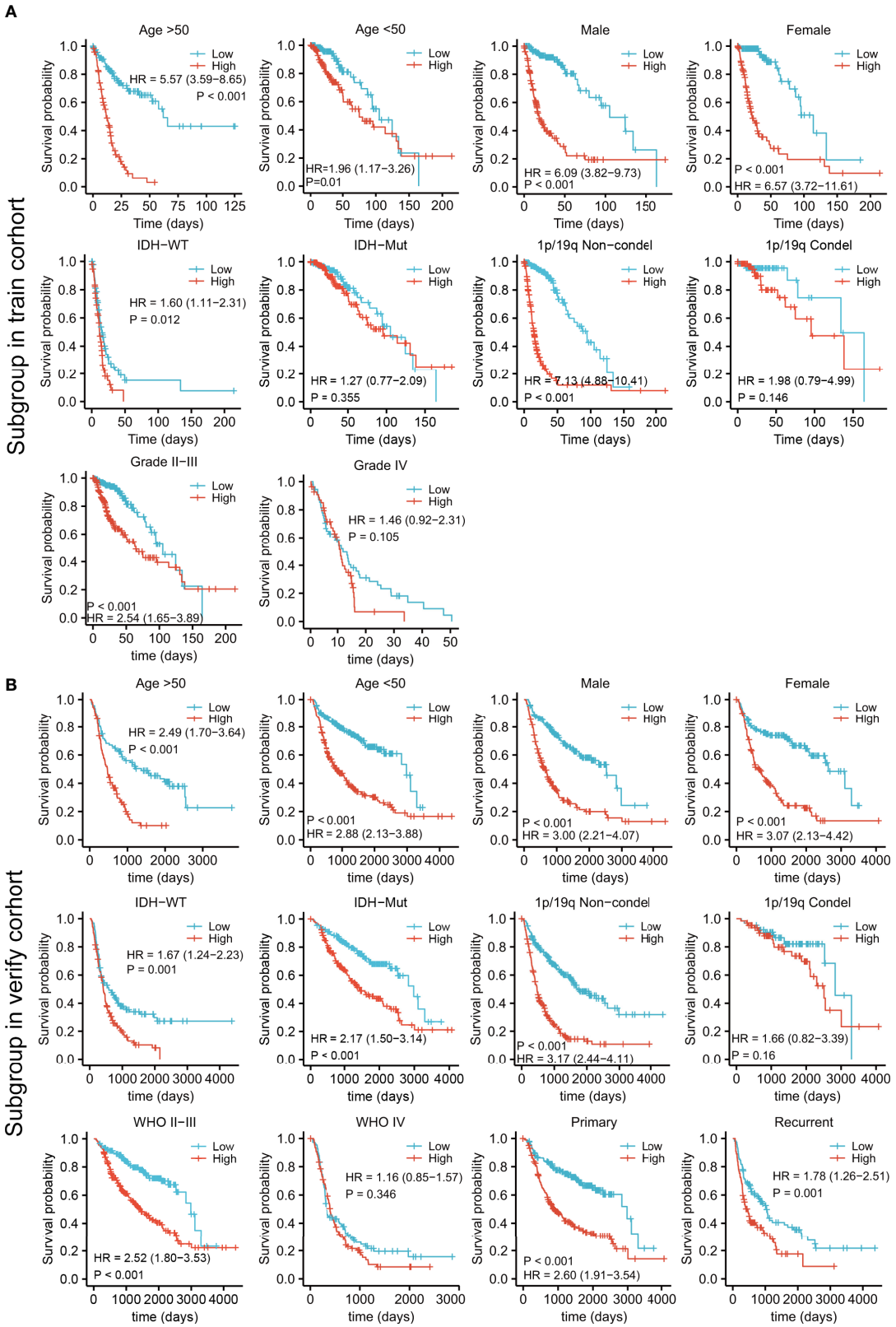

FIGURE 5 | Survival analysis by the risk model in relation to subgroups of clinical features in the training **(A)** and validation cohorts **(B)**.

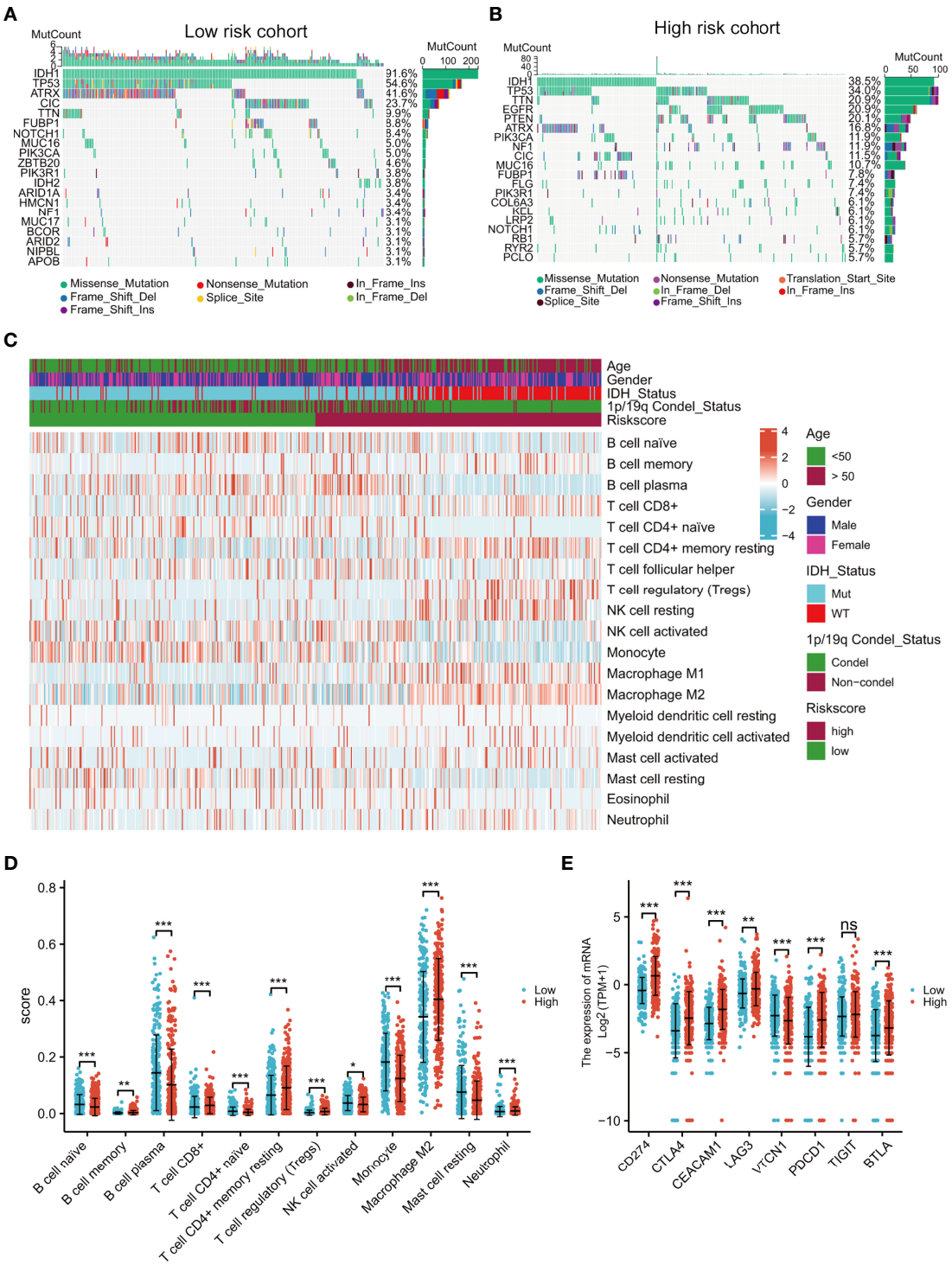

FIGURE 6 | Comprehensive analyses of genomic alterations, immune cell infiltration, and immune checkpoint expression between the different risk groups. Distribution of sex, age, IDH status, 1p/19q condel status, and the top 20 most frequently mutated genes are illustrated for each cohort **(A, B)**. Heatmap showing the CIBERSORT scores of different immune cell distributions in the different subgroups **(C)**. Dot plot showing immune cell CIBERSORT scores and the expression levels of immune checkpoint gene in the high- and low-risk groups **(D, E)**. ns, no significance,*p < 0.05, **p < 0.01, ***p < 0.001.

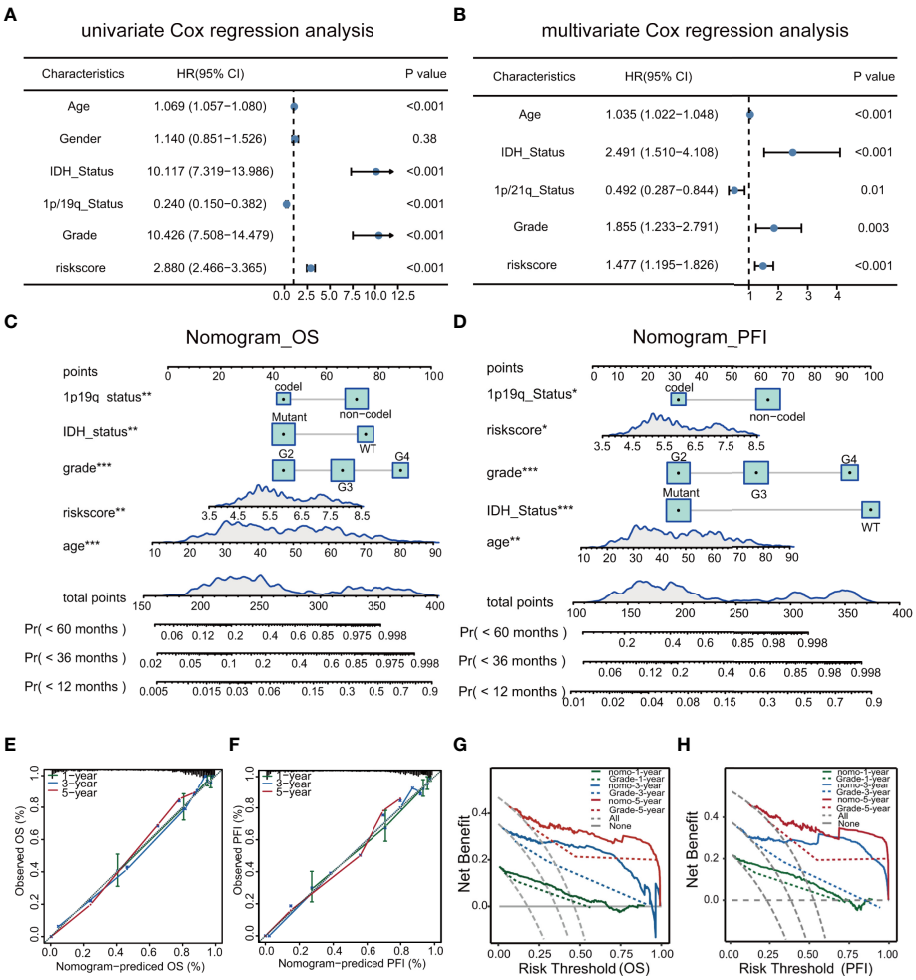

FIGURE 7 | Univariate and multivariate analyses of clinical features in relation to prognosis **(A, B)**. Nomograms for prediction of OS and PFI **(C, D)**. Nomogram calibration using OS and PFI for predicted and actual one- three-, and five-year outcomes **(E, F)**. DCA of nomograms for OS and PFI for one- three-, and five-year survival **(G, H)**.

the high-risk group, this evidence is insufficient for supporting the conclusion that they are effective for treating gliomas. Therefore, iLINCs and CLUE were used to determine which compounds could counteract cancer- or glioma-specific gene expression (i.e., gene expression was increased in tumor tissues but decreased in response to treatment with the compound). We submitted 150 genes with the highest and lowest expression, respectively, to CLUE and 150 genes with the lowest expression to iLINCs. The CLUE results (cMAP scores) were subsequently normalized. The top 20 compounds with the potential to reverse the action of FRGs in high-risk patients are listed in **Figures 9A–C**. Of these, only epirubicin was found to match the GDSC2 results directly, with the other compounds showing similar matches. Thus, we concluded that patients with FRG scores may benefit more from an RTK pathway inhibitor, either by direct inhibition of the RTK or indirect inhibition through targeting downstream effectors such as the PI3K or MAPK pathways.

DISCUSSION

Ferroptosis is a recently described iron-dependent form of PCD, differing from other PCD types such as apoptosis and necroptosis (37). The ferrDB database contains information on all genes linked to ferroptosis and provides the latest resources for research (21). Five ferroptosis-related gene signatures are currently recognized as related to survival in glioma. Gene signatures have been constructed from the investigation of 60-80 candidate genes (9, 38, 39) identified by previous publications. When Zhou and Sun downloaded 173 and 303 FRGs, respectively, from the ferrDB database (40, 41), the overall number of candidate genes was relatively small. The numbers and functional classification of FRGs in the ferrDB are constantly updated as new information becomes available, and new analyses of ferroptosis signatures for glioma have become more necessary. In this study, we applied the latest data including 388 driver, suppressor, and marker genes from the ferrDB database

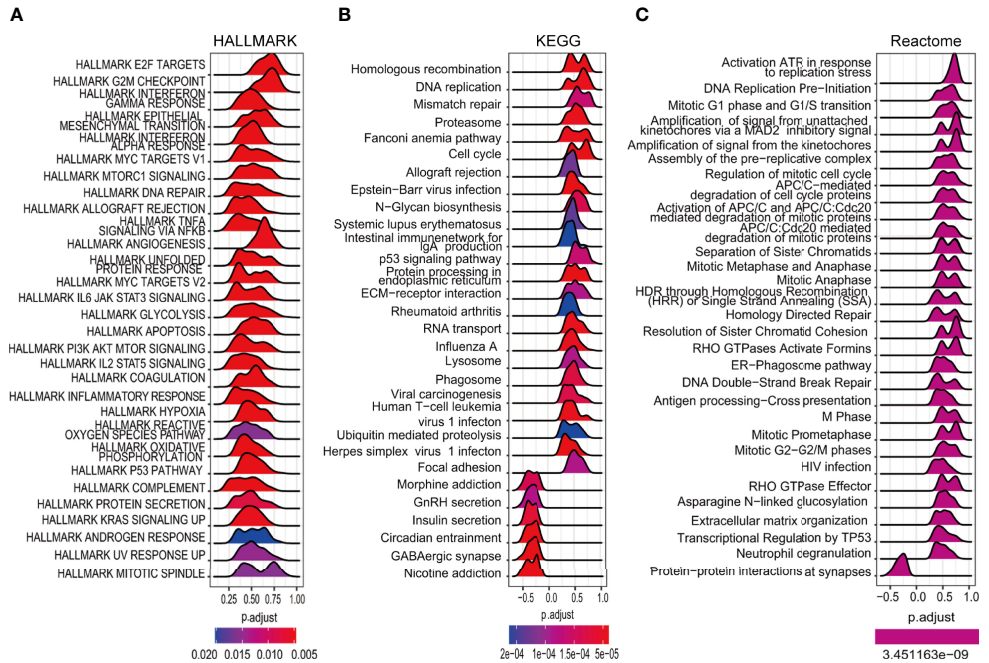

FIGURE 8 | Enrichment analysis of cancer-essential FRG signature genes in the TCGA cohort. The top 30 gene sets of HALLMARK **(A)**, KEGG **(B)**, and Reactome **(C)**.

(**Figure 2A**). At the same time, before the conventional screening of genes using univariate and multivariate Cox regression analysis, we collected data on CRISPR-screened glioma-associated genes from the DepMap portal (**Figure 2A**) and investigated their intersection with the FRGs. This led to the identification of 10 cancer-essential FRGs (ISCU, NFS1, MTOR, EIF2S1, HSPA5, AURKA, RPL8, LONP1, RRM2, and CHMP6) which were closely related to ferroptosis and essential for glioma cell proliferation and survival. The use of the CRISPR screening technique explored potential cancer-essential FRGs, which may shed light on the discovery of targetable FRGs in other tumors or diseases for research.

After multivariate and LASSO analyses, seven cancer-essential FRGs (ISCU, NFS1, MTOR, EIF2S1, HSPA5, AURKA, and RPL8) were used to construct the risk model (**Figures 2B–D**). This model was shown to have stable prognostic prediction capability in both the training and validation cohorts (**Figures 3A–D**) and the subgroups based on clinical features in the validation cohort (**Figure 5**). Further analysis showed that the risk score independently predicted survival in glioma and was effective for predicting both OS and progression-free survival (**Figures 7C–D**). These findings strongly implied that these seven cancer-essential FRGs play important roles in many aspects of glioma development and progression. We further examined the classifications of the risk model genes, finding that three (ISCU, NFS1, and HSPA5) were suppressors of ferroptosis, two (EIF2S1 and AURKA) were marker genes, RPL8 was classified as a driver gene, and MTOR was classified as both a driver and a suppressor gene. Thus, most of the risk model genes were ferroptosis suppressors. On the other hand, all the risk model genes had been identified by CRISPR screening as glioma-associated in glioma cell lines and thus would be involved in the promotion of proliferation (22). In terms of single gene functions, ISCU encodes part of the iron-sulfur (Fe-S) cluster scaffold that synthesizes Fe-S clusters in the mitochondria (42). It has been found that ISCU is targeted by miR-210-3p to block the growth and migration of glioma cells *in vitro* (43). NFS1 encodes several proteins involved in supplying S derived from cysteine to Fe-S clusters and inhibits cysteine transport, triggering ferroptosis and reducing tumor cell growth (44). HSPA5 is involved in protein folding in the endoplasmic reticulum (45), assists in fungal infection of epithelial cells (46), and has been implicated in both proliferation and apoptosis (47). Its expression is promoted by iron in the nasal epithelium (48–50) and is used as a target for >treating chemo-resistant cancers (51). mTOR plays a major role in various metabolic processes, mediating the actions of a variety of hormones, growth factors, and other signaling molecules (52–54). The risk model gene AURKA is involved in cell cycle modulation (55, 56), specifically during mitosis (57), and also regulates phosphorylation of p53/TP53, affecting cancer development (58). In terms of somatic mutation, we found that the frequency of the IDH1 mutation was greater in the low-risk group, in contrast to the higher mutation rates seen in both PTEN and EGFR in the high-risk group (**Figures 6A, B**), suggesting that the mutation frequencies in those genes may have different effects on ferroptosis. Previous studies have shown that IDH-mut glioma patients had a better prognosis than those with wild-type IDH, across all WHO grades (11, 40), that EGFR amplification was correlated with poor prognosis (59), and that PTEN mutations could promote the infiltration of immunosuppressive tumor-associated

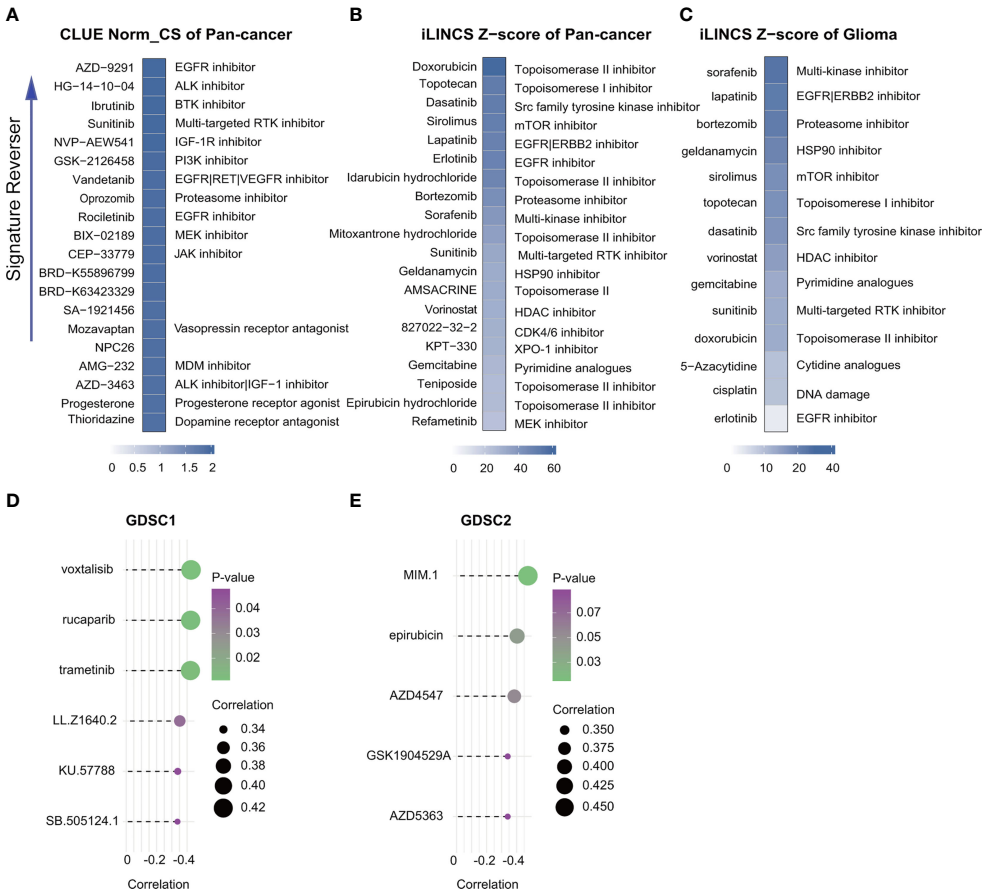

FIGURE 9 | Drug connectivity analysis using alteration-specific transcriptional (CLUE and iLINCS). Pan-cancer in CLUE **(A)**, pan-cancer in iLINCS **(B)**, and glioma in iLINCS **(C)** identifying 20 compounds that enhance or reverse the signature (highlighted with documented mechanisms). Compounds showing negative correlations with AUC values and FRG scores for glioma cells were identified from GDSC1 and GDSC2. **(D, E)**.

macrophages (TAMs) (60). This suggests that FRGs represent good indicators of malignancy-associated glioma characteristics. The analysis of immune cell infiltration showed higher scores for memory B cells, $CD8^+$ T cells, $CtD4^+$ naïve and memory T cells, Tregs, neutrophils, and M2 macrophages in the high-risk group. These results indicated that the patients in the two risk groups have completely different immune microenvironments. Studies have shown that CD4+ T cells, B cells, CD8+ T cells, neutrophils, and M2 macrophages play important roles in the occurrence and malignant progression of glioma (61–63) and that Tregs are closely associated with significant immune suppression in the tumor (64), thus supporting the results of our study. The expression of immune checkpoints was significantly increased in the high-risk group except for VTCN1, indicating a close relationship with glioma immune escape. Tumor immunotherapy is currently an attractive treatment and has achieved good results in other cancers, such as lung cancer. Unfortunately, these have yielded little success clinically, and all clinical trials of immunotherapy have failed. The establishment of the current model may be useful for screening patients for glioma immunotherapy. The enrichment analysis also showed that the model genes were associated with DNA replication and repair and the cell cycle, as well as several signaling pathways closely related to tumor progression (**Figures 8A–C**). Indeed, the high degree of DNA damage and poor repair capacity seen in glioma cells is a trademark feature of cancer and is a determining factor in the growth of tumor cell populations. The gene signature was found to be highly enriched in the cell cycle and DNA damage repair functions; thus, we speculate that these genes play significant parts in cell cycle regulation and tumor development and progression. This suggests an explanation for the influence of FRGs on patient responses, although there may be other reasons also. These genes are thus relevant for the diagnosis and treatment of cancer.

The treatment of malignant brain cancers is challenging. This is especially true of late-stage glioma which is resistant to most traditional types of therapy (65). Recently, an association between ferroptosis-related signatures and drug screening was found in liver cancer (66) and the potential of enhancing treatment efficacy by inducing ferroptosis has attracted attention. Although studies on glioma have focused on the use of ferroptosis to predict prognosis, none have investigated potential drugs (9, 36, 37). Here, we used GDSC1, GDSC2, iLINCS, and CLUE to identify molecules that might reverse the tumor signature, observing that patients with high

FRG scores may benefit more from treatment with an RTK pathway inhibitor, either by direct inhibition of the RTK or indirect inhibition by targeting downstream effectors such as the PI3K or MAPK pathways (**Figure 9**). For primary glioblastoma, bevacizumab (a humanized monoclonal antibody against VEGF-A to block angiogenesis) combined with Stupp is a currently widely used strategy which, although it prolongs the median progression-free survival, does not appear to influence the OS. Using the gene signature for screening patients before deciding on the treatment regimen may improve the efficacy of personalized treatment of glioma.

The study has several limitations. Firstly, ferroptosis-associated pathways are not well understood, and it is possible that the signature genes may function in other pathways as well, for example, in autophagic or immune pathways. Secondly, a major limitation is that we used a public database rather than our own samples; we intend to collect our own glioma samples to further verify the reliability of the research results. Finally, further basic and clinical research is required for verification of the signature application, which will be an important direction of our future research.

To summarize, we identified a seven-gene cancer-essential FRG signature for the prediction of glioma patient prognosis. The signature was found to have an excellent prognostic capability and was utilized for calculating risk scores and drug identification. The model thus has potential in both the diagnosis and management of glioma.

DATA AVAILABILITY STATEMENT

The original contributions presented in the study are included in the article/**Supplementary Material**. Further inquiries can be directed to the corresponding author.

AUTHOR CONTRIBUTIONS

DY and XYW designed the study and analyzed the data. WW, XR, XSW, and JSL collected the data. DY, XR, JF, and JBL drafted and revised the manuscript. XDR, HZ, LC, TL, CZ, and SY revised the images. DY, XYW, and XY revised the manuscript. All authors contributed to the article and approved the submitted version.

FUNDING

This work was supported by the grants from the National Natural Science Foundation of China (No.81872063), Beijing-Tianjin-Hebei Basic Research Cooperation Project (No. 19JCZDJC64200) and Guangxi Natural Science Foundation of China (2018JJA140739).

ACKNOWLEDGMENTS

We thank the team of TCGA, CGGA, GTEx, Depmap, FerrDb, CLUE, LINCS. We also thank Editideas (www.editideas.cn) for its linguistic assistance during the preparation of this manuscript and the R packages compilers.

SUPPLEMENTARY MATERIAL

The Supplementary Material for this article can be found online at: https://www.frontiersin.org/articles/10.3389/fonc.2022.897702/full#supplementary-material

REFERENCES

1. Yuan J, Levitin HM, Frattini V, Bush EC, Boyett DM, Samanamud J, et al. Single-Cell Transcriptome Analysis of Lineage Diversity in High-Grade Glioma. *Genome Med* (2018) 10(1):57. doi: 10.1186/s13073-018-0567-9
2. Lee J, Hoxha E, Song HR. A Novel NFIA-NFkappaB Feed-Forward Loop Contributes to Glioblastoma Cell Survival. *Neuro Oncol* (2017) 19(4):524–34. doi: 10.1093/neuonc/now233
3. Falk Delgado A, De Luca F, van Westen D, Falk Delgado A. Arterial Spin Labeling MR Imaging for Differentiation Between High- and Low-Grade Glioma-a Meta-Analysis. *Neuro Oncol* (2018) 20(11):1450–61. doi: 10.1093/neuonc/noy095
4. Qu S, Liu S, Qiu W, Liu J, Wang H. Screening of Autophagy Genes as Prognostic Indicators for Glioma Patients. *Am J Transl Res* (2020) 12 (9):5320–31.
5. Kieran MW, Goumnerova L, Manley P, Chi SN, Marcus KJ, Manzanera AG, et al. Phase I Study of Gene-Mediated Cytotoxic Immunotherapy With AdV-Tk as Adjuvant to Surgery and Radiation for Pediatric Malignant Glioma and Recurrent Ependymoma. *Neuro Oncol* (2019) 21(4):537–46. doi: 10.1093/neuonc/noy202
6. Yu L, Gui S, Liu Y, Qiu X, Qiu B, Zhang X, et al. Long Intergenic non-Protein Coding RNA 00475 Silencing Acts as a Tumor Suppressor in Glioma Under Hypoxic Condition by Impairing microRNA-449b-5p-Dependent AGAP2 Up-Regulation. *Ther Adv Med Oncol* (2020) 12:1758835920940936. doi: 10.1177/1758835920940936
7. Xu L, Liu H, Yu J, Wang Z, Zhu Q, Li Z, et al. Methylation-Induced Silencing of Maspin Contributes to the Proliferation of Human Glioma Cells. *Oncol Rep* (2016) 36(1):57–64. doi: 10.3892/or.2016.4783
8. Qin EY, Cooper DD, Abbott KL, Lennon J, Nagaraja S, Mackay A, et al. Neural Precursor-Derived Pleiotrophin Mediates Subventricular Zone Invasion by Glioma. *Cell* (2017) 170(5):845–59.e19. doi: 10.1016/j.cell.2017.07.016
9. Chen Z, Wu T, Yan Z, Zhang M. Identification and Validaion of an 11-Ferroptosis Related Gene Signature and Its Correlation With Immune Checkpoint Molecules in Glioma. *Front Cell Dev Biol* (2021) 9:652599. doi: 10.3389/fcell.2021.652599
10. Stoecklein VM, Stoecklein S, Galie F, Ren J, Schmutzer M, Unterrainer M, et al. Resting-State fMRI Detects Alterations in Whole Brain Connectivity Related to Tumor Biology in Glioma Patients. *Neuro Oncol* (2020) 22 (9):1388–98. doi: 10.1093/neuonc/noaa044
11. Tateishi K, Nakamura T, Juratli TA, Williams EA, Matsushita Y, Miyake S, et al. PI3K/AKT/mTOR Pathway Alterations Promote Malignant Progression and Xenograft Formation in Oligodendroglial Tumors. *Clin Cancer Res* (2019) 25(14):4375–87. doi: 10.1158/1078-0432.CCR-18-4144
12. Wang L, Babikir H, Muller S, Yagnik G, Shamardani K, Catalan F, et al. The Phenotypes of Proliferating Glioblastoma Cells Reside on a Single Axis of Variation. *Cancer Discov* (2019) 9(12):1708–19. doi: 10.1158/2159-8290.CD-19-0329
13. Dixon SJ, Lemberg KM, Lamprecht MR, Skouta R, Zaitsev EM, Gleason CE, et al. Ferroptosis: An Iron-Dependent Form of Nonapoptotic Cell Death. *Cell* (2012) 149(5):1060–72. doi: 10.1016/j.cell.2012.03.042

14. Grignano E, Birsen R, Chapuis N, Bouscary D. From Iron Chelation to Overload as a Therapeutic Strategy to Induce Ferroptosis in Leukemic Cells. *Front Oncol* (2020) 10:586530. doi: 10.3389/fonc.2020.586530
15. Asakawa A, Kawade G, Kurata M, Fukuda S, Onishi I, Kinowaki Y, et al. Stratification of Lung Squamous Cell Carcinoma Based on Ferroptosis Regulators: Potential for New Therapeutic Strategies Involving Ferroptosis Induction. *Lung Cancer* (2022) 165:82–90. doi: 10.1016/j.lungcan.2022.01.012
16. Chen J, Li X, Ge C, Min J, Wang F. The Multifaceted Role of Ferroptosis in Liver Disease. *Cell Death Differ* (2022) 29(3):467–80. doi: 10.1038/s41418-022-00941-0
17. Cui W, Zhang J, Wu D, Zhang J, Zhou H, Rong Y, et al. Ponicidin Suppresses Pancreatic Cancer Growth by Inducing Ferroptosis: Insight Gained by Mass Spectrometry-Based Metabolomics. *Phytomedicine* (2022) 98:153943. doi: 10.1016/j.phymed.2022.153943
18. Zhao R, Lv Y, Feng T, Zhang R, Ge L, Pan J, et al. ATF6alpha Promotes Prostate Cancer Progression by Enhancing PLA2G4A-Mediated Arachidonic Acid Metabolism and Protecting Tumor Cells Against Ferroptosis. *Prostate* (2022) 82(5):617–29. doi: 10.1002/pros.24308
19. Zhou A, Fang T, Chen K, Xu Y, Chen Z, Ning X. Biomimetic Activator of Sonodynamic Ferroptosis Amplifies Inherent Peroxidation for Improving the Treatment of Breast Cancer. *Small* (2022) 18(12):e2106568. doi: 10.1002/smll.202106568
20. Yee PP, Wei Y, Kim SY, Lu T, Chih SY, Lawson C, et al. Neutrophil-Induced Ferroptosis Promotes Tumor Necrosis in Glioblastoma Progression. *Nat Commun* (2020) 11(1):5424. doi: 10.1038/s41467-020-19193-y
21. Zhou N, Bao J. FerrDb: A Manually Curated Resource for Regulators and Markers of Ferroptosis and Ferroptosis-Disease Associations. *Database (Oxford)* (2020) 2020:1–8. doi: 10.1093/database/baaa021
22. Meyers RM, Bryan JG, McFarland JM, Weir BA, Sizemore AE, Xu H, et al. Computational Correction of Copy Number Effect Improves Specificity of CRISPR-Cas9 Essentiality Screens in Cancer Cells. *Nat Genet* (2017) 49(12):1779–84. doi: 10.1038/ng.3984
23. Friedman J, Hastie T, Tibshirani R. Regularization Paths for Generalized Linear Models *via* Coordinate Descent. *J Stat Software* (2010) 33(1):1–22. doi: 10.18637/jss.v033.i01
24. Heagerty PJ, Lumley T, Pepe MS. Time-Dependent ROC Curves for Censored Survival Data and a Diagnostic Marker. *Biometrics* (2000) 56(2):337–44. doi: 10.1111/j.0006-341x.2000.00337.x
25. Ceccarelli M, Barthel FP, Malta TM, Sabedot TS, Salama SR, Murray BA, et al. Molecular Profiling Reveals Biologically Discrete Subsets and Pathways of Progression in Diffuse Glioma. *Cell* (2016) 164(3):550–63. doi: 10.1016/j.cell.2015.12.028
26. Mayakonda A, Lin DC, Assenov Y, Plass C, Koeffler HP. Maftools: Efficient and Comprehensive Analysis of Somatic Variants in Cancer. *Genome Res* (2018) 28(11):1747–56. doi: 10.1101/gr.239244.118
27. Li T, Fu J, Zeng Z, Cohen D, Li J, Chen Q, et al. TIMER2.0 for Analysis of Tumor-Infiltrating Immune Cells. *Nucleic Acids Res* (2020) 48(W1):W509–14. doi: 10.1093/nar/gkaa407
28. Gu Z, Eils R, Schlesner M. Complex Heatmaps Reveal Patterns and Correlations in Multidimensional Genomic Data. *Bioinformatics* (2016) 32(18):2847–9. doi: 10.1093/bioinformatics/btw313
29. Love MI, Huber W, Anders S. Moderated Estimation of Fold Change and Dispersion for RNA-Seq Data With Deseq2. *Genome Biol* (2014) 15(12):550. doi: 10.1186/s13059-014-0550-8
30. Wu T, Hu E, Xu S, Chen M, Guo P, Dai Z, et al. Clusterprofiler 4.0: A Universal Enrichment Tool for Interpreting Omics Data. *Innovation (NY)* (2021) 2(3):100141. doi: 10.1016/j.xinn.2021.100141
31. Iasonos A, Schrag D, Raj GV, Panageas KS. How to Build and Interpret a Nomogram for Cancer Prognosis. *J Clin Oncol* (2008) 26(8):1364–70. doi: 10.1200/JCO.2007.12.9791
32. Zhou R, Zeng D, Zhang J, Sun H, Wu J, Li N, et al. A Robust Panel Based on Tumour Microenvironment Genes for Prognostic Prediction and Tailoring Therapies in Stage I-III Colon Cancer. *EBioMedicine* (2019) 42:420–30. doi: 10.1016/j.ebiom.2019.03.043
33. Liu J, Lichtenberg T, Hoadley KA, Poisson LM, Lazar AJ, Cherniack AD, et al. An Integrated TCGA Pan-Cancer Clinical Data Resource to Drive High-Quality Survival Outcome Analytics. *Cell* (2018) 173(2):400–16.e11. doi: 10.1016/j.cell.2018.02.052
34. Yang W, Soares J, Greninger P, Edelman EJ, Lightfoot H, Forbes S, et al. Genomics of Drug Sensitivity in Cancer (GDSC): A Resource for Therapeutic Biomarker Discovery in Cancer Cells. *Nucleic Acids Res* (2013) 41(Database issue):D955–61. doi: 10.1093/nar/gks1111
35. Subramanian A, Narayan R, Corsello SM, Peck DD, Natoli TE, Lu X, et al. A Next Generation Connectivity Map: L1000 Platform and the First 1,000,000 Profiles. *Cell* (2017) 171(6):1437–52.e17. doi: 10.1016/j.cell.2017.10.049
36. Pilarczyk M, Kouril M, Shamsaei B, Vasiliauskas J, Niu W, Mahi N, et al. Connecting Omics Signatures of Diseases, Drugs, and Mechanisms of Actions With iLINCS. *BioRxiv* (2019), 826271. doi: 10.1101/826271
37. Dahlmanns M, Yakubov E, Dahlmanns JK. Genetic Profiles of Ferroptosis in Malignant Brain Tumors and Off-Target Effects of Ferroptosis Induction. *Front Oncol* (2021) 11:783067. doi: 10.3389/fonc.2021.783067
38. Wan RJ, Peng W, Xia QX, Zhou HH, Mao XY. Ferroptosis-Related Gene Signature Predicts Prognosis and Immunotherapy in Glioma. *CNS Neurosci Ther* (2021) 27(8):973–86. doi: 10.1111/cns.13654
39. Zhuo S, Chen Z, Yang Y, Zhang J, Tang J, Yang K. Clinical and Biological Significances of a Ferroptosis-Related Gene Signature in Glioma. *Front Oncol* (2020) 10:590861. doi: 10.3389/fonc.2020.590861
40. Sun W, Yan J, Ma H, Wu J, Zhang Y. Autophagy-Dependent Ferroptosis-Related Signature is Closely Associated With the Prognosis and Tumor Immune Escape of Patients With Glioma. *Int J Gen Med* (2022) 15:253–70. doi: 10.2147/IJGM.S343046
41. Zhou L, Jiang Z, Shi Z, Zhao W, Lu Z, Xie Y, et al. New Autophagy-Ferroptosis Gene Signature Predicts Survival in Glioma. *Front Cell Dev Biol* (2021) 9:739097. doi: 10.3389/fcell.2021.739097
42. Tong WH, Rouault T. Distinct Iron-Sulfur Cluster Assembly Complexes Exist in the Cytosol and Mitochondria of Human Cells. *EMBO J* (2000) 19(21):5692–700. doi: 10.1093/emboj/19.21.5692
43. He H, Liu J, Li W, Yao X, Ren Q, Shen B, et al. MiR-210-3p Inhibits Proliferation and Migration of C6 Cells by Targeting Iscu. *Neurochem Res* (2020) 45(8):1813–24. doi: 10.1007/s11064-020-03043-w
44. Alvarez SW, Sviderskiy VO, Terzi EM, Papagiannakopoulos T, Moreira AL, Adams S, et al. NFS1 Undergoes Positive Selection in Lung Tumours and Protects Cells From Ferroptosis. *Nature* (2017) 551(7682):639–43. doi: 10.1038/nature24637
45. Cuevas EP, Eraso P, Mazon MJ, Santos V, Moreno-Bueno G, Cano A, et al. LOXL2 Drives Epithelial-Mesenchymal Transition *via* Activation of IRE1-XBP1 Signalling Pathway. *Sci Rep* (2017) 7:44988. doi: 10.1038/srep44988
46. Gebremariam T, Liu M, Luo G, Bruno V, Phan QT, Waring AJ, et al. CotH3 Mediates Fungal Invasion of Host Cells During Mucormycosis. *J Clin Invest* (2014) 124(1):237–50. doi: 10.1172/JCI71349
47. Kang JM, Park S, Kim SJ, Kim H, Lee B, Kim J, et al. KIAA1324 Suppresses Gastric Cancer Progression by Inhibiting the Oncoprotein Grp78. *Cancer Res* (2015) 75(15):3087–97. doi: 10.1158/0008-5472.CAN-14-3751
48. Alqarihi A, Gebremariam T, Gu Y, Swidergall M, Alkhazraji S, Soliman SSM, et al. GRP78 and Integrins Play Different Roles in Host Cell Invasion During Mucormycosis. *mBio* (2020) 11(3):e01087–20. doi: 10.1128/mBio.01087-20
49. Gebremariam T, Lin L, Liu M, Kontoyiannis DP, French S, Edwards JEJr., et al. Bicarbonate Correction of Ketoacidosis Alters Host-Pathogen Interactions and Alleviates Mucormycosis. *J Clin Invest* (2016) 126(6):2280–94. doi: 10.1172/JCI82744
50. Liu M, Spellberg B, Phan QT, Fu Y, Fu Y, Lee AS, et al. The Endothelial Cell Receptor GRP78 Is Required for Mucormycosis Pathogenesis in Diabetic Mice. *J Clin Invest* (2010) 120(6):1914–24. doi: 10.1172/JCI42164
51. Huang KC, Chiang SF, Yang PC, Ke TW, Chen TW, Lin CY, et al. ATAD3A Stabilizes GRP78 to Suppress ER Stress for Acquired Chemoresistance in Colorectal Cancer. *J Cell Physiol* (2021) 236(9):6481–95. doi: 10.1002/jcp.30323
52. Hara K, Maruki Y, Long X, Yoshino K, Oshiro N, Hidayat S, et al. Raptor, a Binding Partner of Target of Rapamycin (TOR), Mediates TOR Action. *Cell* (2002) 110(2):177–89. doi: 10.1016/s0092-8674(02)00833-4
53. Kim DH, Sarbassov DD, Ali SM, King JE, Latek RR, Erdjument-Bromage H, et al. mTOR Interacts With Raptor to Form a Nutrient-Sensitive Complex That Signals to the Cell Growth Machinery. *Cell* (2002) 110(2):163–75. doi: 10.1016/s0092-8674(02)00808-5
54. Park IH, Bachmann R, Shirazi H, Chen J. Regulation of Ribosomal S6 Kinase 2 by Mammalian Target of Rapamycin. *J Biol Chem* (2002) 277(35):31423–9. doi: 10.1074/jbc.M204080200

55. Carvalhal S, Ribeiro SA, Arocena M, Kasciukovic T, Temme A, Koehler K, et al. The Nucleoporin ALADIN Regulates Aurora A Localization to Ensure Robust Mitotic Spindle Formation. *Mol Biol Cell* (2015) 26(19):3424–38. doi: 10.1091/mbc.E15-02-0113
56. Marumoto T, Hirota T, Morisaki T, Kunitoku N, Zhang D, Ichikawa Y, et al. Roles of Aurora-A Kinase in Mitotic Entry and G2 Checkpoint in Mammalian Cells. *Genes Cells* (2002) 7(11):1173–82. doi: 10.1046/j.1365-2443.2002.00592.x
57. Marumoto T, Honda S, Hara T, Nitta M, Hirota T, Kohmura E, et al. Aurora-A Kinase Maintains the Fidelity of Early and Late Mitotic Events in HeLa Cells. *J Biol Chem* (2003) 278(51):51786–95. doi: 10.1074/jbc.M306275200
58. Katayama H, Sasai K, Kawai H, Yuan ZM, Bondaruk J, Suzuki F, et al. Phosphorylation by Aurora Kinase A Induces Mdm2-Mediated Destabilization and Inhibition of P53. *Nat Genet* (2004) 36(1):55–62. doi: 10.1038/ng1279
59. Suina K, Tsuchihashi K, Yamasaki J, Kamenori S, Shintani S, Hirata Y, et al. Epidermal Growth Factor Receptor Promotes Glioma Progression by Regulating xCT and GluN2B-Containing N-Methyl-D-Aspartate-Sensitive Glutamate Receptor Signaling. *Cancer Sci* (2018) 109(12):3874–82. doi: 10.1111/cas.13826
60. Chen P, Hsu WH, Chang A, Tan Z, Lan Z, Zhou A, et al. Circadian Regulator CLOCK Recruits Immune-Suppressive Microglia Into the GBM Tumor Microenvironment. *Cancer Discov* (2020) 10(3):371–81. doi: 10.1158/2159-8290.CD-19-0400
61. Brown JM, Recht L, Strober S. The Promise of Targeting Macrophages in Cancer Therapy. *Clin Cancer Res* (2017) 23(13):3241–50. doi: 10.1158/1078-0432.CCR-16-3122
62. Liang J, Piao Y, Holmes L, Fuller GN, Henry V, Tiao N, et al. Neutrophils Promote the Malignant Glioma Phenotype Through S100A4. *Clin Cancer Res* (2014) 20(1):187–98. doi: 10.1158/1078-0432.CCR-13-1279
63. Yin W, Jiang X, Tan J, Xin Z, Zhou Q, Zhan C, et al. Development and Validation of a Tumor Mutation Burden-Related Immune Prognostic Model for Lower-Grade Glioma. *Front Oncol* (2020) 10:1409. doi: 10.3389/fonc.2020.01409
64. Richardson LG, Nieman LT, Stemmer-Rachamimov AO, Zheng XS, Stafford K, Nagashima H, et al. IDH-Mutant Gliomas Harbor Fewer Regulatory T Cells in Humans and Mice. *Oncoimmunology* (2020) 9(1):1806662. doi: 10.1080/2162402X.2020.1806662
65. Yuan J, Peng G, Xiao G, Yang Z, Huang J, Liu Q, et al. Xanthohumol Suppresses Glioblastoma *via* Modulation of Hexokinase 2 -Mediated Glycolysis. *J Cancer* (2020) 11(14):4047–58. doi: 10.7150/jca.33045
66. Chen ZA, Tian H, Yao DM, Zhang Y, Feng ZJ, Yang CJ. Identification of a Ferroptosis-Related Signature Model Including mRNAs and lncRNAs for Predicting Prognosis and Immune Activity in Hepatocellular Carcinoma. *Front Oncol* (2021) 11:738477. doi: 10.3389/fonc.2021.738477

Conflict of Interest: The authors declare that the research was conducted in the absence of any commercial or financial relationships that could be construed as a potential conflict of interest.

Publisher's Note: All claims expressed in this article are solely those of the authors and do not necessarily represent those of their affiliated organizations, or those of the publisher, the editors and the reviewers. Any product that may be evaluated in this article, or claim that may be made by its manufacturer, is not guaranteed or endorsed by the publisher.

frontiers | Frontiers in Pharmacology

ORIGINAL RESEARCH
published: 13 June 2022
doi: 10.3389/fphar.2022.870178

Cisplatin Promotes the Efficacy of Immune Checkpoint Inhibitor Therapy by Inducing Ferroptosis and Activating Neutrophils

Ziwei Zhou[1†], Yiming Zhao[1,2†], Si Chen[1], Guohui Cui[1], Wenkui Fu[1], Shouying Li[1], Xiaorong Lin[1,3] and Hai Hu[1*]*

[1]Department of Oncology, Sun Yat-Sen Memorial Hospital, Sun Yat-sen University, Guangzhou, China, [2]Phase I Clinical Trial Centre, Sun Yat-Sen Memorial Hospital, Sun Yat-sen University, Guangzhou, China, [3]Diagnosis and Treatment Center of Breast Diseases, Shantou Central Hospital, Shantou, China

The combination of immunotherapy with platinum-based chemotherapy has become the first-line treatment for patients with advanced non–small cell lung cancer (NSCLC) with negative driver gene mutations. However, finding an ideal chemotherapeutic regimen for immunotherapy and exploring the underlying mechanism have noticeably attracted clinicians' attention. In this study, we found that cisplatin induced ferroptosis of tumor cells, followed by N1 neutrophil polarization in the tumor microenvironment, which in turn remodeled the "cold" tumor to a "hot" one through enhancing T-cell infiltration and Th1 differentiation. Based on the important role of tumor ferroptosis in the immune-promoting effect of cisplatin, we noticed that the combination of a ferroptosis activator showed a synergistic effect with chemoimmunotherapy of epidermal growth factor receptor (EGFR)-mutant NSCLC, which would be an effective strategy to overcome immunotherapy resistance in NSCLC patients harboring driver mutations.

Keywords: non–small cell lung cancer, cisplatin, ferroptosis, immune checkpoint inhibitors, neutrophils

Edited by:
Jian Chen,
Guilin Medical University, China

Reviewed by:
Bin Xu,
Renmin Hospital of Wuhan University, China
Xin Lu,
University of Notre Dame, United States

***Correspondence:**
Xiaorong Lin
clarelynn_lin@163.com
Hai Hu
huhai@mail.sysu.edu.cn

†*These authors share first authorship*

Specialty section:
This article was submitted to Pharmacology of Anti-Cancer Drugs, a section of the journal Frontiers in Pharmacology

Received: *06 February 2022*
Accepted: *13 April 2022*
Published: *13 June 2022*

Citation:
Zhou Z, Zhao Y, Chen S, Cui G, Fu W, Li S, Lin X and Hu H (2022) Cisplatin Promotes the Efficacy of Immune Checkpoint Inhibitor Therapy by Inducing Ferroptosis and Activating Neutrophils. Front. Pharmacol. 13:870178. doi: 10.3389/fphar.2022.870178

1 INTRODUCTION

Non–small cell lung cancer (NSCLC) remains the leading cause of cancer-related deaths worldwide (Malvezzi et al., 2012; Apetoh et al., 2015; Global Burden of Disease Cancer et al., 2018). Recent development of immune checkpoint inhibitors (ICIs) has revolutionized the treatment of NSCLC and noticeably improved the outcomes in patients with NSCLC. Despite the successful administration of ICIs, only a subgroup of cancer patients can benefit from immune checkpoint blockade therapy. Some patients do not respond to initial immunotherapy, and the majority of responders eventually develop acquired resistance to ICIs. Accumulating preclinical and clinical evidence indicated that chemotherapy regimens, which are capable of inducing anticancer immunity, can be particularly promising partners for use in combination with ICIs (Hanahan and Weinberg, 2011; Pfirschke et al., 2016; Mathew et al., 2018; Emens et al., 2021). Notably, the combination of a platinum-based doublet and pembrolizumab is the first-line treatment of NSCLC without driver mutations (Langer et al., 2016; Gandhi et al., 2018). However, the underline mechanism of platinum-based chemotherapy on promoting anticancer immune response has not been fully clarified yet. Additionally, epidermal growth factor receptor (EGFR)- or anaplastic lymphoma kinase (ALK)-driven mutations showed an inferior response to immunotherapy. The high frequency of inactive tumor-infiltrating lymphocytes, low tumor mutational load (Rizvi et al., 2015), and weak

immunogenicity (Dong et al., 2017) indicate a non-immunogenic or "cold" microenvironment. Thus, exploration of the underlying mechanism of platinum-based chemotherapy on promoting anticancer immune response may lead to the discovery of new solutions to promote ICI outcomes. This knowledge could be significant to developing new combination therapies for patients with NSCLC harboring oncogenic driver mutations and enhance the responses to ICI therapy.

Previous studies indicated that chemotherapeutic agents might induce immunogenic cancer cell death, including pyroptosis (Wang et al., 2017) and ferroptosis (Zhang et al., 2020), with the release of immunostimulating molecules. Research studies revealed that cisplatin could induce different types of cell death, including ferroptosis (Zhang et al., 2020), apoptosis, and pyroptosis. It has been demonstrated that cisplatin-induced pyroptosis plays an important role in enhancing anticancer immune response (Zhang CC. et al., 2019). Ferroptosis is an immunogenic cell death (ICD) which could enhance anticancer immunity in the tumor microenvironment (TME) (Tang et al., 2020). However, the role of ferroptosis in inducing anticancer immune response in NSCLC upon platinum-based chemotherapy has not been evaluated. Herein, we revealed that platinum-based chemotherapy could induce ferroptosis of tumor cells, followed by the activation of anti-tumor neutrophils *in vitro* and *in vivo*, which in turn remodeled the TME through enhancing T-cell infiltration and Th1 differentiation. We also found that a ferroptosis inducer would amplify the anticancer immune response to ICI therapy of NSCLC patients harboring oncogenic driver mutations upon platinum-based chemotherapy.

2 MATERIALS AND METHODS

2.1 Data Collection

The transcriptome data of patients with lung adenocarcinoma (LUAD), lung squamous cell carcinoma (LUSC), bladder urothelial carcinoma (BLCA), breast invasive carcinoma (BRCA), esophageal carcinoma (ESCA), and head and neck squamous cell carcinoma (HNSCC) were downloaded from the Cancer Genome Atlas (TCGA) database *via* the Genomic Data Commons (GDC) data portal [Repository (cancer.gov)]. The RNA-seq gene expression level 3 data were then obtained.

2.2 Correlation Between Ferroptosis and Immune Scores

The marker gene set of the ferroptosis pathway was obtained from the Kyoto Encyclopedia of Genes and Genomes (KEGG) database (**Supplementary Table S3**). Single sample gene set enrichment analysis (ssGSEA) was performed to derive the enrichment score, namely, ferroscore in the present study, of the ferroptosis pathway in each sample using an R package called "GSVA" (Hanzelmann et al., 2013). Immune scores were calculated using the ESTIMATE algorithm (Verhaak et al., 2010). The correlation between ferroscores and immune scores in different types of cancer was assessed by Spearman's correlation analysis.

2.3 Analysis of Immune Cells in the Tumor Microenvironment

The tumor-infiltrating immune cells were estimated using the CIBERSORT analytical tool (Newman et al., 2015). The gene expression signatures for 22 immune cells were obtained from the CIBERSORT analytical tool [CIBERSORT (stanford.edu)]. Only cases with a CIBERSORT p-value < 0.05 were included for further analysis. The difference in immune cells between high-ferroscore and low-ferroscore patients was analyzed *via* the Mann–Whitney U test. The xCell (Aran et al., 2017), a robust computational method that converts bulk transcriptomes to enrichment scores of 64 immune and stromal cells, was also applied to verify the conclusions.

2.4 Gene Ontology and Kyoto Encyclopedia of Genes and Genomes Pathway Enrichment Analysis

Patients were divided into two groups, namely, the Ferroscore-H (high ferroscore) group and the Ferroscore-L (low ferroscore) group, and were compared in terms of the median level of the ferroscore. The "limma" package in R software was used to identify differentially expressed genes (DEGs) in the two groups (Ritchie et al., 2015). A false discovery rate (FDR) < 0.05 combined with |log2 (fold change) | >1 was set as the threshold for the identification of DEGs. All DEGs were analyzed by the GO and KEGG pathway enrichment analyses. An FDR p-value <0.05 was considered statistically significant for the enrichment analysis.

2.5 Gene Set Enrichment Analysis

Gene set enrichment analysis (GSEA) was performed in the ferroscore-H and ferroscore-L groups using the "ClusterProlier" package in R software (Subramanian et al., 2005; Zhang M. et al., 2019). The GO and KEGG pathways were analyzed using this method. Enriched gene sets with a nominal p-value < 0.05 and FDR q < 0.05 were considered to be enrichment significant.

2.6 Cells and Cell Culture

A549 cells and LLC cells from the American Type Culture Collection (ATCC, Manassas, VA, United States) were cultured in a Dulbecco's modified Eagle's medium (DMEM) supplemented with 10% fetal bovine serum (FBS). PC9 cells were maintained in a Roswell Park Memorial Institute (RPMI)-1640 medium supplemented with 10% FBS. Human neutrophils were isolated from the peripheral blood of healthy donors using density gradient centrifugation *via* Percoll (Pharmacia Fine Chemicals, Uppsala, Sweden). Total immune cells are obtained from peripheral blood by lysis of red blood cells. Neutrophils and total immune cells were cultured in a DMEM with 10% FBS.

2.7 Drugs

The chemicals used were as follows: cisplatin (S1166; Selleck Chemicals, Houston, TX, United States), ferrostatin-1-1 (S7243, Selleck), and RSL3 (S8155, Selleck).

2.8 Quantitative Reverse Transcription Polymerase Chain Reaction

Total RNA was extracted using TRIzol reagent (Invitrogen, Carlsbad, CA, United States) and was reversely transcribed into cDNA using a PrimeScript RT Reagent kit (TaKaRa, Tokyo, Japan). The RT-qPCR was performed using a SYBR Premix Ex Taq kit (TaKaRa) according to the manufacturer's instructions. Data were collected and analyzed using LightCycler 480 software (Roche, Basel, Switzerland).

2.9 Cytotoxicity Assay

Calcein-AM–labeled A549 cells or PC9 cells were co-cultured with neutrophils or total immune cells for 8 h. The effector-to-target ratio was 5:1. Co-cultured cells were maintained in 24-well plates. Mixed cells of co-culture system were dyed with 7-AA-D for cell death rate analysis. The death rate of tumor cells was assessed by flow cytometry. The dead tumor cells were considered as calcein and 7-AA-D double-positive cells.

2.10 Lipid Peroxidation Assay

Lipid peroxidation assay was carried out using a lipid peroxidation kit (ab243377; Abcam, Cambridge, United Kingdom) according to the manufacturer's instructions. Briefly, a lipid peroxidation sensor was added to the tumor cell culture medium and incubated for 30 min. After washing with phosphate-buffered saline (PBS), fluorescence was detected in the fluorescein Isothiocyanate (FITC) channel and P-phycoerythrin (PE) channel by flow cytometry. The lipid peroxidation was quantified as the ratio of PE (non-oxidized)/FITC (oxidized)-positive cell count.

2.11 Magnetic Activated Cell Sorting of $CD4^+$ T Cells

Human PBMCs were isolated from the peripheral blood of healthy donors using Ficoll density gradient centrifugation. $CD4^+$ T helper cells were isolated from PBMCs using CD4 microbeads (130-045-101; Miltenyi, Bergisch Gladbach, Germany), a LS Magnetic Column (Miltenyi), and a MiniMACS separator.

2.12 Immunohistochemistry

The IHC staining was performed using Ly-6G (Santa Cruz Biotechnology, Inc., Dallas, TX, United States) and T-bet (Proteintech, Rosemont, IL, United States) antibodies according to standard protocols on formalin-fixed and paraffin-embedded tumor tissues. Immunolabeling was visualized with a mixture of 3,3′-diaminobenzidine (DAB) solution (ZSGB-BIO, Beijing, China), followed by counterstaining with hematoxylin.

2.13 Animal Experiments

6-week-old C57BL/6 mice were purchased from Beijing Vital River Laboratory Animal Technology Co., Ltd. (Beijing, China). Mice were kept in a specific pathogen-free (SPF) animal house at 28°C with 50% humidity. 7 × 106 LLC cells were inoculated into the subcutaneous layer of 6-week-old female C57BL/6 mice ($n = 6$ mice per group). After the xenografts became palpable, mice were injected with 10 mg/kg cisplatin (DDP) or 10 mg/kg DDP plus 10 mg/kg ferrostatin-1-1 intraperitoneally. Anti-PD1 antibody was injected intraperitoneally at a dose of 8 mg/kg 3 days later. After 9 days of observation, the mice were killed. Tumors and harvested organs were subjected to IHC staining.

2.14 Primary Cell Isolation

Cut tumors and get rid of the peripheral tissue. Put the tumor tissue into PBS and wash several times. Use the scalpel to chop the tissue for 5 min. Put the minced tissue into a 50-ml centrifuge tube and add 10 ml/g tissue of DMEM with 300 units/ml collagenase IV and 100 units/ml hyaluronidase for 1 h of shaking at 200 rpm/37°C. Centrifuge at 600 g for 10 min. Re-suspend with 10 ml washing buffer every time until the supernatant is clean and the pellet is white. Wash with DMEM once and re-suspend in 2 ml pre-warmed trypsin. Put into a 35-mm culture dish and incubate at 37°C for 20 min. Gently pipet the solution to mix every 5 min. Add the medium into neutralized trypsin and centrifuge at 1,000 g for 3 min. Re-suspend the pellet in 1–2 ml pre-warmed washing buffer with 5 mg/ml dispase and 0.1 mg/ml DNase I. Gently pipet the solution to mix every 5 min. Add the medium into neutralized trypsin and centrifuge at 1,000 g for 3 min. Re-suspend the pellet in 1–2 ml pre-warmed washing buffer with 5 mg/ml dispase and 0.1 mg/ml DNase I. Gently pipet the solution to mix and incubate at room temperature for 2 min. Briefly centrifuge to achieve the fibers down and then filter through a 70-μm cell strainer to obtain single cell suspension. Centrifuge at 1,000 g for 3 min and re-suspend the cells in a growth medium.

2.15 Enzyme-Linked Immunosorbent Assay

ELISA was performed using human interferon gamma (IFN-γ) (430107; BioLegend, San Diego, CA, United States), human C-X-C Motif Chemokine Ligand 1 (CXCL1) (RAB0116; Sigma-Aldrich, St. Louis, MO, United States), and human C-X-C motif chemokine ligand 2 (CXCL2) (DY276-05; R&D Systems, Minneapolis, MN, United States), according to the manufacturers' protocols.

3 RESULTS

3.1 Cisplatin Promoted Tumor Ferroptosis That Was Correlated With Immune Score

To explore whether cisplatin could trigger ferroptosis to enhance anticancer immune response in NSCLC treatment, we first attempted to indicate whether ferroptosis could be correlated with the tumor immune microenvironment (TIME) of NSCLC using TCGA database. The ferroptosis status was defined as "high" or "low" ferroscore according to the expressions of

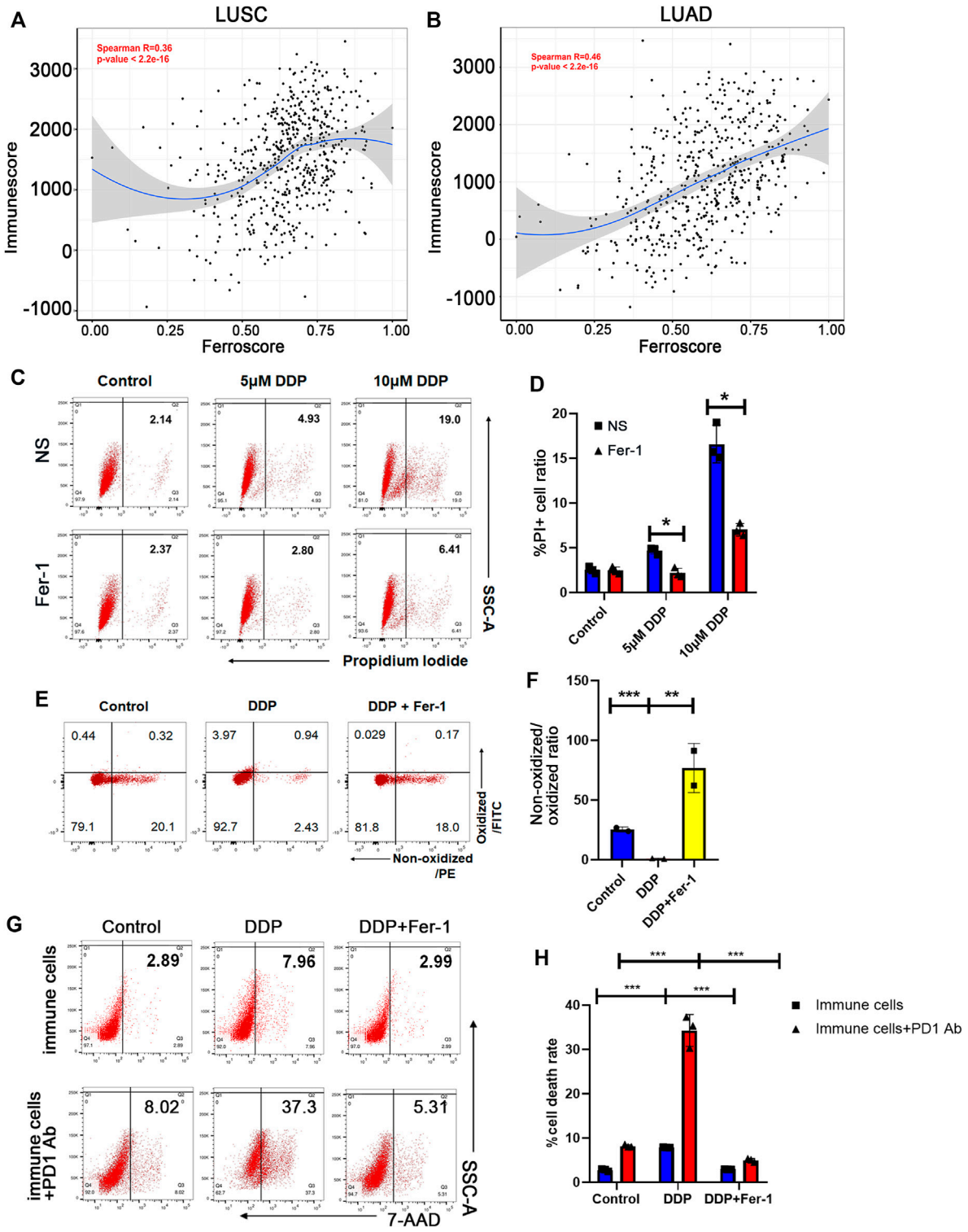

FIGURE 1 | Cisplatin promoted tumor ferroptosis that was correlated with immune score. **(A)** and **(B)** The ferroscore correlated with immunescore in LUSC **(A)** and LUAD **(B)** cohorts of TCGA database. **(C)** Cell death ratio of A549 cells treated with 5 μM cisplatin (DDP) or 10 μM DDP for 8 h measured by flow cytometry (NS: normal saline). **(D)** Quantification of data in **(C)**. **(E)** Lipid peroxidation of A549 cells treated with 10 μM DDP or rescued by 10 μM ferrostatin-1 (Fer-1) for 8 h determined by flow cytometry. **(F)** Quantification of data in **(E)**. The ratio of non-oxidized lipid (PE)/oxidized lipid (FITC) fluorescence intensities decreases in DDP-treated cells, indicating that DDP induces lipid peroxidation, while ferrostatin-1 rescued this effect. **(G)** Cell death ratio of A549 cells co-cultured with immune cells before or after anti-PD1 antibody treatment, determined by flow cytometry. The immune cells were pretreated with supernatant of A549 cells, which were given DDP or DDP plus ferrostatin-1. **(H)** Quantification of data in **(G)**. DDP could increase cytotoxic effect of immune cells and anti-PD1 antibody efficacy, which would be rescued by ferrostatin-1. Bar graphs represent the mean ± SD of indicated samples. $*p < 0.05$, $**p < 0.01$, $***p < 0.001$.

ferroptosis-related genes *via* the KEGG pathway. The TIME status was defined as an immune score featured with different types of immune cells that infiltrated tumor tissues (Verhaak et al., 2010). We revealed that the ferroscore was significantly correlated with immune score both in the LUSC and LUAD cohorts from TCGA database (**Figures 1A,B**). Furthermore, the strong correlation between ferroptosis and enhanced immune cell infiltration was not limited to NSCLC. We found a significant correlation between ferroscore and immune score among different types of cancer, including BLCA, BRCA, ESCA, and HNSCC cohorts in TCGA database (**Supplementary Figures S1A–D**). Cisplatin in combination with immunotherapy is an important treatment option in these tumors. This finding is consistent with our assumption that ferroptosis could act as an enhancement factor to promote the anticancer immune response.

Distinct from other cell death modalities, ferroptosis is marked by iron-dependent lipid peroxidation (Hassannia et al., 2019). In order to indicate whether cisplatin could induce ferroptosis of NSCLC cells, we detected cell death and lipid peroxidation of A549 lung cancer cells upon cisplatin treatment. Our results showed that cisplatin induced A549 cell death in a dose-dependent manner, and about 50% of cell death could be rescued by ferrostatin-1, as a ferroptosis inhibitor (**Figures 1C,D**). In addition, cisplatin also mediated lipid peroxidation and could be rescued by ferrostatin-1 (**Figures 1E,F**), indicating that cisplatin could induce ferroptosis of NSCLC cells. Ferroptosis has been reported to enhance the anticancer immune response (Tang et al., 2020). Then, we examined whether cisplatin-mediated ferroptosis could enhance anti-tumor effect of immune cells and play a synergistic role with ICIs in NSCLC treatment. The supernatants of A549 cells that have been treated with cisplatin or cisplatin + ferrostatin-1 were collected. Immune cells, obtained from peripheral blood after red cell lysis, were pretreated with the supernatants of A549 cells for 24 h. Then, the anti-tumor cytotoxic effect of immune cells was examined by co-culture of A549 cells with these immune cells. Flow cytometry assay was used to assess the cell death ratio of A549 cells, and it was revealed that immune cells pretreated with supernatant of cisplatin-treated NSCLC cells had a significantly stronger cytotoxic effect, whereas the supernatant of cisplatin + ferrostatin-1–treated NSCLC cells could not significantly boost the anti-tumor effect of immune cells (**Figures 1G,H**). Furthermore, immune cells exhibited a stronger anti-tumor ability when pretreatment with programmed cell death protein 1 (PD-1) antibody was performed in the co-culture system (**Figures 1G,H**). The findings mentioned above suggested that cisplatin could induce ferroptosis of NSCLC cells, thereby promoting the anti-tumor cytotoxic ability of immune cells to augment the therapeutic effect of ICIs.

3.2 Neutrophil Activation Pathway Was Significantly Upregulated in the High Ferroscore Cohort

To figure out which type of the immune cells could be involved in the ferroptosis-induced anti-tumor immune response, the infiltration levels of various types of immune cells in the tumor tissues from TCGA database were calculated using the CIBERSORT analytical tool (Newman et al., 2015). We found that neutrophils, resting mast cells, resting dendritic cells, and M2 macrophages were significantly more abundant in the ferroscore-H (high ferroscore) group in both LUSC and LUAD cohorts (**Figures 2A,B**) than in the ferroscore-L (ferroscore low) group. Among these immune cells, neutrophils showed the most prominent enrichment in the ferroscore-H group in both LUSC and LUAD cohorts. Consistently, xCell algorithm (Aran et al., 2017) also demonstrated that the ferroscore-H group was correlated with a higher level of neutrophils (**Supplementary Figure S2**). Moreover, the KEGG pathway and Gene Ontology enrichment analyses of the differentially expressed genes (DEGs) revealed that neutrophil-related pathways, such as neutrophil extracellular trap formation, neutrophil degranulation, and morphological and behavioral changes of neutrophils after being stimulated, were the most activated pathways among the top-ranking pathways in the ferroscore-H group in the LUSC TCGA dataset (**Figures 2C,D**). Furthermore, gene set enrichment analysis (GSEA) was used to examine the correlation between the ferroscore and neutrophil-related pathways. Regulation of neutrophil chemotaxis and migration pathways were strongly correlated with high ferroscore (**Figures 2E,F**). Neutrophils are the most frequent type of innate immune cells and are the first cells to arrive at sites of developing inflammation. It has been shown that neutrophils are often the first cells to arrive both at a wound and during the early initiation phases of carcinogenesis (Feng et al., 2012). Once neutrophils infiltrate tumor tissues, they may undergo polarization to switch to N1/anti-tumor or N2/pro-tumor phenotype induced by the TME (Giese et al., 2019). Thus, we hypothesized that the N1-polarized neutrophils in these tumor tissues could play a key role in the ferroptosis-induced anti-tumor immune response.

Based on the above bioinformatics analysis, we initially put forward the hypothesis that neutrophils play a key role in the anti-tumor immune response induced by ferroptosis. Then we constructed a co-culture system to verify the above hypothesis. The tumor cells pretreated with DDP or DDP + Fer-1 were co-cultured with immune cells (PBMCs + neutrophils) or PBMCs for 12 h, respectively. The tumor death ratio was detected by flow cytometry (**Figure 2G**). The results suggest that the death rate of tumor cells pretreated with DDP is 2 times more than that in the control group with the presence of neutrophils, while Fer-1 can restore the death rate of tumor cells after being attacked by immune cells. However, the death rate of tumor cells did not show obvious change, whether they were pretreated with DDP or DDP + Fer-1 in the co-culture system without neutrophils. The above results indicated that neutrophils play an important role in anti-tumor immune response.

3.3 N1-Polarized Neutrophils Induced by Cisplatin-Mediated Tumor Ferroptosis Exerted an Anti-Tumor Effect

According to the analysis above, we further supposed that cisplatin-based chemotherapy could mediate tumor cell ferroptosis-induced neutrophil infiltration and N1 neutrophil

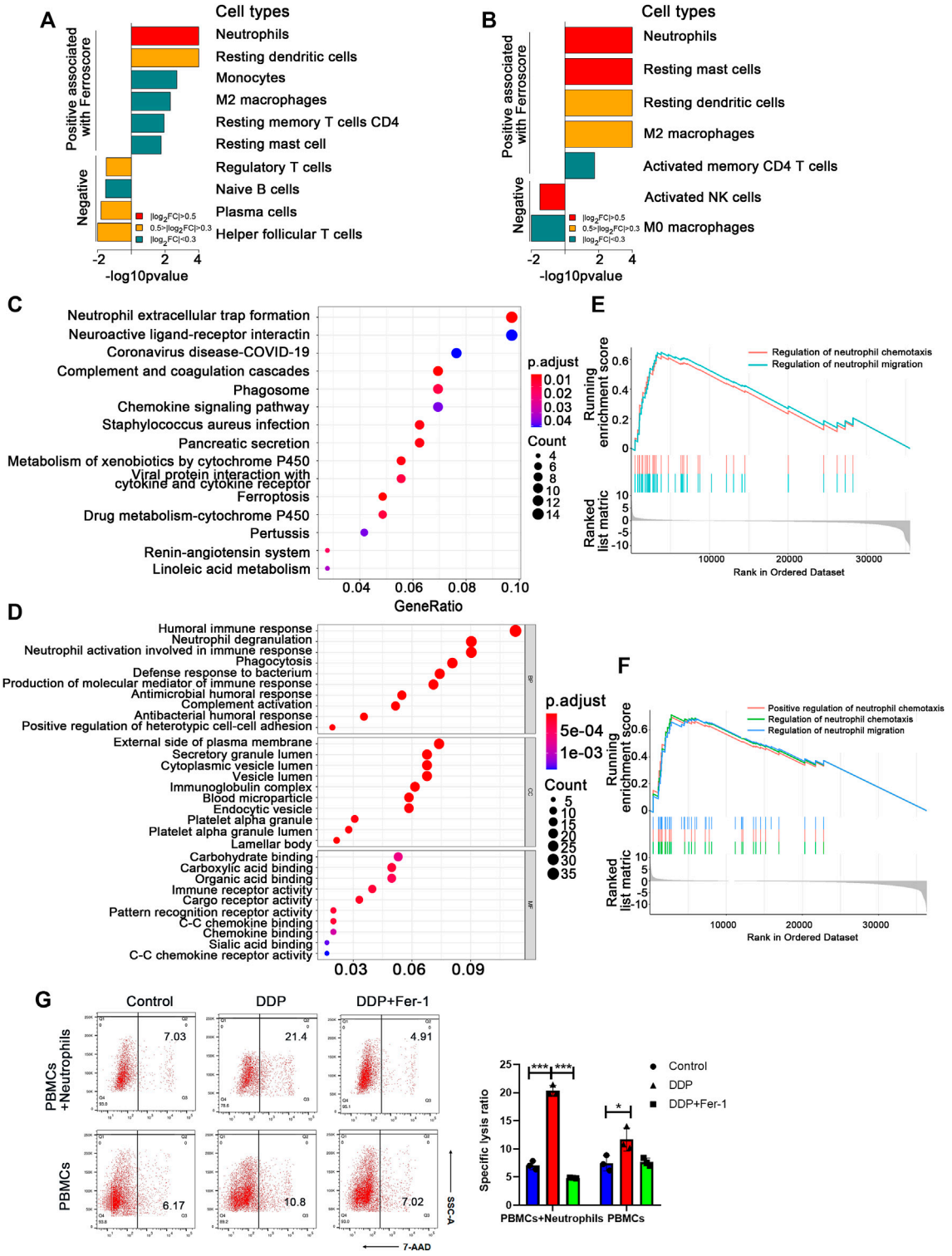

FIGURE 2 | Neutrophil activation pathway was significantly upregulated in the high ferroscore cohort. **(A)** and **(B)** CIBERSORT algorithms analysis showed the cell types, positive and negative, associated with ferroscore in LUSC **(A)** and LUAD **(B)** cohorts (FC: fold change). **(C)** and **(D)** Kyoto Encyclopedia of Genes and Genomes (KEGG) pathway and gene ontology (GO) enrichment analysis of differentially expressed genes between high- and low-ferroscore samples. **(E)** and **(F)** Upregulation of neutrophil migration or chemotaxis-related signature genes in high ferroscore samples relative to low ferroscore samples by gene set enrichment analysis (GSEA) in both LUSC **(E)** and LUAD **(F)** cohort. **(G)** In the presence of neutrophils, DDP pretreatment significantly increased the A549 death ratio, which could be restored by Fer-1. However, DDP pretreatment failed to induce obvious A549 cell death ratio in the absence of neutrophils. $*p < 0.05$, $***p < 0.001$.

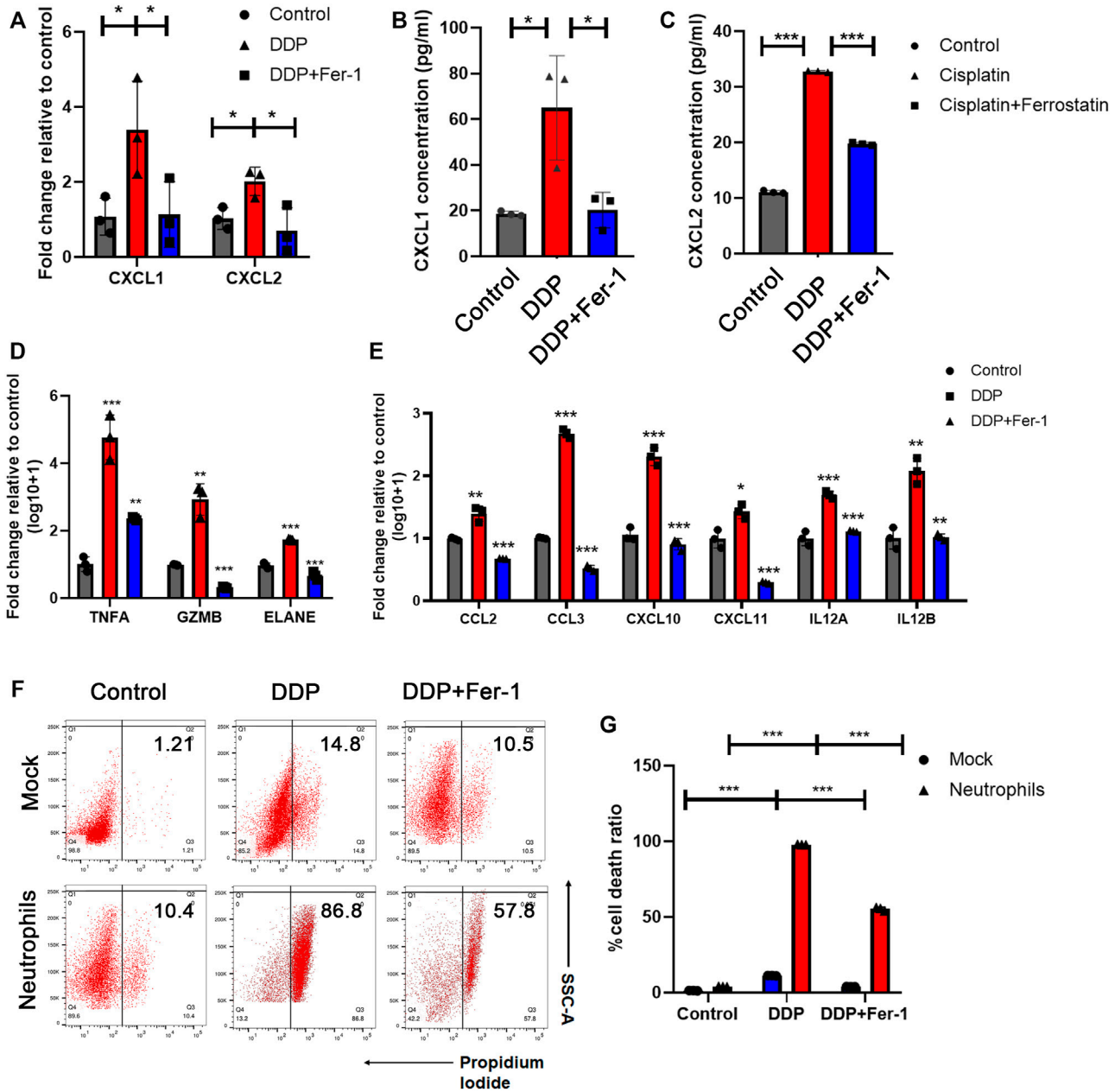

FIGURE 3 | N1-polarized neutrophils induced by cisplatin-mediated tumor ferroptosis exerted an anti-tumor effect. **(A)** Relative mRNA expression of CXCL1 and CXCL2 was tested by RT-qPCR assay in A549 cells treated with 5 μM DDP or rescued by 10 μM ferrostatin-1. **(B)** and **(C)** Concentration of CXCL1 **(B)** and CXCL2 **(C)** released by A549 cells in culture medium, which was tested by ELISA assay. A549 cell were treated with 5 μM DDP or rescued by 10 μM ferrostatin-1. **(D)** and **(E)** Relative mRNA expression of neutrophil cytotoxic markers **(D)** and pro-inflammatory markers **(E)** were tested by RT-qPCR assays in neutrophils co-cultured with A549 cells, which were pretreated with 5 μM DDP or rescued by ferrostatin-1. **(F)** Cell death ratio of A549 cells treated with DDP or rescued by ferrostatin-1 before and after being co-cultured with neutrophils. **(G)** Quantification of data in **(F)**. DDP pretreatment remarkably increases the cytotoxic effect of neutrophils which would be rescued by ferrostatin-1. Bar graphs represent the mean ± SD of indicated samples. $*p < 0.05$, $**p < 0.01$, $***p < 0.001$.

polarization and, thus, enhanced the anti-tumor immune response. In order to validate this assumption, the cytokines for neutrophil recruitment, including CXCL1 and CXCL2 (De Filippo et al., 2013; Paudel et al., 2019), were examined in the cisplatin-treated tumor cells. The RT-qPCR (**Figure 3A**) and ELISA (**Figures 3B,C**) showed that cisplatin-treated A549 cells have higher expression levels of CXCL1 and CXCL2 than the cells without treatment. In addition, the increased RNA and cytokine levels of CXCL1 and CXCL2 could be restored by ferrostatin-1 treatment, suggesting that cisplatin enhanced the expression levels of CXCL1 and CXCL2 expression *via* inducing ferroptosis of tumor cells (**Figures 3A–C**). These findings

supported the idea that cisplatin-mediated tumor cell ferroptosis could recruit neutrophils *via* promoting the expression levels of CXCL1 and CXCL2 in tumor cells.

It has been reported that neutrophils in tumor tissue exhibited an N1/pro-inflammatory phenotype and function as anticancer immune cells (Giese et al., 2019). N1 neutrophils could directly play an anti-tumor role by modulating the expression levels of cytotoxic effectors, including tumor necrosis factor-α (TNF-α) (Balkwill, 2009), granzyme B (GZMB) (Martin et al., 2018), and elastase (ELANE) (Cui et al., 2021). Additionally, N1 neutrophils could be associated with the anti-tumor effects of other immune cells by secreting pro-inflammatory cytokines, such as C-C Motif Chemokine Ligand 2 (CCL2) (Nagarsheth et al., 2017), C-C Motif Chemokine Ligand 3 (CCL3) (Chheda et al., 2016), C-X-C Motif Chemokine Ligand 10 (CXCL10) (Chheda et al., 2016), C-X-C Motif Chemokine Ligand 11 (CXCL11) (Chheda et al., 2016), and interleukin-12 (IL12) (Vignali and Kuchroo, 2012). We attempted to indicate whether cisplatin-mediated tumor cell ferroptosis could induce the anti-tumor pro-inflammatory phenotype of neutrophils. A549 cells were first treated with cisplatin with or without ferrostatin-1 for 8 h. Then, the culture medium was replaced with a fresh medium, and neutrophils were added into the co-culture system for 12 h. We found that cisplatin-pretreated tumor cells stimulate neutrophils which expressed higher levels of cytotoxic effectors, including TNF-α, GZMB, and ELANE (**Figure 3D**), and pro-inflammatory cytokines, such as CCL2, CCL3, CXCL10, CXCL11, and IL12 (**Figure 3E**). However, when tumor cells were pretreated with cisplatin + ferrostatin-1, they could not effectively stimulate neutrophils to express these cytotoxic effectors or pro-inflammatory cytokines (**Figures 3D,E**).

As N1 neutrophils could exert a direct cytotoxic effect on tumor cells (Cui et al., 2021), the cytotoxicity of neutrophils was evaluated by the flow cytometry assay. A549 cells treated with cisplatin showed a moderate cell death, and the presence of ferrostatin-1 partially rescued the cell death (**Figures 3F,G**). When neutrophils were added into the culture system, an overwhelming amount of tumor cell death was observed in the cisplatin treatment group, which could be partially rescued by the presence of ferrostatin-1 (**Figures 3F,G**). The results indicated that cisplatin-mediated tumor cell ferroptosis could recruit neutrophils and boost the pro-inflammatory effects of neutrophils.

3.4 N1-Polarized Neutrophils Induced by Tumor Ferroptosis Promoted T Cell Infiltration and Th1 Differentiation

We found that cisplatin-mediated tumor cell ferroptosis could stimulate the N1-polarized neutrophils. N1-polarized neutrophils could not only directly kill tumor cells but also remodel the TME through pro-inflammatory signals (Eruslanov et al., 2014). We determined whether tumor cell ferroptosis-induced N1-polarized neutrophils could express cytokines to activate T cells for anti-tumor immune response. Chemokines associated with T-cell infiltration were tested on neutrophils that were co-cultured with A549 cells. We found that when neutrophils were co-cultured with cisplatin-pretreated tumor cells, they expressed significantly higher levels of chemokines, such as CXCL9, CXCL10, and CXCL11 (**Figure 4A**), which could be key regulators of recruitment of T cells into tumor tissues (Muller et al., 2010). Consistently, in the ferroscore-H group from TCGA dataset, high expression levels of CX3CR1, CCR5, CXCL9, CXCL10, and CXCL11 were detected (**Figures 4B,C**, **Supplementary Tables S1, S2**), which indicated a higher T-cell infiltration in the TME. Next, the ability of neutrophils to enhance T-cell infiltration was evaluated. A549 cells were pretreated with DDP and then co-cultured with neutrophils. The neutrophils were collected from the co-culture system and seeded into the lower chamber of the transwell system. Calcium-dyed T cells were then seeded into the upper chamber. After 8 h, T cells that moved into the lower chamber were analyzed by flow cytometry, and it was revealed that neutrophils co-cultured with cisplatin-pretreated A549 cells had a stronger potential for T-cell infiltration (**Figures 4D,E**).

In addition to cytokines for T-cell infiltration, we noticed that the levels of IL12A and IL12B were also upregulated in neutrophils that were co-cultured with cisplatin-pretreated A549 cells (**Figure 3E**). IL12A and IL12B are key inducers for the differentiation of naive T cells from Th1 cells (Hsieh et al., 1993). Th1 cells are a subset of helper T cells that have a strong potential to evoke cell-mediated immune response in the TME (Huang et al., 2021). Th1 cell emerged as a new therapeutic target to enhance T-cell infiltration and turning "cold" tumors into "hot" ones. We co-cultured $CD4^+$ T cells sorted by immunomagnetic beads from peripheral blood mononuclear cells (PBMCs) with neutrophils, which were stimulated by ferroptosis A549 cells. RT-qPCR assays demonstrated that CD4+T cells expressed elevated levels of interferon alpha 2 (IFNA2), interferon beta (IFNB), interferon gamma (IFNG), tumor necrosis factor B (TNFB), C-C Motif chemokine receptor 5 (CCR5), and interleukin 2 (IL2) when they were co-cultured with neutrophils that had been co-cultured with cisplatin-pretreated A549 cells (**Figure 4F**). ELISA assay indicated that $CD4^+$ T cells co-cultured with stimulated neutrophils had more IFN-γ secretion (**Figure 4G**), supporting a Th1 differentiation of these T cells. The results mentioned above indicated that cisplatin-treated NSCLC cells could stimulate N1-polarized neutrophils and thus enhanced the T-cell infiltration and Th1 differentiation in the TME to boost the anti-tumor immune response.

Cytotoxic CD8 T lymphocytes (CTL cells) are the most direct and important cell subtype for anti-tumor immunity. Many studies show that the responsiveness of CD8 T cells to tumor cells can be enhanced by neutrophils (Governa et al., 2017; Mysore et al., 2021). Moreover we have revealed that N1 neutrophils have a significant promoting effect on Th1 cells, which play an important role in promoting CTL activation, proliferation, and differentiation into memory T cells (Borst et al., 2018). Therefore, we tested the activation and migration ability of CD8 cells when co-cultured with neutrophils. We constructed a co-culture system of neutrophils and PBMC cells according to the previous method. First, activated neutrophils were placed in the lower transwell chamber, and

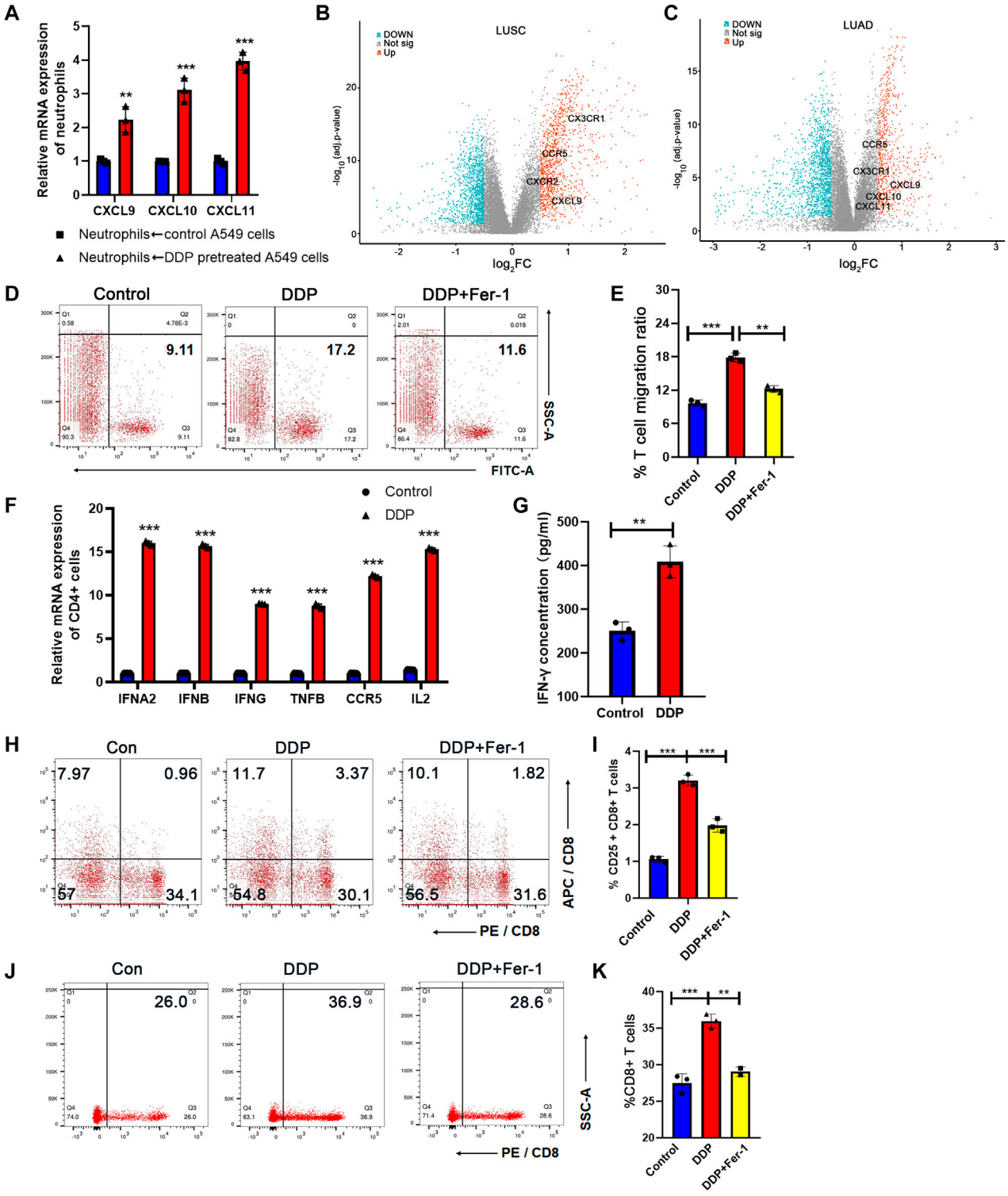

FIGURE 4 | N1-polarized neutrophils induced by tumor ferroptosis promoted T-cell infiltration and Th1 differentiation. **(A)** CXCL9, CXCL10, and CXCL11 mRNA expression levels of neutrophils increase after being co-cultured with DDP-pretreated A549 cells, as measured by RT-qPCR. **(B)** and **(C)** Volcano plot between high- and low-ferroscore groups in LUSC **(B)** and LUAD **(C)** cohorts. Chemokines for T-cell infiltration was highlighted in the plot. **(D)** T-cell migration ratio measured by flow cytometry after being co-cultured in the transwell system with neutrophils. The neutrophils were activated by A549 cells, pretreated with DDP or rescued by ferrostatin-1. **(E)** Quantification of data in **(D)**. **(F)** Markers of Th1 subtypes of CD4-positive T cells were determined by RT-qPCR. The CD4-positive T cells were co-cultured with neutrophils, which are making contact with cisplatin-pretreated A549 cells or ferrostatin-1–rescued A549 cells. **(G)** IFN-γ concentration of CD4-positive T-cell culture medium increased after being co-cultured with neutrophils in the transwell system, measured by ELISA assay. The neutrophils are contacted with cisplatin-pretreated A549 cells or controlled A549 cells. Bar graphs represent the mean ± SD of indicated samples. **(H)** $CD8^+$ T-cell activation measured by flow cytometry after being co-cultured by N1 neutrophils or control neutrophils. **(I)** Quantification of data in **(H)**. **(J)** The proportion of CD8 T cells in the migrated lymphocytes was measured by flow cytometry. **(K)** Quantification of data in **(J)**. $*p < 0.05$, $**p < 0.01$, $***p < 0.001$.

PBMCs were placed in the upper transwell chamber (pore size of 1 μm, to prevent PBMC from entering the lower chamber). CD25 is an important cell surface marker for T-cell activation. After 24 h of co-culture, the proportion of CD8 and CD25 double-positive cells in the upper chamber PBMCs was detected by flow cytometry (**Figures 4H,I**). The results suggested that N1 neutrophiles polarized by tumor cells pretreated with DDP significantly promoted the activation of CD8 cells, while Fer-1 could restore its effect. Next, we used a transwell chamber with a pore size of 5 μm to perform migration assay of CD8 T cells. N1 neutrophiles were placed in the lower chamber. PBMCs were placed in the upper chamber. After 36 h, we used flow cytometry to detect the percentage of CD8 cells in the migrated lymphocytes that entered the lower chamber (**Figures 4J,K**). The results suggested that the percentage of CD8 cells was significantly higher after being attracted by N1 neutrophiles. The above results verify that N1 neutrophils promote the anti-tumor activity of CTLs.

3.5 Cisplatin-Induced Ferroptosis Promoted Efficacy of Immune Checkpoint Inhibitor Therapy *in Vivo*

Clinical trials have shown that different types of lung cancer could benefit from ICI therapy combined with cisplatin-based chemotherapy (Paz-Ares et al., 2020; Rodriguez-Abreu et al., 2021). In order to indicate whether cisplatin-mediated ferroptosis could be involved in synergistic effect of ICI therapy combined with chemotherapy, we attempted to determine whether a ferroptosis inhibitor (ferrostatin-1) could hamper the synergistic efficacy of ICI therapy plus cisplatin in the treatment of Lewis lung carcinoma (LLC) cell lines. C57BL/6 mice were used to inoculate LLC cells. After the tumor cells became palpable, 10 mg/kg cisplatin and 10 mg/kg ferrostatin-1 were administrated intraperitoneally. Then, 8 mg/kg anti-PD1 antibody was injected 3 days later. The tumor growth was significantly inhibited after administration of cisplatin plus anti-PD1 antibody, while cisplatin or PD1 antibody monotherapy showed a moderate anti-tumor efficacy (**Figures 5A,B**, **Supplementary Figures S3A,B**). On the other hand, ferrostatin-1 hampered the synergistic anti-tumor effects of combination of cisplatin and PD1 antibody (**Figures 5A,B**, **Supplementary Figures S3A,B**). After dissection of tumors, tumor cells were isolated, and the ferroptosis status was detected. Flow cytometry showed that cisplatin treatment could effectively induce ferroptosis of tumor cells and ferrostatin-1 would rescue the cisplatin-induced ferroptosis (**Figures 5C–F**). The IHC staining further confirmed that cisplatin treatment increased Ly6 and ICAM1 levels, which presented with N1 neutrophils in the tumors (**Figure 5G**). Additionally, the T-bet level, indicating Th1 cells, was also elevated in the cisplatin treatment group (**Figure 5G**). However, the number of both neutrophils and Th1 cells decreased in the cisplatin plus ferrostatin-1 treatment group compared with the cisplatin treatment group (**Figure 5G**). Collectively, our data suggested that cisplatin-mediated ferroptosis of lung cancer cells could increase neutrophil and Th1 cell enrichment in tumor tissues, thereby promoting the synergistic anti-tumor efficacy of ICI therapy.

3.6 Ferroptosis Induced the Sensitivity of Epidermal Growth Factor Receptor-Mutant Non–Small Cell Lung Cancer to Immunotherapy

The outcomes of clinical trials in the EGFR-mutant NSCLC subgroup showed a generally low response to ICI therapy or ICI therapy plus chemotherapy (Lee et al., 2017). Therefore, there is an urgent need to explore the mechanism of ICI resistance in EGFR-mutant NSCLC. Importantly, neutrophil level in EGFR-mutant NSCLC in TCGA cohort was significantly lower than that in EGFR wild-type cohort, indicating that status of neutrophils could be associated with ICI resistance of EGFR mutant tumors (**Supplementary Figure S4**). Then, A549 cells (EGFR wild-type) and PC9 cells (EGFR-mutant-type with exon 19del) were used to determine whether EGFR mutation could affect cisplatin-induced ferroptosis and the following status of neutrophils. Cisplatin treatment resulted in a higher cell death in A549 cells than in PC9 cells (**Figures 6A,B**). Simultaneously, a noticeably higher lipid peroxidation was observed in A549 cells upon cisplatin treatment than in PC9 cells after cisplatin treatment (**Figures 5C,D**), suggesting a stronger ferroptosis of A549 cells upon cisplatin treatment. On the other hand, RSL3 (a ferroptosis inducer) could further increase ferroptosis of PC9 cells, while it could not additionally increase ferroptosis of A549 cells (**Figures 5A,C**). These results suggested that the cisplatin alone could not effectively induce ferroptosis, whereas its combination with a cisplatin ferroptosis inducer could lead to a high level of ferroptosis in lung cancer cells with EGFR mutation.

Therefore, we hypothesized that EGFR-mutant NSCLC would take advantage from ICI therapy when ferroptosis was induced in tumor tissues. Thus, we pretreated NSCLC cells with cisplatin or cisplatin plus RSL3 to enhance ferroptosis and then co-cultured them with immune cells isolated from the peripheral blood to polarize neutrophils. Subsequently, untreated tumor cells were co-cultured with these neutrophils plus anti-PD1 antibody. We found that immune cells co-cultured with A549 cells pretreated by cisplatin plus RSL3 had a similar efficacy in killing tumor cells to those co-cultured with A549 cells pretreated by cisplatin alone (**Figure 6E**). However, immune cells co-cultured with PC9 cells pretreated by cisplatin plus RSL3 had a higher efficacy in killing tumor cells than those co-cultured with PC9 cells pretreated by cisplatin alone (**Figure 6F**). More importantly, when anti-PD1 antibody was added into the co-culture system, immune cells even showed a higher cytotoxic effect on PC9 cells (**Figure 6F**).

In particular, a few studies (Ma et al., 2021; Xu et al., 2021) have shown that ferroptosis, as a double-edged sword, can dampen anti-tumor immunity by inducing cell death of CD8 T cells. We next wanted to explore the susceptibility of different cells to ferroptosis. We treated A549 cells and different types of immune cells with 5 μM RSL3 for 12 h. The results suggest that tumor cells, compared with immune cells, are more prone to lipid peroxidation (**Supplementary Figures S5A,B**) and cell death

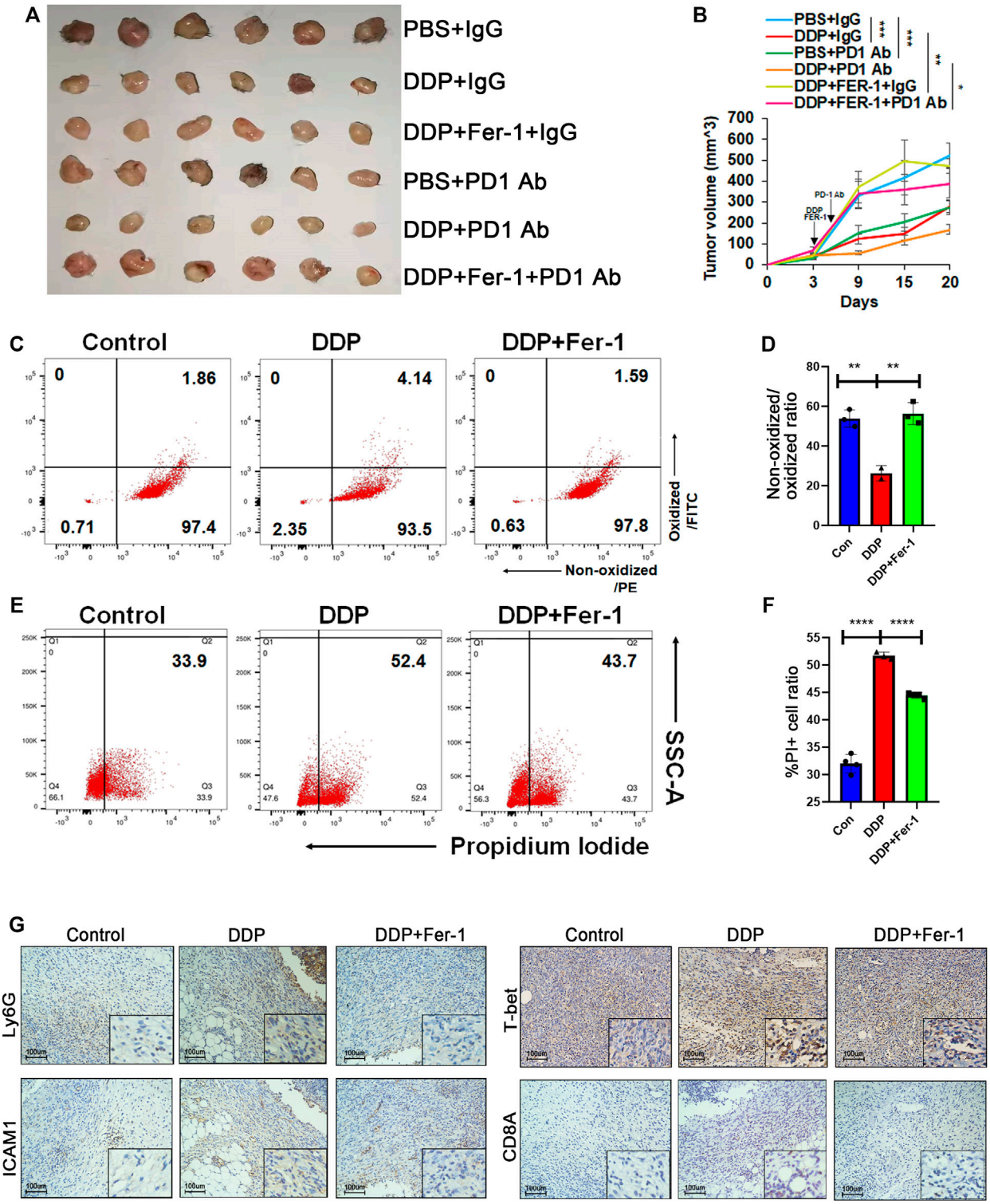

FIGURE 5 | Cisplatin-induced ferroptosis promoted efficacy of ICI therapy *in vivo*. **(A)** and **(B)** Tumor image **(A)** and tumor growth **(B)** of Lewis lung cancer cell (LLC)-bearing C57 mice. When the tumor size was palpable, LLC xenografts were injected with DDP intraperitoneally (5 mg/kg once) and then treated with ferrostatin-1 (10 mg/kg once) or PBS on the same day. Anti-PD1 antibody was injected intraperitoneally the day after DDP or DDP plus ferrostatin-1 administration. Xenografts were harvested 18 days post injection. **(C)** and **(D)** Primary cells were isolated from xenografts 3 days after DDP or DDP plus ferrostatin-1 administration. DDP treatment group showed increased lipid peroxidation while ferrostatin-1 rescued this effect. **(E)** and **(F)** PI staining of primary cells isolated from xenografts indicated that DDP increased cell death ratio while ferrostatin-1 rescued this effect. **(G)** Representative immunohistochemical images of paraffin-embedded xenograft sections. The DDP treatment group showed increased Ly6G and ICAM1 level, which indicated N1 neutrophils. T-bet and CD8A, representing Th1 cells and CD8 T cells, respectively, were also upregulated. Bar graphs represent the mean ± SD of indicated samples. $*p < 0.05$, $**p < 0.01$, $***p < 0.001$.

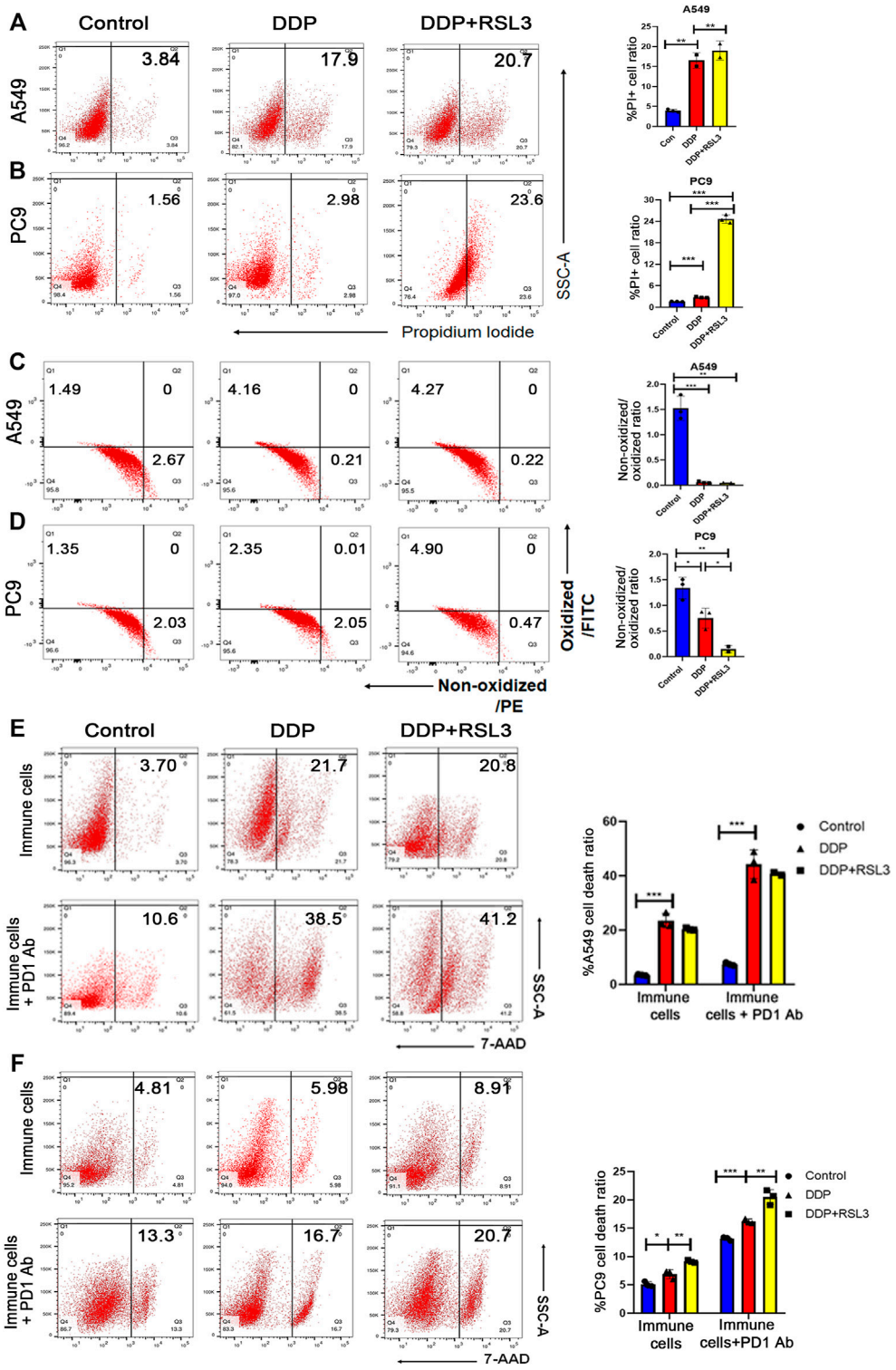

FIGURE 6 | Ferroptosis induced the sensitivity of EGFR-mutant NSCLC to immunotherapy. **(A)** and **(B)** PI staining indicates that more A549 cells die after DDP treatment than PC9 cells. However, DDP plus RSL3 significantly increased cell death ratio in PC9 cells, while RSL3 did not induce a much higher level of cell death in A549 cells. **(C)** and **(D)** Lipid peroxidation assays indicated that A549 cells showed more lipid peroxidation after DDP treatment than PC9 cells. DDP plus RSL3 results in more lipid peroxidation in PC9 cells while RSL3 did not induce much more lipid peroxidation in A549 cells. **(E)** Representative flow cytometry images of A549 cell death ratio in the co-culture system with immune cells. An addition of RSL3 to DDP did not significantly increase cell death level in the co-culture before and after PD1 administration. **(F)** Representative flow cytometry images of PC9 cell death ratio in the co-culture system with immune cells. An addition of RSL3 to DDP significantly increases cell death level in the co-culture before and after PD1 administration. Bar graphs represent the mean ± SD of indicated samples. $*p < 0.05$, $**p < 0.01$, $***p < 0.001$.

(**Supplementary Figures S5C,D**), indicating that tumor cells are the most sensitive to ferroptosis inducers.

Taken together, these results suggested that a ferroptosis inducer could enhance cisplatin-mediated ferroptosis of EGFR-MT NSCLC cells, thereby promoting the anti-tumor immune response of ICI therapy.

4 DISCUSSION

The development of ICIs is revolutionizing cancer treatment (McLaughlin et al., 2020). In most types of cancer, only a minority of patients currently benefit from ICI therapy (Spahn et al., 2020). Intrinsic and acquired resistance to ICIs has stimulated scholars to concentrate on new combination therapies to increase response rates, the depth of remission, and the durability of benefit.

The combination with chemotherapy has proved to be an effective method to enhance immune response of ICIs (Galluzzi et al., 2020). Among the first-line chemo-drugs, cisplatin can kill cancer cells and trigger the release of pro-inflammatory mediators to increase tumor-infiltrating immune cells (Grabosch et al., 2019). The present study went one step forward by describing how cisplatin could induce tumor cell ferroptosis to boost immune response and promote the therapeutic effects of ICIs. According to our study, cisplatin could promote ferroptosis of tumor cells and then enhance the N1 neutrophil polarization. The N1-polarized neutrophils release chemokines to facilitate T-cell infiltration and promote Th1 differentiation in the TME. As the most direct effector of anti-tumor immunity, CD8 T cells are activated under the interaction of N1-type neutrophils or Th1 cells, and their infiltration and proliferation abilities are significantly enhanced.

Ferroptosis is an immunogenic cell death (ICD) (Tang et al., 2020), which is driven by iron accumulation and unrestricted lipid peroxidation (Bertrand, 2017). The interaction between ferroptosis and immunity has been a hot topic since its discovery in 2012. Herein, we found that cisplatin could induce ferroptosis of tumor cells. Ferroptosis could release various damage-associated molecular patterns (DAMPs) or lipid metabolites to regulate the cellular immune response. Our study revealed that cisplatin-mediated cancer cell ferroptosis stimulated cancer cells to release higher levels of cytokines and chemokines for neutrophil recruitment and activation. Additionally, the N1-polarized neutrophils activated by cancer cell ferroptosis showed a stronger anti-tumor potential, which is consistent with the result of a previous study, in which ferroptosis-mediated DAMPs could bind to specific receptors to activate inflammation and start immune cell recruitment of neutrophils and monocytes to initiate a pro-inflammatory TME (Gong et al., 2020).

Studies have shown that radiation therapy (Lhuillier et al., 2019), chemotherapy drugs (Chen and Emens, 2013), and targeted oncogene pathway inhibitors (Sun et al., 2018) could achieve this effect through immunogenic cell death and altered tumor cell biology. In addition to directly promoting the anti-tumor pro-inflammatory phenotype of neutrophils, our findings suggested that the ferroptosis-activated neutrophils could further promote T-cell infiltration *via* secreting CXCL9, CXCL10, and CXCL11 and enhance Th1 differentiation *via* secreting IL12A and IL12B in the TME. Therefore, a "cold" TME would become a "hot" one under the interventions. Our findings further supported that the innate immunity might be a trigger for anti-tumor immunity of the TME. Driver mutations in NSCLC were shown as "cold tumors" (Skoulidis and Heymach, 2019). Therefore, there is an urgent need to develop strategies to turn driver-mutant NSCLC into "hot tumors" *via* increasing the infiltration of tumor antigen-reactive T cells for further effective immunotherapy. The present study revealed that amplification of ferroptosis of NSCLC cells could also enhance the immune response *via* a similar mechanism, suggesting a promising strategy to elevate the sensitivity of ICI therapy to driver mutations in NSCLC.

In this study, *in vitro* experiments showed that the ferroptosis inducer RSL3 mainly caused ferroptosis in tumor cells. This indicated that among various cell subtypes in the TME, tumor cells are more susceptible to ferroptosis. However, we observed that the cell death of lymphocytes also increased after the action of RSL3, although not as much as the increase in the proportion of tumor cells. Tumor cells and T cells have great differences in energy metabolism, redox levels, and maintenance of cell survival. Therefore, how to induce ferroptosis in tumor cells specifically and enhance the anti-tumor immune response of immune cells need further exploration.

In summary, the present study revealed that ferroptosis is a major form of cisplatin-mediated immunogenic cell death, playing a key role in amplifying the immune response of ICI therapy. Moreover, boosting ferroptosis would be a potential method to sensitize driver mutations in NSCLC to ICI therapy.

DATA AVAILABILITY STATEMENT

The original contributions presented in the study are included in the article/**Supplementary Material,** further inquiries can be directed to the corresponding authors.

ETHICS STATEMENT

The animal study was reviewed and approved by the Institutional Animal Care and Use Committee, Sun Yat-Sen University. Written informed consent was obtained from the owners for the participation of their animals in this study.

AUTHOR CONTRIBUTIONS

ZZ: conceptualization, methodology, formal analysis, investigation, writing, and visualization. YZ: conceptualization, data analysis, resources, and writing. SC: software, formal analysis, and methodology. SL: methodology, software, formal analysis, and validation. XL: validation,

supervision, data curation, and funding acquisition. HH: conceptualization, supervision, project administration, and funding acquisition.

FUNDING

This work was supported by grants from the Natural Science Foundation of China (82002823, 82025026, and 81730077) and the Program from Guangdong Basic and Applied Basic Research Foundation (2019A1515110082).

SUPPLEMENTARY MATERIAL

The Supplementary Material for this article can be found online at: https://www.frontiersin.org/articles/10.3389/fphar.2022.870178/full#supplementary-material

REFERENCES

Apetoh, L., Ladoire, S., Coukos, G., and Ghiringhelli, F. (2015). Combining Immunotherapy and Anticancer Agents: the Right Path to Achieve Cancer Cure? *Ann. Oncol.* 26 (9), 1813–1823. doi:10.1093/annonc/mdv209

Aran, D., Hu, Z., and Butte, A. J. (2017). xCell: Digitally Portraying the Tissue Cellular Heterogeneity Landscape. *Genome Biol.* 18 (1), 220. doi:10.1186/s13059-017-1349-1

Balkwill, F. (2009). Tumour Necrosis Factor and Cancer. *Nat. Rev. Cancer* 9 (5), 361–371. doi:10.1038/nrc2628

Bertrand, R. L. (2017). Iron Accumulation, Glutathione Depletion, and Lipid Peroxidation Must Occur Simultaneously during Ferroptosis and Are Mutually Amplifying Events. *Med. Hypotheses* 101, 69–74. doi:10.1016/j.mehy.2017.02.017

Borst, J., Ahrends, T., Bąbała, N., Melief, C. J. M., and Kastenmüller, W. (2018). $CD4^+$ T Cell Help in Cancer Immunology and Immunotherapy. *Nat. Rev. Immunol.* 18 (10), 635–647. doi:10.1038/s41577-018-0044-0

Chen, G., and Emens, L. A. (2013). Chemoimmunotherapy: Reengineering Tumor Immunity. *Cancer Immunol. Immunother.* 62 (2), 203–216. doi:10.1007/s00262-012-1388-0

Chheda, Z. S., Sharma, R. K., Jala, V. R., Luster, A. D., and Haribabu, B. (2016). Chemoattractant Receptors BLT1 and CXCR3 Regulate Antitumor Immunity by Facilitating $CD8^+$ T Cell Migration into Tumors. *J. Immunol.* 197 (5), 2016–2026. doi:10.4049/jimmunol.1502376

Cui, C., Chakraborty, K., Tang, X. A., Zhou, G., Schoenfelt, K. Q., Becker, K. M., et al. (2021). Neutrophil Elastase Selectively Kills Cancer Cells and Attenuates Tumorigenesis. *Cell* 184 (12), 3163–e21. doi:10.1016/j.cell.2021.04.016

De Filippo, K., Dudeck, A., Hasenberg, M., Nye, E., van Rooijen, N., Hartmann, K., et al. (2013). Mast Cell and Macrophage Chemokines CXCL1/CXCL2 Control the Early Stage of Neutrophil Recruitment during Tissue Inflammation. *Blood* 121 (24), 4930–4937. doi:10.1182/blood-2013-02-486217

Dong, Z. Y., Zhang, J. T., Liu, S. Y., Su, J., Zhang, C., Xie, Z., et al. (2017). EGFR Mutation Correlates with Uninflamed Phenotype and Weak Immunogenicity, Causing Impaired Response to PD-1 Blockade in Non-small Cell Lung Cancer. *Oncoimmunology* 6 (11), e1356145. doi:10.1080/2162402X.2017.1356145

Emens, L. A., Molinero, L., Loi, S., Rugo, H. S., Schneeweiss, A., Diéras, V., et al. (2021). Atezolizumab and Nab-Paclitaxel in Advanced Triple-Negative Breast Cancer: Biomarker Evaluation of the IMpassion130 Study. *J. Natl. Cancer Inst.* 113 (8), 1005–1016. doi:10.1093/jnci/djab004

Eruslanov, E. B., Bhojnagarwala, P. S., Quatromoni, J. G., Stephen, T. L., Ranganathan, A., Deshpande, C., et al. (2014). Tumor-associated Neutrophils Stimulate T Cell Responses in Early-Stage Human Lung Cancer. *J. Clin. Invest.* 124 (12), 5466–5480. doi:10.1172/JCI77053

Feng, Y., Renshaw, S., and Martin, P. (2012). Live Imaging of Tumor Initiation in Zebrafish Larvae Reveals a Trophic Role for Leukocyte-Derived PGE_2. *Curr. Biol.* 22 (13), 1253–1259. doi:10.1016/j.cub.2012.05.010

Galluzzi, L., Humeau, J., Buqué, A., Zitvogel, L., and Kroemer, G. (2020). Immunostimulation with Chemotherapy in the Era of Immune Checkpoint Inhibitors. *Nat. Rev. Clin. Oncol.* 17 (12), 725–741. doi:10.1038/s41571-020-0413-z

Gandhi, L., Rodríguez-Abreu, D., Gadgeel, S., Esteban, E., Felip, E., De Angelis, F., et al. (2018). Pembrolizumab Plus Chemotherapy in Metastatic Non-small-cell Lung Cancer. *N. Engl. J. Med.* 378 (22), 2078–2092. doi:10.1056/NEJMoa1801005

Giese, M. A., Hind, L. E., and Huttenlocher, A. (2019). Neutrophil Plasticity in the Tumor Microenvironment. *Blood* 133 (20), 2159–2167. doi:10.1182/blood-2018-11-844548

Global Burden of Disease Cancer, C., Fitzmaurice, C., Akinyemiju, T. F., Al Lami, F. H., Alam, T., Alizadeh-Navaei, R., et al. (2018). Global, Regional, and National Cancer Incidence, Mortality, Years of Life Lost, Years Lived with Disability, and Disability-Adjusted Life-Years for 29 Cancer Groups, 1990 to 2016: A Systematic Analysis for the Global Burden of Disease Study. *JAMA Oncol.* 4 (11), 1553–1568. doi:10.1001/jamaoncol.2018.2706

Gong, T., Liu, L., Jiang, W., and Zhou, R. (2020). DAMP-sensing Receptors in Sterile Inflammation and Inflammatory Diseases. *Nat. Rev. Immunol.* 20 (2), 95–112. doi:10.1038/s41577-019-0215-7

Governa, V., Trella, E., Mele, V., Tornillo, L., Amicarella, F., Cremonesi, E., et al. (2017). The Interplay between Neutrophils and $CD8^+$ T Cells Improves Survival in Human Colorectal Cancer. *Clin. Cancer Res.* 23 (14), 3847–3858. doi:10.1158/1078-0432.CCR-16-2047

Grabosch, S., Bulatovic, M., Zeng, F., Ma, T., Zhang, L., Ross, M., et al. (2019). Cisplatin-induced Immune Modulation in Ovarian Cancer Mouse Models with Distinct Inflammation Profiles. *Oncogene* 38 (13), 2380–2393. doi:10.1038/s41388-018-0581-9

Hanahan, D., and Weinberg, R. A. (2011). Hallmarks of Cancer: the Next Generation. *Cell* 144 (5), 646–674. doi:10.1016/j.cell.2011.02.013

Hänzelmann, S., Castelo, R., and Guinney, J. (2013). GSVA: Gene Set Variation Analysis for Microarray and RNA-Seq Data. *BMC Bioinformatics* 14, 7. doi:10.1186/1471-2105-14-7

Hassannia, B., Vandenabeele, P., and Vanden Berghe, T. (2019). Targeting Ferroptosis to Iron Out Cancer. *Cancer Cell* 35 (6), 830–849. doi:10.1016/j.ccell.2019.04.002

Hsieh, C. S., Macatonia, S. E., Tripp, C. S., Wolf, S. F., O'Garra, A., and Murphy, K. M. (1993). Development of TH1 CD4+ T Cells through IL-12 Produced by Listeria-Induced Macrophages. *Science* 260 (5107), 547–549. doi:10.1126/science.8097338

Huang, D., Chen, X., Zeng, X., Lao, L., Li, J., Xing, Y., et al. (2021). Targeting Regulator of G Protein Signaling 1 in Tumor-specific T Cells Enhances Their Trafficking to Breast Cancer. *Nat. Immunol.* 22 (7), 865–879. doi:10.1038/s41590-021-00939-9

Langer, C. J., Gadgeel, S. M., Borghaei, H., Papadimitrakopoulou, V. A., Patnaik, A., Powell, S. F., et al. (2016). Carboplatin and Pemetrexed with or without Pembrolizumab for Advanced, Non-squamous Non-small-cell Lung Cancer: a Randomised, Phase 2 Cohort of the Open-Label KEYNOTE-021 Study. *Lancet Oncol.* 17 (11), 1497–1508. doi:10.1016/S1470-2045(16)30498-3

Lee, C. K., Man, J., Lord, S., Links, M., Gebski, V., Mok, T., et al. (2017). Checkpoint Inhibitors in Metastatic EGFR-Mutated Non-small Cell Lung Cancer-A Meta-Analysis. *J. Thorac. Oncol.* 12 (2), 403–407. doi:10.1016/j.jtho.2016.10.007

Lhuillier, C., Rudqvist, N. P., Elemento, O., Formenti, S. C., and Demaria, S. (2019). Radiation Therapy and Anti-tumor Immunity: Exposing Immunogenic Mutations to the Immune System. *Genome Med.* 11 (1), 40. doi:10.1186/s13073-019-0653-7

Ma, X., Xiao, L., Liu, L., Ye, L., Su, P., Bi, E., et al. (2021). CD36-mediated Ferroptosis Dampens Intratumoral $CD8^+$ T Cell Effector Function and Impairs Their Antitumor Ability. *Cell Metab* 33 (5), 1001–e5. doi:10.1016/j.cmet.2021.02.015

Malvezzi, M., Bertuccio, P., Levi, F., La Vecchia, C., and Negri, E. (2012). European Cancer Mortality Predictions for the Year 2012. *Ann. Oncol.* 23 (4), 1044–1052. doi:10.1093/annonc/mds024

Martin, A., Seignez, C., Racoeur, C., Isambert, N., Mabrouk, N., Scagliarini, A., et al. (2018). Tumor-derived Granzyme B-Expressing Neutrophils Acquire Antitumor Potential after Lipid A Treatment. *Oncotarget* 9 (47), 28364–28378. doi:10.18632/oncotarget.25342

Mathew, M., Enzler, T., Shu, C. A., and Rizvi, N. A. (2018). Combining Chemotherapy with PD-1 Blockade in NSCLC. *Pharmacol. Ther.* 186, 130–137. doi:10.1016/j.pharmthera.2018.01.003

McLaughlin, M., Patin, E. C., Pedersen, M., Wilkins, A., Dillon, M. T., Melcher, A. A., et al. (2020). Inflammatory Microenvironment Remodelling by Tumour Cells after Radiotherapy. *Nat. Rev. Cancer* 20 (4), 203–217. doi:10.1038/s41568-020-0246-1

Müller, M., Carter, S., Hofer, M. J., and Campbell, I. L. (2010). Review: The Chemokine Receptor $CXCR_3$ and its Ligands $CXCL_9$, $CXCL_{10}$ and $CXCL_{11}$ in Neuroimmunity-Aa Tale of Conflict and Conundrum. *Neuropathol. Appl. Neurobiol.* 36 (5), 368–387. doi:10.1111/j.1365-2990.2010.01089.x

Mysore, V., Cullere, X., Mears, J., Rosetti, F., Okubo, K., Liew, P. X., et al. (2021). FcγR Engagement Reprograms Neutrophils into Antigen Cross-Presenting Cells that Elicit Acquired Anti-tumor Immunity. *Nat. Commun.* 12 (1), 4791. doi:10.1038/s41467-021-24591-x

Nagarsheth, N., Wicha, M. S., and Zou, W. (2017). Chemokines in the Cancer Microenvironment and Their Relevance in Cancer Immunotherapy. *Nat. Rev. Immunol.* 17 (9), 559–572. doi:10.1038/nri.2017.49

Newman, A. M., Liu, C. L., Green, M. R., Gentles, A. J., Feng, W., Xu, Y., et al. (2015). Robust Enumeration of Cell Subsets from Tissue Expression Profiles. *Nat. Methods* 12 (5), 453–457. doi:10.1038/nmeth.3337

Paudel, S., Baral, P., Ghimire, L., Bergeron, S., Jin, L., DeCorte, J. A., et al. (2019). CXCL1 Regulates Neutrophil Homeostasis in Pneumonia-Derived Sepsis Caused by Streptococcus Pneumoniae Serotype 3. *Blood* 133 (12), 1335–1345. doi:10.1182/blood-2018-10-878082

Paz-Ares, L., Vicente, D., Tafreshi, A., Robinson, A., Soto Parra, H., Mazières, J., et al. (2020). A Randomized, Placebo-Controlled Trial of Pembrolizumab Plus Chemotherapy in Patients with Metastatic Squamous NSCLC: Protocol-Specified Final Analysis of KEYNOTE-407. *J. Thorac. Oncol.* 15 (10), 1657–1669. doi:10.1016/j.jtho.2020.06.015

Pfirschke, C., Engblom, C., Rickelt, S., Cortez-Retamozo, V., Garris, C., Pucci, F., et al. (2016). Immunogenic Chemotherapy Sensitizes Tumors to Checkpoint Blockade Therapy. *Immunity* 44 (2), 343–354. doi:10.1016/j.immuni.2015.11.024

Ritchie, M. E., Phipson, B., Wu, D., Hu, Y., Law, C. W., Shi, W., et al. (2015). Limma powers Differential Expression Analyses for RNA-Sequencing and Microarray Studies. *Nucleic Acids Res.* 43 (7), e47. doi:10.1093/nar/gkv007

Rizvi, N. A., Hellmann, M. D., Snyder, A., Kvistborg, P., Makarov, V., Havel, J. J., et al. (2015). Cancer Immunology. Mutational Landscape Determines Sensitivity to PD-1 Blockade in Non-small Cell Lung Cancer. *Science* 348 (6230), 124–128. doi:10.1126/science.aaa1348

Rodríguez-Abreu, D., Powell, S. F., Hochmair, M. J., Gadgeel, S., Esteban, E., Felip, E., et al. (2021). Pemetrexed Plus Platinum with or without Pembrolizumab in Patients with Previously Untreated Metastatic Nonsquamous NSCLC: Protocol-Specified Final Analysis from KEYNOTE-189. *Ann. Oncol.* 32 (7), 881–895. doi:10.1016/j.annonc.2021.04.008

Skoulidis, F., and Heymach, J. V. (2019). Co-occurring Genomic Alterations in Non-small-cell Lung Cancer Biology and Therapy. *Nat. Rev. Cancer* 19 (9), 495–509. doi:10.1038/s41568-019-0179-8

Spahn, S., Roessler, D., Pompilia, R., Gabernet, G., Gladstone, B. P., Horger, M., et al. (2020). Clinical and Genetic Tumor Characteristics of Responding and Non-responding Patients to PD-1 Inhibition in Hepatocellular Carcinoma. *Cancers (Basel)* 12 (12), 3830. doi:10.3390/cancers12123830

Subramanian, A., Tamayo, P., Mootha, V. K., Mukherjee, S., Ebert, B. L., Gillette, M. A., et al. (2005). Gene Set Enrichment Analysis: a Knowledge-Based Approach for Interpreting Genome-wide Expression Profiles. *Proc. Natl. Acad. Sci. U S A.* 102 (43), 15545–15550. doi:10.1073/pnas.0506580102

Sun, Z., Fu, Y. X., and Peng, H. (2018). Targeting Tumor Cells with Antibodies Enhances Anti-tumor Immunity. *Biophys. Rep.* 4 (5), 243–253. doi:10.1007/s41048-018-0070-2

Tang, R., Xu, J., Zhang, B., Liu, J., Liang, C., Hua, J., et al. (2020). Ferroptosis, Necroptosis, and Pyroptosis in Anticancer Immunity. *J. Hematol. Oncol.* 13 (1), 110. doi:10.1186/s13045-020-00946-7

Verhaak, R. G., Hoadley, K. A., Purdom, E., Wang, V., Qi, Y., Wilkerson, M. D., et al. (2010). Integrated Genomic Analysis Identifies Clinically Relevant Subtypes of Glioblastoma Characterized by Abnormalities in PDGFRA, IDH1, EGFR, and NF1. *Cancer Cell* 17 (1), 98–110. doi:10.1016/j.ccr.2009.12.020

Vignali, D. A., and Kuchroo, V. K. (2012). IL-12 Family Cytokines: Immunological Playmakers. *Nat. Immunol.* 13 (8), 722–728. doi:10.1038/ni.2366

Wang, Y., Gao, W., Shi, X., Ding, J., Liu, W., He, H., et al. (2017). Chemotherapy Drugs Induce Pyroptosis through Caspase-3 Cleavage of a Gasdermin. *Nature* 547 (7661), 99–103. doi:10.1038/nature22393

Xu, S., Chaudhary, O., Rodríguez-Morales, P., Sun, X., Chen, D., Zappasodi, R., et al. (2021). Uptake of Oxidized Lipids by the Scavenger Receptor CD36 Promotes Lipid Peroxidation and Dysfunction in $CD8^+$ T Cells in Tumors. *Immunity* 54 (7), 1561–e7. doi:10.1016/j.immuni.2021.05.003

Zhang, C. C., Li, C. G., Wang, Y. F., Xu, L. H., He, X. H., Zeng, Q. Z., et al. (2019a). Chemotherapeutic Paclitaxel and Cisplatin Differentially Induce Pyroptosis in A549 Lung Cancer Cells *via* Caspase-3/GSDME Activation. *Apoptosis* 24 (3-4), 312–325. doi:10.1007/s10495-019-01515-1

Zhang, M., Zhu, K., Pu, H., Wang, Z., Zhao, H., Zhang, J., et al. (2019b). An Immune-Related Signature Predicts Survival in Patients with Lung Adenocarcinoma. *Front. Oncol.* 9, 1314. doi:10.3389/fonc.2019.01314

Zhang, X., Sui, S., Wang, L., Li, H., Zhang, L., Xu, S., et al. (2020). Inhibition of Tumor Propellant Glutathione Peroxidase 4 Induces Ferroptosis in Cancer Cells and Enhances Anticancer Effect of Cisplatin. *J. Cel Physiol* 235 (4), 3425–3437. doi:10.1002/jcp.29232

Conflict of Interest: The authors declare that the research was conducted in the absence of any commercial or financial relationships that could be construed as a potential conflict of interest.

Publisher's Note: All claims expressed in this article are solely those of the authors and do not necessarily represent those of their affiliated organizations, or those of the publisher, the editors, and the reviewers. Any product that may be evaluated in this article, or claim that may be made by its manufacturer, is not guaranteed or endorsed by the publisher.

GLOSSARY

ALK anaplastic lymphoma kinase
ATCC American type culture collection
BLCA bladder urothelial carcinoma
BRCA breast invasive carcinoma
CCL2 C-C motif chemokine ligand 2
CCL3 C-C motif chemokine ligand 3
CCR5 C-C motif chemokine receptor 5
CXCL1 C-X-C motif chemokine ligand 1
CXCL2 C-X-C motif chemokine ligand 2
CXCL10 C-X-C motif chemokine ligand 10
CXCL11 C-X-C motif chemokine ligand 11
DAMPs damage-associated molecular patterns
DDP cisplatin
DEG differentially expressed gene
EGFR epidermal growth factor receptor
ELANE elastase
ELISA enzyme-linked immunosorbent assay
ESCA esophageal carcinoma
FDR false discovery rate
GDC Genomic Data Commons
GO gene ontology
GSEA gene set enrichment analysis
GZMB granzyme B
HNSCC head and neck squamous cell carcinoma
ICD immunogenic cell death
ICIs immune checkpoint inhibitors
IFNA2 interferon alpha 2
IFNB interferon beta
IFN-γ interferon gamma
IHC immunohistochemistry
IL2 interleukin 2
IL12 interleukin-12
KEGG Kyoto Encyclopedia of Genes and Genomes
LLC Lewis lung carcinoma
LUAD lung adenocarcinoma
LUSC lung squamous cell carcinoma
MACS magnetic activated cell sorting
NSCLC non–small cell lung cancer
PBMCs peripheral blood mononuclear cells
PD-1 programmed cell death protein 1
RT-qPCR quantitative reverse transcription polymerase chain reaction
ssGSEA single sample gene set enrichment analysis
TCGA The Cancer Genome Atlas
TIME tumor immune microenvironment
TME tumor microenvironment
TNF-α tumor necrosis factor-α
TNFB tumor necrosis factor B

frontiers | Frontiers in Pharmacology

REVIEW
published: 17 June 2022
doi: 10.3389/fphar.2022.905501

The Organelle-Specific Regulations and Epigenetic Regulators in Ferroptosis

Yixuan Zhang[1], *Mingrui Li*[1], *Yiming Guo*[1], *Shuang Liu*[2] *and Yongguang Tao*[1,3,4,5]*

[1]*Hunan Key Laboratory of Cancer Metabolism, Hunan Cancer Hospital and The Affiliated Cancer Hospital of Xiangya School of Medicine, Central South University, Changsha, China,* [2]*Department of Oncology, Institute of Medical Sciences, National Clinical Research Center for Geriatric Disorders, Xiangya Hospital, Central South University, Changsha, China,* [3]*NHC Key Laboratory of Carcinogenesis, Cancer Research Institute and School of Basic Medicine, Central South University, Changsha, China,* [4]*Key Laboratory of Carcinogenesis and Cancer Invasion, Ministry of Education, Department of Pathology, Xiangya Hospital, School of Basic Medicine, Central South University, Changsha, China,* [5]*Hunan Key Laboratory of Early Diagnosis and Precision Therapy in Lung Cancer, Department of Thoracic Surgery, Second Xiangya Hospital, Central South University, Changsha, China*

Ferroptosis is fairly different from other types of cell-death in biochemical processes, morphological changes and genetics as a special programmed cell-death. Here we summarize the current literatures on ferroptosis, including the cascade reaction of key material metabolism in the process, dysfunction of organelles, the relationship between different organelles and the way positive and negative key regulatory factors to affect ferroptosis in the epigenetic level. Based on material metabolism or epigenetic regulation, it is obvious that the regulatory network of ferroptosis is interrelated and complex.

Keywords: ferroptosis, epigenetics, cancer, organelles, post-translational modification, metabolism

OPEN ACCESS

Edited by:
Jiaoti Huang,
Duke University, United States

Reviewed by:
Charareh Pourzand,
University of Bath, United Kingdom
Cheng Qiu,
Shandong University, China

***Correspondence:**
Yongguang Tao
taoyong@csu.edu.cn

Specialty section:
This article was submitted to Pharmacology of Anti-Cancer Drugs, a section of the journal Frontiers in Pharmacology

Received: *27 March 2022*
Accepted: *26 May 2022*
Published: *17 June 2022*

Citation:
Zhang Y, Li M, Guo Y, Liu S and Tao Y (2022) The Organelle-Specific Regulations and Epigenetic Regulators in Ferroptosis. Front. Pharmacol. 13:905501. doi: 10.3389/fphar.2022.905501

1 INTRODUCTION

Cell death is the universal outcome of cells. In the 1970s, cell death was segmented into apoptosis (type I), autophagy (type II) and necrosis (type III) on the basis of the early classification of cell morphology (Kroemer et al., 2005). In 2012, The Nomenclature Committee on Cell Death (NCCD) recommended molecular events in the death process replace cell morphology as a defining distinction (Kroemer et al., 2005). Compared with type III cell necrosis, the death process of type I and II is more orderly and complexly regulated. After the concept of programmed death was put forward, apoptosis and programmed death are often regarded as the same way. However, nowadays, people have gradually discovered that programmed death also includes some different death modes that do not rely on caspase like apoptosis, including ferroptosis. Ferroptosis was formally come up in 2012, used to describe RSLs-induced programmed cell death different from apoptosis (Dixon et al., 2012), depending on the iron and characterized by the reactive oxygen species (ROS) accumulating (Li et al., 2020). Different from necroptosis mediated by the combination of death receptor and death receptor ligand (Liu X. et al., 2021), the key central links of ferroptosis are iron-overload and ROS accumulation. First, the iron accumulating. Iron metabolism disorder causes Fenton reaction in cells, and then produces a mass of reactive oxygen species. The second stage is the imbalance of antioxidant system induced by the increasing of ROS (Leng et al., 2021). For such a new type of cell death that has many differences from the traditional way of death in biochemical metabolism and the morphology, how ferroptosis is triggered, how ferroptosis is inhibited, and the relation between ferroptosis and others are being explored (Cao and Dixon, 2016). As regard to ferroptosis, we will discuss and summarize its metabolic regulatory pathways, and how to affect the functional structure of organelles, its important key regulatory factors and epigenetic regulation pathways.

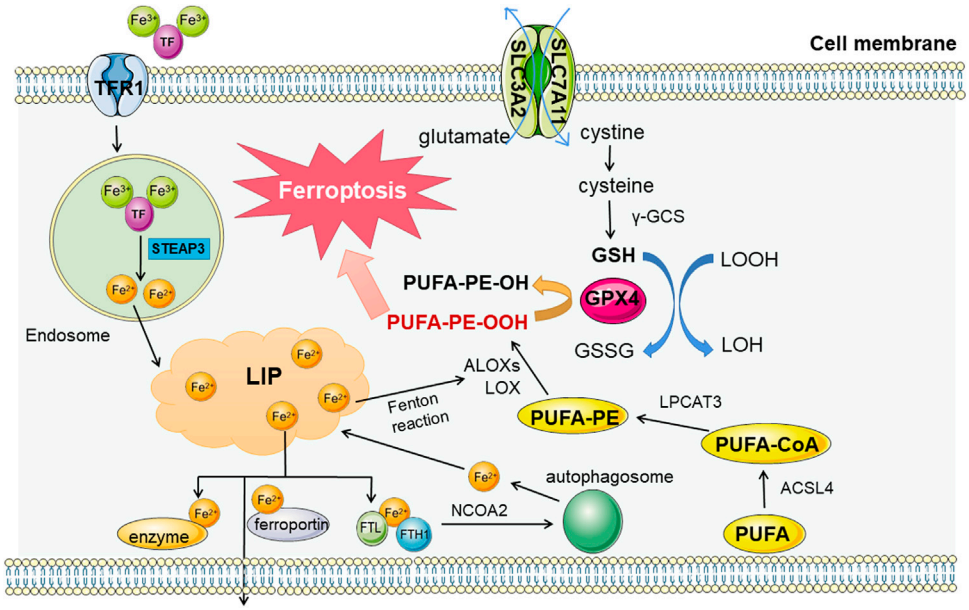

FIGURE 1 | Regulation pathways in ferroptosis. There are three main metabolic pathways related to ferroptosis, iron metabolism, lipid metabolism and amino acid metabolism. The first two metabolites mainly promote the occurrence of ferroptosis, while the metabolites of amino acids (taking cysteine as an example) mainly play a role in resisting material peroxidation and ferroptosis. Fe^{3+} enters the cell through transferrin receptor 1 (TFR1) and is reduced to Fe^{2+} in lysosome. After entering the free iron pool, it can promote the formation and destruction of lipid peroxides, and hinder the removal of iron (including synthase, expelling and binding to ferritin storage) can lead to the overload of free iron. In addition, lipid peroxidation products are affected by Acyl-CoA synthetase long-chain family member 4 (ACSL4), lysophosphatidylcholine acyltransferase 3 (LPCAT3), Arachidonic acid lipoxygenases (ALOXS) and other enzymes, and are also catalyzed by Fe2+ Fenton reaction. Lipid peroxides produced have a central position in the process of ferroptosis. As a representative of antioxidant capacity, cysteine metabolic pathway can reduce lipid peroxides by Reduced glutathione (GSH). The coordination of the three maintain the stability of the internal environment, and the collapse of the balance will lead to the cascade reaction of ferroptosis.

2 REGULATION OF METABOLIC PATHWAYS IN FERROPTOSIS

2.1 Iron Metabolism

In vivo, iron is a vital metal element which is involved in biosynthesis and enzymatic reaction. Iron in human body is often divided into two types, functional iron (such as hemoglobin iron, transferrin iron) and stored iron (such as ferritin, hemosiderin). Firstly, Fe^{2+} is usually the initial way that enters into vivo, and is absorbed in the small intestine. After being oxidized by ceruloplasmin, it becomes Fe^{3+} iron that is easy to transport and binds to intracellular transferrin (TF) (Fuqua et al., 2012) to form TF-$[Fe^{3+}]_2$-TFR1, which is swallowed into the cells through the transferrin receptor 1 (TFR1) on the cell membrane. In the cells, TF-$[Fe^{3+}]_2$-TFR1 was reduced by iron reductase six-transmembrane epithelial antigen of prostate 3 (STEAP3) in lysosomes, and gathered in the intracellular labile iron pool (LIP) through the divalent metal transporter 1 (DMT1) (Torti and Torti, 2013). Then, Fe^{2+} can participate in different physiological processes, like the formation of functional enzymes, binding to ferritin temporarily stored, or through ferroportin discharged cells back to the blood medium (Chen J. et al., 2022).

Iron metabolic abnormalities *in vivo* is mainly due to abnormal iron input and discharge obstacles, triggering free iron accumulation in LIP. Then it leads Fenton reaction to generate lots of ROS, inducing ferroptosis (Liu J. et al., 2021). Ferroptosis inducers erastin or RSL3 can inhibit the antioxidant system and induce ferroptosis by promoting iron accumulation, and a variety of components mediating iron transport and utilization have been confirmed to affect the process of ferroptosis through regulation (**Figure 1**).

At the same time, as a storage unit, ferritin can also be degraded by autophagy mediated by nuclear receptor coactivator 4 (NCOA4), leading to the substantial increase in free iron (Hou et al., 2016) and subsequent cascade reactions. And the sensitivity to ferroptosis reflected in the earliest RAS-deficient cells of concern is also related to the subunits of ferroptosis (Yang and Stockwell, 2008).

2.2 Lipid Metabolism

Another important link of ferroptosis is lipid peroxidation. The Fenton reaction induced by iron overload can cause a large amount of ROS accumulation, and the free radicals in ROS can react with intracellular lipids to obtain a hydrogen atom from the allyl carbon in the lipid structure, forming lipid peroxide (ROOH) and generating a new free radical concurrently, and continuously circulating (Gaschler and Stockwell, 2017). In this process, the continuously-generated lipid peroxides are toxic, reflecting in two aspects-one is the destruction of biofilm. As an important component of the membrane, after lipid

peroxidation, the membrane's physical properties as a biofilm and cell recognition function will be affected (Catalá and Díaz, 2016), resulting in a series of physiological disorders of cells. On the other hand, lipid peroxide itself and its degradation products are also toxic (Kappus, 1987). Lipidomics has proved that polyunsaturated fatty acids (PUFA) can be preferentially oxidized by lipid peroxides, and this feature gives PUFA an important position in lipid metabolism related to ferroptosis. And similarly, the supplementation of PUFA can delay the ferroptosis process to a certain extent (Yang et al., 2016). This also shows to some extent that the content of PUFA can affect the degree of lipid peroxidation and determine the sensitivity of cells to ferroptosis (Magtanong et al., 2019).

Arachidonic acid (AA) and adrenaline (AdA), ω-6 fatty acids, are also the PUFAs most prone to lipid peroxidation (Tarangelo and Dixon, 2019). AA/AdA is converted into PUFA-CoA after acyl-CoA synthetase long-chain family member 4 (ACSL4) is added with an acyl group, and then it is converted into polyunsaturated fatty acids-phosphatidylethanolamine (PUFA-PEs) through lysophosphatidylcholine acyltransferase 3 (LPCAT3) catalysis (Zhang H. et al., 2021). PUFA-PES, an important substrate in the lipid peroxidation pathway, is oxidized to PUFA-PE-OOH under the action of lipoxygenase (ALOX) as a lipid peroxide to drive the ferroptosis process (Capelletti et al., 2020). This oxidation of ALOX can be enhanced by the Fenton reaction product of free iron and reversed by the important antioxidant component GPX4 in the amino acid metabolic pathway mentioned later (Xu et al., 2021), indicating the balance regulation function between different metabolic pathways.

ALOX is not only involved in lipid peroxidation, but also can be used as the target of classical ferroptosis regulators such as p53 for systematic regulation (Chu et al., 2019). Significant down-regulation of ALOX inhibits erastin-induced and RSL3-induced ferroptosis, and accordingly up-regulation of ALOX accelerates ferroptosis (Shintoku et al., 2017). While ACSL4 is involved in driving ferroptosis, it can also be used as a biomarker for ferroptosis (Yuan et al., 2016). Similarly, cytochrome P450 oxidoreductases with similar functions can also scavenge excessive lipid peroxides (Zou et al., 2020). These studies suggest that lipid synthase can not only adjust lipid oxidation but also take part in other links involved in ferroptosis to influent the cell-death progress.

2.3 Amino Acid Metabolism

GSH, composed of glutamic acid, has a significant application in the oxidation resistance ways against ferroptosis (Kuang et al., 2020). Cysteine, as a precursor of GSH, is also participating in the resistance to cell oxidation. On the one hand, it has its own antioxidant effect, on the other hand, the conversion of cystine to cysteine will affect the synthesis of glutathione (GSH) as a rate-limiting step (Lu, 2009). Transporter system Xc-can output glutamate in exchange for cystine accumulation by obtaining sufficient cystine to ensure intracellular cysteine supply for GSH synthesis (Bannai, 1986). It consists of solute carrier family three member 2 (SLC3A2) and solute carrier family seven member 11 (SLC7A11), of which SLC7A11 plays an active key role in ferroptosis (Sato et al., 1999).

Another vital antioxidant component of ferroptosis called glutathione peroxidase (GPX), a family of enzymes, worked as a cofactor of GSH to reduce excessive intracellular peroxides. However, only glutathione peroxidase 4 (GPX4) has a reduction effect on lipid peroxides (Forcina and Dixon, 2019), so the liveness of GPX4 is the basic of anti-lipid peroxide ability in ferroptosis (Ursini and Maiorino, 2020).

The collapse of this antioxidant line of defense is often a significant part of the ferroptosis process. The system Xc-responsible for input is often up-regulated in cancer cells due to the excessive demand for nutrients, but this effect can be blocked by the classical ferroptosis inducer erastin. The inhibition of erastin on SLC7A11 causes the depletion of intracellular cysteine, thereby affecting the production of GSH and the function of GPX4, which will lead to the disorder of antioxidant program in cells (Wang L. et al., 2020). In addition to the inhibition of system Xc-from the source, some small molecular inhibition and direct binding inhibition with GPX4 can also trigger ferroptosis. The target of ferroptosis inducer (1S, 3R) -RSL3 is GPX4, which can induce ferroptosis by inhibiting its phospholipid peroxidase activity (Yang et al., 2014). These studies indicate that the lack or depletion of nutrients, especially amino acids, has adverse effects on cells. Reducing the number of cells through the ferroptosis pathway may be the spontaneous choice of cancer cells under such adverse conditions, and can also provide new ideas for cancer treatment.

3 INVOLVEMENT OF ORGANELLES IN FERROPTOSIS

3.1 Ferroptosis in Mitochondria

Mitochondria is an important organelle for energy metabolism and ATP production in cells. There is a substantial connection between the generation of oxygen free radicals in mitochondria and programmed cell death (Liu and Shi, 2020). The function of the molecules and proteins in mitochondria in the process of ferroptosis has long been indeterminate. In ferroptosis cells, mitochondria often show significant morphological changes, including mitochondrial enlargement and crista disappearance (Doll et al., 2017), and the mitochondrial membrane potential abnormality may happen (Maru et al., 2022), suggesting that changes in normal mitochondrial function are closely associated with ferroptosis. Obviously, some mitochondrial-targeting chemicals have good inhibitory effect on ferroptosis (Krainz et al., 2016) (**Figure 2**).

The metabolism in mitochondria is the predominant source of reactive oxygen species (ROS) in cells. Complex II and complex III exist in mitochondrial inner membrane. The electrons produced in oxidative phosphorylation can leak and produce superoxide (O_2·-) through complex II and complex III. Under the catalysis of superoxide dismutase (SOD), O_2—disproportionately reacts to produce H_2O_2 and further generates OH through the Fenton reaction. The production of ROS affects the normal function of mitochondria and the redox state of other organelles (Zhang B. et al., 2022). System Xc-is a transporter presenting on the cell membrane, cystine import by system Xc-is

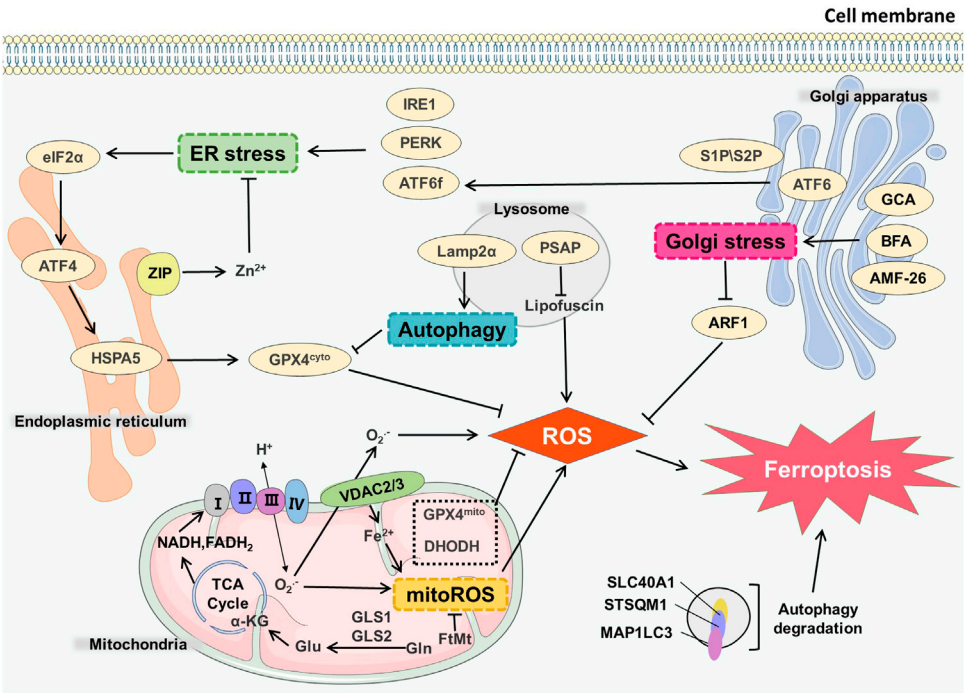

FIGURE 2 | Organelles and ferroptosis. GLS1/GLS2 catalyzes Gln in the mitochondrial matrix to generate Glu, which is involved in TCA cycle to produce NADH and FADH2. After ETC, peroxides and mitoROS were generated. VDAC2/3 on the mitochondrial membrane mediated the maintenance of the steady state of Fe^{2+} in mitochondria, which also affected the generation process of mitoROS, and ultimately led to ferroptosis. GCA, BFA, AMF-26 induce Golgi stress and affect ferroptosis. Endoplasmic reticulum stress receptors such as PERK, ATF6, IRE1 can also cause endoplasmic reticulum stress-mediated ferroptosis. Autophagy degradation in lysosomes directly infulences the occurrence of ferroptosis. Lamp2α can inhibit GPX4 by affecting autophagy process, thereby increasing the level of ROS. PSAP can also affect lipofuscin and promote ROS generation.

simultaneously accompanied by glutamine export. The decomposition of glutamine can produce α-ketoglutarate, which participates in the tricarboxylic acid cycle (TCA) cycle occurring in the mitochondrial matrix and mimic the death-inducing activity of L-Gln, thereby regulating the ferroptosis (Gao et al., 2015). Suppression of TCA cycle or electron transfer chain (ETC) can effectively reduce the production of lipid peroxides (Zhao et al., 2022), thereby reducing the occurrence of ferroptosis, indicating that ferroptosis is related to abnormal ROS production. At the same time, glutamine decomposition can generate intermediates of the TCA cycle which induces mitochondrial membrane hyperpolarization, and it may reflect the increase of ETC activity and ROS generation (Tang E. et al., 2021). Mitochondrial membrane hyperpolarization may reflect increased ETC activity and ROS generation (Bonanno et al., 2022).

GPX4 is one of the most important enzymes involved in ferroptosis, and it weakens the toxicity of lipid peroxides to maintain the homeostasis of phospholipid bilayers and resist oxidative damage. However, during the ferroptosis induced by GPX4 inhibition, mitochondria is non-essential (Gao et al., 2019). Some enzymes, such as monoamine oxidase and α-ketoglutarate dehydrogenase, in the catalytic process can also produce ROS (Adam-Vizi and Tretter, 2013). Coenzyme Q10 (CoQ10), a regulator of mitochondrial permeability transition pore (mPTP) as a key part of ETC, inhibits the occurrence of ferroptosis (Ernster and Forsmark-Andrée, 1993). Myristylation recruits ferroptosis suppressor protein 1 (FSP1) to mediate the reduction of NADH-dependent CoQ10, and this process inhibits the transmission of lipid peroxides to prevent ferroptosis. Exogenous supplement of CoQ10 can also protect cells from oxidative stress (Bersuker et al., 2019; Rizzardi et al., 2021).

Mitochondria are closely involved in the formation of intracellular iron homeostasis. The free state and redox state of intracellular iron affect the occurrence of ferroptosis. Voltage-dependent anion channels (VDAC) participate in the regulation of the transport of iron in mitochondria, and erastin destroys the expression of VDAC2 and VDAC3 (Yagoda et al., 2007). Down-regulation of mitochondrial VDACs can also effectively inhibit ferroptosis (Yang and Stockwell, 2008). Mitochondrial ferritin (FtMt) controls the size of mitochondrial LIP and attenuates the level of ROS. Also FtMt can significantly inhibit ferroptosis induced by erastin, and maintain the level of Bcl-2 and mitochondrial membrane potential to diminish caspase three expression (Wang YQ. et al., 2016; Gao et al., 2017).

Dihydroorotate dehydrogenase (DHODH) is an enzyme expressed in the mitochondrial inner membrane, which catalyzes the *de novo* synthesis of pyrimidine nucleotides, the deletion of DHODH can induce cell death in cells with high GPX4 expression without causing lipid peroxidation, and this process can be rescued by supplementing uridine (Vasan et al.,

2020). In cell lines with low GPX4 expression such as NCI-H226, even when supplemented with uridine, DHODH can still induce lipid peroxidation and ferroptosis. The cell lines could not be cultured for a long time, indicating that DHODH acts in parallel to GPX4 in ferroptosis whereas the inhibition of DHODH has no impact on the expression of GPX4. It also suppresses lipid peroxidation by reducing CoQ to CoQH2, suggesting that DHODH and mitochondrial GPX4 constitute the two main defense mechanisms of lipid peroxide detoxification in mitochondria (Mao et al., 2021).

However, there is also some evidence against the main role of mitochondria in ferroptosis. Cell lines lacking mitochondrial DNA (ρ0 cell lines) have no significant difference in ferroptosis sensitivity compared with their parental cell lines. By evaluating the distribution of ferrostatin-1 and ferrostatins in organelles, it is found that mitochondria are not necessary to inhibit ferroptosis (Gaschler et al., 2018). Therefore, to further investigate the role of mitochondrial metabolism in ferroptosis model is necessary, and to clarify whether mitochondrial and mitochondrial-related signaling pathways can be used as effective targets for regulating ferroptosis.

3.2 Ferroptosis in Endoplasmic Reticulum

Endoplasmic reticulum (ER) is a complex membrane system performing the functions of protein, lipid and carbohydrate synthesis. The ER is spatially and functionally connected to other organelles such as the mitochondria, lysosomal system, etc (Daniele and Schiaffino, 2014). The stability of endoplasmic reticulum structure and function directly affects the normal function of other organelles. ER stress occurs when the cells deal with the misfolded or unfolded proteins in endoplasmic reticulum as well as calcium ion balance disorders (Lei et al., 2022). For example, unfolded protein response (UPR) can be initiated through three signaling pathways, separately mediated by three transmembrane ER receptors, AMP-dependent transcription factor (ATF6), inosital-requiring enzyme-1 (IRE1) and protein kinase R-like ER kinase (PERK) (Zanetti et al., 2022). Amino-terminal cytoplasmic fragment (ATF6f) produced by the cleavage of ATF6 is involved in mediating ER protein folding. IRE1 oligomerization forms IRE1 RNase, inducing regulated IRE1-dependent decay (RIDD). ATF6 phosphorylates eukaryotic translation initiation factor 2 (eIF2α) and up-regulates ATF4, ATF4 controls the expression of related genes such as C/EBP-homologous protein (CHOP) (McGrath et al., 2021).

ER stress is closely related to ferroptosis in many cases, such as acute kidney injury (Li et al., 2022), type II diabetes (Sha et al., 2021), and tumors (Sun et al., 2015; Zhu et al., 2017). Several lines of evidence highlight that erastin can induce ER stress through the activation of eIF2α/ATF4 signaling pathway (Dixon et al., 2014), while sorafenib can activate IRE1 and p-ERK, but the activation of p-ERK has a protective effect on cells (Rahmani et al., 2007). Dihydroartemisinin (DHA) can activate ATF4 by promoting the level of p-ERK in glioma cells, thereby increasing the level of heat shock protein family A (Hsp70) member five HSPA5. HSPA5 has the effect of up-regulating the GPX4, which results in protecting glioma cells from ferroptosis, indicating the activation of ATF4 strengthens the drug resistance of glioma (Chen Y. et al., 2019). p-ERK-mediated ATF4 activation can also protect pancreatic cancer cells from ferroptosis (Dixon et al., 2014), and evidence shows that cystine starvation can increase the phosphorylation of eIF2α, as well as the expression of ATF4, in human triple negative breast cancer (TNBC) cells, resulting in ferroptosis (Chen et al., 2017).

There are other pathways besides the ER stress that affect the occurrence of ferroptosis. For example, ZIP7 controls zinc transport from the ER to the cytoplasm (MacKenzie and Bergdahl, 2022), a reduction in ZIP7 expression will cause ferroptosis protection. This process may be related to the involvement of zinc in ER and nuclear communication (Chen PH. et al., 2021). Exogenous monounsaturated fatty acids (MUFA) can reduce the production of lipid peroxides on ER membrane, and this ACSL3-dependent process induces ferroptosis-resistance (Magtanong et al., 2019).

ER has a certain contact with other organelles. ER and mitochondria can be linked through mitochondrial-associated ER membrane (MAM) (Means and Katz, 2021). Hence, MAM is essential for the maintenance of intracellular calcium homeostasis and cell survival (Lee and Min, 2018). Therefore, the future study should give attention to the more precise delineation of the signal network between endoplasmic reticulum and other organelles.

3.3 Ferroptosis in Golgi Apparatus

This membranous organelle is involved in the secretory function and glycosylation of proteins. Golgi disruptors, including brefeldin A (BFA), golgicide A (GCA), and 2-methylcoprophilinamide (AMF-26, also called M-COPA), can act on Golgi to cause oxidative stress. The production of superoxide and peroxide induces ferroptosis. The lipid peroxides accumulate after Golgi stress happens, which also lessen the intracellular glutathione. Antioxidants, reactive oxygen species scavengers and GPX4 can promote ferroptosis-resistant cells stage induced in Golgi stress, indicating that reducing the production of lipid peroxides is beneficial to maintain the steady state of secretion pathway (Alborzinia et al., 2018). Golgi-associated small GTPase ADP ribosylation factor 1 (ARF1) can reduce the production of lipid peroxides. When Golgi stressors and low doses of ferroptosis inducers are applied at the same time, ferroptosis inducers can significantly reduce the effect of the Golgi stressors on inducing cell death (Alborzinia et al., 2018). This process may be related to the common antioxidant regulation and feedback mechanism such as the transsulfuration pathway initiated by cells, which enhance viability upon Golgi stressors (Alborzinia et al., 2018). Therefore, it is speculated that during ferroptosis, the normal function of Golgi apparatus is affected, resulting in the destruction of cell secretion and the steady state of lipid ROS generation.

3.4 Ferroptosis in Lysosome

Autophagy, a lysosomal degradation pathway that degrades ferritin in cells, induces ferroptosis (Hou et al., 2016; Kang and Tang, 2017). Blocking the function of cathepsin and H^+-ATPase can limit ferroptosis (Gao et al., 2018). Ferroptosis often occurs when the function of GPX4 is inhibited or insufficient.

Studies have shown that erastin increases the expression of lysosome-associated membrane protein 2α (Lamp2α), which promotes molecular chaperone-mediated autophagy and down-regulate GPX4 (Wu et al., 2019). Following the treatment of cells with lysosome activity inhibitors, the outbreaks of lysosome ROS are significantly reduced, and the lipid peroxides in the perinuclear space are also significantly attenuated, suggesting that lysosomes may participate in ferroptosis by regulating ROS generation (Torii et al., 2016; Kumar et al., 2021).

Ferroptosis activators (erastin and RSL3) decrease GPX4 expression in human tumor cell lines. RSL3 up-regulates the microtubule-associated protein one light chain three beta (MAP1LC3B-II) or down-regulates sequestosome 1 (SQSTM1) (Liu J. et al., 2019). Accordingly, it increases the level of intracellular iron ions and promotes the occurrence of ferroptosis (Li et al., 2021). Furthermore, autophagy degradation of intracellular lipid droplets is conducive to the accumulation of free fatty acids, promoting ferroptosis in RSL3-induced cells (Bai et al., 2019).

The targeted fluorescent probe used in erastin-treated HT1080 cells shows the intracellular iron homeostasis has been changed, and the increase of unstable Fe2+ in lysosomes leads to ferroptosis (Hirayama et al., 2019). The decrease in the expression of lysosomal protein prosaposin (PSAP) could trigger the formation of lipofuscin, which promotes the accumulation of iron and ROS, leading to ferroptosis (Tian et al., 2021). Studies have also shown that NTP-activated ringer's lactate (PAL) can cause NO-mediated lysosomal damage, triggering ferroptosis in malignant mesothelioma cells (Jiang et al., 2021b). Recent insights show that ferroptosis is dependent on autophagy, which is a lysosome-mediated process of recycling cellular components. Therefore, future studies can further explore the autophagy-based induction of ferroptosis in tumor cells.

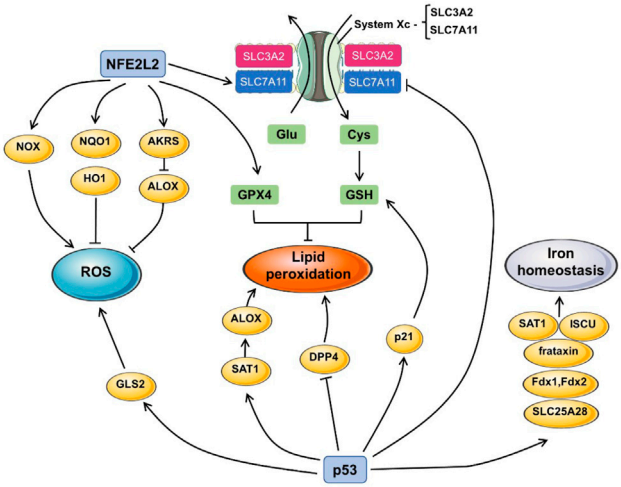

FIGURE 3 | The pathway of p53 and Nrf2 in ferroptosis. The generation of ROS, lipid peroxidation and iron homeostasis are the indispensable course in triggering ferroptosis. Nrf2 and p53 participate in ferroptosis by influencing the expression of a series of downstream proteins. For example, Nrf2 promotes the expression of GPX4 and upregulates the expression or the function of solute carrier family seven member 11 (SLC7A11) to exert influence on lipid peroxidation. Nrf2 also activates NADPH oxidases (NOX), NAD(P)H quinone dehydrogenase 1 (NQO1), heme oxygenase 1 (HO1), aldosterone reductases (AKRS), which all contribute to the production of ROS, resulting in ferroptosis. GLS2 induced by p53 inhibit the depletion of ROS. P53 also promote the synthesis of Spermidine/spermine N1-acetyltransferase 1 (SAT1) and dipeptidyl peptidase 4 (DPP4), which enhance the lipid peroxidation. P53 also regulates frataxin, ferredoxin one and 2 (Fdx1/Fdx2), iron-sulfur cluster assembly enzyme (ISCU), SAT1, the activation of those molecules contributes to iron homeostasis.

4 KEY REGULATORS OF FERROPTOSIS

4.1 Transcription Factor NRF2

Nrf2 is an essential transcription factor with antioxidant function, and its content remains at a low level through three different E3—ubiquitin ligase complexes, Kelch-like ECH-associated protein 1-Cullin 3-Ring box 1 (KEAP1-CUL3-RBX1), (SKP1, CUL1, and F-box protein)/β-Transducin repeats-containing protein (SCF/β-TrCP) and synovin/Hrd1 (Li et al., 2019; Wu et al., 2020). Kelch ECH-associated protein 1 (KEAP1) is one of the main negative regulatory factors of Nrf2 (Bellezza et al., 2018). Normally, KEAP1 regulates NRF2 activity by targeting ubiquitination and proteasome-dependent degradation, which interact and remain in the cytoplasm (Huang et al., 2010; Baird and Yamamoto, 2020). Under oxidative stress, the cysteine residues of KEAP1 were modified and then lost the ability to degrade Nrf2 (Taguchi et al., 2011). Nrf2 dissociates from Keap1 and accumulates in the nucleus to activate other protective genes in anti-oxidative stress response (Deshmukh et al., 2017) (**Figure 3**).

Given the role of NRF2 in multiple key pathways against oxidative stress, it is not difficult to imagine the effect of Nrf2 on iron cell death. For the first time in hepatocellular carcinoma (HCC), researches have demonstrated the effectiveness of Nrf2 in protecting cells from ferroptosis, this pathway can also be used by ferroptosis activators including sorafenib, which stabilizes NFE2L2 in human HCC cells by inhibiting the formation of NFE2L2-KRAP1 complexes. This process is further regulated by SQSTM1/p62. P62, a kind of ubiquitin-binding protein, competes with NRF2 in the Kelch motif of KEAP1 and increases the content of downstream Nrf2 by inactivation of Keap1. It also shows that the regulation of Nrf2 by KEAP1 will be competitively interfered by many KEAP1-binding proteins (Sun et al., 2016; Nam and Keum, 2019).

There are many downstream genes of Nrf2, which mainly inhibit the occurrence of ferroptosis through several groups of targeted genes with different targets, including iron metabolism, intermediate metabolism and GSH synthesis/metabolism, and no matter what kind of mode, they all involve antioxidant reaction elements (ARE) (Rojo de la Vega et al., 2018; Dodson et al., 2019). As a typical anti-oxidative stress molecule, the enhanced Nrf2 can upregulate multiple ROS inhibitor (Guo et al., 2021), thereby protecting cells from oxidative stress. In iron metabolism, existing studies have found that Nrf2-regulated genes involved in iron metabolism can affect several links including heme synthesis,

hemoglobin catabolism, iron storage and iron output (Kerins and Ooi, 2018). Nrf2 can regulate iron/heme metabolism pathway, and Heme oxygenase 1 (HO1) is an enzyme catalyzing the conversion of heme to choline which is related to it (Balla et al., 2007; Kerins and Ooi, 2018). HO-1, a targeted gene of Nrf2 participates in the induction of ferroptosis and accelerates erastin-induced ferroptosis (Kwon et al., 2015; Chang et al., 2018). Nrf2-HO-1 pathway also has moderating effect on intracellular iron concentration (LIP) (Tomiotto-Pellissier et al., 2018), but it needs further study to see whether this pathway is the main one to regulate free iron concentration. However, the role of HO-1 has both positive and negative regulatory directions, which is often concerned about the protective effect of HO-1 on cells. The specific regulatory direction may depend on the pathological state and internal environment of the cell itself.

In iron storage, ferritin is a protein formed of light chain (FTL) and heavy chain (FTH1) subunits (Muhoberac and Vidal, 2019), which participates in iron storage, which can also be affected by Nrf2 (Sun et al., 2016; Muhoberac and Vidal, 2019). As for the iron transport related heme transporter solute carrier family 48 member 1(SLC48A1), Nrf2 also plays an up-regulated role in SLC48A1's participating in ferroptosis (Campbell et al., 2013).

In the intermediate metabolism of intracellular substances, NADPH is indispensable for the reduction and oxidation of substrates. NADPH, NADPH oxidase and its homologous NOX family are also affected by Nrf2 (Bedard and Krause, 2007). Nrf2 can produce ROS through NADPH oxidase, leading to the accumulation of ROS, which also plays a similar role in the NOX family. On the other hand, aldosterone reductases (AKRs) gene family (AKR1C1/3) is also regulated by Nrf2 (Gagliardi et al., 2019).

In terms of GSH metabolism, Nrf2 can regulate GSH production by affecting glutamate-cysteine ligase (GCL) and GCL-catalyzed/modified subunit (GCLC/GCLM). Also regulated by Nrf2 are the subunit SLC7A11 of cystine/glutamate transporter xCT, and GPX4 downstream of GSH, which exert a profound influence on the production and function of GSH (Fan et al., 2017; Shin et al., 2018; Jin et al., 2019).

4.2 TP53

Mutational activation of the TP53 is one of the most common genetic alteration in human cancer (Hoang and Landi, 2022). As an anti-oncogene, TP53 is involved in all aspects of normal physiological activities of cells, including the regulation of glycolysis and oxidative phosphorylation, and the regulation of ROS generation (Kruiswijk et al., 2015). Its translation product p53 is a specific DNA-binding protein with the function of transcription factors, which participates in various cell stress and cell cycle, and also mediates cell senescence and death (Laptenko and Prives, 2006). Ferroptosis is characterized by iron-dependent lipoperoxide accumulation, and p53 can participate in the occurrence of ferroptosis by affecting iron metabolism and lipid metabolism.

Iron homeostasis interacts with the expression of p53. Excessive iron could reduce p53 expression level, whereas the iron polyporphyrin heme could restrain the combination between p53 and DNA, promoting the export of p53 from the nucleus and degradation in the cytoplasm (Shen et al., 2014). After human lymphocytes were treated with deferoxamine (DFX), p53 increased but its downstream target protein was not affected (Kim et al., 2007). In addition, p53 can up-regulate the expression of frataxin, which affects the iron homeostasis in mitochondria and prevents the occurrence of iron overload (Shimizu et al., 2014). P53 also affects the expression of ferredoxin reductase (FDXR) (Zhang Y. et al., 2022). FDXR transfers the reduction equivalent obtained from NADPH to ferredoxin 1 and 2 (Fdx1, Fdx2) (Brandt and Vickery, 1992). Fdx1 is involved in steroid metabolism and the synthesis of iron sulfur protein. The limitation of Fdx2 function leads to increased iron uptake in cells and iron accumulation in mitochondria (Sheftel et al., 2010). P53 can also induce the expression of iron-sulfur cluster assembly enzyme (ISCU). ISCU inhibits the binding of iron regulatory protein 1 (IRP1) to ferritin heavy peptide 1 (FTH1) and promotes the translation of FTH1, which will increase intracellular iron storage (Funauchi et al., 2015).

P53 affects systemic lipid metabolism by promoting intestinal lipid absorption (Goldstein et al., 2012), and it also plays a vital role in intracellular lipid metabolism. P53 can bind with glucose-6-phosphate dehydrogenase to inhibit NADPH formation. Since NADPH is an important auxiliary factor in fatty acid synthesis, its synthesis limitation directly affects lipid synthesis (Jiang et al., 2011). P53 also affects sterol regulatory element binding protein-1(SREBP-1), regulating the lipid synthesis through the IGF-1-AKT-mTOR pathway (Yahagi et al., 2003; Feng and Levine, 2010).

In addition, p53 can inhibit the expression of solute carrier family seven member 11 (SLC7A11) (Ritzenthaler et al., 2022), SLC7A11 is an important part of the cystine/glutamate antiporter, so the decrease of SLC7A11 expression inhibits the cystine ingestion and sensitizes cells to ferroptosis (Jiang et al., 2015). Since SLC7A11 can specifically bind and inhibit ALOX12 (arachidonate 12-lipoxygenase, an enzyme in another pathway other than GPX4-mediated effect on intracellular lipoperoxide level, p53 indirectly affects the activity of ALOX12 and influences the lipoperoxide level in the cytoplasm (Kappus, 1987). Phosphate-activated glutaminase (GLS2) can promote glutamine decomposition and reduce intracellular ROS level, and P53 affects intracellular antioxidant capacity by regulating GLS2 expression (Suzuki et al., 2010; Shi et al., 2022). Another study showed that the decrease of p53 expression in colorectal cancer accumulates Dipeptidyl peptidase 4 (DPP4) in nuclear, and facilitates membrane lipid peroxidation and leads to ferroptosis (Xie et al., 2017). Polyamines are closely associated with the occurrence of cancer (Gerner and Meyskens, 2004). Spermidine/spermine N1-acetyltransferase 1 (SAT1) is a limiting enzyme that controls the metabolism of polyamines. P53 activation can significantly upregulate the expression level of SAT1. Cells with high expression of SAT1 die after ROS treatment. This process can be suppressed by ferroptosis inhibitor Ferrostatin-1. Meanwhile, the expression level of ALOX15 is promoted. After the SAT1 expression was knocked down in p53-induced ferroptosis, the expression of ALOX15 was

attenuated. It is speculated that ALOX15 may be a downstream molecule of SAT1 (Ou et al., 2016). p53 forms a complex with soluble carrier family 25 member 28 (SLC25A28) and activates SLC25A28, affecting the function of ETC and iron homeostasis, leading to ferroptosis in hepatic stellate cells (HSCs) (Zhang et al., 2020). P21, a downstream molecule of p53, can also interact with CDK and enhance cell resistance to ferroptosis in some tumor cell lines (Venkatesh et al., 2020).

Since p53 has effects on the adjustment of different target genes expression under different environmental backgrounds, the role of p53 in the occurrence of ferroptosis is very complex. This most widely studied gene, can be a powerful target for future treatment in ferroptosis (Liu and Gu, 2022). The bidirectional control of ferroptosis is context-dependent, so the role and regulation of p53 in the occurrence of ferroptosis still need further study.

5 EPIGENETIC REMODELERS IN FERROPTOSIS

5.1 Non-Coding RNAs

Non-coding RNAs are divided into several categories, long non-coding (lnc) RNA NEAT1 regulates the sensitivity of non-small cell lung cancer (NSCLC) to iron-dependent lipid peroxide accumulation by affecting the acyl-CoA synthetase long-chain family member 4 (ACSL4), thereby affecting the resistance of cancer cells to ferroptosis (Wu and Liu, 2021). MiRNA-17-92 can also reduce the erastin-induced ferroptosis in endothelial cells with the help of the A20-ACSL4 axis (Xiao et al., 2019).

In the meantime, the mutual regulatory pathways of different types of non-coding RNAs often have value in ferroptosis. In rat pulmonary fibrosis tissues, silencing of lncRNA ZFAS1 affects miR-150-5p, resulting in down-regulation of SLC38A1, thereby attenuating lipid peroxidation and ferroptosis induced by bleomycin (BLM) and transforming growth factor-β1 (TGF-β1). lncRNA PVT1 in cerebral ischemia/reperfusion (I/R) can reduce the binding of miR-214 to PVT1 and TP53 3′UTR by restraining the expression of miR-214, thereby enhancing ferroptosis. This pathway has a positive feedback regulation mechanism, and different coding RNAs also interact in this process (Yang et al., 2020b; Lu et al., 2020). Chloramphenone can suppress lncPVT1, and weaken the effect of miR-214-3p on GPX4, thereby accelerating ferroptosis (He et al., 2021). lncRNA LINC00336, as a competitive endogenous RNA (ceRNA), combines with the ELAV-like RNA-binding protein 1 (ELAVL1). ELAVL1 can inhibit ferroptosis in lung cancer cells, and ELAVL1 itself also promotes this process by stabilizing LINC00336 transcription. LINC00336 can also regulate cystathionine-β-synthase (CBS) by affecting microRNA 6852 (MIR6852), and CBS can trigger the ferroptosis process of cancer cells (Wang et al., 2019). The ectopic expression of metallothionein 1D pseudogene (MT1DP) can increase the sensitivity of lung cancer cells to erastin-induced ferroptosis by down-regulating NRF2, while up-regulating MDA and ROS levels to promote ferroptosis (Gai et al., 2020).

While up-regulating caspase-3 to promote cell apoptosis, LINC00618 can also promote ferroptosis by increasing the free iron content and ROS accumulation in cells. This phenomenon that LINC00618 is regulated by lymph-specific helicase (LSH) confirms that the regulation of non-coding RNA in the field of ferroptosis can also be affected by other epigenetic pathways. In view of the key role of LSH in ferroptosis-related chromatin remodeling and DNA methylation modification pathway, it cannot be ignored (Wang Z. et al., 2021; Chen X. et al., 2022).

On the other hand, LSH can down-regulate the expression of lncP53RRA, and P53RRA can bind to Ras GTPase activator protein binding protein 1 (G3BP1). The decrease of P53RRA leads to the replacement of P53 from G3BP1, and P53 being retained in the nucleus more It will also results in subsequent cell cycle arrest and ferroptosis (Mao et al., 2018). The regulation of LSH on LINC00618 and P53RRA on ferroptosis pathway also reflects the cross of different epigenetic modification pathways to some extent.

A large number of lncRNAs not only play a role in ferroptosis, a considerable number of indicators can be used as prognostic factors for ferroptosis through the investigation of cancer genome map (TCGA) database. For example, 25 lncRNAs are found to be the independent prognostic factors in head and neck cancer (HNSCC) (Tang Y. et al., 2021).

5.2 Chromatin Remodeling Factors

Chromatin remodeling usually depends on the covalent modification of nucleosomes. Using ATP as the energy source, this process works in adjusting cell cycle progressing, cell movement and nuclear hormone signal transduction (Dawson and Kouzarides, 2012). Through genome sequence analysis, chromatin remodeling complex dysfunction is widespread in major cancers, and complex mutations and other genetic changes often occur (Zhang et al., 2016). LSH, as a chromatin remodeling protein, belongs to the chromatin remodeling ATPase SNF2 family, and generally plays a stabilizing role by maintaining an appropriate DNA methylation level (He et al., 2016; Jiang et al., 2017; Xiao et al., 2017; Chen L. et al., 2019; Liu et al., 2020; Chen X. et al., 2022). Studies have shown that LSH can also take part in the metabolic paths associated with ferroptosis to achieve regulatory purposes, except for the above-mentioned pathways that control non-coding RNAs to participate in ferroptosis. For example, LSH inhibits ferroptosis by up-regulating the enrichment of WD40 protein WDR76 (nuclear WD40 protein) on lipid metabolism-related genes, thereby reducing iron accumulation and lipid ROS load (Jiang et al., 2017). These studies show that chromatin remodeling mainly affects the expression level of ferroptosis-related genes through gene expression regulation mode, thereby regulating ferroptosis.

5.3 Post-Translational Modifications and Ferroptosis

5.3.1 Protein Ubiquitination and Ferroptosis

Similarly, the resistance and induction of cells to ferroptosis are also related to the ubiquitination process. Neuronal precursor cell-expressed developmentally downregulated 4 (Nedd4), as a

ubiquitin ligase of the conserved HECT domain E3, can promote voltage-dependent anion channel (VDAC) ubiquitination and degradation by unifying with VDAC, which can lead to ferroptosis resistance in the treatment with erastin, an ferroptosis inducer. The treatment of erastin can trigger the transcriptional activation of Nedd4 in melanoma cells, leading to the degrading of VDAC2/3, the target of erastin (Yang et al., 2020a). However, deubiquitinases have opposite effects on ferroptosis. For example, deubiquitinase ubiquitin hydrolase OTUB1 can maintain SLC7A11's stability through direct interaction with it, and this process does not depend on the participation of P53 (Liu T. et al., 2019).

On the other hand, deubiquitinase can have different effects on ferroptosis. For example, deubiquitinase ubiquitin hydrolase OTUB1 can directly interact with and maintain the stability of SLC7A11, and this process does not depend on the participation of P53 (Liu T. et al., 2019).

Ubiquitination modification is common in various diseases, and the ubiquitination of key factors of ferroptosis is participate in the procedure of ferroptosis-related diseases like diabetic retinopathy (DR) (Zhang J. et al., 2021), impaired cognitive dysfunction (POCD) (Zhao et al., 2021) and ischemia/reperfusion (I/R) (Tang LJ. et al., 2021). Ubiquitination modification also widely exists in several major metabolic processes related to ferroptosis. In terms of iron metabolism, FPN1, the only iron-exporting protein on the cytoplasmic membrane, has been confirmed to be able to be ubiquitinated and thus affect its function. For example, ubiquitin ligase RNF217 mediates the degradation of iron-exporting protein FPN and regulates iron homeostasis (Jiang et al., 2021a). As for the lipid metabolism, tumor suppressor BRCA1-associated protein 1 (BAP1) reduces the binding rate of SLC7A11 promoter to H2A-ub, and inhibits SLC7A11 and cystine uptake by deubiquitinating enzyme (DUB) encoded by BAP1, contributing to lipid peroxidation and ferroptosis (Zhang et al., 2018). E3 ubiquitin ligase named Tripartite motif-containing protein 26 (TRIM26) can promote SLC7A11 ubiquitination and degradation in HCC to promote lipid peroxidation and ferroptosis downstream (Zhu et al., 2021). The latest development of mass spectrometry can qualitatively and quantitatively analyze the ubiquitination of cancer specimens, which has a positive significance for revealing the causes of abnormal protein expression of cancer genes (Faktor et al., 2019).

The ubiquitination process also has a significant effect on the ferroptosis's key regulatory factors. For example, Nrf2, the main negative regulatory factor of ferroptosis, can be deubiquitinated by ubiquitin-specific-processing protease 11 (USP11) to increase the stability of its own proteins, so as to better participate in the process of ferroptosis (Meng et al., 2021). On the contrary, Quiescin sulfhydryl oxidase 1 (QSOX1) can indirectly inhibit the activity of Nrf2 by ubiquitinizing Epidermal growth factor receptor (EGFR) (Sun et al., 2021).

5.3.2 Protein Methylation and Ferroptosis

As a dynamic regulation mechanism, protein methylation is widely present in histone and non-histone post-translational modifications (Hamamoto et al., 2015), which has considerable influence on cell cycle, apoptosis and cancer progression. More attention has been paid to histone methylation modification, such as histone H3 lysine nine demethylase B (KDM3B). SLC7A11, as one of the subunits of Xc-, can be used as a downstream factor of ferroptosis inhibitor. kDM3B can inhibit ferroptosis caused by Erastin, an ferroptosis inducer, by activating SLC7A11 (Wang Y. et al., 2020). Similarly, ferroptosis also take part in the pathway that SET domain bifurcated 1 (SETDB1) regulates epithelial-mesenchymal transition (EMT) in lung cancer. For cells without EMT, SETDB1 indirectly induces downstream E-cadherin downregulation by catalyzing the histone H3 lysine nine trimethylation (H3K9me3) of the main EMT transcription factor Snai1, thereby increasing ferroptosis (Liu et al., 2022). (+) -JQ1 can reduce the expression of histone lysine methyltransferase G9a by epigenetic way, thereby inhibiting Bromodomain-containing protein 4 (BRD4), a tumor-driven bromodomain protein that is often highly expressed in tumors, to regulate ferritin phagocytosis, iron accumulation and reactive oxygen species production (Sui et al., 2019).

For the modification of non-histone proteins, studies have shown that the methylation modification of non-histone proteins can regulate the process of cancer, and the specific effects vary according to different substrates (Wei et al., 2014). The role of non-histone methylation in ferroptosis and possible pathways needs to be further explored.

5.3.3 Protein Acetylation

The lysine acetylation process takes effect in lots of biological phenomena, and one included is ferroptosis. Acetylation of P53 has a considerable effect on its influence on apoptosis and ferroptosis. Studies have shown that the acetylated mutant p53 3KR retains its iron-induced death function though it loses its ability to regulate cell cycle and other aspects (Jiang et al., 2015). The acetylation of proteins will affect functions, and the adjustment of the degree of acetylation will also have different effects, which partly depends on the site of acetylation. When the acetylation of K98 (p53 4KR98) on P53 is lost, there is only a slight functional effect. When K98 and K117/161/162 acetylation (p53 3KR) are eliminated simultaneously, the downstream function mediated by p53 is significantly inhibited, including downstream molecules such as GLS2 and SLC7A11 (Wang SJ. et al., 2016). Sodium hydrosulfide (NaHS) can significantly alleviate ferroptosis in prefrontal cortex (PFC) of diabetic mice. This is mainly because NaHS can decrease the iron accumulation and oxidative stress, and GPX4 and SLC7A11can also be enhanced by NaHS. In addition, the effect of NaHS on alleviating anxiety in diabetic mice is based on its inhibition of ferroptosis in central nervous cells, and also involves the participation of protein acetylation. NaHS can boost the sirtuin 6 (Sirt6) in microglia and the deacetylation of H3 lysine9 (H3K9ac) by Sirt6, thereby reducing the expression of H3K9ac. This process can reduce the degree of neuroinflammation in diabetic mice, reduce iron accumulation caused by pro-inflammatory reaction, and further inhibit ferroptosis (Wang Y. et al., 2021).

5.3.4 Protein Glycosylation

The role of glycosylation modification of proteins in ferroptosis may not be emphatically discussed. During cell transformation, the main types of protein glycosylation changes are O-glycan (GalNAc-Ser/Thr) and N-glycan (Rodrigues et al., 2018). The down regulation of GALNT14, which is up-regulated in ovarian cancer, inhibits the activity of mTOR pathway through O-glycosylation of EGFR, thereby inhibiting ferroptosis in ovarian cancer cells (Lee et al., 2020). Lysosome-associated membrane protein 2 (LAMP2) is a highly glycosylated lysosome membrane protein. E participating in the autophagy process of cells, LAMP2 can also affect the process of ferroptosis. New researches have uncovered that the lack of LAMP2 is in connected with ROS. LAMP2—KD (LAMP knock-down) reduces the concentration of cytosolic cysteine, while cysteine starvation can lead to decreased antioxidant capacity and mitochondrial lipid peroxidation. Supplementation of cysteine can restore GSH and prevent cell death caused by LAMP knockdown (Lee et al., 2020).

6 CONCLUSION

The principal axis of ferroptosis mechanism is as the sequence, iron accumulation, ROS accumulation and then lipid peroxidation. It involves the metabolic process of various substances and the participation of different organelles. The general pathway to inhibit ferroptosis is how to cut the spindle before the toxicity of cells cannot be reversed, or to reverse the harm caused as much as possible by supplementing raw materials or reducing components. In different diseases, the treatment methods targeting ferroptosis can also be different. The up-regulation of ferroptosis in tumors will help reduce cancer cells (Chen X. et al., 2021), and for diseases such as ischemia reperfusion, ferroptosis needs to be avoided as much as possible (Lillo-Moya et al., 2021). Among the three main metabolic pathways, the accumulation of iron in the central ganglia and the overloaded lipid peroxides promote ferroptosis (directing oxidation), while amino acids (represented by cysteine) play a role in reduction and remediation. Among the metabolic of different substances, how to influence the synergy and antagonism forces of ferroptosis above in order to achieve the desired results of treatment, will be an interesting topic.

Ferroptosis is a programmed cell death process involving cell lipid metabolism, ROS production and intracellular LIP changes. With the passive participation of organelles, these messes finally guide to the cell membrane rupture. At present, we have got somewhere in the molecular occurrence and regulation mechanism of ferroptosis. However, it remains other questions to be figured out. What role does mitochondrial metabolic process play in ferroptosis-related signaling pathways, and whether the related pathways in mitochondria can be used as targets of future drug researches and developments. Whether balance of the lipid metabolism can be maintained by reducing the occurrence of endoplasmic reticulum stress, and the results can further adjust the endoplasmic reticulum-mediated intercellular communication process. in addition, as to the study of organelles, how to design molecular probes in order to further study the changes of Golgi apparatus in the process of ferroptosis, and how to understand the role of lysosomes in autophagy and ferroptosis-whether they affect each other or are independent of each other. These questions still need further research to answer.

Overall, the regulatory network of ferroptosis can be roughly divided into two interrelated directions-non-epigenetic methods, dependant on metabolism and regulation of various factors, and the other is the epigenetic methods. Epigenetics involves a wide range and details, for example, its modification can involve all aspects of translation-The structural adjustment of the chromatin as a whole, the micro-regulation of DNA and RNA, and the influence of all aspects of post-translational modification downstream of the central law. Meanwhile, the mechanisms and methods of modification are not monotonous-different perssads can participate in the modification, and non-coding RNA can regulate each process under different conditions. The links between different steps make it a huge network. At the same level, different ways of post-translational modification are related and influenced mutually. Distinct epigenetic factors also maintain at different levels within the same pathway, such as transcription, translation and modification (Dai et al., 2020). These phenomena can describe how epigenetic regulation creates a complex and extensive delicate balance. And whether there are other regulatory mechanisms in this course, and how the relationships is like between epigenetic and non-epigenetic patterns, are also the research about the epigenetic regulations of ferroptosis that needs to be explored further in the future.

In addition, at the level of post-translational modification, its modifying targets are often divided into histone and non-histone (Yang et al., 2021), and the former has received more attention than the latter due to its closer relationship with genetic materials. It can be predicted that how epigenetic regulators affect non-histone proteins is a complex area of exploration. Similarly, the glycosylation modification is rarely mentioned. It is also a future direction that whether there are any other pathways to guide ferroptosis and whether they have the same status as important modification methods such as ubiquitination.

Finally, the regulatory factor network of ferroptosis, the unknown downstream targets and other details are not clear, but it will undoubtedly provide us with more new treatment directions a new perspective different from the previous cell death network and more new treatment directions, which will motivate new research, and the new technology of curing ferroptosis-related diseases.

AUTHOR CONTRIBUTIONS

YZ, ML, SL, and YT, drafted the manuscript and prepared the figures. YG participated in the discussion and the modification. All authors read and approved the final manuscript.

FUNDING

This work was supported by the National Natural Science Foundation of China (82072594, YT.; 82073097, 81874139, SL), Natural Science Foundation of Hunan Province, and Hunan Provincial Key Area R&D Programs (2021SK2013, YT).

REFERENCES

Adam-Vizi, V., and Tretter, L. (2013). The Role of Mitochondrial Dehydrogenases in the Generation of Oxidative Stress. *Neurochem. Int.* 62 (5), 757–763. doi:10.1016/j.neuint.2013.01.012

Alborzinia, H., Ignashkova, T. I., Dejure, F. R., Gendarme, M., Theobald, J., Wölfl, S., et al. (2018). Golgi Stress Mediates Redox Imbalance and Ferroptosis in Human Cells. *Commun. Biol.* 1, 210. doi:10.1038/s42003-018-0212-6

Bai, Y., Meng, L., Han, L., Jia, Y., Zhao, Y., Gao, H., et al. (2019). Lipid Storage and Lipophagy Regulates Ferroptosis. *Biochem. Biophys. Res. Commun.* 508 (4), 997–1003. doi:10.1016/j.bbrc.2018.12.039

Baird, L., and Yamamoto, M. (2020). The Molecular Mechanisms Regulating the KEAP1-NRF2 Pathway. *Mol. Cell Biol.* 40 (13), e00099–20. doi:10.1128/mcb.00099-20

Balla, J., Vercellotti, G. M., Jeney, V., Yachie, A., Varga, Z., Jacob, H. S., et al. (2007). Heme, Heme Oxygenase, and Ferritin: How the Vascular Endothelium Survives (And Dies) in an Iron-Rich Environment. *Antioxid. Redox Signal* 9 (12), 2119–2137. doi:10.1089/ars.2007.1787

Bannai, S. (1986). Exchange of Cystine and Glutamate across Plasma Membrane of Human Fibroblasts. *J. Biol. Chem.* 261 (5), 2256–2263. doi:10.1016/s0021-9258(17)35926-4

Bedard, K., and Krause, K. H. (2007). The NOX Family of ROS-Generating NADPH Oxidases: Physiology and Pathophysiology. *Physiol. Rev.* 87 (1), 245–313. doi:10.1152/physrev.00044.2005

Bellezza, I., Giambanco, I., Minelli, A., and Donato, R. (2018). Nrf2-Keap1 Signaling in Oxidative and Reductive Stress. *Biochim. Biophys. Acta Mol. Cell Res.* 1865 (5), 721–733. doi:10.1016/j.bbamcr.2018.02.010

Bersuker, K., Hendricks, J. M., Li, Z., Magtanong, L., Ford, B., Tang, P. H., et al. (2019). The CoQ Oxidoreductase FSP1 Acts Parallel to GPX4 to Inhibit Ferroptosis. *Nature* 575 (7784), 688–692. doi:10.1038/s41586-019-1705-2

Bonanno, J. A., Shyam, R., Choi, M., and Ogando, D. G. (2022). The H+ Transporter SLC4A11: Roles in Metabolism, Oxidative Stress and Mitochondrial Uncoupling. *Cells* 11 (2), 197. doi:10.3390/cells11020197

Brandt, M. E., and Vickery, L. E. (1992). Expression and Characterization of Human Mitochondrial Ferredoxin Reductase in *Escherichia coliEscherichia coli*. *Arch. Biochem. Biophys.* 294 (2), 735–740. doi:10.1016/0003-9861(92)90749-m

Campbell, M. R., Karaca, M., Adamski, K. N., Chorley, B. N., Wang, X., and Bell, D. A. (2013). Novel Hematopoietic Target Genes in the NRF2-Mediated Transcriptional Pathway. *Oxid. Med. Cell Longev.* 2013, 120305. doi:10.1155/2013/120305

Cao, J. Y., and Dixon, S. J. (2016). Mechanisms of Ferroptosis. *Cell Mol. Life Sci.* 73 (11-12), 2195–2209. doi:10.1007/s00018-016-2194-1

Capelletti, M. M., Manceau, H., Puy, H., and Peoc'h, K. (2020). Ferroptosis in Liver Diseases: An Overview. *Int. J. Mol. Sci.* 21 (14), 4908. doi:10.3390/ijms21144908

Catalá, A., and Díaz, M. (2016). Editorial: Impact of Lipid Peroxidation on the Physiology and Pathophysiology of Cell Membranes. *Front. Physiol.* 7, 423. doi:10.3389/fphys.2016.00423

Chang, L. C., Chiang, S. K., Chen, S. E., Yu, Y. L., Chou, R. H., and Chang, W. C. (2018). Heme Oxygenase-1 Mediates BAY 11-7085 Induced Ferroptosis. *Cancer Lett.* 416, 124–137. doi:10.1016/j.canlet.2017.12.025

Chen, J., Li, X., Ge, C., Min, J., and Wang, F. (2022a). The Multifaceted Role of Ferroptosis in Liver Disease. *Cell Death Differ.* 29, 467–480. doi:10.1038/s41418-022-00941-0

Chen, L., Shi, Y., Liu, N., Wang, Z., Yang, R., Yan, B., et al. (2019a). DNA Methylation Modifier LSH Inhibits P53 Ubiquitination and Transactivates P53 to Promote Lipid Metabolism. *Epigenetics Chromatin* 12 (1), 59. doi:10.1186/s13072-019-0302-9

Chen, M. S., Wang, S. F., Hsu, C. Y., Yin, P. H., Yeh, T. S., Lee, H. C., et al. (2017). CHAC1 Degradation of Glutathione Enhances Cystine-Starvation-Induced Necroptosis and Ferroptosis in Human Triple Negative Breast Cancer Cells via the GCN2-eIF2α-ATF4 Pathway. *Oncotarget* 8 (70), 114588–114602. doi:10.18632/oncotarget.23055

Chen, P. H., Wu, J., Xu, Y., Ding, C. C., Mestre, A. A., Lin, C. C., et al. (2021a). Zinc Transporter ZIP7 Is a Novel Determinant of Ferroptosis. *Cell Death Dis.* 12 (2), 198. doi:10.1038/s41419-021-03482-5

Chen, X., Kang, R., Kroemer, G., and Tang, D. (2021b). Broadening Horizons: the Role of Ferroptosis in Cancer. *Nat. Rev. Clin. Oncol.* 18 (5), 280–296. doi:10.1038/s41571-020-00462-0

Chen, X., Li, Y., Rubio, K., Deng, B., Li, Y., Tang, Q., et al. (2022b). Lymphoid-specific Helicase in Epigenetics, DNA Repair and Cancer. *Br. J. Cancer* 126 (2), 165–173. doi:10.1038/s41416-021-01543-2

Chen, Y., Mi, Y., Zhang, X., Ma, Q., Song, Y., Zhang, L., et al. (2019b). Dihydroartemisinin-induced Unfolded Protein Response Feedback Attenuates Ferroptosis via PERK/ATF4/HSPA5 Pathway in Glioma Cells. *J. Exp. Clin. Cancer Res.* 38 (1), 402. doi:10.1186/s13046-019-1413-7

Chu, B., Kon, N., Chen, D., Li, T., Liu, T., Jiang, L., et al. (2019). ALOX12 Is Required for P53-Mediated Tumour Suppression through a Distinct Ferroptosis Pathway. *Nat. Cell Biol.* 21 (5), 579–591. doi:10.1038/s41556-019-0305-6

Dai, C., Chen, X., Li, J., Comish, P., Kang, R., and Tang, D. (2020). Transcription Factors in Ferroptotic Cell Death. *Cancer Gene Ther.* 27 (9), 645–656. doi:10.1038/s41417-020-0170-2

Daniele, T., and Schiaffino, M. V. (2014). Organelle Biogenesis and Interorganellar Connections: Better in Contact Than in Isolation. *Commun. Integr. Biol.* 7, e29587. doi:10.4161/cib.29587

Dawson, M. A., and Kouzarides, T. (2012). Cancer Epigenetics: from Mechanism to Therapy. *Cell* 150 (1), 12–27. doi:10.1016/j.cell.2012.06.013

Deshmukh, P., Unni, S., Krishnappa, G., and Padmanabhan, B. (2017). The Keap1-Nrf2 Pathway: Promising Therapeutic Target to Counteract ROS-Mediated Damage in Cancers and Neurodegenerative Diseases. *Biophys. Rev.* 9 (1), 41–56. doi:10.1007/s12551-016-0244-4

Dixon, S. J., Lemberg, K. M., Lamprecht, M. R., Skouta, R., Zaitsev, E. M., Gleason, C. E., et al. (2012). Ferroptosis: an Iron-dependent Form of Nonapoptotic Cell Death. *Cell* 149 (5), 1060–1072. doi:10.1016/j.cell.2012.03.042

Dixon, S. J., Patel, D. N., Welsch, M., Skouta, R., Lee, E. D., Hayano, M., et al. (2014). Pharmacological Inhibition of Cystine-Glutamate Exchange Induces Endoplasmic Reticulum Stress and Ferroptosis. *Elife* 3, e02523. doi:10.7554/eLife.02523

Dodson, M., Castro-Portuguez, R., and Zhang, D. D. (2019). NRF2 Plays a Critical Role in Mitigating Lipid Peroxidation and Ferroptosis. *Redox Biol.* 23, 101107. doi:10.1016/j.redox.2019.101107

Doll, S., Proneth, B., Tyurina, Y. Y., Panzilius, E., Kobayashi, S., Ingold, I., et al. (2017). ACSL4 Dictates Ferroptosis Sensitivity by Shaping Cellular Lipid Composition. *Nat. Chem. Biol.* 13 (1), 91–98. doi:10.1038/nchembio.2239

Ernster, L., and Forsmark-Andrée, P. (1993). Ubiquinol: an Endogenous Antioxidant in Aerobic Organisms. *Clin. Investig.* 71 (8 Suppl. l), S60–S65. doi:10.1007/bf00226842

Faktor, J., Pjechová, M., Hernychová, L., and Vojtěšek, B. (2019). Protein Ubiquitination Research in Oncology. *Klin. Onkol.* 32 (Suppl. um 3), 56–64. doi:10.14735/amko20193S

Fan, Z., Wirth, A. K., Chen, D., Wruck, C. J., Rauh, M., Buchfelder, M., et al. (2017). Nrf2-Keap1 Pathway Promotes Cell Proliferation and Diminishes Ferroptosis. *Oncogenesis* 6 (8), e371. doi:10.1038/oncsis.2017.65

Feng, Z., and Levine, A. J. (2010). The Regulation of Energy Metabolism and the IGF-1/mTOR Pathways by the P53 Protein. *Trends Cell Biol.* 20 (7), 427–434. doi:10.1016/j.tcb.2010.03.004

Forcina, G. C., and Dixon, S. J. (2019). GPX4 at the Crossroads of Lipid Homeostasis and Ferroptosis. *Proteomics* 19 (18), e1800311. doi:10.1002/pmic.201800311

Funauchi, Y., Tanikawa, C., Yi Lo, P. H., Mori, J., Daigo, Y., Takano, A., et al. (2015). Regulation of Iron Homeostasis by the P53-ISCU Pathway. *Sci. Rep.* 5, 16497. doi:10.1038/srep16497

Fuqua, B. K., Vulpe, C. D., and Anderson, G. J. (2012). Intestinal Iron Absorption. *J. Trace Elem. Med. Biol.* 26 (2-3), 115–119. doi:10.1016/j.jtemb.2012.03.015

Gagliardi, M., Cotella, D., Santoro, C., Corà, D., Barlev, N. A., Piacentini, M., et al. (2019). Aldo-keto Reductases Protect Metastatic Melanoma from ER Stress-independent Ferroptosis. *Cell Death Dis.* 10 (12), 902. doi:10.1038/s41419-019-2143-7

Gai, C., Liu, C., Wu, X., Yu, M., Zheng, J., Zhang, W., et al. (2020). MT1DP Loaded by Folate-Modified Liposomes Sensitizes Erastin-Induced Ferroptosis via Regulating miR-365a-3p/NRF2 axis in Non-small Cell Lung Cancer Cells. *Cell Death Dis.* 11 (9), 751. doi:10.1038/s41419-020-02939-3

Gao, G., Zhang, N., Wang, Y. Q., Wu, Q., Yu, P., Shi, Z. H., et al. (2017). Mitochondrial Ferritin Protects Hydrogen Peroxide-Induced Neuronal Cell Damage. *Aging Dis.* 8 (4), 458–470. doi:10.14336/ad.2016.1108

Gao, H., Bai, Y., Jia, Y., Zhao, Y., Kang, R., Tang, D., et al. (2018). Ferroptosis Is a Lysosomal Cell Death Process. *Biochem. Biophys. Res. Commun.* 503 (3), 1550–1556. doi:10.1016/j.bbrc.2018.07.078

Gao, M., Monian, P., Quadri, N., Ramasamy, R., and Jiang, X. (2015). Glutaminolysis and Transferrin Regulate Ferroptosis. *Mol. Cell* 59 (2), 298–308. doi:10.1016/j.molcel.2015.06.011

Gao, M., Yi, J., Zhu, J., Minikes, A. M., Monian, P., Thompson, C. B., et al. (2019). Role of Mitochondria in Ferroptosis. *Mol. Cell* 73 (2), 354–e3. e353. doi:10.1016/j.molcel.2018.10.042

Gaschler, M. M., Hu, F., Feng, H., Linkermann, A., Min, W., and Stockwell, B. R. (2018). Determination of the Subcellular Localization and Mechanism of Action of Ferrostatins in Suppressing Ferroptosis. *ACS Chem. Biol.* 13 (4), 1013–1020. doi:10.1021/acschembio.8b00199

Gaschler, M. M., and Stockwell, B. R. (2017). Lipid Peroxidation in Cell Death. *Biochem. Biophys. Res. Commun.* 482 (3), 419–425. doi:10.1016/j.bbrc.2016.10.086

Gerner, E. W., and Meyskens, F. L., Jr. (2004). Polyamines and Cancer: Old Molecules, New Understanding. *Nat. Rev. Cancer* 4 (10), 781–792. doi:10.1038/nrc1454

Goldstein, I., Ezra, O., Rivlin, N., Molchadsky, A., Madar, S., Goldfinger, N., et al. (2012). p53, a Novel Regulator of Lipid Metabolism Pathways. *J. Hepatol.* 56 (3), 656–662. doi:10.1016/j.jhep.2011.08.022

Guo, Y., Hu, M., Ma, J., Chinnathambi, A., Alharbi, S. A., Shair, O. H. M., et al. (2021). Protective Effect of Panaxydol against Repeated Administration of Aristolochic Acid on Renal Function and Lipid Peroxidation Products via Activating Keap1-Nrf2/ARE Pathway in Rat Kidney. *J. Biochem. Mol. Toxicol.* 35 (1), e22619. doi:10.1002/jbt.22619

Hamamoto, R., Saloura, V., and Nakamura, Y. (2015). Critical Roles of Non-histone Protein Lysine Methylation in Human Tumorigenesis. *Nat. Rev. Cancer* 15 (2), 110–124. doi:10.1038/nrc3884

He, G. N., Bao, N. R., Wang, S., Xi, M., Zhang, T. H., and Chen, F. S. (2021). Ketamine Induces Ferroptosis of Liver Cancer Cells by Targeting lncRNA PVT1/miR-214-3p/GPX4. *Drug Des. Devel Ther.* 15, 3965–3978. doi:10.2147/dddt.S332847

He, X., Yan, B., Liu, S., Jia, J., Lai, W., Xin, X., et al. (2016). Chromatin Remodeling Factor LSH Drives Cancer Progression by Suppressing the Activity of Fumarate Hydratase. *Cancer Res.* 76 (19), 5743–5755. doi:10.1158/0008-5472.Can-16-0268

Hirayama, T., Miki, A., and Nagasawa, H. (2019). Organelle-specific Analysis of Labile Fe(ii) during Ferroptosis by Using a Cocktail of Various Colour Organelle-Targeted Fluorescent Probes. *Metallomics* 11 (1), 111–117. doi:10.1039/c8mt00212f

Hoang, P. H., and Landi, M. T. (2022). DNA Methylation in Lung Cancer: Mechanisms and Associations with Histological Subtypes, Molecular Alterations, and Major Epidemiological Factors. *Cancers (Basel)* 14 (4), 961. doi:10.3390/cancers14040961

Hou, W., Xie, Y., Song, X., Sun, X., Lotze, M. T., Zeh, H. J., 3rd, et al. (2016). Autophagy Promotes Ferroptosis by Degradation of Ferritin. *Autophagy* 12 (8), 1425–1428. doi:10.1080/15548627.2016.1187366

Huang, J., Tabbi-Anneni, I., Gunda, V., and Wang, L. (2010). Transcription Factor Nrf2 Regulates SHP and Lipogenic Gene Expression in Hepatic Lipid Metabolism. *Am. J. Physiol. Gastrointest. Liver Physiol.* 299 (6), G1211–G1221. doi:10.1152/ajpgi.00322.2010

Jiang, L., Kon, N., Li, T., Wang, S. J., Su, T., Hibshoosh, H., et al. (2015). Ferroptosis as a P53-Mediated Activity during Tumour Suppression. *Nature* 520 (7545), 57–62. doi:10.1038/nature14344

Jiang, L., Wang, J., Wang, K., Wang, H., Wu, Q., Yang, C., et al. (2021a). RNF217 Regulates Iron Homeostasis through its E3 Ubiquitin Ligase Activity by Modulating Ferroportin Degradation. *Blood* 138 (8), 689–705. doi:10.1182/blood.2020008986

Jiang, L., Zheng, H., Lyu, Q., Hayashi, S., Sato, K., Sekido, Y., et al. (2021b). Lysosomal Nitric Oxide Determines Transition from Autophagy to Ferroptosis after Exposure to Plasma-Activated Ringer's Lactate. *Redox Biol.* 43, 101989. doi:10.1016/j.redox.2021.101989

Jiang, P., Du, W., Wang, X., Mancuso, A., Gao, X., Wu, M., et al. (2011). p53 Regulates Biosynthesis through Direct Inactivation of Glucose-6-Phosphate Dehydrogenase. *Nat. Cell Biol.* 13 (3), 310–316. doi:10.1038/ncb2172

Jiang, Y., Mao, C., Yang, R., Yan, B., Shi, Y., Liu, X., et al. (2017). EGLN1/c-Myc Induced Lymphoid-specific Helicase Inhibits Ferroptosis through Lipid Metabolic Gene Expression Changes. *Theranostics* 7 (13), 3293–3305. doi:10.7150/thno.19988

Jin, Y., Huang, Z. L., Li, L., Yang, Y., Wang, C. H., Wang, Z. T., et al. (2019). Quercetin Attenuates Toosendanin-Induced Hepatotoxicity through Inducing the Nrf2/GCL/GSH Antioxidant Signaling Pathway. *Acta Pharmacol. Sin.* 40 (1), 75–85. doi:10.1038/s41401-018-0024-8

Kang, R., and Tang, D. (2017). Autophagy and Ferroptosis - What's the Connection? *Curr. Pathobiol. Rep.* 5 (2), 153–159. doi:10.1007/s40139-017-0139-5

Kappus, H. (1987). Oxidative Stress in Chemical Toxicity. *Arch. Toxicol.* 60 (1-3), 144–149. doi:10.1007/bf00296968

Kerins, M. J., and Ooi, A. (2018). The Roles of NRF2 in Modulating Cellular Iron Homeostasis. *Antioxid. Redox Signal* 29 (17), 1756–1773. doi:10.1089/ars.2017.7176

Kim, B. M., Choi, J. Y., Kim, Y. J., Woo, H. D., and Chung, H. W. (2007). Desferrioxamine (DFX) Has Genotoxic Effects on Cultured Human Lymphocytes and Induces the P53-Mediated Damage Response. *Toxicology* 229 (3), 226–235. doi:10.1016/j.tox.2006.10.022

Krainz, T., Gaschler, M. M., Lim, C., Sacher, J. R., Stockwell, B. R., and Wipf, P. (2016). A Mitochondrial-Targeted Nitroxide Is a Potent Inhibitor of Ferroptosis. *ACS Cent. Sci.* 2 (9), 653–659. doi:10.1021/acscentsci.6b00199

Kroemer, G., El-Deiry, W. S., Golstein, P., Peter, M. E., Vaux, D., Vandenabeele, P., et al. (2005). Classification of Cell Death: Recommendations of the Nomenclature Committee on Cell Death. *Cell Death Differ.* 12 (Suppl. 2), 1463–1467. doi:10.1038/sj.cdd.4401724

Kruiswijk, F., Labuschagne, C. F., and Vousden, K. H. (2015). p53 in Survival, Death and Metabolic Health: a Lifeguard with a Licence to Kill. *Nat. Rev. Mol. Cell Biol.* 16 (7), 393–405. doi:10.1038/nrm4007

Kuang, F., Liu, J., Tang, D., and Kang, R. (2020). Oxidative Damage and Antioxidant Defense in Ferroptosis. *Front. Cell Dev. Biol.* 8, 586578. doi:10.3389/fcell.2020.586578

Kumar, S., Sánchez-Álvarez, M., Lolo, F. N., Trionfetti, F., Strippoli, R., and Cordani, M. (2021). Autophagy and the Lysosomal System in Cancer. *Cells* 10 (10), 2752. doi:10.3390/cells10102752

Kwon, M. Y., Park, E., Lee, S. J., and Chung, S. W. (2015). Heme Oxygenase-1 Accelerates Erastin-Induced Ferroptotic Cell Death. *Oncotarget* 6 (27), 24393–24403. doi:10.18632/oncotarget.5162

Laptenko, O., and Prives, C. (2006). Transcriptional Regulation by P53: One Protein, Many Possibilities. *Cell Death Differ.* 13 (6), 951–961. doi:10.1038/sj.cdd.4401916

Lee, J. J., Ishihara, K., Notomi, S., Efstathiou, N. E., Ueta, T., Maidana, D., et al. (2020). Lysosome-associated Membrane Protein-2 Deficiency Increases the Risk of Reactive Oxygen Species-Induced Ferroptosis in Retinal Pigment Epithelial Cells. *Biochem. Biophys. Res. Commun.* 521 (2), 414–419. doi:10.1016/j.bbrc.2019.10.138

Lee, S., and Min, K. T. (2018). The Interface between ER and Mitochondria: Molecular Compositions and Functions. *Mol. Cells* 41 (12), 1000–1007. doi:10.14348/molcells.2018.0438

Lei, Y., Huang, Y., Wen, X., Yin, Z., Zhang, Z., and Klionsky, D. J. (2022). How Cells Deal with the Fluctuating Environment: Autophagy Regulation under Stress in Yeast and Mammalian Systems. *Antioxidants (Basel)* 11 (2), 304. doi:10.3390/antiox11020304

Leng, Y., Luo, X., Yu, J., Jia, H., and Yu, B. (2021). Ferroptosis: A Potential Target in Cardiovascular Disease. *Front. Cell Dev. Biol.* 9, 813668. doi:10.3389/fcell.2021.813668

Li, J., Cao, F., Yin, H. L., Huang, Z. J., Lin, Z. T., Mao, N., et al. (2020). Ferroptosis: Past, Present and Future. *Cell Death Dis.* 11 (2), 88. doi:10.1038/s41419-020-2298-2

Li, J., Liu, J., Xu, Y., Wu, R., Chen, X., Song, X., et al. (2021). Tumor Heterogeneity in Autophagy-dependent Ferroptosis. *Autophagy* 17 (11), 3361–3374. doi:10.1080/15548627.2021.1872241

Li, N., Wang, Y., Wang, X., Sun, N., and Gong, Y. H. (2022). Pathway Network of Pyroptosis and its Potential Inhibitors in Acute Kidney Injury. *Pharmacol. Res.* 175, 106033. doi:10.1016/j.phrs.2021.106033

Li, R., Jia, Z., and Zhu, H. (2019). Regulation of Nrf2 Signaling. *React. Oxyg. Species (Apex)* 8 (24), 312–322. doi:10.20455/ros.2019.865

Lillo-Moya, J., Rojas-Solé, C., Muñoz-Salamanca, D., Panieri, E., Saso, L., and Rodrigo, R. (2021). Targeting Ferroptosis against Ischemia/Reperfusion Cardiac Injury. *Antioxidants (Basel)* 10 (5), 667. doi:10.3390/antiox10050667

Liu, J., Yang, M., Kang, R., Klionsky, D. J., and Tang, D. (2019a). Autophagic Degradation of the Circadian Clock Regulator Promotes Ferroptosis. *Autophagy* 15 (11), 2033–2035. doi:10.1080/15548627.2019.1659623

Liu, J., Kang, R., and Tang, D. (2021a). Signaling Pathways and Defense Mechanisms of Ferroptosis. *Febs J.* 1, 1. doi:10.1111/febs.16059

Liu, N., Yang, R., Shi, Y., Chen, L., Liu, Y., Wang, Z., et al. (2020). The Cross-Talk between Methylation and Phosphorylation in Lymphoid-specific Helicase Drives Cancer Stem-like Properties. *Signal Transduct. Target Ther.* 5 (1), 197. doi:10.1038/s41392-020-00249-w

Liu, T., Jiang, L., Tavana, O., and Gu, W. (2019b). The Deubiquitylase OTUB1 Mediates Ferroptosis via Stabilization of SLC7A11. *Cancer Res.* 79 (8), 1913–1924. doi:10.1158/0008-5472.Can-18-3037

Liu, T., Xu, P., Ke, S., Dong, H., Zhan, M., Hu, Q., et al. (2022). Histone Methyltransferase SETDB1 Inhibits TGF-β-Induced Epithelial-Mesenchymal Transition in Pulmonary Fibrosis by Regulating SNAI1 Expression and the Ferroptosis Signaling Pathway. *Arch. Biochem. Biophys.* 715, 109087. doi:10.1016/j.abb.2021.109087

Liu, X., Xie, X., Ren, Y., Shao, Z., Zhang, N., Li, L., et al. (2021b). The Role of Necroptosis in Disease and Treatment. *MedComm (2020)* 2 (4), 730–755. doi:10.1002/mco2.108

Liu, Y., and Shi, Y. (2020). Mitochondria as a Target in Cancer Treatment. *MedComm (2020)* 1 (2), 129–139. doi:10.1002/mco2.16

Liu, Y., and Gu, W. (2022). p53 in Ferroptosis Regulation: the New Weapon for the Old Guardian. *Cell Death Differ.* 29, 895–910. doi:10.1038/s41418-022-00943-y

Lu, J., Xu, F., and Lu, H. (2020). LncRNA PVT1 Regulates Ferroptosis through miR-214-Mediated TFR1 and P53. *Life Sci.* 260, 118305. doi:10.1016/j.lfs.2020.118305

Lu, S. C. (2009). Regulation of Glutathione Synthesis. *Mol. Asp. Med.* 30 (1-2), 42–59. doi:10.1016/j.mam.2008.05.005

MacKenzie, S., and Bergdahl, A. (2022). Zinc Homeostasis in Diabetes Mellitus and Vascular Complications. *Biomedicines* 10 (1), 139. doi:10.3390/biomedicines10010139

Magtanong, L., Ko, P. J., To, M., Cao, J. Y., Forcina, G. C., Tarangelo, A., et al. (2019). Exogenous Monounsaturated Fatty Acids Promote a Ferroptosis-Resistant Cell State. *Cell Chem. Biol.* 26 (3), 420–e9. e429. doi:10.1016/j.chembiol.2018.11.016

Mao, C., Liu, X., Zhang, Y., Lei, G., Yan, Y., Lee, H., et al. (2021). DHODH-mediated Ferroptosis Defence Is a Targetable Vulnerability in Cancer. *Nature* 593 (7860), 586–590. doi:10.1038/s41586-021-03539-7

Mao, C., Wang, X., Liu, Y., Wang, M., Yan, B., Jiang, Y., et al. (2018). A G3BP1-Interacting lncRNA Promotes Ferroptosis and Apoptosis in Cancer via Nuclear Sequestration of P53. *Cancer Res.* 78 (13), 3484–3496. doi:10.1158/0008-5472.Can-17-3454

Maru, D., Hothi, A., Bagariya, C., and Kumar, A. (2022). Targeting Ferroptosis Pathways: A Novel Strategy for Cancer Therapy. *Ccdt* 22, 234–244. doi:10.2174/1568009622666220211122745

McGrath, E. P., Centonze, F. G., Chevet, E., Avril, T., and Lafont, E. (2021). Death Sentence: The Tale of a Fallen Endoplasmic Reticulum. *Biochim. Biophys. Acta Mol. Cell Res.* 1868 (6), 119001. doi:10.1016/j.bbamcr.2021.119001

Means, R. E., and Katz, S. G. (2021). Balancing Life and Death: BCL-2 Family Members at Diverse ER-Mitochondrial Contact Sites. *Febs J.* 1, 1. doi:10.1111/febs.16241

Meng, C., Zhan, J., Chen, D., Shao, G., Zhang, H., Gu, W., et al. (2021). The Deubiquitinase USP11 Regulates Cell Proliferation and Ferroptotic Cell Death via Stabilization of NRF2 USP11 Deubiquitinates and Stabilizes NRF2. *Oncogene* 40 (9), 1706–1720. doi:10.1038/s41388-021-01660-5

Muhoberac, B. B., and Vidal, R. (2019). Iron, Ferritin, Hereditary Ferritinopathy, and Neurodegeneration. *Front. Neurosci.* 13, 1195. doi:10.3389/fnins.2019.01195

Nam, L. B., and Keum, Y. S. (2019). Binding Partners of NRF2: Functions and Regulatory Mechanisms. *Arch. Biochem. Biophys.* 678, 108184. doi:10.1016/j.abb.2019.108184

Ou, Y., Wang, S. J., Li, D., Chu, B., and Gu, W. (2016). Activation of SAT1 Engages Polyamine Metabolism with P53-Mediated Ferroptotic Responses. *Proc. Natl. Acad. Sci. U. S. A.* 113 (44), E6806–e6812. doi:10.1073/pnas.1607152113

Rahmani, M., Davis, E. M., Crabtree, T. R., Habibi, J. R., Nguyen, T. K., Dent, P., et al. (2007). The Kinase Inhibitor Sorafenib Induces Cell Death through a Process Involving Induction of Endoplasmic Reticulum Stress. *Mol. Cell Biol.* 27 (15), 5499–5513. doi:10.1128/mcb.01080-06

Ritzenthaler, J. D., Torres-Gonzalez, E., Zheng, Y., Zelko, I. N., Van Berkel, V., Nunley, D. R., et al. (2022). The Profibrotic and Senescence Phenotype of Old Lung Fibroblasts Is Reversed or Ameliorated by Genetic and Pharmacological Manipulation of Slc7a11 Expression. *Am. J. Physiology-Lung Cell. Mol. Physiology* 322, L449–L461. doi:10.1152/ajplung.00593.2020

Rizzardi, N., Liparulo, I., Antonelli, G., Orsini, F., Riva, A., Bergamini, C., et al. (2021). Coenzyme Q10 Phytosome Formulation Improves CoQ10 Bioavailability and Mitochondrial Functionality in Cultured Cells. *Antioxidants (Basel)* 10 (6), 927. doi:10.3390/antiox10060927

Rodrigues, J. G., Balmaña, M., Macedo, J. A., Poças, J., Fernandes, Â., de-Freitas-Junior, J. C. M., et al. (2018). Glycosylation in Cancer: Selected Roles in Tumour Progression, Immune Modulation and Metastasis. *Cell Immunol.* 333, 46–57. doi:10.1016/j.cellimm.2018.03.007

Rojo de la Vega, M., Chapman, E., and Zhang, D. D. (2018). NRF2 and the Hallmarks of Cancer. *Cancer Cell* 34 (1), 21–43. doi:10.1016/j.ccell.2018.03.022

Sato, H., Tamba, M., Ishii, T., and Bannai, S. (1999). Cloning and Expression of a Plasma Membrane Cystine/glutamate Exchange Transporter Composed of Two Distinct Proteins. *J. Biol. Chem.* 274 (17), 11455–11458. doi:10.1074/jbc.274.17.11455

Sha, W., Hu, F., Xi, Y., Chu, Y., and Bu, S. (2021). Mechanism of Ferroptosis and its Role in Type 2 Diabetes Mellitus. *J. Diabetes Res.* 2021, 9999612. doi:10.1155/2021/9999612

Sheftel, A. D., Stehling, O., Pierik, A. J., Elsässer, H. P., Mühlenhoff, U., Webert, H., et al. (2010). Humans Possess Two Mitochondrial Ferredoxins, Fdx1 and Fdx2, with Distinct Roles in Steroidogenesis, Heme, and Fe/S Cluster Biosynthesis. *Proc. Natl. Acad. Sci. U. S. A.* 107 (26), 11775–11780. doi:10.1073/pnas.1004250107

Shen, J., Sheng, X., Chang, Z., Wu, Q., Wang, S., Xuan, Z., et al. (2014). Iron Metabolism Regulates P53 Signaling through Direct Heme-P53 Interaction and Modulation of P53 Localization, Stability, and Function. *Cell Rep.* 7 (1), 180–193. doi:10.1016/j.celrep.2014.02.042

Shi, P., Song, C., Qi, H., Ren, J., Ren, P., Wu, J., et al. (2022). Up-regulation of IRF3 Is Required for Docosahexaenoic Acid Suppressing Ferroptosis of Cardiac Microvascular Endothelial Cells in Cardiac Hypertrophy Rat. *J. Nutr. Biochem.* 104, 108972. doi:10.1016/j.jnutbio.2022.108972

Shimizu, R., Lan, N. N., Tai, T. T., Adachi, Y., Kawazoe, A., Mu, A., et al. (2014). p53 Directly Regulates the Transcription of the Human Frataxin Gene and its Lack of Regulation in Tumor Cells Decreases the Utilization of Mitochondrial Iron. *Gene* 551 (1), 79–85. doi:10.1016/j.gene.2014.08.043

Shin, D., Kim, E. H., Lee, J., and Roh, J. L. (2018). Nrf2 Inhibition Reverses Resistance to GPX4 Inhibitor-Induced Ferroptosis in Head and Neck Cancer. *Free Radic. Biol. Med.* 129, 454–462. doi:10.1016/j.freeradbiomed.2018.10.426

Shintoku, R., Takigawa, Y., Yamada, K., Kubota, C., Yoshimoto, Y., Takeuchi, T., et al. (2017). Lipoxygenase-mediated Generation of Lipid Peroxides Enhances Ferroptosis Induced by Erastin and RSL3. *Cancer Sci.* 108 (11), 2187–2194. doi:10.1111/cas.13380

Sui, S., Zhang, J., Xu, S., Wang, Q., Wang, P., and Pang, D. (2019). Ferritinophagy Is Required for the Induction of Ferroptosis by the Bromodomain Protein BRD4 Inhibitor (+)-JQ1 in Cancer Cells. *Cell Death Dis.* 10 (5), 331. doi:10.1038/s41419-019-1564-7

Sun, J., Zhou, C., Zhao, Y., Zhang, X., Chen, W., Zhou, Q., et al. (2021). Quiescin Sulfhydryl Oxidase 1 Promotes Sorafenib-Induced Ferroptosis in Hepatocellular Carcinoma by Driving EGFR Endosomal Trafficking and Inhibiting NRF2 Activation. *Redox Biol.* 41, 101942. doi:10.1016/j.redox.2021.101942

Sun, X., Ou, Z., Chen, R., Niu, X., Chen, D., Kang, R., et al. (2016). Activation of the P62-Keap1-NRF2 Pathway Protects against Ferroptosis in Hepatocellular Carcinoma Cells. *Hepatology* 63 (1), 173–184. doi:10.1002/hep.28251

Sun, X., Ou, Z., Xie, M., Kang, R., Fan, Y., Niu, X., et al. (2015). HSPB1 as a Novel Regulator of Ferroptotic Cancer Cell Death. *Oncogene* 34 (45), 5617–5625. doi:10.1038/onc.2015.32

Suzuki, S., Tanaka, T., Poyurovsky, M. V., Nagano, H., Mayama, T., Ohkubo, S., et al. (2010). Phosphate-activated Glutaminase (GLS2), a P53-Inducible Regulator of Glutamine Metabolism and Reactive Oxygen Species. *Proc. Natl. Acad. Sci. U. S. A.* 107 (16), 7461–7466. doi:10.1073/pnas.1002459107

Taguchi, K., Motohashi, H., and Yamamoto, M. (2011). Molecular Mechanisms of the Keap1–Nrf2 Pathway in Stress Response and Cancer Evolution. *Genes cells.* 16 (2), 123–140. doi:10.1111/j.1365-2443.2010.01473.x

Tang, E., Liu, S., Zhang, Z., Zhang, R., Huang, D., Gao, T., et al. (2021a). Therapeutic Potential of Glutamine Pathway in Lung Cancer. *Front. Oncol.* 11, 835141. doi:10.3389/fonc.2021.835141

Tang, L. J., Zhou, Y. J., Xiong, X. M., Li, N. S., Zhang, J. J., Luo, X. J., et al. (2021b). Ubiquitin-specific Protease 7 Promotes Ferroptosis via Activation of the p53/TfR1 Pathway in the Rat Hearts after Ischemia/reperfusion. *Free Radic. Biol. Med.* 162, 339–352. doi:10.1016/j.freeradbiomed.2020.10.307

Tang, Y., Li, C., Zhang, Y. J., and Wu, Z. H. (2021c). Ferroptosis-Related Long Non-coding RNA Signature Predicts the Prognosis of Head and Neck Squamous Cell Carcinoma. *Int. J. Biol. Sci.* 17 (3), 702–711. doi:10.7150/ijbs.55552

Tarangelo, A., and Dixon, S. J. (2019). *Lipid Metabolism and Ferroptosis*, 1–26. doi:10.1007/978-3-030-26780-3_1

Tian, R., Abarientos, A., Hong, J., Hashemi, S. H., Yan, R., Dräger, N., et al. (2021). Genome-wide CRISPRi/a Screens in Human Neurons Link Lysosomal Failure to Ferroptosis. *Nat. Neurosci.* 24 (7), 1020–1034. doi:10.1038/s41593-021-00862-0

Tomiotto-Pellissier, F., Alves, D. R., Miranda-Sapla, M. M., de Morais, S. M., Assolini, J. P., da Silva Bortoleti, B. T., et al. (2018). Caryocar Coriaceum Extracts Exert Leishmanicidal Effect Acting in Promastigote Forms by Apoptosis-like Mechanism and Intracellular Amastigotes by Nrf2/HO-1/ferritin Dependent Response and Iron Depletion: Leishmanicidal Effect of Caryocar Coriaceum Leaf Exracts. *Biomed. Pharmacother.* 98, 662–672. doi:10.1016/j.biopha.2017.12.083

Torii, S., Shintoku, R., Kubota, C., Yaegashi, M., Torii, R., Sasaki, M., et al. (2016). An Essential Role for Functional Lysosomes in Ferroptosis of Cancer Cells. *Biochem. J.* 473 (6), 769–777. doi:10.1042/bj20150658

Torti, S. V., and Torti, F. M. (2013). Iron and Cancer: More Ore to Be Mined. *Nat. Rev. Cancer* 13 (5), 342–355. doi:10.1038/nrc3495

Ursini, F., and Maiorino, M. (2020). Lipid Peroxidation and Ferroptosis: The Role of GSH and GPx4. *Free Radic. Biol. Med.* 152, 175–185. doi:10.1016/j.freeradbiomed.2020.02.027

Vasan, K., Werner, M., and Chandel, N. S. (2020). Mitochondrial Metabolism as a Target for Cancer Therapy. *Cell Metab.* 32 (3), 341–352. doi:10.1016/j.cmet.2020.06.019

Venkatesh, D., Stockwell, B. R., and Prives, C. (2020). p21 Can Be a Barrier to Ferroptosis Independent of P53. *Aging (Albany NY)* 12 (18), 17800–17814. doi:10.18632/aging.103961

Wang, L., Liu, Y., Du, T., Yang, H., Lei, L., Guo, M., et al. (2020a). ATF3 Promotes Erastin-Induced Ferroptosis by Suppressing System Xc(). *Cell Death Differ.* 27 (2), 662–675. doi:10.1038/s41418-019-0380-z

Wang, M., Mao, C., Ouyang, L., Liu, Y., Lai, W., Liu, N., et al. (2019). Long Noncoding RNA LINC00336 Inhibits Ferroptosis in Lung Cancer by Functioning as a Competing Endogenous RNA. *Cell Death Differ.* 26 (11), 2329–2343. doi:10.1038/s41418-019-0304-y

Wang, S. J., Li, D., Ou, Y., Jiang, L., Chen, Y., Zhao, Y., et al. (2016a). Acetylation Is Crucial for P53-Mediated Ferroptosis and Tumor Suppression. *Cell Rep.* 17 (2), 366–373. doi:10.1016/j.celrep.2016.09.022

Wang, Y., Wang, S., Xin, Y., Zhang, J., Wang, S., Yang, Z., et al. (2021a). Hydrogen Sulfide Alleviates the Anxiety-like and Depressive-like Behaviors of Type 1 Diabetic Mice via Inhibiting Inflammation and Ferroptosis. *Life Sci.* 278, 119551. doi:10.1016/j.lfs.2021.119551

Wang, Y., Zhao, Y., Wang, H., Zhang, C., Wang, M., Yang, Y., et al. (2020b). Histone Demethylase KDM3B Protects against Ferroptosis by Upregulating SLC7A11. *FEBS Open Bio* 10 (4), 637–643. doi:10.1002/2211-5463.12823

Wang, Y. Q., Chang, S. Y., Wu, Q., Gou, Y. J., Jia, L., Cui, Y. M., et al. (2016b). The Protective Role of Mitochondrial Ferritin on Erastin-Induced Ferroptosis. *Front. Aging Neurosci.* 8, 308. doi:10.3389/fnagi.2016.00308

Wang, Z., Chen, X., Liu, N., Shi, Y., Liu, Y., Ouyang, L., et al. (2021b). A Nuclear Long Non-coding RNA LINC00618 Accelerates Ferroptosis in a Manner Dependent upon Apoptosis. *Mol. Ther.* 29 (1), 263–274. doi:10.1016/j.ymthe.2020.09.024

Wei, H., Mundade, R., Lange, K. C., and Lu, T. (2014). Protein Arginine Methylation of Non-histone Proteins and its Role in Diseases. *Cell Cycle* 13 (1), 32–41. doi:10.4161/cc.27353

Wu, H., and Liu, A. (2021). Long Non-coding RNA NEAT1 Regulates Ferroptosis Sensitivity in Non-small-cell Lung Cancer. *J. Int. Med. Res.* 49 (3), 3000605521996183. doi:10.1177/0300060521996183

Wu, Y., Zhang, S., Gong, X., Tam, S., Xiao, D., Liu, S., et al. (2020). The Epigenetic Regulators and Metabolic Changes in Ferroptosis-Associated Cancer Progression. *Mol. Cancer* 19 (1), 39. doi:10.1186/s12943-020-01157-x

Wu, Z., Geng, Y., Lu, X., Shi, Y., Wu, G., Zhang, M., et al. (2019). Chaperone-mediated Autophagy Is Involved in the Execution of Ferroptosis. *Proc. Natl. Acad. Sci. U. S. A.* 116 (8), 2996–3005. doi:10.1073/pnas.1819728116

Xiao, D., Huang, J., Pan, Y., Li, H., Fu, C., Mao, C., et al. (2017). Chromatin Remodeling Factor LSH Is Upregulated by the LRP6-Gsk3β-E2f1 Axis Linking Reversely with Survival in Gliomas. *Theranostics* 7 (1), 132–143. doi:10.7150/thno.17032

Xiao, F. J., Zhang, D., Wu, Y., Jia, Q. H., Zhang, L., Li, Y. X., et al. (2019). miRNA-17-92 Protects Endothelial Cells from Erastin-Induced Ferroptosis through Targeting the A20-ACSL4 axis. *Biochem. Biophys. Res. Commun.* 515 (3), 448–454. doi:10.1016/j.bbrc.2019.05.147

Xie, Y., Zhu, S., Song, X., Sun, X., Fan, Y., Liu, J., et al. (2017). The Tumor Suppressor P53 Limits Ferroptosis by Blocking DPP4 Activity. *Cell Rep.* 20 (7), 1692–1704. doi:10.1016/j.celrep.2017.07.055

Xu, C., Sun, S., Johnson, T., Qi, R., Zhang, S., Zhang, J., et al. (2021). The Glutathione Peroxidase Gpx4 Prevents Lipid Peroxidation and Ferroptosis to Sustain Treg Cell Activation and Suppression of Antitumor Immunity. *Cell Rep.* 35 (11), 109235. doi:10.1016/j.celrep.2021.109235

Yagoda, N., von Rechenberg, M., Zaganjor, E., Bauer, A. J., Yang, W. S., Fridman, D. J., et al. (2007). RAS-RAF-MEK-dependent Oxidative Cell Death Involving Voltage-dependent Anion Channels. *Nature* 447 (7146), 864–868. doi:10.1038/nature05859

Yahagi, N., Shimano, H., Matsuzaka, T., Najima, Y., Sekiya, M., Nakagawa, Y., et al. (2003). p53 Activation in Adipocytes of Obese Mice. *J. Biol. Chem.* 278 (28), 25395–25400. doi:10.1074/jbc.M302364200

Yang, G., Yuan, Y., Yuan, H., Wang, J., Yun, H., Geng, Y., et al. (2021). Histone Acetyltransferase 1 Is a Succinyltransferase for Histones and Non-histones and Promotes Tumorigenesis. *EMBO Rep.* 22 (2), e50967. doi:10.15252/embr.202050967

Yang, W. S., Kim, K. J., Gaschler, M. M., Patel, M., Shchepinov, M. S., and Stockwell, B. R. (2016). Peroxidation of Polyunsaturated Fatty Acids by Lipoxygenases Drives Ferroptosis. *Proc. Natl. Acad. Sci. U. S. A.* 113 (34), E4966–E4975. doi:10.1073/pnas.1603244113

Yang, W. S., SriRamaratnam, R., Welsch, M. E., Shimada, K., Skouta, R., Viswanathan, V. S., et al. (2014). Regulation of Ferroptotic Cancer Cell Death by GPX4. *Cell* 156 (1-2), 317–331. doi:10.1016/j.cell.2013.12.010

Yang, W. S., and Stockwell, B. R. (2008). Synthetic Lethal Screening Identifies Compounds Activating Iron-dependent, Nonapoptotic Cell Death in Oncogenic-RAS-Harboring Cancer Cells. *Chem. Biol.* 15 (3), 234–245. doi:10.1016/j.chembiol.2008.02.010

Yang, Y., Luo, M., Zhang, K., Zhang, J., Gao, T., Connell, D. O., et al. (2020a). Nedd4 Ubiquitylates VDAC2/3 to Suppress Erastin-Induced Ferroptosis in Melanoma. *Nat. Commun.* 11 (1), 433. doi:10.1038/s41467-020-14324-x

Yang, Y., Tai, W., Lu, N., Li, T., Liu, Y., Wu, W., et al. (2020b). lncRNA ZFAS1 Promotes Lung Fibroblast-To-Myofibroblast Transition and Ferroptosis via Functioning as a ceRNA through miR-150-5p/SLC38A1 axis. *Aging (Albany NY)* 12 (10), 9085–9102. doi:10.18632/aging.103176

Yuan, H., Li, X., Zhang, X., Kang, R., and Tang, D. (2016). Identification of ACSL4 as a Biomarker and Contributor of Ferroptosis. *Biochem. Biophys. Res. Commun.* 478 (3), 1338–1343. doi:10.1016/j.bbrc.2016.08.124

Zanetti, M., Xian, S., Dosset, M., and Carter, H. (2022). The Unfolded Protein Response at the Tumor-Immune Interface. *Front. Immunol.* 13, 823157. doi:10.3389/fimmu.2022.823157

Zhang, B., Pan, C., Feng, C., Yan, C., Yu, Y., Chen, Z., et al. (2022a). Role of Mitochondrial Reactive Oxygen Species in Homeostasis Regulation. *Redox Rep.* 27 (1), 45–52. doi:10.1080/13510002.2022.2046423

Zhang, C., Lu, J., and Zhang, P. (2016). The Roles of Chromatin Remodeling Proteins in Cancer. *Curr. Protein Pept. Sci.* 17 (5), 446–454. doi:10.2174/1389203717666160122120713

Zhang, H., Zhang, E., and Hu, H. (2021a). Role of Ferroptosis in Non-alcoholic Fatty Liver Disease and its Implications for Therapeutic Strategies. *Biomedicines* 9 (11), 1660. doi:10.3390/biomedicines9111660

Zhang, J., Qiu, Q., Wang, H., Chen, C., and Luo, D. (2021b). TRIM46 Contributes to High Glucose-Induced Ferroptosis and Cell Growth Inhibition in Human Retinal Capillary Endothelial Cells by Facilitating GPX4 Ubiquitination. *Exp. Cell Res.* 407 (2), 112800. doi:10.1016/j.yexcr.2021.112800

Zhang, Y., Shi, J., Liu, X., Feng, L., Gong, Z., Koppula, P., et al. (2018). BAP1 Links Metabolic Regulation of Ferroptosis to Tumour Suppression. *Nat. Cell Biol.* 20 (10), 1181–1192. doi:10.1038/s41556-018-0178-0

Zhang, Y., Mohibi, S., Vasilatis, D. M., Chen, M., Zhang, J., and Chen, X. (2022b). Ferredoxin Reductase and P53 Are Necessary for Lipid Homeostasis and Tumor Suppression through the ABCA1-SREBP Pathway. *Oncogene* 41, 1718–1726. doi:10.1038/s41388-021-02100-0

Zhang, Z., Guo, M., Shen, M., Kong, D., Zhang, F., Shao, J., et al. (2020). The BRD7-P53-Slc25a28 axis Regulates Ferroptosis in Hepatic Stellate Cells. *Redox Biol.* 36, 101619. doi:10.1016/j.redox.2020.101619

Zhao, L., Gong, H., Huang, H., Tuerhong, G., and Xia, H. (2021). Participation of Mind Bomb-2 in Sevoflurane Anesthesia Induces Cognitive Impairment in Aged Mice via Modulating Ferroptosis. *ACS Chem. Neurosci.* 12 (13), 2399–2408. doi:10.1021/acschemneuro.1c00131

Zhao, Y., Liu, Y., Xu, Y., Li, K., Zhou, L., Qiao, H., et al. (2022). The Role of Ferroptosis in Blood-Brain Barrier Injury. *Cell Mol. Neurobiol.* 1, 1. doi:10.1007/s10571-022-01197-5

Zhu, S., Zhang, Q., Sun, X., Zeh, H. J., 3rd, Lotze, M. T., Kang, R., et al. (2017). HSPA5 Regulates Ferroptotic Cell Death in Cancer Cells. *Cancer Res.* 77 (8), 2064–2077. doi:10.1158/0008-5472.Can-16-1979

Zhu, Y., Zhang, C., Huang, M., Lin, J., Fan, X., and Ni, T. (2021). TRIM26 Induces Ferroptosis to Inhibit Hepatic Stellate Cell Activation and Mitigate Liver Fibrosis through Mediating SLC7A11 Ubiquitination. *Front. Cell Dev. Biol.* 9, 644901. doi:10.3389/fcell.2021.644901

Zou, Y., Li, H., Graham, E. T., Deik, A. A., Eaton, J. K., Wang, W., et al. (2020). Cytochrome P450 Oxidoreductase Contributes to Phospholipid Peroxidation in Ferroptosis. *Nat. Chem. Biol.* 16 (3), 302–309. doi:10.1038/s41589-020-0472-6

Conflict of Interest: The authors declare that the research was conducted in the absence of any commercial or financial relationships that could be construed as a potential conflict of interest.

Publisher's Note: All claims expressed in this article are solely those of the authors and do not necessarily represent those of their affiliated organizations, or those of the publisher, the editors and the reviewers. Any product that may be evaluated in this article, or claim that may be made by its manufacturer, is not guaranteed or endorsed by the publisher.

frontiers | Frontiers in Pharmacology

TYPE Review
PUBLISHED 15 August 2022
DOI 10.3389/fphar.2022.902302

OPEN ACCESS

EDITED BY
Xu Chen,
Guilin Medical University, China

REVIEWED BY
Qiang Wang,
Nanjing Drum Tower Hospital, China
Gabriel Adelman Cipolla,
Federal University of Paraná, Brazil

*CORRESPONDENCE
Yi Wang,
hbyiwang@126.com
Zhao Feng Liang,
liangzhaofeng@ujs.edu.cn

†These authors have contributed equally to this work

SPECIALTY SECTION
This article was submitted to Pharmacology of Anti-Cancer Drugs, a section of the journal Frontiers in Pharmacology

RECEIVED 23 March 2022
ACCEPTED 28 June 2022
PUBLISHED 15 August 2022

CITATION
Lu L, Chen B, Xu Y, Zhang X, Jin L, Qian H, Wang Y and Liang ZF (2022), Role of ferroptosis and ferroptosis-related non-coding RNAs in the occurrence and development of gastric cancer.
Front. Pharmacol. 13:902302.
doi: 10.3389/fphar.2022.902302

Role of ferroptosis and ferroptosis-related non-coding RNAs in the occurrence and development of gastric cancer

Ling Lu[1†], Bei Chen[2,3†], Yumeng Xu[2], Xinyi Zhang[2], Longtao Jin[1], Hui Qian[2], Yi Wang[4*] and Zhao Feng Liang[2*]

[1]Child Healthcare Department, The Fourth Affiliated Hospital of Jiangsu University, Zhenjiang, JS, China, [2]Jiangsu Key Laboratory of Medical Science and Laboratory Medicine, School of Medicine, Jiangsu University, Zhenjiang, JS, China, [3]Suzhou Science and Technology Town Hospital, Suzhou, JS, China, [4]Department of Urology, the Second Hospital of Anhui Medical University, Hefei, China

Gastric cancer (GC) is a malignant cancer of the digestive tract and is a life-threatening disease worldwide. Ferroptosis is a newly discovered form of regulated cell death, which involves the accumulation of iron-dependent lipid peroxides. It has been found that ferroptosis plays an important regulatory role in the occurrence, development, drug resistance, and prognosis of GC. Non-coding RNAs (ncRNAs) play a critical role in the occurrence and progression of a variety of diseases including GC. In recent years, the role of ferroptosis and ferroptosis-related ncRNAs (miRNA, lncRNA, and circRNA) in the occurrence, development, drug resistance, and prognosis of GC has attracted more and more attention. Herein, we briefly summarize the roles and functions of ferroptosis and ferroptosis-related ncRNAs in GC tumorigenesis, development, and prognosis. We also prospected the future research direction and challenges of ferroptosis and ferroptosis-related ncRNAs in GC.

KEYWORDS

gastric cancer, ferroptosis, noncoding RNA, mechanisms, function

Introduction

Cell death is strictly regulated by complex intracellular and extracellular signals, and is very important for various physiological and pathological processes, including growth, development, and tumorigenesis. The imbalance between abnormal proliferation and cell death of cancer cells is an important basis for the biological characteristics of malignancy. Ferroptosis is a newly discovered form of regulated cell death, which involves the accumulation of iron-dependent lipid peroxides and leads to fatal cell damage (Zhang et al., 2020). Ferroptosis, a unique form of nonapoptotic-regulated cell death caused by overwhelming iron-dependent lipid peroxides, is considered an emerging cancer suppression mechanism for gastric cancer (GC) (Ma et al., 2022).

GC is one of the most common malignant cancers that seriously affect human health in the world. Although great progress has been made in the diagnosis and treatment of GC

in recent years, there is still lack of effective diagnostic markers, and the prognosis of advanced GC is not optimistic. Studies have started to reveal the essential role of ferroptosis in GC (Lee et al., 2020; Zhang et al., 2020; Guan et al., 2022; Ma et al., 2022). Ferroptosis plays an important regulatory role in the occurrence, development, invasion, migration, diagnosis, drug resistance, and prognosis of GC (Gomaa et al., 2019; Zhang et al., 2020; Liu Y. et al., 2021; Guan et al., 2022). Increasing evidence has shown that non-coding RNA (ncRNAs) play a crucial role in the occurrence and development of GC. NcRNAs are important regulators of gene expression and contribute to the promotion of a large number of human diseases. In general, miRNAs negatively regulate gene expression by binding to the 3′ untranslated region of the target messenger RNAs (mRNAs), resulting in mRNA silencing or degradation (Luo et al., 2019; Yan and Bu, 2021). Long noncoding RNAs (lncRNAs) are a class of potentially-coding RNA transcripts, which have the functions of regulating gene expression by inhibiting the mRNA translation, modulating the mRNA stability, or as competing endogenous RNAs (ceRNAs) by acting as miRNA sponges (Li et al., 2020a; Yan and Bu, 2021). Circular RNAs (circRNAs) are mainly produced by the reverse splicing of exons of precursor mRNAs. The functions of circRNAs are mainly ceRNA or miRNA sponging, binding with proteins, regulation of precursor mRNAs (pre-mRNA) splicing, regulation of parental gene expression, and potential translation templates for proteins or peptides (Yan and Bu, 2021; Zhang Y. et al., 2022). MiRNAs, lncRNAs, and circRNAs may have other ways to regulate the expression of mRNAs or proteins jointly or competitively. NcRNAs play a key role in GC occurrence and development with disruption of their function including gene splicing and transcription as well as biological processes related to ferroptosis, cell differentiation, migration, apoptosis, and immune response (Wei et al., 2020; Tang et al., 2021; Ye et al., 2021).

However, the role of ncRNAs associated with ferroptosis in GC has not been systematically discussed. Herein, we analyzed and discussed the relationship between ferroptosis, ferroptosis-related ncRNAs, and GC. This review summarized the role of ferroptosis and ferroptosis-related ncRNAs in the occurrence, development, drug resistance, and prognosis of GC, which may provide a new basis for the early diagnosis and treatment of GC.

Ferroptosis and gastric cancer

Ferroptosis is a newly defined form of programmed cell death characterized by iron-dependent peroxide lipid accumulation (Shao et al., 2021). Fe^{3+} enters cells and is reduced to Fe^{2+} through STEAP3. Then, the divalent metal transporter 1 (DMT1) leads to the release of Fe^{2+} from endosomes, leading to the accumulation of ROS, which induce lipid peroxidation and ferroptosis (Jiang N. et al., 2021; Zhang C. et al., 2022). Glutathione peroxidase 4 (GPX4)-mediated lipid peroxidation pathway plays an important role in inhibiting ferroptosis. GPX4 converts glutathione (GSH) into oxidized glutathione (GSSG) and reduces lipid peroxidation (Jiang N. et al., 2021; Zhang C. et al., 2022).

GC is a malignant tumor that causes a great burden globally, and its molecular mechanism is not very clear. Dysregulation of the balance between cell proliferation and death is a central feature of GC. Studies have found that ferroptosis plays a critical role in the carcinogenesis and progression of GC (Gomaa et al., 2019; Liu Y. et al., 2021). The levels of ferroptosis were related to a variety of prognosis and cancer immune characteristics, which might be conducive to the individualized treatment of GC (Ma et al., 2021).

Ferroptosis played a regulatory role in GC by affecting the biological characteristics of GC cells, such as proliferation, migration, and apoptosis. Ferritinophagy-induced ferroptosis and the KEAP1/NRF2/HO-1 pathway was involved in the epithelial-to-mesenchymal transition (EMT) process of GC cells (Guan et al., 2022). Lee et al. demonstrated that the biosynthetic pathway of polyunsaturated fatty acids determines the sensitivity of GC to ferroptosis (Lee et al., 2020). The data of Sun et al. expounded that perilipin-2 promotes the proliferation or apoptosis of GC cells by modifying the ferroptosis pathway (Sun et al., 2020). It was reported that cytoplasmic polyadenylation element binding protein 1 (CPEB1) enhanced erastin-induced ferroptosis in GC cells by inhibiting TWIST1, and then promotes GC cells metastasis and angiogenesis (Wang J. et al., 2021). The above studies showed that ferroptosis plays an important role in the occurrence and development of GC, and its specific role and mechanism need to be further explored.

The drug resistance of patients with advanced GC seriously affects the effect of chemotherapy. Many studies suggested that ferroptosis could enhance the sensitivity of GC cells to chemotherapeutic drugs. Zhang et al. demonstrated that miR-522 secreted by cancer-associated fibroblasts (CAFs) suppressed ferroptosis and promoted chemoresistance in GC (Zhang et al., 2020). The results revealed that apatinib could induce lipid peroxidation through SREBP-1a-mediated GPX4, and regulate multidrug resistance and ferroptosis of GC cells (Zhao et al., 2021). Activating transcription factor 3 (ATF3) made GC cells sensitive to cisplatin by blocking NRF2/KEAP1/XCT pathway transduction and inducing ferroptosis, which provides a promising treatment for overcoming the chemoresistance of GC (Fu et al., 2021). The silent information regulator 6 (SIRT6) silencing overcomes resistance to sorafenib via promoting ferroptosis in GC (Cai et al., 2021).

Ferroptosis was expected to be used in the treatment and prognosis of GC (Liu S. J. et al., 2021; Huo et al., 2021). Shao et al. screened 10 ferroptosis-related markers (SP1, MYB, ALDH3A2, KEAP1, AIFM2, ITGB4, TGFBR1, MAP1LC3B, NOX4, and ZFP36), which could well predict the prognosis and immunotherapy of GC (Shao et al., 2021). Studies have shown

that by changing the activation degree of ferroptosis, GC cells and the microenvironment can be formed (Xiao et al., 2021a). Ferroptosis-related genes *NOX4, CHAC1,* and *HIF1A* were the prognostic biomarkers of gastric adenocarcinoma (Xiao et al., 2022). In addition, it was also found that the ferroptosis pattern in GC is related to the characteristics of immune microenvironment (Jiang X. et al., 2021; Liu S. J. et al., 2021; Wang F. et al., 2021). The establishment of markers associated with ferroptosis will help to predict the biological characteristics of GC and select the appropriate treatment for GC patients. However, there are still many problems to be solved in the application of ferroptosis to the clinical diagnosis and treatment of GC.

Ferroptosis was the major mechanism mediating antitumor activity, which was expected to become a promising compound for the treatment of GC (Liu Y. et al., 2021; Zhang L. et al., 2022; Ye et al., 2022). Jiyuan oridonin A, a naturally occurring ent-kaurane diterpenoid, induced ferroptosis through the autophagy pathway, suggesting that the induction of ferroptosis may be the main mechanism mediating the antitumor activity of Jiyuan oridonin A and its derivatives (Liu Y. et al., 2021). The results showed that Yiqi Huayu Decoction (a Chinese herbal medicine formula) could induce GC ferroptosis through the JAK2-STAT3 pathway and ACSl4 (Song et al., 2022). The data of Zhang et al. suggested that 6-Thioguanine (6-TG) performed as a potential novel compound for GC treatment via inducing ferroptosis (Zhang J et al., 2022). Tanshinone IIA, a pharmacologically active component isolated from Chinese herb, induced ferroptosis in GC cells by affecting the expression of p53-mediated SLC7A11 (Guan et al., 2020). Ma et al. demonstrated that the activating MAT2A-ACSL3 pathway could protect GC cells from ferroptosis2. However, it is not clear how ferroptosis plays a crucial role in the occurrence, development, and diagnosis of GC. Recent studies have found that ncRNAs may play a key role in this process.

Ferroptosis-related non-coding RNA and gastric cancer

More and more evidences have shown that ferroptosis-related ncRNAs play critical roles in the occurrence, development, treatment, and prognosis of GC. We summarized and analyzed the role of ferroptosis-related ncRNAs in the occurrence, progression, and drug resistance of GC.

Ferroptosis-related miRNA and gastric cancer

Ferroptosis is an iron-dependent mediated necrosis, which plays a decisive role in the occurrence and development of GC. It is reported that miRNAs play an important role in the multiple stages of GC (Li et al., 2020b; Wang J. et al., 2022). Studies suggested that miRNAs regulate the ferroptosis process of GC cells. We summarized the role of ferroptosis-related miRNAs in the occurrence, development, prognosis, and drug resistance of GC.

ALOX15 was closely related to the production of lipid peroxidation in GC cells, and miR-522 was a potential inhibitor of ALOX15. Zhang et al. demonstrated that CAFs secrete exosomal miR-522 to inhibit ferroptosis by blocking ALOX15 and lipid peroxidation accumulation (Zhang et al., 2020). GC stem cells are the main cause of metastasis and drug resistance of GC. It was found that the miR-375/SLC7A11 axis could stimulate ferroptosis, thus reducing the stemness of GC cells (Ni et al., 2021). The study of Niu et al. confirmed that physcion 8-O-β-glucopyranoside plays an important role in promoting ferroptosis by regulating miR-103a-3p/GLS2, so as to highlight its therapeutic potential in GC (Niu et al., 2019). Levobupivacaine has potential anticancer properties. Levobupivacaine, a local anesthetic, induced ferroptosis of GC cells and inhibited the growth of GC cells through the miR-489-3p/SLC7A11 axis (Mao et al., 2021). Propofol can inhibit the proliferation and induce the apoptosis of GC cells. Propofol induced ferroptosis and inhibited malignant phenotypes of GC cells via the miR-125b-5p/STAT3 axis (Liu Y. P. et al., 2021). The data of Gomaa et al. identified a new mechanism mediating miR-4715-3p silencing and AURKA induction in upper gastrointestinal adenocarcinoma. The inhibition of AURKA or reconstitution of miR-4715-3p inhibited GPX4 and induced cell death, suggesting a link between AURKA and ferroptosis (Gomaa et al., 2019).

Ferroptosis has been proved to play an important role in the pathogenesis of GC. MiRNAs have regulatory function in GC cells and have potential diagnostic and prognostic value in the occurrence and development of GC. Ferroptosis-related miRNAs have potential clinical application prospect in the diagnosis, personalized treatment, and prognosis of GC (Table 1).

Ferroptosis-related lncRNA and gastric cancer

LncRNAs and ferroptosis play a crucial role in the occurrence and development of GC (Jiang N. et al., 2021). In this part, we focus on the role and mechanism of ferroptosis-related lncRNAs in the occurrence and development of GC.

It is reported that the lncBDNF-AS/WDR5/FBXW7 axis regulated ferroptosis and mediated peritoneal metastasis of GC through VDAC3 ubiquitination (Huang et al., 2022). The experiment of Wang et al. confirmed that lncLASTR mediated the proliferation and migration of GC cells through the regulation of ferroptosis (Wang G. et al., 2022). GC stem cells

TABLE 1 Overview of the role of ferroptosis-related miRNAs in GC.

MiRNA	Expression status	Relationship with autophagy	Target	Type of biomarker	References
miR-522	Upregulated	Inhibited ferroptosis	ALOX15	Chemo- resistance	Zhang et al. (2020)
miR-375	Upregulated	Triggered ferroptosis	SLC7A11	Stemness of GC	Ni et al. (2021)
miR-103a-3p	Downregulated	Promoted ferroptosis	GLS2	Development and prognosis	Niu et al. (2019)
miR-489-3p	Upregulated	Enhanced ferroptosis	SLC7A11	Development and treatment	Mao et al. (2021)
miR-125b-5p	Upregulated	Enhanced ferroptosis	STAT3	Development	Liu Y. P. et al. (2021)
miR-4715-3p	Downregulated	Enhanced ferroptosis	AURKA/GPX4	Development and prognosis	Gomaa et al. (2019)

TABLE 2 Overview of the role of ferroptosis-related lncRNAs in GC.

LncRNA	Expression status	Relationship with autophagy	Target	Type of biomarker	References
lncBDNF-AS	Upregulated	Inhibited ferroptosis	WDR5/FBXW7	Development	Huang et al. (2022)
lncLASTR	Upregulated	Inhibited ferroptosis	GPX4	Occurrence, development, and prognostic	Wang G. et al. (2022)
lncFERO	Upregulated	Inhibited ferroptosis	hnRNPA1/SCD1	Development, resistance, and treatment	Zhang et al. (2021)
lncA2M-AS1, C2orf27A, and ZNF667-AS1	Upregulated	Inhibited ferroptosis	hub FRGs (MYB, PSAT1, TP53, and LONP1)	Treatment and prognostic	Yao et al. (2021)
17 ferroptosis-related lncRNAs	Differential expression			Treatment and prognostic	Pan et al. (2021)
20 ferroptosis-related lncRNAs	Differential expression			Diagnostic and prognostic	Chen W. et al. (2021)
AP000695.2, AL365181.3, and LINC01615	Upregulated			Treatment and prognostic	Zhang S. et al. (2022)
AP003392.1, AC245041.2, AP001271.1, and BOLA3-AS1	Expression correlated with clinical features			Treatment and prognostic	Wei et al. (2021)
17 ferroptosis-related lncRNAs	Differential expression		cytoskeleton, WNT and PI3K/mTOR	Development, treatment, and prognostic	Xiao et al. (2021b)
10 ferroptosis-related lncRNAs	Differential expression			Prognostic and resistance	Lai et al. (2021)
TMEM105, PVT1, LOC646588, FLJ22447, and DLEU1	Differential expression			Treatment and prognostic	Chen X. et al. (2021)

(GCSC) are the main cause of the occurrence and prognosis of GC. Zhang et al. suggested that GC cell-derived exosomal lncFERO controls the tumorigenicity of GCSC by inhibiting ferroptosis, suggesting that the targeted exosomal lncFERO/hnRNPA1/SCD1 combined chemotherapy may be a promising GCSC based therapeutic strategy (Zhang et al., 2021). Yao et al. found that lncRNAs (A2M-AS1, C2orf27A, and ZNF667-AS1) targeted ferroptosis-related genes and impaired the activation of $CD4^+$ T cells in GC, which provides a new strategy of GC immunotherapy (Yao et al., 2021). *Pan* et al. prognostic model based on the 17 ferroptosis-related lncRNAs may improve the overall survival prediction of GC (Pan et al., 2021). These ferroptosis-related lncRNAs may play an important role in the immune infiltration of GC, which may help to determine the personalized prognosis and treatment of GC patients (Chen W. et al., 2021). Zhang et al. also established a ferroptosis-related lncRNA model that could predict the prognosis of stomach adenocarcinoma patients (Zhang S. et al., 2022). There are other prediction models showing ferroptosis-related lncRNAs associated with drug resistance, immunity, and tumor microenvironment changes in GC (Chen X. et al., 2021; Lai et al., 2021; Xiao et al., 2021b; Wei et al., 2021; Zhang S. et al., 2022).

Ferroptosis-related lncRNAs are differentially expressed in different stages of GC, which can provide a basis for ferroptosis-related lncRNAs clinical application in the diagnosis, treatment, and prognosis of GC. These studies suggest that ferroptosis-related lncRNAs can be used as potential markers for the progression, prognosis, personalized treatment, and drug resistance of GC (Table 2).

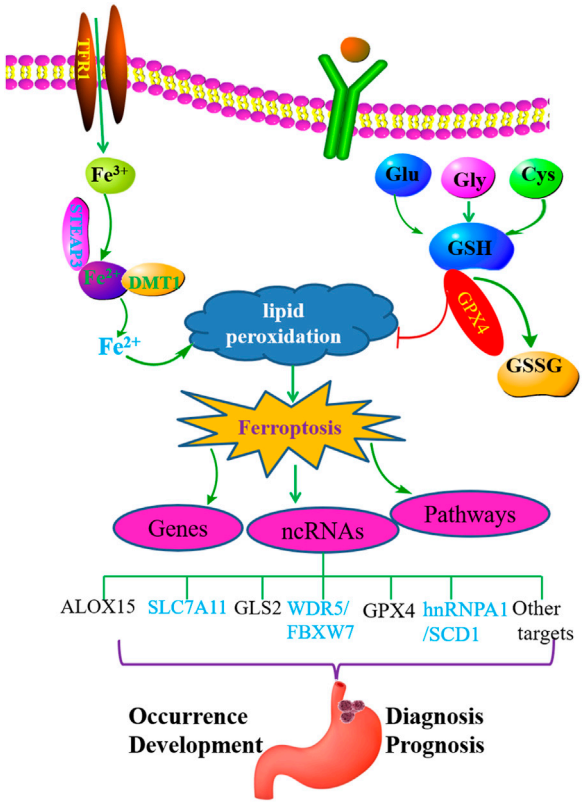

FIGURE 1
Ferroptosis plays an important role in GC and may regulate the occurrence and development of gastric cancer by interacting with related ncRNAs.

Ferroptosis-related circRNAs and gastric cancer

Multiple circRNAs have been verified to act as essential regulators in the occurrence and progression of GC. As new prognostic biomarkers, ferroptosis-related circRNAs will be broad application prospects in GC diagnosis, individualized treatment, microenvironment, drug resistance, and immunotherapy in the future. Herein, we summarized the role of ferroptosis-related circRNAs in GC.

The expression level of circ0008035 was upregulated in GC tissues and cells. Li et al. reported that circ0008035 repressed ferroptosis and affected the proliferation and apoptosis of GC cells by up-regulating *EIF4A1* via sponging miR-599 (Li C. et al., 2020). Circ0000190 was down regulated in GC tissues and cell lines, indicating a poor prognosis of GC patients. Circ0000190 overexpression suppressed GC cell proliferation and migration by inducing ferroptosis (Jiang et al., 2022).

Summary and the challenges

Ferroptosis plays an important role in the pathogenesis of GC. NcRNAs play a crucial role in the occurrence, development, treatment, and drug resistance of GC. However, the relationship between ferroptosis, ferroptosis-related ncRNAs, and GC has not been well summarized and clarified. In recent years, the understanding of the relationship between ferroptosis, ferroptosis-related ncRNAs, and GC has advanced rapidly. Based on the abovementioned overview , we conclude that ferroptosis and ferroptosis-related ncRNAs play essential roles in the occurrence and prognosis of GC (Figure 1). Ferroptosis-related ncRNAs are expected to be used as potential clinical markers of GC.

However, to achieve clinical application, there are still many aspects to be improved and many challenges to be solved in the future research. First, the regulatory mechanism between ferroptosis and ferroptosis-related ncRNAs are not very clear. In the future, we believe that the role and mechanism of ferroptosis-related ncRNAs in GC may become one of the research focuses. Second, the mechanisms of generation and selection of ferroptosis-related ncRNAs are still unclear. Clarifying the mechanism of ferroptosis ncRNA generation, selection and degradation may be an important link in promoting its clinical application. Third, at present, there are only few studies on ferroptosis-related ncRNAs in the occurrence and prognosis of GC. It is necessary to further explore the role of more ncRNAs in GC. Furthermore, the research and verification of large-scale population tissue samples need to be carried out before clinical application. The reproducibility, specificity, and sensitivity of ferroptosis-related ncRNA detection and application need to be further evaluated. In addition, exosomes can carry mRNAs, ncRNAs, proteins, and other components to participate in the cell-cell communication. Whether ferroptosis related ncRNAs can affect the microenvironment of GC through exosomes, and then play key roles in the occurrence, prognosis, and drug resistance of GC needs to be explored.

Based on the abovementioned studies, we also speculated the potential future development direction of ferroptosis and ferroptosis-related ncRNAs in GC. First, developing experimental methods or detection techniques of ferroptosis and ferroptosis-related ncRNAs, so that they can be better used in the early diagnosis of GC, monitoring progress, drug resistance, and prognosis. Second, liquid biopsy is more and more widely used in GC and other cancers. It is particularly important to detect ferroptosis-related ncRNAs in blood or exosomes, and analyze the relationship between these abnormally expressed ncRNAs and the occurrence, development, drug resistance, and prognosis of GC. Last, as a potential therapeutic target for GC, giving better use of ferroptosis-related ncRNAs in diagnosis and treatment may

help to prolong the survival time and improve the quality of life of GC patients.

Author contributions

LL, BC, and ZL designed research and wrote the manuscript. YX, XZ, and LJ participated in data collection and analysis. HQ, YW and ZL contributed to the writing and revisions.

Funding

This work was supported by the National Natural Science Foundation of China (no. 81602883), project of social development in Zhenjiang (No. SH2021045), "Jinshan Doctor" medical field talent training plan of Zhenjiang, Foundation for Excellent Young Teachers of Jiangsu University, Clinical Medical Science and Technology Development Foundation of Jiangsu University (No. JLY2021013), Medical Research Collaborative Innovation Joint Fund of The Second Affiliated Hospital of Anhui Medical University and Center for Medical Physics, Chinese Academy of Sciences (LHJJ202003), and Suzhou Science and Technology Town Hospital Pre-Research Fund (No. szkjcyy2022002).

Conflict of interest

The authors declare that the research was conducted in the absence of any commercial or financial relationships that could be construed as a potential conflict of interest.

Publisher's note

References

Cai, S., Fu, S., Zhang, W., Yuan, X., Cheng, Y., Fang, J., et al. (2021). SIRT6 silencing overcomes resistance to sorafenib by promoting ferroptosis in gastric cancer. *Biochem. Biophys. Res. Commun.* 577, 158–164. doi:10.1016/j.bbrc.2021.08.080

Chen, W., Feng, Z., Huang, J., Fu, P., Xiong, J., Cao, Y., et al. (2021). Identification of ferroptosis-related long noncoding RNA and construction of a novel prognostic signature for gastric cancer. *Dis. Markers* 2021, 7724997. doi:10.1155/2021/7724997

Chen, X., Zhu, Z., Li, X., Yao, X., and Luo, L. (2021). The ferroptosis-related noncoding RNA signature as a novel prognostic biomarker in the tumor microenvironment, immunotherapy, and drug screening of gastric adenocarcinoma. *Front. Oncol.* 11, 778557. doi:10.3389/fonc.2021.778557

Fu, D., Wang, C., Yu, L., and Yu, R. (2021). Induction of ferroptosis by ATF3 elevation alleviates cisplatin resistance in gastric cancer by restraining Nrf2/Keap1/xCT signaling. *Cell. Mol. Biol. Lett.* 26 (1), 26. doi:10.1186/s11658-021-00271-y

Gomaa, A., Peng, D., Chen, Z., Soutto, M., Abouelezz, K., Corvalan, A., et al. (2019). Epigenetic regulation of AURKA by miR-4715-3p in upper gastrointestinal cancers. *Sci. Rep.* 9 (1), 16970. doi:10.1038/s41598-019-53174-6

Guan, Z., Chen, J., Li, X., and Dong, N. (2020). Tanshinone IIA induces ferroptosis in gastric cancer cells through p53-mediated SLC7A11 down-regulation. *Biosci. Rep.* 40 (8), BSR20201807. doi:10.1042/BSR20201807

Guan, D., Zhou, W., Wei, H., Wang, T., Zheng, K., Yang, C., et al. (2022). Ferritinophagy-mediated ferroptosis and activation of keap1/Nrf2/HO-1 pathway were conducive to EMT inhibition of gastric cancer cells in action of 2, 2'-Di-pyridineketone hydrazone dithiocarbamate butyric acid ester. *Oxid. Med. Cell. Longev.* 2022, 3920664. doi:10.1155/2022/3920664

Huang, G., Xiang, Z., Wu, H., He, Q., Dou, R., Lin, Z., et al. (2022). The lncRNA BDNF-AS/WDR5/FBXW7 axis mediates ferroptosis in gastric cancer peritoneal metastasis by regulating VDAC3 ubiquitination. *Int. J. Biol. Sci.* 18 (4), 1415–1433. doi:10.7150/ijbs.69454

Huo, J., Wu, L., and Zang, Y. (2021). Eight-gene prognostic signature associated with hypoxia and ferroptosis for gastric cancer with general applicability. *Epigenomics* 13 (11), 875–890. doi:10.2217/epi-2020-0411

Jiang, M., Mo, R., Liu, C., and Wu, H. (2022). Circ_0000190 sponges miR-382-5p to suppress cell proliferation and motility and promote cell death by targeting ZNRF3 in gastric cancer. *J. Biochem.*, mvac003. doi:10.1093/jb/mvac003

Jiang, N., Zhang, X., Gu, X., Li, X., and Shang, L. (2021). Progress in understanding the role of lncRNA in programmed cell death. *Cell Death Discov.* 7 (1), 30. doi:10.1038/s41420-021-00407-1

Jiang, X., Liu, F., Liu, P., Yan, Y., Lan, S., Zhuang, K., et al. (2021). Ferroptosis patterns correlate with immune microenvironment characterization in gastric cancer. *Int. J. Gen. Med.* 14, 6573–6586. doi:10.2147/IJGM.S331291

Lai, D., Tan, L., Zuo, X., Liu, D., Jiao, D., Wan, G., et al. (2021). Prognostic ferroptosis-related lncRNA signatures associated with immunotherapy and chemotherapy responses in patients with stomach cancer. *Front. Genet.* 12, 798612. doi:10.3389/fgene.2021.798612

Lee, J. Y., Nam, M., Son, H. Y., Hyun, K., Jang, S. Y., Kim, J. W., et al. (2020). Polyunsaturated fatty acid biosynthesis pathway determines ferroptosis sensitivity in gastric cancer. *Proc. Natl. Acad. Sci. U. S. A.* 117 (51), 32433–32442. doi:10.1073/pnas.2006828117

Li, C., Tian, Y., Liang, Y., and Li, Q. (2020). Circ_0008035 contributes to cell proliferation and inhibits apoptosis and ferroptosis in gastric cancer via miR-599/EIF4A1 axis. *Cancer Cell Int.* 20 (1), 84. doi:10.1186/s12935-020-01168-0

Li, Y., Li, G., Guo, X., Yao, H., Wang, G., Li, C., et al. (2020). Non-coding RNA in bladder cancer. *Cancer Lett.* 485, 38–44. doi:10.1016/j.canlet.2020.04.023

Li, Y., Tian, Z., Tan, Y., Lian, G., Chen, S., Chen, S., et al. (2020). Bmi-1-induced miR-27a and miR-155 promote tumor metastasis and chemoresistance by targeting RKIP in gastric cancer. *Mol. Cancer* 19 (1), 109. doi:10.1186/s12943-020-01229-y

Liu, S. J., Yang, Y. B., Zhou, J. X., Lin, Y. J., Pan, Y. L., Pan, J. H., et al. (2021). A novel ferroptosis-related gene risk signature for predicting prognosis and immunotherapy response in gastric cancer. *Dis. Markers* 2021, 2385406. doi:10.1155/2021/2385406

Liu, Y., Song, Z., Liu, Y., Ma, X., Wang, W., Ke, Y., et al. (2021). Identification of ferroptosis as a novel mechanism for antitumor activity of natural product derivative a2 in gastric cancer. *Acta Pharm. Sin. B* 11 (6), 1513–1525. doi:10.1016/j.apsb.2021.05.006

Liu, Y. P., Qiu, Z. Z., Li, X. H., and Li, E. Y. (2021). Propofol induces ferroptosis and inhibits malignant phenotypes of gastric cancer cells by regulating miR-125b-5p/STAT3 axis. *World J. Gastrointest. Oncol.* 13 (12), 2114–2128. doi:10.4251/wjgo.v13.i12.2114

Luo, Y. J., Huang, Q. M., Ren, Y., Liu, Z. L., Xu, C. F., Wang, H., et al. (2019). Non-coding RNA in drug resistance of gastric cancer. *World J. Gastrointest. Oncol.* 11 (11), 957–970. doi:10.4251/wjgo.v11.i11.957

Ma, J., Hu, X., Yao, Y., Wu, L., Sheng, C., Chen, K., et al. (2021). Characterization of two ferroptosis subtypes with distinct immune

infiltration and gender difference in gastric cancer. *Front. Nutr.* 8, 756193. doi:10.3389/fnut.2021.756193

Ma, M., Kong, P., Huang, Y., Wang, J., Liu, X., Hu, Y., et al. (2022). Activation of MAT2A-ACSL3 pathway protects cells from ferroptosis in gastric cancer. *Free Radic. Biol. Med.* 181, 288–299. doi:10.1016/j.freeradbiomed.2022.02.015

Mao, S. H., Zhu, C. H., Nie, Y., Yu, J., and Wang, L. (2021). Levobupivacaine induces ferroptosis by miR-489-3p/SLC7A11 signaling in gastric cancer. *Front. Pharmacol.* 12, 681338. doi:10.3389/fphar.2021.681338

Ni, H., Qin, H., Sun, C., Liu, Y., Ruan, G., Guo, Q., et al. (2021). MiR-375 reduces the stemness of gastric cancer cells through triggering ferroptosis. *Stem Cell Res. Ther.* 12 (1), 325. doi:10.1186/s13287-021-02394-7

Niu, Y., Zhang, J., Tong, Y., Li, J., and Liu, B. (2019). Physcion 8-O-beta-glucopyranoside induced ferroptosis via regulating miR-103a-3p/GLS2 axis in gastric cancer. *Life Sci.* 237, 116893. doi:10.1016/j.lfs.2019.116893

Pan, J., Zhang, X., Fang, X., and Xin, Z. (2021). Construction on of a ferroptosis-related lncRNA-based model to improve the prognostic evaluation of gastric cancer patients based on bioinformatics. *Front. Genet.* 12, 739470. doi:10.3389/fgene.2021.739470

Shao, Y., Jia, H., Li, S., Huang, L., Aikemu, B., Yang, G., et al. (2021). Comprehensive analysis of ferroptosis-related markers for the clinical and biological value in gastric cancer. *Oxid. Med. Cell. Longev.* 2021, 7007933. doi:10.1155/2021/7007933

Song, S., Wen, F., Gu, S., Gu, P., Huang, W., Ruan, S., et al. (2022). Network Pharmacology study and experimental validation of Yiqi Huayu decoction inducing ferroptosis in gastric cancer. *Front. Oncol.* 12, 820059. doi:10.3389/fonc.2022.820059

Sun, X., Yang, S., Feng, X., Zheng, Y., Zhou, J., Wang, H., et al. (2020). The modification of ferroptosis and abnormal lipometabolism through overexpression and knockdown of potential prognostic biomarker perilipin2 in gastric carcinoma. *Gastric Cancer* 23 (2), 241–259. doi:10.1007/s10120-019-01004-z

Tang, X. H., Guo, T., Gao, X. Y., Wu, X. L., Xing, X. F., Ji, J. F., et al. (2021). Exosome-derived noncoding RNAs in gastric cancer: functions and clinical applications. *Mol. Cancer* 20 (1), 99. doi:10.1186/s12943-021-01396-6

Wang, F., Chen, C., Chen, W. P., Li, Z. L., and Cheng, H. (2021). Development and validation of a novel ferroptosis-related gene signature for predicting prognosis and the immune microenvironment in gastric cancer. *Biomed. Res. Int.* 2021, 6014202. doi:10.1155/2021/6014202

Wang, G., Sun, L., Wang, S., Guo, J., Xiao, R., Li, W., et al. (2022). Ferroptosisrelated long noncoding RNAs and the roles of LASTR in stomach adenocarcinoma. *Mol. Med. Rep.* 25 (4), 118. doi:10.3892/mmr.2022.12634

Wang, J., Wang, T., Zhang, Y., Liu, J., Song, J., Han, Y., et al. (2021). CPEB1 enhances erastin-induced ferroptosis in gastric cancer cells by suppressing twist1 expression. *IUBMB life* 73 (9), 1180–1190. doi:10.1002/iub.2525

Wang, J., Ge, J., Wang, Y., Xiong, F., Guo, J., Jiang, X., et al. (2022). EBV miRNAs BART11 and BART17-3p promote immune escape through the enhancer-mediated transcription of PD-L1. *Nat. Commun.* 13 (1), 866. doi:10.1038/s41467-022-28479-2

Wei, L., Sun, J., Zhang, N., Zheng, Y., Wang, X., Lv, L., et al. (2020). Noncoding RNAs in gastric cancer: implications for drug resistance. *Mol. Cancer* 19 (1), 62. doi:10.1186/s12943-020-01185-7

Wei, J., Zeng, Y., Gao, X., and Liu, T. (2021). A novel ferroptosis-related lncRNA signature for prognosis prediction in gastric cancer. *BMC cancer* 21 (1), 1221. doi:10.1186/s12885-021-08975-2

Xiao, S., Liu, X., Yuan, L., Chen, X., and Wang, F. (2021). Expression of ferroptosis-related genes shapes tumor microenvironment and pharmacological profile in gastric cancer. *Front. Cell Dev. Biol.* 9, 694003. doi:10.3389/fcell.2021.694003

Xiao, S., Liu, X., Yuan, L., and Wang, F. (2021). A ferroptosis-related lncRNAs signature predicts prognosis and therapeutic response of gastric cancer. *Front. Cell Dev. Biol.* 9, 736682. doi:10.3389/fcell.2021.736682

Xiao, R., Wang, S., Guo, J., Liu, S., Ding, A., Wang, G., et al. (2022). Ferroptosis-related gene NOX4, CHAC1 and HIF1A are valid biomarkers for stomach adenocarcinoma. *J. Cell. Mol. Med.* 26 (4), 1183–1193. doi:10.1111/jcmm.17171

Yan, H., and Bu, P. (2021). Non-coding RNA in cancer. *Essays Biochem.* 65 (4), 625–639. doi:10.1042/EBC20200032

Yao, F., Zhan, Y., Pu, Z., Lu, Y., Chen, J., Deng, J., et al. (2021). LncRNAs target ferroptosis-related genes and impair activation of CD4(+) T cell in gastric cancer. *Front. Cell Dev. Biol.* 9, 797339. doi:10.3389/fcell.2021.797339

Ye, J., Li, J., and Zhao, P. (2021). Roles of ncRNAs as ceRNAs in gastric cancer. *Genes* 12 (7), 1036. doi:10.3390/genes12071036

Ye, Y., Li, X., Feng, G., Ma, Y., Ye, F., Shen, H., et al. (2022). 3, 3'-Diindolylmethane induces ferroptosis by BAP1-IP3R axis in BGC-823 gastric cancer cells. *Anticancer. Drugs* 33 (4), 362–370. doi:10.1097/CAD.0000000000001270

Zhang, C., Liu, X., Jin, S., Chen, Y., and Guo, R. (2022). Ferroptosis in cancer therapy: a novel approach to reversing drug resistance. *Mol. Cancer* 21 (1), 47. doi:10.1186/s12943-022-01530-y

Zhang, H., Deng, T., Liu, R., Ning, T., Yang, H., Liu, D., et al. (2020). CAF secreted miR-522 suppresses ferroptosis and promotes acquired chemo-resistance in gastric cancer. *Mol. Cancer* 19 (1), 43. doi:10.1186/s12943-020-01168-8

Zhang, H., Wang, M., He, Y., Deng, T., Liu, R., Wang, W., et al. (2021). Chemotoxicity-induced exosomal lncFERO regulates ferroptosis and stemness in gastric cancer stem cells. *Cell Death Dis.* 12 (12), 1116. doi:10.1038/s41419-021-04406-z

Zhang, J., Gao, M., Niu, Y., and Sun, J. (2022). From DNMT1 degrader to ferroptosis promoter: Drug repositioning of 6-Thioguanine as a ferroptosis inducer in gastric cancer. *Biochem. Biophys. Res. Commun.* 603, 75–81. doi:10.1016/j.bbrc.2022.03.026

Zhang, L., Li, C., Zhang, Y., Zhang, J., and Yang, X. (2022). Ophiopogonin B induces gastric cancer cell death by blocking the GPX4/xCT-dependent ferroptosis pathway. *Oncol. Lett.* 23 (3), 104. doi:10.3892/ol.2022.13224

Zhang, S., Zheng, N., Chen, X., Du, K., Yang, J., Shen, L., et al. (2022). Establishment and validation of a ferroptosis-related long non-coding RNA signature for predicting the prognosis of stomach adenocarcinoma. *Front. Genet.* 13, 818306. doi:10.3389/fgene.2022.818306

Zhang, Y., Zhang, X., Xu, Y., Fang, S., Ji, Y., Lu, L., et al. (2022). Circular RNA and its roles in the occurrence, development, diagnosis of cancer. *Front. Oncol.* 12, 845703. doi:10.3389/fonc.2022.845703

Zhao, L., Peng, Y., He, S., Li, R., Wang, Z., Huang, J., et al. (2021). Apatinib induced ferroptosis by lipid peroxidation in gastric cancer. *Gastric Cancer* 24 (3), 642–654. doi:10.1007/s10120-021-01159-8

Advantages of publishing in Frontiers

OPEN ACCESS
Articles are free to read for greatest visibility and readership

FAST PUBLICATION
Around 90 days from submission to decision

HIGH QUALITY PEER-REVIEW
Rigorous, collaborative, and constructive peer-review

TRANSPARENT PEER-REVIEW
Editors and reviewers acknowledged by name on published articles

Frontiers
Avenue du Tribunal-Fédéral 34
1005 Lausanne | Switzerland

Visit us: www.frontiersin.org
Contact us: frontiersin.org/about/contact

REPRODUCIBILITY OF RESEARCH
Support open data and methods to enhance research reproducibility

DIGITAL PUBLISHING
Articles designed for optimal readership across devices

FOLLOW US
@frontiersin

IMPACT METRICS
Advanced article metrics track visibility across digital media

EXTENSIVE PROMOTION
Marketing and promotion of impactful research

LOOP RESEARCH NETWORK
Our network increases your article's readership